

ISTANBUL TECHNICAL UNIVERSITY ★ GRADUATE SCHOOL

**DESIGN OF SEAFARER-CENTRIC SAFETY SYSTEM; MENTAL
WORKLOAD (MWL) PREDICTION**



Ph.D. THESIS

Bariş ÖZSEVER

Maritime Transportation Engineering Department

Maritime Transportation Engineering Programme

JANUARY 2022

ISTANBUL TECHNICAL UNIVERSITY ★ GRADUATE SCHOOL

**DESIGN OF SEAFARER-CENTRIC SAFETY SYSTEM; MENTAL
WORKLOAD (MWL) PREDICTION**

Ph.D. THESIS

**Bariř ÖZSEVER
(512152011)**

Maritime Transportation Engineering Department

Maritime Transportation Engineering Programme

Thesis Advisor: Prof. Dr. Leyla TAVACIOĐLU

JANUARY 2022

İSTANBUL TEKNİK ÜNİVERSİTESİ ★ LİSANSÜSTÜ EĞİTİM ENSTİTÜSÜ

**GEMİ İNSANI-MERKEZLİ EMNİYET SİSTEMİNİN TASARIMI; MENTAL İŞ
YÜKÜ ÖNGÖRÜSÜ**

DOKTORA TEZİ

**Bariş ÖZSEVER
(512152011)**

Deniz Ulaştırma Mühendisliği Anabilim Dalı

Deniz Ulaştırma Mühendisliği Programı

Tez Danışmanı: Prof. Dr. Leyla TAVACIOĞLU

OCAK 2022

Barış ÖZSEVER, a Ph.D. student of İTÜ Graduate School student ID 512152011, successfully defended the thesis/dissertation entitled “DESIGN OF SEAFARER-CENTRIC SAFETY SYSTEM; MENTAL WORKLOAD (MWL) PREDICTION”, which he prepared after fulfilling the requirements specified in the associated legislations, before the jury whose signatures are below.

Thesis Advisor : **Prof. Dr. Leyla TAVACIOĞLU**
İstanbul Technical University

Jury Members : **Prof. Dr. Mustafa Ersel KAMAŞAK**
İstanbul Technical University

Asst. Prof. Dr. Erdem BİLGİLİ
Piri Reis University

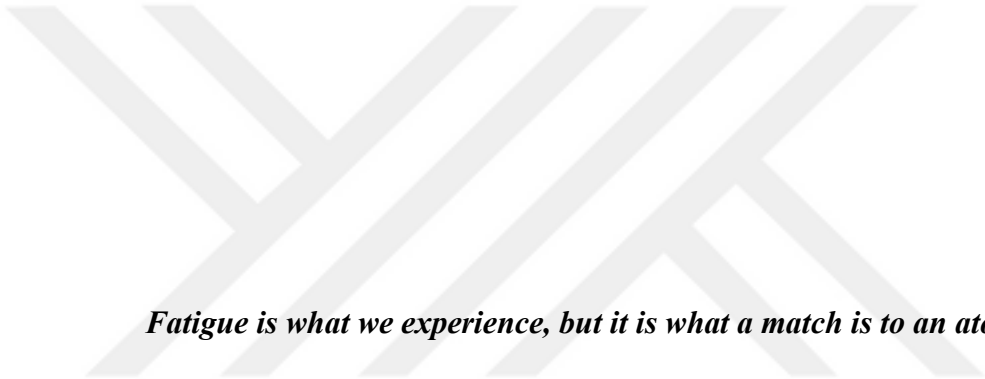
Assoc. Prof. Dr. Tanzer SATIR
İstanbul Technical University

Assoc. Prof. Dr. Özgür Bilgin TOPÇUOĞLU
İstanbul Kent University

Date of Submission : 14.12.2021

Date of Defense : 06.01.2022





Fatigue is what we experience, but it is what a match is to an atomic bomb.

(Laura Hillenbrand)



FOREWORD

I would like to thank my dear advisor Prof. Dr. Leyla TAVACIOĞLU for her interest and support in all processes from the design to the execution and analysis of the study and Res. Asst. Neslihan GÖKMEN for her support in the analysis of the data. I would also like to thank my jury members Prof. Dr. Mustafa Ersel KAMAŞAK and Asst. Prof. Dr. Erdem BİLGİLİ for their critical guidance and contributions during the progress of the thesis. I would like to thank the personnel of Piri Reis University Simulator Centre for providing the necessary environment for me to take the measurements. I would like to thank to my dear colleagues and dear PRU graduates who had their time for my measurements and participated as subjects. I would also like to thank the Dean of the PRU Maritime Faculty for motivating and supporting me to finish my doctorate thesis as soon as possible.

I would like to express my endless thanks to my closest friends (parallel universe team) who have been listening relentlessly the troubles I have experienced during the thesis for years, and to Büşra, who is my home mate from this team, who has not withheld her loud voice during my studies and who has always uttered sentences that could be taken anywhere by saying "Did you mouth", but whose friendship I always felt in my heart, to my friends from the Trabzon Student Solidarity, whose support I always felt, where we come together at the tables of the sun even though we are in different cities, to my comrades at Umut-Sen for their patience, for whom I could not be with them in most of the activities and movements due to this busyness and I reserve their right to criticize me at this point. Starting with my dear little nephew Derin, who said "he is working, busy" when I could not be reached, I would like to thank my sister, my dear mother, whose support I always felt, my comrade father, who motivated me with his jokes and my dear sweetheart makes me see beautiful things in my dream.

Note: This study was supported by Scientific Research Projects Department of Istanbul Technical University (Project Number: 41710) and by TUBITAK 1002 - Short Term R&D Funding Program (Project Number: 119E460).

January 2022

Barış ÖZSEVER
(Research Assistant)



TABLE OF CONTENTS

	<u>Page</u>
FOREWORD	ix
TABLE OF CONTENTS	xi
ABBREVIATIONS	xv
SYMBOLS	xvii
LIST OF TABLES	xix
LIST OF FIGURES	xxi
SUMMARY	xxv
ÖZET	xxix
1. INTRODUCTION	1
1.1 Seafarer-Centric Safety System.....	5
1.2 Autonomous Ships and the Necessity of Physiological Monitorization of Operators in Future.....	6
1.3 Purpose of the Thesis	7
1.4 Limitations and Assumptions of the Thesis	8
2. THEORETICAL AND CONCEPTUAL FRAMEWORK	9
2.1 Workload Theory	9
2.1.1 Malleable attentional resources theory (MART)	15
2.1.2 The role of situation awareness theory on workload	15
2.1.3 Officer workload	17
2.1.4 Vigilance	19
2.1.5 Inverted U principle	20
2.2 The Summary of The Theories Used in This Study.....	21
2.3 Measures of Mental Workload	22
2.3.1 Subjective workload measures	26
2.3.2 Performance-based measures	27
2.3.3 Task loading assessment	30
2.3.4 Physiological measures	33
2.3.4.1 Cardiovascular activity.....	36
2.3.4.2 Electrodermal activity	44
2.3.4.3 Ocular activity	49
2.3.4.4 Other central, peripheral and biochemical activities.....	52
2.3.4.5 The choice of physiological measures for the study	57
2.3.5 Classification and decision-making techniques	57
3. METHODOLOGY	67
3.1 Sampling Strategy and Subjects	67
3.2 Mental Workload Prediction System Layout.....	68
3.3 Simulated Ship Environment	70
3.3.1 Navigation tasks	71
3.3.1.1 Task load assessment of navigation scenarios	74
3.3.2 Cargo operation tasks	75
3.3.2.1 Task load assessment of cargo operation scenarios	80
3.4 Measurement Details	83

3.4.1 Performance measurement	83
3.4.1.1 Performance measurement for navigation tasks.....	83
3.4.1.2 Performance measurement for cargo operation tasks	89
3.4.1.3 Validation of the performance measurement method	93
3.4.2 Physiological measurement.....	94
3.4.2.1 PPG.....	94
3.4.2.2 EDA.....	95
3.4.2.3 Eye movements and eye tracking.....	95
3.4.3 Subjective workload assessment	95
3.5 Analysis of Data and Computerized Process.....	96
3.5.1 Transformation process	96
3.5.1.1 PPG signal	96
3.5.1.2 EDA signal	99
3.5.1.3 Eye data	101
3.5.1.4 Normalization of extracted features	102
3.5.2 Dimension reduction and/or feature selection.....	102
3.5.3 Classification.....	102
4. RESULTS.....	105
4.1 Analysis of Subjective Workload Assessment Results	105
4.1.1 NASA-TLX scores of the subjects performing navigation scenario.....	105
4.1.2 NASA-TLX scores of the subjects performing cargo operation scenario	106
4.2 Analysis of Performance Measurement Results.....	107
4.2.1 Navigation tasks	107
4.2.2 Cargo operation tasks	110
4.2.3 Validation results of performance measurement method.....	112
4.2.4 Determination of the red line for task load level.....	113
4.3 Analysis of Physiological Measurement Results	114
4.3.1 Analysis of physiological responses during navigation tasks	115
4.3.2 Analysis of physiological responses during cargo operation tasks	125
4.4 Feature Selection Results	131
4.5 Classification Results	133
4.5.1 Within task classification	133
4.5.1.1 Navigation task.....	133
4.5.1.2 Cargo operation task.....	135
4.5.2 Cross task classification	140
4.6 Determining the Red Lines of Task Demands	142
5. CONCLUSIONS.....	145
5.1 Practical Application of This Study	148
REFERENCES.....	151
APPENDICES	161
APPENDIX A: Voluntary Participation Form	162
APPENDIX B: NASA Task Load Index (Rating)	163
APPENDIX C: NASA Task Load Index (Weighting)	164
APPENDIX D: All Subjective Assessments of the Subjects	165
APPENDIX E: SPSS ANOVA Analysis Outputs of NASA-TLX Scores.....	167
APPENDIX F: Calculation Details of Performance Scores.....	169
APPENDIX G: Coordinates of the ROC Curves of Developed Officer Performance Model	186
APPENDIX H: Data Collected During the Study.....	187

APPENDIX I: SPSS t-Test Outputs of Physiological Data Between Low and High Task Load	214
APPENDIX J: Divergence Values of Physiological Features	222
APPENDIX K: Matlab Code for Eye Features	224
APPENDIX L: Matlab Code for ANN Classification	225
APPENDIX M: <i>MSE</i> Values of Validation Data Sets	227
CURRICULUM VITAE.....	231





ABBREVIATIONS

A/C	: Alteration of Course
AECD	: Average Eye Closure Duration
ANS	: Autonomic Nervous System
ANN	: Artificial Neural Network
ANOVA	: Analysis of Variance
AOI	: Area of Interest
AUC	: Area Under Curve
BM	: Bending Moment
C	: Control
CDA	: Continuous Decomposition Analysis
CNS	: Central Nervous System
COG	: Course Over Ground
COLREG	: International Regulations for Preventing Collisions at Sea
CPA	: Closest Point of Approach
CSSI	: Cognitive Seafarer-Ship Interface
ECDIS	: Electronic Chart Display and Information System
ECG	: Electrocardiography
EDA	: Electrodermal Activity
EEG	: Electroencephalogram
EMG	: Electromyography
EOG	: Electrooculography
GSR	: Galvanic Skin Response
HR	: Heart Rate
HRV	: Heart Rate Variability
HRVAS	: Heart Rate Variability Analysis Software
IBI	: Interbeat Interval
IMO	: International Maritime Organization
IRF	: Impulse Response Function
ISO	: International Organization for Standardization
KNN	: K-Nearest Neighbour
LF/HF	: The ratio of LF to HF power
LSP	: Lomb-Scargle Periodogram
M	: Mean
MART	: Malleable Attentional Resources Theory
min.	: minutes
MSE	: Mean Squared Error
MWL	: Mental Workload
NASA-TLX	: NASA Task Load Index
NC	: No control
nm	: nautical mile
NN	: Normal-to-Normal (beat-to-beat)
NR	: No response
NS-SCRs	: Non-Specific Skin Conductance Responses
OFM-COG	: Operator Function Model - Cognitive Task Analysis

PERCLOS	: Percentage of Eye Closure
PerLPD	: Percentage of Large Pupil Dilation
PNS	: Peripheral Nervous System
PPG	: Photoplethysmogram
PSD	: Power Spectral Density
ROC	: Receiver Operating Characteristic
SA	: Situational Awareness
SC	: Skin Conductance
SCL	: Skin Conductance Level
SCR	: Skin Conductance Response
SD	: Standard Deviation
SF	: Shearing Force
SNS	: Sympathetic Nervous System
SVM	: Support Vector Machine
TARGETS	: Targeted Acceptable Responses to Generated Events or Tasks
TCPA	: Time to Closest Point of Approach
TTP	: Trough-to-Peak
VHF	: Marine Very High Frequency radio
wp	: way point
wrw	: within response window
XTE	: Cross Track Error

SYMBOLS

P_T	: Performance score for related task
p	: Probability value
t	: Time
w_α, w_ν	: Importance weights of navigation and cargo operation tasks
φ_i	: Physiological measurables
σ_k	: Task load parameters
γ_α	: Safety critical task scores
η_ν	: Trackkeeping / operational task scores
Ψ_j'	: Cognitive indicators
Ψ_j''	: Task load indicators



LIST OF TABLES

	<u>Page</u>
Table 2.1 : Integration of SA model into maritime context.	17
Table 2.2 : The integration of SA model into chemical tanker cargo operation.	18
Table 2.3 : Mental workload and fatigue studies in maritime domain.	24
Table 2.4 : Cognitive task transactions and the human information processing resources.	32
Table 2.5 : The classification accuracies stated in the studies in literature.	65
Table 3.1 : Classification of variables.	70
Table 3.2 : Performance parameters for navigation scenario.	73
Table 3.3 : The OFM-COG analysis for navigation tasks used in this thesis.	76
Table 3.4 : Performance parameters for cargo operation scenario.	80
Table 3.5 : The OFM-COG analysis for cargo operation tasks used in this thesis. ..	81
Table 3.6 : Fuzzy numbers corresponding to the importance weights.	84
Table 3.7 : Navigaiton performance results of 3 experts during the trials.	85
Table 3.8 : The limits corresponding to the score values evaluated by experts for navigation scenario.	86
Table 3.9 : The evaluations of the experts for parameter weights of whole navigation scenario and the quantification of weight evaluations.	88
Table 3.10 : Cargo operation performance results of 3 experts during the trials.	90
Table 3.11 : The limits corresponding to the score values evaluated by experts for cargo operation scenario.	91
Table 3.12 : The evaluations of the experts for parameter weights of whole cargo operation scenario and the quantification of weight evaluations.	92
Table 3.13 : Confusion matrix of used ROC technique for validation of performance measurement method.	94
Table 3.14 : Definition and description of HRV features.	98
Table 3.15 : Definition and description of EDA features.	101
Table 3.16 : Definition and description of pupil diameter and blink rate features.	101
Table 4.1 : ANOVA of NASA-TLX scores among 4 navigation steps.	105
Table 4.2 : ANOVA of NASA-TLX scores among 3 cargo operation steps.	106
Table 4.3 : Correlation between performance score and task load level for navigation tasks.	110
Table 4.4 : Correlation between performance score and task load level for cargo operation tasks.	112
Table 4.5 : Area under the curve statistics for navigation tasks.	113
Table 4.6 : Area under the curve statistics for cargo operation tasks.	113
Table 4.7 : t-Test of performance data between low and high task load for navigation tasks.	114
Table 4.8 : t-Test of performance data between low and high task load for cargo operation tasks.	114
Table 4.9 : Correlations between task load and other measures for navigation tasks.	119

Table 4.10 : t-Test of physiological data between low and high task load for navigation tasks.	124
Table 4.11 : Correlations between task load and other measures for cargo operation tasks.	127
Table 4.12 : t-Test of physiological data between low and high task load for cargo operation tasks.	131
Table 4.13 : Average <i>MSE</i> values of validation data sets of partitions (navigation task without feature selection).	133
Table 4.14 : Average <i>MSE</i> values of validation data sets of partitions (navigation task with feature selection).	135
Table 4.15 : Average <i>MSE</i> values of validation data sets of partitions (cargo operation task without feature selection).	137
Table 4.16 : Average <i>MSE</i> values of validation data sets of partitions (cargo operation task with feature selection).	138
Table 4.17 : Summary of classification results.	142
Table D.1 : All subjective assessments of the subjects and their calculations.	165
Table J.1 : Divergence values of features for navigation tasks.	222
Table J.2 : Divergence values of features for cargo operation tasks.	223
Table M.1 : <i>MSE</i> values of validation data sets (navigation task without feature selection).	227
Table M.2 : <i>MSE</i> values of validation data sets (navigation task with feature selection).	228
Table M.3 : <i>MSE</i> values of validation data sets (cargo operation task without feature selection).	229
Table M.4 : <i>MSE</i> values of validation data sets (cargo operation task with feature selection).	230

LIST OF FIGURES

	<u>Page</u>
Figure 1.1 : The stress-strain-effects model of ISO 10075-1	3
Figure 1.2 : The future Seafarer-Centric Safety System design.	5
Figure 1.3 : Mental workload prediction system layout.	7
Figure 2.1 : Relation between resources, demands and task performance	10
Figure 2.2 : Relation between task performance and behavioural activity	11
Figure 2.3 : Mental effort applied by operator over time t	11
Figure 2.4 : The effect of increasing level of skill to mental work.....	12
Figure 2.5 : Schematic representation of Wickens’ model	14
Figure 2.6 : The relationship between task demand and resource supply associated with mental workload and performance.....	14
Figure 2.7 : The relationship between performance and task demand with regards to MART	15
Figure 2.8 : Model of situation awareness.	16
Figure 2.9 : Resemblance of 4 stages of information processing theory with situation awareness theory.	16
Figure 2.10 : An example of bridge console.	18
Figure 2.11 : An example of cargo control room.....	19
Figure 2.12 : Inverted U function of Yerkes-Dodson principle for relationship between arousal and performance	20
Figure 2.13 : The relationship between arousal and performance.	21
Figure 2.14 : Two anatomical distinct structure: Central Nervous System and Peripheral Nervous System.	34
Figure 2.15 : General pattern of autonomic innervation	37
Figure 2.16 : Simultaneously recorded ECG (black coloured) and PPG (blue coloured) signal.....	37
Figure 2.17 : Welch and Lomb-Scargle Periodograms (a) and samples of PSD generated from PPG-derived HRV for resting and stress conditions (b).....	40
Figure 2.18 : Samples of TFD generated from PPG-derived HRV for resting and stress conditions	42
Figure 2.19 : Poincare Plot (a) and detrended fluctuation analysis (b) of IBI data ..	43
Figure 2.20 : CNS determiners of EDA	45
Figure 2.21 : Electrode placements for EDA recording.....	46
Figure 2.22 : Graphical representation of EDA components.....	46
Figure 2.23 : Sample EDA raw signal from rest and active trials	47
Figure 2.24 : Phasic driver extraction with continuous decomposition analysis	49
Figure 2.25 : The parts of eye (pointed with yellow line) and the basic dimensions used for MWL prediction (pointed with red lines and a circle).	50
Figure 2.26 : Neurophysiological basis of EEG generation. A coronal slice of brain (a), an expanded view of cerebral gyri and sulci in relations to the scalp, skull, and cerebral spinal fluid (CSF) (b), a schematic illustration of cortical pyramidal cells within the critical mantle (c).	52
Figure 2.27 : Decision making blocks for pattern recognition.	58

Figure 2.28 : The distribution of vectors with low divergence value (a) and high divergence value (b).	59
Figure 2.29 : Basic decision function for 2 classes distribution.	61
Figure 2.30 : The classification of discriminant functions.	62
Figure 2.31 : The effect of neighbourhood to KNN classification.	62
Figure 2.32 : The structure of perceptron.	63
Figure 3.1 : Research model of the thesis.	67
Figure 3.2 : Mental workload prediction system layout.	69
Figure 3.3 : Bridge simulator (a), recording the subject performance (b).	71
Figure 3.4 : Liquefied Cargo Handling Simulator (a), recording the subject performance (b).	72
Figure 3.5 : Navigation area used in simulator with route legs and performance measurement areas as stated in steps.	73
Figure 3.6 : Detailed step organization with the routes of own ship and target ships; step 1 (a), step 2 (b), step 3 (c) and step 4 (d)	74
Figure 3.7 : Task loading of navigation scenario.	75
Figure 3.8 : The cargo operation scenario with cargo plans of final conditions.	79
Figure 3.9 : The deck view (a) and the general plan (b) of the chemical tanker.	79
Figure 3.10 : Task loading of cargo operation scenario.	83
Figure 3.11 : Optical Pulse Sensor of GSR unit (a) and recording the PPG data (b).	94
Figure 3.12 : GSR unit (a) and recording the GSR data (b).	95
Figure 3.13 : Eye tracking headset (a), recording the eye movement and tracking data (b).	96
Figure 3.14 : Inter-beat interval conversion from raw PPG signal.	97
Figure 3.15 : HRV extraction from IBI data	97
Figure 3.16 : HRVAS software graphical user interface.	98
Figure 3.17 : Feature extraction from EDA raw data with different methods	100
Figure 3.18 : Continuous Decomposition Analysis (CDA) for raw EDA signal.	100
Figure 3.19 : Tonic EDA (black coloured) and phasic EDA (blue coloured) trends.	100
Figure 3.20 : Partitions of data set for navigation tasks.	103
Figure 3.21 : Partitions of data set for cargo operation tasks.	103
Figure 4.1 : Boxplot of NASA-TLX total scores among 4 navigation steps.	105
Figure 4.2 : Boxplot of NASA-TLX total scores among 3 cargo operation steps.	106
Figure 4.3 : The performance-task load graphic of subject ID 01.	107
Figure 4.4 : The performance-task load graphic of subject ID 02.	107
Figure 4.5 : The performance-task load graphic of subject ID 03.	107
Figure 4.6 : The performance-task load graphic of subject ID 04.	108
Figure 4.7 : The performance-task load graphic of subject ID 05.	108
Figure 4.8 : The performance-task load graphic of subject ID 06.	108
Figure 4.9 : The performance-task load graphic of subject ID 07.	108
Figure 4.10 : The performance-task load graphic of subject ID 09.	109
Figure 4.11 : The performance-task load graphic of subject ID 10.	109
Figure 4.12 : The performance-task load graphic of subject ID 12.	109
Figure 4.13 : The performance-task load graphic of subject ID 14.	109
Figure 4.14 : The performance-task load graphic of subject ID 16.	110
Figure 4.15 : The performance-task load graphic of subject ID 8.	110
Figure 4.16 : The performance-task load graphic of subject ID 11.	111
Figure 4.17 : The performance-task load graphic of subject ID 13.	111

Figure 4.18 : The performance-task load graphic of subject ID 15.	111
Figure 4.19 : The performance-task load graphic of subject ID 17.	111
Figure 4.20 : ROC curve graphic of developed officer performance model for navigation tasks (a) and cargo operation tasks (b).	112
Figure 4.21 : The distinction of task load level for navigation tasks.	113
Figure 4.22 : The distinction of task load level for cargo operation tasks.	113
Figure 4.23 : The comparison of data between low and high task load for subject ID 03.	116
Figure 4.24 : The comparison of data between low and high task load for subject ID 10.	117
Figure 4.25 : The comparison of data between low and high performance for subject ID 06.	118
Figure 4.26 : The comparison of data between low and high task load for subject ID 8.	126
Figure 4.27 : Divergence values of features for navigation tasks.	132
Figure 4.28 : Divergence values of features for cargo operation tasks.	132
Figure 4.29 : <i>MSE</i> values of various network structures in partition 2 (navigation task without feature selection).	133
Figure 4.30 : Confusion matrix and ROC curve graphics of ANN classifier (navigation task without feature selection).	134
Figure 4.31 : Confusion matrix and ROC curve graphic of KNN classifier (navigation task without feature selection).	134
Figure 4.32 : <i>MSE</i> values of various network structures in partition 2 (navigation task with feature selection).	135
Figure 4.33 : Confusion matrix and ROC curve graphics of ANN classifier (navigation task with feature selection).	136
Figure 4.34 : Confusion matrix and ROC curve graphic of Linear Discriminant classifier (navigation task with feature selection).	136
Figure 4.35 : <i>MSE</i> values of various network structures in partition 3 (cargo operation task without feature selection).	137
Figure 4.36 : Confusion matrix and ROC curve graphics of ANN classifier (cargo operation task without feature selection).	138
Figure 4.37 : Confusion matrix and ROC curve graphic of SVM classifier (cargo operation task without feature selection).	138
Figure 4.38 : <i>MSE</i> values of various network structures in partition 1 (cargo operation task with feature selection).	139
Figure 4.39 : Confusion matrix and ROC curve graphics of ANN classifier (cargo operation task with feature selection).	139
Figure 4.40 : Confusion matrix and ROC curve graphic of Logistic Regression classifier (cargo operation task with feature selection).	140
Figure 4.41 : Partition of data used in cross task classification.	140
Figure 4.42 : Confusion matrix and ROC curve graphics of ANN classifier (cross task classification with feature selection).	141
Figure 4.43 : Confusion matrix and ROC curve graphic of Subspace KNN classifier (cross task classification with feature selection).	141
Figure 4.44 : Detailed navigational inputs of “Task Load Estimator” in CSSI.	143
Figure 5.1 : The detailed future Seafarer-Centric Safety System design.	149
Figure E.1 : Descriptives of NASA-TLX scores for navigation scenario.	167
Figure E.2 : ANOVA of NASA-TLX scores for navigation scenario.	167
Figure E.3 : Descriptives of NASA-TLX scores for cargo operation scenario.	168

Figure E.4 : ANOVA of NASA-TLX scores for cargo operation scenario.....	168
Figure F.1 : Calculation details of performance score for navigation tasks.	169
Figure F.2 : Calculation details of performance score for cargo operation tasks. ..	181
Figure G.1 : Coordinates of the ROC curves for navigaiton tasks (a) and cargo operation tasks (b).	186
Figure H.1 : Data collected during the study.	187
Figure I.1 : t-Test of physiological data between low and high task load for navigation tasks.	214
Figure I.2 : t-Test of physiological data between low and high task load for cargo operation tasks.....	218



DESIGN OF SEAFARER-CENTRIC SAFETY SYSTEM; MENTAL WORKLOAD (MWL) PREDICTION

SUMMARY

It is known that human factor has a major effect on maritime casualties that cause great harm to environment, economy and maritime sector. It was stated that while human error is the primary contributor of accidents, a good part of collisions and groundings were related to mental workload (MWL) of watchkeeping officers. Automation, mechanization and the introduction of new technologies had changed the working conditions together with reducing the number of crew and increasing the MWL of operators. This clearly indicates that human element related issues will continue to be one of the major issues in marine transportation assets. In maritime-related studies, it has been analysed mostly how the ship's environment, working period and other factors affect the seafarers. Almost all maritime-related studies couldn't have a potential to develop MWL prediction system for maritime operations aspect. However, lots of studies on drivers and pilots, have produced successful results for MWL prediction. Taking into consideration the fact that MWL has major contribution to maritime casualties, the development of real-time MWL prediction system is vitally essential for ships.

By implementing the similar measurement techniques used in the studies on drivers and pilots, to maritime transportation, this study aims to classify the physiological responses of the operators that can produce an output for state of officer on duty as "Safe" or "Risky" from the collected physiological data and task load data during the seaborne operations. This study predicated on the theories which are the statement "minimum performance requires sufficient behavioural activity" of Sheridan and Simpson (1979) together with inverted U function of Yerkes and Dodson (1908) which presents the relationship between arousal and performance. Moreover, the theory of Young et al. (2015) which presents the relationship among mental workload, performance, task demand and resource supply and indicates the overload region, guides this study in terms of building the structure of the experimental research. By being predicated on the above-mentioned theories, this study aimed to design Cognitive Seafarer - Ship Interface (CSSI) which is a main part of Seafarer-Centric Safety System. The physiological data of the 17 junior deck officers (12 subjects performed navigation scenario, 5 subjects performed cargo operation scenario) was recorded according to the design. By being correlated with the performance of the officer, the change of physiological responses of the subjects were analysed in low and high task load levels. The medical decision-making process, which deduced "Safe" or "Risky", was run for this change. For performance measurement that is a part of triangulated measurement strategy (Wierwille and Eggemeier, 1993), Officer Performance Model which is used for MWL classification, was developed for navigation and cargo operation tasks. Additionally, the inputs of Task Load Estimator were defined as data transcription from navigational aids according to results of classification. In summary, the following process were done and results were found.

Firstly, the navigation and cargo operation scenarios were created to simulate ship environment. The difficulty level of navigation scenario was gradually adjusted (in order to prevent acquired skill) according to traffic density, visibility and geography by combining in 4 steps. The difficulty level of cargo operation scenario was gradually adjusted according to type and number of operation and operation period corresponding to a real cargo operation by combining in 3 steps. Task load assessments of the scenarios were carried out according to Operator Function Model (OFM-COG) and its sample implications in literature.

The results of NASA-TLX scores of the subjects supported the increase of task load levels of the scenarios. ANOVA results showed that there are significant differences in the NASA-TLX scores of 5 different dimensions and in total, among 4 steps which have different task load levels for navigation scenario. Similarly, ANOVA results showed that there are significant differences in the NASA-TLX scores of 3 different dimensions and in total among 3 steps which have different task load levels for cargo operation scenario. According to the subjective assessments of the subjects, MWL increased during the both of navigation and cargo operation scenarios.

Secondly, ROC curve analysis was performed for validation of developed officer performance model. Recorded performances of the participants were evaluated as “safe” and “risky” for each task by one ocean going Master expert for navigation tasks and by one ocean going Chief Officer for cargo operation tasks. According to the ROC curve analysis, developed officer performance model was validated with high significance and AUC values. These results showed that the developed officer performance model can be used in any study focused on performance measurement in navigation and chemical tanker cargo operations.

Being validated measurement method, performances of the subjects showed that there is a negative significant correlation between performance score and task load in both of navigation and cargo operation tasks. With the distinction of the task load as high task load and low task load, the performance scores were also found significantly different in low and high task loads for both of navigation and cargo operation tasks.

Thirdly, physiological responses of the subjects were often differentiated between low and high task loads. Although the change of time-based heart rate variability (HRV) features was not found meaningful according to literature during the increase of task load, the change of frequency-based, time-frequency and nonlinear HRV features were found significant and meaningful during the increase of task load. Moreover, the change of some electrodermal activity (EDA) features and some eye responses were found significant in this study. However, the change of EDA responses was not found strongly correlated with the increase of task load. This can be explained by the fact that electrodermal activity occurs in stressful conditions rather than mental workload. The “frustration” scores of the NASA-TLX supported the fact that the subjects didn’t feel so stressed during the tasks. On the other hand, the change of pupil diameter features was found significant and meaningful during the increase of task load in navigation tasks but in cargo operation tasks. Additionally, the change of blink frequency features varied across the scenarios. The variable results of eye responses are thought that the selectivity of eye blinks and pupil diameter to MWL is low according to literature. Additionally, the reason of the fact that the change of some eye features was significant during the increase of task load is thought to be related with the characteristics of eye responses that pupil diameter change is correlated highly with error rate and blink rate increases in incorrect responses rather than correct responses.

Therefore, these significances can be explained with the decrease of performance together arising from the increase of task load. On the other hand, the correlations between HRV and EDA features, HRV and eye features, EDA and eye features were found significant and meaningful in mental workload theory.

Classification process was carried out with artificial neural network (ANN) code and “Classification Learner” tool of Matlab 2020a. Although the results of the classifications of the subjects’ physiological responses on high and low task loads in this study did not give very good accuracies, compared with the studies in literature, they gave sufficient results. The classification accuracies, 75.7% in testing, 83.3% in all for navigation tasks, 80.0% in testing, 92.5% in all for cargo operation tasks and 61.3% in testing, 77.0% in all for cross-task classification have been found similar to those stated in the related studies whose mental workload and stress classification accuracies vary between 70.48% and 98%.

According to classification efforts of physiological responses on high task load and low task load levels and performance scores of the subjects, the red lines of task demand became appear in this study. Continuing from the aim of Orlandi and Brooks (2018) and the contributions to MWL prediction in marine engine operations of Yan et al. (2019), the red lines of task demand in ship navigation was tried to determine in this study. Classification of physiological responses and the distinction of the task loads according to the performances of the subjects have ensured the task load to be separated as high task load and low task load.

Thus, the inputs of the Cognitive Seafarer-Ship Interface (CSSI) were formed with the outputs of high task load details for navigation and the physiological responses given as features (classified in this study). CSSI processes the task loading together with physiological data of the officer and gives an output as “Risky” for safety of navigation in “The future Seafarer-Centric Safety System design” to be used on ships or at the Shore Control Centre for autonomous ships in future.

Consequently, this study will contribute to literature, being the first study in terms of predicting MWL for navigation and cargo operations in maritime transportation. In addition, this study will be a guide for future studies as it reveals the design of the “Seafarer-Centric Safety System” to be developed in order to minimize maritime casualties.



GEMİ İNSANI-MERKEZLİ EMNİYET SİSTEMİNİN TASARIMI; MENTAL İŞ YÜKÜ ÖNGÖRÜSÜ

ÖZET

Çevreye, ekonomiye ve denizcilik sektörüne büyük zararlar veren deniz kazalarında insan faktörünün büyük bir etkisi olduğu bilinmektedir. İnsan hatalarının kazaların başlıca sebebi olduğu belirtilirken, çatışma ve karaya oturma olaylarının nedenlerinin önemli bir kısmının vardiya zabitlerinin mental iş yükü (MWL) ile ilgili olduğu belirtilmektedir. Otomasyon, mekanizasyon ve yeni teknolojilerin girmesi çalışma koşullarını değiştirdi. Değişen çalışma koşullarında gemi personel sayısı azaldı ve dolayısıyla vardiya zabitlerinin mental iş yükleri arttı. Bu durum, insan unsuru ile ilgili konuların deniz taşımacılığında önemli konulardan biri olmaya devam edeceğini açıkça göstermektedir. Denizcilikle ilgili yapılan çalışmalarda daha çok gemi ortamının, çalışma süresinin ve diğer faktörlerin denizcileri nasıl etkilediği analiz edilmiştir. Denizcilikle ilgili hemen hemen tüm çalışmalar, denizcilik operasyonları açısından mental iş yükü ile ilgili bir uyarı sistemi geliştirme potansiyeline sahip değildir. Bununla birlikte, sürücüler ve pilotlar üzerinde yapılan birçok çalışma, mental iş yükü ölçümlerinde başarılı sonuçlar vermiştir. Mental iş yükünün deniz kazalarına büyük etkisi olduğu göz önüne alındığında, gerçek zamanlı bir mental iş yükü öngörü sisteminin geliştirilmesi gemiler için hayati önem taşımaktadır.

Bu çalışma, sürücü ve pilotlar üzerinde yapılan çalışmalarda kullanılan benzer ölçüm tekniklerini deniz taşımacılığına da uygulayarak, denizcilik operasyonları süresince toplanan fizyolojik ve iş yükü verilerinden vardiya zabitinin durumuna dair “Emniyetli” veya “Riskli” çıkarımı üretebilecek bir fizyolojik veri sınıflaması yapmayı amaçlamaktadır. Bu çalışma, Sheridan ve Simpson'ın (1979) “asgari performans yeterli davranışsal aktivite gerektirir” önermesi ile uyarılma ve performans arasındaki ilişkiyi ortaya koyan Yerkes ve Dodson'ın (1908) ters U eğrisi teorilerini temel almaktadır. Ayrıca, Young ve arkadaşlarının (2015) mental iş yükü, performans, görev talebi ve mental kaynak arzı arasındaki ilişkiyi ortaya koyan ve aşırı yüklenme bölgesini gösteren teorisi, bu çalışmanın deneysel araştırma yapısını oluşturması açısından temelini oluşturmuştur. Bu çalışma, yukarıda bahsedilen teorilere dayanılarak, Gemi İnsanı - Merkezli Emniyet Sisteminin ana parçası olan Bilişsel Gemi İnsanı - Gemi Arayüzü (CSSI) tasarlamayı amaçlamış ve bu amaçla simulator ortamında 17 güverte zabitinin (12 katılımcı seyir senaryosunu, 5 katılımcı kimyasal tanker yük operasyonu senaryosunu icra etmişlerdir) fizyolojik verileri tasarıma göre kaydedilmiştir. Katılımcıların performansları ile ilişkilendirilerek düşük ve yüksek iş yükü seviyelerinde katılımcıların fizyolojik tepkilerinin değişimi analiz edilmiştir. Bu değişim için “Emniyetli” veya “Riskli” çıkarımı yapan “Tıbbi Karar Verme” süreci yürütülmüştür. Mental iş yükü sınıflandırmasında kullanılmak üzere, üçlü ölçüm stratejisinin bir parçası olan performans ölçümü için (Wierwille ve Eggemeier, 1993), seyir ve yük operasyon görevlerini içeren Vardiya Zabiti Performans Modeli geliştirilmiştir. Ayrıca sınıflandırma sonuçlarına göre, iş yükü estimator girdileri seyir yardımcılarından veri transkripsiyonu olarak tanımlanmıştır. Özetle tez boyunca aşağıdaki süreçler işletilmiş ve ilgili sonuçlara ulaşılmıştır.

İlk olarak, gemi ortamını simüle etmek için seyir ve yük operasyonu senaryoları oluşturulmuştur. Seyir senaryosunun zorluk seviyesi (kazanılan beceriyi önlemek için) trafik yoğunluğu, görüş ve coğrafi bölgeye göre kademeli olarak ayarlanarak senaryo 4 aşamada birleştirilerek oluşturulmuştur. Yük operasyonu senaryosunun zorluk seviyesi ise, operasyon tipi ve sayısı ile gerçek bir yük operasyonunda denk gelen farklı operasyon süreçlerine göre kademeli olarak ayarlanarak senaryo 3 aşamada birleştirilerek oluşturulmuştur. Senaryoların iş yükü değerlendirmeleri ise Operatör Fonksiyon Modeli (OFM-COG) ve bu modelin literatürdeki örnek uygulamalarına göre yapılmıştır.

Katılımcıların mental iş yüklerini ölçmek üzere kullanılan NASA-TLX anket sonuçları, senaryoların iş yükü seviyelerinin artışı destekler niteliktedir. ANOVA sonuçları, seyir senaryosu için farklı iş yükü seviyelerine sahip 4 aşama arasında 5 farklı boyutta ve toplamda NASA-TLX sonuçlarında önemli farklılıklar olduğunu göstermiştir. Benzer şekilde ANOVA sonuçları, yük operasyonu senaryosu için farklı iş yükü seviyelerine sahip 3 aşama arasında 3 farklı boyutta ve toplamda NASA-TLX sonuçlarında önemli farklılıklar olduğunu göstermiştir. Katılımcıların subjektif değerlendirmelerine göre, hem seyir hem de yük operasyonu senaryoları sırasında mental iş yükleri artmıştır.

İkinci olarak, geliştirilen vardiya zabiti performans modelinin doğrulanması için ROC eğri analizi yapılmıştır. Katılımcıların kaydedilen performansları, seyir görevleri için bir uzakyol kaptanı tarafından, yük operasyonu görevleri için kimyasal tanker tecrübeli bir uzakyol birinci zabiti tarafından "emniyetli" ve "riskli" olarak değerlendirildi. ROC eğrisi analizine göre, geliştirilen vardiya zabiti performans modeli yüksek anlamlılık ve AUC değerleri ile doğrulanmıştır. Bu sonuçlar, geliştirilen vardiya zabiti performans modelinin seyir ve kimyasal tanker yük operasyonlarında performans ölçümüne odaklanan herhangi bir çalışmada kullanılabileceğini göstermiştir.

Doğrulanmış performans ölçüm metodu ile katılımcıların performansları, hem seyir hem de yük operasyonu görevlerinde performans sonuçları ile iş yükü arasında negatif ve anlamlı bir ilişki olduğunu göstermiştir. İş yükünün yüksek iş yükü ve düşük iş yükü olarak ayrılmasıyla, hem seyir hem de yük operasyonu görevleri için düşük ve yüksek iş yüklerinde performans sonuçları da önemli ölçüde farklı bulunmuştur.

Üçüncü olarak, katılımcıların fizyolojik tepkileri genellikle düşük ve yüksek iş yükleri arasında değişiklik göstermiştir. İş yükünün artması sırasında zaman bazlı kalp hızı değişkenliği (HRV) özniteliklerinin değişimi literatüre göre anlamlı bulunmazken, frekans bazlı, zaman-frekans ve doğrusal olmayan HRV özniteliklerindeki değişim anlamlı bulunmuştur. Ayrıca bu çalışmada bazı elektrodermal aktivite (EDA) özniteliklerinin ve bazı göz tepkilerinin değişimi de anlamlı bulunmuştur. Fakat, elektrodermal aktivitedeki değişimin, iş yükündeki artışla olan ilişkisi güçlü bir şekilde değerlendirilememiştir. Bu, elektrodermal aktivitenin mental iş yükünden ziyade stresli koşullarda ortaya çıkmasıyla açıklanabilir. Ayrıca, NASA-TLX'in "frustrasyon" sonuçları, katılımcıların görevler sırasında çok stresli hissetmediği sonucunu desteklemiştir. Öte yandan, iş yükünün artması sırasında katılımcıların gözbebeklerindeki değişim, seyir görevlerinde anlamlı bulunurken yük operasyonu görevlerinde anlamlı bulunmamıştır. Ek olarak, göz kırpma frekansındaki değişim senaryolar arasında değişiklik göstermiştir. Göz tepkilerinin değişken sonuçlarının, literatüre göre göz kırpma frekansının ve göz bebeği çapının mental iş yükünde seçiciliğinin düşük olmasından kaynaklandığı düşünülmektedir. Ayrıca, iş yükünün artması sırasında bazı göz tepkilerindeki değişimin anlamlı bulunması, göz

hareketlerinin karakteristik özellikleri ile açıklanabilir ki gözbebeğindeki değişim, görevlerdeki hata oranı ile yüksek ilişkilidir ve göz kırpma frekansı görevler süresince verilen doğru aksiyonlardan ziyade yanlış aksiyonlarda artmaktadır. Dolayısıyla bu anlamlılıklar, iş yükünün artması sonucunda performansın azalmasıyla birlikte açıklanabilir. Öte yandan, HRV ve EDA, HRV ve göz hareketleri, EDA ve göz hareketleri arasındaki ilişkiler mental iş yükü teorilerine göre anlamlı bulunmuştur.

Sınıflama işlemleri yapay sinir ağları (YSA) kodu ve Matlab 2020a'nın "Classification Learner" aracı ile gerçekleştirilmiştir. Katılımcıların, yüksek ve düşük iş yüklerindeki fizyolojik tepkilerinin sınıflama sonuçları çok yüksek değerler vermese de literatürdeki çalışmalarla karşılaştırıldığında yeterli sonuçlar vermiştir. Seyir görevlerinde toplanan veriler için testte %75.7, tümünde %83.3, yük operasyonu görevlerinde toplanan veriler için testte %80.0, tümünde %92.5 ve görevler arası sınıflandırmada testte %61.3, tümünde %77.0 bulunan sınıflama başarıları, mental iş yükü ve stres sınıflamaları yapılan çalışmalardaki sınıflama başarıları ile benzerlik göstermiştir. Bu çalışmalardaki sınıflama başarıları %70.48 ile %98 arasında bir değer almaktadır.

Yüksek iş yükü ve düşük iş yükü seviyelerindeki fizyolojik tepkilerin sınıflama çabalarına ve katılımcıların performans sonuçlarına göre, bu çalışmada bir vardiya zabitanın emniyetli bir şekilde görev yapabileceği maksimum iş yükü belirlenmiştir. Orlandi ve Brooks'un (2018) amacından ve Yan ve arkadaşlarının (2019) gemi makineleri operasyonlarında mental iş yükü ölçümü katkılarından devam ederek, bu çalışmada gemi seyirinde iş yükünün kırmızı çizgileri belirlenmeye çalışılmıştır. Fizyolojik tepkilerin sınıflanabilmesi ve katılımcıların performanslarının iş yüküne göre keskin bir şekilde ayrılabilmesi, iş yükünün yüksek iş yükü ve düşük iş yükü olarak ayrılmasını sağlamıştır.

Böylece, Bilişsel Gemi İnsanı - Gemi Arayüzü'nün (CSSI) girdileri, seyir için yüksek iş yükü estimator çıktıları ve öznitelikleri ile belirtilen fizyolojik tepkilerin çıktıları ile oluşturulmuştur. Bu doktora tezi ile CSSI, gemilerde veya otonom gemiler için Kıyı Kontrol Merkezlerinde kullanılmak üzere "Geleceğin Gemi İnsanı - Merkezli Emniyet Sistemi tasarımı" nda, iş yükünü vardiya zabitanın fizyolojik verileri ile birlikte işleyerek ve seyir emniyeti için "Riskli" olarak uyarı verebilecek bir arayüz olarak tanımlanmıştır.

Sonuç olarak, bu çalışma deniz taşımacılığında seyir ve yük operasyonları için mental iş yükünün öngörülebilmesi açısından ilk olması vesilesiyle literatüre katkı sağlayacaktır. Ayrıca bu çalışma, deniz kazalarını en aza indirebilecek bir "Gemi İnsanı - Merkezli Emniyet Sistemi" nin tasarımını ortaya koyması bakımından ileride yapılacak çalışmalara yol gösterecektir.



1. INTRODUCTION

While human error is the primary contributor of accidents where about 85% of all accidents were caused by human error (Kurt et al., 2016), it was stated that 16% of collisions, 30% of groundings were related to mental workload (MWL) of watchkeeping officers (Akhtar and Bouwer Utne, 2015) in furtherance the determination that technology and automation have reduced the number of crew and increased the workload of officers (Grech et al., 2008; Louie and Doolen, 2007). This clearly indicates that human element related issues will continue to be one of the major issues in marine transportation assets.

International Maritime Organization (IMO) published a circular named as “Guidance on Fatigue Mitigation and Management” in 2001. Main objective of this circular is to develop marine safety culture by addressing the issue of fatigue. Human element was underlined as a contributing factor in maritime casualties just like the Exxon Valdez disaster. In effects of fatigue for ship’s officer, inability to concentrate, diminished decision-making ability, poor memory, slow response, loss of control bodily movements, mood change and attitude change were stated in circular. Boring, repetitive work and excessive work load were some of the causes of these performance impairments (IMO, 2001).

One step forward, Maritime Labour Convention 2006 (MLC 2006) set the minimum requirements for living and working conditions of seafarers including the minimum standards for cabin and other places, health protection, working and rest hours. It was aimed that the external conditions which cause fatigue or stress are tried to diminished onboard ship together with protecting the seafarers’ rights (MLC, 2006).

From global perspective, automation, mechanization and the introduction of new technologies had changed the working conditions together with increasing the MWL of operators. Thus, International Organization for Standardization (ISO) set the standards on MWL with ISO 10075 series to develop a standard on terminology and basic concepts, determine ergonomic principles and measurement method principles.

Firstly, ISO 10075 defines the “mental” as informational cognitive, and emotional process in the human being. Mental stress has also been defined as “the total of all assessable influences impinging upon a human being from external sources and affecting it mentally” in ISO 10075 (Koukoulaki and Boy, 2002) similar to definitions of “stress” stated in literature as the stressor factors which are the external conditions threatening the human being (Fisher, 1984; Lazarus, 1966).

ISO 10075 uses the stress-strain-effects model to simplify the relation between the stress (stressor factors), mental strain and the effects of that (Figure 1.1). In the components of “Task requirements” there are sustained attention, information processing, responsibility, duration, temporal pattern and temporal position of action, task content and danger. These are underlined because of that the seaborne operations involve the same task requirement components. According to the model, mental strain is “immediate effect of mental stress within the individual depending on their current condition”. As the consequences of mental strain, the effects are divided to two different components as facilitating and impairing. In short term effects of mental strain, while activation, learning and warming-up effects are facilitating effects, mental fatigue and fatigue-like states as reduced vigilance, mental satiation and monotony are impairing effects. Mental fatigue is “temporary impairment of mental and physical functional efficiency, depending on the intensity, duration, and temporal pattern of the preceding mental strain”. Monotony is “slowly developing state of reduced activation which is mainly associated with drowsiness, tiredness, decrease and fluctuations in performance, reductions in adaptability and responsiveness”. Reduced vigilance is “a state with reduced activation and detection performance mainly associated with monitoring tasks offering only little variation” (ISO, 2017). Therefore, both of overload and underload is important in ergonomic principles due to their impairing effects (Koukoulaki and Boy, 2002). This statement was early offered by inverted U principle (Yerkes and Dodson, 1908) and the MWL studies have been based on this principle (Kahneman, 1973; Sheridan and Simpson, 1979; Young et al., 2015) that is detailed explained in chapter 2 of this thesis.

In the section of design principles of ISO 10075 (ISO, 2000), it is mostly underlined that both high workload demand and low workload demand that causes monotony or satiation, should be avoided. In complexity of work demands, decision support systems should be used in ergonomic principle.

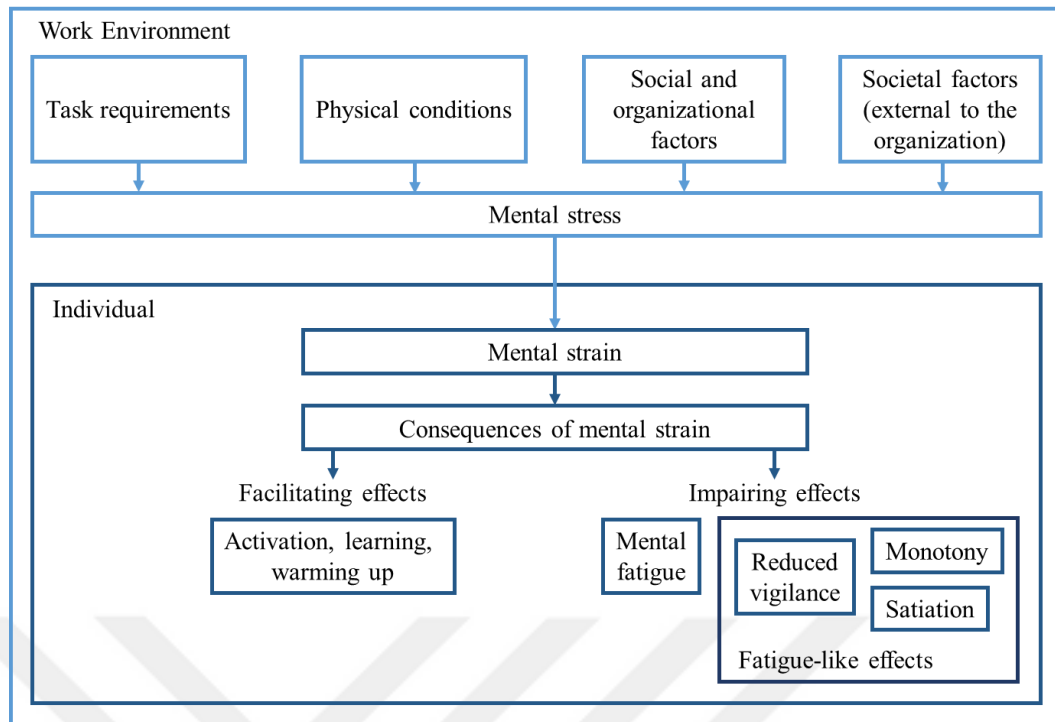


Figure 1.1 : The stress-strain-effects model of ISO 10075-1, adapted from (ISO, 2017).

ISO 10075 Part 3 is concerned with measurement aspects (ISO, 2004). It is stated that standardized, valid, reliable and easy to handle diagnostic measurement methods are needed to measure MWL. While subjective measurements are not sufficient alone, psychophysiological measurements need specialised professional training. How the methods can be developed that are usable by non-experts, acceptable, valid and reliable is the question of this part (Koukoulaki and Boy, 2002). This part is based on a three-dimensional model. First dimension involves stress-strain-effects process, second dimension involves the measurement techniques which are psychophysiology, subjective scaling, performance assessment and job and task analysis. These measurement techniques are detailed in chapter 2 of this thesis. Third dimension is the precision level of the measurement. However, the validation of the measurement methods has been still a problem to assess MWL (Nachreiner, 1999).

Recent studies show that authors have get to first base on measurement techniques to assess MWL and stress for mostly drivers. Healey and Picard (2005) developed a stress detection system for drivers with ECG, EDA, EMG and respiration measurements and reported the accuracy of the system as 97%. Borghini et al. (2014) have designed the system for both drivers and pilots with EEG and EOG measurements, and have achieved 89% MWL classification accuracy with only EEG features. This was 98%

for air traffic controllers with same measurements and ANN classification (Wilson and Russell, 2003). Moreover, Singh et al. (2013) used EDA and PPG measurements in real-time stress detection system design for drivers and they stated the predictive ability as 89.23%. The above-mentioned and similar studies focus on maximizing classification performance and minimizing measurement instruments.

In maritime-related studies, it has been analysed mostly how the ship's environment, working period and other factors affect the seafarers. Maurier et al. (2011) stated that fatigue negatively affects awareness and attention of seafarer in their study conducted in simulator with the aid of psychophysiological data. Yılmaz et al. (2013) analysed that increase in working hours caused fatigue and insomnia via EEG, SpO₂ and ECG measurements. Tac et al. (2013) examined the effects of the seafarer's cognitive performance with EEG on the operational processes in ship environment under certain stressor factors such as fatigue, insomnia, temperature and noise. Özsever and Tavacıoğlu (2018) observed that when seafarer's circadian rhythm is changed more frequently, they experience more drowsiness based upon EDA and HRV measures and their reaction times decrease. Lützhöft and Sri (2012) wrote a software (MARTHA) that involves working and resting hours of seafarers for fatigue detection. Culley et al. (2015) revised the software with the risk index by adding shift (watchkeeping hours) alterations. However, these studies were not able to implement real time fatigue / workload detection based on instantaneous physiological data. Wu et al. (2017) associated the EEG and the HRV data, obtained from 10 participants in engine control room simulator, with MWL as task difficulty increased. Orlandi and Brooks (2018) applied similar method to ship pilots and reached similar results. Yan et al. (2019) used eye response measurement to predict MWL for engine department tasks. With the ANN classification success of eye response data and subjective ratings together with decreased performance results, the authors stated that eye response measurement can be used to predict MWL.

The maritime-related studies except last three ones, couldn't have a potential to develop MWL prediction system for maritime operations aspect. However, lots of studies on drivers and pilots, have produced successful results for MWL prediction. Taking into consideration the fact that MWL has major contribution to maritime casualties, the development of real-time MWL prediction system is vitally essential for ships. With the help of developed MWL prediction system, in future, the dynamic

monitorization system such Seafarer-Centric Safety System, which consists of the operational variables together with physiological variables of the operator, can be applicable in ships.

1.1 Seafarer-Centric Safety System

As a future perspective, Seafarer-Centric Safety System focuses mainly the safety of the ship by taking the considerations of operational parameters which are navigational ones, if the operation is navigation or cargo operational ones if the operation is cargo operation, and physiological parameters of the responsible operator. Therefore, the system needs the operational data from related equipment and the physiological data of the operator. Figure 1.2 presents a sample Seafarer-Centric Safety System design for navigation. Considering the fact that operator manages the operation on ship or at the Shore Control Centre for autonomous ships, the Cognitive Seafarer-Ship Interface (CSSI) concept should include the variables of related operation and physiological variables of the operator and accomplished interface processing which gives a signal for safety of ship as “Safe” or “Risky”. The success of the CSSI processing is the success of the early warning system for ships according to the design.

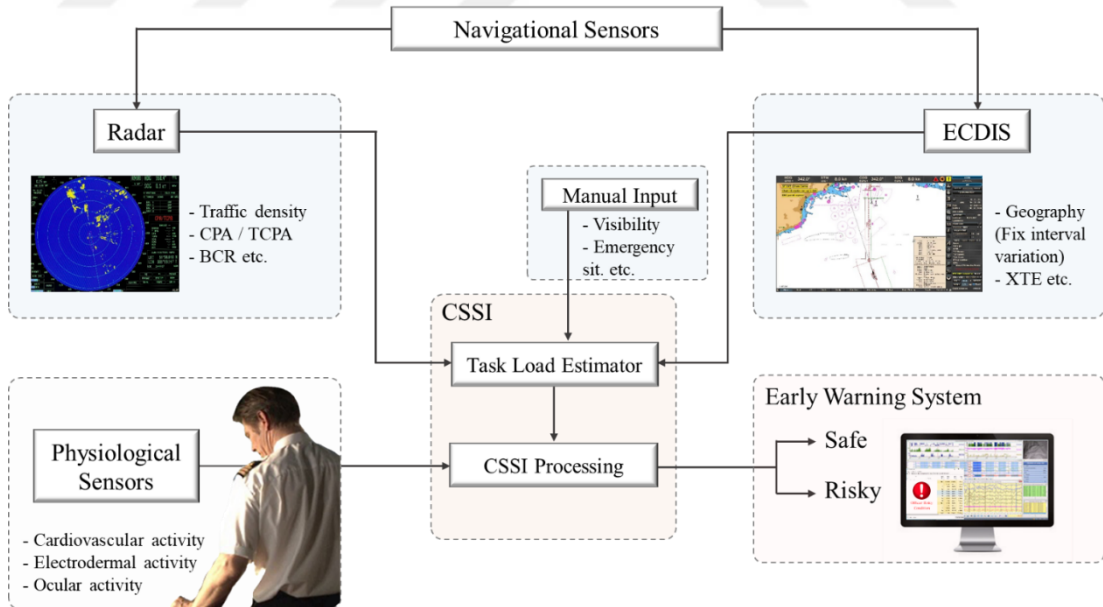


Figure 1.2 : The future Seafarer-Centric Safety System design.

Task load estimator takes the traffic density data from Radar, geographical load, which is determined with fix interval, from ECDIS, visibility or other variables data from manual input option and calculates the task loading. CSSI process the task loading

together with physiological data of the officer and gives an output as “Safe” or “Risky” for safety of navigation in this sample design. Similar study for aircrafts was conducted by Liu et al. (2016). Cognitive pilot-aircraft interface was designed with environmental variables of flight and physiological variables of the pilot. Interface can give an output to adjust the level of auto pilot considering the mental strain of pilot and the task load of environmental variables of flight.

1.2 Autonomous Ships and the Necessity of Physiological Monitorization of Operators in Future

Physiological monitorization named as MWL prediction in this thesis, is essential in maritime-related operations even if the operations are controlled by manned vessels. With the increase of automation in bridge designs, situation awareness of watchkeeping officers has decreased as in the example of auto pilot failure; half of the test subjects couldn't recognize the automation failure in the study (Pazouki et al., 2018).

The importance of human element was emphasized for new autonomous ships at the 99th session of Maritime Safety Committee meeting (May 16-25, 2018). IMO (International Maritime Organization) Secretary-General Kitack Lim highlighted the importance of being flexible in using new technologies to improve the efficiency of shipping, “while at the same time keeping in mind the role of the human element and the need to maintain safe navigation, further reducing the number of marine casualties and incidents.” The most important thing that can be inferred from this statement is the fact that on board autonomous ships human element will not cease to exist. Within the four autonomous ship categories projected by IMO, only the fully autonomous ships will be operating with no seafarers on board or ashore. All the other three categories will require seafarers to be present either on board or ashore for remote controlling (IMO, 2018).

Authors stated in their study that most prominent issue for Shore Control Centre Operator (SCCO) is reduced situation awareness due to limited sense of the ship (Burmeister et al., 2014; Man et al., 2015; Wahlström et al., 2015). The other issues were also stated as information overload due to the plurality of ships and ship sensors, boredom, constant reorientation to new tasks, delays in control and monitoring

(Wahlström et al., 2015). Physiological monitorization will be more important for autonomous ships due to the above-mentioned reasons.

1.3 Purpose of the Thesis

There have been studies focusing on assessing the cognitive states of operators in terms of their mental workload levels as well as their drowsiness through physiological measurements. The innovation site of the thesis is implementing the similar measurement techniques to maritime transportation for designing Cognitive Seafarer – Ship Interface. This study aims to classify the physiological responses of the operators that can produce an output for state of officer on duty as “Safe” or “Risky” from the collected physiological data and task load data during the seaborne operations. It is aimed to reach the following objectives with the study to be carried out throughout the thesis:

- Designing Cognitive Seafarer - Ship Interface (CSSI) which is a main part of Seafarer-Centric Safety System. The physiological data of the officer will be recorded according to the design. By being correlated with the performance of the officer, the change of physiological responses of the subjects will be analysed in low and high task load levels. The medical decision-making process, which will deduce “Safe” or “Risky”, will be run for this change (Figure 1.3). High accuracy of classification will show the success of the design.

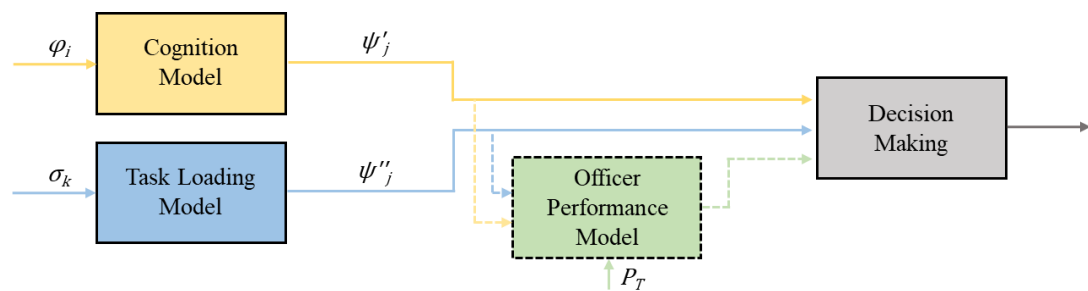


Figure 1.3 : Mental workload prediction system layout.

- Defining the inputs of Task Load Estimator (Figure 1.2) as data transcription from navigational aids according to results of classification.
- Developing Officer Performance Model for navigation and cargo operation tasks which is used for MWL classification.

1.4 Limitations and Assumptions of the Thesis

In this thesis study, “mental workload prediction” refers to task-related fatigue and fatigue-like effects caused by mental strain specified in the stress-strain-effects model of ISO 10075-1 (Figure 1.1).

Limitations and assumptions of the thesis are stated below:

- Simulator environment was chosen for measurements due to fact that measurement on real environment on board is dangerous and is difficult to obtain repeatable results of operator errors.
- The sample group for this research consists of junior deck officers who have minimum one contract sea service. Although it is known that most of maritime accidents result from the deficiencies in cooperation of Master-Pilot-Officer during pilotage or manoeuvre, in one-third of all accidents one officer keeps watch at the bridge (Yıldırım et al., 2019). On the other hand, experience is a major contributor for coping with stressor factors (Jeżewska and Iversen, 2012; Salyga and Kusleikaite, 2011). Considering all of above-mentioned reasons, junior officers are selected for this research and the measurements were taken from the subjects in simulators as if they keep watch alone at the bridge.
- It is assumed that all subjects, who have minimum one contract sea service, have sufficient knowledge to handle navigation and cargo operation tasks.
- One of the limits of the thesis is that the sample group consists of only junior deck officers. Universal usability of the MWL prediction system for all ranks of seafarers and for all specified seaborn operations has to be researched in future studies.
- Other limitation is that developed MWL prediction system is only based on mental strain and mental fatigue. In future, the related systems should be able to detect sleep-drowsiness states and/or other fatigue-like effects.

2. THEORETICAL AND CONCEPTUAL FRAMEWORK

Mental workload (MWL) can be defined as the amount of mental effort and it is related to information processing and decision making. In literature, the words such as attention, stress, arousal, activation, workload, physiological response, behavioural activity, cognitive ability are used in similar areas. As MWL can only be inferred, not directly measured, other measures such task performance measurement, physiological response have been analysed to infer MWL.

Information processing and task performance items has been subjects of physiological and cognitive theories. They use same terminology at many times. It is stated that there is an integration between these theories (Sanders, 1983; De Waard 1996). From the view of this theoretical point, cognitive (mental) workload should be studied and overemphasised to determine which theoretical approaches to adopt and develop measurement techniques. In brief, cognitive workload can be defined as the number of mental resources an individual needs to handle a particular task in his / her environment. The difference of limited amount cognitive resource and environmental demand is a ground of human error in occupational areas (Embrey et al., 2006).

First part of this section contains theoretical approach to workload. Second part presents the summary of the theories used in this study. Last part includes the measures of MWL and medical decision-making techniques.

2.1 Workload Theory

Workload is defined simplistically as a demand placed upon humans. Demand is specified by the aim of task performance. So, the workload is the effect of demand on the individual in terms of stages used in energetics and information processing. More specifically, workload is the amount of information processing capacity used for task performance. (De Waard, 1996). It points out two components; stress that is task demand and strain that is effect on the individual. While stress comprises multiple demand factors, strain indicates the use of available resources for those demands (Young et al., 2015).

The first information processing theory was proposed by Broadbent (Embrey et al., 2006). The theory, single-channel hypothesis, suggests that there is a single-channel processor that can only select one sensory input at a time for intentional processing, that means limited capacity. However, this hypothesis fails on all tasks requiring selective or divided attention. It was accepted that human cognition should be thought as a limited capacity processor rather than a limited capacity channel, overtime. Although O'Donnell and Eggemeier argued that there is no difference between capacity and resource, Wickens stated that capacity is the maximum of processing capacity and resource is mental effort to improve processing efficiency (as cited in De Waard, 1996). Moray asserted that performance is affected by the limitation of the central processor, not the limitations on input channels (Embrey et al., 2006). So, the capacity could be divided among different processors by this view. This theory is called resource theory.

Single resource theory is simplistically based on the balance between supply and demand (Embrey et al., 2006). When resource demands exceed available supply, performance is assumed to be decreased (Figure 2.1). According to Kahneman (1973), the cognitive system has a single pool of limited capacity. Large amounts of resources are required for difficult tasks, especially when these tasks are coupled with concurrent tasks. On the contrary, easy and automated tasks require less resource with time sharing efficiency.

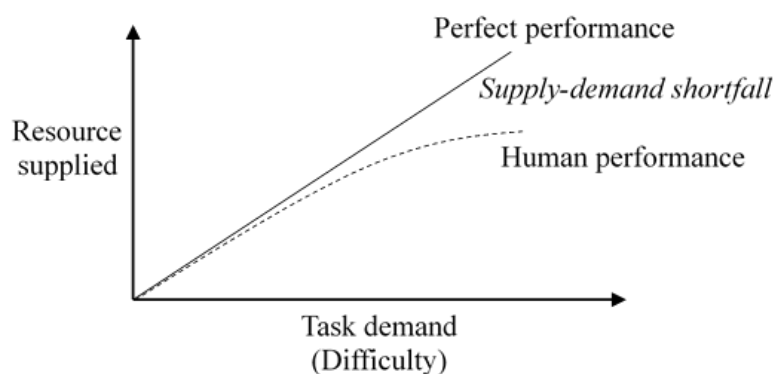


Figure 2.1 : Relation between resources, demands and task performance, adapted from (Embrey et al., 2006).

Kahneman (1973) argued that in the cognitive system, difficult and complex tasks increase the arousal level, providing additional resources to cope with these tasks. In the light of this information, MWL can be monitored with the aid of physiological data collection in terms of autonomic nervous system activation. Kahneman (1973)'s

approach, in terms of being measurable, was not considered sufficient alone, but has been adopted by other researchers (De Waard, 1996; Young and Stanton, 2002).

From Kahneman (1973)'s viewpoint that resource supply needs sufficient arousal level, Sheridan and Simpson (1979) tried to formulate the relation of behavioural (arousal) activity, mental effort and performance. They underlined that MWL is neither performance nor task demand. They stated that acceptable minimum performance ($P_{i \min}$) requires sufficient behavioural activity (B_i) (Figure 2.2).

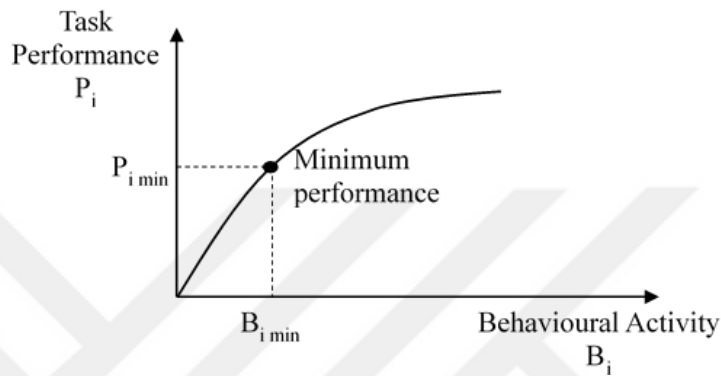


Figure 2.2 : Relation between task performance and behavioural activity, adapted from (Sheridan and Simpson, 1979).

They assumed that there is a monotonic relationship between work load and behavioural activity and work load cannot be measured, only inferred. They also stated that mental work identified with task i can be extended in time (Figure 2.3). Thus, mental work load (M^P_i) is the time integral of mental effort (\acute{M}^P_i);

$$\acute{M}^P_i(t) = \int_0^t \acute{M}^P_i(t). dt \quad (2.1)$$

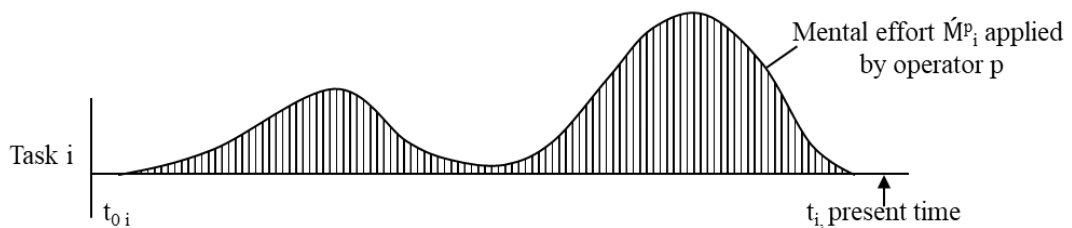


Figure 2.3 : Mental effort applied by operator over time t , adapted from (Sheridan and Simpson, 1979).

Similar to the lack of a simple relationship between performance and effort invested (De Waard, 1996), there is no constant relationship between behavioural effort and mental effort (Sheridan and Simpson, 1979). Practice, experience, operator's state can affect the performance. Similarly, increasing level of skill can make individual need

less mental effort (Figure 2.4). In order to prevent acquired skill, tasks were sequentially complicated within a certain period of time in this study.

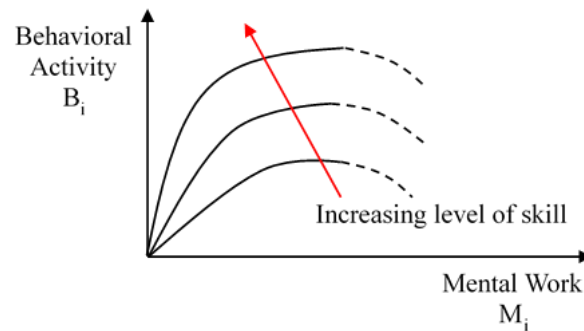


Figure 2.4 : The effect of increasing level of skill to mental work, adapted from (Sheridan and Simpson, 1979).

Sheridan and Simpson (1979) put forth two constraints for the task completion optimization:

- i. The behavioural activity for task i is a function of the mental work expended on that task (Figure 2.4).
- ii. The performance achieved on task i is a function of behavioural activity expended on that task (Figure 2.2).

In the information processing theory, a series of stages involved the process from information uptake to convert reaction, are performed in computational process which will be detailed in chapter 2.1.2. The researchers, who interpret energetic and computational models, stated that efficiency of computational process affected by the energetic resources (De Waard, 1996). According to Pribram & McGuiness, these energetic resources are arousal, activation (behavioural activity) and effort (mental work) which is not processing effort, is being active in the case of attention (as cited in De Waard, 1996).

MWL, the effect of demand on operator, is an interaction between operator and task structure. Complexity and difficulty are the main characteristics of demand. Complexity is the number of stages of processing and difficulty is processing effort and it is related to number of resources (De Waard, 1996). MWL, in terms of demand / resource balance, is a product of the resources available to meet the task demands (Young et al., 2015). Demand is determined by the aim to be achieved by the task performance and cannot be associated precisely to workload. Assessment of workload is combined with task difficulty as much as the operator experiences since the operator

can give several reactions to the task demands such as adaptation or giving up (De Waard, 1996). Thus, MWL is a multidimensional construct and is determined by task characteristics (e.g., performance, demand), operator characteristics (e.g., attention, skill) and environmental factors (Young et al., 2015).

Although task performance cannot alone indicate any change in workload, suboptimal workload leads to errors and incidents. Suboptimal workload can be described either overload or underload (Young et al., 2015). With the aid of the relationship between mental work and behavioural activity (Sheridan and Simpson, 1979), physiological measurements can indicate mental work (De Waard, 1996; Embrey et al., 2006; Kahneman, 1973).

Young et al. (2015) stated that physiological response (behavioural activity) cannot alone indicate any change in workload. Work load is born upon availability of resource supply to meet task demands rather than physiological response level. They stated that if cognitive system has a single pool of limited capacity, work load would be easily detected in case of any change in behavioural activity according to Kahneman (1973)'s viewpoint. However, cognitive system is a multiple channel processor and each processor has its own internal capacity (Wickens, 2008). The name of this theory is Multiple Resource Theory.

Wickens (2008) argued that mental resources are divided among several competing tasks. Mental resources have three dichotomous dependent or independent resource pools (Figure 2.5). According to Multiple Resource Theory, when two different tasks that use different resource pools appear, operative time-sharing performance should occur. Although two tasks, that occur at same time, seem to raise workload, if they use different resource pools workload may not tend to rise with the aid of time-sharing efficiency. Thus, changes in MWL may not be quantitatively observed in Wickens' model.

Multiple resource theory is utilizable for interference between tasks but contradictory for multidimensionality that cause reveals the need to add new dimensions when existing dimensions are not enough (De Waard, 1996).

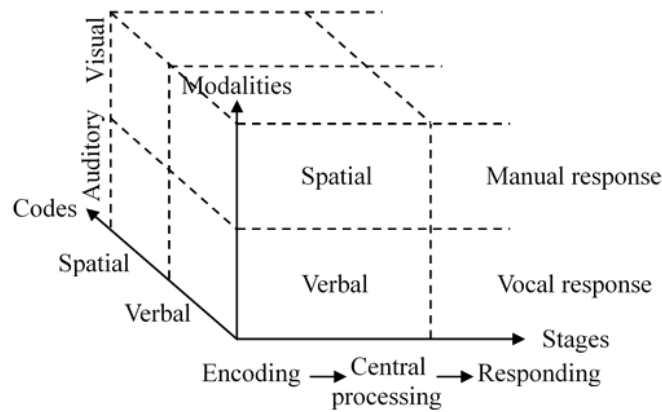


Figure 2.5 : Schematic representation of Wickens' model, adapted from (Embrey et al., 2006).

Another situation that makes the measurement of the workload difficult is related to controlled or automatic (nonattention) information processing. Mental effort is related to just controlled mode of information processing (De Waard, 1996). According to Young et al. (2015), MWL is identified by the balance of automatic and controlled processing. Automatic processing releases attentional resources for other tasks that reduces mental work load.

Young et al. (2015) stated the relationship between performance, task demand and resource supply (that is activation level according to De Waard (1996)) in Figure 2.6. However, both of them is coherent with Kahneman (1973)'s viewpoint.

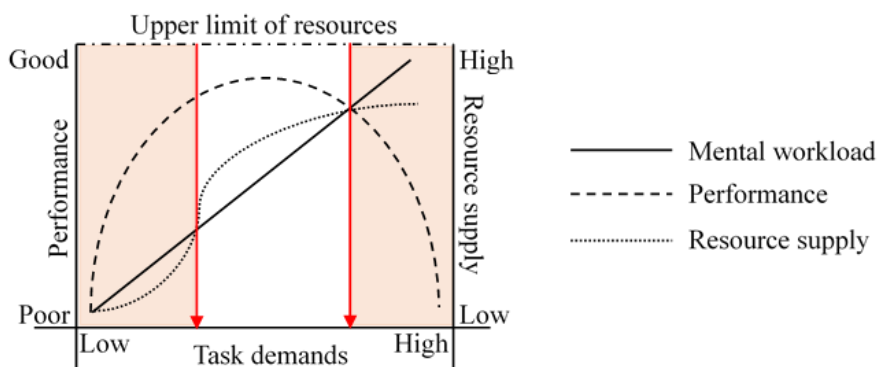


Figure 2.6 : The relationship between task demand and resource supply associated with mental workload and performance, adapted from (Young et al., 2015).

The left region of the red lines is called the 'reserve capacity' (underload) and right region is called the 'overload' region (Figure 2.6). In underload region task demands could be misperceived by operator and it could lead to performance decrement. Alternatively, in overload region when task demands exceed the resource supply, performance could be decreased. Resource supply is based on activation and/or effort

and brain oxygenation could reflect a quantitative measure of attentional measures in connection with mental effort (Young et al., 2015).

2.1.1 Malleable attentional resources theory (MART)

Underload needs to be focused more because of that is more difficult to detect than overload. The upper limit capacity of an operator has been based on task circumstance. If the task is low demand task, operator cannot cope with any critical situation when he/she has suddenly faced with increased demand. MART clarifies why mental underload can lead to performance impairment (Young and Stanton, 2002).

The theory can be modelled as in Figure 2.7. Increased demand leads to sharp performance decrease. This theory is more acceptable in maritime because of that contains automation systems. Watchkeeping officer may not cope with the situation in case of any failure in automation systems or being exposed to unexpected danger when his/her attention decreases in non-traffic area with auto-pilot.

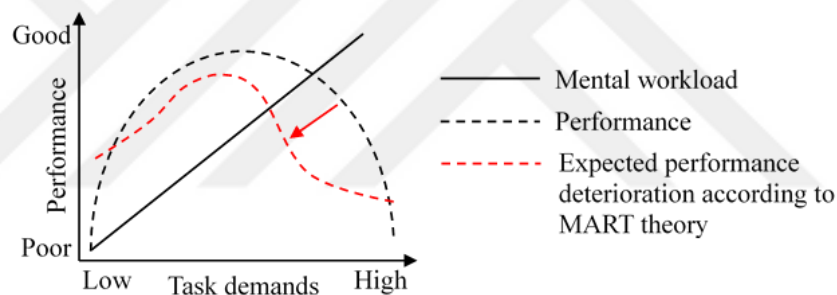


Figure 2.7 : The relationship between performance and task demand with regards to MART, adapted from (Young and Stanton, 2002).

2.1.2 The role of situation awareness theory on workload

Situation awareness (SA) is a predominant concern in information processing. Working memory and attention are key factors that limit operators from acquiring and interpreting information from the environment to convert it to reaction. Endsley (2017) used the following definition for SA; “Situation awareness is the perception of the elements in the environment within a volume of time and space, the comprehension of their meaning, and the projection of their status in the near future.” (p. 36).

Decision and action take place after three stages of SA. In Endsley (2017)’s SA model (Figure 2.8), “perception” points to the question “What is it doing”, “comprehension” to “Why is it doing that” and “projection” to “What will it do next”.

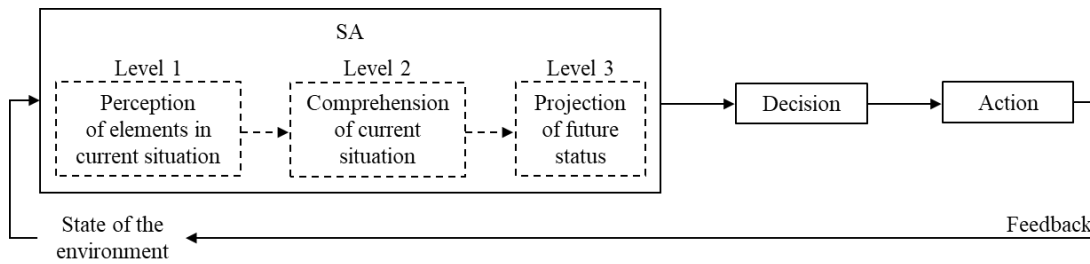


Figure 2.8 : Model of situation awareness, adapted from (Endsley, 2017).

The model of SA is used as “encoding - central processing – responding” in Wickens (2008) multiple resource theory (presented in Figure 2.5) and similarly De Waard (1996) presented this process as the energetic magnetic activity of brain. It can be seen in Figure 2.9 that “Stimulus pre-processing” and “feature extraction” seem to be part of SA. Moreover, authors stated that it is possible to know which brain mechanisms are active in various information processing stages (De Waard, 1996).

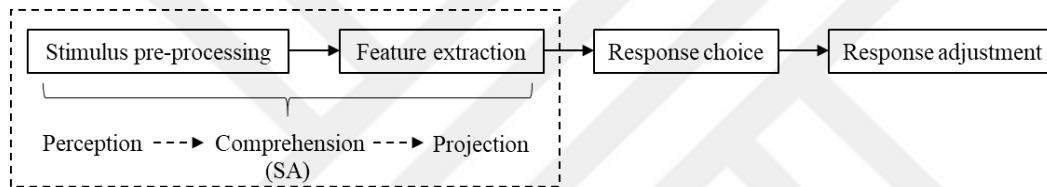


Figure 2.9 : Resemblance of 4 stages of information processing theory (De Waard, 1996) with situation awareness theory.

Errors can occur in all stages and can affect the task performance. However, the relationship between SA and performance is not always directed. Although it is known that incomplete or insufficient SA causes poor performance, it is stated in a study that when operators realized their poor SA, they were able to adjust their behaviour to eliminate the possibility of poor performance (Endsley, 2017).

Endsley (2017) stated the relationship between workload and SA with the following comparisons;

- i. Low SA with low workload; inattentiveness, low motivation or vigilance problem.
- ii. Low SA with high workload; erroneous or incomplete perception and integration of information.
- iii. High SA with low workload; ideal state.
- iv. High SA with high workload; working hard but being successful in task.

Thus, SA and workload can be varied because of characteristics of task, operator and environmental factors. If effort increases but demand exceeds the operator’s limited capacity, a decrement in SA can be expected.

2.1.3 Officer workload

Safety of navigation and safe operation are crucial in terms of avoiding incidents and accidents in maritime. It is stated that operator errors that cause accidents can occur at all levels according to Endsley (2017)’s model. In literature, these levels have been investigated in terms of navigation parameters in mostly collision situations. Table 2.1 presents how the SA model has been integrated into maritime context.

Table 2.1 : Integration of SA model into maritime context.

Authors	The cases for levels		
	Level 1	Level 2	Level 3
Schuffel et al. (1989)	(Perception) Identification of targets	(Information processing) Track keeping automated path prediction on ARPA	(Motor control) Decision on tracks, set-point control
Grech et al. (2008)	(Perception) Presence of other vessels	(Comprehension) Will courses intersect? Any risk of collision? Which ship is going to give way?	(Execution) Actions to avoid collision
Gould et al. (2009)	(Cognitive mapping) Understanding of the surrounding environment	(Decision-making) Planning the actions based on route information	(Decision-execution) Decisions are transferred into physical behaviours by giving order to rudder and engine
Cordon et al. (2017)	(Perception) Traffic on course	(Comprehension) IMO regulations to prevent collisions	(Projection) Predicted dangerous manoeuvres, radio contact with other vessels / VTS

Grech et al. (2008) illustrated SA with anti-collision work on board a ship. Firstly, other vessels must be detected. In level 2, their courses must be determined whether there is a danger of collision or not. Watchkeeping officer must determine which ship is going to give way according to International Regulations for Preventing Collisions at Sea (COLREG). In level 3, action must be taken in order to avoid collision and officer must be sure that manoeuvre has the intended effect.

Figure 2.10 presents that the bridge console where watchkeeping officer controls the ship. The main controlled equipment and items on bridge by watchkeeping officer are stated on the figure.



Figure 2.10 : An example of bridge console.

Similarly, SA model can be integrated into cargo operations of ship. Table 2.2 presents the integration of SA model into chemical tanker cargo operation. Figure 2.11 presents that the cargo control room (CCR) where officer performs the cargo operation. The main controlled equipment in CCR is stated on the figure.

Table 2.2 : The integration of SA model into chemical tanker cargo operation.

Situation	Perception	Comprehension	Projection
Manifold pressure	Increase of pressure	Cargo lines linked correctly to each other? All related valves open? Being aware the distance of lines and height of shore tank.	Reduce the pump rpm in discharging operation or increase the number of tanks in loading operation
Cargo temperature	Suddenly rise of temperature	Being aware of polymerization. Chemical reaction may have been occurred.	Stop operation. Cooling the tank. Using the inhibitor.
Ballast operation	Critical list or trim occurs	Being aware of shearing force and bending moment limits. Present ballast tanks levels. Being aware of loading / discharging steps	Load or discharge ballast contrariwise. Reduce the rate of cargo operation.

All parameters should be respectively considered in order to determine officer workload. In this study, all these stages were stated to relate the behavioural activity of the officer with his / her performance in navigation and cargo operations. Operator

Function Model (OFM-COG) was adapted to determine task load of the simulation tasks (See detailed information in chapter 2.3.3.) The classification used in the model similar with SA model helps in determining the task difficulties and complexities of the simulation tasks and calculating the inferred workload.

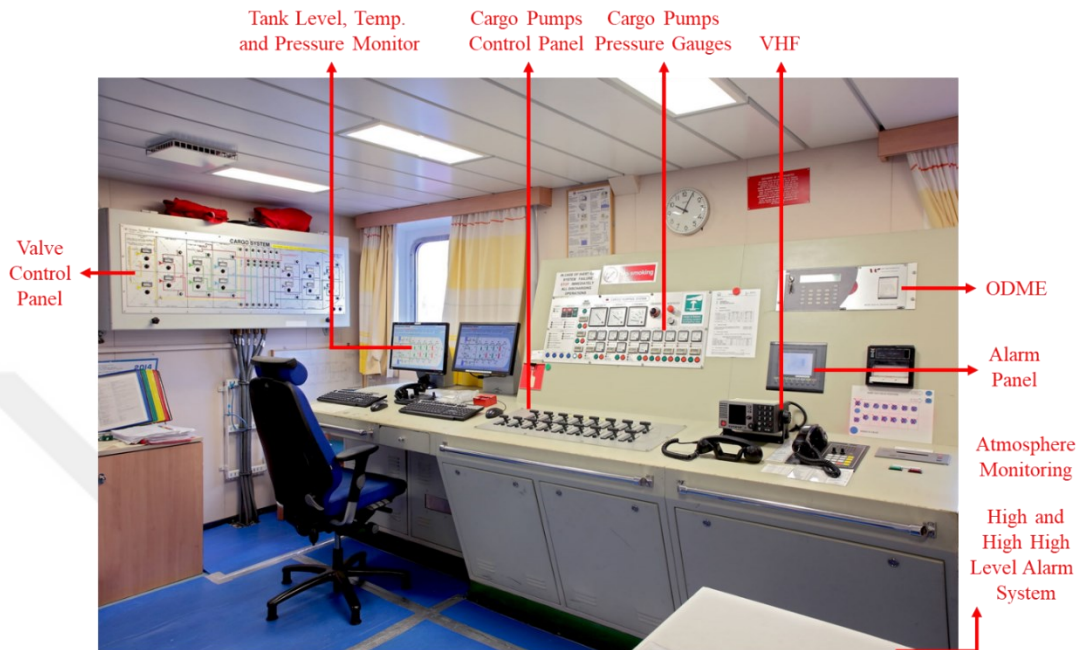


Figure 2.11 : An example of cargo control room.

2.1.4 Vigilance

Vigilance is the state of keeping of a individual's attention and long-standing alert to target stimuli. The efficiency of task performance depends upon several factors. These factors for watchkeeping tasks are stated below (Embrey et al., 2006):

- i. The sensory modality of the target signal; signals are detected via auditory, visual or cutaneous stimulation.
- ii. The salience or detectability of signal; amplitude and duration of signal are determinative for detectability.
- iii. Stimulus uncertainty; position, time or nature of signal can affect the response time to signal detection.
- iv. Background context; performance degradation is more pronounced when high frequency background events occur.

- v. Stimulus complexity; fast, effortless and skill-based behaviours occur in automatic processes. On the contrary, slow, effortful and capacity limited behaviours occur in controlled processes.

2.1.5 Inverted U principle

When the environmental demands increase, MWL increases correspondingly and human information processing system cannot cope with large amounts of environmental demands in cognitive strain condition. On the contrary, when the environmental demand is low, an individual tends to become less vigilant and his / her attention cannot direct to needed environmental demand due to less stimulation. The relationship between performance on related task demand and mental arousal can be described with reference to Yerkes and Dodson (as cited in Tavacıoğlu, 1999). They observed on mice that weak and strong stimulus cause slow habit-formation. Thus, the optimal task performance takes place at a medium level of mental arousal and weak performances are related to higher and lower arousal levels according to the law called Yerkes-Dodson principle. There is a linear relationship between performance and arousal in simple tasks whilst there is a curvilinear relationship in complex tasks according to Yerkes and Dodson (1908) (Figure 2.12a).

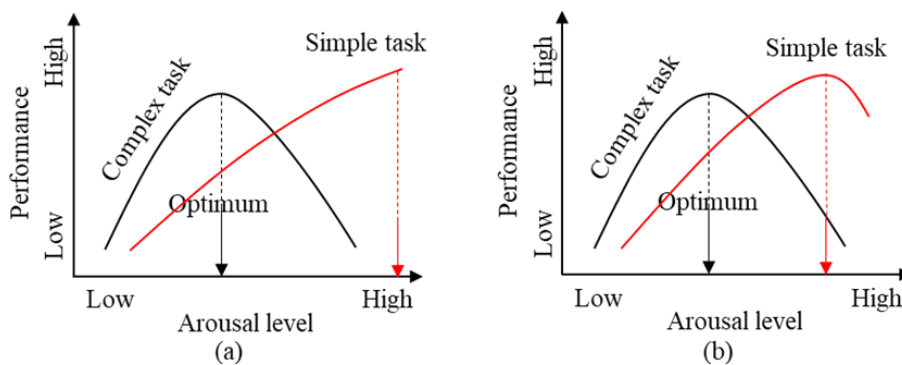


Figure 2.12 : Inverted U function of Yerkes-Dodson principle for relationship between arousal and performance, adapted from (Diamond et al., 2007).

However, there shouldn't be a linear relationship in simple tasks according to Diamond et al. (2007) (Figure 2.12b). High arousal cause performance degradation regardless of task difficulty.

2.2 The Summary of The Theories Used in This Study

In this study, the following theoretical assumptions have been used as a result of the theoretical approach mentioned in the previous section.

- i. MWL (M_i^P) is the time integral of mental effort (\dot{M}_i^P) (Equation 2.1, Figure 2.3).
- ii. The behavioural activity for task i is a function of the mental work expanded on that task (Figure 2.4);

$$B_i = f(M_i) \quad (2.2)$$

Tasks were sequentially complicated within a certain period of time in this study in order to prevent increasing level of skill that can make individual need less mental effort.

- iii. Acceptable minimum performance requires sufficient resource supply and behavioural activity (arousal) (B_i). Yerkes and Dodson (1908) stated that the optimal task performance takes place at a medium level of mental arousal and weak performances are related to higher and lower arousal levels. However, high stimulation (arousal level) is needed for optimal performance of simple tasks. Same behavioural activity at tasks of which difficulty levels are different, may not be sufficient for minimum performance (Figure 2.13).

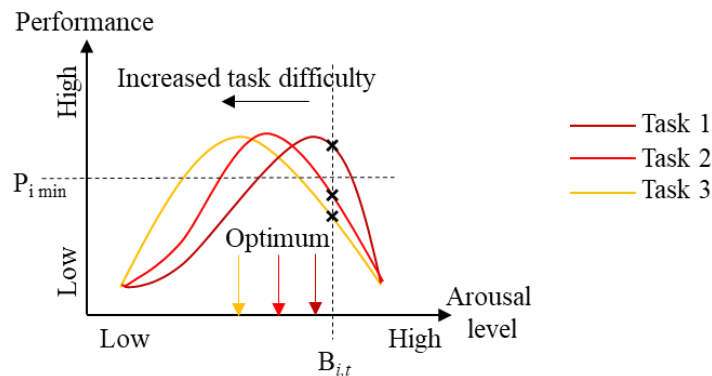


Figure 2.13 : The relationship between arousal and performance.

- iv. The relations among performance, task demand and resource supply are as the model of Young et al. (2015) (Figure 2.6). However, arousal level takes the place of resource supply according to assumption ii and iii.

Consequently, when task demand is very low, operator should give more attention to tasks to detect any change in environmental conditions. When task demand is

moderate, higher performances of operator can be seen at this stage and the relationship between arousal and performance is formally closer to inverted U shape. It is assumed that the performance decreases as the complexity and difficulty of task increase. At last stage, best performance takes place at medium level of arousal. Moreover, MWL increases when task demand increases as stated in Figure 2.6.

2.3 Measures of Mental Workload

The main goal of MWL measurement is to evaluate the effect of task demands on human operator. There are 4 measurement strategy for MWL assessment. First one is subjective measurement that bases on the own subjective evaluation of operator. Self-report rating scales were used to quantify the workload assessment. Second one is performance measurement that measures workload through fluctuation in task performance. Third one is physiological measurement and last one is task loading assessment which adopts engineering perspective to estimate workload within cognitive structure (Embrey et al., 2006). According to Wierwille and Eggemeier (1993), there are three major empirical measurement methods which are subjective, physiological and task performance measures. These are also the components of triangulated measurement strategy.

In maritime human factor research, there are several data collection methods. The ones related with MWL or fatigue are mainly physiological, physical (eye movement etc.), environmental measures, performance analysis in simulator environment, interviews, questionnaires, observations and log books, accident / incident analysis and computer-aided design / evaluations. To collect human factor data and choose the appropriate method in maritime domain, following general aspects should be considered (Grech et al., 2008);

- where to conduct the study,
- what to examine,
- what measures to record,
- who to study,
- how to collect the data,
- how to analyse the data,

- study requirements (practical, reliable, valid, free from contamination unplanned or unintended influences).

In the studies related to MWL / fatigue in maritime, the measures for mainly navigation tasks and few engine and cargo operation tasks have been analysed. Table 2.3 presents the related maritime studies indicating the measurement strategies.

Most of researchers didn't apply the triangulated measurement strategy in their studies and they used mostly EEG measurements for workload assessment. Performance measurements were conducted either with primary task performance, which is related to the ship specific tasks, or secondary task performance. The contradiction between primary and secondary task performances appears in subjective workload measurement and EEG measurements (Wu et al., 2017). Participants reported higher MWL in n-back tasks (secondary task) than in primary tasks while they had lower alpha wave suppression in n-back tasks than in primary tasks. Primary task of the study required more than one information processing channel while the secondary task required only one. As the structure of multidimensional limited cognitive resource model (Wickens, 2008), MWL increases when task demand increases in tasks used only one information processing channel. Apart from that, most of researchers used either primary task performance measurements or non-ship specific task performance measurements which are mostly related to cognitive functions of operators (Table 2.3).

Generally, there are two groups of techniques to measure workload. First one is arousal-related measures such as subjective, performance and physiological measures. It is thought that a global measure of MWL is possible and it is comparable to single-resource use. This technique is applicable in many cases. The other group is more diagnostic and is linked to multiple resource theory. Some of physiological measures and secondary task techniques belong in this group (De Waard, 1996).

The choice of workload measure depends on some properties. Sensitivity (ability to detect changes in workload levels), diagnosticity, primary task intrusion (by secondary task), those are essential according to De Waard (1996), implementation requirements and operator acceptance are the properties of workload measurement techniques (Embrey et al., 2006). Wickens added two properties – 'selectivity' (between mental workload and physical workload) and 'bandwidth and reliability' (to identify upper and lower performance limits) to the list of criteria (as cited in Embrey et al, 2006).

Table 2.3 : Mental workload and fatigue studies in maritime domain.

Authors	Subjects	Measures			Results
		Subjective	Physiological	Performance	
Cook and Shipley (1980)	7 marine pilots	Self-Report Affect Questionnaire	Body temperature ECG EDA Reaction time	-	The mean of fatigue is either high activation / stimulation or low vigilance. Monotonous tasks decrease the vigilance of ship pilots.
Robert et al. (2003)	12 non-seafarer students and graduates	Subjective Rating of Mental Workload (MWL)	-	Primary; 6 generic scenarios with the crossing collision threat and target behaviour variables. Secondary; maintaining engine oil temperature within tolerance limits.	Secondary task method can be used to assess cognitive demands in a simulated maritime task environment. Higher levels of collision threat were found to be associated with increased MWL and with impaired performance on the secondary task.
Lützhöft and Dukic (2007)	6 students and experienced officer	-	Eye tracking (AOI, % of gaze, mean glance duration, scan path, number of glances per minute)	-	Authors indicated the relationship between eye tracking data and workload. However, they didn't find significant difference between students and experienced officers.
Gould et al. (2009)	20 senior students	NASA - TLX	HRV EDA	TARGETS method (expert evaluation, course deviation, ship control) within the variables of geography, visibility and traffic density.	Navigating with ECDIS significantly improved the course-keeping performance and HRV and EDA measurements indicated higher workload in using paper charts.
Maurier et al. (2011)	40 officers	Food, wake and sleep diaries Karolinska Sleepiness Scale (KSS)	EEG EOG Actiwatch Psychomotor Vigilance Task (PVT) Stroop Test	Activity data allowing the analysis of area use and movements performed by the participants in bridge, cargo control room and engine room simulators.	6 on / 6 off watch pattern has negative impact on officers in terms of fatigue and performance. EEG measurements indicated that sleepiness and fatigue increased at the end of the 00-06 watch.
Yilmaz et al. (2013)	7 officers	-	EEG	Routine bridge operational check lists	Increase in working hours caused fatigue and sleepiness and decrease in performance of routine operational tasks.
Muczyński et al. (2013)	10 captains, officers and students	-	Eye tracking (AOI, fixation freq., saccade freq., blink freq.)	Simple navigation scenario consists of overtaking and bypassing of ships in a narrow canal.	Experienced subjects with best performance results had lowest MWL.

Table 2.3 (continued) : Mental workload and fatigue studies in maritime domain.

Authors	Subjects	Measures			Results
		Subjective	Physiological	Performance	
Tac et al. (2013)	12 Seafarers	-	EEG	Cognitive Test	Cognitive performance and reaction time deteriorate through fatigue and sleepiness.
Bjørneseth et al. (2014)	8 Dynamic Position (DP) Operator	Post-experiment interview	Eye-tracking (fixation, saccadic movements, pupillary response, eye blink rate, scanpath)	-	Expert operators do spend more time during the operation, fixating on the outside environment and important equipment. DPO's pupillary response increases when reaching a critical phase of the operation.
Liu et al. (2017)	4 students	-	EEG	Stroop Colour word test	The participant, who played the Master role in Bridge team, had the highest stress and workload. EEG shows higher sensitivity than HRV.
Wu et al. (2017)	10 students and graduates	NASA – TLX	EEG HRV	Primary; 4 engine department tasks with different levels of difficulty. Secondary; n-back task for quantifying working memory.	Participants reported higher MWL in n-back tasks than in MEPS tasks while they had lower alpha wave suppression in n-back tasks than in MEPS tasks.
Orlandi and Brooks (2018)	10 Marine Pilots	NASA-TLX Likert Scale	EEG HRV Eye-tracking (pupil dilation)	Simulated berthing / unberthing operation tasks with the variables of port familiarity, difficulty and manoeuvre phase.	Workload increased as the difficulty level of berthing increased and/or the pilots completed the berthings in unfamiliar ports. Physiological responses could indirectly monitor levels of mental workload.
Özsever and Tavacıoğlu (2018)	14 seafarers	-	EDA HRV	2-choice reaction time test	When seafarer's circadian rhythm is changed more frequently, they experience more drowsiness. The synchronization of EDA and HRV contributed to assess individual's arousal mood and activation state.
Murai et al. (2018)	4 seafarers	-	ECG	Simple navigation scenario in the narrow channel.	LF/HF value was useful index for MWL that was used for a real time evaluation.
Yan et al. (2019)	27 students	NASA-TLX, SWAT	Eye-tracking (pupil dilation, blink rate, fixation rate, saccadic rate)	2 engine department tasks (operation time and number of errors)	Eye response data and subjective ratings were classified with ANN. The results were correlated with decreased performance results. As a result, eye response is sensitive to MWL.

High sensitivity does not mean always high diagnosticity. For instance, pupil diameter is sensitive but not diagnosable for MWL. The diagnosticity of secondary task performance is higher than pupil diameter (De Waard, 1996). Besides, being global of sensitivity and transferability are the other important properties of workload measurement techniques (Wierwille and Eggemeier, 1993). Hereby, the workload measurement technique should have the properties as high reliability, preferably in a wide bandwidth, low primary task intrusion and high sensitivity (De Waard, 1996).

2.3.1 Subjective workload measures

Subjective measurement techniques are mostly used in estimating MWL. There are several scales for MWL measurement but three of them are thoroughly analysed in literature. Modified Cooper-Harper Scale (MCH) was mainly concerned with physical workload. In this scale, there is a simplistic assumption that performance of operator has a linear relation with the effort operator made on task. Low workload is desirable for task but low vigilance and sustain attention can indicate low workload according to scale. NASA Task Load Index (NASA-TLX) has 6 sub-scales for measurement. Mental, physical and temporal loads are task related, performance and effort loads are behavioural and skill related, frustration is individual related. Participants weight the sub-scales after they complete scoring the index. So, this measure has multidimensional structure and priority choice of workload types. Subjective Workload Assessment Technique (SWAT) has 3 sub-scales as mental effort load, time load and psychological stress load. SWAT scale involves two-step procedure same as NASA-TLX in terms of weighting the sub-scales. Authors stated that two-step procedure has negative effect on measurement duration for SWAT and TLX scales. Besides, simple univariate scales are more sensitive than SWAT/TLX scales in variation in task difficulty (Embrey et al., 2006).

MCH, TLX and SWAT are globally sensitive measures of operator workload. They have been used mostly for flight simulation environment (Wierwille and Eggemeier, 1993). According to the authors, TLX is more sensitive than SWAT at lower workload levels. Besides, TLX is more user acceptance scale because of that the implementation of SWAT scale takes 1 hour.

The relation between subjective workload and task performance is not always significant as well as between physiological and subjective ones (Young et al., 2015).

Operator may not feel the workload during low task demand but performance can decrease caused by monotonous jobs. Actually, operator should more attention at this stage. Similarly, operator may quit from the task or give high activation during high task demand. Both of cases cause to performance decrement. Actual effort and workload experienced are not always in parallel and they are not always distinctive. Therefore, one of the MWL scales, Rating Scale Mental Effort (RSME) which has scale between 'no effort' and 'extreme effort', has a problem to detect workload but it was found more sensitive than TLX. It was stated that this outcome may be associated to confusion caused by sub-scales of TLX (De Waard, 1996). According to Author, Raw Task Load Index (RTLX) as well as RSME is more sensitive than TLX because of that RTLX does not necessitate task paired comparison weights.

As a result, TLX (see column 3 of Table 2.3) and SWAT have been mostly used in MWL studies although they have 2-step procedures for evaluating workload that cause confusion. As the implementation of SWAT takes more time than TLX, it seems that the use of TLX is more applicable for this study.

2.3.2 Performance-based measures

In literature, there are 2 types of performance measurement methods. One of them is primary task performance that measures the total effectiveness of human-machine interaction. It mainly considers response latency, error rates, accuracy of response and time taken to complete the task (De Waard, 1996). Secondary task is mainly related to cognitive process and provides a measure of spare capacity. As the decrement of primary performance is not directly linked to workload, both tasks should be used concurrently to estimate workload (Embrey et al., 2006).

According to Wickens (2008), both tasks should use same resource. For example, audial warnings have not an effect on the driver workload measurement (De Waard, 1996). Therefore, light test can be used for secondary performance measurement because of that vehicle handling that is primary performance is a visual task (Young et al., 2015). Additionally, using of secondary task performance increase the workload. If the intrusion of primary task performance is not desirable, the use of secondary task performance can be risky because of possible compromises of secondary task to system safety. Besides, operator acceptance decreases with secondary task performance.

The expectation of primary task performance is the decrease of speed and accuracy and the increase of workload. The disadvantage of method can be variance of the results due to operator's ability. In secondary task measurement, information processing and response functions such as perception, memory, motor output are assessed. However, sensitivity and intrusion should be considered when using the secondary tasks. An alternative method to use of external tasks is the embedded task. This task is a part of the normal system operation (Wierwille and Eggemeier, 1993). Routine or emergency radio communication can be an example of embedded task for navigation or cargo operation at terminal.

Other alternative method that can be used to assess workload is reference task measurement. This measure involves pre and post measurements using some task batteries (De Waard, 1996).

In maritime, lots of primary and secondary task measurement methods have been used to assess MWL (see Table 2.3). Wu et al. (2017) performed 4 engine department tasks with different levels of difficulty. These are transferring diesel oil from settling tank to service tank, preparing and starting the central cooling system, starting diesel engine of no. 2 generator and starting lubrication oil purifier. Authors considered the operation time for measurement of performance. For secondary task measurement, n-back task measurement was used to quantify working memory. Number of mistaken responses and total time in seconds were considered for measurement of secondary task performance.

In another study conducted on workload assessment of marine pilots, port familiarity, difficulty of manoeuvre (adjusting the safety limits) and manoeuvre phase were selected as variables for primary task measurement. Pre and post physiological measurements were applied in order to determine MWL of marine pilots (Orlandi and Brooks, 2018).

Gould et al. (2009) used the variables as geography, visibility and traffic density for navigation scenario with 4 different levels of difficulty. TARGETS method was implemented to assess primary performances of officers by expert evaluations. Task-generated (observable safety-critical navigation tasks) and event-generated (responses to external objects such as safe passing criteria; these are evaluated as "just acceptable or not" by experts) evaluation criteria were implemented by experts. Additionally,

course deviation (XTE) and ship control (speed, rudder angle, turn rate) measures were considered in the study.

Collision threat, target behaviour and traffic were used as variables for navigation scenario, which was conducted as 6 minutes and 18 times, in another study (Robert et al., 2003). CPA and TCPA, track keeping, rule following, course changes, target acquisitions, test manoeuvre, bearings taken and headings entered were considered for primary task performance parameters. For example, keeping the CPA value less than 0.5 nm (nautical miles) is collision while less than 0.8 nm is near miss and more than 1 nm is good performance. Authors also performed the secondary task measurement that is “to maintain engine oil temperature within tolerance limits” adding to primary task.

Similar to the study of Gould et al. (2009), visibility, traffic density, geography, equipmental condition and speed restriction were determined as difficulty variables in the study of Grabowski and Sanborn (2003). Less XTE, fewer manoeuvring order command, fewer communication and more CPA were evaluated as good performance parameters in the study. Similarly, XTE, mean speed, mean frequency of engine rudder and course orders, mean frequency of fixes and CPA were chosen as performance measures for the landfall approach in earlier study (Cook et al., 1981).

Kim et al. (2010) evaluated the operators in 3 main parameters; collision avoidance ability, decision making time and degree of deviation. They performed the criteria according to only COLREG rules. Position fixing, control of ship speed and course, look out of other vessels, collision avoidance and radio communication (Embrey et al., 2006), determine position, COLREG compliance, detection range of targets, CPA, communication and attention, position report (Kircher and Lutzhoft, 2011) were evaluated in performance measurements conducted in the studies. Schuffel et al. (1989) used simpler method to assess workload of officers; XTE for primary task and continuous memory task for secondary task.

Generally, safety aspects of navigation and ship handling parameters have been used for performance measurement in maritime. Navigation scenarios have been varied being used different level of difficulties in mostly visibility, traffic density and geography parameters. However, there is no performance measurement method for cargo operation of chemical tankers. In this study, a comprehensive performance

measurement method will be tried to form with experts for chemical tanker cargo operations.

2.3.3 Task loading assessment

Task loading method has an engineering approach to workload assessment. This method aims to measure workload predicated on the estimation of task demands matched against the resources needed to meet the demands. There are two approaches for task loading methodology; time-based loading model and cognitive transaction model (Embrey et al., 2006).

Time-based evaluation assumes that workload is a function of the time required to perform the task. In this model, the number and durations of tasks to be carried out should be determined in specific time line. Secondly, the duration of watch or total work time of operator should be specified. So, workload can be calculated as ratio of total duration of task to the duration of watch. This method was first used for nuclear reprocessing facility and later refined to be used for measuring task demands in automated chemical process control room (Embrey et al., 2006).

Another task load method is Task Analysis Workload (TAWL). This method was developed within the context of military operations and it can be only used where time constraint is taken for being an important performance influencing factor (Embrey et al., 2006).

The third one is Operator Function Model (OFM) which is one of the cognitive task analysis methods. This method has been specifically used in maritime context to assess the workload deductions of ship-based automation systems. It is predicated on a state-transition type of task analysis. Information processing model which is similar to SA model in terms of information processing stages as perception, comprehension and projection, is used to drive the analysis (Embrey et al., 2006). Lee and Sanquist (2000) extended the model (which has known as OFM-COG) adding cognitive transactions that indicate cognitive load on operator and proposed 9 resource types associated with the cognitive transaction:

- Perceptual Sensitivity (Level 1)
- Perceptual Discrimination (Level 1)
- Working Memory (Level 1)

- Response Precision (Level 1)
- Selective Attention (Level 2)
- Sustained Attention (Level 2)
- Distributed Attention (Level 2)
- Long-term Memory (Level 3)
- Processing Strategy (Level 3)

The levels of resources state the information processing categories which are respectively information acquisition, handling and interpretation as well as in SA model (perception-comprehension-projection). Lee and Sanquist (2000) used Miller's terminology for cognitive task transaction and their information processing resources (Table 2.4) to describe the information transformations and control activities required for system operation. They adapted Miller's terminology for OFM-COG in maritime context. For OFM-COG analysis of track-keeping subfunction with ECDIS example, determining position is a "Identify/Acquisition" cognitive agent task. However, this process occurs automatically as Global Positioning System (GPS) data is input and the current position is output. Similarly, in "Code/Handling" stage, recording position occurs automatically as plotted on ECDIS. In "Test/Interpretation" stage, monitoring progress uses the perception and working memory of human information processing resources to detect deviation between actual and planned position (see for more explanations; (Lee and Sanquist, 2000)). Whereas frequency count of cognitive tasks in total for track-keeping with ECDIS is only one (that is "Test/Interpretation"), this is seven for track-keeping with charts and without GPS data.

OFM-COG can be adapted to cargo operations in similar way. For example, in tank topping operation, tank level monitoring is a "Input select/Acquisition" cognitive agent task to close required cargo valves ("Edit/Handling"), then being sure that cargo flow is stopped, is a "Test/Interpretation" cognitive agent task. In total, the frequency count of cognitive tasks for the exemplified operation is three.

Table 2.4 : Cognitive task transactions and the human information processing resources, adapted from (Lee and Sanquist, 2000).

Cognitive Agent Task	General Category of Information Processing	Human Information Processing Resources
1. <i>Input select.</i> Selecting what to pay attention to next.	Acquisition	Selective attention, Perceptual sensitivity
2. <i>Filter.</i> Straining out what does not matter.	Acquisition	Selective attention
3. <i>Detect.</i> Is something there?	Acquisition	Perceptual sensitivity, Distributed attention
4. <i>Search.</i> Looking for something	Acquisition	Sustained attention, Perceptual sensitivity
5. <i>Identify.</i> What is it and what is its name?	Acquisition/Interpret	Perceptual discrimination, Long-term memory, Working memory
6. <i>Message.</i> A collection of symbols sent as a meaningful statement.	Handling	Response precision
7. <i>Queue to channel.</i> Lining up to process in the future.	Handling	Working memory, Processing strategies
8. <i>Code.</i> Translating the same thing from one from to another.	Handling	Response precision, Working memory, Long-term memory
9. <i>Transmit.</i> Moving something from one place to another.	Handling	Response precision
10. <i>Store.</i> Keeping something intact for future use.	Handling	Working memory, Long-term memory
11. <i>Store in Buffer.</i> Holding something temporarily.	Handling	Working memory, Processing strategies
12. <i>Compute.</i> Figuring out a logical or mathematical answer to a defined problem.	Handling	Processing strategies, Working memory
13. <i>Edit.</i> Arranging or correcting things according to rules.	Handling	Long-term memory, Selective attention
14. <i>Display.</i> Showing something that makes sense.	Handling	Response precision
15. <i>Purge.</i> Getting rid of the irrelevant data.	Handling	Selective attention
16. <i>Reset.</i> Getting ready for some different action.	Handling	Selective attention, Response precision
17. <i>Count.</i> Keeping track of how many.	Handling/Interpretation	Sustained attention, Working memory
18. <i>Control.</i> Changing an action according to plan.	Handling/Interpretation	Response precision
19. <i>Decide/Select.</i> Choosing a response to fit the situation.	Interpret	Long-term memory, Processing strategy
20. <i>Plan.</i> Matching resources in time to expectations.	Interpret	Working memory, Processing strategy
21. <i>Test.</i> Is it what it should be?	Interpret	Perceptual sensitivity, Working memory, Long-term memory
22. <i>Interpret.</i> What does it mean?	Interpretation	Long-term memory, Sustained attention
23. <i>Categorize.</i> Defining and naming a group of things.	Interpretation	Long-term memory, Perceptual sensitivity
24. <i>Adapt/Learn.</i> Making and remembering new responses to a learned situation.	Interpretation	Long-term memory
25. <i>Goal image.</i> A picture of a task well done.	Interpretation	Long-term memory, Processing strategies

Briefly, time-based evaluations cannot consider the weight of information processing. For cognitive transaction models, TAD is more complex than OFM-COG because of

that expert judgment is needed for almost all stages. On the other hand, OFM-COG has been generally used in maritime context.

In this study, OFM-COG analysis is used for task loading assessment. The level of complexities or difficulties of tasks used in this thesis, were determined according to the model and quantified based on the frequency count of cognitive tasks in similar way stated in the study of Lee and Sanquist (2000).

2.3.4 Physiological measures

In human physiology, there are two anatomical distinct structure: central nervous system (CNS), which is composed of spinal cord and brain, and peripheral nervous system, which consists of the nerves and ganglion out of brain and spinal cord (Figure 2.14). Peripheral nervous system is divided to two nervous system as somatic, which is related to the voluntary muscles activation, and autonomic nervous system (ANS), which controls involuntary responses to regulate physiological functions. ANS is also divided into the sympathetic nervous system (SNS) and the parasympathetic nervous system (PNS). While PNS maintains bodily functions, SNS is active in emergency reactions (De Waard, 1996). SNS sends signals to the brain, which will command "fight or flight" in the face of emergency and stressful situations. By stimulating the hypothalamus, digestion stops, blood flows from the internal organs into the muscles and the heart rate increased. After the danger or emergency, PNS is activated and tries to return the body to its routine functioning. Breathing and heart rate become normal. PNS performs non-urgent recovery tasks such as the elimination of bodily wastes, providing the protective measures for the vision system (such as tears and pupil constriction) and the long-term preservation of body energy (Gerrig et al., 2010).

Most organs are dually innervated by both the parasympathetic and sympathetic nervous systems. SNS and PNS can be independently active, mutually active or coactive (De Waard, 1996).

MWL causes the changes in human performance and behaviour those are nearly related to the physiological and biochemical changes in the body which are based on humoral regulation, nervous regulation and autoregulation. Lean and Shan (2012) classified the measures according to their control and activation principles as;

- peripheral physiological,

- central physiological,
- biochemical.

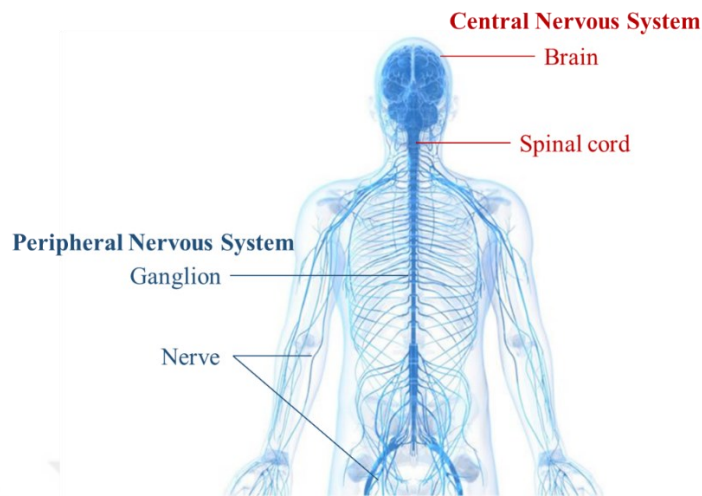


Figure 2.14 : Two anatomical distinct structure: Central Nervous System and Peripheral Nervous System.

While central physiological evaluations involve brain and eye activity measurements such as EEG (electroencephalography), and EOG (electrooculography) (De Waard, 1996; Lean and Shan, 2012), peripheral physiological evaluations involve following measures those reflect the activity of autonomic nervous system (Alberdi et al., 2016; De Waard, 1996; Embrey et al., 2006; Lean and Shan, 2012):

- ECG (electrocardiogram); involves the measures of HRV (heart rate variability), HR (heart rate)
- EDA (electrodermal activity) or GSR (galvanic skin response)
- Pupil diameter
- EEB (Endogenous eye blinks); involves eyeblink rate, blink duration and eye blink latency
- BVP (blood volume pulse) or PPG (photoplethysmography)
- Blood pressure
- Respiration
- Skin temperature
- EMG (electromyography)

Authors classified the measures as physical and physiological in the studies mainly related to stress measurements (Alberdi et al., 2016; Sharma and Gedeon, 2012). Physical reactions can be observed without any instruments, but advanced instruments have been used for data analysis. Adding to pupil diameter, blink rates, the following measures are classified as physical measures:

- Behaviour, gesture and interaction
- Facial features including facial expressions, eye gaze, voice

The last MWL evaluation is biochemical evaluation. Mostly, the following hormones have been used in workload studies (De Waard, 1996; Lean and Shan, 2012):

- Catecholamines (adrenaline, noradrenaline)
- Cortisol
- Immunoglobulin A

There are 4 dimensions that researchers should consider when using physiological metrics. These are the evaluations of invasive versus non-invasive, real-time versus delayed, natural context versus artificial lab and subjective versus objective. While subjective measurements can be easily collected, the scoring of the indexes by participants can not reflect the truth in reliance on retrospective memory. On the other hand, objective measurements reflect the real-time states of participants. However, arousal data may not express alone about the state of human, they should be combined with other measurements. For the dimension of real-time versus delayed, the measures such as EEG, pupil dilation are better for real-time assessment. However, EDA has more delayed response than EEG and pupil dilation. The place, where the measurement occurs, has an important role on the state assessment. While subjective measurements, facial recognition can be easily done in natural context, the physiological measurements need the laboratory conditions. However, advance in technology enables the physiological measurements execute easily in natural context by the aid of Bluetooth technology, ergonomic portable instruments. The last dimension is invasiveness. The brain imaging technics such as MEG (magnetoencephalography) and PET (brain positron emission tomography) need the laboratory environment and the participants cannot be relaxed during the

measurements. While pupil dilation, subjective assessment are non-invasive measures, facial recognition, EDA and EEG are close to invasive (Bergstrom et al., 2014).

To identify workload peaks, relatively short durations should be considered. While HRV is not suitable to detect workload peaks, event-related potentials (ERP) from EEG data are suitable. On the other hand, there is no certainty for sensitivity of performance and physiological measures to workload peaks (De Waard, 1996).

Briefly, as the advantage side of the physiological measurements, they do not require overt response. However, the disadvantage of those is needing specialized equipment (De Waard, 1996).

2.3.4.1 Cardiovascular activity

Cardiovascular system is essential for human body. It is composed of the heart and the vasculature. The heart supplies a consistent flow of oxygenated blood by sending it to the lungs and then to rest of the body (Berntson et al., 2007). The heart is clearly affected by autonomic nervous system (Alberdi et al., 2016). The cardiovascular system is under the control of both parasympathetic and sympathetic divisions of the ANS. Both parasympathetic and sympathetic neurons release acetylcholine onto nicotinic receptors (N_N) at the peripheral ganglia (Figure 2.15). Sympathetic neurons secrete norepinephrine onto beta 1 adrenergic (β_1) receptors while parasympathetic neurons secrete acetylcholine onto cholinergic (M) receptors. These processes vary in temporal dynamics according to related neurons. Parasympathetic system has a more rapid rise, a shorter latency of action and a higher frequency capacity. This is the base of selectivity of vagal control of heart which means high frequency heart rate variability (Berntson et al., 2007).

The electrocardiogram (ECG) is the recording the electrical activity generated by heart on the body surface (Alberdi et al., 2016). Cardiac cycle is an event from one beat to the next beat in the heart. Another recording method of heart activity, blood volume pulse (BVP) is the measure of the volume of blood passes over specific area (finger etc.). It can be detected with the aid of photoplethysmography (PPG) sensor (Sharma and Gedeon, 2012). Figure 2.16 presents the one beat of ECG and PPG signal. RRI and PPI represent the cardiac beat-to-beat interval.

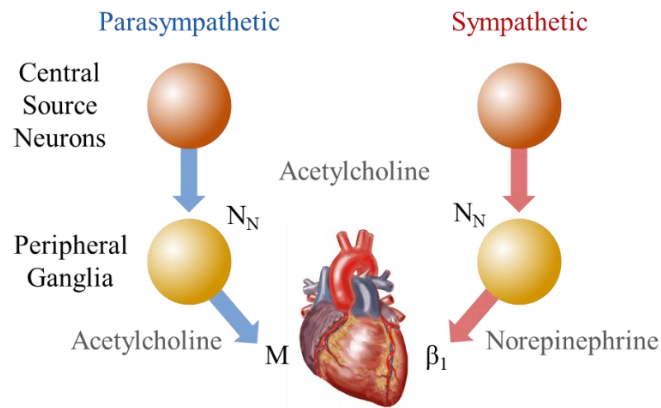


Figure 2.15 : General pattern of autonomic innervation, adapted from (Berntson et al., 2007).

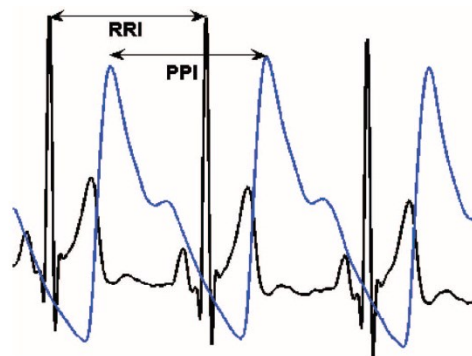


Figure 2.16 : Simultaneously recorded ECG (black coloured) and PPG (blue coloured) signal, adapted from (Berntson et al., 2007; Selvaraj et al., 2008).

Cardiovascular activity is more correlated with stress than EMG and respiration. However, the ECG and PPG data cannot be directly compared across multiple people. The measurements should be standardised with some baseline measurements (Sharma and Gedeon, 2012). According to Embrey et al. (2006), stressful events cause considerable variation in the cardiovascular reactions. The variation can be analysed with the comparison of shifting averages relative to prevalent bandwidth norms.

The heart period, which is the time between adjacent heart beats, and heart rate (HR) is a conversion of heart period as beats per minutes. However, heart rate and heart period are not linearly related to each other. Whereas heart period is sensitive to short-term cardiac responses, heart rate is sensitive to the effects of parasympathetic and sympathetic branches interactions (Berntson et al., 2007). Inter beat interval (IBI) which is extracted from RRI and PPI data from ECG and PPG signal respectively, is average time duration of heart beats within that time period and heart rate variability (HRV) is the variation in IBI or temporal variation between series of successive heart beats (Embrey et al., 2006). HRV is useful feature of cardiovascular activity and has

successful classification accuracies in MWL and stress levels (Alberdi et al., 2016). HR increases when task demand increases (Backs et al., 2000; De Rivecourt et al., 2008; De Waard, 1996; Embrey et al., 2006), in multi task conditions (Fournier et al., 1999), during additional memory load (Finsen et al., 2001), when requiring problem solving (Splawn and Miller, 2013) or stressful condition increases (Alberdi et al., 2016; Sharma and Gedeon, 2012), HR increases and HRV decreases (Alberdi et al., 2016; De Waard, 1996; Embrey et al., 2006; Sharma and Gedeon, 2012).

Additionally, there is no significant differences between ECG and PPG parameters which are detailed below, in HRV analysis. There is a high degree agreement between two measurement methods (Selvaraj et al., 2008). HRV metrics include the time-domain, frequency domain, time-frequency and non-linear analysis (Aimie-Salleh et al., 2019; Ramshur, 2010; Selvaraj et al., 2008).

In time domain analysis, NN (normal-to-normal, beat-to-beat) intervals have been analysed and the following features have been extracted (Alberdi et al., 2016; Shaffer and Ginsberg, 2017):

- Mean of heart rate
- Standard deviation of NN intervals (SDNN) (Equation 2.3)
- Root mean square successive difference (RMSSD) (Equation 2.4)
- NN intervals differing by more than 50 ms (NN50)
- Percentage of the number of successive NN intervals varying more than 50ms from the previous interval (pNN50)
- Standard deviation of the averages of NN interval in all 5-min segments (SDANN)
- HRV triangular index (HRVti) (Equation 2.5)
- Triangular interpolation of IBI interval histogram (TINN) (Equation 2.6)

$$SDNN = \sqrt{\frac{1}{N-1} \sum_{n=1}^N [NN_n - mean(NN)]^2} \quad (2.3)$$

$$RMSSD = \sqrt{\frac{1}{N-2} \sum_{n=3}^N [I(n) - I(n-1)]^2} \quad (2.4)$$

where N is total window length and NN is normal-to-normal time interval (Aimie-Salleh et al., 2019).

$$HRV_{ti} = \frac{N_{IBI}}{Y} \quad (2.5)$$

$$TINN = M - N \quad (2.6)$$

where N_{IBI} is the total number of IBI (NN) intervals, Y is the maximum value of density distribution of IBI, M and N values represent the minimum and maximum values of a triangle which is shaped on IBI histogram graphic, on the time axis (Ramshur, 2010).

Continuous feedback between peripheral autonomic receptors and the CNS leads to irregularities in HR. Decrease of HRV is more sensitive to increase in workload than increase of HR. Whereas HRV decreases and HR increases in physical load, HRV decreases and HR has no change in mental load (Brookings et al., 1996; De Waard, 1996). On the other hand, Lean and Shan (2012) stated that the increase of HR with the decrease of HRV is associated with an increase of difficulty of task demand.

Frequency domain methods decompound the variance of overall heart rate period into specific frequency bands. Quantifying the variance within the IBI series is done by calculating the power spectrum density (PSD). Estimation of PSD has been carried out using Fourier transform, autoregressive modelling etc. One of the methods is Welch periodogram that is based on discrete Fourier transform (Ramshur, 2010):

$$DFT_x(f) = \sum_{n=0}^{N-1} X(n)e^{-i2\pi fn} \quad (2.7)$$

The periodogram that is extension of DFT is calculated to estimate PSD of a time series as below:

$$P(f) = \frac{1}{N} \left| \sum_{n=0}^{N-1} X(n)e^{-i2\pi fk/L} \right|^2 \quad k = 0, 1, \dots, L-1. \quad (2.8)$$

Modified periodogram, which is incorporating a weighted windowing function, is calculated to reduce spectral leakage as stated below:

$$P_M(f) = \frac{1}{MU} \left| \sum_{n=0}^{N-1} X(n)w(n)e^{-i2\pi fn} \right|^2 \quad i = 0, 1, \dots, L-1. \quad (2.9)$$

where $U = 1/M \sum_{N=0}^{M-1} w^2(n)$. Finally, PSD by the Welch periodogram is calculated as stated below:

$$P_W(f) = \frac{1}{N} \sum_{i=0}^{N-1} P_{M,i}(f) \quad (2.10)$$

where $P_{M,i}(f)$ is the i^{th} modified periodogram of the data series (Ramshur, 2010).

Another method is Lomb-Scargle periodogram (LSP). LSP estimates the frequency spectrum by fitting the least squares of sinusoids to the data. Unlike Welch periodogram, LSP doesn't use the weighted windowing functions. The LSP for real-valued data sequence X of length N for random times t_n is calculated as stated below:

$$P_{LS}(f) \equiv \frac{1}{2\sigma^2} \left\{ \frac{[\sum_{n=1}^N (X(t_n) - \bar{x}) \cos(2\pi f(t_n - \tau))]^2}{\sum_{n=1}^N \cos^2(2\pi f(t_n - \tau))} + \frac{[\sum_{n=1}^N (X(t_n) - \bar{x}) \sin(2\pi f(t_n - \tau))]^2}{\sum_{n=1}^N \sin^2(2\pi f(t_n - \tau))} \right\}$$

where $\tau \equiv \tan^{-1} \left(\frac{\sum_{n=1}^N \sin(4\pi f t_n)}{\sum_{n=1}^N \cos(4\pi f t_n)} \right)$ (2.11)

where \bar{x} and σ^2 are the mean and variance of the time series (Ramshur, 2010). Figure 2.17 presents the above-mentioned frequency domain methods and a sample PSD-frequency graphic for resting and stress conditions.

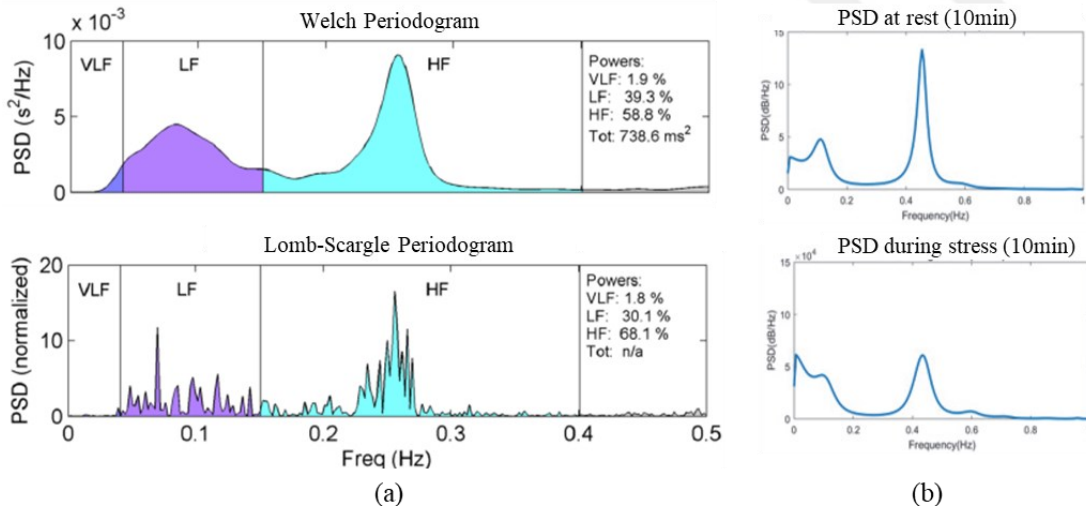


Figure 2.17 : Welch and Lomb-Scargle Periodograms, adapted from (Ramshur, 2010) (a) and samples of PSD generated from PPG-derived HRV for resting and stress conditions, adapted from (Aimie-Salleh et al., 2019) (b).

In frequency analysis, the following features with above-mentioned methods have been extracted in literature (Aimie-Salleh et al., 2019; Ramshur, 2010; Shaffer and Ginsberg, 2017):

- Absolute spectral powers of low, mid and high frequencies

- Percentage of frequency bands to the sum of the bands
- Normalized frequency bands to total power
- The ratio of low frequency to high frequency
- Peak frequencies in frequency bands

The frequency band is divided into three frequency band, these are low frequency (0.02-0.06 Hz) that is related to body temperature, mid frequency (0.07-0.14 Hz) that is related to short-term blood pressure, and last one, high frequency (0.15-0.50 Hz) that is related to respiratory and PNS influenced fluctuations. Decrease in mid and high frequencies is associated with an increase in mental effort and task demand (Veltman and Gaillard, 1998). Mid frequency is most sensitive in low workload areas (De Waard, 1996). While sympathetic control increases the low frequency (LF) being under the control of cardiac sympathetic nervous, parasympathetic control affects high frequency (HF) being associated with vagal components of ANS including respiratory and cardiac vagal nervous (Alberdi et al., 2016; Berntson et al., 2007; Lean and Shan, 2012). The increase of LF/HF by the increase of LF together with the decrease of HF is associated with MWL (Lean and Shan, 2012) and stress (Alberdi et al., 2016; Sharma and Gedeon, 2012). However, the decrease of LF in high task difficulty were stated by authors (Delaney and Brodie, 2000; Lehrer et al., 2010; Splawn and Miller, 2013).

Generally, the energy ratio of LF (0-0.08 Hz, 0.04-0.15Hz or 0.05-0.15 Hz) to HF (0.15-0.5 Hz or 0.16-0.4 HZ) (Sharma and Gedeon, 2012), the ratio of HF to all frequencies, total energy of the spectrum, energies of certain frequency bands (ULF, VLF, LF, HF) (Alberdi et al., 2016) have been used as features of ECG signal. Adding to above mentioned features, sum of LF power, sum of HF power, LF/HF, HF/AF, normalized mean, standard deviation, wavelet mean and wavelet standard deviation (Chen et al., 2017), total (LF+MF+HF), MF/HF, (LF+MF)/HF, (LF+MF) / total and median of HRV (Chueh et al., 2012) have been used for feature extraction.

Like frequency-domain analysis, time-frequency analysis is carried out with low, mid and high frequency bands and the features of those. Despite the methods used in frequency bands, windowed periodograms are used in time-frequency analysis. Moreover, continuous wavelet transform (CWT) (Equation 2.12 and 2.13) and discrete wavelet transform are used to analyse non-stationary signals in HRV analysis

(Ramshur, 2010). Figure 2.18 presents a sample time-frequency analysis for resting and stress conditions.

$$W(\tau, \alpha) = \frac{1}{\sqrt{\alpha}} \int_{-\infty}^{\infty} x(t) \Psi^* \left(\frac{t - \tau}{\alpha} \right) dt \quad (2.12)$$

where $\Psi^*(t)$ is the complex conjugate of the mother wavelet $\Psi(t)$, α is the dilation parameter, and τ is the location parameter. CWT coefficients equals the $W(\tau, \alpha)$ for given time τ . The instantaneous power of the frequency band $[f_1 f_2]$ can be calculated as stated below:

$$P_{CWT}(t) = \frac{1}{C_{\Psi}} \int_{\alpha_1}^{\alpha_2} |W(t, \alpha)|^2 \frac{d\alpha}{\alpha^2} = \frac{1}{C_{\Psi} f_{\Psi}} \int_{f_1}^{f_2} \left| W(t, \frac{f_{\Psi}}{f}) \right|^2 df \quad (2.13)$$

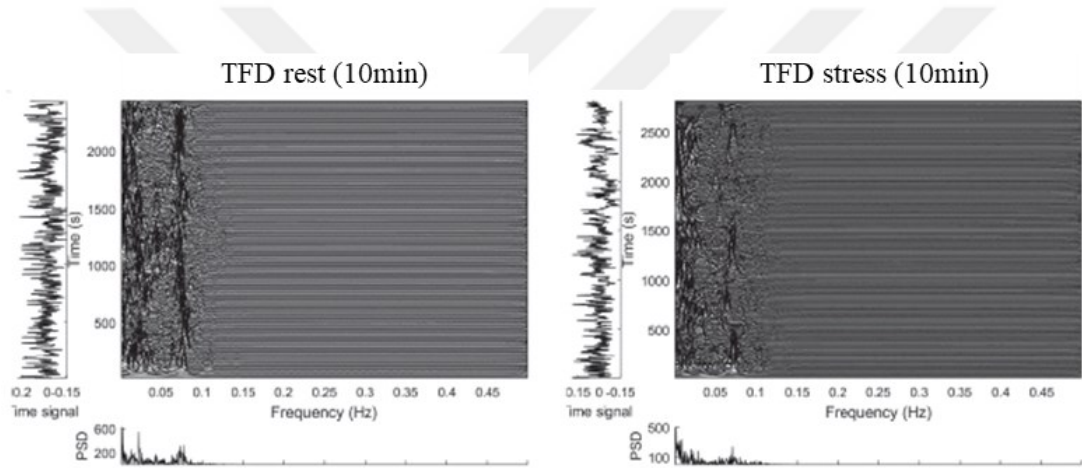


Figure 2.18 : Samples of TFD generated from PPG-derived HRV for resting and stress conditions, adapted from (Aimie-Salleh et al., 2019).

Spectral analysis of HRV has been used as an index of cognitive, MWL in literature. However, it can be influenced by speech (De Waard, 1996). In literature, the increase of HRV was stated in high complexity tasks for longer durations (Fairclough et al., 2005; Gao et al., 2013). Although, HRV is lacked sufficient sensitivity and diagnosticity according to Nickel and Nachreiner (2003), HRV in HF changes when difficulty changes (Brookings et al., 1996). Moreover, HRV in MF band has a significant change during tasks compared to baseline (Fallahi et al., 2016). However, this is more sensitive for the task from low to intermediate, not at high levels (De Rivecourt et al., 2008).

Besides, there are following non-linear features in literature (Aimie-Salleh et al., 2019; Alberdi et al., 2016; Ramshur, 2010; Shaffer and Ginsberg, 2017):

- Standard deviations in Poincare plot (Figure 2.19a)
- Sample entropy (Equation 2.14)
- Shannon entropy
- Complexity (C) that is randomness of NN intervals and tone (T) that is sympathovagal balance
- Alpha values of detrended fluctuation analysis (Equation 2.15 and Figure 2.19b)

$$SampEn(m,r,N) = -\ln[\phi^{m+1}(r)/\phi^m(r)] \quad (2.14)$$

where $\phi^m(r) = (N - m)^{-1} \sum_{i=1}^{N-m} C_i^m$, $C_i^m = n_i^m / (N - m)$, N is the sample value of the IBI signal, m and $m+1$ represent the length of vectors/sequences taken from IBI signal.

$$F(n) = \sqrt{\frac{1}{N} \left(\sum_{k=1}^N [y(k) - y_n(k)]^2 \right)} \quad (2.15)$$

where $y(k) = \sum_{i=1}^k [IBI(i) - \overline{IBI}]$ and is the k th value of the integrated series, $IBI(i)$ is the i th interbeat interval, \overline{IBI} is the average interbeat interval for the entire time series, $y_n(k)$ represents the value of separated segment of length n (Ramshur, 2010).

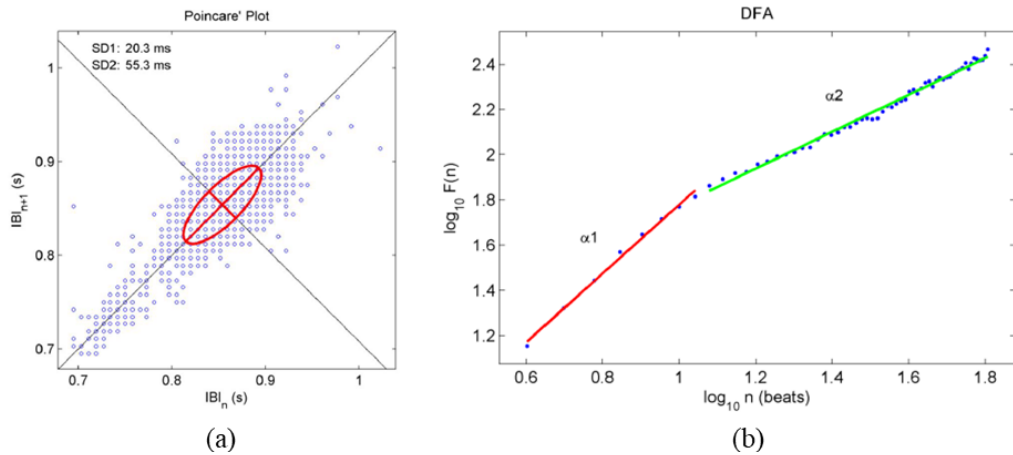


Figure 2.19 : Poincare Plot (a) and detrended fluctuation analysis (b) of IBI data, adapted from (Ramshur, 2010).

From other recording methods of cardiovascular activity, blood pressure (BP) is the pressure of the blood against the inner walls of the veins. BP increases with stress (Sharma and Gedeon, 2012) but is not a good indicator as well as HRV. BP is regulated peripherally and is affected by local functions in working muscles. Therefore, it may

camouflage the changes of MWL. Systolic blood pressure (SBP), diastolic blood pressure (DBP), mean and standard deviation are mostly used features (Alberdi et al., 2016).

2.3.4.2 Electrodermal activity

Electrodermal activity (EDA) or skin conductance response (SCR) or galvanic skin response (GSR) reflects the change in the electrical properties of the skin under increased cognitive workload or physical activity, arousal, emotion (Alberdi et al., 2016). Besides, it reflects changes in the level of activation generated during on attention (Lajante et al., 2012). EDA occurs at the process from attention, emotion, information processing to normal-abnormal behaviours (Dawson et al., 2007). Electrodermal activity is a reliable indicator of stress. Additionally, EDA has strong correlation with cognitive load and working performance (Sharma and Gedeon, 2012). Basically, EDA reflects the fight or flight response (Bergstrom et al., 2014). In contrast to heart rate, electrodermal activity is controlled by only sympathetic nervous system (Kettunen et al., 1998). Therefore, it is mostly sensitive to stress, excitement, engagement, frustration and anger (Bergstrom et al., 2014) and EDA is a good physiological indicator of arousal related stress-strain process (Embrey et al., 2006). EDA and HRV are the best correlates of real time stress (Alberdi et al., 2016) and the synchronization of EDA and HRV is associated with verbal activity, variability of arousal ratings and prevailing activation mood, so this synchronization is mainly associated with arousal (Kettunen et al., 1998). For MWL measurement, EDA is sensitive to sudden stimulus and the duration of the response increases in stressful conditions (Collet et al., 2014). Additionally, EDA increases when task difficulty increases (Miyake et al., 2009).

Eccrine and apocrine sweat glands are the forms of sweat glands in the human body. Eccrine sweat glands are active for thermoregulation. However, eccrine sweat glands located on palmar and plantar surfaces are responsive to psychologically significant stimuli than thermal stimuli. There are three independent pathways those lead to production of EDA (presented in Figure 2.20). The first one is the influences from limbic system and hypothalamus. Second one involves contralateral cortical and basal ganglion influences. One of the pathways is excitatory control by the premotor cortex and other one involves both excitatory and inhibitory influences originated in the

frontal cortex. Third one is the activation of reticular formation in the brain stem. Briefly, there are evidence that central control of EDA is associated with attention and emotional process (Dawson et al., 2007).

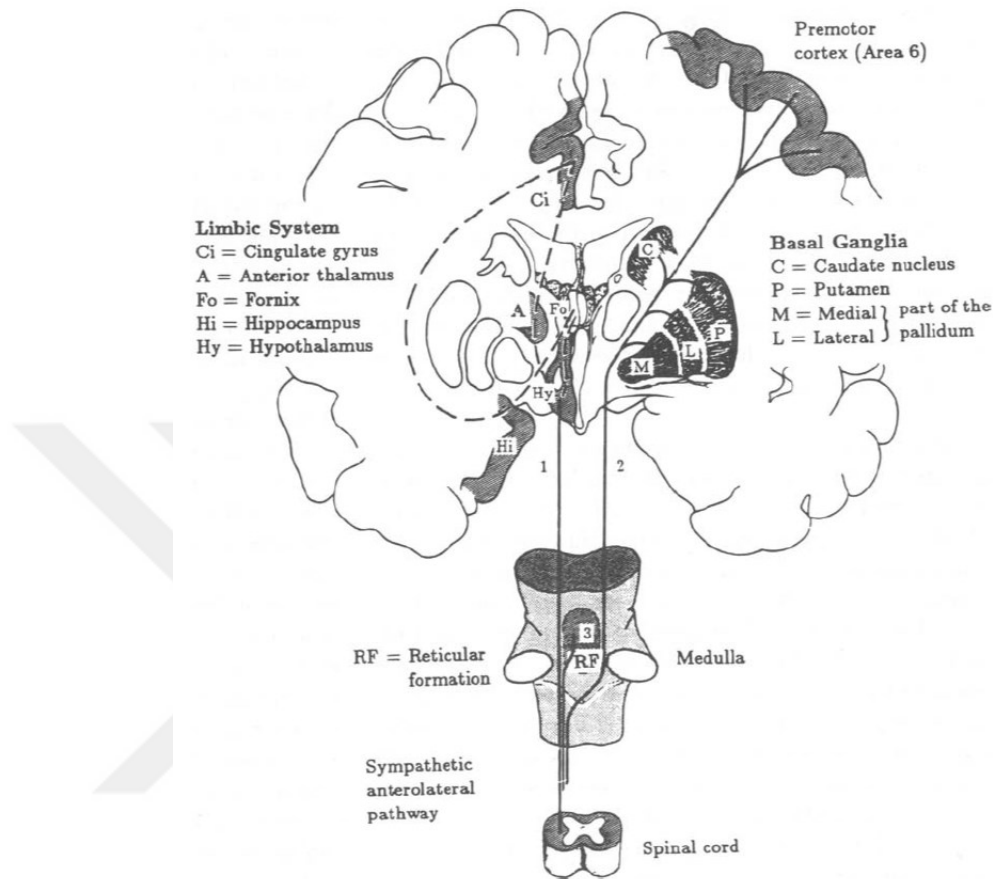


Figure 2.20 : CNS determiners of EDA, adapted from (Dawson et al., 2007).

Electrodermal recordings are generally taken from locations on the palms of the hands. There are many possible placements (presented in Figure 2.21) those are medial (#1) and distal (#2) phalanges of the fingers and thenar and hypothenar (#3) eminences. The greatest level of the reactivity was found at the distal site where a large number of active sweat glands are located. Before measurement, hands should be washed with nonabrasive soap and skin should be kept clean and dry. Ambient temperature should be the room temperature, 23°C in order to prevent undesirable increase in sweating due to high ambient temperature (Dawson et al., 2007).

EDA is composed of tonic, which is slow, and phasic activity which is rapid secretions in response to a discrete stimulus (Bergstrom et al., 2014). Skin conductance level (SCL) that is tonic activity, occurs at 2-20 μS , has 1-3 μS changes in SCL in a specific

time (Dawson et al., 2007; Lajante et al., 2012) and skin conductance response that is phasic activity, generates 0.1-1.0 μS changes in amplitude (Dawson et al., 2007).

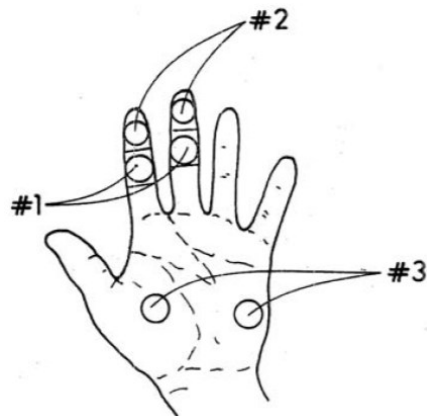


Figure 2.21 : Electrode placements for EDA recording, adapted from (Dawson et al., 2007).

Defining the SCR in a raw EDA data is little complicated. Normally, minimum values between .01 and .05 μS increases in 5s or fewer duration have been used to define SCR (Blain et al., 2010). But there are nonspecific or spontaneous (NS-SCRs) and specific SCRs those should be differentiated correctly. NS-SCRs occur in the rate between 1 and 3 per minute while the person is at rest. Latency window (presented in Figure 2.22) is also defined for SCRs and should be in the interval between 1-3 s or 1-4 s. SCR rise time is generally 1-3 s, SCR half recovery time is generally 2-10 s (Dawson et al., 2007). Rise time should be less than recovery time to define a SCR (Bergstrom et al., 2014). Figure 2.23 presents the raw EDA signals at the rest state and active state. Red circles on the rest trail graphic means the NS-SCRs and the red circles on the active trail graphic means the specific SCRs.

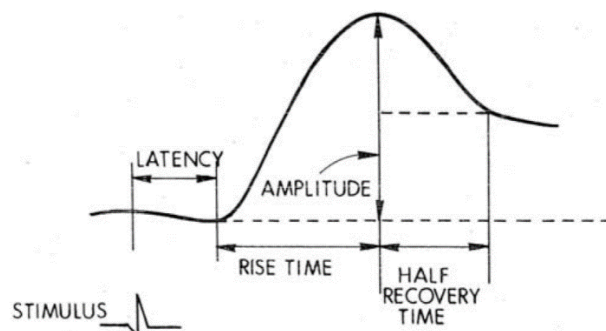


Figure 2.22 : Graphical representation of EDA components, adapted from (Dawson et al., 2007).

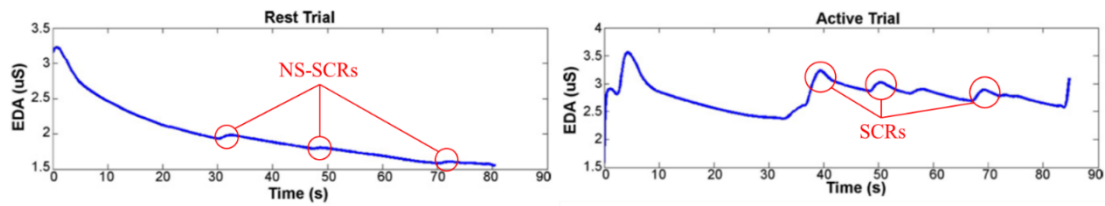


Figure 2.23 : Sample EDA raw signal from rest and active trials, adapted from (Blain et al., 2010).

EDA raw data requires minimal calculations such as mean and sum. On the other hand, complex measures are known that are more successive than mean and sum (Sharma and Gedeon, 2012). Generally, mean EDA value, the range and the number of SCRs have been used for feature extraction of EDA signal. However, first difference of EDA signal and the centroid of the EDA first difference histogram by using derivative of EDA signal were found more successive to detect emotional state of the person (Blain et al., 2010). Additionally, the following features have been used in literature (Alberdi et al., 2016):

- Mean amplitude and standard deviation of mean amplitude
- Minimum and maximum values
- Root mean square (RMS)
- Rising time (tRise)
- Difference between first value and the maximum (DiffMax) and difference between first value and the minimum (DiffMin)
- Position of maximum (MaxPos) and position of minimum (MinPos)
- Zero crossings (ZC)
- Number of peaks
- Peak height
- Half recovery time (tRecovery)
- The sum of magnitudes, the sum of response duration and the sum of estimated areas under the response (areaResp)
- Kurtosis, skewness and smoothed first derivate average (Diffavg)

- SCR amplitude (Aq), duration (Dq) and the average area under the rising half of SCRs (areaRise)

The other features are generated from the superposition (namely SC) of SCL and SCR. One of them is overall level of SC. However, this method ignores the EDA signal property as the components of tonic and phasic activity. The other one is mean change score of SC (Lajante et al., 2012). To prevent skewness and leptokurtosis of EDA magnitude and amplitude (for SCL or SCR), logarithmic transformation is often used (Dawson et al., 2007).

To assess SCRs, there are some extraction methods in literature. One of them is standard min-max or trough-to-peak analysis. Extraction is carried out according to values from local minimum to local maximum. However, there are common errors on quantification of SCR amplitude such as underestimation of amplitude and misattribution with respect to response window (Benedek and Kaernbach, 2010). The more reliable method, continuous decomposition analysis (CDA) reflects the SCL and SCR. The integral of the area under of SCR, the ISCR generates more reliable measure stimulus-related phasic activity (Lajante et al., 2012).

To extract phasic sympathetic activity of the EDA signal decomposition of skin conductance (SC) data is performed (Figure 2.24). This process is based on standard deconvolution algorithm performed on SC data with impulse response function (IRF) (temporal vicinity of the SCR peak) which is based on Bateman function (Equation 2.17):

$$SC = (\text{Driver}_{\text{tonic}} + \text{Driver}_{\text{phasic}}) * \text{IRF} \quad (2.16)$$

$$\text{IRF} = C. \left(e^{-\frac{t}{\tau_1}} - e^{-\frac{t}{\tau_2}} \right) \quad (2.17)$$

where τ_1 and τ_2 are 0.75 and 2 for standard IRF. To estimate phasic activity, tonic activity should be estimated. Although the tonic activity is observed in the absence of phasic activity, SCRs can overlap the tonic activity. Therefore, driver is smoothed by convolution with a gauss window ($\sigma=200\text{ms}$) and peak detection is performed with a difference of $\delta \geq 0.2 \mu\text{S}$ between local minimum and local maximum. The areas which are not detected SCRs are considered non-overlapped tonic driver. Then, interpolation is carried out with 10s-time grids to estimate tonic driver for total time range. Phasic driver can be found in equation 2.16 after that tonic driver is found. The process is performed with pre-defined parameters of IRF. However, optimization of τ values

should be carried out on Bateman function to increase goodness of the model. Finally, tonic and phasic activity of EDA are reconstructed (Benedek and Kaernbach, 2010).

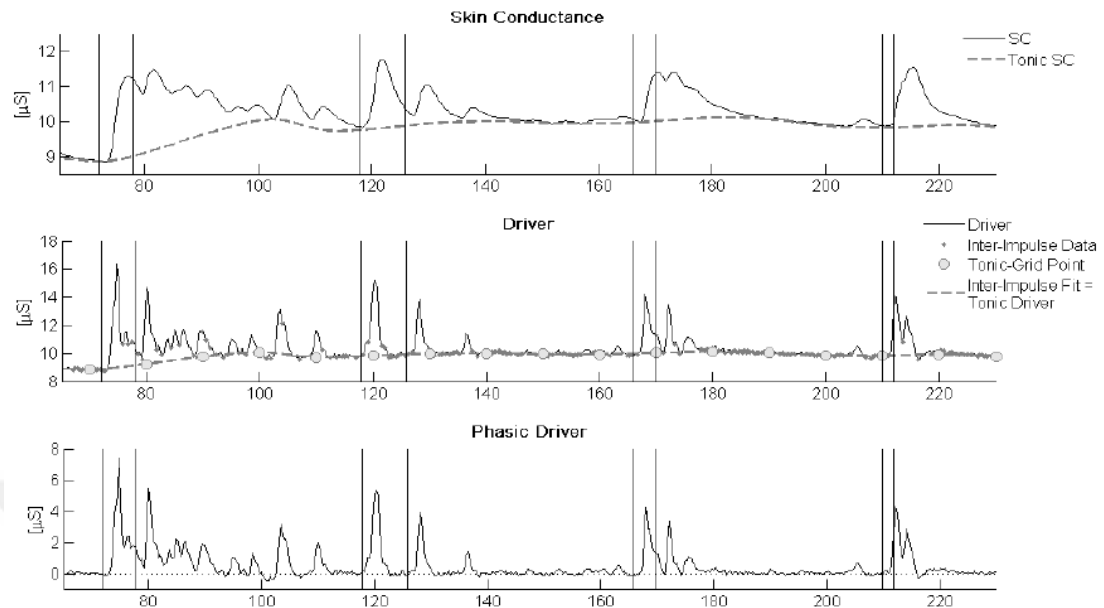


Figure 2.24 : Phasic driver extraction with continuous decomposition analysis, adapted from (Benedek and Kaernbach, 2010).

Although electrodermal activity is a sensitive index of MWL according to Lean and Shan (2012), it is global sensitive and not very selective (De Waard, 1996). It should be noted that EDA shows the intensity of arousal but not the valence (Bergstrom et al., 2014).

Peak rise time (t_{Rise}) and the peak amplitude (A_q) have been mostly used for stress and emotion detection researches in literature (Healey and Picard, 2005; Katsis et al., 2008; Parnandi et al., 2013; Singh et al., 2013). Moreover, sum of the peak number, sum of the startle magnitude, sum of the rising duration and sum of the rising area (Chen et al., 2017), mean amplitude of SCR, rate of SCR, mean abs first difference and mean rise duration of SCR (Katsis et al., 2008) were used in the studies. EDA and HRV were most closely correlated with driver stress in respect of the theory stated in Kettunen et al. (1998).

2.3.4.3 Ocular activity

Ocular activity can be recorded with the aid of developed eye movement recording techniques. One of them is electrooculogram (EOG). Eye is an electrical dipole. The axis of this dipole and the optical axis of the eye are nearly collinear. The retina is more negative than the cornea. The difference, roughly 6mV results from the electrical

activity of photoreceptors and the neurons in the retina. This way allows the EOG measurement on the skin. Adding to EOG, infrared reflection devices (IRD), scleral search coil and video-oculography (VOG) are the other eye movement recording techniques (Eggert, 2007).

The features of ocular activity are based on the following functions of eye and basic dimensions of eye used in video recording techniques presented in Figure 2.25:

- Eye gaze
- Pupil diameter
- Eye blink

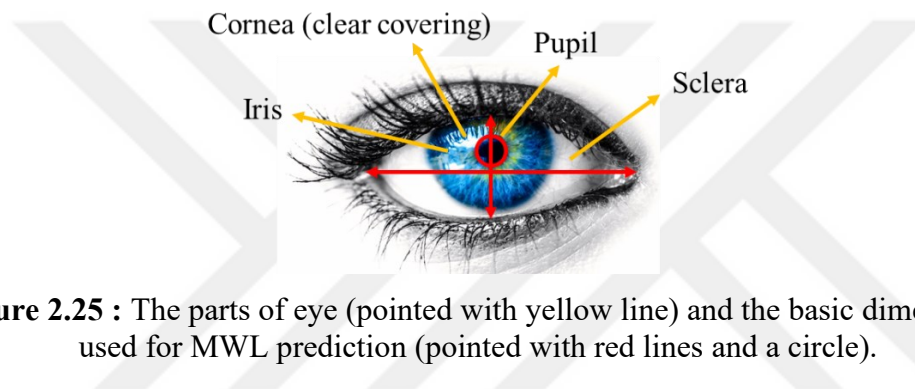


Figure 2.25 : The parts of eye (pointed with yellow line) and the basic dimensions used for MWL prediction (pointed with red lines and a circle).

Eye gaze spatial distribution is positively correlated with stress levels. Human eye focuses more under stressful conditions (Alberdi et al., 2016; Sharma and Gedeon, 2012). Dwell time and fixation duration also increases when workload increases (Lean and Shan, 2012). On the other hand, peak velocity of saccadic eye movement is decreased, duration of saccades is increased when mental work load increases (Di Stasi et al., 2012). However, it is differed depend on task characteristics, they were observed as decreased when task demand increased in flight task (De Rivecourt et al., 2008). Commonly used eye gaze features are stated below (Alberdi et al., 2016; Sharma and Gedeon, 2012):

- Gaze spatial distribution (GazeDis)
- Percentage of saccadic eye movement (PerSac)

Additionally, mean, standard deviation of fixation duration, the number of forward and backward tracking fixations, the distance an eye covered and proportion of the time eye fixated on different regions of the computer screen have been used for eye gaze feature (Alberdi et al., 2016).

Pupil diameter and endogenous eye blinks are related to workload. Pupil dilation occurs when task demand increases (Causse et al., 2010), but gives insufficient data to state the magnitude of arousal (Embrey et al., 2006), moreover it cannot give any sign whether the arousal is negative or positive (Bergstrom et al., 2014; Sharma and Gedeon, 2012). So, it is not diagnostic (De Waard, 1996). Pupil dilation is an autonomic sympathetic nervous system response that covers attention, interest or emotion (Bergstrom et al., 2014). On the contrary, pupil constriction occurs as a result of parasympathetic-innervated muscles (De Waard, 1996). Pupil diameter change is also correlated highly with error rate (Gao et al., 2013). The following pupil features have been used in literature (Alberdi et al., 2016; Sharma and Gedeon, 2012):

- Mean of pupil diameter, max-min values, standard deviation
- Percentage of large pupil dilation (PerLPD)
- Pupil ratio variation (PRV)

Endogenous eye blinks can be measured by corneal-reflection techniques, EOG or video scanning. Those consist of three parameters; eye blink rate, blink duration and eye blink latency (speed of response of the blink following presentation of stimuli). Eye blink rate decreases when continued monitoring is required (Brookings et al., 1996; Ryu and Myung, 2005; Sirevaag et al., 1993; Veltman and Gaillard, 1996; Wilson, 2002) while closure duration and eye blink latency decrease with increased task demand (De Waard, 1996; Embrey et al., 2006). In high MWL, eye blink interval is longest and blink duration is shortest (Borghini et al., 2014; Hwang et al., 2008; Lean and Shan, 2012; Veltman and Gaillard, 1996). Moreover, blink frequency increases under stressful conditions, higher stress causes faster eye closure (Alberdi et al., 2016; Sharma and Gedeon, 2012). In a study, the increase of mental fatigue and MWL caused the decrease of blink rate (Liu et al., 2016). Sharma and Gedeon (2012) stated that the opposite results about the blink frequency exist in literature. According to Holland and Tarlow (1972) blink rate increases in incorrect responses rather than correct responses.

Ocular activity is more sensitive to visual demands not auditory or cognitive. The selectivity of eye blinks to workload is low just as pupil diameter (De Waard, 1996). Mostly used features for eye blink are stated below (Alberdi et al., 2016):

- Blink rate (frequency)

- Average eye closure speed (AECS)
- Percentage of eye closure (PERCLOS)

2.3.4.4 Other central, peripheral and biochemical activities

The brain which is located in the head, is the centre of the nervous. There are different imaging techniques for brain activities. These are hemodynamic (fMRI), metabolic (PET) and electromagnetic (EEG, MEG). While real-time data can be collected via EEG, this is hard to say for fMRI (Pizzagalli, 2007). EEG has high temporal resolution, needs lower intrusive equipment and lower costs. EEG signals can be collected during synaptic excitations and inhibitions of dendrites (Sharma and Gedeon, 2012). Excitatory and inhibitory post-synaptic potentials in cortical pyramidal neurons are assumed to generate scalp-recorded EEG oscillations. Tens of thousands of pyramidal cortical neurons should be activated synchronously to generate an EEG oscillation. An excitatory post-synaptic potential (EPSP) is generated at the cell soma; (see Figure 2.26) local excitation (+ and -) leads to a tangential current flow. Extracellular currents (dashed lines) are produced by the post-synaptic potentials at cortical pyramidal cells and they are perpendicular to the cortical surface. This way produces a positive field potential at the cortical surface (Pizzagalli, 2007).

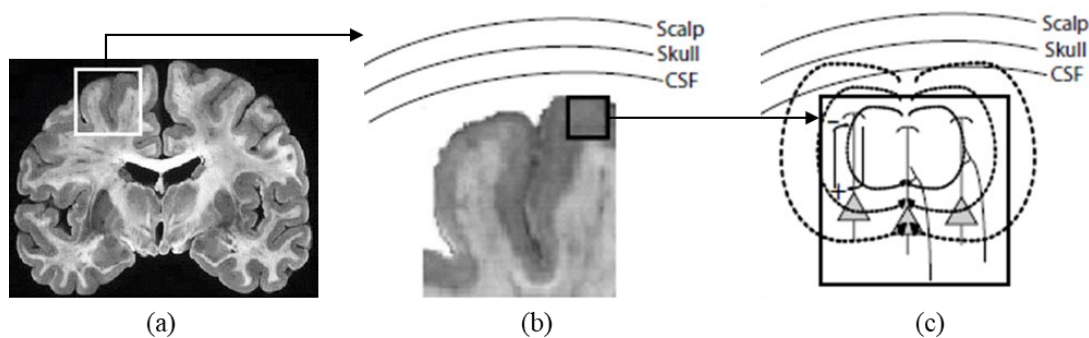


Figure 2.26 : Neurophysiological basis of EEG generation. A coronal slice of brain (a), an expanded view of cerebral gyri and sulci in relations to the scalp, skull, and cerebral spinal fluid (CSF) (b), a schematic illustration of cortical pyramidal cells within the cortical mantle (c), adapted from (Pizzagalli, 2007).

In the EEG studies, waveforms are characterized by frequency, amplitude, shape and sites of the scalp (Sharma and Gedeon, 2012). In many studies, normative EEG activities have been stated with frequencies and the sites of the brain related to state of the human.

Delta wave (1-4 Hz) appears in sleep, deep sleep conditions and there is inverse relation between delta and glucose metabolism. Delta activity is mainly an inhibitory rhythm (De Waard, 1996; Posner et al., 2007; Sharma and Gedeon, 2012). Theta wave (4-8 Hz) appears in two types of wakefulness conditions adding to sleep conditions. Decreased alertness (drowsiness) (De Waard, 1996; Posner et al., 2007; Sharma and Gedeon, 2012) and impaired information processing in widespread scalp distribution reveal theta activity. Other type is frontal midline theta activity which is related to mental effort, focused attention and effective stimulus processing, those are correlated glucose metabolism. Theta activity also appears in oscillation transmissions between different limbic structures. Theta activity may serve a gating function on the information processing flow in limbic regions (Posner et al., 2007). Alpha wave (8-13 Hz) appears mainly in relaxed and wakefulness conditions (Alberdi et al., 2016; De Waard, 1996; Posner et al., 2007; Sharma and Gedeon, 2012). Its greatest amplitudes appear over posterior and parietal regions during resting period eye-closed. Alpha activity diminishes by eye-opening because of mental concentration and sudden alerting (Posner et al., 2007). While alpha activity decreases, beta activity increases in these cognitive and emotional process (Alberdi et al., 2016) or in the stressful conditions (Sharma and Gedeon, 2012). Beta wave (13-30 Hz) replaces alpha rhythm during cognitive activity with symmetrical fronto-central distribution and increases with attention and vigilance (Posner et al., 2007) or anxiety (Sharma and Gedeon, 2012). In the stressful conditions high beta power seem at the anterior temporal sites (Alberdi et al., 2016). Gamma (36-44 Hz) activity is associated with object recognition, arousal, attention, top-down modulation of sensory process and other cognitive functions. In sleep-wake cycle, systematic decrease in gamma occurs. While highest gamma activity states the wakefulness, intermediate gamma activity states REM stage and lowest gamma activity states the slow-wave sleep. Gamma activity is a direct indicator of activation by means of glucose metabolism (Posner et al., 2007).

In the sense of MWL, theta activity on central, parietal, frontal and temporal sites of the brain is sensitive to difficulty levels of MWL. Theta activity increases at those sites when difficulty increases. In low workload conditions alpha activity increases. Beta 1 activity appears on F7 and T4 in overload condition, on T6 in high workload condition. Beta 1 and delta increase on Fz, F3, Pz, F7 and T4 in low-medium workload conditions. Delta is lower in high workload conditions (Lean and Shan, 2012). In dual

tasks, theta increases, alpha decreases (De Waard, 1996). Alpha event-related desynchronization and theta event-related synchronization with task demand is relevant to attentional resource allocation and sensory-motor processing. However, this is not sensitive to multiple task workload, is sensitive to single-task workload. Beta/alpha, beta/(alpha+theta), left temporal alpha/central alpha and left occipital alpha/right occipital alpha have been used for mental task engagement, and beta/(alpha+theta) gave the best accuracy in a study stated in (Lean and Shan, 2012). P300 (one of the event related potentials) and wavelet transform of theta+alpha+beta (Sharma and Gedeon, 2012) have been used for MWL evaluation. Theta activity on FC3, FC4 and C4 increases during mental arithmetic tasks. In dynamical perspective, nonlinear indices of EEG signals such as correlation dimension, Lyapunov exponent and approximate entropy reflect the cognitive and mental activation of cerebral cortical networks. Relative wavelet pocket energy in alpha on P3, P4, Pz, O1, O2 and Oz decreases while beta increases. It should be noted that changes in brain activity occurred earlier than autonomic nervous system (Lean and Shan, 2012).

In mostly driver and pilot MWL / stress detection studies there are similar results of frequency meanings. When task demands increase, theta increases on frontal (especially for time pressure tasks) and central scalp (Borghini et al., 2014). Increase in theta with decrease in alpha was found to be associated with the increase of the accuracy of the performance (Borghini et al., 2014). When working memory load increases, alpha decreases on parietal sites (Fournier et al., 1999; Ryu and Myung, 2005). In monotonous driving tasks, increase in delta, theta and alpha on occipital areas was observed. Alpha increases in resting state. While focusing and in time pressure, theta increases on frontal and central scalp areas. Increased MWL causes mental fatigue and alpha and delta increases and beta decreases at this stage. According to Myrden and Chau (2017), the frontal and central electrodes are important for fatigue detection, posterior alpha band and frontal beta band activity for frustration detection and posterior alpha band activity for attention detection.

It can be seen that EEG activity cannot be easily analysed and needs more trials of the features of frequencies and scalp areas. It has been stated that no consensus has been reached related to best algorithms and features for detection (Borghini et al., 2014). On the other hand, specific low amplitude potentials may point out task demands. Disruption of the rhythmic pattern that can be attributed to the brain's reaction to an

external event (Embrey et al., 2006), the event-related potentials (ERP) are suitable to detect workload peaks (De Waard, 1996). One of the ERP features, P3 (P300), is sensitive to perceptual / central processing load (De Waard, 1996; Embrey et al., 2006), but not affected by response / motor system (Embrey et al., 2006). Therefore, it has high diagnosticity to cognitive processing. P300 amplitude increases in response to unexpected task-relevant stimuli and task complexity. First or second negative waves of N1 and N2 and second or third positive waves of P2 and P3 (P300) are related to cognitive activities. Mismatch negativity (MMN) measures the function of central auditory processing, allocation of attention and level of workload (Lean and Shan, 2012). Poor signal to noise ratio and individual variability are the disadvantages of this feature. Briefly, ERP figures out the dynamic changes in MWL (De Waard, 1996).

Skin temperature is another physiological measurement. Skin temperature varies in different conditions such as fever, physical exertion, malnutrition and physiological changes. Localized changes in blood flow caused by arterial blood pressure or vascular resistance, has an effect on the change of skin temperature and this mechanism is influenced by autonomic nervous system (Alberdi et al., 2016). Sharma and Gedeon (2012) stated that skin temperature is negatively correlated with stress. However, there are coincident and opposite findings in literature; finger temperature increases in stressful conditions. Facial features such as nose and forehead are the effective indicators of stress and fatigue. Skin temperature difference between nose and forehead is a sensitive index of MWL (Lean and Shan, 2012). Whereas nasal skin temperature decreases during negative emotions, facial temperature increases with stress. Minimum, maximum and standard deviation are the mostly used features of skin temperature (Alberdi et al., 2016).

Electromyogram (EMG) is the electrical activity of the muscles. Stress causes to involuntary reaction on trapezius (Sharma and Gedeon, 2012) and facial muscles. Tonic activity of facial muscles is related to mental effort. In detail, lateral frontalis muscle responses to mental effort and corrugator supercilia muscle responses to emotional changes (De Waard, 1996). While EMG amplitudes increases, number of gaps decreases (Alberdi et al., 2016).

Stress and fatigue cause the change of speed and depth of respiration. It can be measured by pneumotachograph. However, this method is intrusive and respiration is not a good indicator as well as EDA and HRV (Alberdi et al., 2016; Sharma and

Gedeon, 2012). Cognitive effort has a small but significant increase in energy expenditure of respiration. Respiration rate increases when memory load or temporal demands increases and in stressful conditions. Ventilation per minute that is respiration rate times tidal volume, increases with mental effort while respiration rate increases and tidal volume decreases. It is also found that respiration rate decreased when cognitive activity increased. Respiration is also affected by speech and physical effort (De Waard, 1996). In a study conducted during landing operation, spectral energies of respiration in the mid and high band were largest and high workload caused slow respiratory (Lean and Shan, 2012).

Facial expression has been also analysed for fatigue and stress detection by using visual techniques together with head movements. Eye brow activity, mouth activity and smile intensity are the features of facial expression (Alberdi et al., 2016). The increase of head and mouth movements indicates the increase of stress (Sharma and Gedeon, 2012).

Voice is another stress indicator. Change in pitch (fundamental frequency) and in speaking rate, the spectral and energy variations of the glottal pulse are the common detection points (Alberdi et al., 2016). The increase of stress causes the increase in range and rapid fluctuations in pitch, the increase in energy for high frequency voice components and greater proportions of high frequency components (Sharma and Gedeon, 2012).

Stress has an effect on the endocrine and immune system allowing to release adrenaline hormone from adrenal cortex and cortisol hormone from adrenal medulla (Alberdi et al., 2016) by SNS stimulation (De Waard, 1996). Catecholamines those are adrenal cortical steroid cortisol, noradrenaline (NA) and adrenaline (A) are the mostly analysed hormones in fatigue and stress studies. The hormones are measured from urine, blood and saliva samples (Alberdi et al., 2016; De Waard, 1996; Lean and Shan, 2012). Cortisol levels increase with stress (Alberdi et al., 2016). In mental load, adrenaline increases, noradrenaline and dopamine hormones are constant (Lean and Shan, 2012). A and NA increase in effortful coping, while those together with cortisol increase in effortful distress. Whereas NA responses mostly to physical effort, A responses to mental effort. It is stated that when the ratio of NA to A is greater than or equal to 5 it means physical effort, when the ratio of NA to A is between 2 and 3 it means mental effort. However, NA increases with emotional stress, cortisol increases

with low control tasks and A and NA increase with high control tasks (De Waard, 1996). Briefly, the analysis of hormone levels does not involve the continuous monitoring. Therefore, event-related detection cannot be done effectively. This method is intrusive, costly and slow (Alberdi et al., 2016; De Waard, 1996).

2.3.4.5 The choice of physiological measures for the study

Charles and Nixon (2019) evaluated the measures which are electro cardiac, respiration, skin, blood pressure, eye response and brain activity measures, according to their specifications and limitations and stated following findings:

- The measures exclude eye response, some electro cardiac activities, skin measures and brain activity are affected by respiration, speech, training and experience. However, skin measure and blood pressure are sensitive to time of day and affected by ambient temperature or humidity and participant age or gender.
- Only eye response and respiration are sensitive to errors or poor performance.
- Electro cardiac activity and respiration differentiates MWL between higher or lower task load. But most of them is sensitive to changes in MWL from increasing task demand.
- Eye response has higher predictivity of MWL for visual task demands.
- All measures exclude brain activity is appropriate for shorter task duration (<5 min.).
- Eye response, skin measures, electro cardiac activity in time domain and respiration are sensitive to a sudden stimulus.

According to capabilities of the measures stated in this chapter and above-mentioned findings, eye response, electro cardiac and skin measures were selected for MWL measurement in this study. Moreover, the time of day, the level of training and experience and participant age or gender were confined with the measurement time and sample group of subjects.

2.3.5 Classification and decision-making techniques

Before classifying the collected data, some issues should be taken into consideration. Data collection and the quality of the data are the essential parameters for

classification. Data must be relevant, complete, accurate, appropriately represented, sufficiently detailed, timely, and must retain sufficient contextual information to support decision making. Sensor placement, sampling frequency of the data are the other issues. Nyquist sampling frequency has been implemented to data collection process. According to the approach, sampling frequency should be greater than or equal to two times maximum frequency. Another issue is noise. In order to eliminate instrumental noise, some filters have been used such as Butterworth low-pass filter, wavelet decomposition, Kalman filters, wiener filters and median filters. For artefact removal, regression analysis, least mean squares, independent component analysis (ICA) and principal component analysis (PCA) have been used (Alberdi et al., 2016).

When multimodal data is used for classification, some problems such as lack of data and having different dimensions, can affect the classification accuracy. It is better to process separately the data and merge in the final decision step in such cases. Moreover, synchronization is essential issue for multimodal data. Another problem is big data in the aspect of storage. Dimension reduction, feature extraction, segmentation windows (use of sliding window techniques is recommended) and feature selection have been used to eliminate the problems (Alberdi et al., 2016). Figure 2.27 presents the general illustration of pattern recognition including the processes such as dimension reduction, feature extraction.

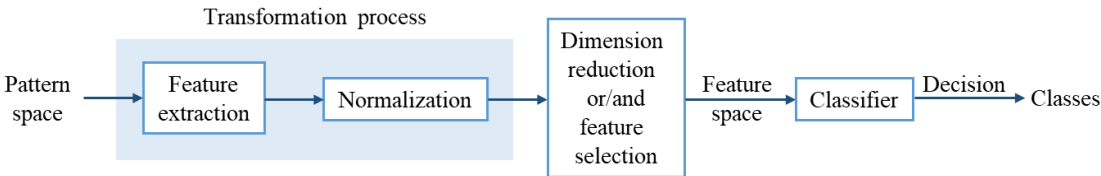


Figure 2.27 : Decision making blocks for pattern recognition.

In previous section, normalization and feature extraction methods for EEG, EDA, ECG and ocular activity signals have been stated. Next processes are dimension reduction and feature selection (Figure 2.27). Generally, the method of feature extraction is determined according to discernment of researcher. However, some elements of feature space may not have significant information. Irrelevant features may cause the classifier structure to overgrow. Therefore, dimension reduction or/and feature selection methods have been used to select significant features for classification. Divergence analysis, which is the ratio of between-class scatter matrix to within-class

scatter matrix, has been mostly used for feature selection (Devijver and Kittler, 1982). Following equations are used for divergence calculations:

$$W_i^j = \sum_t (\beta_i^{tj} - \mu_i^j) \cdot (\beta_i^{tj} - \mu_i^j)^T; j = 1, 2, \dots, K; i = 1, 2, \dots, n \quad (2.18)$$

$$\mu_i = \sum_{k=1}^K \mu_i^k \quad (2.19)$$

$$W_i = \sum_{k=1}^K W_i^k \quad (2.20)$$

$$B_i = \sum_{k=1}^K (\mu_i - \mu_i^k) \cdot (\mu_i - \mu_i^k)^T \quad (2.21)$$

$$D_i = \text{tr}((W_i)^{-1} B_i) \quad (2.22)$$

where β_i^{tj} is i-dimensional t-th feature vector of the j-th class, μ_i^j is the mean value of the i-dimensional feature vectors of the j-th class, W_i^j is within-class scatter matrix of the j-th class, B_i is between-class scatter matrix, K is number of classes, D_i is the divergence value at the i-th dimension, $\text{tr}(\cdot)$ is trace operation applied to the matrix obtained after the division. Low divergence values mean that the vectors are scattered in feature space while high divergence values mean that the vectors are clustered in feature space (Figure 2.28). Therefore, the features, which give high divergence values, should be selected in order to improve classification accuracy.

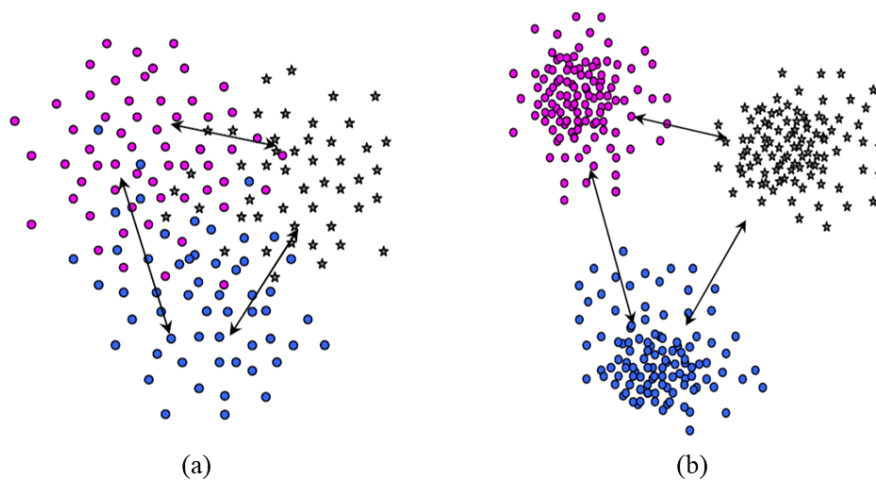


Figure 2.28 : The distribution of vectors with low divergence value (a) and high divergence value (b).

Generally, divergence value increases when the dimension of vector increases. On the other hand, 2-dimension has the opportunity for comparing the classifiers in visual. It can be seen in Figure 2.28, there are 2 dimensions and 3 classes as an example of distribution of classes.

Next step in decision-making blocks (Figure 2.27) is classification. Mostly used classifiers are stated below:

- Decision functions
- Bayesian decision theory
- K-nearest neighbour (KNN)
- Artificial neural networks (ANN)
- Support vector machines (SVM)
- Logistic regression
- Markov chains and hidden Markov models
- Fuzzy techniques

Classifiers make a decision about cluster membership of the feature vectors. The functions are defined for representing the cluster borders. Most known decision function is stated below (Duda et al., 2012):

$$d(x) = w_0 + w_1.x_1 + w_2.x_2 + \dots + w_n.x_n \quad (2.23)$$

where x is the accessing vector and $d(x)$ defines a hyper-plane in n-dimension space. Hyper-plane divides the feature space two patches. The x vector has a negative or positive value according to $d(x)$ function based on the distance of the vector to plane.

Following equation presents the rule of function:

$$f(d(x)) = \begin{cases} +1 & d(x) \geq 0 \\ -1 & \text{otherwise} \end{cases} \quad (2.24)$$

Figure 2.29 is an example for a decision function as 2-dimension with 2 classes. It can be seen that when the x vector has positive value, the vector is the member of C_1 according to $d(x)$ function. However, one straight line is not often adequate to determine the borders of clusters. In this case, more than one decision function may be used for determining the borders.

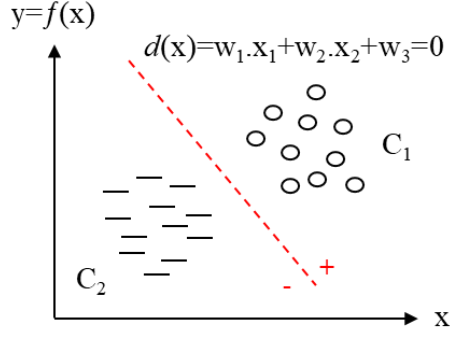


Figure 2.29 : Basic decision function for 2 classes distribution.

Other classifier is Bayesian decision theory and can be used only when distribution is statistically significant. As a priori information, $P(w_i)$ is the probabilities for classes, $p(\underline{\beta}|w_i)$ is the conditional probability density and $\underline{\beta}$ is the feature vector. By this way, the conditional probability, $P(w_i|\underline{\beta})$, the element is in class i is defined as below (Duda et al., 2012):

$$P(w_i|\underline{\beta}) = \frac{p(\underline{\beta}|w_i) \cdot P(w_i)}{p(\underline{\beta})} \quad (2.25)$$

For 2 classes, the penalty is defined as being an action of i -th class while being a member of class j . Therefore, the penalty is defined as following equation:

$$\Lambda(\alpha_i|\underline{\beta}) = \Lambda_{ij} \text{ (penalty)} \quad (2.26)$$

By the meaning of the equation, $\Lambda_{ii} = 0$ and $\Lambda_{jj} = 0$. Expected error or conditional risk function can be defined as the following equation as a result of the occurrence of the α_i action:

$$R(\alpha_i|\underline{\beta}) = \sum_{j=1}^M \Lambda_{ij} \cdot P(w_j|\underline{\beta}); \quad i=1, 2, \dots, M \quad (2.27)$$

Then, discriminant function $d_i(\underline{\beta})$ is defined in consideration of that the risk function is smallest:

$$d_i(\underline{\beta}) = -R(\alpha_i|\underline{\beta}) \quad (2.28)$$

As shown in Figure 2.30, class decision for i -th class is given with maximum $d_i(\underline{\beta})$. At last, discriminant function takes its final shape with mahalanobis distance equation:

$$d_i(\underline{\beta}) = \frac{1}{\sigma^2} \cdot \mu_i^T \cdot \underline{\beta} - \frac{\mu_i \cdot \mu_i^T}{2\sigma^2} + \ln P(w_i) \quad (2.29)$$

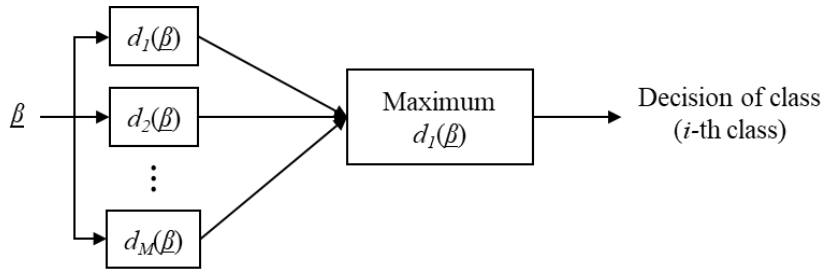


Figure 2.30 : The classification of discriminant functions.

KNN is another classifier which uses mostly the Euclidean distance. Assessing vector is labelled according to the class labels of K number neighbours in terms of Euclidean distance. There is a problem in conditions that feature vectors are not clustered. There is no priori information. Firstly, K number nearest neighbour is found for assessing vector. Then, the class labels are analysed and the label of majority is decided as class label. The distance of assessing vector to feature vectors of K number neighbours is not considered. Determining the number of neighbours is essential for classification accuracy (Duda et al., 2012). Figure 2.31 presents an example for different classification results according to the number of neighbours.

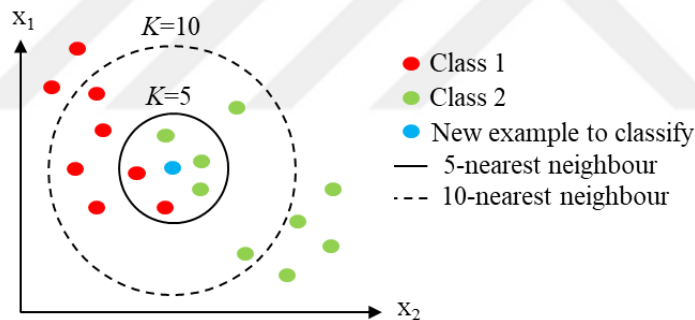


Figure 2.31 : The effect of neighbourhood to KNN classification.

As can be seen in Figure 2.31, when K is determined as 5, new example is classified in class 2. However, when K is determined as 10, it is classified in class 1.

ANN has been often used for classification in literature. This classifier has lots of advantages such as feedforward and backpropagation options, high process speed, generalization ability. The classifier has a structure like a neuron which consists of similar input and output structure (Fausett, 1994; Polikar, 2006). Figure 2.32 represents the general structure of ANN (perceptron) with the following mathematical statement of perceptron:

$$\begin{aligned}
 net &= \sum_{i=0}^d w_{ji} \cdot x_i = \mathbf{x}^T \cdot \mathbf{w} + w_0 \\
 y &= f(net)
 \end{aligned}
 \tag{2.30}$$

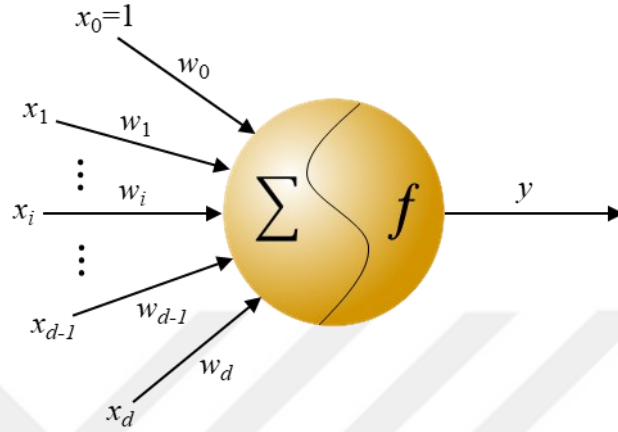


Figure 2.32 : The structure of perceptron, adapted from (Polikar, 2006).

While first part of equation 2.30 represents the linear weighted sum function consisting of assessing vector (x_i), and associated weight (w_i), second part of this equation represents the non-linear activation function of which output is represented by binary codes (Polikar, 2006):

$$f(net) = \begin{cases} 1, & \text{if } net \geq 0 \\ 0, & \text{otherwise} \end{cases}
 \tag{2.31}$$

The process of perceptron training includes the modifying the weights and finding the best w_i . In literature, there are several training algorithms to form the relationship of input and output. These algorithms have been categorized based on their learning methods; supervised and unsupervised. Multi-layer perceptron (MLP), grow and learn (GAL) restricted coulomb energy (RCE) are the supervised neural networks. Kohonen self-organizing map (SOM) is one of the unsupervised neural networks. Each neural network consists of the nodes, input layer, hidden layers and output layer. The number of hidden layers and nodes vary to the structure of the problem (Fausett, 1994).

Sharma and Gedeon (2012) stated that small number of hidden layers may not classify the complex patterns. On the other hand, large number of layers can cause over-parameterization. Apart from above-mentioned classifiers, support vector machines (SVM) have been used for classifying linear and non-linear primary measures and used to model emotions based on mostly EEG data. Katsis et al. (2008) reported that SVM

had accuracy of 79,3% within the emotion categories which were high stress, low stress, disappointment and euphoria for drivers. In another study, support vector data description and support vector clustering techniques have been used to classify 3 MWL classes which are low, normal and high with EEG data (Yin and Zhang, 2014). Besides, Markov chains and hidden Markov models that is time-domain process and has prior information from previous cases, have been used to recognize and predict behavioural changes. Another classification technique, Fuzzy has been used to model workload with heart rate signals (Sharma and Gedeon, 2012).

There are some problems in classification the workload or emotions such as analysing the data within task or different tasks. Baldwin and Penaranda (2012) stated that the classification accuracy of the comparison of 2 distinct levels of task difficulty within task was higher than that is conducted for different (cross) tasks. The other issue is individual differences. In the study which is conducted for emotional recognition with ECG, EDA and skin temperature data, the problem, individual differences, was eliminated by using multivariate ANOVA (MANOVA) before classification. The feature vectors were seen to be well-clustered (Chueh et al., 2012).

Table 2.5 presents the classification accuracies stated in sample studies conducted for mostly drivers with the signals used for measurement and classification techniques. It can be seen that the measurements were conducted with 24 subjects in most. This table consists of classified stress, mental workload and emotion targets. ANN and SVM were the best classifiers and their accuracy rates varied between 70% and 99%.

Table 2.5 : The classification accuracies stated in the studies in literature.

Authors	Target	Classes	Subj.	Elicitation	Signals	Classifiers	Accuracy
Wilson and Russell (2003)	Mental workload	4	7	Air traffic control tasks	EEG, EOG	ANN and SWDA	ANN: 98%
Healey and Picard (2005)	Stress	3	24	Real-time driving	ECG, EDA, EMG and respiration	Linear discriminant function	Accuracy: 97%
Hwang et al. (2008)	Mental workload	2	13	Simulated nuclear power plant tasks	Eye response, HRV, blood pressure	Group method of data handling	Validity of proposed model: $R^2=0.84$
Katsis et al. (2008)	Emotion	4	10	Car driving simulation	ECG, EDA, EMG and respiration	Adaptive neuro-fuzzy inference system (ANFIS) and SVM	ANFIS: 76.7% SVM: 79.3%
Baldwin and Penaranda (2012)	Mental workload	2	15	Working memory task	EEG, EOG	ANN	Within task: 87,1% Cross task: 44,8%
Chueh et al. (2012)	Emotion	3	10	Laboratory	ECG, skin temperature, EDA	Bayesian network learning, naive Bayesian classification, SVM, decision tree of C4.5, Logistic model and KNN	Logistic model: 74,76% SVM: 70,48%
Singh et al. (2013)	Stress	3	19	Real-time driving	HRV from PPG signals and EDA	ANN	Predictive ability: 89.23%
Yin and Zhang (2014)	Mental workload	3	6	Simulated spacecraft tasks	EEG	Support vector clustering (SVC) and Support vector data description (SVDD)	SVC-SVDD: 79,54%
Guo et al. (2016)	Mental Fatigue	2	20	Car driving simulation	EEG, ECG and reaction time	SVM	EEG: 86%
Chen et al. (2017)	Stress	3	14	Real-time driving	ECG, EDA and respiration	SVM, ELM	99% at per-drive level and 89% in cross-drive validation
Han et al. (2020)	Mental states	4	8	Flight simulation	EEG and PPMs (ECG, Respiration, EDA)	Multimodal deep learning (MDL)	EEG: 77,7% PPMs: 72,5% EEG & PPMs: 85,2%



3. METHODOLOGY

The study is based on the measurement in real-like environment and the analysis of the data to classify the physiological responses of the operators that can produce an output for state of officer on duty as “Safe” or “Risky” in mental workload prediction. The research model of the thesis is presented in Figure 3.1. According to the model, first attempt was to create navigation and cargo operation scenarios. In measurement process, triangulated measurement strategy (Wierwille and Eggemeier, 1993) with task loading assessment was applied to the thesis. In computerized process, transformation and classification techniques for measured data were applied.

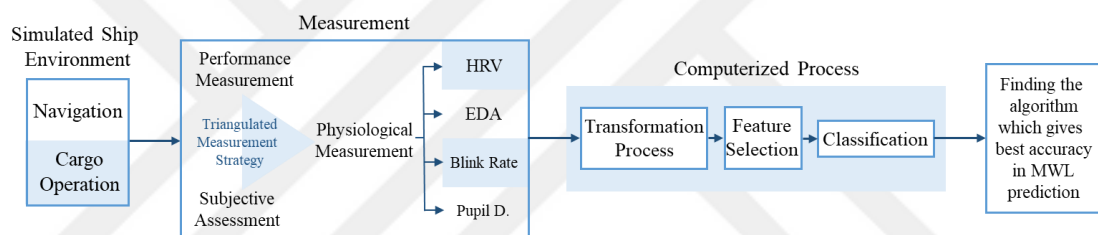


Figure 3.1 : Research model of the thesis.

Therefore, the chapter of methodology involves the following sub-chapters:

- Sampling strategy and subjects
- Mental workload prediction system layout
- Simulated ship environment
- Measurement details
- Analysis of data and computerized process

3.1 Sampling Strategy and Subjects

The sample group consists of junior deck officers who were randomly selected. 17 subjects (6 female) were recruited to study (12 subjects performed navigation scenario, 5 subjects performed cargo operation scenario). At least, subjects must have had an Oceangoing Watchkeeping Officer certificate and one contract sea experience as

officer in merchant ships. The mean age was 28.41 ($SD = 5.02$) and the mean period of service of subjects was 13.12 months ($SD = 9.12$). All subjects gave informed consent form (Appendix A) to be participant before performing the tasks in simulator. This study was approved by Medical and Engineering Sciences Human Research Ethics Committee of Istanbul Technical University.

3.2 Mental Workload Prediction System Layout

Mental workload prediction system, presented in Figure 3.2, has the main components which are named as “Cognition Model”, “Task Loading Model” and an oriented component which is named as “Officer Performance Model”. The most representative members of the system are listed in Table 3.1. Cognitive states of officers correspond to a set of the physiological variables of the officers, which is described as:

$$\psi'_{j,t} = f(\varphi_{i,t}) \quad (3.1)$$

Task loading model were formed according to Officer Function Model (OFM-COG) which is detailed in chapter 3.3.1.1. and 3.3.2.1. According to the model, the output ψ''_j was calculated from the complexity weights of the inputs σ_k .

These changes of cognitive states and performance scores were analysed in tasks which have high task load level. The importance weights of the performance parameters, which are specified in chapter 3.4.1.1. and 3.4.1.2., were determined by experts with fuzzy logic for each step of the scenarios, and the performance scores of the subjects were equal to the weighted sum of these parameters:

$$P_T = \sum_{\alpha=1}^p w_{\alpha} \cdot \gamma_{\alpha} + \sum_{\nu=1}^q w_{\nu} \cdot \eta_{\nu} \quad (3.2)$$

where w_{α} represents the weights of safety critical tasks and w_{ν} represents the weights of operational tasks. In addition, subjective workload assessments were compared with the cognitive status of the officer. It was assumed that the subject was familiar with the parameters for the performance evaluation of the specified tasks and tried to perform these tasks during the scenarios. The areas on the simulator screen tracked by the officer were monitored by Eye Tracker device for this assumption.

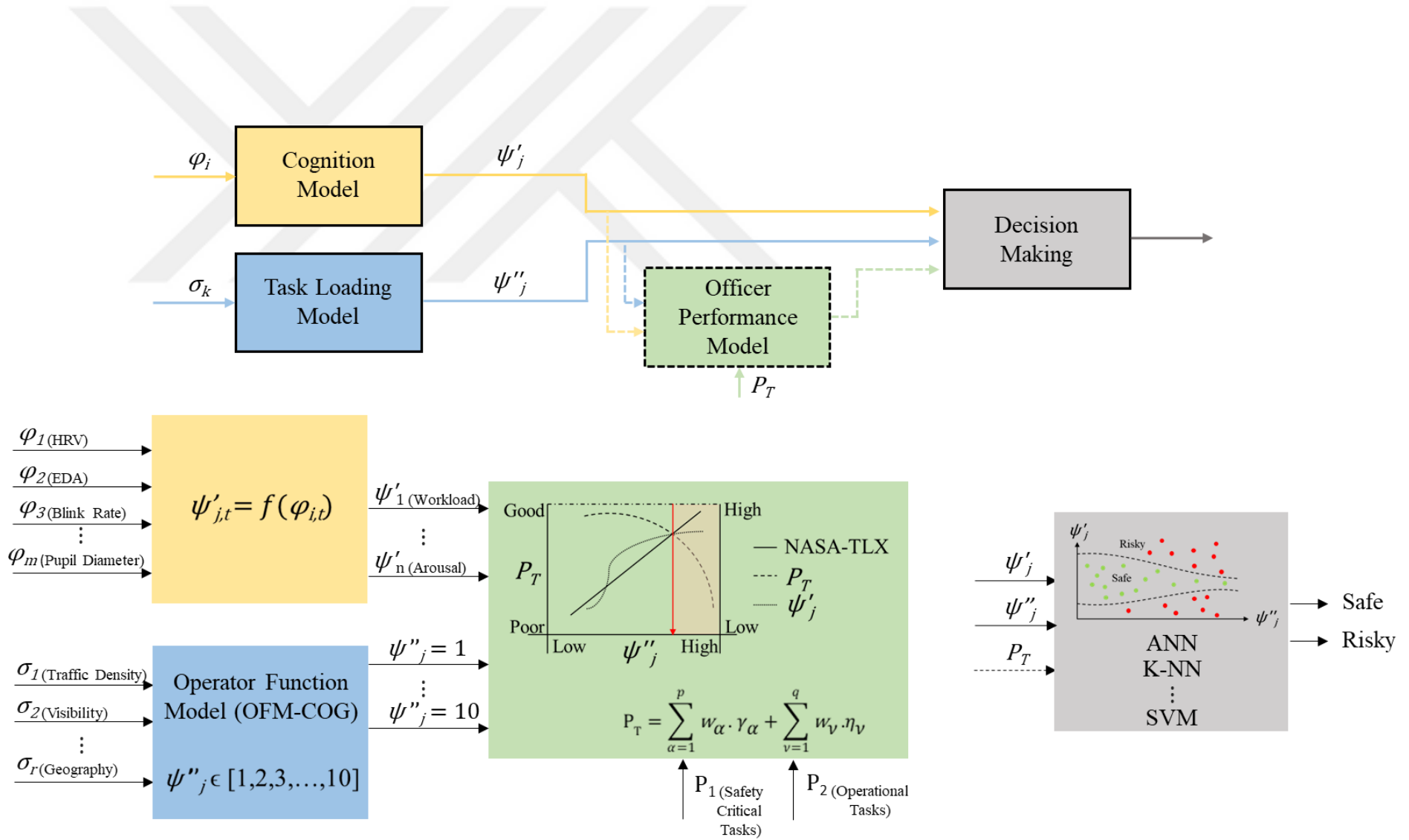


Figure 3.2 : Mental workload prediction system layout.

During the “Decision Making” process (specified in chapter 3.5.3), cognitive states ψ'_j were classified in 2 groups which are “Safe” and “Risky” represented the distinction of task loads ψ''_j as low task load and high task load respectively in training data set. In test data set, ψ'_j was tried to classified with high accuracy as “Safe” and “Risky” according to distinction of task load level ψ''_j (Figure 3.2).

Table 3.1 : Classification of variables.

Name	Symbol	Variables
Physiological measurables	$\varphi_i i \in [1, m]$	Heart rate variability (HRV) Electrodermal activity (EDA) Blink rate, pupil diameter
Task load parameters	$\sigma_k k \in [1, r]$	Traffic density, visibility and geography for navigation Type and number of operation and operation period for cargo operation
Safety critical task scores	$\gamma_\alpha \alpha \in [1, p]$	Scores for navigation Scores for cargo operation
Trackkeeping / operational task scores	$\eta_v v \in [1, q]$	Scores for navigation Scores for cargo operation
Cognitive indicators	$\psi'_j j \in [1, n]$	Workload, arousal
Task load indicators	$\psi''_j j \in [1, \dots, 10]$	Task difficulty numbered as 1, 2, ..., 10

3.3 Simulated Ship Environment

The study was conducted in bridge simulator and Liquefied Cargo Handling Simulator of Piri Reis University with navigation tasks based on Malacca Strait passage and cargo operation tasks based on different types of chemicals.

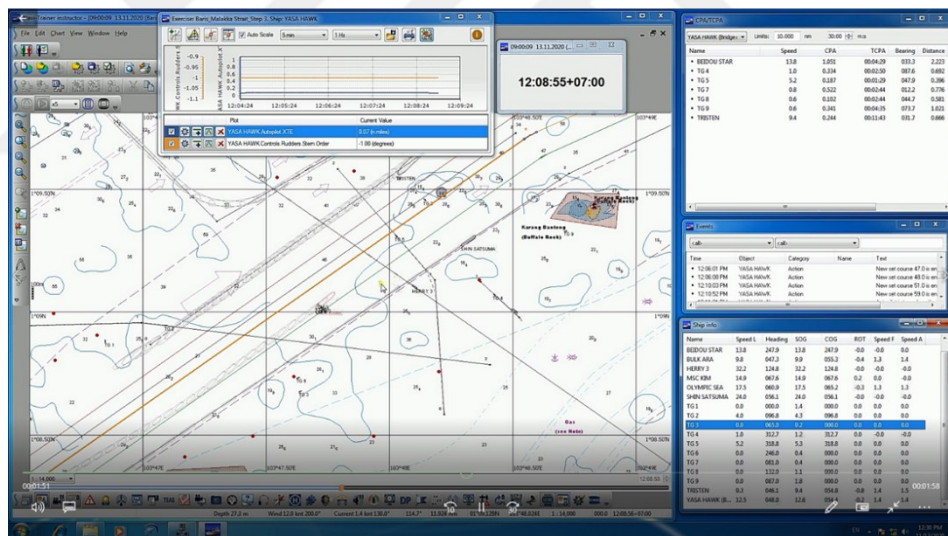
Subjects performed the navigation tasks in bridge simulator (Figure 3.3a). The ship which was used for trials is a chemical tanker which has 183.0m length over all, 32.2m breadth with 60976.0t displacement and 13.0m maximum draft. The simulator has three screens which are ECDIS, RADAR and Conning Display that contains visual settings and auto pilot panel adding to one engine telegraph, one steering wheel. Navigational data was sampled at 1 Hz (TRANSAS, 2014). Additionally, the whole performance of subject as tracks on charts and other variables were recorded as video format from the computer located in control room (Figure 3.3b).

Subjects performed the cargo operation tasks in Liquefied Cargo Handling Simulator (Figure 3.4a). The ship was used for trials is IMO type-1 chemical tanker (its length overall is 161.12m. and its displacement is 28921 tonnes) with 28 cargo tanks. The simulator has the functions which are remote controlling of valves and pumps,

performing on deck and inside tank jobs, monitoring the ship's stress and stability conditions (TRANSAS, 2012). The whole performances of subjects were recorded as video format from the computer located in trainer's desk (Figure 3.4b).



(a)



(b)

Figure 3.3 : Bridge simulator (a), recording the subject performance (b).

3.3.1 Navigation tasks

In chapter 2.3.2, it is stated that navigation scenarios have been varied being used different level of difficulties in mostly visibility, traffic density and geography parameters (Gould et al., 2009; Grabowski and Sanborn, 2003). In this study, the difficulty level of navigation scenario was gradually adjusted (in order to prevent acquired skill) according to traffic density, visibility and geography by combining in 4 steps as:

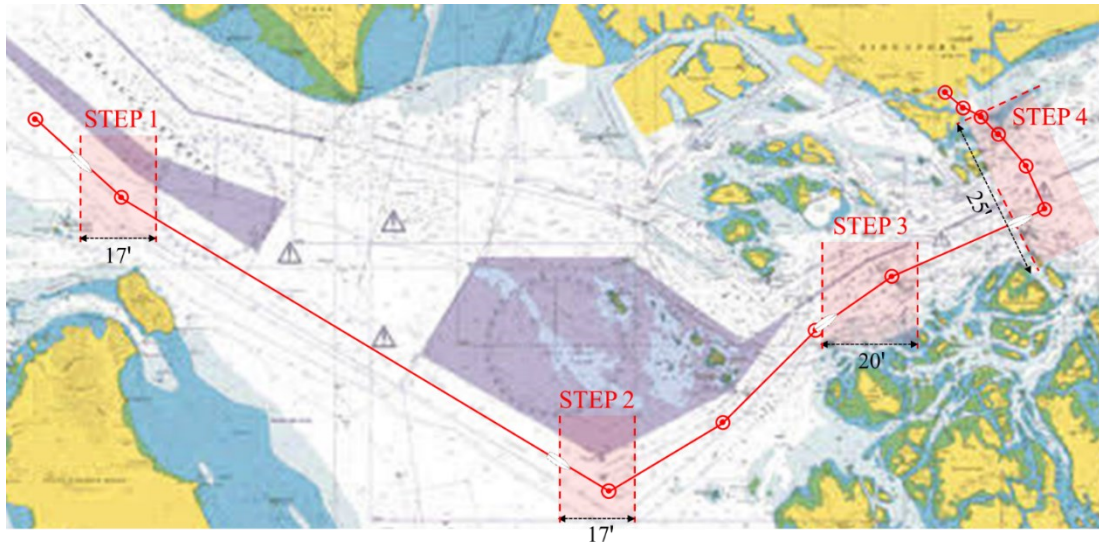


Figure 3.5 : Navigation area used in simulator with route legs and performance measurement areas as stated in steps. Image obtained from Admiralty Chart BA 3833.

Performance parameters were determined according to issues stated in literature (see chapter 2.1.3 and 2.3.2) and the opportunities of simulator environment (Table 3.2).

Table 3.2 : Performance parameters for navigation scenario.

Type of task	Main parameters	Detailed parameters	Symbol
Safety critical navigation tasks	Collision avoidance	Keeping a safe CPA	γ_{11}
		Rule following (COLREG)	γ_{12}
		Detection range of targets	γ_{13}
		Time to response	γ_{14}
		Communication & true reaction	γ_{15}
	Identify and communicate navigation landmarks		γ_2
	Identify hazards (report & action)		γ_3
Trackkeeping tasks	Crosstrack variability (XTE)		η_1
	Time to return to course		η_2
	Ship control	Rudder angle	η_{31}
		Turn radius	η_{32}
	Radar performance		η_4

In first step, contacting one vessel on starboard bow side (Figure 3.6a), making correct manoeuvre, course alteration and then returning to course are carried out by subjects. In second step, vessel traffic becomes moderate. Contacting two vessels on head in same separation zone (Figure 3.6b), course alteration to starboard to keep safe CPA, identifying the fishing nets and fishing boats, course alteration for way point with hand steering mode and safe passage from buoys are carried out by subjects. In third step,

adding to moderate traffic density, visibility decreases and geographical conditions make navigation hard for subjects. Firstly, keeping the vessel clear from fishing nets on starboard and port side, contacting two vessels which make short cut in separation on port bow side with one vessel on head in same separation zone (Figure 3.6c), then contacting one fishing boat on starboard bow side, altering course to starboard to avoid collision and contacting one vessel on starboard bow side are carried out by subjects. In last step, contacting one vessel which makes short cut in separation and one vessel on opposite side of separation prior to alteration course for making short cut and proceeding to port (Figure 3.6d) is carried out by subjects. Then, visibility decreases more in this period. After making short cut, geographical conditions become hard by currents making the vessel way through to northeast. There are fishing nets, fishing boats and one ferry make the navigation hard. Conducting another vessel on starboard side and avoiding collision with her are carried out by subjects.

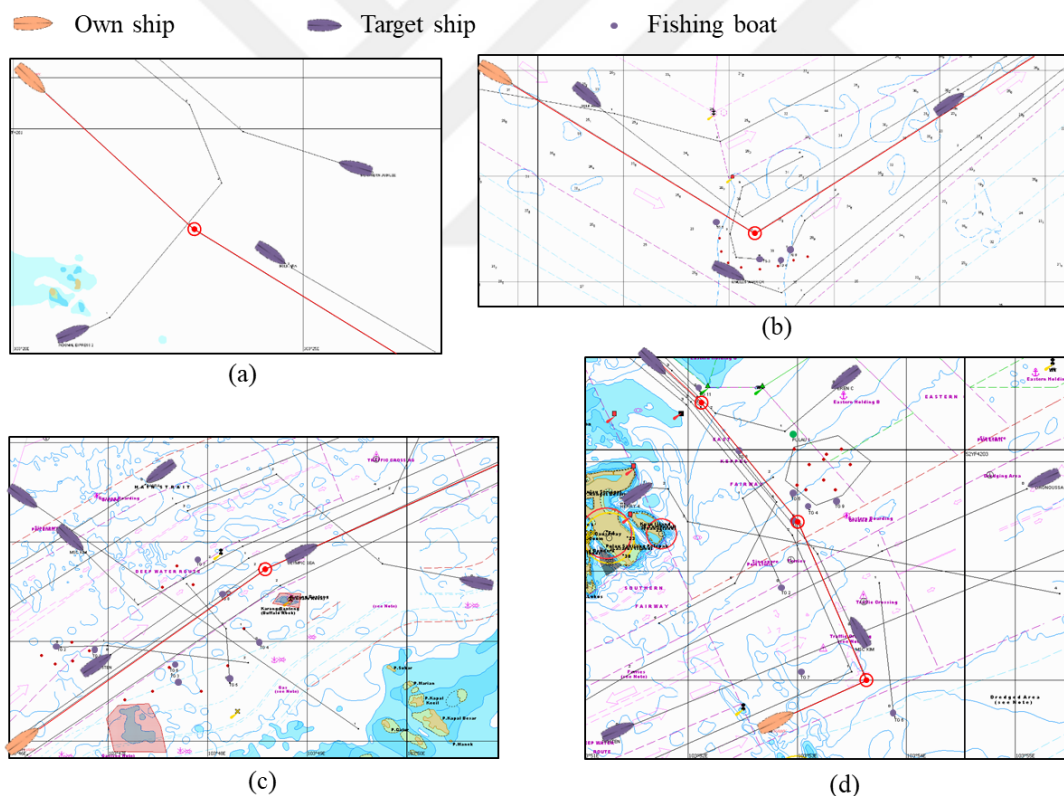


Figure 3.6 : Detailed step organization with the routes of own ship and target ships; step 1 (a), step 2 (b), step 3 (c) and step 4 (d). Chart screenshot authorized by TRANSAS.

3.3.1.1 Task load assessment of navigation scenarios

In this study, task load assessment was carried out according to Operator Function Model (OFM-COG) and its sample implications in literature (Lee and Sanquist, 2000).

Detailed information is stated in chapter 2.3.3. According to the model, the task loads of the navigation scenarios used in this thesis were calculated and detailed stated in Table 3.3, and figured out in Figure 3.7.

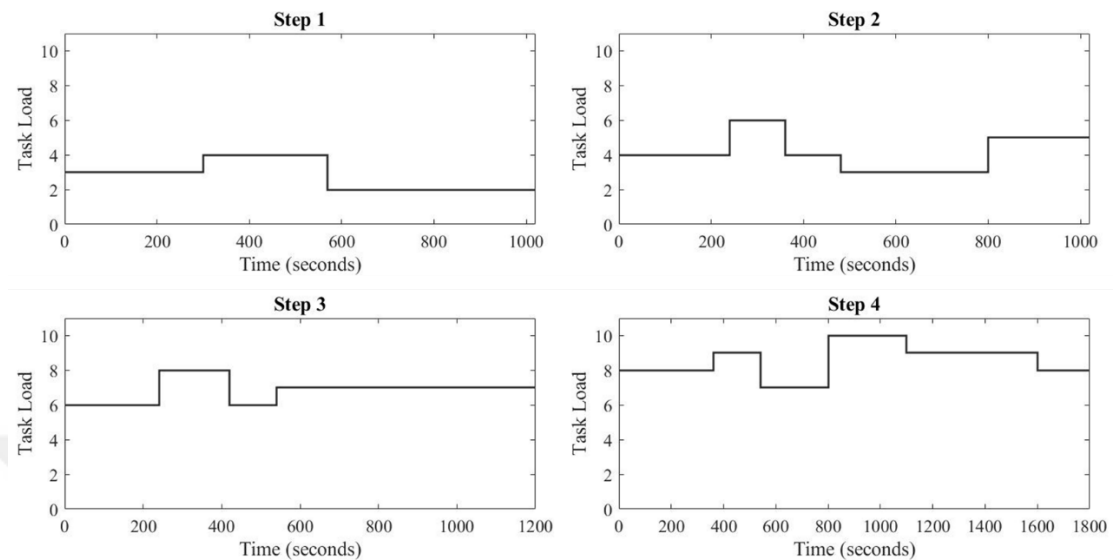


Figure 3.7 : Task loading of navigation scenario.

3.3.2 Cargo operation tasks

The difficulty level of cargo operation scenario was gradually adjusted according to type and number of operation and operation period corresponding to a real cargo operation. The steps of cargo operation scenario those are represented with cargo plans of final conditions of steps in Figure 3.8, are stated as:

- Step 1; 1 parcel cargo loading to 3 tanks
- Step 2; 2 parcels cargo loading to 5 tanks, 2 tanks topping off and inert operation in 3 tanks
- Step 3; 2 parcels cargo loading to 5 tanks, 1 parcel cargo discharging from 2 tanks and 5 tanks (2 parcels) topping off

Subjects performed the cargo operation scenario in a simulated IMO type-1 chemical tanker (presented in Figure 3.9) having 28 cargo tanks because of that this type chemical tankers carry a lot of type cargo and has the opportunity to be handled lots of operations simultaneously.

Performance parameters were determined according to issues stated in chapter 2.1.3, developed scenario and the opportunities of simulator environment (Table 3.4).

Table 3.3 : The OFM-COG analysis for navigation tasks used in this thesis.

Step	Task (sec.)	Task description	OFM function	Frequency count of the navigation tasks			
				Acquisition	Handling	Interpretation	Total
1	T1 (0-300)	Proceed to next waypoint with minimum XTE and detect the target on starboard bow side	Track-keeping with ECDIS Identify target with RADAR	1 (Identify)	0	2 (Interpret) (Categorize)	3
	T2 (300-420)	React for collision avoidance	Consider course change	1 (Input select)	1 (Compute)	2 (Interpret) (Decide)	4
	T3 (420-570)	Make visible course change to starboard	Target evaluation Course execution	0 0	1 (Compute) 1 (Count)	1 (Categorize) 1 (Goal image)	4
	T4 (570-780)	Proceed with safe CPA	Track-keeping with ECDIS Target evaluation	0 0	0 0	1 (Test) 1 (Categorize)	2
	T5 (780-1020)	Return to planned course	Course execution	0	1 (Queue to channel)	1 (Select)	2
2	T1 (0-120)	Proceed to next waypoint with minimum XTE and detect the targets on head	Track-keeping with ECDIS Identify target with RADAR	1 (Identify)	0	3 (Test) (Interpret) (Categorize)	4
	T2 (120-240)	Alter the course for safe CPA and for avoiding the fishing nets	Consider course change	1 (Input select)	1 (Compute)	2 (Interpret) (Decide)	4
	T3 (240-360)	Proceed with safe CPA and detect the target on starboard bow side	Track-keeping with ECDIS Target evaluation Identify target	0 0 1 (Identify)	0 0 0	1 (Test) 1x2 (Categorize) 2 (Interpret) (Categorize)	6
	T4 (360-480)	Proceed with safe CPA	Track-keeping with ECDIS Target evaluation	0 0	0 0	1 (Test) 3 (Categorize)	4
	T5 (480-800)	Proceed with safe CPA and not be out of the traffic separation	Course execution	0	1 (Queue to channel)	1 (Select)	3
	T6 (800-1020)	Alter the course to port for next waypoint and detect the fishing boat targets	Target evaluation Course execution Identify target	0 0 1 (Identify)	0 0 0	1 (Categorize) 1 (Select) 2 (Interpret) (Categorize)	5
3	T1 (0-240)	Proceed to next waypoint with minimum XTE by considering the fishing nets Detect the targets on port bow side	Track-keeping with ECDIS Identify target (fishing nets) Identify target	0 1 (Identify) 1 (Identify)	0 0 0	1 (Test) 2 (Interpret) (Categorize) 1 (Categorize)	6
	T2 (240-300)	Alter the course for safe CPA and for avoiding the fishing nets	Track-keeping with ECDIS Consider course change Target evaluation	0 1 (Input select) 1 (Identify)	0 1 (Compute) 0	1 (Test) 2 (Interpret) (Decide) 1x2 (Categorize)	8
	T3 (300-420)	Proceed with safe CPA and not be out of the traffic separation	Course execution Target evaluation Identify target	0 0 1 (Identify)	1 (Queue to channel) 0 0	1 (Select) 3 (Categorize) 2 (Interpret) (Categorize)	8

Table 3.3 (continued) : The OFM-COG analysis for navigation tasks used in this thesis.

Step	Task (sec.)	Task description	OFM function	Frequency count of the navigation tasks				
				Acquisition	Handling	Interpretation	Total	
3	T4 (420-540)	Proceed with safe CPA in decreased visibility and not be out of the traffic separation	Track-keeping with ECDIS	0	0	1 (Test)	6	
			Target evaluation Identify target	0 2 (Detect) (Identify)	0 0	1 (Categorize) 2 (Interpret) (Categorize)		
	T5 (540-840)	Proceed with safe CPA and detect the target on starboard bow side	Track-keeping with ECDIS	0	0	1 (Test)	7	
			Consider course change	2 (Detect) (Input select)	1 (Compute)	2 (Interpret) (Decide)		
	T6 (840-1200)	Detect the target on starboard bow side and react for collision avoidance	Identify hazards	0	0	1 (Categorize)	7	
			Track-keeping with ECDIS Consider course change	0 2 (Detect) (Input select)	0 1 (Compute)	1 (Test) 2 (Interpret) (Decide)		
			Target evaluation	0	0	1 (Categorize)		
4	T1 (0-360)	Proceed to next waypoint with minimum XTE Detect the targets on port bow side	Track-keeping with ECDIS	0	0	1 (Test)	8	
			Identify target with RADAR	1 (Detect) 1x2 (Identify)	0	2x2 (Interpret) (Categorize)		
	T2 (360-540)	Alter the course to port for next waypoint and proceed with safe CPA	Course execution	0	1 (Queue to channel)	1 (Select)	9	
			Identify target Target evaluation	2 (Detect) (Identify) 0	0 0	2 (Interpret) (Categorize) 3 (Categorize)		
	T3 (540-800)	Alter the course to starboard for safe CPA	Track-keeping with ECDIS	0	0	1 (Test)	7	
			Consider course change	2 (Detect) (Input select)	1 (Compute)	2 (Interpret) (Decide)		
				Target evaluation	0	0	1 (Categorize)	
	T4 (800-1100)	Return to planned course considering the current and detect the targets on port bow side	Course execution	1 (Detect)	1 (Queue to channel)	1 (Select)	10	
			Identify target	1 (Detect) 1x2 (Identify)	0	2x2 (Interpret) (Categorize)		
	T5 (1100-1250)	Proceed with safe CPA to fishing targets in more decreased visibility, detect the target on starboard side	Course execution	1 (Detect)	1 (Queue to channel)	1 (Select)	9	
Identify target (fishing nets) Identify target			1 (Detect) 2 (Detect) (Identify)	0 0	1 (Categorize) 2 (Interpret) (Decide)			
T6 (1250-1350)	Detect the fishing targets and proceed with safe CPA	Consider course change	2 (detect) (Input select)	1 (Compute)	2 (Interpret) (Decide)	9		
		Target evaluation Course execution	0 1 (Detect)	0 1 (Queue to channel)	1 (Categorize) 1 (Select)			

Table 3.3 (continued) : The OFM-COG analysis for navigation tasks used in this thesis.

Step	Task (sec.)	Task description	OFM function	Frequency count of the navigation tasks			Total
				Acquisition	Handling	Interpretation	
4	T7 (1350-1600)	Detect the fishing targets and proceed with safe CPA	Consider course change	2 (detect) (Input select)	1 (Compute)	2 (Interpret) (Decide)	9
			Target evaluation	0	0	1 (Categorize)	
	T8 (1600-1800)	Proceed to Loading Port with minimum XTE	Course execution	1 (Detect)	1 (Queue to channel)	1 (Select)	8
			Identify target	2 (Detect) (Identify)	0	2 (Interpret) (Categorize)	
		Target evaluation	0	0	1 (Categorize)		

10P	5P	8P	7P	6P	5P	4P	3P	2P	1P
0,000 MT 0,000 CBM 0,0%	MAL 470,320 MT 536,323 CBM 97,0%	0,000 MT 0,000 CBM 0,0%	721,280 MT 820,594 CBM 97,0%	0,000 MT 0,000 CBM 0,0%	MAL 154,850 MT 183,34 CBM 96,0%	0,000 MT 0,000 CBM 0,0%	304,210 MT 346,379 CBM 96,0%	0,000 MT 0,000 CBM 0,0%	0,000 MT 0,000 CBM 0,0%
1108,772 CBM	570,246 CBM	753,278 CBM	915,902 CBM	838,272 CBM	373,895 CBM	393,272 CBM	612,623 CBM	975,492 CBM	667,968 CBM
0,000 MT 0,000 CBM 0,0%	0,000 MT 0,000 CBM 0,0%	0,000 MT 0,000 CBM 0,0%	0,000 MT 0,000 CBM 0,0%	0,000 MT 0,000 CBM 0,0%	0,000 MT 0,000 CBM 0,0%	0,000 MT 0,000 CBM 0,0%	0,000 MT 0,000 CBM 0,0%	0,000 MT 0,000 CBM 0,0%	0,000 MT 0,000 CBM 0,0%
10S	5S	8S	7S	6S	5S	4S	3S	2S	1S
0,000 MT 0,000 CBM 0,0%	MAL 242,430 MT 307,379 CBM 90,0%	0,000 MT 0,000 CBM 0,0%	721,280 MT 820,594 CBM 97,0%	0,000 MT 0,000 CBM 0,0%	MAL 295,000 MT 375,048 CBM 96,0%	0,000 MT 0,000 CBM 0,0%	307,850 MT 349,549 CBM 95,0%	0,000 MT 0,000 CBM 0,0%	0,000 MT 0,000 CBM 0,0%
1113,003 CBM	620,246 CBM	753,278 CBM	915,902 CBM	838,272 CBM	382,485 CBM	393,078 CBM	312,424 CBM	915,688 CBM	677,474 CBM

- STEP 1**
- 15'
 - 3 tanks Methanol loading, ■
 - Cont. loading, 1 tank changing ■

10P	5P	8P	7P	6P	5P	4P	3P	2P	1P
482,600 MT 555,792 CBM 115,000%	XLP MAL 470,320 MT 536,323 CBM 97,0%	0,000 MT 0,000 CBM 0,0%	721,280 MT 820,594 CBM 97,0%	0,000 MT 0,000 CBM 0,0%	MAL 246,500 MT 292,501 CBM 96,0%	0,000 MT 0,000 CBM 0,0%	304,210 MT 346,379 CBM 96,0%	0,000 MT 0,000 CBM 0,0%	0,000 MT 0,000 CBM 0,0%
1108,772 CBM	623,524 CBM	753,278 CBM	915,902 CBM	838,272 CBM	332,081 CBM	393,078 CBM	350,242 CBM	975,492 CBM	667,968 CBM
0,000 MT 0,000 CBM 0,0%	0,000 MT 0,000 CBM 0,0%	0,000 MT 0,000 CBM 0,0%	0,000 MT 0,000 CBM 0,0%	0,000 MT 0,000 CBM 0,0%	0,000 MT 0,000 CBM 0,0%	0,000 MT 0,000 CBM 0,0%	0,000 MT 0,000 CBM 0,0%	0,000 MT 0,000 CBM 0,0%	0,000 MT 0,000 CBM 0,0%
10S	5S	8S	7S	6S	5S	4S	3S	2S	1S
486,650 MT 570,443 CBM 117,000%	XLP MAL 470,320 MT 536,323 CBM 97,0%	0,000 MT 0,000 CBM 0,0%	721,280 MT 820,594 CBM 97,0%	0,000 MT 0,000 CBM 0,0%	MAL 295,000 MT 375,048 CBM 96,0%	0,000 MT 0,000 CBM 0,0%	307,850 MT 349,549 CBM 95,0%	0,000 MT 0,000 CBM 0,0%	0,000 MT 0,000 CBM 0,0%
1113,003 CBM	623,524 CBM	753,278 CBM	915,902 CBM	838,272 CBM	332,081 CBM	393,078 CBM	350,242 CBM	915,688 CBM	677,474 CBM

- STEP 2**
- 18'
 - 3 P-Xylene tanks inerting ■
 - 2 Methanol tanks topping off ■
 - 2 tanks Methanol, 3 tanks P-Xylene loading ■ ■
 - 3 P-Xylene tanks inerting ■

10P	5P	8P	7P	6P	5P	4P	3P	2P	1P
537,280 MT 540,285 CBM 92,0%	XLP MAL 470,320 MT 536,323 CBM 97,0%	0,000 MT 0,000 CBM 0,0%	721,280 MT 820,594 CBM 97,0%	0,000 MT 0,000 CBM 0,0%	MAL 195,000 MT 237,048 CBM 96,0%	0,000 MT 0,000 CBM 0,0%	157,070 MT 178,555 CBM 45,0%	212,250 MT 248,845 CBM 25,0%	0,000 MT 0,000 CBM 0,0%
1108,772 CBM	623,524 CBM	753,278 CBM	915,902 CBM	838,272 CBM	330,285 CBM	393,078 CBM	352,242 CBM	975,492 CBM	667,968 CBM
0,000 MT 0,000 CBM 0,0%	0,000 MT 0,000 CBM 0,0%	0,000 MT 0,000 CBM 0,0%	0,000 MT 0,000 CBM 0,0%	0,000 MT 0,000 CBM 0,0%	0,000 MT 0,000 CBM 0,0%	0,000 MT 0,000 CBM 0,0%	0,000 MT 0,000 CBM 0,0%	0,000 MT 0,000 CBM 0,0%	0,000 MT 0,000 CBM 0,0%
10S	5S	8S	7S	6S	5S	4S	3S	2S	1S
535,440 MT 540,285 CBM 92,0%	XLP MAL 470,320 MT 536,323 CBM 97,0%	0,000 MT 0,000 CBM 0,0%	721,280 MT 820,594 CBM 97,0%	0,000 MT 0,000 CBM 0,0%	MAL 195,000 MT 237,048 CBM 96,0%	0,000 MT 0,000 CBM 0,0%	157,070 MT 178,555 CBM 45,0%	212,250 MT 248,845 CBM 25,0%	0,000 MT 0,000 CBM 0,0%
1113,003 CBM	623,524 CBM	753,278 CBM	915,902 CBM	838,272 CBM	332,081 CBM	393,078 CBM	352,242 CBM	915,688 CBM	677,474 CBM

- STEP 3**
- 23'
 - 2 Methanol tanks topping off, loading comp. ■
 - 1 P-Xylene tank topping off, additional 1 tank loading ■
 - 2 tanks Benzene discharging ■
 - 2 P-Xylene tanks topping off ■

Figure 3.8 : The cargo operation scenario with cargo plans of final conditions.

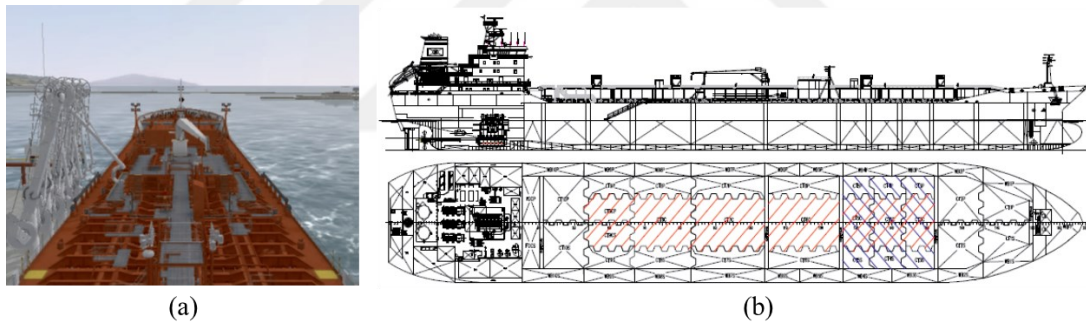


Figure 3.9 : The deck view (a) and the general plan (b) of the chemical tanker. View screenshot authorized by TRANSAS.

The duration of first step is about 15 minutes. One parcel (methanol) loading to three tanks and de-ballasting are the tasks of the first step. In ten minutes, the operation of tank shifting is expected to carry out by subjects. The parameters should be considered by subjects in step 1 are $\gamma_1, \gamma_2, \gamma_3, \gamma_4, \gamma_5, \gamma_6, \eta_1, \eta_2, \eta_4$ (detailed in Table 3.4). The duration of second step is about 18 minutes. Two parcels (methanol and p-xylene) loading to five tanks in total and de-ballasting are the tasks of the second step. Inerting operation in three tanks is expected to carry out by subjects before p-xylene loading. Additionally, the operation of tank topping for two methanol tanks is expected to carry out by subjects. The parameters should be considered by subjects in step 2 are $\gamma_7, \gamma_8, \eta_3$ addition to first step. The duration of third step is about 23 minutes. two parcels

(methanol and p-xylene) loading to five tanks in total, one parcel (benzene) discharging from two tanks and de-ballasting are the tasks of the third step. The operations of tank topping for two methanol tanks and completion of methanol loading, tank topping for three p-xylene tanks in total and tank shifting amongst p-xylene tanks are expected to carry out by subjects. Additionally, subjects are expected to prepare the valves and lines of the tanks to be discharged. The parameters should be considered by subjects in step 3 are those stated in previous steps except γ_7 and η_3 .

Table 3.4 : Performance parameters for cargo operation scenario.

Type of task	Main parameters	Symbol
Safety critical operation tasks	List / Trim monitoring	γ_1
	Shearing Force (SF) / Bending Moment (BM) monitoring	γ_2
	Manifold pressure	γ_3
	Tank pressure	γ_4
	Line up from manifold to cargo tanks	γ_5
	Initial rate	γ_6
	Atmosphere monitoring	γ_7
	Topping of tanks	γ_8
Operational tasks	Ballast operation	η_1
	Loading / Discharging rate	η_2
	Inerting	η_3
	Operating pumps	η_4
	Tank heating	η_5
	Stripping	η_6

3.3.2.1 Task load assessment of cargo operation scenarios

In similar way, task load assessment was carried out according to Operator Function Model (OFM-COG). There are no similar implications for cargo operation in literature. However, it was tried to define the cargo operation tasks according to the model. Detailed information is stated in chapter 2.3.3. The task loads of the cargo operation scenarios used in this thesis were calculated and detailed stated in Table 3.5, and figured out in Figure 3.10.

Table 3.5 : The OFM-COG analysis for cargo operation tasks used in this thesis.

Step	Task (sec.)	Task description	OFM function	Frequency count of the navigation tasks			
				Acquisition	Handling	Interpretation	Total
1	T1 (0-300)	Check the status of continued Methanol loading to three tanks	Level monitoring	0	0	1 (Test)	2
	Monitoring the safety parameters		0	0	1 (Test)		
	T2 (300-540)	Do proper ballast operation to keep vessel upright	Level monitoring	0	0	1 (Test)	4
	Monitoring the safety parameters		0	0	1 (Test)		
	T3 (540-600)	Do proper tank change according to planned cargo operation	List / trim correction	1 (Search)	0	1 (Control)	5
	Level monitoring		0	0	1 (Test)		
	Monitoring the safety parameters		0	0	1 (Test)		
	Handling operation		1 (Search)	1 (Edit)	1 (Test)		
	T4 (600-900)	Check the status of continued Methanol loading to three tanks and do proper ballast operation to keep vessel upright	Level monitoring	0	0	1 (Test)	4
	Monitoring the safety parameters		0	0	1 (Test)		
List / trim correction	1 (Search)		0	1 (Control)			
2	T1 (0-120)	Check the status of continued Methanol loading to three tanks and continued inerting operation for PX tanks	Level monitoring	0	0	1x2 (Test)	3
	Monitoring the safety parameters		0	0	1 (Test)		
	T2 (120-360)	Do proper ballast operation to keep vessel upright adding to continued operation	Level monitoring	0	0	1x2 (Test)	5
	Monitoring the safety parameters		0	0	1 (Test)		
	List / trim correction		1 (Search)	0	1 (Control)		
	T3 (360-720)	Do proper tank topping operation for one methanol tank	Level monitoring	1 (Input select)	1 (Edit)	1x2 (Test)	7
	Monitoring the safety parameters		0	0	1 (Test)		
	List / trim correction		1 (Search)	0	1 (Control)		
	Level monitoring		1 (Input select)	0	1x2 (Test)		
	T4 (720-840)	Do proper tank topping and tank changing operation for methanol tanks	Monitoring the safety parameters	0	0	1 (Test)	8
	List / trim correction (mon.)		0	0	1 (Test)		
	Handling operation		1 (Search)	1 (edit)	1 (Test)		
	Level monitoring		0	0	1x2 (Test)		
	T5 (840-900)	Check the status of continued Methanol loading to two tanks and continued inerting operation for PX tanks	Monitoring the safety parameters	0	0	1 (Test)	5
List / trim correction	1 (Search)		0	1 (Control)			
Level monitoring	0		0	1x2 (Test)			
T6 (900-960)	Commence PX loading	Monitoring the safety parameters	0	0	1 (Test)	7	
List / trim correction (mon.)		0	0	1 (Test)			
Handling operation		1 (Search)	1 (edit)	1 (Test)			

Table 3.5 (continued) : The OFM-COG analysis for cargo operation tasks used in this thesis.

Step	Task (sec.)	Task description	OFM function	Frequency count of the navigation tasks			
				Acquisition	Handling	Interpretation	Total
2	T7 (960-1080)	Check the status of continued PX loading and Methanol loading to two tanks and continued inerting operation for PX tanks	Level monitoring	0	0	1x3 (Test)	5
			Monitoring the safety parameters	0	0	1 (Test)	
			List / trim correction (mon.)	0	0	1 (Test)	
T1 (0-120)	Check the status of continued PX loading and Methanol loading to two tanks	Level monitoring	0	0	1x2 (Test)	4	
		Monitoring the safety parameters	0	0	1 (Test)		
		List / trim correction (mon.)	0	0	1 (Test)		
T2 (120-300)	Check the status of continued PX loading and Methanol loading to two tanks	Level monitoring	0	0	1x2 (Test)	4	
		Monitoring the safety parameters	0	0	1 (Test)		
		List / trim correction (mon.)	0	0	1 (Test)		
T3 (300-420)	Do proper tank topping operation for one methanol tank	Level monitoring	1 (Input select)	1 (Edit)	1x2 (Test)	6	
		Monitoring the safety parameters	0	0	1 (Test)		
		List / trim correction (mon.)	0	0	1 (Test)		
T4 (420-540)	Check the status of continued PX loading to three tanks and Methanol loading to one tank	Level monitoring	1 (Input select)	0	1x2 (Test)	8	
		Monitoring the safety parameters	0	0	1 (Test)		
		List / trim correction (mon.)	0	0	1 (Test)		
3	T5 (540-600)	Commence loading for one more PX tank Do proper tank topping operation for last methanol tank and	Handling operation	1 (Search)	1 (Edit)	1 (Test)	7
			Level monitoring	1 (Input select)	1 (Edit)	1x2 (Test)	
			Monitoring the safety parameters	0	0	1 (Test)	
T6 (600-780)	Commence Benzene discharging	List / trim correction	1 (Search)	0	1 (Control)	9	
		Level monitoring	1 (Input select)	0	1 (Test)		
		Monitoring the safety parameters	1 (Input select)	0	1 (Test)		
T7 (780-1080)	Do proper tank topping operation for one PX tank	List / trim correction (mon.)	0	1 (count)	1 (Test)	6	
		Handling operation	1 (Search)	1 (Edit)	1 (Test)		
		Level monitoring	1 (Input select)	1 (Edit)	1x2 (Test)		
T8 (1080-1380)	Do proper tank topping and tank changing operation for PX tanks	Monitoring the safety parameters	0	0	1 (Test)	11	
		List / trim correction (mon.)	0	0	1 (Test)		
		List / trim correction (mon.)	0	0	1 (Test)		
			Handling operation	1x2 (Search)	1x2 (edit)	1x2 (Test)	

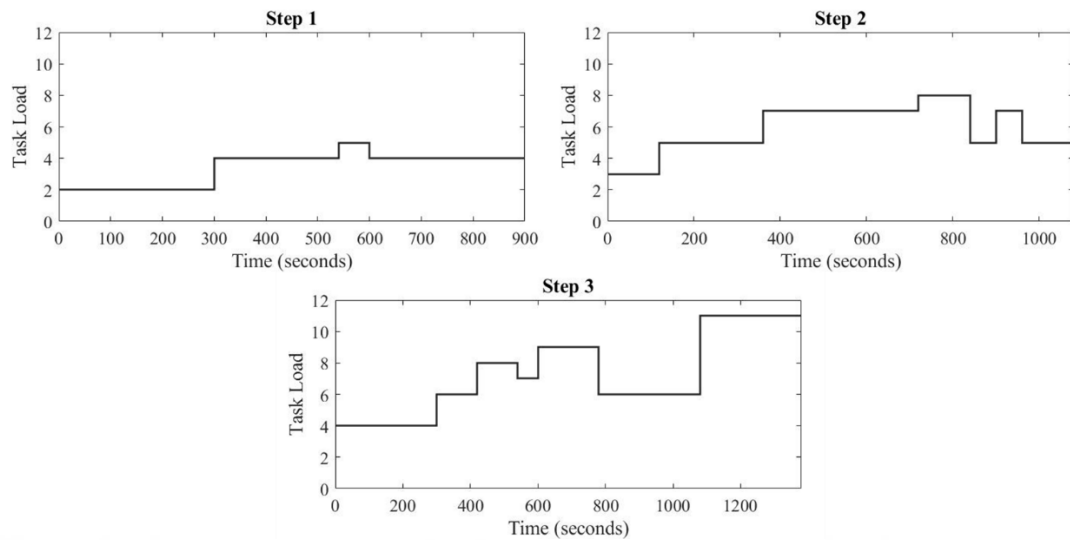


Figure 3.10 : Task loading of cargo operation scenario.

3.4 Measurement Details

It was stated that triangulated measurement strategy was implemented to this study. This involves performance measurement, physiological measurement and subjective assessment. This chapter includes the detailed procedures of these measurements.

3.4.1 Performance measurement

3.4.1.1 Performance measurement for navigation tasks

The speed of own vessel is 10 to 13 knots and the XTE is 0.05 nm during the whole steps. Subjects performed the navigation with auto pilot, but they can use hand steering for big course alterations and in emergency cases. The tasks of each step were separately evaluated and their evaluation parameters were specified. Table 3.7 represents optimum performance results of 3 experts during the trials.

After the trails were completed by experts, they set the limits for each criterion and for each specific tasks of steps as well as “just acceptable or not” stated in the study of Gould et al. (2009). In this study, performances of the subjects were scored as 0 and 1 or 0, 0.5 and 1 for safety critical navigation and trackkeeping tasks. Table 3.8 represents the limits corresponding to the score values (stated with red colour) evaluated by experts. Subjects were evaluated according to the values stated in Table 3.8.

Navigation performances were evaluated by using the targeted acceptable responses to generated events or tasks (TARGETS) method (Fowlkes et al., 1994). Differently, targets corresponding to the events were weighted according to the degree of importance in related event / task. Moreover, the performance results of the participants were scored as 0, 0.5 and 1 against the evaluation “just acceptable or not”. By the way, it was aimed to make performance measurement quantify in this study. In literature, Kim et al. (2010) tried to make performance measurement quantify, but they used constant limits for performances and that evaluation was not sufficient for variable navigational conditions. In a similar way stated in the study of Gould et al. (2009), tasks were evaluated separately as safety critical and trackkeeping in this study. Those were stated as task generated activities which are “observable safety-critical navigation tasks” and event-generated activities which are “responses to external objects” (Gould et al., 2009). Differently, performance scores were equal to the weighted sum of the scores of all parameters of both activities in this study.

The navigation parameters were stated in Table 3.2. 3 experts scored the importance weights of each parameter for each step and for each task with fuzzy numbers (Table 3.6) because of that the level of importance of navigation parameters can vary to the navigational conditions.

Table 3.6 : Fuzzy numbers corresponding to the importance weights, adapted from (Buckley and Eslami, 2002).

Linguistic expression	Fuzzy numbers
Very Low (VL)	(0.1, 0.1, 0.3)
Low (L)	(0.1, 0.3, 0.5)
Medium (M)	(0.3, 0.5, 0.7)
High (H)	(0.5, 0.7, 0.9)
Very High (VH)	(0.7, 0.9, 0.9)

The averages of weights for each parameter were calculated with following equation;

$$w_j = \frac{1}{E} [w_j^1 (+) w_j^2 (+) \dots (+) w_j^E] \quad (3.3)$$

where E is the number of experts and w_j is the weight of j^{th} parameter. The averages of all membership functions (lower, middle and upper values) are calculated according to the equation 3.3. Next step is defuzzification;

$$A_j = \frac{l + 4m + u}{6} \quad (3.4)$$

Table 3.7 : Navigaiton performance results of 3 experts during the trials.

Step	Tasks (secs)	Difficulty			Safety critical navigation task parameters							Trackkeeping task parameters				
		The number of targets (target ID)	Vsby. (nm)	Fix interval (min.)	CPA / TCPA (nm/min) (γ 11)	Heading ($^{\circ}$) (γ 12)	Detection range of targets (nm) (γ 13)	Time to response (min) (γ 14)	Comm. & true react. (γ 15)	Identify landmarks (γ 2)	Identify hazards (γ 3)	XTE (nm) (η 1)	Return to course (new heading) ($^{\circ}$) (η 2)	Turn radius (rad/nm) (η 31)	Rudder angle ($^{\circ}$) (η 32)	Radar (nm) (η 4)
1	T1 (0-300)	1	10	5	0.18/11'	133	3.5	-	-	-	-	0.05	-	0.54	-	6
	T2 (300-420)	1	10	5	0.23/10'	133	-	TCPA 10'	VHF/ trial	-	-	0.05	-	0.54	-	6
	T3 (420-570)	1	10	5	-	>133	-	TCPA 8'	A/C to stb	-	-	-	-	0.54	-	6
	T4 (570-780)	1	10	5	1.0/5'	133+ x	-	-	-	-	-	-	-	0.54	-	6
	T5 (780-1020)	1	10	5	0.8/2'	113	-	-	-	-	-	-	-2x	0.54	-	6
2	T1 (0-120)	2	10	3		122						0.05	-	0.54	-	3
		(Detroit)			0.37/4'		0.8	-	-							
		(Ara)			0.29/10'		0.9	-	VHF							
	T2 (120-240)	2	10	3	-	>122	-	TCPA 8'	A/C to stb	-	F. nets	-	-	0.54	-	3
	T3 (240-360)	3	10	3		145								0.54	-	3
		(Detroit)			0.32/0'		-	-	-							
		(Ara)			0.73/1'		-	-	-							
	(Olympic)			1.24/8'		3.5	-	-								
T4 (360-480)	3	10	3	1.47/5'	145	-	-	-	-	-	-	-	0.54	-	3	
T5 (480-800)	3	10	3	1.0/2'	A/C to P	-	-	-	Sep.	-	-	-	0.54	-	3	
T6 (800-1020)	2+ f. boats	10	3	Hand steering for wp			-	-	Sep.	F. buoys	-	-	-	10-15	3	
3	T1 (0-240)	2	5	2		55					F. nets	0.05	-	0.54	-	3
		(Triesten)			0.15/11'		1.1	-	-							
		(MSC Kim)			0.33/6'		1.85	<2 min.	VHF							
	T2 (240-300)	3	5	1		55				-	.15s, .4p	0.05	-	0.54	-	3
		(Satsuma)			0.08/2'		0.4	-	A/C to port							
	T3 (300-420)	4	5	1		45				-	.15s, .4p	-	-	0.54	-	3
		(Satsuma)			0.16/0'											
T4 (420-540)	3	3	1		45	0.8	-	-	-		-	-	0.54	-	3	
	(Herry 3 and fishing boats)				-											
T5 (540-840)	4	3	1		>45	-	-	A/C to stb	-	Shallow	-	-	0.54	-	3	
T6 (840-1200)	4	3	3		55				Sep.	-	-	-	0.34	-	3	
	(Cecela S)				0.12/3'	1.5	<10 sec.	A/C to stb								

Table 3.7 (continued) : Navigaiton performance results of 3 experts during the trials.

Step	Tasks (secs)	Difficulty			Safety critical navigation task parameters						Trackkeeping task parameters				
		The number of targets (target ID)	Vsby. (nm)	Fix interval (min.)	CPA / TCPA (nm/min) ($\gamma11$)	Heading ($^{\circ}$) ($\gamma12$)	Detection range of targets (nm) ($\gamma13$)	Time to response (min) ($\gamma14$)	Comm. & true react. ($\gamma15$)	Identify landmarks ($\gamma2$)	Identify hazards ($\gamma3$)	XTE (nm) ($\eta1$)	Return to course (new heading) ($^{\circ}$) ($\eta2$)	Turn radius (rad/nm) ($\eta31$)	Rudder angle ($^{\circ}$) ($\eta32$)
4	T1 (0-360)	4	3	1		66					0.05	-	0.34	-	3
		(MSC Kim)			0.89/1'		1	-	-						
	T2 (360-540)	4	3	1	Hand steering for wp									10-20	3
		(Dhonoussa)			0.9/5'		3	-	-						
	T3 (540-800)	4	3	1	0.3/1'	350	-	<10 sec.	A/C to stb				0.34	-	3
	T4 (800-1100)	4	1.5	1	>0.1/0'	-	-	-	-		Current/Herry4/fishing b.		0.34	-	3
	T5 (1100-1250)	5	0.8	1	0.24/4'	-	1.22	-	-		F. nets		0.34	-	3
	T6 (1250-1350)	5	0.8	1	>0.2/0'	-	-	-	A/C to stb		F. nets		0.34	-	3
T7 (1350-1600)	5	0.8	1	0.02/1'	-	-	<10 sec.	A/C to port		Shallow		-	-	3	
T8 (1600-1800)	4	0.8	1	-	-	-	-	-	Buoys	current	0.05	-	0.34	-	3

Table 3.8 : The limits corresponding to the score values evaluated by experts for navigation scenario.

Step	Tasks (secs)	Safety critical navigation task parameters						Trackkeeping task parameters					
		CPA / TCPA (nm/min) ($\gamma11$)	Heading ($^{\circ}$) ($\gamma12$)	Detection range of targets (nm) ($\gamma13$)	Time to response (TCPA) ($\gamma14$)	Comm. & true react. ($\gamma15$)	Identify landmarks ($\gamma2$)	Identify hazards ($\gamma3$)	XTE (nm) ($\eta1$)	return to course (new heading) ($^{\circ}$) ($\eta2$)	Turn radius (rad/nm) ($\eta31$)	Rudder angle ($^{\circ}$) ($\eta32$)	Radar (nm) ($\eta4$)
1	T1 (0-300)	-		0; <2, 0.5; 2-3, 1; >3		-			0; >0.1				
	T2 (300-420)	-		0; <6, 0.5; 6-8, 1; >8		0; NR, 1; Stb		0.5; 0.05-0.1					
								1; <0.05					
	T3 (420-570)	-	0; P, 1; S	0; <4, 0.5; 4-6, 1; >6		0; <5, 1; >5					0; S		1; 6
	T4 (570-780)	0; <0.5, 0.5;									1; IS		
T5 (780-1020)	0.5-0.8, 1; >0.8							0; /-2x(-5+5), 0.5; -2x(-5+5), 1; -2x					
2	T1 (0-120)	-						0; >0.1					
	(Detroit)	-	0; <0.5, 0.5; 0.5-0.6,					0.5; 0.05-0.1, 1; <0.05			0; S		1; 3
	(Ara)	-	1; >0.7	0; <5, 0.5; 5-7,		0; P				1; IS			
T2 (120-240)	-	0; <-10, 1; >+10		1; >7	1; A/C to stb								

Table 3.8 (continued) : The limits corresponding to the score values evaluated by experts for navigation scenario.

Step	Tasks (secs)	Safety critical navigation task parameters							Trackkeeping task parameters				
		CPA / TCPA (nm/min) (γ_{11})	Heading ($^{\circ}$) (γ_{12})	Detection range of targets (nm) (γ_{13})	Time to response (TCPA) (γ_{14})	Comm. & true react. (γ_{15})	Identify landmarks (γ_2)	Identify hazards (γ_3)	XTE (nm) (η_1)	return to course (new heading) ($^{\circ}$) (η_2)	Turn radius (rad/nm) (η_{31})	Rudder angle ($^{\circ}$) (η_{32})	Radar (nm) (η_4)
2	T3 (240-360)	0; <+10, 1; >+10	-	-	-	-	-	-	-	-	-	-	-
	(Detroit)	0; <0.1, 0.5; 0.1-0.3, 1; >0.3	-	-	-	-	-	-	-	-	-	-	-
	(Ara)	0; <0.4, 0.5; 0.4-0.6, 1; >0.6	-	-	-	-	-	-	-	-	-	-	-
	(Olympic)	0; <2, 0.5; 2-3, 1; >3	-	-	-	-	-	-	-	-	0; S	-	-
	T4 (360-480)	0; <0.5, 0.5; 0.5-1, 1; >1	0; <+10, 1; >+10	-	-	-	-	-	-	-	1; IS	-	1; 3
	T5 (480-800)	1; >1	0; S, 1; P	-	-	-	0; out,	-	-	-	-	-	-
T6 (800-1020)	-	-	-	-	-	1; in	1; range > 0.1	-	-	-	1; IS	-	
3	T1 (0-240)	-	-	-	-	-	-	-	-	-	-	-	-
	(Triesten)	-	0; <0.5, 0.5; 0.5-1, 1; >1	-	-	-	-	0; out,	0; >0.1	-	-	-	-
	(MSC Kim)	-	0; <1, 0.5; 1-1.5, 1; >1.5	0; <3, 0.5; 3-4, 1; >4	0; NR, 1; VHF	-	1; NC	0.5; 0.05-0.1	1; <0.05	-	-	-	-
	T2 (240-300)	0; <0.3, 0.5; 0.3-0.4, 1; >0.4	-	-	-	0; A/C to stb	1; range > 0.1	-	-	-	-	-	1; 3
	T3 (300-420)	0; <0.1, 0.5; 0.1-0.5, 1; >0.5	1; <45	-	-	-	-	1; range > 0.1	-	-	0; S	-	-
	T4 (420-540)	0; <0.4, 0.5; 0.4-0.6, 1; >0.6	-	-	-	-	1; range > 0.1	-	-	1; IS	-	-	-
T5 (540-840)	-	-	-	-	1; A/C to stb	1; range > 0.1	-	-	-	-	-	-	
T6 (840-1200)	0; <0.3, 0.5; 0.3-0.5, 1; >0.5	1; >55	0; <0.5, 0.5; 0.5-1, 1; >1	1; <10s	1; A/C to stb	0; out, 1; in	-	-	-	-	-	-	
4	T1 (0-360)	-	-	-	-	-	-	0; >0.1	-	-	-	-	-
	(MSC Kim)	-	0; <0.5, 0.5; 0.5-1, 1; >1	-	-	-	-	0.5; 0.05-0.1	1; <0.05	-	-	-	-
	T2 (360-540)	-	-	-	-	-	-	-	-	-	1; IS	-	-
	(Dhonoussa)	-	0; <2, 0.5; 2-2.5, 1; >2.5	-	-	-	-	-	-	-	-	-	-
	T3 (540-800)	0; <0.2, 0.5; 0.2-0.3, 1; >0.3	-	-	1; <10s	1; A/C to stb	-	-	-	-	0; S	-	1; <3
	T4 (800-1100)	0; <0.1, 1; >0.1	-	-	-	-	1; A/C to port	-	-	1; IS	-	-	-
	T5 (1100-1250)	-	-	0; <0.6, 0.5; 0.6-0.8, 1; >0.8	-	-	1; range > 0.1	-	-	-	-	-	-
	T6 (1250-1350)	0; <0.1, 0.5; 0.1-0.2, 1; >0.2	-	-	-	1; A/C to stb	-	-	-	-	-	-	-
T7 (1350-1600)	0; <0.1, 1; >0.1	-	-	1; <10s	1; A/C to port	0; out, 1; in	1; range > 0.1	-	-	-	1; IS	-	
T8 (1600-1800)	-	-	-	-	-	0; out, 1; in	1; respon.	1; <0.05	-	-	-	-	

Table 3.9 : The evaluations of the experts for parameter weights of whole navigation scenario and the quantification of weight evaluations.

Steps	Experts	Task																																				
		Parameter																																				
		Weights of parameter																																				
		T1				T2				T3				T4				T5																				
γ_{13}	η_1	η_{31}	η_4	γ_{14}	γ_{15}	η_1	η_{31}	η_4	γ_{12}	γ_{14}	γ_{15}	η_{31}	η_4	γ_{11}	η_{31}	η_4	γ_{11}	η_2	η_{31}	η_4																		
1	Exp. 1	H	M	L	M	H	H	M	L	M	VH	VH	VH	M	M	VH	L	M	M	H	M	M																
	Exp. 2	VH	M	L	H	VH	VH	VL	H	H	VH	VH	VH	H	H	VH	H	H	VH	M	M	H																
	Exp. 3	VH	VH	H	H	VH	VH	M	H	VH	VH	VH	VH	VH	VH	VH	M	H	M	H	M	M																
	$w_{a,v}$.32	.25	.18	.25	.25	.25	.12	.17	.21	.22	.22	.22	.17	.17	.43	.25	.32	.27	.27	.22	.24																
2	Exp. 1	VH	H	L	L	H	H	H	VH	L	M	VH	H	VH	L	H	VH	H	L	M	H	H	VH	L	M	H	VH	M	M									
	Exp. 2	VH	VH	H	H	VH	VH	VH	VH	H	VH	VH	VH	VH	H	VH	VH	VH	H	VH	VH	VH	H	H	VH	M	H	H	VH									
	Exp. 3	VH	VH	H	H	VH	H	VH	VH	H	VH	VH	VH	VH	H	VH	VH	VH	H	VH	H	M	VH	H	H	VH	VH	H	VH									
	$w_{a,v}$.24	.22	.16	.16	.22	.20	.22	.23	.15	.20	.22	.21	.22	.14	.21	.29	.27	.19	.25	.21	.20	.23	.16	.20	.24	.28	.22	.26									
3	Exp. 1	VH	H	H	H	M	L	M	VH	VH	H	M	L	M	VH	H	M	L	M	H	H	L	M	VH	H	M	M	VH	M	VH	VH	VH	H	H	M			
	Exp. 2	VH	VH	VH	VH	M	H	VH	VH	VH	VH	M	H	VH	VH	VH	H	H	VH	VH	VH	H	VH	VH	VH	H	VH	VH	VH	VH	VH	VH	H	VH				
	Exp. 3	VH	VH	VH	VH	H	H	VH	VH	VH	VH	M	M	VH	VH	H	M	M	VH	VH	VH	M	VH	M	VH	M	VH	H	VH	VH	VH	VH	VH	M	VH			
	$w_{a,v}$.16	.16	.16	.16	.11	.11	.14	.20	.20	.19	.12	.12	.17	.25	.22	.16	.15	.22	.28	.28	.18	.26	.26	.28	.20	.26	.13	.12	.13	.13	.14	.13	.10	.12			
4	Exp. 1	VH	M	M	H	VH	H	M	VH	VH	VH	M	M	H	VH	M	M	VH	H	M	M	VH	H	M	M	VH	VH	VH	VH	VH	H	M	H	H	M	M	M	
	Exp. 2	VH	L	VH	VH	VH	H	VH	VH	VH	VH	H	VH	H	H	H	VH	VH	H	H	VH	VH	VH	H	VH	VH	VH	H	H	H	VH	H	VH	M	VH	VH		
	Exp. 3	VH	M	M	VH	VH	VH	VH	VH	VH	VH	VH	VH	VH	VH	VH	VH	VH	VH	VH	VH	VH	VH	VH	H	VH	VH	VH	VH	VH	VH	VH	VH	VH	VH	H	VH	VH
	$w_{a,v}$.31	.16	.23	.30	.37	.32	.31	.21	.22	.22	.17	.18	.25	.27	.23	.25	.28	.25	.23	.24	.28	.27	.21	.24	.15	.15	.15	.14	.14	.14	.13	.21	.22	.16	.21	.20	

The following equation is used to normalize the weights of the related parameter;

$$w_{\alpha,v} = \frac{w_j}{\sum w_i} \quad (3.5)$$

where w_α is the weights of safety critical navigation task parameters and w_v is the weights of trackkeeping task parameters.

Table 3.9 presents the evaluations of the experts for parameters weights of whole scenario and the quantification of weight evaluations ($w_{\alpha,v}$) as the results of the equations stated before.

Then, the performance score of the subject can be calculated with the equation 3.2 (see chapter 3.2) where γ_α is the score value for safety critical navigation tasks and η_v is the score value for trackkeeping tasks as stated with red colour in Table 3.8.

3.4.1.2 Performance measurement for cargo operation tasks

Table 3.10 represents optimum performance results of 3 experts during the trials. In a similar way with performance measurement for navigation tasks, experts set the limits for each criterion and for each specific task of steps. In this study, performances of the subjects were scored as 0 and 1 or 0, 0.5 and 1 for safety critical operation tasks and operational tasks. Table 3.11 represents the limits corresponding to the score values (stated with red colour) evaluated by experts. Subjects were evaluated according to the values stated in Table 3.11.

The cargo operation parameters were stated in Table 3.4. 3 experts scored the importance weights of each parameter for each step and for each period with fuzzy numbers just like in performance measurement for navigation tasks.

Table 3.12 presents the evaluations of the experts for parameter weights of whole scenario and the quantification of weight evaluations ($w_{\alpha,v}$) as the results of the equations stated in previous sub-chapter.

In a similar way for navigation tasks, the performance score of the subject can be calculated with the equation 3.2 (See chapter 3.2) where γ_α is the score value for safety critical operation tasks and η_v is the score value for operational tasks as stated with red colour in Table 3.11.

Table 3.10 : Cargo operation performance results of 3 experts during the trials.

Step	Task (secs)	Difficulty		Safety critical operation task parameters							Operational task parameters						
		Type and number of operations	Actual operation period	List / Trim mon. (γ1)	SF/BM mon. (γ2)	Man. press. (bar) (γ3)	Tank pressure (γ4)	Line up (γ5)	Initial rate (m ³ /h) (γ6)	Atmosphere monitoring (O ₂ conc.) (γ7)	Topping of tanks (γ8)	Ballast operation (η1)	Loading / Discharging rate (m ³ /h) (η2)	Inert. (η3)	Opr. pumps (η4)	Tank heat. (°C) (η5)	Strip. (η6)
1	T1 (0-300)	1 loading	-	0 / 0.8	62 / 72	<10	P/V val.	CC	-	-	-	-	900	-	-	-	-
	T2 (300-540)	1 loa.+ball.	-	0.2 P	62 / 72	<10	P/V val.	CC	-	-	-	5 W	900	-	2-3 j.p.	-	-
	T3 (540-600)	1 loa.+ball.	tank cha.	0.1 P	62 / 72	>10	P/V val.	CC	80	-	-	-	900	-	-	-	-
	T4 (600-900)	1 loa.+ball.	-	0 / 0.9	62 / 71	>10	P/V val.	CC	-	-	-	5 W	900	-	2-3 j.p.	-	-
2	T1 (0-120)	1 loa.+inert	-	0 / 1.2	62 / 74	<10	P/V val.	CC	-	3C < 5%	-	-	600	3C	-	-	-
	T2 (120-360)	1 loa.+inert+ball.	-	0.2 S	62 / 74	<10	P/V val.	CC	-	3C < 5%	-	5W / 9W	600	3C	2-3 j.p.	-	-
	T3 (360-720)	1 loa.+inert+ball.	tank top.	0.1 S	62 / 74	<10	P/V val.	CC	-	9W > 5%	5S 96%	5W / 9W	600	9W	2-3 j.p.	-	-
	T4 (720-840)	1 loa.+inert+ball.	top.+cha.	0	62 / 74	<10	P/V val.	CC	-	9W > 5%	9P 97%	5W / 9W	400	9W	2-3 j.p.	-	-
	T5 (840-900)	1 loa.+inert+ball.	-	0	62 / 74	<10	P/V val.	CC	-	9W < 5%	-	9W	400	9W	2-3 j.p.	-	-
	T6 (900-960)	2 loa.+inert+ball.	-	0	62 / 75	<10	P/V val.	CC+10P+3C	80	5C > 5%	-	9W/FPT	400 / 700	5C	2-3 j.p.	-	-
	T7 (960-1080)	2 loa.+inert+ball.	-	0 / 1.2	62 / 75	<10	P/V val.	CC+10P+3C	-	5C < 5%	-	FPT	400 / 700	5C	2-3 j.p.	-	-
3	T1 (0-120)	2 loa.+ball.	-	0.15S / 2.7	70 / 77	<10	P/V val.	CC+10P+3C	-	-	-	9S	400 / 700	-	2-3 j.p.	-	-
	T2 (120-300)	2 loa.+ball.	-	0.15 S	70 / 77	<10	P/V val.	CC+10P+3C	-	-	-	9S	200 / 700	-	2-3 j.p.	-	-
	T3 (300-420)	2 loa.+ball.	tank top.	0.1 S	70 / 77	<10	P/V val.	CC+10P+3C	-	-	5P 98%	9S	100 / 700	-	2-3 j.p.	-	-
	T4 (420-540)	2 loa.+ball.	tank cha.	0.1 S	70 / 77	<10	P/V val.	CC+10P+3C+5C	80	-	-	9S	100 / 700	-	2-3 j.p.	-	-
	T5 (540-600)	2 loa.+ball.	tank top.	0.1 S	71 / 77	<10	P/V val.	CC+10P+3C+5C	-	-	9S 97%	7W	700	-	2-3 j.p.	-	-
	T6 (600-780)	1 loa.+1 dis.+ball.	tank prep	0	71 / 77	<10	P/V val.	10P+3C+5C+3P	80	-	-	7W	700 / 80	-	3 j.p.	-	-
	T7 (780-1080)	1 loa.+1 dis.+ball.	tank top.	0	71 / 77	<10	P/V val.	10P+3C+5C+3P	-	-	3C 85%	7W	700 / 400	-	3 j.p.	-	-
	T8 (1080-1380)	1 loa.+1 dis.+ball.	top.+cha.	0	72 / 77	<10	P/V val.	10P+5C+3P+2P	80	-	10W 92%	7W	700 / 400	-	3 j.p.	-	-

Table 3.11 : The limits corresponding to the score values evaluated by experts for cargo operation scenario.

Step	Task (secs)	Safety critical operation task parameters								Operational task parameters					
		List / Trim mon. (γ1)	SF/BM mon. (γ2)	Man. pressure (bar) (γ3)	Tank pressure (γ4)	Line up (γ5)	Initial rate (m ³ /h) (γ6)	Atmosphere monitoring (γ7)	Topping of tanks (%) (γ8)	Ballast operation (η1)	Loading / Discharging rate (m ³ /h) (diff.) (η2)	Inerting (O ₂ conc.) (η3)	Opr. pumps (m ³ /h) (η4)	Tank heating (°C) (η5)	Stripping (η6)
1	T1 (0-300)						-	-	-	-	-	-	-	-	-
	T2 (300-540)	0; >0.4	0; >80	0; >12	0; NR	1; CC	-	-	-	0; 5S, 1; 5P	0; >20,	-	0; <250,0.5;250-300,1;>300	-	-
	T3 (540-600)	1; <0.4	1; <80	1; <12	1; C		1; <80	-	-	-	0.5;0-20,	-	-	-	-
	T4 (600-900)									0; 5P, 1; 5S	1; 0	-	0; <250,0.5;250-300,1;>300	-	-
2	T1 (0-120)						-	-	-	-	-	0;>6, 0.5;>5, 1;4-5	-	-	
	T2 (120-360)						-	-	-	0.5; 9W,	-	0;>5, 0.5;>4.5, 1;4-4.5	-	-	
	T3 (360-720)					1; CC	-	-	0;#96,1;=96	1; 5W	-	0;>6, 0.5;>5.5, 1;4-5.5	-	-	
	T4 (720-840)						-	-	0;#97,1;=97	0.5; 5W,	0; >20,	0;>6,0.5;>5.	-	-	
	T5 (840-900)	0; >0.4	0; >80	0; >12	0; NR		-	0; NR	-	1; 9W	0.5;0-20,	5,1;4-5.5	0; <250, 0.5;250-300,	-	-
	T6 (900-960)	1; <0.4	1; <80	1; <12	1; C		1; <80	1; C	-	-	1; 0	0;>6,0.5;>5.	1;>300	-	-
	T7 (960-1080)					1; CC+10P+3C	-	-	-	0.5; 9W,	-	5, 1;4-5.5	-	-	
3	T1 (0-120)						-	-	-	-	-	0;>5,0.5;>4.5	-	-	
	T2 (120-300)					1; CC+10P+3C	-	-	-	-	-	-	-	-	
	T3 (300-420)						-	-	0;#98,1;=98	1; 9S	-	0; <250,	-	-	
	T4 (420-540)	0; >0.4	0; >80	0; >12	0; NR	1; CC+10P+	1; <80	-	-	-	0; >20,	-	0.5;250-	-	-
	T5 (540-600)	1; <0.4	1; <80	1; <12	1; C	3C+5C	-	-	0;#97,1;=97	-	0.5;0-20,	-	300,	-	-
	T6 (600-780)					1; 10P+3C+	1; <80	-	-	-	1; 0	-	1;>300	-	-
	T7 (780-1080)					5C+3P	-	-	0;#85,1;=85	0; 9W,	-	-	-	-	-
	T8 (1080-1380)					1;10P+5C+3P+2P	1; <80	-	0;#92,1;=92	1; 7W	-	-	-	-	-

Table 3.12 : The evaluations of the experts for parameter weights of whole cargo operation scenario and the quantification of weight evaluations.

Steps	Experts	Task																																														
		Parameter																																														
		Weights of parameter																																														
		T1						T2						T3						T4																												
		γ_1	γ_2	γ_3	γ_4	γ_5	η_2	γ_1	γ_2	γ_3	γ_4	γ_5	η_1	η_2	η_4	γ_1	γ_2	γ_3	γ_4	γ_5	γ_6	η_2	γ_1	γ_2	γ_3	γ_4	γ_5	η_1	η_2	η_4																		
1	Exp. 1	L	VL	H	H	L	M	M	VL	H	H	L	H	M	H	L	VL	VH	M	VH	H	H	M	VL	H	H	L	H	M	H																		
	Exp. 2	L	L	M	H	VH	M	M	M	M	H	VH	H	M	VH	H	L	VH	VH	VH	H	H	M	M	H	H	H	H	M	H																		
	Exp. 3	M	M	H	H	VH	M	VH	M	H	VH	M	VH	M	VH	VH	H	VH	VH	VH	VH	H	H	M	H	H	M	H	M	H																		
	$w_{\alpha,v}$.11	.10	.20	.22	.21	.16	.12	.08	.13	.15	.11	.15	.10	.16	.12	.08	.17	.15	.17	.15	.16	.12	.08	.15	.15	.10	.15	.10	.15																		
2	Exp. 1	L	VL	H	M	L	H	M	H	M	VL	H	M	L	H	H	M	H	H	M	VL	VH	H	VH	M	VH	M	H	L	M	L	VL	M	H	VH	M	VH	L	H	L	M							
	Exp. 2	M	M	H	H	H	H	M	H	M	L	M	H	M	H	H	M	M	H	M	L	H	VH	H	H	VH	M	H	M	H	M	VL	H	H	H	M	VH	H	VH	M	H							
	Exp. 3	H	M	H	H	M	VH	H	H	VH	H	M	M	M	VH	VH	M	VH	VH	H	M	VH	VH	VH	H	VH	H	M	H	H	H	H	H	H	VH	H	VH	H	H	H								
	$w_{\alpha,v}$.10	.08	.15	.14	.12	.15	.11	.15	.09	.05	.10	.11	.08	.13	.13	.09	.10	.12	.07	.04	.11	.12	.11	.09	.13	.07	.10	.07	.09	.07	.02	.10	.11	.12	.08	.13	.08	.12	.07	.10							
3	Exp. 1	L	VL	M	H	L	VH	L	H	H	M	L	VL	H	H	VH	VH	M	M	H	M	M	L	VL	H	H	M	H	M	H	M	H	M	H	M	H	M											
	Exp. 2	M	VL	H	H	H	M	H	H	M	H	L	M	VH	VH	VH	VH	L	M	H	M	H	VL	L	M	H	M	L	L	H	L	M	L	H	L	M	L	M										
	Exp. 3	H	H	H	H	M	H	H	M	H	M	H	H	VH	VH	VH	VH	VH	H	VH	VH	M	H	H	M	M	M	H	H	M	H	M	H	M	H	M	H	M	H	M								
	$w_{\alpha,v}$.08	.03	.11	.13	.10	.11	.10	.12	.11	.11	.05	.06	.12	.12	.13	.13	.06	.07	.10	.07	.09	.04	.06	.12	.14	.11	.10	.08	.14	.10	.10	.11	.10	.08	.14	.10	.11										
3	Exp. 1	L	L	H	H	M	M	M	M	L	L	H	H	M	M	H	M	L	L	H	H	M	VH	M	H	M	L	L	H	H	VH	VH	M	H	M	L	L	H	H	M	VH	VH	M	H	M			
	Exp. 2	L	M	H	H	M	M	M	M	L	M	M	M	L	M	M	M	M	L	M	L	VH	L	M	L	L	L	M	H	H	VH	L	H	M	L	H	M	L	M	H	M	VH	VH	L	H	H		
	Exp. 3	VH	H	M	M	M	H	M	H	H	H	H	M	H	VH	H	H	H	VH	VH	M	VH	H	VH	H	H	H	VH	VH	VH	VH	H	VH	H	M	M	M	M	M	VH	VH	VH	VH	M	VH	M		
	$w_{\alpha,v}$.11	.12	.14	.14	.12	.13	.11	.13	.10	.11	.14	.14	.10	.13	.15	.13	.10	.10	.12	.13	.08	.16	.09	.13	.09	.07	.07	.12	.13	.14	.15	.09	.13	.10	.11	.10	.13	.13	.06	.10	.10						
3	Exp. 1	L	L	H	H	M	VH	H	H	M	L	L	H	H	VH	VH	M	H	H	L	L	H	H	M	VH	M	H	H	L	L	H	M	VH	VH	VH	L	M	H	L	M	H	M	VH	VH	L	H	H	
	Exp. 2	L	M	M	H	M	VH	L	L	M	M	L	VH	VH	VH	H	L	VH	H	L	L	H	H	M	VH	L	M	H	M	M	H	H	M	VH	VH	L	H	H	M	M	M	M	M	VH	VH	L	H	H
	Exp. 3	H	H	M	H	M	VH	H	H	M	M	M	VH	VH	VH	VH	H	VH	H	M	M	M	M	M	M	M	M	M	M	M	M	M	M	M	M	M	M	M	M	M	M	M	M	M	M	M	M	M
	$w_{\alpha,v}$.08	.10	.11	.13	.09	.17	.11	.11	.10	.07	.06	.13	.13	.14	.14	.08	.13	.12	.07	.07	.13	.13	.10	.17	.09	.11	.13	.07	.12	.11	.11	.13	.13	.06	.10	.10	.13	.13	.06	.10	.10						

3.4.1.3 Validation of the performance measurement method

After the completion of experiments, performances were evaluated by different experts who is an ocean- going master for navigation scenario and an ocean-going chief officer for cargo operation scenario to assess the actions “just acceptable or not”. These evaluations were matched with the performance scores. The ratio of true positive to false positive was analysed in ROC curves with the help of the thresholds set to performance score value. It was expected to assess the performances of officers with the help of the statistically significant threshold value of performance score.

A receiver operating characteristic (ROC) is a technique for evaluating classifiers based on their performance (Fawcett, 2006). Graphical plot of sensitivity (true positive rate) (Equation 3.6) is used to analyse the tendency of true positive and false positive rates (Equation 3.7).

$$\text{True positive rate} = \frac{\text{Positives correctly classified}}{\text{Total positives}} \quad (3.6)$$

$$\text{False positive rate} = \frac{\text{Negatives incorrectly classified}}{\text{Total negatives}} \quad (3.7)$$

The area under the ROC curve (AUC) is a statistical metric to show the accuracy of the classification. AUC value represents the classification performance - excellent ($AUC > 0.9$), good ($0.8 < AUC < 0.9$), fair ($0.6 < AUC < 0.8$) and failed (below 0.6) test (Singh et al., 2013).

The popular method has been used to evaluate the classification success of classifiers in stress / fatigue / drowsy levels of drivers, pilots in literature. Singh et al. (2013) used the ROC graph to evaluate the classifiers for 3-class stress levels. They matched the designated stress levels according to traffic conditions with classification results based on the subjects’ physiological data. In this study, positive, negative and hypothesized cases are stated in Table 3.13. The performance scores are calculated according to developed performance model. The “Safe” and “Risky” are the evaluations of experts and they represent the real positive and negative cases in this technique.

According to equation 3.6 and 3.7, true positive rate is a ratio of TP to TP+FN and false positive rate is a ratio of FP to FP+TN as stated in Table 3.13.

Table 3.13 : Confusion matrix of used ROC technique for validation of performance measurement method.

		Actual	
		Positive	Negative
Predicted	Positive	TP • Expert evaluation as “Safe” • Performance score above the threshold	FP • Expert evaluation as “Risky” • Performance score above the threshold
	Negative	FN • Expert evaluation as “Safe” • Performance score below the threshold	TN • Expert evaluation as “Risky” • Performance score below the threshold

3.4.2 Physiological measurement

The physiological measures and the specifications of equipment used in this study are stated below.

3.4.2.1 PPG

Optical pulse sensor of GSR (EDA) unit used in this study, measures the photoplethysmogram (PPG) signal from a finger or ear-lobe to estimate heart rate. This measurement is used to evaluate PPG signal and to convert the PPG signal to heart rate. This unit contains electronics attached a velcro cuff for finger with a cable length of 9 inch (Figure 3.11a).

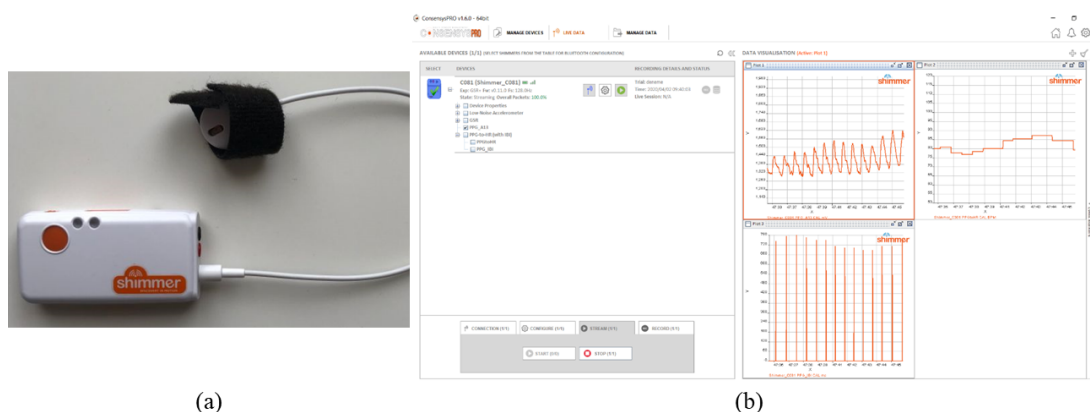


Figure 3.11 : Optical Pulse Sensor of GSR unit (a) and recording the PPG data (b).

Sampling rate of 100 Hz or greater is recommended to provide good performance in user guide. The ConsensusPRO software allows that PPG data is converted to heart rate and IBI signal (Figure 3.11b) ("Optical Pulse Sensor User Guide," 2016).

3.4.2.2 EDA

The main function of the GSR (EDA) unit is the measure galvanic skin response, also known as electro dermal activity with two reusable electrodes attached to two fingers of one hand (Figure 3.12a). By increasing skin conductance (decreasing skin resistance) in response to internal and external stimuli, the flow of electrical current between positive and negative ions becomes more rapidly.



Figure 3.12 : GSR unit (a) and recording the GSR data (b).

The unit was designed to resolve skin conductance levels from $0.2\mu\text{S}$ to $125\mu\text{S}$ ($4.7\text{M}\Omega$ to $8\text{k}\Omega$ resistance). Sampling rate of 0-5 Hz for tonic measurements with 0.03-5 Hz for phasic measurements is suggested in user guide. 2 Ag/AgCl electrodes are used. The surface area of the electrodes should be kept to a minimum; 1 cm^2 are ideal ("GSR+ User Guide," 2018).

3.4.2.3 Eye movements and eye tracking

Eye tracking headset has 1 eye camera and 1 world camera (Figure 3.13a). The sampling frequency of eye camera is 200Hz at $192\times 192\text{px}$ and this is 30Hz at 1080p , 60Hz at 720p , 120Hz at 480p for world camera (URL-1).

With the help of the headset, the gaze positions can be recorded (Figure 3.13b). Additionally, the headset has pupil detector, by setting min and max areas of pupil, and blink detection.

3.4.3 Subjective workload assessment

According to the comparison of the subjective workload assessment tools (See chapter 2.3.1), NASA Task Load Index (NASA-TLX) was chosen for this study. NASA-TLX is a multidimensional task load assessment tool, developed by Hart and Staveland

(1988). NASA-TLX has 6 sub-scales which are mental, physical and temporal loads (task related), performance and effort (behavioural and skill related) and frustration (individual related). Subjects weight the sub-scales to determine the intensity of each factor to total workload (Hart, 1986).



Figure 3.13 : Eye tracking headset (a), recording the eye movement and tracking data (b).

The explanations of sub-scales are stated in appendix B. NASA-TLX has two-step procedure. First step is comparative evaluation of the sub-scales in terms of contribution of scales to total workload. Subjects used the form (Appendix C) that consists 15 dual comparisons of 6 sub-scales by marking the sub-scale which is thought to be more dominant to other one. According to comparisons, the sub-scales are weighted from 0 to 5. In second step, subjects evaluate the sub-scales independently from 0 to 20 (Appendix B). Finally, the weighted sum of the task load assessment is found as a score between 0 and 100 (Hart, 1986).

3.5 Analysis of Data and Computerized Process

This chapter covers the transformation process which are normalization and feature extraction of the physiologic signals, the techniques used for classification of data and decision-making process.

3.5.1 Transformation process

3.5.1.1 PPG signal

For HRV feature extraction from PPG signal, there are some steps to be performed. Firstly, PPG raw data was converted to IBI signal by The ConsensusPRO software and this IBI signal was transferred to new chart for indicating the variability (Figure 3.14).

Then, Heart Rate Variability Analysis Software (HRVAS) developed by Ramshur (2010), was used to perform transformation process of IBI data in Matlab R2014a. Figure 3.15 presents the transformation process of IBI data and extraction of HRV features.

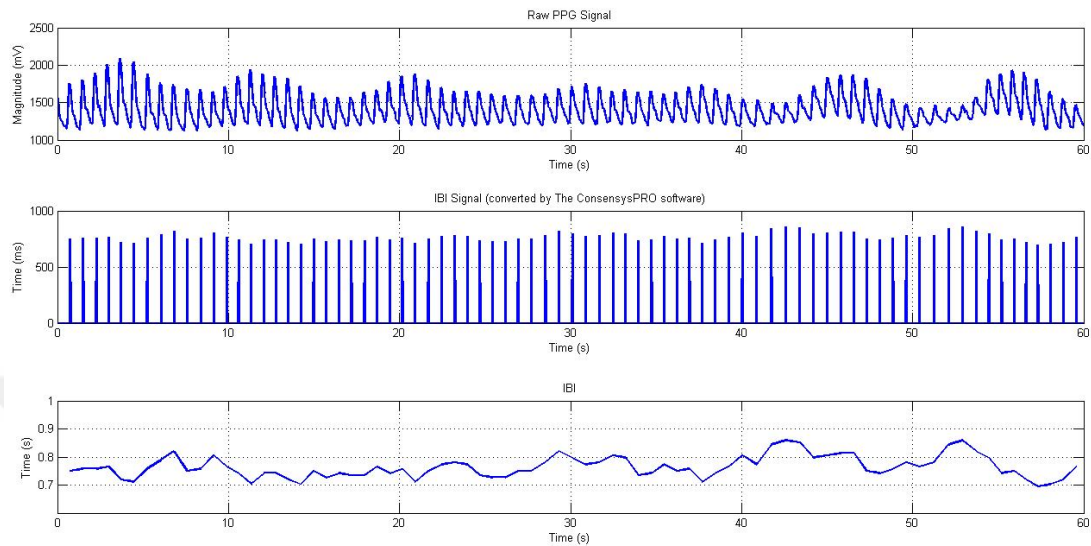


Figure 3.14 : Inter-beat interval conversion from raw PPG signal.

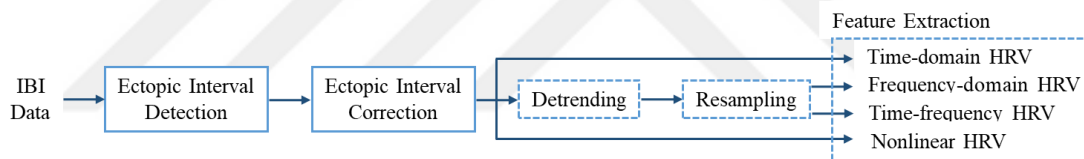


Figure 3.15 : HRV extraction from IBI data, adapted from (Ramshur, 2010).

Ectopic beats mean one or more abnormal beats on IBI signals. To detect ectopic beats, percentage filter (20%) and standard deviation (3 SD) filter were used. To correct ectopic beats, removal function was used. Detrending is used to remove low frequency trends on IBI signal. There are several methods in literature; linear, polynomial, wavelet, wavelet packet detrending and smoothing (Ramshur, 2010). In this study, wavelet detrending was implemented by using discrete wavelet transform. For signal stationary, resampling was used with linear interpolation. Figure 3.16 presents HRVAS software graphical user interface with a sample processed IBI signal analysis.

According to reviewed literature (stated in chapter 2.3.4.1), the studies where the detailed HRV measurements were conducted (Aimie-Salleh et al., 2019; Moraes et al., 2018; Ramshur, 2010; Selvaraj et al., 2008) and the contents of the HRVAS software, HRV features were extracted as stated in Table 3.14. The features were analysed in time domain, frequency domain, time-frequency and nonlinear domain.

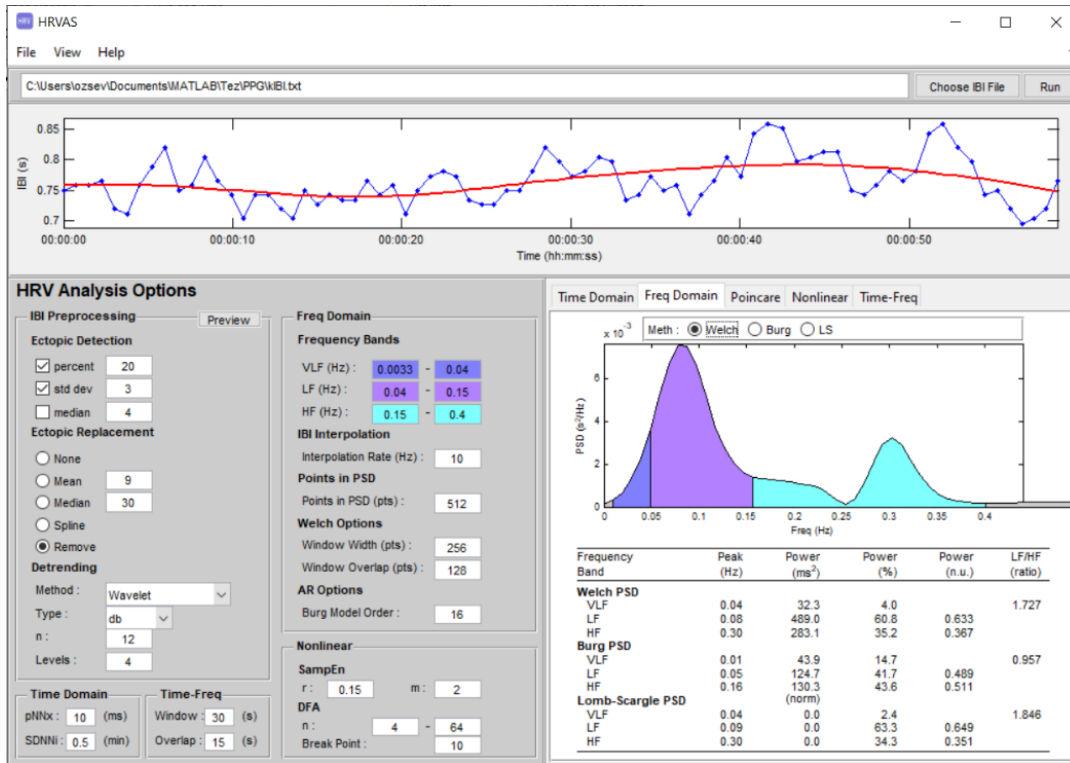


Figure 3.16 : HRVAS software graphical user interface.

Table 3.14 : Definition and description of HRV features.

Domain	Feature	Equation / Description	Abbreviation
Time-based	HR	Mean of heart rate	hrv_hr
	SDNN	Standard deviation of NN intervals	hrv_sdnnn
	RMSSD	Root mean square of the successive differences	hrv_rmssd
	pNN50	Percentage of NN50 count	hrv_pnn50
	HRVti	Integral of the density of IBI histogram divided by its height	hrv_hrvti
	TINN	The triangular interpolation of the NN interval histogram	hrv_tinn
Frequency-based (Welch Periodogram)	aLF	Absolute spectral power of low frequency (0.04-0.15 Hz)	hrv_fwalf
	aHF	Absolute spectral power of high frequency (0.15-0.4 Hz)	hrv_fwahf
	atotal	Absolute total band power	hrv_fwatotal
	pLF	Low frequency percentage of the sum of aLF and aHF	hrv_fwplf
	pHF	High frequency percentage of the sum of aLF and aHF	hrv_fwphf
	nLF	Normalized low frequency to total power	hrv_fwnlf
	nHF	Normalized high frequency to total power	hrv_fwnhf
	LF/HF	The ratio of low frequency to high frequency	hrv_fwlhfh
Frequency-based (Lomb-Scargle Periodogram)	peakLF	Peak frequency in low frequency band	hrv_fwpeaklf
	peakHF	Peak frequency in high frequency band	hrv_fwpeakhf
	aLF	Absolute spectral power of low frequency (0.04-0.15 Hz)	hrv_flself
	aHF	Absolute spectral power of high frequency (0.15-0.4 Hz)	hrv_flsahf
	atotal	Absolute total band power	hrv_flsatotal
	pLF	Low frequency percentage of the sum of aLF and aHF	hrv_flsplf
	pHF	High frequency percentage of the sum of aLF and aHF	hrv_flsphf
	nLF	Normalized low frequency to total power	hrv_flsnlf
nHF	Normalized high frequency to total power	hrv_flsnhf	
LF/HF	The ratio of low frequency to high frequency	hrv_flslhfh	
peakLF	Peak frequency in low frequency band	hrv_flspeaklf	
peakHF	Peak frequency in high frequency band	hrv_flspeakhf	

Table 3.14 (continued) : Definition and description of HRV features.

Domain	Feature	Equation / Description	Abbreviation
Time-frequency based (Wavelet transform)	aLF	Absolute spectral power of low frequency (0.04-0.15 Hz)	hrv_tfwalf
	aHF	Absolute spectral power of high frequency (0.15-0.4 Hz)	hrv_tfwahf
	atotal	Absolute total band power	hrv_tfwatotal
	pLF	Low frequency percentage of the sum of aLF and aHF	hrv_tfwplf
	pHF	High frequency percentage of the sum of aLF and aHF	hrv_tfwphf
	nLF	Normalized low frequency to total power	hrv_tfwnlf
	nHF	Normalized high frequency to total power	hrv_tfwnhf
	LF/HF	The ratio of low frequency to high frequency	hrv_tfwlfhf
	peakLF	Peak frequency in low frequency band	hrv_tfwpeaklf
	peakHF	Peak frequency in high frequency band	hrv_tfwpeakhf
Time-frequency (Lomb-Scargle Periodogram)	aLF	Absolute spectral power of low frequency (0.04-0.15 Hz)	hrv_tflsalf
	aHF	Absolute spectral power of high frequency (0.15-0.4 Hz)	hrv_tflsahf
	atotal	Absolute total band power	hrv_tflsatotal
	pLF	Low frequency percentage of the sum of aLF and aHF	hrv_tflsplf
	pHF	High frequency percentage of the sum of aLF and aHF	hrv_tflsphf
	nLF	Normalized low frequency to total power	hrv_tflsnlf
	nHF	Normalized high frequency to total power	hrv_tflsnhf
	LF/HF	The ratio of low frequency to high frequency	hrv_tflslfhf
	peakLF	Peak frequency in low frequency band	hrv_tflspeaklf
	peakHF	Peak frequency in high frequency band	hrv_tflspeakhf
Non-linear	SD1	Poincaré plot SD perpendicular the line of identity	hrv_nlsd1
	SD2	Poincaré plot standard deviation along the line of identity	hrv_nlsd2
	SampEn	Sample entropy, which measures the regularity and complexity of a time series	hrv_nlsampen
	DFA $\alpha 1$	Detrended fluctuation analysis, which describes short-term fluctuations	hrv_nlalpha1
	DFA $\alpha 2$	Detrended fluctuation analysis, which describes long-term fluctuations	hrv_nlalpha2

3.5.1.2 EDA signal

To analysis EDA raw data, there are some methods to be performed. Ledalab was used to perform these methods and feature extraction. This software is a Matlab-based software. Firstly, the data which is taken from The ConsensusPRO software, was converted as importable GSR data for Ledalab software:

```
data.conductance = Shimmer_C081_GSR_Skin_Conductance_CAL(:, :);
data.time = (1:45689)/128;
data.timeoff = 0;
data.event = [];
save('mydata', 'data')
```

Then, Ledalab was run and data was imported. Down sampling to 8 Hz (Factor 16) was carried out because of that the sampling frequency was 128 Hz with PPG measurement. After the above-mentioned steps were carried out, transformation process of EDA data was started as stated in Figure 3.17.

Butterworth-lowpass filter with 1 Hz lower cut-off frequency was implemented and artifacts were visually inspected and corrected. Then, CDA analysis was run. Figure 3.18 presents the sample CDA analysis from EDA raw data (SC data) to obtain phasic

and tonic drivers. Figure 3.19 presents the tonic and phasic EDA trends after the implementation of CDA analysis and adding event markers.

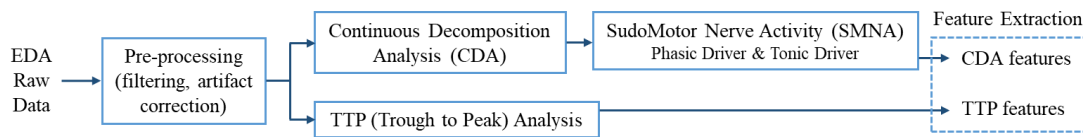


Figure 3.17 : Feature extraction from EDA raw data with different methods; CDA analysis is adapted from (Benedek and Kaernbach, 2010; Greco et al., 2014), TTP analysis is adapted from (Enewoldsen, 2016).

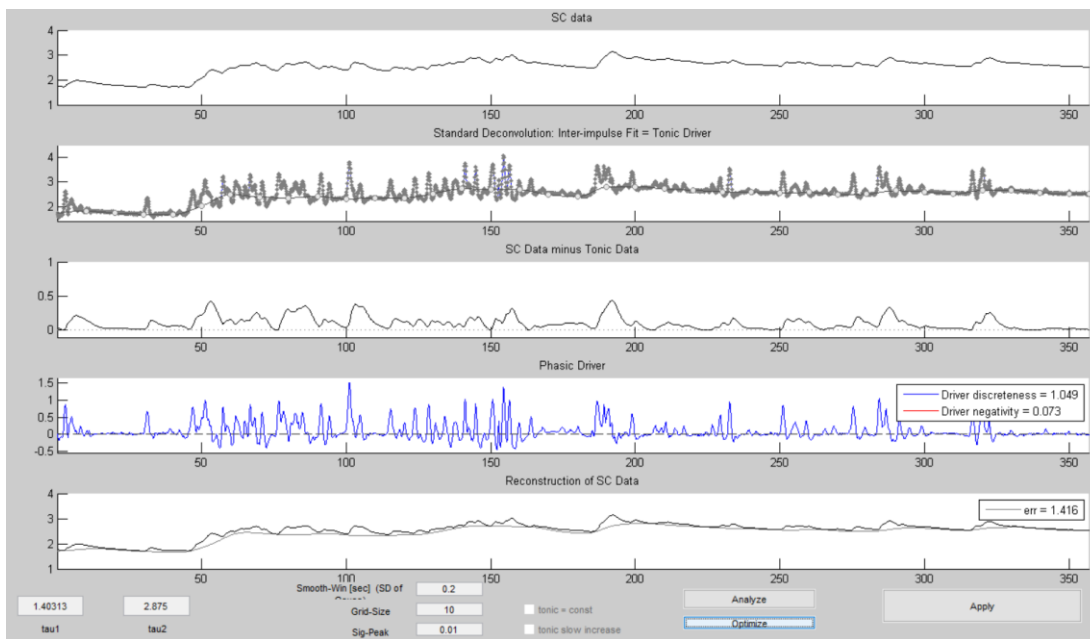


Figure 3.18 : Continuous Decomposition Analysis (CDA) for raw EDA signal.

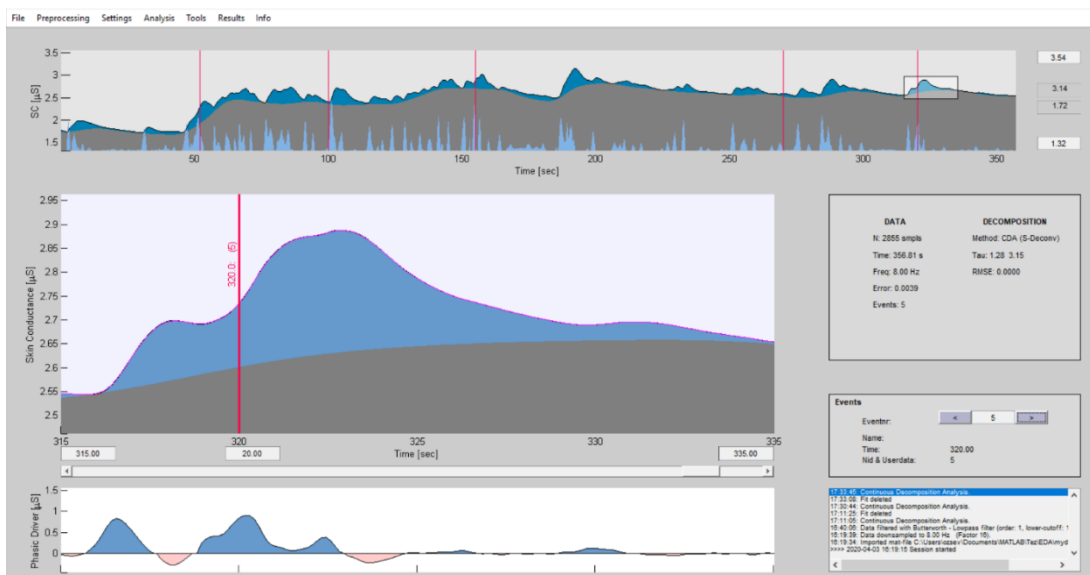


Figure 3.19 : Tonic EDA (black coloured) and phasic EDA (blue coloured) trends.

According to reviewed literature (stated in chapter 2.3.4.2) and the contents of the Ledalab software, the EDA features were extracted as stated in Table 3.15.

Table 3.15 : Definition and description of EDA features.

Feature	Equation / Description	Abbreviation
nSCR (CDA)	Number of significant SCRs within response window (wrw) according to CDA	eda_cdanscr
AmpSum (CDA)	Sum of SCR-amplitudes of significant SCRs wrw (reconvolved from corresponding phasic driver-peaks)	eda_cdaampsum
SCR (CDA)	Average phasic driver wrw. This score represents phasic activity wrw most accurately, but does not fall back on classic SCR amplitudes	eda_cdascr
ISCR (CDA)	Area (i.e., time integral) of phasic driver wrw. It equals SCR multiplied by size of response window	eda_cdaiscr
Phasic Max (CDA)	Maximum value of phasic activity wrw	eda_cdamax
Tonic (CDA)	Mean tonic activity wrw (of decomposed tonic component)	eda_cdatonic
nSCR (TTP)	Number of significant SCRs within response window (wrw) according to TTP	eda_ttpnscr
AmpSum (TTP)	Sum of SCR-amplitudes of significant SCRs wrw	eda_ttpampsum
Mean	Mean SC value within response window	eda_sc

Due to fact that there is more than one feature value within response windows (task duration for this thesis), “average” and “max” values have been extracted for the features “AmpSum (CDA)”, “SCR (CDA)”, “ISCR (CDA)”, “Phasic Max (CDA)”, “Tonic (CDA)”, “AmpSum (TTP)” and “Mean” and indicated with “a” and “m” letters at the end of the related abbreviations (e.g., eda_scra and eda_scrm). Therefore, there are totally 16 EDA features extracted.

3.5.1.3 Eye data

Data set which is imported from Pupil Core Software, includes the pupil diameter and blink data. Firstly, down sampling to 60 Hz was carried out for pupil diameter data;

```
A=load('pd.txt');
A0=downsample(A,2,0);
```

Then, according to reviewed literature (stated in chapter 2.3.4.3), the pupil diameter and blink rate features were extracted in Matlab R2014a (code is presented in Appendix K) as stated in Table 3.16.

Table 3.16 : Definition and description of pupil diameter and blink rate features.

Feature	Equation / Description	Abbreviation
Mean	Mean of pupil diameter	pd_mean
Standard deviation	Standard deviation of pupil diameter	pd_std
PerLPD	Percentage of large pupil dilation	pd_lpd
Blink rate	Blink rate as frequency	br_freq
AECD	Average eye closure duration	br_aecd
PERCLOS	Percentage of eye closure	br_perclos

3.5.1.4 Normalization of extracted features

Min-max normalization was applied in order to eliminate individual differences between the subjects and to observe the physiological change during the tasks. Following equation was performed for normalization;

$$\psi'_{j_normalized} = \frac{\psi'_{it} - \psi'_{j_min}}{\psi'_{j_max} - \psi'_{j_min}} \quad (3.8)$$

where ψ'_{j_min} and ψ'_{j_max} are the minimum and maximum values of related extracted feature within the measured data of the subject. Normalized features have been indicated with “n” letter at the beginning of the related abbreviations (e.g., n_hrv_hr).

3.5.2 Dimension reduction and/or feature selection

In total, 73 physiological features were extracted in this study. Divergence analysis (detailed in chapter 2.3.5) was performed for feature selection in Matlab R2014a:

```
for i=1:1:73
    feai=features(:,i);
    safei=feai(1:135);
    riskyi=feai(136:283);
    Bi=(mean(feai)'-(mean(safei)'))^2+(mean(feai)'-(mean(riskyi)'))^2;
    Wi=var(safei)'+var(riskyi)';
    D(i)=Bi/Wi
end
```

Additionally, to correlate the divergence values, t-test was performed for extracted features in SPSS 24. The features have a significant value is less than 0.01 were selected for classification.

3.5.3 Classification

In this study, standard feed-forward ANN code (stated in Appendix L) has been used in Matlab R2014a. While physiological features form the input layer, two task load levels form the output layer. In ANN structure, 2 hidden layers have been used, a *tansig* transfer function have been used for hidden layers. Additionally, *trainlm* training function has been used as training method. Due to small number of samples, k-fold cross-validation method has been used to examine the performance of neural network in prediction model. Data has been divided into 6 partitions. Each partition has been trained and its performance has been tested with validation data set. Best partition has been selected according to average mean square error (*MSE*) values. Partitions of the

data sets are stated in Figure 3.20 and Figure 3.21 for navigation tasks and cargo operation tasks, respectively. The number of testing and validation data corresponds to 2 subjects for each and the number of training data corresponds to 7 subjects in partitions of data set for navigation tasks (Figure 3.20). The number of testing and validation data corresponds to 1 subject for each and the number of training data corresponds to 3 subjects in partitions of data set for cargo operation tasks (Figure 3.21).

1	Testing (37)	Validation (37)	Training (129)	
2	Testing (37)	Training (132)		Validation (34)
3	Training (130)		Testing (39)	Validation (34)
4	Training (130)		Validation (39)	Testing (34)
5	Validation (37)	Training (132)		Testing (34)
6	Validation (37)	Testing (37)	Training (129)	

Figure 3.20 : Partitions of data set for navigation tasks.

1	Testing (15)	Validation (14)	Training (51)	
2	Testing (15)	Training (47)		Validation (18)
3	Training (46)		Testing (16)	Validation (18)
4	Training (46)		Validation (16)	Testing (18)
5	Validation (15)	Training (47)		Testing (18)
6	Validation (15)	Testing (14)	Training (51)	

Figure 3.21 : Partitions of data set for cargo operation tasks.

After the selection of best partition, *MSE* values of training and testing data sets corresponding to the number of neurons have been noted to determine best classification structure of ANN.

Similarly, other classification techniques (detailed in chapter 2.3.5) have been performed by using “Classification Learner” tool box of Matlab R2020a. Due to small number of samples, k-fold cross validation (6 folds) have been used for each run. Classification accuracies and AUC values of ROC curves have been noted.

Classification accuracies have been noted separately as the classification with feature selection and without feature selection for both of navigation and cargo operation tasks. These classification accuracies have been evaluated as within task classification. The samples of cargo operation tasks have been also classified with the ANN structure

formed for navigation tasks. This classification has been evaluated as cross task classification.



4. RESULTS

4.1 Analysis of Subjective Workload Assessment Results

4.1.1 NASA-TLX scores of the subjects performing navigation scenario

All subjective assessments of the subjects are presented in Appendix D. According to the Table D.1, subject ID 1,2,3,4,5,6,7,9,10,12,14 and 16 performed navigation scenario in experimental study. The NASA-TLX scores of each step evaluated by the subjects have been statistically analysed and summarized in Table 4.1. ANOVA results show that there are significant differences in the NASA-TLX scores of 5 different dimensions and in total, among 4 steps which have different task load levels, i.e., MD ($p < 0.01$), P ($p < 0.05$), TD ($p < 0.01$), E ($p < 0.01$), F ($p < 0.01$) and total ($p < 0.01$). Figure 4.1 shows the boxplots of the distribution of total scores among 4 steps.

Table 4.1 : ANOVA of NASA-TLX scores among 4 navigation steps.

	Step 1 ($M \pm SD$)	Step 2 ($M \pm SD$)	Step 3 ($M \pm SD$)	Step 4 ($M \pm SD$)	p
Mental demands	3.33 ± 2.15	10.22 ± 4.04	14.28 ± 5.71	20.03 ± 6.34	$<0.001^{**}$
Performance	5.61 ± 5.16	5.17 ± 2.94	6.89 ± 4.21	10.00 ± 5.04	0.045^*
Temporal demands	0.83 ± 1.19	6.36 ± 7.11	9.72 ± 7.21	14.53 ± 10.53	$<0.001^{**}$
Efforts	3.33 ± 2.56	6.97 ± 4.89	9.39 ± 4.89	14.72 ± 5.68	$<0.001^{**}$
Frustration	1.50 ± 1.27	6.31 ± 5.89	7.08 ± 5.23	13.75 ± 10.41	0.001^{**}
NASA-TLX score	14.61 ± 8.97	35.03 ± 16.16	47.36 ± 14.24	73.03 ± 10.20	$<0.001^{**}$

*. $p \leq 0.05$, **. $p \leq 0.01$.

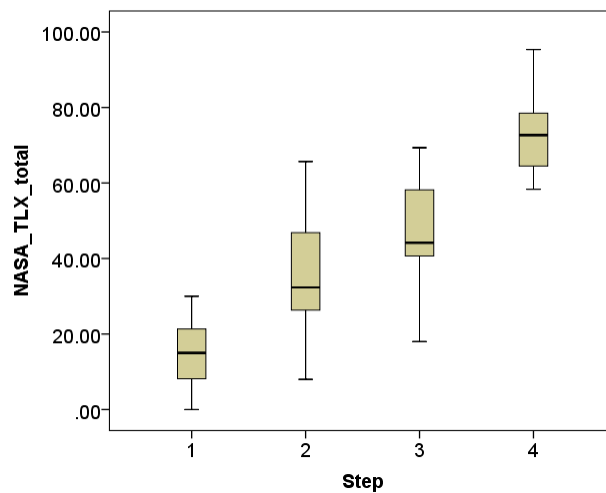


Figure 4.1 : Boxplot of NASA-TLX total scores among 4 navigation steps.

All statistical analysis of NASA-TLX assessments for navigation scenario are presented in Figure E.1 and Figure E.2 of Appendix E.

4.1.2 NASA-TLX scores of the subjects performing cargo operation scenario

According to the Table D.1, subject ID 8,11,13,15 and 17 performed cargo operation scenario in experimental study. The NASA-TLX scores of each step evaluated by the subjects have been statistically analysed and summarized in Table 4.2. ANOVA results show that there are significant differences in the NASA-TLX scores of mental demand ($p < 0.01$), temporal demand ($p < 0.05$), effort ($p < 0.01$) and in total ($p < 0.01$) among 3 steps which have different task load levels. Figure 4.2 shows the boxplots of the distribution of total scores among 3 steps.

Table 4.2 : ANOVA of NASA-TLX scores among 3 cargo operation steps.

	Step 1 ($M \pm SD$)	Step 2 ($M \pm SD$)	Step 3 ($M \pm SD$)	p
Mental demands	5.60 ± 1.74	11.93 ± 4.23	18.00 ± 3.70	<0.001**
Performance	4.60 ± 2.97	5.13 ± 2.78	4.27 ± 0.92	0.851
Temporal demands	2.93 ± 1.21	9.93 ± 4.76	16.33 ± 10.43	0.025*
Efforts	5.27 ± 2.81	11.40 ± 4.40	19.27 ± 6.49	0.002**
Frustration	4.40 ± 4.78	8.53 ± 6.69	16.93 ± 11.97	0.094
NASA-TLX score	22.80 ± 7.45	46.93 ± 10.13	74.80 ± 9.70	<0.001**

*. $p \leq 0.05$, **. $p \leq 0.01$.

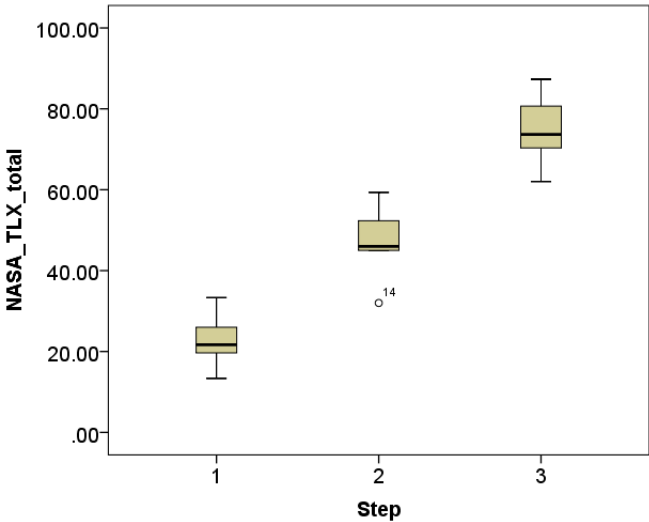


Figure 4.2 : Boxplot of NASA-TLX total scores among 3 cargo operation steps.

All statistical analysis of NASA-TLX assessments for cargo operation scenario are presented in Figure E.3 and Figure E.4 of Appendix E.

4.2 Analysis of Performance Measurement Results

4.2.1 Navigation tasks

The performances of the subjects were evaluated according to the performance parameters stated in Table 3.2 (in chapter 3) and calculated by the equation 3.4 (stated in chapter 3). Subjects performed the tasks which are detailed in Table 3.3. The performance-task load graphics of the all subjects are presented in Figure 4.3-4.14. Additionally, the weights of the performance parameters and the scores corresponding to the weights for each task and step are detailed for each subject in Appendix F.

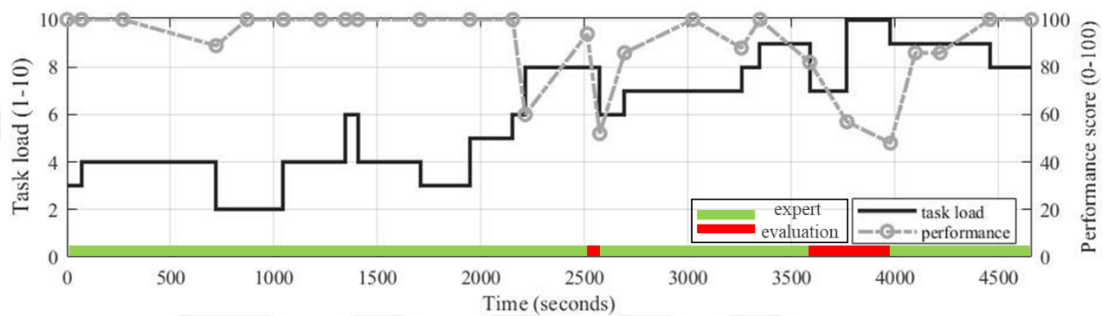


Figure 4.3 : The performance-task load graphic of subject ID 01.

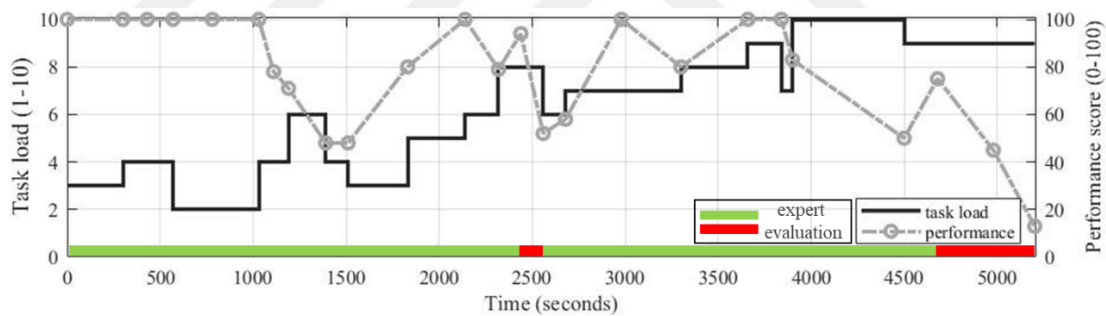


Figure 4.4 : The performance-task load graphic of subject ID 02.

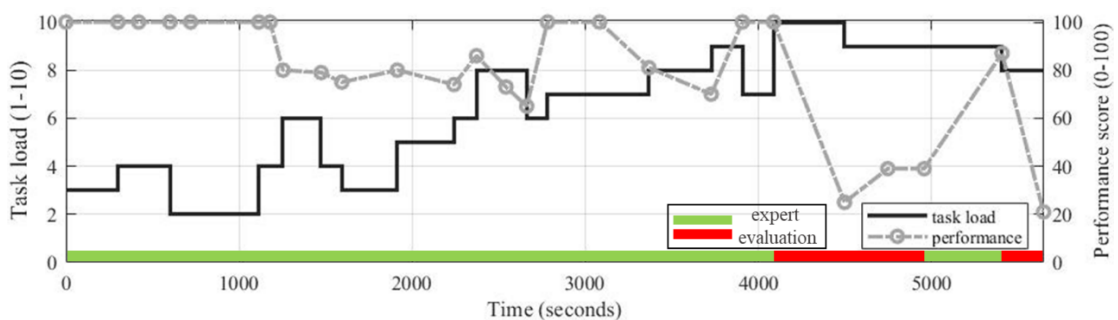


Figure 4.5 : The performance-task load graphic of subject ID 03.

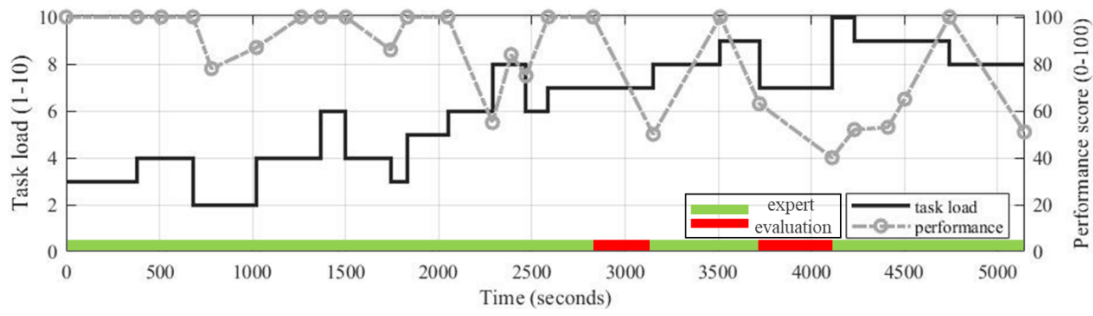


Figure 4.6 : The performance-task load graphic of subject ID 04.

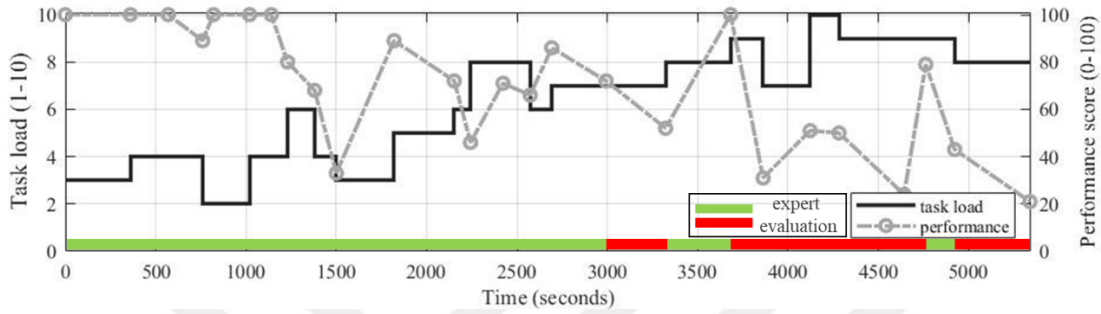


Figure 4.7 : The performance-task load graphic of subject ID 05.

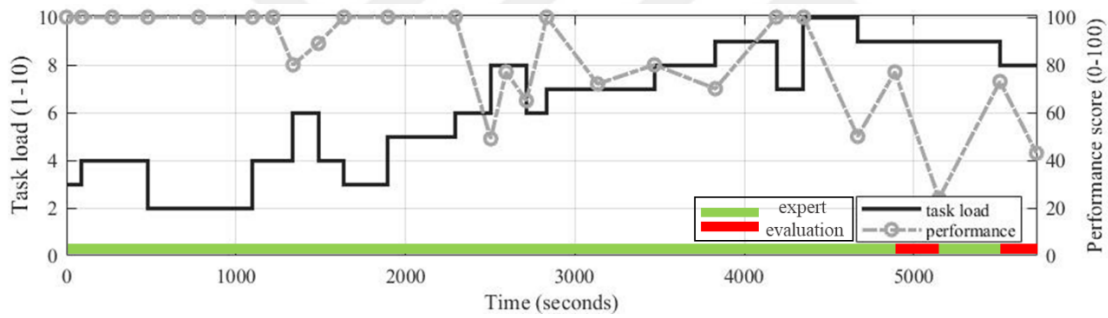


Figure 4.8 : The performance-task load graphic of subject ID 06.

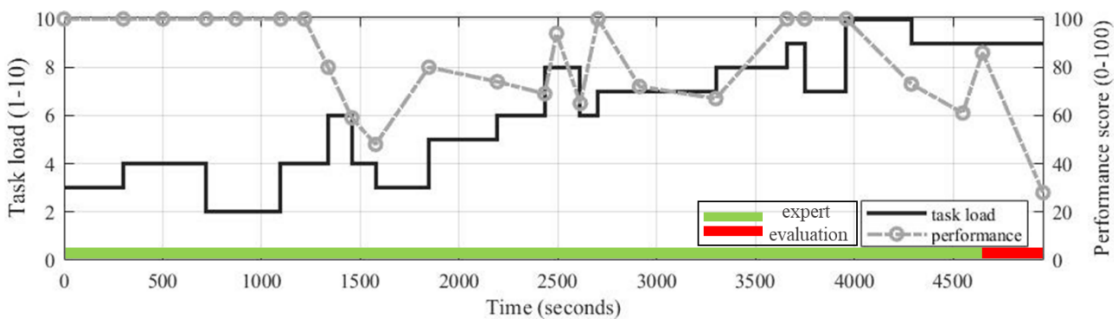


Figure 4.9 : The performance-task load graphic of subject ID 07.

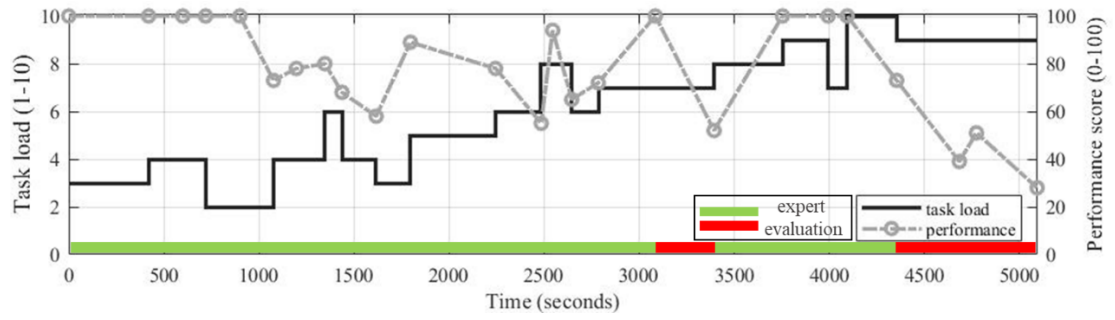


Figure 4.10 : The performance-task load graphic of subject ID 09.

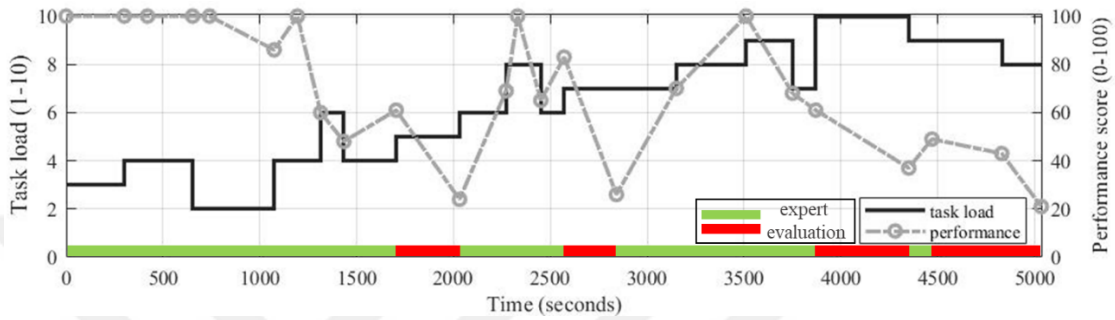


Figure 4.11 : The performance-task load graphic of subject ID 10.

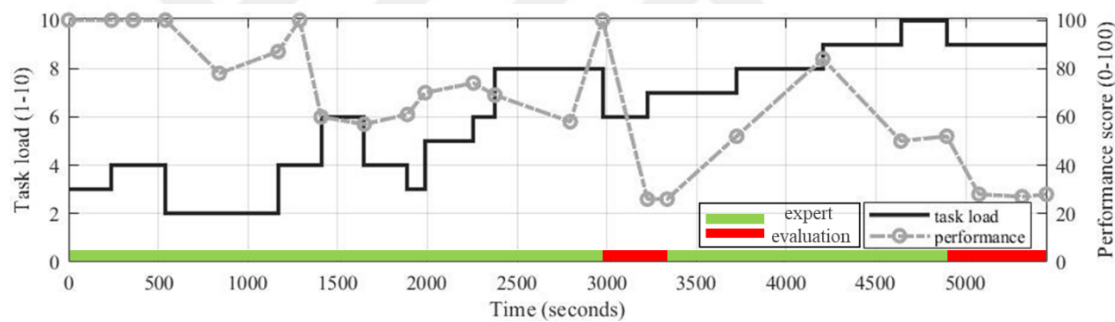


Figure 4.12 : The performance-task load graphic of subject ID 12.

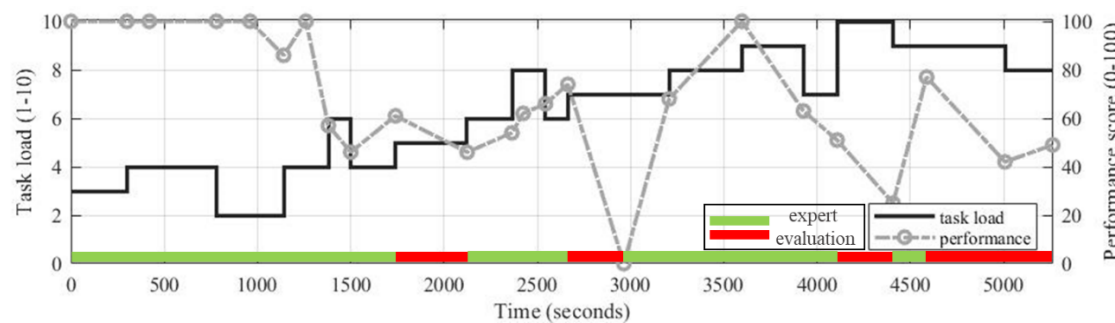


Figure 4.13 : The performance-task load graphic of subject ID 14.

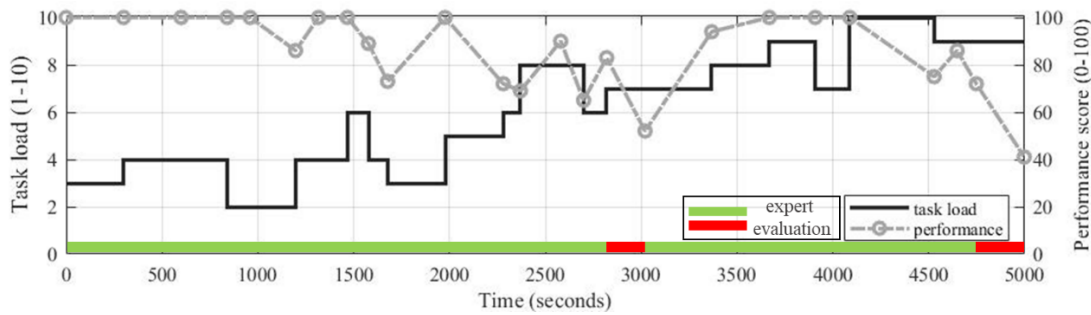


Figure 4.14 : The performance-task load graphic of subject ID 16.

Statistically, performance data show that there is a negative significant correlation between performance score and task load ($p < 0.01$). Correlation analysis are presented in Table 4.3.

Table 4.3 : Correlation between performance score and task load level for navigation tasks.

		Performance score	Task load level
Performance score	Spearman's rho Correlation	1.000	
	Sig. (1-tailed)		
Task load level	Spearman's rho Correlation	-0.485**	1.000
	Sig. (1-tailed)	<0.001	

** . Correlation is significant at the 0.01 level (1-tailed).

4.2.2 Cargo operation tasks

The performances of the subjects were evaluated according to the performance parameters stated in Table 3.4 (in chapter 3) and calculated by the equation 3.4 (stated in chapter 3). Subjects performed the tasks which are detailed in Table 3.5. The performance-task load graphics of the all subjects are presented in Figure 4.15-4.19. Additionally, the weights of the performance parameters and the scores corresponding to the weights for each task and step are detailed for each subject in Appendix F.

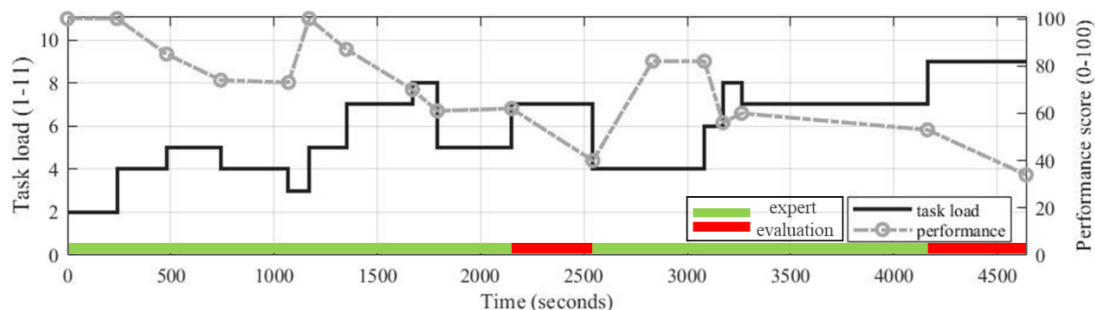


Figure 4.15 : The performance-task load graphic of subject ID 8.

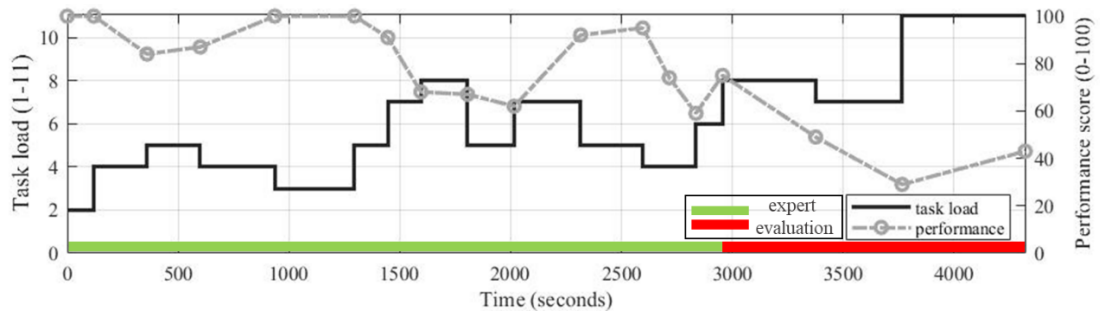


Figure 4.16 : The performance-task load graphic of subject ID 11.

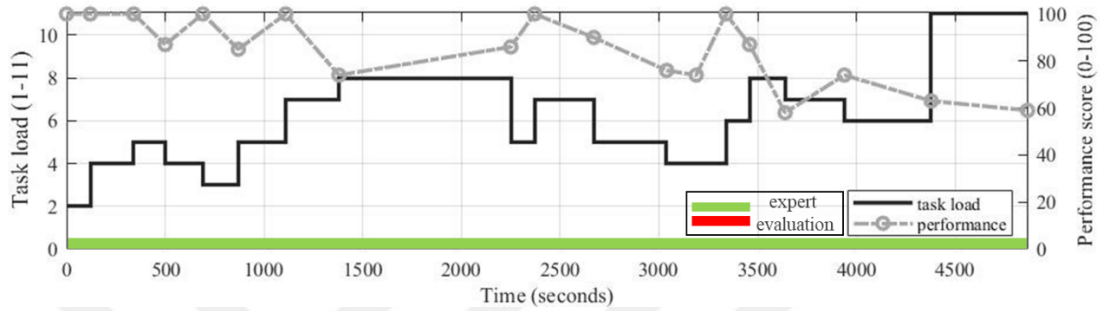


Figure 4.17 : The performance-task load graphic of subject ID 13.

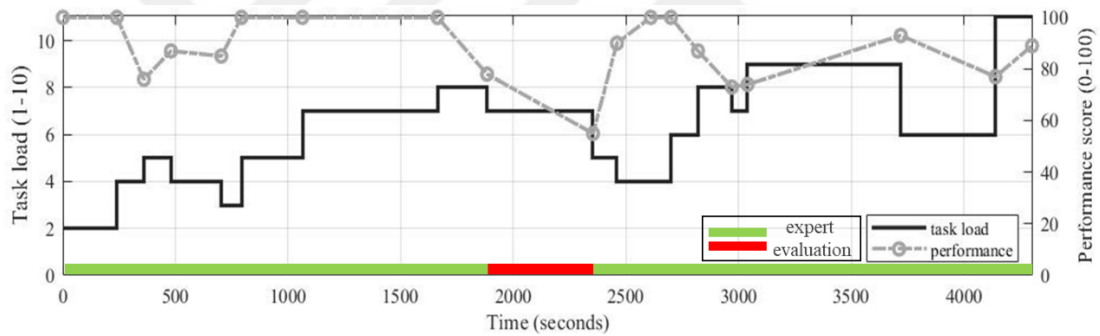


Figure 4.18 : The performance-task load graphic of subject ID 15.

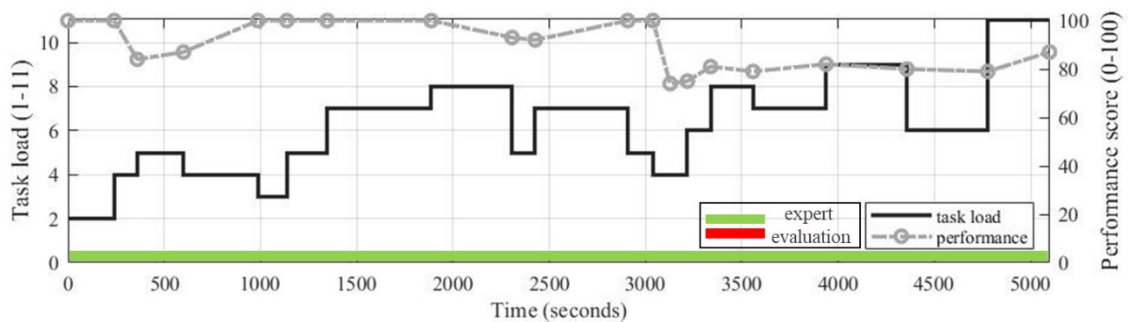


Figure 4.19 : The performance-task load graphic of subject ID 17.

Statistically, performance data show that there is a negative significant correlation between performance score and task load ($p < 0.01$). Correlation analysis are presented in Table 4.4.

Table 4.4 : Correlation between performance score and task load level for cargo operation tasks.

		Performance score	Task load level
Performance score	Spearman's rho Correlation	1.000	
	Sig. (1-tailed)		
Task load level	Spearman's rho Correlation	-0.484**	1.000
	Sig. (1-tailed)	<0.001	

** . Correlation is significant at the 0.01 level (1-tailed).

4.2.3 Validation results of performance measurement method

ROC curve analysis has been performed for validation of developed officer performance model. Recorded performances of the participants were evaluated as “safe” and “risky” for each task by one ocean going Master expert for navigation task and by one ocean going Chief Officer for cargo operation tasks. According to the analysis, the value of AUC is 0.983 ($p < 0.0001$) (Sensitivity; 92.7, Specificity; 93) and the cut-off value is 52.5 for the navigation tasks. Similarly, the value of AUC is 0.998 ($p < 0.0001$) (Sensitivity; 98.8, Specificity; 100) and the cut-off value is 55 for the cargo operation tasks.

ROC curves are stated for navigation and cargo operation tasks in Figure 4.20. Table 4.5 and Table 4.6 present the area under the curve statistics for navigation and cargo operation tasks respectively. Coordinates of the curves are detailed in Appendix G for both of tasks.

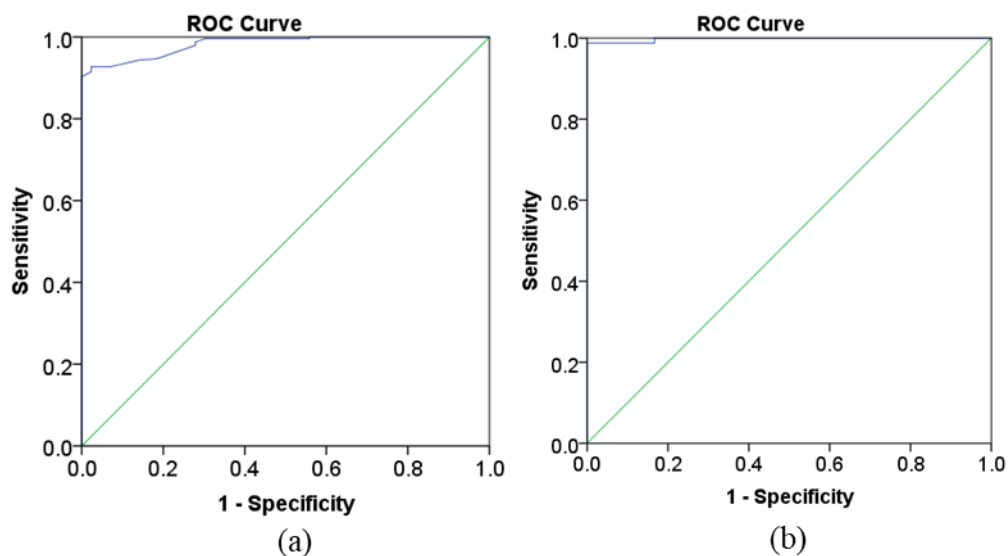


Figure 4.20 : ROC curve graphic of developed officer performance model for navigation tasks (a) and cargo operation tasks (b).

Table 4.5 : Area under the curve statistics for navigation tasks.

Area	Std. Error ^a	Asymptotic Sig. ^b	Asymptotic 95% Confidence Interval	
			Lower Bound	Upper Bound
0.983	0.006	<0.001	0.971	0.994

- a. Under the nonparametric assumption
- b. Null hypothesis: true area=0.5

Table 4.6 : Area under the curve statistics for cargo operation tasks.

Area	Std. Error ^a	Asymptotic Sig. ^b	Asymptotic 95% Confidence Interval	
			Lower Bound	Upper Bound
0.998	0.003	<0.001	0.991	1.000

- a. Under the nonparametric assumption
- b. Null hypothesis: true area=0.5

4.2.4 Determination of the red line for task load level

Performance results show that the “risky” evaluations of the experts centre upon the specific task load level. For navigation tasks, the number and percentage of “risky” evaluations become distinct where the task load level is greater than or equal to 7 (Figure 4.21). The similar distinction appears for cargo operation tasks (Figure 4.22).

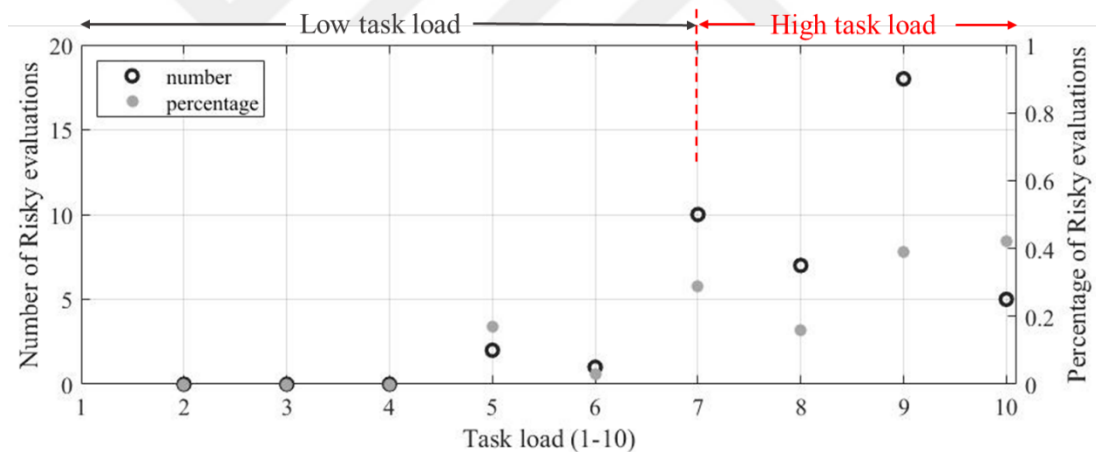


Figure 4.21 : The distinction of task load level for navigation tasks.

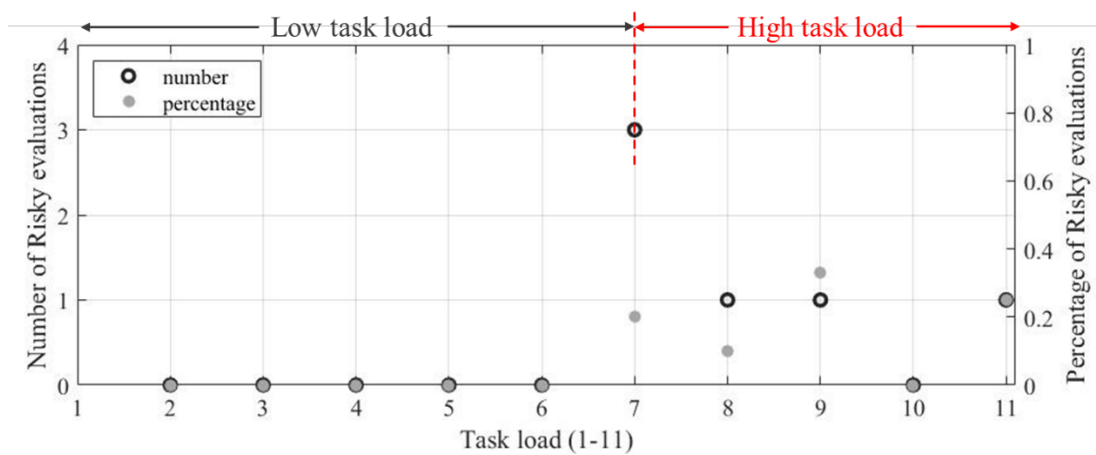


Figure 4.22 : The distinction of task load level for cargo operation tasks.

Statistically, the performance scores have been found significantly different ($t = 6.663$; $p < 0.01$) in low and high task loads for navigation tasks (Table 4.7). Similarly, the performance scores are significantly different ($t = 3.95$; $p < 0.01$) in low and high task loads for cargo operation tasks (Table 4.8).

Table 4.7 : t-Test of performance data between low and high task load for navigation tasks.

	Low task load ($M \pm SD$)	High task load ($M \pm SD$)	p
Performance score	85.19 \pm 18.692	67.43 \pm 25.235	<0.001**

** $. p \leq 0.01$.

Table 4.8 : t-Test of performance data between low and high task load for cargo operation tasks.

	Low task load ($M \pm SD$)	High task load ($M \pm SD$)	p
Performance score	86.88 \pm 12.785	71.50 \pm 19.784	<0.001**

** $. p \leq 0.01$.

4.3 Analysis of Physiological Measurement Results

In total, the measurement process has been conducted with 12 subjects in Bridge simulator and with 5 subjects in tanker simulator. Physiological measurement couldn't be done for only participant ID 12. The whole data collected during the study is stated in Appendix H. Orange colour on the column of "Participant ID" indicates the measurement conducted in tanker simulator while white colour does in bridge simulator. Yellow colour on the column of "Task No" indicates the beginning of utilizable physiological data of the subject. The stages above yellow row has been assumed as adaptation period of subject to simulator environment. If there is missing or unreliable data (shown with pink highlight) at any task of steps due to the difficulty in data collection or feature extraction, the data at the relevant task have not included in the analysis and the relevant data set is shown with grey font colour in Figure H.1. Thus, 203x73 data set as rows x column (physiological features) has been constituted for navigation tasks and 80x73 data set has been constituted for cargo operation tasks in total.

73 physiological features (stated in Figure H.1) have been extracted according to the methods which are detailed in chapter 3.5.1 of the thesis. As a part of transformation process, min-max normalization that is detailed in chapter 3.5.1.4, was performed for physiological features. Differently, the features which are pLF, pHF, nLF, nHF, nSCR

(CDA), Phasic Max (CDA), nSCR (TTP), standard deviation of pupil diameter and PerLPD have been analysed with their own values on the grounds that the related features do not differentiate between individuals or already normalized.

4.3.1 Analysis of physiological responses during navigation tasks

Physiological responses of the subjects have been often differentiated between low and high task loads. Figure 4.23 and 4.24 are examples of difference between low task load and high task load. In HRV section of the figures, it can be seen that low frequency increases while high frequency decreases in high task load. In EDA section of the figures, EDA responses are higher in high task load. Moreover, pupil diameter increases and blink rate and its features decrease in high task load. On the other hand, Figure 4.25 presents an example of difference between low performance and high performance in high task load. Although the task load level is high for both of examples compared in this figure, low frequency increases while high frequency decreases, EDA responses increase, pupil diameter increases and blink rate and its features decrease in the period where the subject has low performance scores and the action of the subject is evaluated as “Risky”.

To analyse the relation among task load, performance and physiological responses statistically, correlation analysis has been performed in SPSS 24. Significant correlations are stated in Table 4.9. It should be noted that there no whole correlations in this table. Significant and meaningful correlations are stated. Firstly, it can be seen in HRV and HR features that there is a negative significant correlation between heart rate (hrv_hr) and task load, positive significant correlation between heart rate and performance and positive significant correlation between heart rate variability (HRV features) and task load. Although, this result does not support the literature (detailed in chapter 2.3.4.1), it is stated that HRV is more sensitive than HR and whereas HRV decreases and HR increases in physical load, HRV decreases and HR has no change in mental load (Brookings et al., 1996; De Waard, 1996). Besides, it should be noted that the increase of HRV was stated in high complexity tasks for longer durations (Fairclough et al., 2005; Gao et al., 2013). The other time-based HR features (hrv_sdnn, hrv_rmssd, hrv_pnn50 and hrv_tinn) were expected to be negative correlated with heart rate according to literature that they happened.

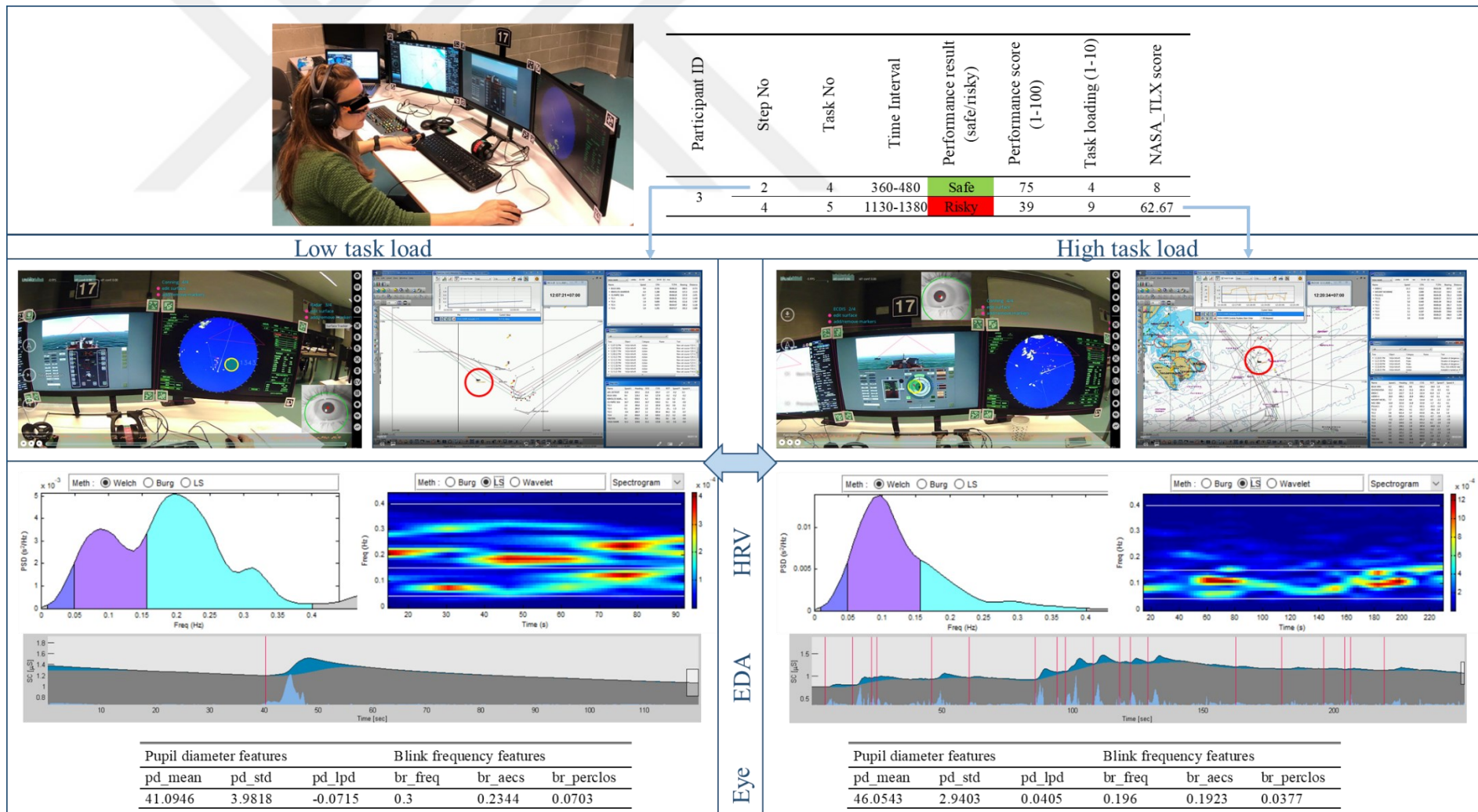


Figure 4.23 : The comparison of data between low and high task load for subject ID 03.

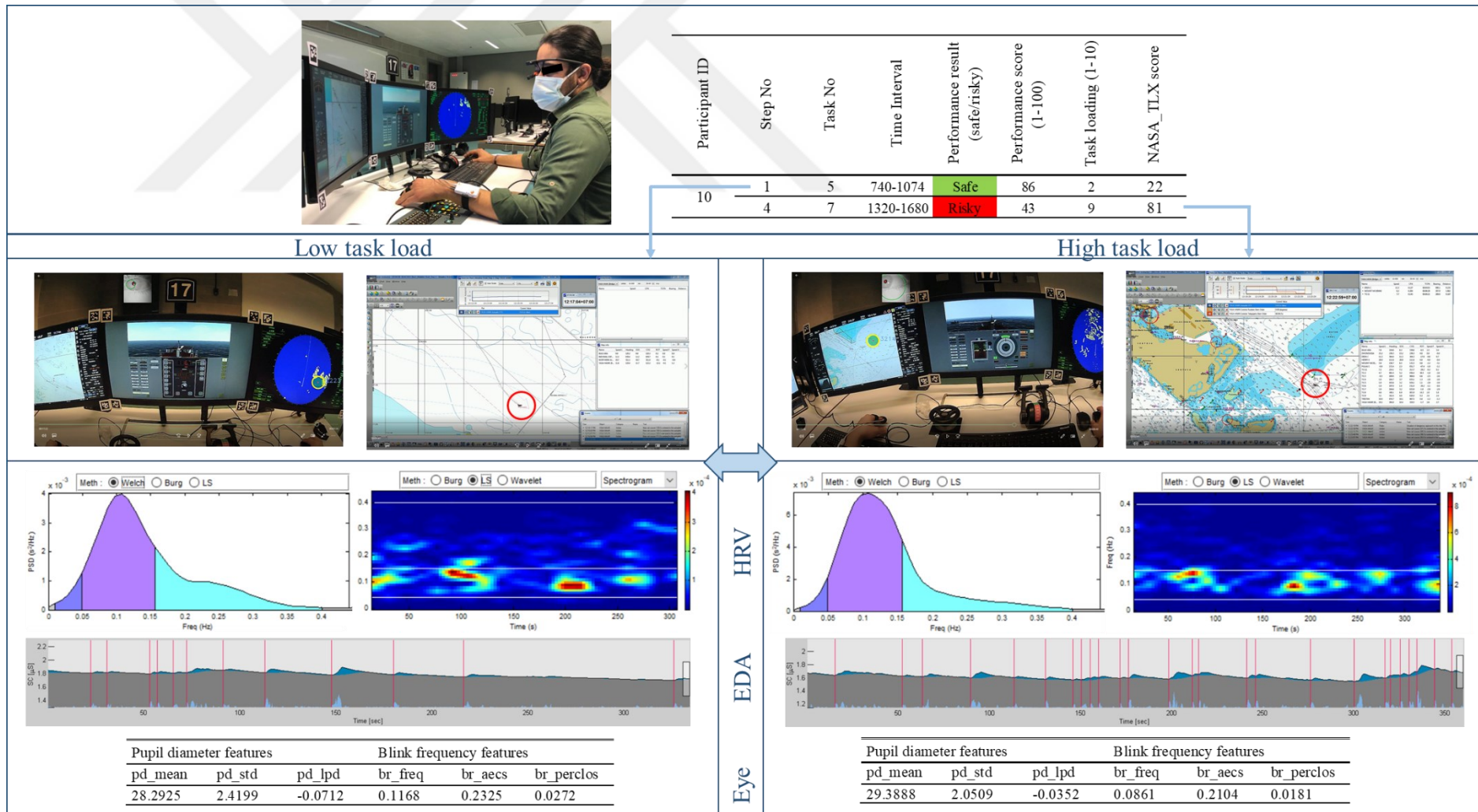


Figure 4.24 : The comparison of data between low and high task load for subject ID 10.

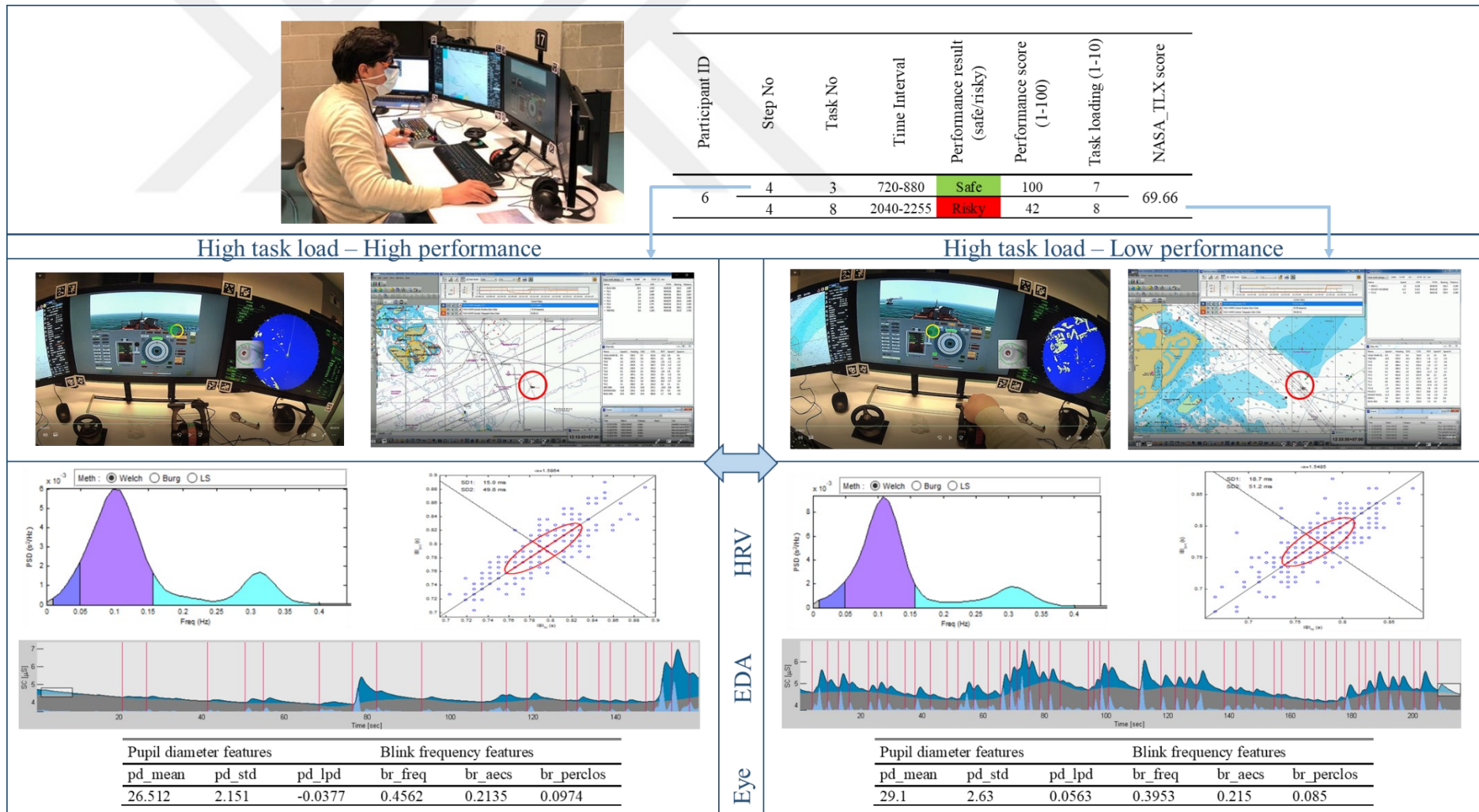


Figure 4.25 : The comparison of data between low and high performance for subject ID 06.

Table 4.9 : Correlations between task load and other measures for navigation tasks.

		performance_score	task_load	n_hrv_hr	n_hrv_sdn	n_hrv_rmssd	n_hrv_pnn50	n_hrv_tinn	n_hrv_fwalf	n_hrv_fwahf	n_hrv_fwatotal	hrv_fwplf	hrv_fwphf	n_hrv_fwlfhf	n_hrv_flsalf	n_hrv_nlsd1	n_hrv_nlsd2	n_hrv_tflsalf	n_hrv_tflsahf	n_hrv_tflsatotal
performance_score	Spearman's rho	1																		
	Sig. (2-tailed)																			
task_load	Spearman's rho		1																	
	Sig. (2-tailed)																			
n_hrv_hr	Spearman's rho	.196**	-.163*	1																
	Sig. (2-tailed)	0.005	0.020																	
n_hrv_sdn	Spearman's rho	-.203**	.215**		1															
	Sig. (2-tailed)	0.004	0.002																	
n_hrv_rmssd	Spearman's rho	-.227**	.208**			1														
	Sig. (2-tailed)	0.001	0.003																	
n_hrv_pnn50	Spearman's rho	-.215**	.233**				1													
	Sig. (2-tailed)	0.002	0.001																	
n_hrv_tinn	Spearman's rho	-.211**	.184**					1												
	Sig. (2-tailed)	0.003	0.008																	
n_hrv_fwalf	Spearman's rho	-.165*	.233**	-.207**	.708**	.667**	.629**	.275**	1											
	Sig. (2-tailed)	0.019	0.001	0.003	0.000	0.000	0.000	0.000												
n_hrv_fwahf	Spearman's rho	-.250**	.197**	-.401**	.633**	.770**	.681**	.381**	.552**	1										
	Sig. (2-tailed)	0.000	0.005	0.000	0.000	0.000	0.000	0.000	0.000											
n_hrv_fwatotal	Spearman's rho	-.201**	.229**	-.278**	.758**	.734**	.684**	.469**	.967**	.694**	1									
	Sig. (2-tailed)	0.004	0.001	0.000	0.000	0.000	0.000	0.000	0.000	0.000										
hrv_fwplf	Spearman's rho	-0.055	0.078				.148*	.213**	.285**		.164*	1								
	Sig. (2-tailed)	0.436	0.270				0.035	0.002	0.000		0.020									
hrv_fwphf	Spearman's rho	0.078	-0.085				-.142*	-.243**	-.270**		-.171*	-.973**	1							
	Sig. (2-tailed)	0.269	0.230				0.043	0.000	0.000		0.015	0.000								
n_hrv_fwlfhf	Spearman's rho	0.005	0.102		.251**			.254**	.543**		.423**	.284**	-.243**	1						
	Sig. (2-tailed)	0.946	0.149		0.000			0.000	0.000		0.000	0.000	0.000							
n_hrv_flsalf	Spearman's rho		.145*		.232**	.214**	.169*								1					
	Sig. (2-tailed)		0.039		0.001	0.002	0.016													
n_hrv_nlsd1	Spearman's rho	-.229**	.206**	-.462**	.683**	1.000**	.896**	.421**	.663**	.770**	.730**				.215**	1				
	Sig. (2-tailed)	0.001	0.003	0.000	0.000	0.000	0.000	0.000	0.000	0.000	0.000				0.002					
n_hrv_nlsd2	Spearman's rho	-.204**	.220**	-.164*	.996**	.644**	.618**	.624**	.697**	.610**	.743**			.263**	.231**		1			
	Sig. (2-tailed)	0.003	0.002	0.020	0.000	0.000	0.000	0.000	0.000	0.000	0.000			0.000	0.001	0.022				
n_hrv_tflsalf	Spearman's rho	-.162*	.247**	-.211**	.729**	.644**	.597**	.494**								.639**	.721**	1		
	Sig. (2-tailed)	0.021	0.000	0.002	0.000	0.000	0.000	0.000								0.000	0.000			
n_hrv_tflsahf	Spearman's rho	-.237**	.215**	-.379**	.673**	.762**	.666**	.390**								.760**	.646**	.644**	1	
	Sig. (2-tailed)	0.001	0.002	0.000	0.000	0.000	0.000	0.000								0.000	0.000	0.000		
n_hrv_tflsatotal	Spearman's rho	-.190**	.241**	-.292**	.761**	.711**	.639**	.485**								.707**	.748**	.967**	.782**	1
	Sig. (2-tailed)	0.007	0.001	0.000	0.000	0.000	0.000	0.000								0.000	0.000	0.000	0.000	

Table 4.9 (continued) : Correlations between task load and other measures for navigation tasks.

		performance_score	task_load	n_hrv_hr	n_hrv_sdmn	n_hrv_rmssd	n_hrv_pnn50	n_hrv_tinn	n_hrv_fwalf	n_hrv_fwahf	n_hrv_fwatotal	hrv_fwplf	hrv_fwphf	n_hrv_fwlfhf	n_hrv_flsalf	n_hrv_nlsdl	n_hrv_nlsd2	n_hrv_tflsalf	n_hrv_tflsahf	n_hrv_tflsatotal
n_hrv_tfwalf	Spearman's rho	-.158*	.253**	-.186**	.740**	.677**	.650**	.474**												
	Sig. (2-tailed)	0.024	0.000	0.008	0.000	0.000	0.000	0.000												
n_hrv_tfwahf	Spearman's rho	-.229**	.224**	-.348**	.649**	.756**	.660**	.396**												
	Sig. (2-tailed)	0.001	0.001	0.000	0.000	0.000	0.000	0.000												
n_hrv_tfwatotal	Spearman's rho	-.180*	.252**	-.246**	.765**	.736**	.687**	.474**												
	Sig. (2-tailed)	0.010	0.000	0.000	0.000	0.000	0.000	0.000												
eda_cdanscr	Spearman's rho					.189**	.248**					.509**	-.506**							
	Sig. (2-tailed)					0.007	0.000					0.000	0.000							
n_eda_cdaampsuma	Spearman's rho						.157*							.168*						
	Sig. (2-tailed)						0.025							0.050	0.017					
n_eda_cdaampsumm	Spearman's rho													-.177*						
	Sig. (2-tailed)													0.011						
n_eda_cdascra	Spearman's rho					.145*	.197**				.139*			.161*			.145*			
	Sig. (2-tailed)					0.039	0.005				0.048			0.021			0.039			
n_eda_cdascrm	Spearman's rho			-.150*				.182**						.181**						
	Sig. (2-tailed)			0.033				0.010						0.010						
n_eda_cdaiscra	Spearman's rho					.145*	.197**				.139*			.161*			.145*			
	Sig. (2-tailed)					0.039	0.005				0.048			0.021			0.039			
n_eda_cdaiscrm	Spearman's rho			-.150*				.182**						.181**						
	Sig. (2-tailed)			0.033				0.010						0.010						
n_eda_cdamaxa	Spearman's rho													.153*	.162*					
	Sig. (2-tailed)													0.030	0.021					
eda_cdamaxm	Spearman's rho			-.141*								.209**	-.261**							
	Sig. (2-tailed)			0.045								0.003	0.000							
n_eda_cdatonica	Spearman's rho		.157*				.164*			.151*										
	Sig. (2-tailed)		0.025				0.019			0.031										
n_eda_cdatonicm	Spearman's rho		.154*		.144*		.171*	.172*												.146*
	Sig. (2-tailed)		0.028		0.040		0.015	0.014												0.037
n_eda_sca	Spearman's rho		.152*		.153*		.167*	.143*		.149*										.156*
	Sig. (2-tailed)		0.030		0.029		0.017	0.042		0.033										0.026
n_eda_scm	Spearman's rho		.154*		.161*		.209**	.154*							.167*					.161*
	Sig. (2-tailed)		0.028		0.022		0.003	0.028							0.017					0.022
n_pd_mean	Spearman's rho	-.165*			.208**	.169*	.140*	.150*	.175*	.143*							.172*	.213**		.175*
	Sig. (2-tailed)	0.019			0.003	0.016	0.046	0.033	0.012	0.042							0.014	0.002		0.013
pd_std	Spearman's rho				.204**													.189**		
	Sig. (2-tailed)				0.004													0.007		
pd_lpd	Spearman's rho		.158*			.166*	.179*		.155*								.172*			
	Sig. (2-tailed)		0.025			0.018	0.011		0.028								0.014			

Table 4.9 (continued) : Correlations between task load and other measures for navigation tasks.

		n_hrv_tfwalf	n_hrv_tfwahf	n_hrv_tfwatotal	eda_cdanscr	n_eda_cdaampsuma	n_eda_cdaampsumm	n_eda_cdascra	n_eda_cdascrm	n_eda_cdaisera	n_eda_cdaiscrm	n_eda_cdamaxa	eda_cdamaxm	n_eda_cdatonica	n_eda_cdatonicm	n_eda_sca	n_eda_scm	n_pd_mean	pd_std	pd_lpd
n_hrv_tfwalf	Spearman's rho Sig. (2-tailed)	1																		
n_hrv_tfwahf	Spearman's rho Sig. (2-tailed)	.581** 0.000	1																	
n_hrv_tfwatotal	Spearman's rho Sig. (2-tailed)	.969** 0.000	.709** 0.000	1																
eda_cdanscr	Spearman's rho Sig. (2-tailed)				1															
n_eda_cdaampsuma	Spearman's rho Sig. (2-tailed)					1														
n_eda_cdaampsumm	Spearman's rho Sig. (2-tailed)						1													
n_eda_cdascra	Spearman's rho Sig. (2-tailed)							1												
n_eda_cdascrm	Spearman's rho Sig. (2-tailed)								1											
n_eda_cdaisera	Spearman's rho Sig. (2-tailed)									1										
n_eda_cdaiscrm	Spearman's rho Sig. (2-tailed)										1									
n_eda_cdamaxa	Spearman's rho Sig. (2-tailed)											1								
eda_cdamaxm	Spearman's rho Sig. (2-tailed)												1							
n_eda_cdatonica	Spearman's rho Sig. (2-tailed)													1						
n_eda_cdatonicm	Spearman's rho Sig. (2-tailed)														1					
n_eda_sca	Spearman's rho Sig. (2-tailed)															1				
n_eda_scm	Spearman's rho Sig. (2-tailed)																1			
n_pd_mean	Spearman's rho Sig. (2-tailed)		.168* 0.017	.149* 0.034										.180* 0.010	.170* 0.015	.157* 0.026	.152* 0.031	1		
pd_std	Spearman's rho Sig. (2-tailed)				-.298** 0.000														1	
pd_lpd	Spearman's rho Sig. (2-tailed)					.311** 0.000								.261** 0.000	.268** 0.000	.237** 0.001	.255** 0.000			1

Table 4.9 (continued) : Correlations between task load and other measures for navigation tasks.

		performance_score	task_load	n_hrv_hr	n_hrv_sdmn	n_hrv_rmssd	n_hrv_pnn50	n_hrv_tinn	n_hrv_fwalf	n_hrv_fwahf	n_hrv_fwatotal	hrv_fwplf	hrv_fwphf	n_hrv_fwlfhf	n_hrv_flsalf	n_hrv_nlsd1	n_hrv_nlsd2	n_hrv_tflsalf	n_hrv_tflsahf	n_hrv_tflsatal
n_br_freq	Spearman's rho				.192**	.176*	.167*		.230**		.205**			.212**		.173*	.182**	.204**	.155*	.196**
	Sig. (2-tailed)				0.006	0.012	0.018		0.001		0.003			0.002		0.013	0.009	0.004	0.027	0.005
n_br_aecd	Spearman's rho	.167*	-.218**									-.191**	.194**	.162*						
	Sig. (2-tailed)	0.017	0.002									0.006	0.005	0.021						
n_br_perclos	Spearman's rho							.175*			.139*			.225**						
	Sig. (2-tailed)		0.022					0.013			0.048			0.001						

Table 4.9 (continued) : Correlations between task load and other measures for navigation tasks.

		n_hrv_tfwalf	n_hrv_tfwahf	n_hrv_tfwatotal	eda_cdanscr	n_eda_cdaampsuma	n_eda_cdaampsumm	n_eda_cdasra	n_eda_cdasrmm	n_eda_cdaiscra	n_eda_cdaiscrm	n_eda_cdamaxa	eda_cdamaxm	n_eda_cdatonica	n_eda_cdatoniem	n_eda_sca	n_eda_scm	n_pd_mean	pd_std	pd_lpd
n_br_freq	Spearman's rho	.215**		.189**		.183**	.181**	.299**	.160*	.299**	.160*	.231**	.222**							
	Sig. (2-tailed)	0.002		0.007		0.009	0.010	0.000	0.023	0.000	0.023	0.001	0.001							-.147*
n_br_aecd	Spearman's rho		-.143*			.203**		.217**	.168*	.217**	.168*	.246**	.140*							
	Sig. (2-tailed)		0.042			0.004		0.002	0.016	0.002	0.016	0.000	0.046							-.203**
n_br_perclos	Spearman's rho					.223**	.178*	.313**	.190**	.313**	.190**	.258**	.254**							
	Sig. (2-tailed)					0.001	0.011	0.000	0.007	0.000	0.007	0.000	0.000							-.259**
																				0.000
																				0.039
																				0.007
																				-.167*
																				0.017

Despite of the time-based HRV features, the frequency-based and time-frequency HRV features have been found to be more meaningful according to literature. Although absolute spectral powers of LF and HF (hrv_fwalf, hrv_fwahf, hrv_fwatotal, n_hrv_flsalf, hrv_tflsalf, hrv_tflsahf, hrv_tflsatotal, hrv_tfwalf, hrv_tfwahf, hrv_tfwatotal) increase together, the percentage of LF (hrv_fwplf) increases and the percentage of HF (hrv_fwphf) decreases when task load increases. The increase of LF/HF (hrv_fwlhfh) together with the increase of LF and the decrease of HF is significantly correlated with the increase of EDA responses (eda_cdaampsuma, eda_cdascra, eda_cdascrm, eda_cdaiscra, n_eda_cdaiscrm, eda_cdamaxa) that this situation occurs in high task load according to literature.

From non-linear HRV features, nlsd2 (Poincaré plot standard deviation along the line of identity) has been found highly positive correlated with task load and negative correlated with performance score. It is also significantly correlated with LF/HF and EDA responses that nlsd2 increases together with other MWL measures when task load increases. This result supports the literature (Martin et al., 2016).

Some EDA features (eda_cdatonica, eda_cdatonicm, eda_sca, eda_scm) are significantly correlated with task load that EDA response increases when task load increases. Additionally, some EDA features (eda_cdaampsuma, eda_cdascra, eda_cdascrm, eda_cdaiscra, eda_cdaiscrm, eda_cdamaxa) which are the components of the phasic activity, have been found positive significantly correlated with LF/HF (hrv_fwlhfh) that increases by the increase of MWL. These results also support the literature (See chapter 2.3.4.2).

Some eye responses have been significant in this study. Large pupil dilation (pd_lpd) is positive correlated with task load. Additionally, the mean of pupil diameter (pd_mean) and large pupil dilation (pd_lpd) have been found positive significantly correlated with some time-based HRV features (hrv_sdn, hrv_rmssd, hrv_pnn50, hrv_tinn), non-linear HRV features (hrv_nlsd1, hrv_nlsd2) and EDA features (eda_cdatonica, eda_cdatonicm, eda_sca, eda_scm). These results support the literature on the grounds that pupil diameter increases when MWL increases (See chapter 2.3.4.3). The features of blink rate (br_aecd, br_perclos) are negative significantly correlated with task load and LF (hrv_fwplf). br_aecd is also positive significantly correlated with HF. This result support the literature that eye blink interval is longest and blink duration is shortest in high MWL (See chapter 2.3.4.4). However, this correlation is not meaningful on the positive significant correlation between blink rate features and LF/HF (hrv_fwlhfh). Because, this correlation is expected

to be negative on the grounds that LF/HF increases when MWL increase. On the other hand, blink rate features have been found positive significantly correlated with EDA features (eda_cdaampsuma, eda_cdaampsumm, eda_cdascra, eda_cdascra, eda_cdascrm, eda_cdaiscra, eda_cdaiscrm, eda_cdamaxa, eda_cdamaxm) that blink frequency increases under stressful conditions according to literature (Alberdi et al., 2016; Sharma and Gedeon, 2012). It should be noted that EDA response is more observable in stressful conditions.

Statistically, 40 physiological features in total have been found significantly different in low and high task loads for navigation tasks (Table 4.10). Whole SPSS *t*-Test output is stated in Appendix I.

Table 4.10 : *t*-Test of physiological data between low and high task load for navigation tasks.

	Low task load (<i>M</i> ± <i>SD</i>)	High task load (<i>M</i> ± <i>SD</i>)	<i>p</i>
n_hrv_hr	0.551 ± 0.294	0.432 ± 0.269	0.003**
n_hrv_sdn	0.417 ± 0.271	0.545 ± 0.255	0.001**
n_hrv_rmssd	0.390 ± 0.268	0.479 ± 0.247	0.015*
n_hrv_pnn50	0.305 ± 0.289	0.414 ± 0.287	0.008**
n_hrv_tinn	0.419 ± 0.288	0.541 ± 0.276	0.003**
n_hrv_fwalf	0.351 ± 0.268	0.486 ± 0.267	<0.001**
n_hrv_fwahf	0.344 ± 0.260	0.446 ± 0.264	0.007**
n_hrv_fwatotal	0.360 ± 0.262	0.490 ± 0.264	0.001**
hrv_fwplf	61.28 ± 14.68	65.14 ± 11.20	0.042*
hrv_fwphf	34.31 ± 16.32	29.82 ± 12.74	0.035*
hrv_fwnlf	0.644 ± 0.163	0.688 ± 0.128	0.038*
hrv_fwnhf	0.356 ± 0.163	0.312 ± 0.128	0.038*
n_hrv_fwpeaklf	0.551 ± 0.317	0.452 ± 0.260	0.018*
n_hrv_flsalf	0.444 ± 0.264	0.547 ± 0.278	0.008**
hrv_flsphf	34.65 ± 16.25	30.43 ± 13.61	0.046*
hrv_flsnlf	0.651 ± 0.162	0.692 ± 0.136	0.048*
hrv_flsnhf	0.349 ± 0.162	0.308 ± 0.136	0.048*
n_hrv_nlsd1	0.390 ± 0.268	0.477 ± 0.246	0.017*
n_hrv_nlsd2	0.413 ± 0.268	0.545 ± 0.256	<0.001**
n_hrv_tflsalf	0.337 ± 0.261	0.474 ± 0.273	<0.001**
n_hrv_tflsahf	0.365 ± 0.295	0.475 ± 0.268	0.006**
n_hrv_tflsatotal	0.357 ± 0.261	0.492 ± 0.273	<0.001**
hrv_tflsplf	59.73 ± 14.50	63.67 ± 11.39	0.037*
hrv_tflsphf	37.03 ± 15.65	32.61 ± 12.38	0.031*
hrv_tflsnlf	0.619 ± 0.157	0.663 ± 0.124	0.034*
hrv_tflsnhf	0.381 ± 0.157	0.337 ± 0.124	0.034*
n_hrv_tflslfhf	0.418 ± 0.260	0.506 ± 0.266	0.020*
n_hrv_tfalf	0.362 ± 0.275	0.522 ± 0.284	<0.001**
n_hrv_tfahf	0.361 ± 0.275	0.488 ± 0.270	0.001**
n_hrv_tfwatotal	0.381 ± 0.270	0.538 ± 0.287	<0.001**

*. *p* ≤ 0.05; **. *p* ≤ 0.01.

Table 4.10 (continued) : t-Test of physiological data between low and high task load for navigation tasks.

	Low task load ($M \pm SD$)	High task load ($M \pm SD$)	p
hrv_tfwplf	63.75 ± 15.81	68.26 ± 12.85	0.031*
hrv_tfwphf	35.90 ± 15.99	31.33 ± 13.06	0.031*
hrv_tfwnlf	0.640 ± 0.160	0.686 ± 0.130	0.031*
hrv_tfwnhf	0.360 ± 0.160	0.314 ± 0.130	0.031*
n_eda_cdatonica	0.484 ± 0.320	0.572 ± 0.304	0.046*
n_eda_cdatonicm	0.481 ± 0.307	0.570 ± 0.283	0.035*
n_eda_scm	0.474 ± 0.308	0.570 ± 0.283	0.022*
pd_lpd	0.002 ± 0.053	0.031 ± 0.078	0.002**
n_br_aecd	0.494 ± 0.332	0.338 ± 0.285	0.001**
n_br_perclos	0.456 ± 0.275	0.380 ± 0.262	0.045*

*. $p \leq 0.05$; **. $p \leq 0.01$.

4.3.2 Analysis of physiological responses during cargo operation tasks

Physiological responses of the subjects have been often differentiated between low and high task loads in cargo operation tasks same as in navigation tasks. Figure 4.26 is an example of difference between low task load and high task load. In HRV section of the figures, it can be seen that low frequency increases while high frequency decreases in high task load. In EDA section of the figures, EDA responses are higher in high task load. However, eye responses have not been meaningful unlike in navigation tasks.

To analyse the relation among task load, performance and physiological responses statistically, correlation analysis has been performed in SPSS 24. Significant correlations are stated in Table 4.11. It should be noted that there no whole correlations in this table. Significant and meaningful correlations are stated. For time-based HRV features similar results with in navigation tasks have been observed.

The frequency-based and time-frequency HRV features have also similar results as in navigation tasks. For example, the peak frequency of HF (hrv_fwpeakhf) is negative significantly correlated with task load and EDA features.

From non-linear HRV features, nlsd1 (Poincaré plot SD perpendicular the line of identity) and nlsd2 have positive significant correlation with task load. These non-linear HRV features have also positive significant correlations with other HRV features and EDA features same as in navigation tasks.

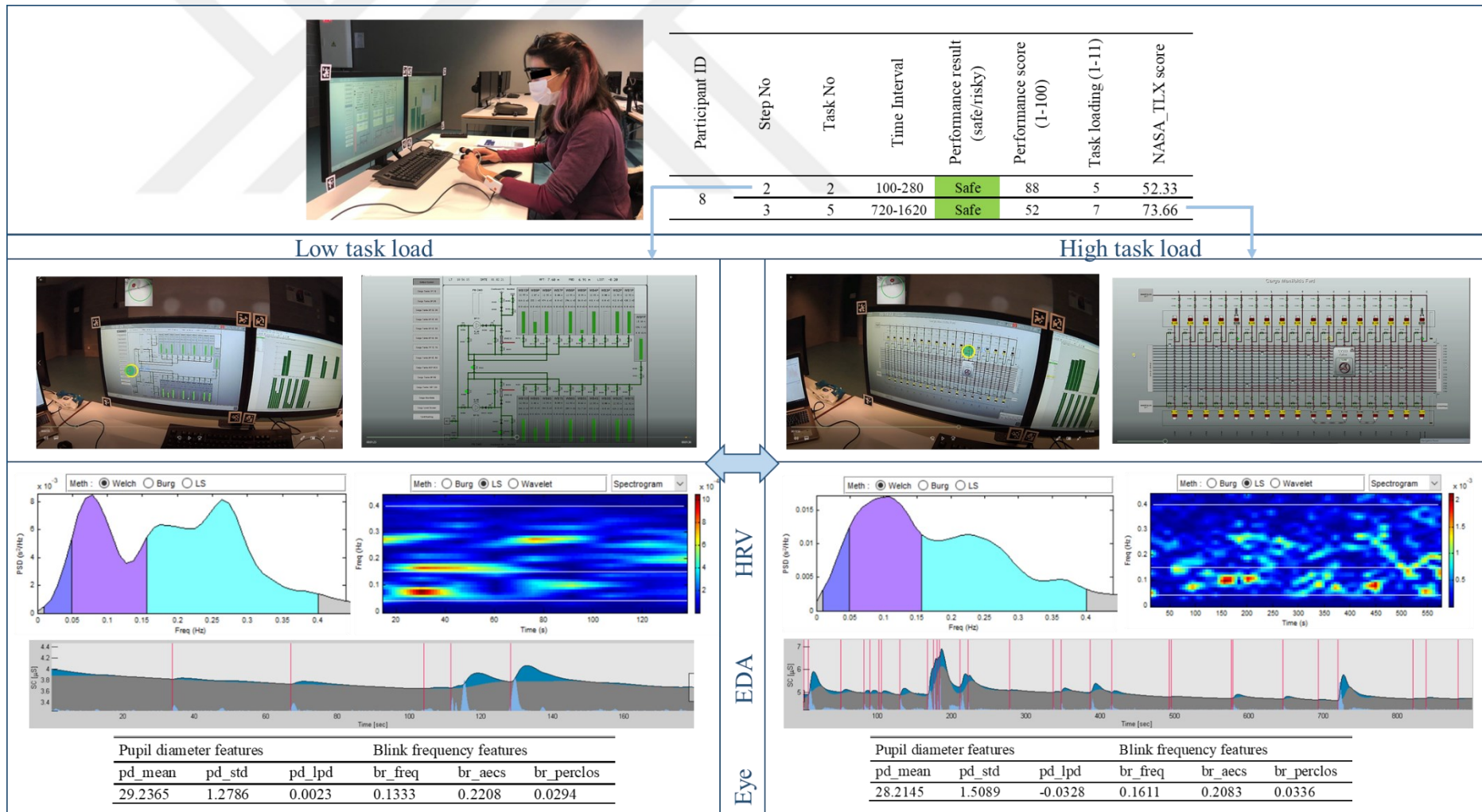


Figure 4.26 : The comparison of data between low and high task load for subject ID 8.

Table 4.11 (continued) : Correlations between task load and other measures for cargo operation tasks.

		performance_score	task_load	n_hrv_hr	n_hrv_sdmn	n_hrv_rmsd	n_hrv_pnn50	n_hrv_tinn	n_hrv_fwalf	n_hrv_fwahf	n_hrv_fwatotal	n_hrv_fwlhlf	n_hrv_fwpeakhf	n_hrv_nlsd1	n_hrv_nlsd2	n_hrv_tflsalf	n_hrv_tflsahf	n_hrv_tflsatal	n_hrv_tfwalf	n_hrv_tfwahf
n_hrv_tfwatotal	Spearman's rho		.351**		.894**	.686**	.577**	.556**						.684**	.868**				.944**	.701**
	Sig. (2-tailed)		0.001		0.000	0.000	0.000	0.000						0.000	0.000				0.000	0.000
hrv_tfwplf	Spearman's rho																		.234*	
	Sig. (2-tailed)																		0.037	
hrv_tfwphf	Spearman's rho																		-.239*	
	Sig. (2-tailed)																		0.033	
eda_cdanscr	Spearman's rho	.220*																		
	Sig. (2-tailed)	0.050																		
n_eda_cdascra	Spearman's rho	-.297**	.236*	-.277*											.243*					
	Sig. (2-tailed)	0.007	0.035	0.013											0.030					
n_eda_cdascrm	Spearman's rho		.264*	-.260*																
	Sig. (2-tailed)		0.018	0.020																
n_eda_cdaiscra	Spearman's rho	-.297**	.236*	-.277*											.243*					
	Sig. (2-tailed)	0.007	0.035	0.013											0.030					
n_eda_cdaiscrm	Spearman's rho		.264*	-.260*																
	Sig. (2-tailed)		0.018	0.020																
n_eda_cdamaxa	Spearman's rho										.261*									
	Sig. (2-tailed)										0.019									
eda_cdamaxm	Spearman's rho		-.288**								.252*									
	Sig. (2-tailed)		0.010								0.024									
n_eda_cdatonica	Spearman's rho																			
	Sig. (2-tailed)																			
n_eda_cdatonicm	Spearman's rho		-.297**						.265*				-.228*	.252*	.275*				.267*	
	Sig. (2-tailed)		0.007						0.018				0.042	0.024	0.014				0.017	
n_eda_ttpampsuma	Spearman's rho																			
	Sig. (2-tailed)																			
n_eda_ttpampsumm	Spearman's rho																			
	Sig. (2-tailed)																			
n_eda_sca	Spearman's rho																			
	Sig. (2-tailed)																			
n_eda_scm	Spearman's rho																			
	Sig. (2-tailed)																			
n_pd_mean	Spearman's rho		-.234*										.260*							
	Sig. (2-tailed)		0.037										0.020							
pd_std	Spearman's rho			-.338**		.253*			.264*								.232*			.265*
	Sig. (2-tailed)			0.002		0.024			0.018								0.039			0.017
pd_lpd	Spearman's rho	.221*											.222*							
	Sig. (2-tailed)	0.049											0.048							

Table 4.11 (continued) : Correlations between task load and other measures for cargo operation tasks.

		n_hrv_ tfwatotal	hrv_ tfwplf	hrv_ tfwphf	eda_ cdanscr	n_eda_ cdascra	n_eda_ cdascrm	n_eda_ cdaiscra	n_eda_ cdaiscrm	n_eda_ cdamaxa	eda_ cdamaxm	n_eda_ cdatonica	n_eda_ cdatonicm	n_eda_ ttpampsuma	n_eda_ ttpampsumm	n_eda_ sca	n_eda_ scm	n_ pd_mean	pd_ std	pd_ lpd
n_hrv_tfwatotal	Spearman's rho Sig. (2-tailed)	1																		
hrv_tfwplf	Spearman's rho Sig. (2-tailed)		1																	
hrv_tfwphf	Spearman's rho Sig. (2-tailed)		-.999**	1																
eda_cdanscr	Spearman's rho Sig. (2-tailed)		.375**	-.378**	1															
n_eda_cdascra	Spearman's rho Sig. (2-tailed)		0.001	0.001		1														
n_eda_cdascrm	Spearman's rho Sig. (2-tailed)						1													
n_eda_cdaiscra	Spearman's rho Sig. (2-tailed)							1												
n_eda_cdaiscrm	Spearman's rho Sig. (2-tailed)								1											
n_eda_cdamaxa	Spearman's rho Sig. (2-tailed)									1										
eda_cdamaxm	Spearman's rho Sig. (2-tailed)										1									
n_eda_cdatonica	Spearman's rho Sig. (2-tailed)											1								
n_eda_cdatonicm	Spearman's rho Sig. (2-tailed)												1							
n_eda_ttpampsuma	Spearman's rho Sig. (2-tailed)	.226*												1						
n_eda_ttpampsumm	Spearman's rho Sig. (2-tailed)	0.044													1					
n_eda_sca	Spearman's rho Sig. (2-tailed)															1				
n_eda_scm	Spearman's rho Sig. (2-tailed)	.223*	.243*	-.245*													1			
n_pd_mean	Spearman's rho Sig. (2-tailed)													.244*				1		
pd_std	Spearman's rho Sig. (2-tailed)		-.281*	.278*		.391**	.391**	.456**	.488**					.029					1	
pd_lpd	Spearman's rho Sig. (2-tailed)		0.012	0.013		0.000	0.000	0.000	0.000					.363**						1
					.323**															
					0.003															

Table 4.11 (continued) : Correlations between task load and other measures for cargo operation tasks.

	performance_score	task_load	n_hrv_hr	n_hrv_sdmn	n_hrv_rmssd	n_hrv_pnn50	n_hrv_tinn	n_hrv_fwalf	n_hrv_fwahf	n_hrv_fwtotal	n_hrv_fwlfhf	n_hrv_fwpeakhf	n_hrv_nlsd1	n_hrv_nlsd2	n_hrv_tflsalf	n_hrv_tflsahf	n_hrv_tflsatal	n_hrv_tfwalf	n_hrv_tfwahf	
n_br_freq	Spearman's rho				.336**	.267*			.256*											
	Sig. (2-tailed)				0.002	0.017			0.022											
n_br_aecd	Spearman's rho											.243*								
	Sig. (2-tailed)											0.030								
n_br_perclos	Spearman's rho												.336**							
	Sig. (2-tailed)												0.002							
															.227*					
															0.043					
																				.228*
																				0.042

Table 4.11 (continued) : Correlations between task load and other measures for cargo operation tasks.

	n_hrv_tfwtotal	hrv_tfwplf	hrv_tfwphf	eda_cdanscr	n_eda_cdasra	n_eda_cdasrm	n_eda_cdaiscra	n_eda_cdaiscrm	n_eda_cdamaxa	eda_cdamaxm	n_eda_cdatonica	n_eda_cdatoniem	n_eda_tfpampsuma	n_eda_tfpampsumm	n_eda_sca	n_eda_scm	n_pd_mean	pd_std	pd_lpd
n_br_freq																	.269*	.385**	
																	0.016	0.000	
n_br_aecd											.263*								
											0.018								
n_br_perclos											.233*								
											0.037								
															.244*				
															0.029				
																	.311**	.288**	.229*
																	0.005	0.009	0.041

It can be seen in Table 4.11 that some EDA features (eda_cdascra, eda_cdascrm, eda_cdaiscra, eda_cdaiscrm,) are significantly correlated with task load that EDA response increases when task load increases. Additionally, the correlation between EDA and HRV features are meaningful according to literature; the increase of EDA response (eda_ttpampsuma) is correlated with the increase of LF (hrv_tfwalf) and the decrease of HF (hrv_fwpeakhf).

Contrary to the results in the navigational tasks, the changes of pupil diameter (pd_mean) have not been meaningful; it is positive significantly correlated with the peak frequency of HF (hrv_fwpeakhf). Similarly, standard deviation of pupil diameter (pd_std) is positive significantly correlated with HF (hrv_tfwphf) and negative significantly correlated with LF (hrv_tfwplf). This result does not support the literature. On the other hand, large pupil dilation (pd_lpd) is positive significantly correlated with EDA response (eda_cdanscr); this supports the literature. The results of the correlations between blink rate features and other physiological features are similar with those in navigation tasks.

Statistically, 10 physiological features in total have been found significantly different in low and high task loads for cargo operation tasks (Table 4.12). Whole SPSS *t*-Test output is stated in Appendix I.

Table 4.12 : *t*-Test of physiological data between low and high task load for cargo operation tasks.

	Low task load (<i>M</i> ± <i>SD</i>)	High task load (<i>M</i> ± <i>SD</i>)	<i>p</i>
n_hrv_hr	0.482 ± 0.306	0.314 ± 0.219	0.005**
n_hrv_sdn	0.429 ± 0.277	0.585 ± 0.268	0.014*
n_hrv_rmssd	0.423 ± 0.303	0.584 ± 0.253	0.015*
n_hrv_pnn50	0.435 ± 0.301	0.613 ± 0.231	0.006**
n_hrv_tinn	0.427 ± 0.263	0.589 ± 0.270	0.009**
n_hrv_nlsd1	0.426 ± 0.305	0.586 ± 0.254	0.016*
n_hrv_nlsd2	0.430 ± 0.289	0.582 ± 0.278	0.022*
n_hrv_tfwahf	0.410 ± 0.286	0.545 ± 0.245	0.032*
n_hrv_tfwpeakhf	0.407 ± 0.406	0.154 ± 0.308	0.002**
n_pd_mean	0.532 ± 0.306	0.365 ± 0.245	0.008**

*. *p* ≤ 0.05; **. *p* ≤ 0.01.

4.4 Feature Selection Results

Feature selection has been carried out with the help of divergence analysis which is detailed in chapter 3.5.2. The results of divergence analysis for navigation tasks are graphed in Figure 4.27. All divergence values of the analysis are stated in Appendix J. Being compared with *t*-Test results (Table 4.10), 13 features (n_hrv_tfwalf,

4.5 Classification Results

4.5.1 Within task classification

4.5.1.1 Navigation task

In ANN classification without feature selection, the partitioned data sets (detailed in chapter 3.5.3) have been trained for various network structures with different number of iterations. Table 4.13 presents the average *MSE* values in all network structures (from 1 to 35) of validation data sets for each partition. The all *MSE* values are presented in Appendix M. It can be seen that in Table 4.13, partition 2 has minimum average *MSE*. Therefore, partition 2 has selected as a suitable partition.

Table 4.13 : Average *MSE* values of validation data sets of partitions (navigation task without feature selection).

Partition 1	Partition 2	Partition 3	Partition 4	Partition 5	Partition 6
0.2662	0.2374	0.2597	0.2543	0.2547	0.2792

To determine best network structure, the *MSE* values of training and testing data sets of partition 2 have been evaluated. These values are given in Figure 4.29. It can be seen in this figure that 73-15-15-1 network structure has minimum training and testing error. Therefore, this structure has selected as a suitable network structure for this classification.

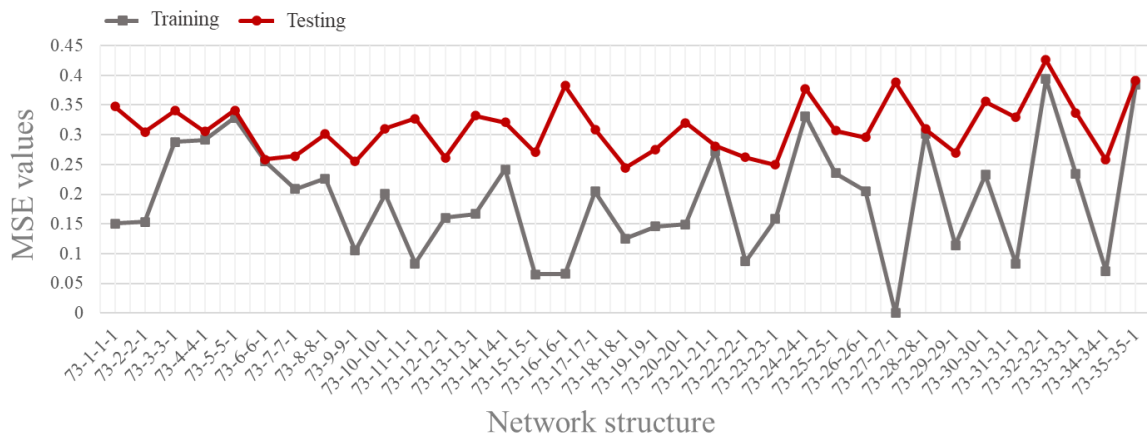


Figure 4.29 : *MSE* values of various network structures in partition 2 (navigation task without feature selection).

The results of the ANN classification with the 73-15-15-1 network structure showed that the classification accuracy is 83.7% in all (training; 92.4%, testing; 64.9%). Figure 4.30 presents the confusion matrix and ROC curve graphics of the related structure. The results of other classifiers performed by “Classification Learner” tool box of the software showed

that KNN has the maximum accuracy (68.0%). Figure 4.31 presents the confusion matrix and ROC curve graphic of the KNN classifier. SVM followed the KNN as classification accuracy (66.5%).

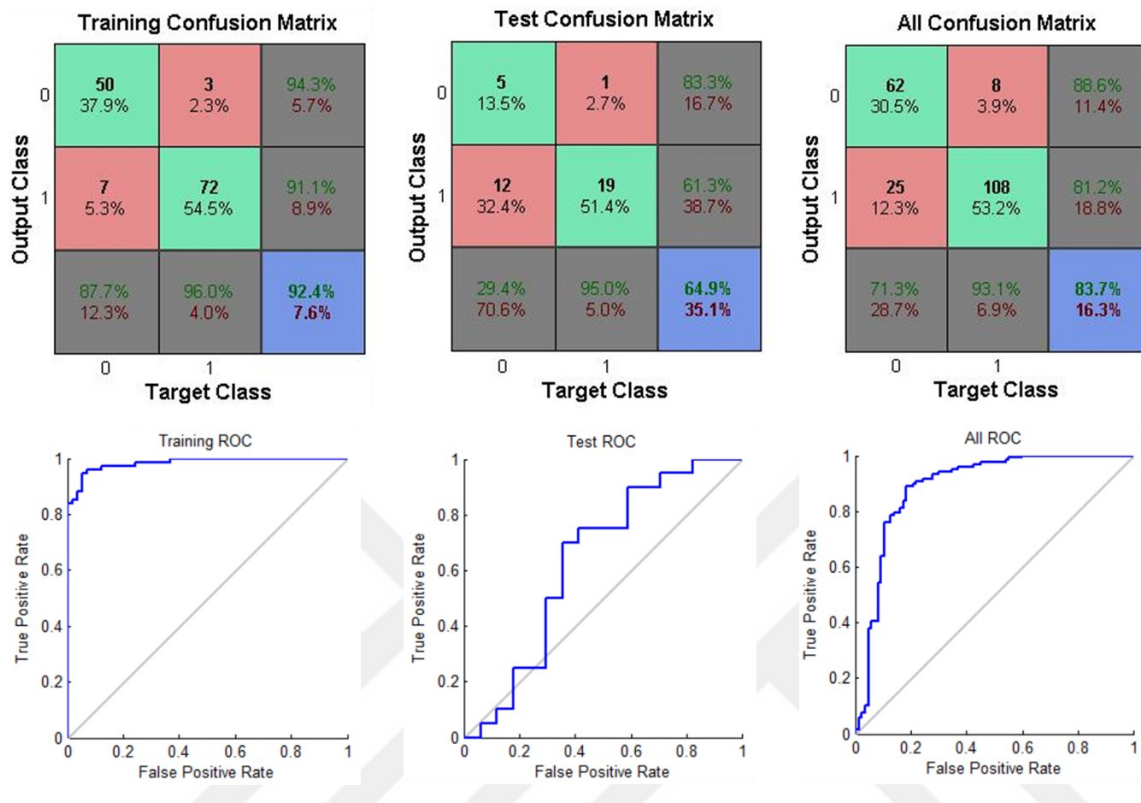


Figure 4.30 : Confusion matrix and ROC curve graphics of ANN classifier (navigation task without feature selection).

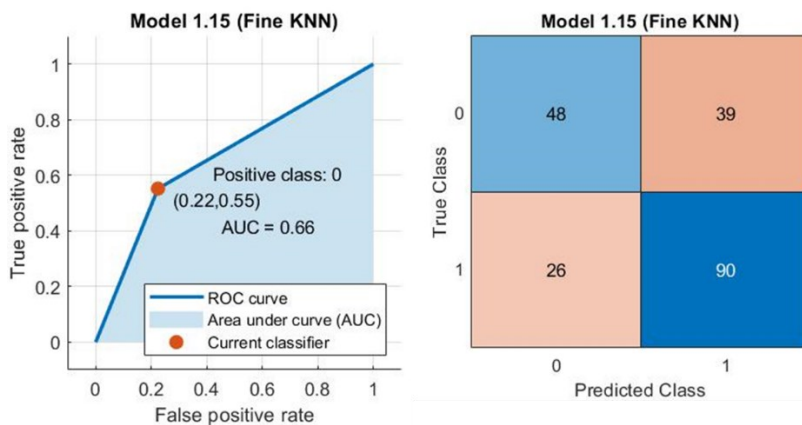


Figure 4.31 : Confusion matrix and ROC curve graphic of KNN classifier (navigation task without feature selection).

On the other hand, the results of classifications with selected features (detailed in chapter 4.4) have provided better classification accuracies (especially in testing). Similarly, the partitioned data set has been trained for various network structures with different number of iterations in ANN classification. Table 4.14 presents the average *MSE* values in all

network structures (from 1 to 26) of validation data sets for each partition. It can be seen that in Table 4.14, partition 2 has minimum average *MSE*. Therefore, partition 2 has selected as a suitable partition.

Table 4.14 : Average *MSE* values of validation data sets of partitions (navigation task with feature selection).

Partition 1	Partition 2	Partition 3	Partition 4	Partition 5	Partition 6
0.2989	0.2217	0.2241	0.2698	0.2661	0.2729

The *MSE* values of training and testing data sets of partition 2 are given in Figure 4.32. It can be seen in this figure that 13-19-19-1 network structure has minimum training and testing error. Therefore, this structure has selected as a suitable network structure for this classification.

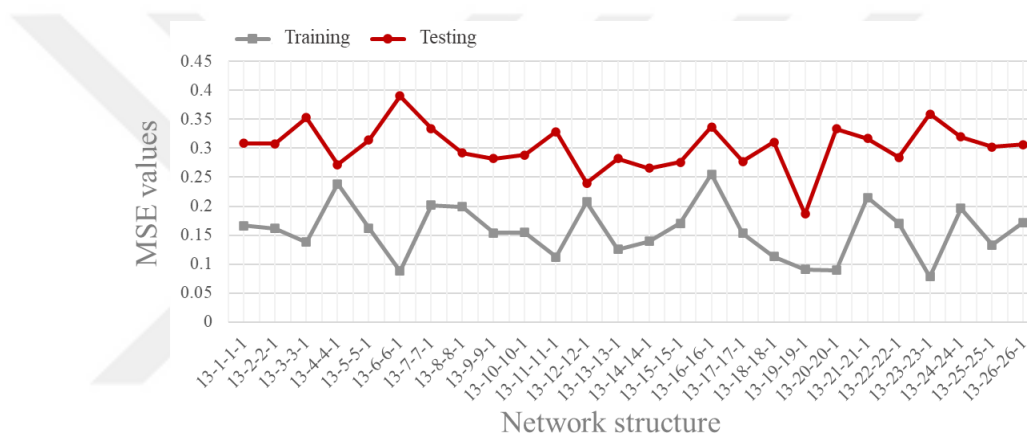


Figure 4.32 : *MSE* values of various network structures in partition 2 (navigation task with feature selection).

The results of the ANN classification with the 13-19-19-1 network structure showed that the classification accuracy is 83.3% in all (training; 90.2%, testing; 75.7%). Figure 4.33 presents the confusion matrix and ROC curve graphics of the related structure.

The results of other classifiers performed by “Classification Learner” tool box of the software showed that Linear Discriminant has the maximum accuracy (70.4%). Figure 4.34 presents the confusion matrix and ROC curve graphic of the Linear Discriminant classifier. Logistic Regression followed the Linear Discriminant as classification accuracy (69.5%).

4.5.1.2 Cargo operation task

Same steps have been performed for the data set of cargo operation tasks. The partitioned data set has been trained for various network structures with different number of iterations

in ANN classification. Table 4.15 presents the average *MSE* values in all network structures (from 1 to 35) of validation data sets for each partition. It can be seen that in Table 4.15, partition 3 has minimum average *MSE*. Therefore, partition 3 has selected as a suitable partition.

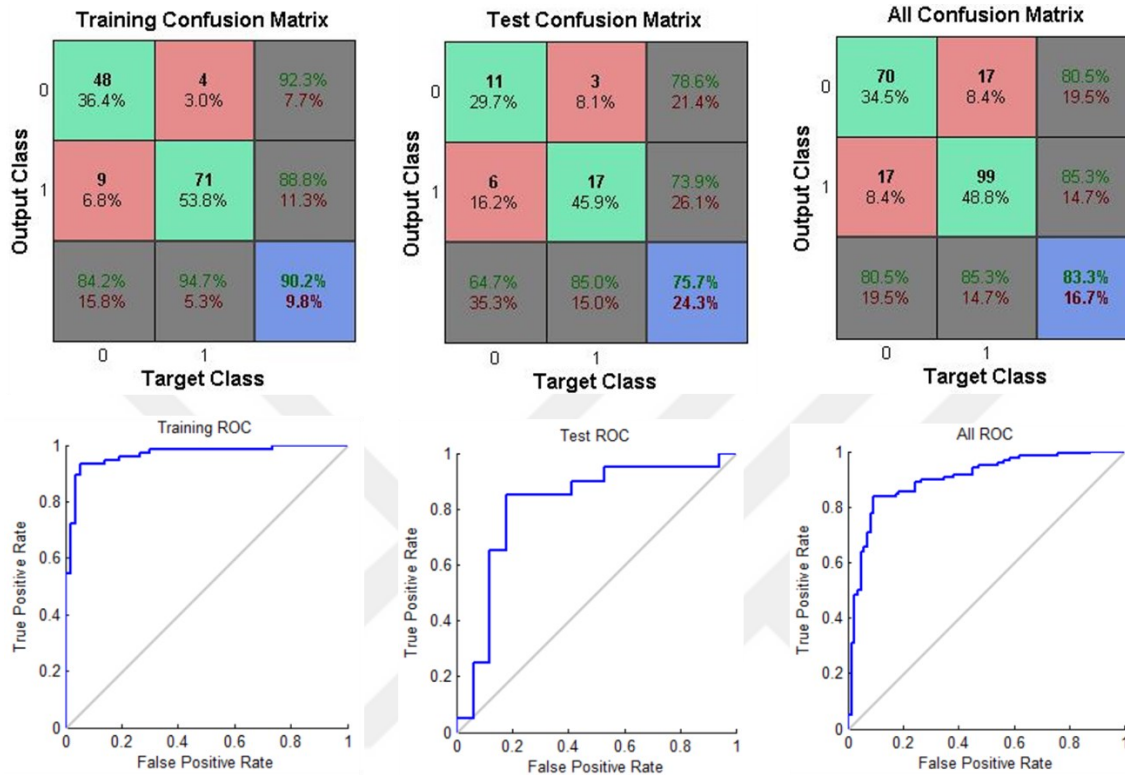


Figure 4.33 : Confusion matrix and ROC curve graphics of ANN classifier (navigation task with feature selection).

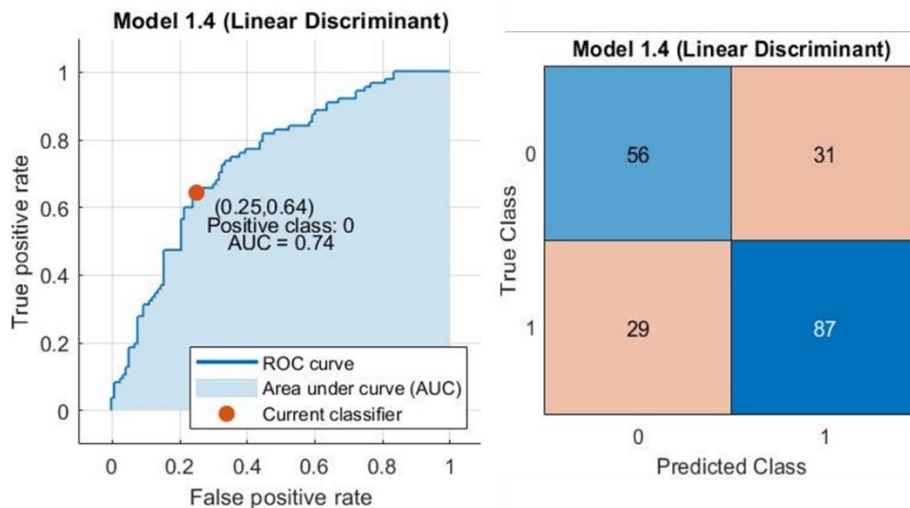


Figure 4.34 : Confusion matrix and ROC curve graphic of Linear Discriminant classifier (navigation task with feature selection).

Table 4.15 : Average *MSE* values of validation data sets of partitions (cargo operation task without feature selection).

Partition 1	Partition 2	Partition 3	Partition 4	Partition 5	Partition 6
0.2180	0.1893	0.1876	0.2374	0.2505	0.2389

The *MSE* values of training and testing data sets of partition 3 are given in Figure 4.35. It can be seen in this figure that 73-30-30-1 network structure has minimum training and testing error. Therefore, this structure has selected as a suitable network structure for this classification.

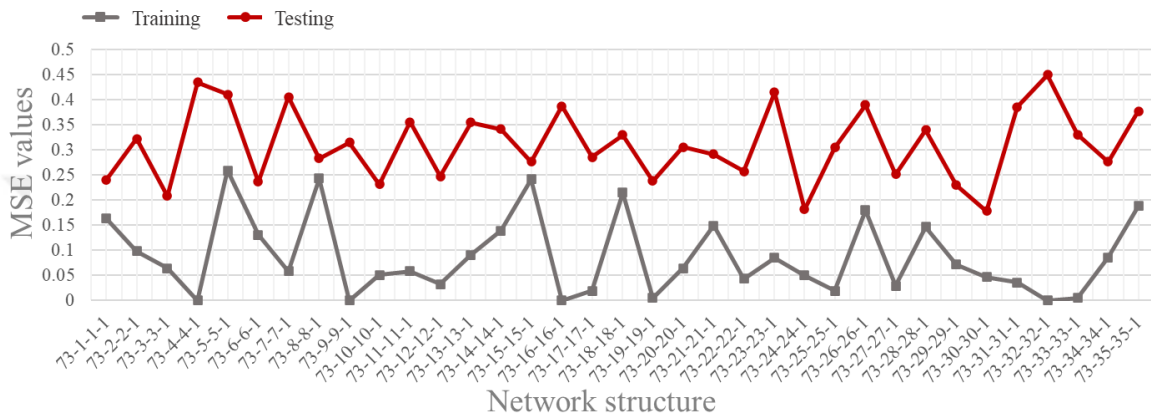


Figure 4.35 : *MSE* values of various network structures in partition 3 (cargo operation task without feature selection).

The results of the ANN classification with the 73-30-30-1 network structure showed that the classification accuracy is 87.5% in all (training; 95.7%, testing; 75.0%). Figure 4.36 presents the confusion matrix and ROC curve graphics of the related structure.

The results of other classifiers performed by “Classification Learner” tool box of the software showed that SVM has the maximum accuracy (68.8%). Figure 4.37 presents the confusion matrix and ROC curve graphic of the SVM classifier.

On the other hand, the results of classifications with selected features (detailed in chapter 4.4) have provided better classification accuracies (especially in testing) same as in navigation tasks. Similarly, the partitioned data set has been trained for various network structures with different number of iterations in ANN classification. Table 4.16 presents the average *MSE* values in all network structures (from 1 to 20) of validation data sets for each partition. It can be seen that in Table 4.16, partition 1 has minimum average *MSE*. Therefore, partition 1 has selected as a suitable partition.

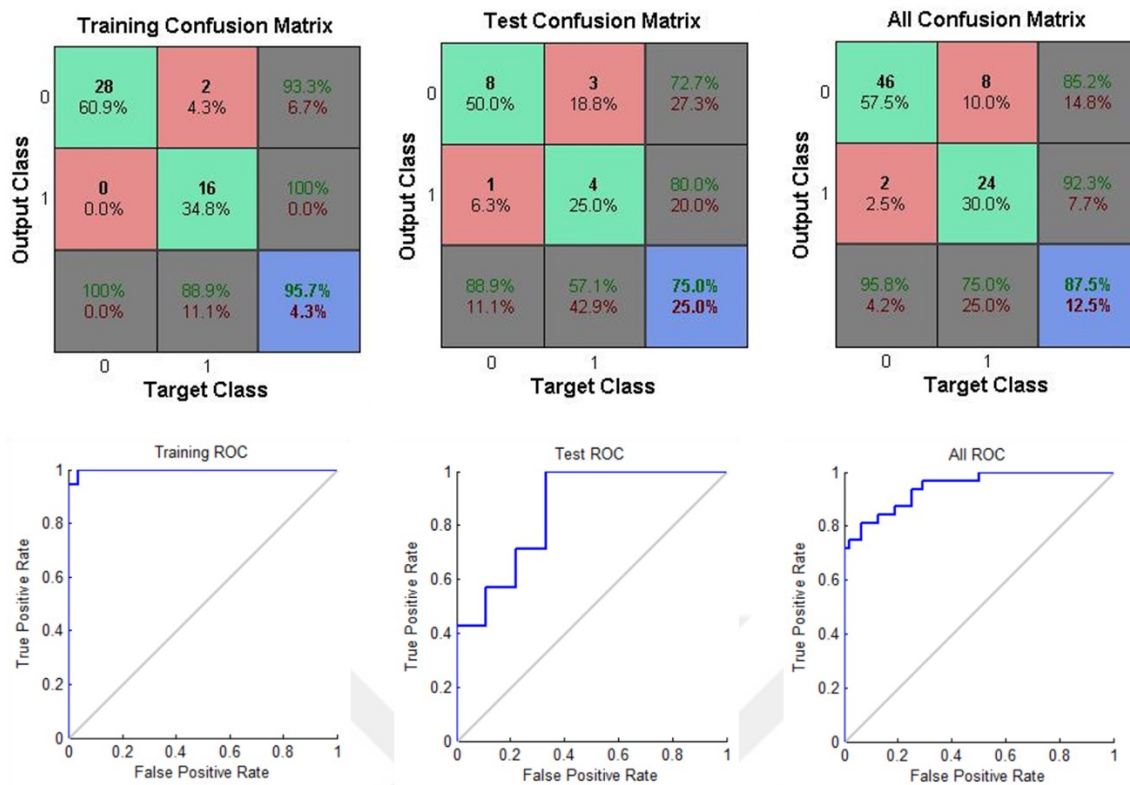


Figure 4.36 : Confusion matrix and ROC curve graphics of ANN classifier (cargo operation task without feature selection).

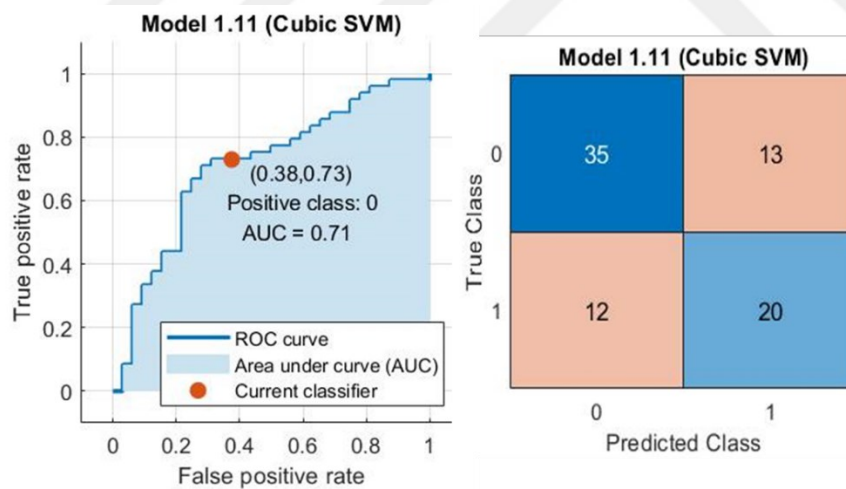


Figure 4.37 : Confusion matrix and ROC curve graphic of SVM classifier (cargo operation task without feature selection).

Table 4.16 : Average *MSE* values of validation data sets of partitions (cargo operation task with feature selection).

Partition 1	Partition 2	Partition 3	Partition 4	Partition 5	Partition 6
0.1758	0.2036	0.1875	0.1870	0.2298	0.2109

The *MSE* values of training and testing data sets of partition 1 are given in Figure 4.38. It can be seen in this figure that 10-14-14-1 network structure has minimum training and

testing error. Therefore, this structure has selected as a suitable network structure for this classification.

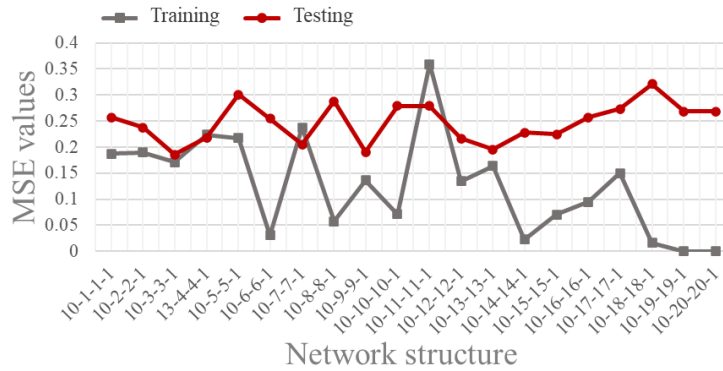


Figure 4.38 : MSE values of various network structures in partition 1 (cargo operation task with feature selection).

The results of the ANN classification with the 10-14-14-1 network structure showed that the classification accuracy is 92.5% in all (training; 98.0%, testing; 80.0%). Figure 4.39 presents the confusion matrix and ROC curve graphics of the related structure.

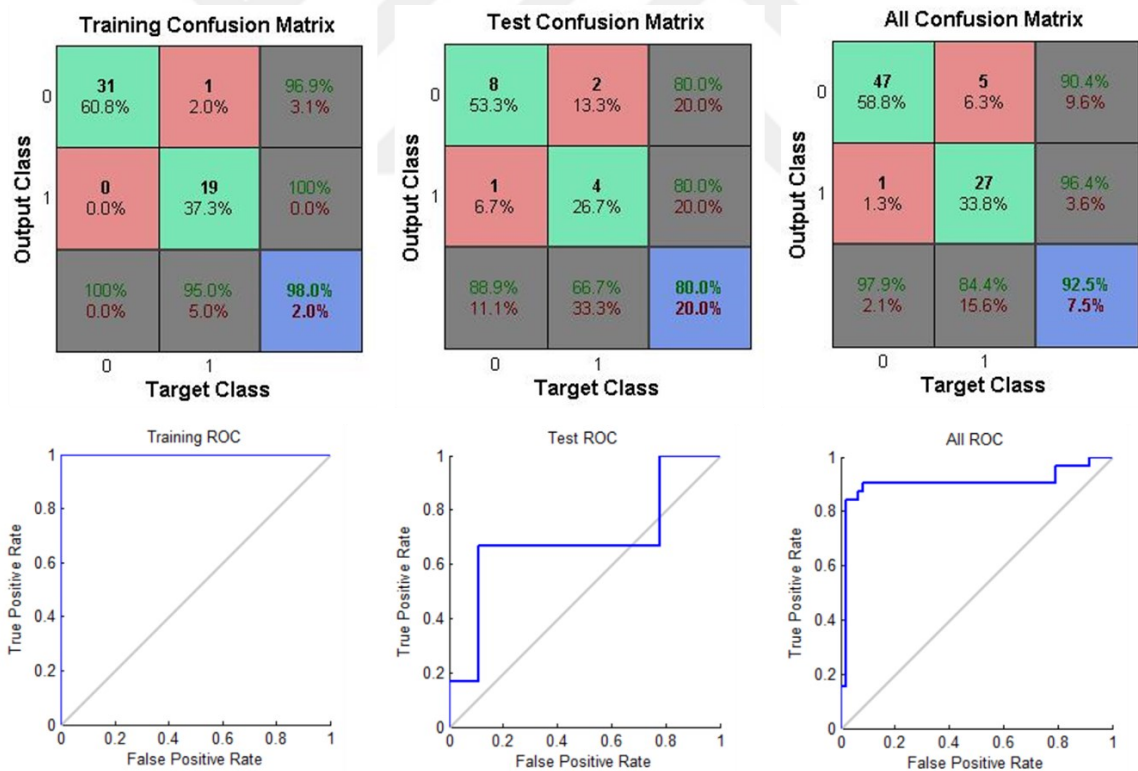


Figure 4.39 : Confusion matrix and ROC curve graphics of ANN classifier (cargo operation task with feature selection).

The results of other classifiers performed by “Classification Learner” tool box of the software showed that Logistic Regression has the maximum accuracy (77.5%). Figure

4.40 presents the confusion matrix and ROC curve graphic of the Logistic Regression classifier. KNN and Linear Discriminant followed the Logistic Regression as classification accuracy (75.0%).

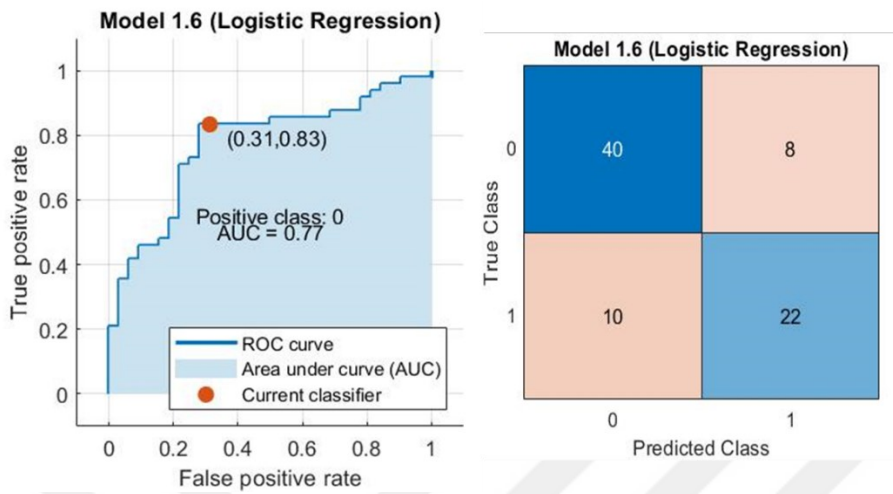


Figure 4.40 : Confusion matrix and ROC curve graphic of Logistic Regression classifier (cargo operation task with feature selection).

4.5.2 Cross task classification

Cross task classification has been performed by testing the data of cargo operation tasks with training and validation data sets of navigation tasks (Partition is given in figure 4.41).

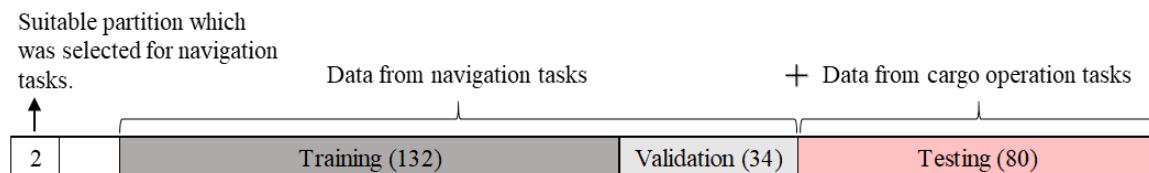


Figure 4.41 : Partition of data used in cross task classification.

The results of the ANN classification with the 13-19-19-1 network structure (this structure has been provided the best classification accuracy in navigation tasks) showed that the classification accuracy is 77.0% in all (training; 90.2%, testing; 61.3%). Figure 4.42 presents the confusion matrix and ROC curve graphics of the related structure. The results of other classifiers performed by “Classification Learner” tool box of the software showed that Subspace KNN has the maximum accuracy (67.8%). Figure 4.43 presents the confusion matrix and ROC curve graphic of the Subspace KNN classifier.

In another MWL study which was conducted for working memory tasks by 15 subjects (Baldwin and Penaranda, 2012), the classification accuracies of ANN were found as 87.1% for within task and 44.8% for cross task. The result of this study has better

classification accuracy in especially cross task (75.7% and 80.0% testing accuracies for within task, 61.3% testing accuracy for cross task) when compared with the similar study.

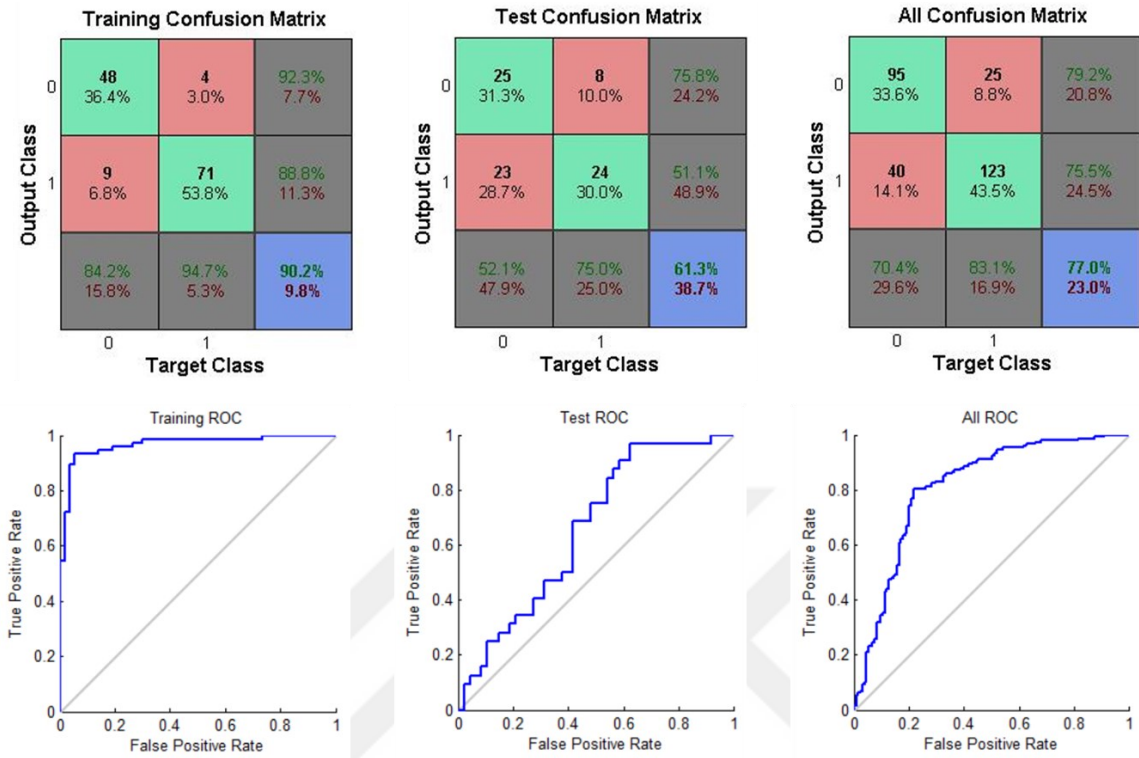


Figure 4.42 : Confusion matrix and ROC curve graphics of ANN classifier (cross task classification with feature selection).

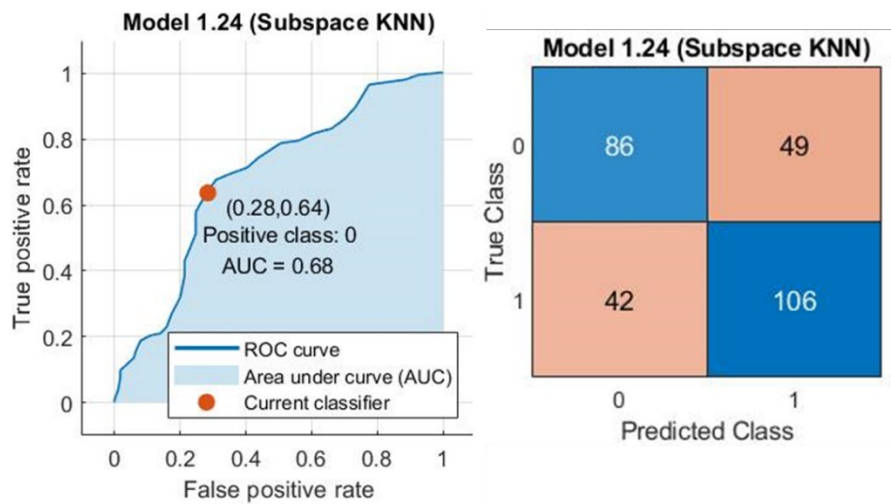


Figure 4.43 : Confusion matrix and ROC curve graphic of Subspace KNN classifier (cross task classification with feature selection).

In general, although the results of the classifications in this study did not give very good accuracies, compared with the studies indicated in Table 2.5, they gave sufficient results. As can be seen in Table 2.5, mental workload and stress classification accuracies vary

between 70.48% and 98%. The results of this study are summarized in Table 4.17, it is seen that the classification accuracies are similar to the related studies in the literature.

Table 4.17 : Summary of classification results.

Data	ANN (test/all)	Other classifiers (accuracy)
Navigation tasks without feature selection	64.9% / 83.7%	KNN; 68.0%
Within task Navigation tasks with feature selection	75.7% / 83.3%	Linear Discriminant; 70.4%
Cargo operation tasks without feature selection	75.0% / 87.5%	SVM; 68.8%
Cargo operation tasks with feature selection	80.0% / 92.5%	Logistic Regression; 77.5%
Cross task Cargo operation tasks (testing) adding to navigation tasks (training and validation)	61.3% / 77.0%	Subspace KNN; 67.8%

4.6 Determining the Red Lines of Task Demands

According to classification efforts of physiological responses on high task load and low task load levels and performance scores of the subjects, the red lines of task demands can become appear in this study. What the concrete conditions of the overload region theorized by Young et al. (2015) is a question and wondered by researchers. Moreover, Orlandi and Brooks (2018) tried to define an upper red line of the task demands during berthing and unberthing operations of ships. Continuing from the aim of Orlandi and Brooks (2018) and the contributions to MWL prediction in marine engine operations of Yan et al. (2019), the red lines of task demand in ship navigation have been tried to determine in this study. Classification of physiological responses and the distinction of the task loads (see chapter 4.2.4) according to the performances of the subjects have ensured the task load to be separated as high task load and low task load. Concrete conditions of high task load have been detailed in Table 3.3 (the tasks of which task load level is greater than or equal to 7) and the “Difficulty” column of Table 3.7 for navigation tasks.

Concrete conditions of high task load for navigation have been generalized and summarized in Figure 4.44 according to the results of this study. Thereby, the “Task Load Estimator” stated in “The future Seafarer-Centric Safety System design” (Figure 1.2) has been detailed. It is seen in Figure 4.44 that data from the navigational sensors (ECDIS, Radar and manual input) provides 8 “risky” conditions to be evaluated in task load estimator. According to the results of this study, these 8 “risky” conditions and the riskier conditions where the inputs are higher than the limits in blue boxes stated in this figure, can be input of the Cognitive Seafarer-Ship Interface (CSSI) concept that process the task loading together with physiological data of the officer and gives an output as “Risky” for safety of navigation in this sample design. This system design is detailed in chapter 5.1.

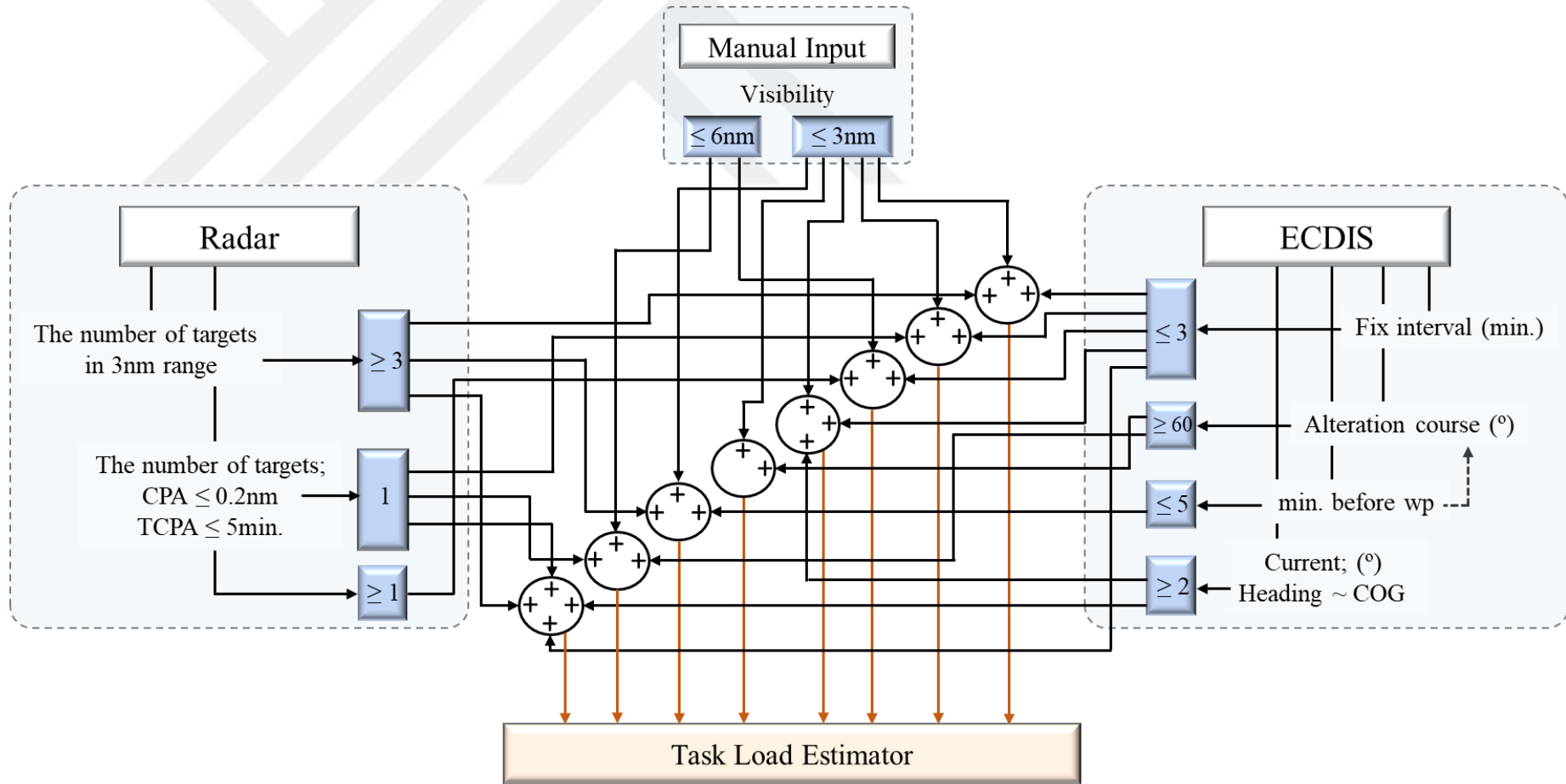


Figure 4.44 : Detailed navigational inputs of “Task Load Estimator” in CSSI.



5. CONCLUSIONS

It is known that human factor has a major effect on maritime casualties that cause great harm to environment, economy and maritime sector. It was stated that while human error is the primary contributor of accidents, a good part of collisions and groundings were related to mental workload (MWL) of watchkeeping officers. Automation, mechanization and the introduction of new technologies had changed the working conditions together with reducing the number of crew and increasing the MWL of operators. This clearly indicates that human element related issues will continue to be one of the major issues in marine transportation assets. In maritime-related studies, it has been analysed mostly how the ship's environment, working period and other factors affect the seafarers. Almost all maritime-related studies couldn't have a potential to develop MWL prediction system for maritime operations aspect. However, lots of studies on drivers and pilots, have produced successful results for MWL prediction. Taking into consideration the fact that MWL has major contribution to maritime casualties, the development of real-time MWL prediction system is vitally essential for ships.

The innovation site of the thesis is implementing the similar measurement techniques used in the studies on drivers and pilots, to maritime transportation for designing Cognitive Seafarer – Ship Interface. This study aims to classify the physiological responses of the operators that can produce an output for state of officer on duty as “Safe” or “Risky” from the collected physiological data and task load data during the seaborne operations.

This study predicated on the theories which are the statement “minimum performance requires sufficient behavioural activity” of Sheridan and Simpson (1979) together with inverted U function of Yerkes and Dodson (1908) which presents the relationship between arousal and performance. Moreover, the theory of Young et al. (2015) which presents the relationship among mental workload, performance, task demand and resource supply (Figure 2.6) and indicates the overload region, guides this study in terms of building the structure of the experimental research. By being predicated on

the above-mentioned theories, this study aimed to design Cognitive Seafarer - Ship Interface (CSSI) which is a main part of Seafarer-Centric Safety System. The physiological data of the officer was recorded according to the design. By being correlated with the performance of the officer, the change of physiological responses of the subjects were analysed in low and high task load levels. The medical decision-making process, which deduced “Safe” or “Risky”, was run for this change (Figure 3.2). For performance measurement that is a part of triangulated measurement strategy (Wierwille and Eggemeier, 1993), Officer Performance Model was developed for navigation and cargo operation tasks which is used for MWL classification. Additionally, the inputs of Task Load Estimator (Figure 1.2) were defined as data transcription from navigational aids according to results of classification. In summary, the following process were done and results were found.

Firstly, the navigation and cargo operation scenarios were created to simulate ship environment. The difficulty level of navigation scenario was gradually adjusted (in order to prevent acquired skill) according to traffic density, visibility and geography by combining in 4 steps. The difficulty level of cargo operation scenario was gradually adjusted according to type and number of operation and operation period corresponding to a real cargo operation by combining in 3 steps. Task load assessments of the scenarios were carried out according to Operator Function Model (OFM-COG) and its sample implications in literature (Lee and Sanquist, 2000). It can be seen that the task loads of the scenarios were gradually increased.

The results of NASA-TLX scores of the subjects supported the increase of task load levels of the scenarios. ANOVA results showed that there are significant differences in the NASA-TLX scores of 5 different dimensions and in total, among 4 steps which have different task load levels for navigation scenario. Similarly, ANOVA results showed that there are significant differences in the NASA-TLX scores of 3 different dimensions and in total among 3 steps which have different task load levels for cargo operation scenario. According to the subjective assessments of the subjects, MWL increased during the both of navigation and cargo operation scenarios.

Secondly, ROC curve analysis was performed for validation of developed officer performance model. Recorded performances of the participants were evaluated as “safe” and “risky” for each task by one ocean going Master expert for navigation tasks and by one ocean going Chief Officer for cargo operation tasks. According to the ROC

curve analysis, developed officer performance model was validated with high significance and AUC values. These results showed that the developed officer performance model can be used in any study focused on performance measurement in navigation and chemical tanker cargo operations.

Being validated measurement method, performances of the subjects showed that there is a negative significant correlation between performance score and task load in both of navigation and cargo operation tasks. With the distinction of the task load as high task load and low task load, the performance scores were also found significantly different in low and high task loads for both of navigation and cargo operation tasks.

Thirdly, physiological responses of the subjects were often differentiated between low and high task loads. Although the change of time-based HRV features was not found meaningful according to literature during the increase of task load, the change of frequency-based, time-frequency and nonlinear HRV features were found significant and meaningful during the increase of task load. Moreover, the change of some EDA features and some eye responses were found significant in this study. However, the change of EDA responses was not found strongly correlated with the increase of task load. This can be explained by the fact that electrodermal activity occurs in stressful conditions rather than mental workload. The “frustration” scores of the NASA-TLX supported the fact that the subjects didn’t feel so stressed during the tasks. On the other hand, the change of pupil diameter features was found significant and meaningful during the increase of task load in navigation tasks but in cargo operation tasks. Additionally, the change of blink frequency features varied across the scenarios. The variable results of eye responses are thought that the selectivity of eye blinks and pupil diameter to MWL is low according to literature. Additionally, the reason of the fact that the change of some eye features was significant during the increase of task load is thought to be related with the characteristics of eye responses that pupil diameter change is correlated highly with error rate and blink rate increases in incorrect responses rather than correct responses. Therefore, these significances can be explained with the decrease of performance together arising from the increase of task load. On the other hand, the correlations between HRV and EDA features, HRV and eye features, EDA and eye features were found significant and meaningful in mental workload theory. For example, the increase of LF/HF (hrv_fwlhfh) together with the increase of LF and the decrease of HF was found to be significantly correlated with

the increase of EDA responses (eda_cdaampsuma, eda_cdasra, eda_cdasrm, eda_cdaisra, n_eda_cdaisrm, eda_cdamaxa) that this situation occurs in high task load.

Classification process was carried out with ANN code and “Classification Learner” tool of Matlab 2020a. Although the results of the classifications of the subjects’ physiological responses on high and low task loads in this study did not give very good accuracies, compared with the studies indicated in Table 2.5, they gave sufficient results. The classification accuracies, 75.7% in testing, 83.3% in all for navigation tasks, 80.0% in testing, 92.5% in all for cargo operation tasks and 61.3% in testing, 77.0% in all for cross-task classification have been found similar to those stated in the related studies. As can be seen in Table 2.5, mental workload and stress classification accuracies vary between 70.48% and 98%.

According to classification efforts of physiological responses on high task load and low task load levels and performance scores of the subjects, the red lines of task demand became appear in this study. Continuing from the aim of Orlandi and Brooks (2018) and the contributions to MWL prediction in marine engine operations of Yan et al. (2019), the red lines of task demand in ship navigation was tried to determine in this study. Classification of physiological responses and the distinction of the task loads according to the performances of the subjects have ensured the task load to be separated as high task load and low task load. Concrete conditions of high task load for navigation were generalized and summarized in Figure 4.44 according to the results of this study. Thereby, the “Task Load Estimator” stated in “The future Seafarer-Centric Safety System design” (Figure 1.2) has been detailed.

5.1 Practical Application of This Study

The system which is named as “The future Seafarer-Centric Safety System design” (Figure 1.2) needs the operational data from related equipment and the physiological data of the operator. The outputs of high task load details for navigation and the physiological responses given as features (classified in this study) can be input of the Cognitive Seafarer-Ship Interface (CSSI) concept that process the task loading together with physiological data of the officer and gives an output as “Risky” for safety of navigation in this sample design. Figure 5.1 presents the sample design to be used on ships or at the Shore Control Centre for autonomous ships in future.

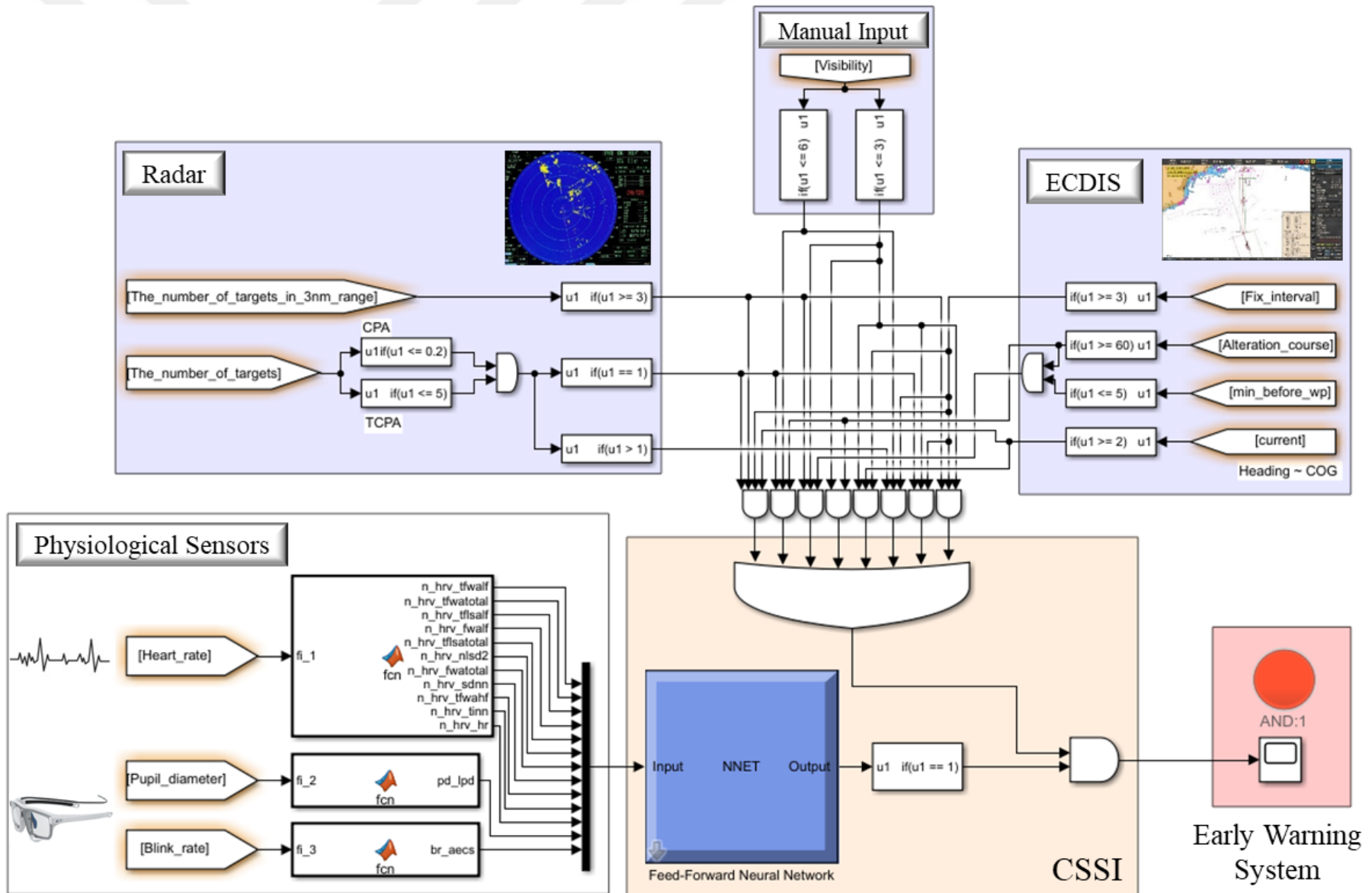


Figure 5.1 : The detailed future Seafarer-Centric Safety System design (created in Matlab 2020a Simulink).

According to the design, task load estimator processes the data which are the possible combinations of the outputs from ECDIS, Radar and manual input. These combinations stated in this design, are the high task load indicators which have been tested in this study. Therefore, the combinations that can be evaluated as high task load should be increased in future studies. At the same time, neural network stated in CSSI, processes the inputs which are physiological features extracted from physiological sensors and gives an output according to the structure of ANN. When the output of neural network is “1” (indicated as “Risky” in this study) and one of the possible combinations exists in task load estimator, CSSI gives an output for early warning system to be activated. It was stated before that similar study for aircrafts was conducted by Liu et al. (2016). Cognitive pilot-aircraft interface was designed with environmental variables of flight and physiological variables of the pilot. Interface can give an output to adjust the level of auto pilot considering the mental strain of pilot and the task load of environmental variables of flight.

Consequently, this study will contribute to literature, being the first study in terms of predicting MWL for navigation and cargo operations in maritime transportation. In addition, this study will be a guide for future studies as it reveals the design of the “Seafarer-Centric Safety System” to be developed in order to minimize maritime casualties.

REFERENCES

- Aimie-Salleh, N., Ghani, N. A. A., Hasanudin, N., & Shafie, S. N. S.** (2019). Heart Rate Variability Recording System Using Photoplethysmography Sensor. In *Autonomic Nervous System Monitoring*. IntechOpen.
- Akhtar, M. J., & Bouwer Utne, I.** (2015). Common patterns in aggregated accident analysis charts from human fatigue-related groundings and collisions at sea. *Maritime Policy & Management*, 42(2), 186-206.
- Alberdi, A., Aztiria, A., & Basarab, A.** (2016). Towards an automatic early stress recognition system for office environments based on multimodal measurements: A review. *Journal of biomedical informatics*, 59, 49-75.
- Backs, R. W., Navidzadeh, H. T., & Xu, X.** (2000). *Cardiorespiratory indices of mental workload during simulated air traffic control*. Paper presented at the Proceedings of the Human Factors and Ergonomics Society Annual Meeting.
- Baldwin, C. L., & Penaranda, B.** (2012). Adaptive training using an artificial neural network and EEG metrics for within-and cross-task workload classification. *NeuroImage*, 59(1), 48-56.
- Benedek, M., & Kaernbach, C.** (2010). A continuous measure of phasic electrodermal activity. *Journal of neuroscience methods*, 190(1), 80-91.
- Bergstrom, J. R., Duda, S., Hawkins, D., & McGill, M.** (2014). Physiological Response Measurements *Eye Tracking in User Experience Design* (pp. 81-108): Elsevier.
- Berntson, G. G., Quigley, K. S., & Lozano, D.** (2007). Cardiovascular psychophysiology. *Handbook of psychophysiology*, 3, 182-210.
- Bjørneseth, F. B., Clarke, L., Dunlop, M., & Komandur, S.** (2014). Towards an understanding of operator focus using eye-tracking in safety-critical maritime settings. In *International Conference on Human Factors in Ship Design & Operation*.
- Blain, S., Power, S. D., Sejdic, E., Mihailidis, A., & Chau, T.** (2010). A cardiorespiratory classifier of voluntary and involuntary electrodermal activity. *Biomedical engineering online*, 9(1), 11.
- Borghini, G., Astolfi, L., Vecchiato, G., Mattia, D., & Babiloni, F.** (2014). Measuring neurophysiological signals in aircraft pilots and car drivers for the assessment of mental workload, fatigue and drowsiness. *Neuroscience & Biobehavioral Reviews*, 44, 58-75.
- Brookings, J. B., Wilson, G. F., & Swain, C. R.** (1996). Psychophysiological responses to changes in workload during simulated air traffic control. *Biological Psychology*, 42(3), 361-377.

- Buckley, J. J., & Eslami, E.** (2002). *An introduction to fuzzy logic and fuzzy sets* (Vol. 13). Springer Science & Business Media.
- Burmeister, H.-C., Bruhn, W., Rødseth, Ø. J., & Porathe, T.** (2014). Autonomous unmanned merchant vessel and its contribution towards the e-Navigation implementation: The MUNIN perspective. *International Journal of e-Navigation and Maritime Economy*, 1, 1-13.
- Causse, M., Sénard, J.-M., Démonet, J. F., & Pastor, J.** (2010). Monitoring cognitive and emotional processes through pupil and cardiac response during dynamic versus logical task. *Applied psychophysiology and biofeedback*, 35(2), 115-123.
- Charles, R. L., & Nixon, J.** (2019). Measuring mental workload using physiological measures: a systematic review. *Applied ergonomics*, 74, 221-232.
- Chen, L.-l., Zhao, Y., Ye, P.-f., Zhang, J., & Zou, J.-z.** (2017). Detecting driving stress in physiological signals based on multimodal feature analysis and kernel classifiers. *Expert systems with applications*, 85, 279-291.
- Chueh, T.-H., Chen, T.-B., Lu, H. H.-S., Ju, S.-S., Tao, T.-H., & Shaw, J.-H.** (2012). Statistical prediction of emotional states by physiological signals with manova and machine learning. *International Journal of Pattern Recognition and Artificial Intelligence*, 26(04), 1250008.
- Collet, C., Salvia, E., & Petit-Boulanger, C.** (2014). Measuring workload with electrodermal activity during common braking actions. *Ergonomics*, 57(6), 886-896.
- Cook, R. C., Marino, K. L., & Cooper, R. B.** (1981). *A Simulator Study of Deepwater Port Shiphandling and Navigation Problems in Poor Visibility* (No. EA-80-U-099). Eclectech Associates Inc North Stonington Ct.
- Cook, T., & Shipley, P.** (1980). Human factors studies of the working hours of UK ship's pilots: 1. A field study of fatigue. *Applied ergonomics*, 11(2), 85-92.
- Cordon, J. R., Mestre, J. M., & Walliser, J.** (2017). Human factors in seafaring: The role of situation awareness. *Safety science*, 93, 256-265.
- Culley, K. E., Kern, D. J., & Phaneuf, M.** (2015). Are a “can do” Attitude and a can of Red Bull Enough? Workload and Fatigue in High-stakes, High-demand Carrier Sortie Operations. *Procedia Manufacturing*, 3, 3062-3069.
- Dawson, M. E., Schell, A. M., & Fillion, D. L.** (2007). The electrodermal system. *Handbook of psychophysiology*, 2, 200-223.
- De Rivecourt, M., Kuperus, M., Post, W., & Mulder, L.** (2008). Cardiovascular and eye activity measures as indices for momentary changes in mental effort during simulated flight. *Ergonomics*, 51(9), 1295-1319.
- De Waard, D.** (1996). *The measurement of drivers' mental workload*: Groningen University, Traffic Research Center Netherlands.
- Delaney, J., & Brodie, D.** (2000). Effects of short-term psychological stress on the time and frequency domains of heart-rate variability. *Perceptual and motor skills*, 91(2), 515-524.

- Devijver, P. A., & Kittler, J.** (1982). *Pattern recognition: A statistical approach*: Prentice Hall.
- Di Stasi, L. L., Renner, R., Catena, A., Cañas, J. J., Velichkovsky, B. M., & Pannasch, S.** (2012). Towards a driver fatigue test based on the saccadic main sequence: A partial validation by subjective report data. *Transportation research part C: emerging technologies*, 21(1), 122-133.
- Diamond, D. M., Campbell, A. M., Park, C. R., Halonen, J., & Zoladz, P. R.** (2007). The temporal dynamics model of emotional memory processing: a synthesis on the neurobiological basis of stress-induced amnesia, flashbulb and traumatic memories, and the Yerkes-Dodson law. *Neural plasticity*, 2007.
- Duda, R. O., Hart, P. E., & Stork, D. G.** (2012). *Pattern classification*: John Wiley & Sons.
- Eggert, T.** (2007). Eye movement recordings: methods *Neuro-Ophthalmology* (Vol. 40, pp. 15-34): Karger Publishers.
- Embrey, D., Blackett, C., Marsden, P., & Peachey, J.** (2006). Development of a human cognitive workload assessment tool. *MCA Final Report, Lancashire*, 1-253.
- Endsley, M. R.** (2017). Toward a theory of situation awareness in dynamic systems In *Situational Awareness* (pp. 9-42). Routledge.
- Enewoldsen, N.** (2016). *Analysis of the quality of electrodermal activity and heart rate data recorded in daily life over a period of one week with an E4 wristband*. University of Twente.
- Fairclough, S. H., Venables, L., & Tattersall, A.** (2005). The influence of task demand and learning on the psychophysiological response. *International Journal of Psychophysiology*, 56(2), 171-184.
- Fallahi, M., Motamedzade, M., Heidarimoghadam, R., Soltanian, A. R., & Miyake, S.** (2016). Effects of mental workload on physiological and subjective responses during traffic density monitoring: A field study. *Applied ergonomics*, 52, 95-103.
- Fausett, L. V.** (1994). *Fundamentals of neural networks: architectures, algorithms, and applications*. Prentice-Hal, Inc.
- Fawcett, T.** (2006). An introduction to ROC analysis. *Pattern recognition letters*, 27(8), 861-874.
- Finsen, L., Sogaard, K., Jensen, C., Borg, V., & Christensen, H.** (2001). Muscle activity and cardiovascular response during computer-mouse work with and without memory demands. *Ergonomics*, 44(14), 1312-1329.
- Fisher, S.** (1984). *Stress and the perception of control*: Erlbaum.
- Fournier, L. R., Wilson, G. F., & Swain, C. R.** (1999). Electrophysiological, behavioral, and subjective indexes of workload when performing multiple tasks: manipulations of task difficulty and training. *International Journal of Psychophysiology*, 31(2), 129-145.

- Fowlkes, J. E., Lane, N. E., Salas, E., Franz, T., & Oser, R.** (1994). Improving the measurement of team performance: The TARGETs methodology. *Military Psychology, 6*(1), 47-61.
- Gao, Q., Wang, Y., Song, F., Li, Z., & Dong, X.** (2013). Mental workload measurement for emergency operating procedures in digital nuclear power plants. *Ergonomics, 56*(7), 1070-1085.
- Gerrig, R. J., Zimbardo, P. G., Zimbardo, P. G., Psychologue, E. U., & Zimbardo, P. G.** (2010). *Psychology and life* (Vol. 20). Boston: Pearson.
- Gould, K. S., Røed, B. K., Saus, E.-R., Koefoed, V. F., Bridger, R. S., & Moen, B. E.** (2009). Effects of navigation method on workload and performance in simulated high-speed ship navigation. *Applied ergonomics, 40*(1), 103-114.
- Grabowski, M., & Sanborn, S. D.** (2003). Human performance and embedded intelligent technology in safety-critical systems. *International journal of human-computer studies, 58*(6), 637-670.
- Grech, M., Horberry, T., & Koester, T.** (2008). *Human factors in the maritime domain*. CRC press.
- Greco, A., Valenza, G., Lanata, A., Rota, G., & Scilingo, E. P.** (2014). Electrodermal activity in bipolar patients during affective elicitation. *IEEE journal of biomedical and health informatics, 18*(6), 1865-1873.
- GSR+ User Guide.** (2018). (Revision 1.13 ed.): Shimmer.
- Guo, M., Li, S., Wang, L., Chai, M., Chen, F., & Wei, Y.** (2016). Research on the relationship between reaction ability and mental state for online assessment of driving fatigue. *International journal of environmental research and public health, 13*(12), 1174.
- Han, S.-Y., Kwak, N.-S., Oh, T., Lee, S.-W.** (2020). Classification of pilots' mental states using a multimodal deep learning network. *Biocybernetics and Biomedical Engineering, 40*(1), 324-336.
- Hart, S. G.** (1986). NASA Task load Index (TLX). Volume 1.0; Paper and pencil package.
- Hart, S. G., & Staveland, L. E.** (1988). Development of NASA-TLX (Task Load Index): Results of empirical and theoretical research. In *Advances in psychology* (Vol. 52, pp. 139-183). North-Holland.
- Healey, J. A., & Picard, R. W.** (2005). Detecting stress during real-world driving tasks using physiological sensors. *IEEE Transactions on intelligent transportation systems, 6*(2), 156-166.
- Holland, M. K., & Tarlow, G.** (1972). Blinking and mental load. *Psychological Reports, 31*(1), 119-127.
- Hwang, S.-L., Yau, Y.-J., Lin, Y.-T., Chen, J.-H., Huang, T.-H., Yenn, T.-C., Hsu, C.-C.** (2008). Predicting work performance in nuclear power plants. *Safety science, 46*(7), 1115-1124.
- IMO** (2001). Guidance on fatigue mitigation and management. *MSC/Circ. 1014*: IMO London.

- IMO** (2018). *Maritime Safety Committee (MSC), 100th session, 3-7 December 2018*. Retrieved October 08, 2019 from <http://www.imo.org/en/MediaCentre/MeetingSummaries/MSC/Pages/MSC-100th-session.aspx>
- ISO** (2000). *10075-2: Ergonomic principles related to mental workload–Part 2: Design principles*. CEN, Brussels.
- ISO** (2004). *10075-3: Ergonomic principles related to mental workload–Part 3: Principles and requirements concerning methods for measuring and assessing mental workload*. CEN, Brussels.
- ISO** (2017). *10075-1: Ergonomic principles related to mental workload–Part 1: General issues and concepts, terms and definitions*. CEN, Brussels.
- Jeżewska, M., & Iversen, R.** (2012). Stress and fatigue at sea versus quality of life. Gdansk, 11 June 2012. II International Congress on Maritime, Tropical, and Hyperbaric Medicine. *International maritime health*, 63(2), 106-115.
- Kahneman, D.** (1973). *Attention and effort* (Vol. 1063): Citeseer.
- Katsis, C. D., Katertsidis, N., Ganiatsas, G., & Fotiadis, D. I.** (2008). Toward emotion recognition in car-racing drivers: A biosignal processing approach. *IEEE Transactions on Systems, Man, and Cybernetics-Part A: Systems and Humans*, 38(3), 502-512.
- Kettunen, J., Ravaja, N., Näätänen, P., Keskiivaara, P., & Keltikangas-Järvinen, L.** (1998). The synchronization of electrodermal activity and heart rate and its relationship to energetic arousal: A time series approach. *Biological Psychology*, 48(3), 209-225.
- Kim, H., Kim, H., & Hong, S.** (2010). Collision Scenario-based Cognitive Performance Assessment for Marine Officers.
- Kircher, A., & Lutzhoft, M.** (2011). Performance of seafarers during extended simulation runs. In *International Conference on human factors in ship design and operation* (pp. 53-59).
- Koukoulaki, T., & Boy, S.** (2002). *Globalizing technical standards: impact and challenges for occupational health and safety*: European Trade Union Technical Bureau for Health and Safety.
- Kurt, R. E., Khalid, H., Turan, O., Houben, M., Bos, J., & Helvacioğlu, I. H.** (2016). Towards human-oriented norms: Considering the effects of noise exposure on board ships. *Ocean Engineering*, 120, 101-107.
- Lajante, M., Droulers, O., Dondaine, T., & Amarantini, D.** (2012). Opening the “black box” of electrodermal activity in consumer neuroscience research. *Journal of Neuroscience, Psychology, and Economics*, 5(4), 238.
- Lazarus, R. S.** (1966). *Psychological stress and the coping process*. McGraw-Hill.
- Lean, Y., & Shan, F.** (2012). Brief review on physiological and biochemical evaluations of human mental workload. *Human Factors and Ergonomics in Manufacturing & Service Industries*, 22(3), 177-187.

- Lee, J. D., & Sanquist, T. F.** (2000). Augmenting the operator function model with cognitive operations: Assessing the cognitive demands of technological innovation in ship navigation. *IEEE Transactions on Systems, Man, and Cybernetics-Part A: Systems and Humans*, 30(3), 273-285.
- Lehrer, P., Karavidas, M., Lu, S.-E., Vaschillo, E., Vaschillo, B., & Cheng, A.** (2010). Cardiac data increase association between self-report and both expert ratings of task load and task performance in flight simulator tasks: An exploratory study. *International Journal of Psychophysiology*, 76(2), 80-87.
- Liu, J., Gardi, A., Ramasamy, S., Lim, Y., & Sabatini, R.** (2016). Cognitive pilot-aircraft interface for single-pilot operations. *Knowledge-Based Systems*, 112, 37-53.
- Liu, Y., Subramaniam, S. C. H., Sourina, O., Liew, S. H. P., Krishnan, G., Konovessis, D., & Ang, H. E.** (2017, September). EEG-based mental workload and stress recognition of crew members in maritime virtual simulator: a case study. In *2017 International Conference on Cyberworlds (CW)* (pp. 64-71). IEEE.
- Louie, V. W., & Doolen, T. L.** (2007). A study of factors that contribute to maritime fatigue. *Marine Technology*, 44(2), 82-92.
- Lützhöft, M., & Dukic, T.** (2007). *Show me where you look and I'll tell you if you're safe: Eye tracking of maritime watchkeepers*. Paper presented at the Proceedings of the 39th Nordic Ergonomics Society Conference.
- Lützhöft, M., & Sri, T. Å.** (2012). Fatigue Management Toolkit.
- Man, Y., Lundh, M., Porathe, T., & MacKinnon, S.** (2015). From desk to field-Human factor issues in remote monitoring and controlling of autonomous unmanned vessels. *Procedia Manufacturing*, 3, 2674-2681.
- Martin, J., Schneider, F., Kowalewskij, A., Jordan, D., Hapfelmeier, A., Kochs, E., . . . Schulz, C.** (2016). Linear and non-linear heart rate metrics for the assessment of anaesthetists' workload during general anaesthesia. *BJA: British Journal of Anaesthesia*, 117(6), 767-774.
- Maurier, P., Barnett, M., Pekcan, C., Gatfield, D., Corrigan, P., & Clarke, G.** (2011). "Fatigue and Performance in Bridge and Engine Control Room Watchkeeping on a 6on/6off Watch Regime".
- Miyake, S., Yamada, S., Shoji, T., Takae, Y., Kuge, N., & Yamamura, T.** (2009). Physiological responses to workload change. A test/retest examination. *Applied ergonomics*, 40(6), 987-996.
- MLC** (2006). *Maritime Labour Convention*: ILO.
- Moraes, J. L., Rocha, M. X., Vasconcelos, G. G., Vasconcelos Filho, J. E., De Albuquerque, V. H. C., & Alexandria, A. R.** (2018). Advances in photoplethysmography signal analysis for biomedical applications. *Sensors*, 18(6), 1894.

- Muczyński, B., Gucma, M., Bilewski, M., & Zalewski, P.** (2013). Using eye tracking data for evaluation and improvement of training process on ship's navigational bridge simulator. *Zeszyty Naukowe/Akademia Morska w Szczecinie* (33 (105)), 75--78.
- Murai, K., Higuchi, K., Fujita, T., Maenaka, K., Saiki, T., & Takizawa, Y.** (2018). *Development of a Real-time Evaluation Support System Using Physiological Index: Case Study of a Simulator-based Ship Handling Exercise*. Paper presented at the 2018 IEEE International Conference on Teaching, Assessment, and Learning for Engineering (TALE).
- Myrden, A., & Chau, T.** (2017). A passive EEG-BCI for single-trial detection of changes in mental state. *IEEE Transactions on Neural Systems and Rehabilitation Engineering*, 25(4), 345-356.
- Nachreiner, F.** (1999). International Standards on Mental Work-Load. *Industrial Health*, 37(2), 125-133.
- Nickel, P., & Nachreiner, F.** (2003). Sensitivity and diagnosticity of the 0.1-Hz component of heart rate variability as an indicator of mental workload. *Human factors*, 45(4), 575-590.
- Optical Pulse Sensor User Guide.** (2016). (Revision 1.6 ed.): Shimmer.
- Orlandi, L., & Brooks, B.** (2018). Measuring mental workload and physiological reactions in marine pilots: Building bridges towards redlines of performance. *Applied ergonomics*, 69, 74-92.
- Özsever, B., & Tavacıoğlu, L.** (2018). Analysing the effects of working period on psychophysiological states of seafarers. *International maritime health*, 69(2), 84-93.
- Parnandi, A., Son, Y., & Gutierrez-Osuna, R.** (2013, September). A control-theoretic approach to adaptive physiological games. In *2013 Humaine Association Conference on Affective Computing and Intelligent Interaction* (pp. 7-12). IEEE.
- Pazouki, K., Forbes, N., Norman, R. A., & Woodward, M. D.** (2018). Investigation on the impact of human-automation interaction in maritime operations. *Ocean Engineering*, 153, 297-304.
- Pizzagalli, D. A.** (2007). Electroencephalography and high-density electrophysiological source localization. *Handbook of psychophysiology*, 3, 56-84.
- Polikar, R.** (2006). Pattern Recognition. *Wiley Encyclopedia of Biomedical Engineering*.
- Posner, M. I., Rueda, M. R., & Kanske, P.** (2007). 18 probing the mechanisms of attention. In *Handbook of psychophysiology* (p. 410). Cambridge University Press.
- Ramshur, J. T.** (2010). *Design, evaluation, and application of heart rate variability analysis software (HRVAS)*. University of Memphis Memphis, TN.
- Robert, G., Hockey, J., Healey, A., Crawshaw, M., Wastell, D. G., & Sauer, J.** (2003). Cognitive demands of collision avoidance in simulated ship control. *Human factors*, 45(2), 252-265.

- Ryu, K., & Myung, R.** (2005). Evaluation of mental workload with a combined measure based on physiological indices during a dual task of tracking and mental arithmetic. *International Journal of Industrial Ergonomics*, 35(11), 991-1009.
- Salyga, J., & Kusleikaite, M.** (2011). Factors influencing psychoemotional strain and fatigue, and relationship of these factors with health complaints at sea among Lithuanian seafarers. *Medicina (Kaunas)*, 47(12), 675-681.
- Sanders, A.** (1983). Towards a model of stress and human performance. *Acta psychologica*, 53(1), 61-97.
- Schuffel, H., Boer, J., & Van Breda, L.** (1989). The ship's wheelhouse of the nineties: the navigation performance and mental workload of the officer of the watch. *The Journal of Navigation*, 42(1), 60-72.
- Selvaraj, N., Jaryal, A., Santhosh, J., Deepak, K. K., & Anand, S.** (2008). Assessment of heart rate variability derived from finger-tip photoplethysmography as compared to electrocardiography. *Journal of medical engineering & technology*, 32(6), 479-484.
- Shaffer, F., & Ginsberg, J.** (2017). An overview of heart rate variability metrics and norms. *Frontiers in public health*, 5, 258.
- Sharma, N., & Gedeon, T.** (2012). Objective measures, sensors and computational techniques for stress recognition and classification: A survey. *Computer methods and programs in biomedicine*, 108(3), 1287-1301.
- Sheridan, T. B., & Simpson, R. W.** (1979). *Toward the definition and measurement of the mental workload of transport pilots*. Cambridge, Mass.: Massachusetts Institute of Technology, Dept. of Aeronautics and Astronautics, Flight Transportation Laboratory, [1979].
- Singh, R. R., Conjeti, S., & Banerjee, R.** (2013). A comparative evaluation of neural network classifiers for stress level analysis of automotive drivers using physiological signals. *Biomedical Signal Processing and Control*, 8(6), 740-754.
- Sirevaag, E. J., Kramer, A. F., Wickens, C. D., Reisweber, M., Strayer, D. L., & Grenell, J. F.** (1993). Assessment of pilot performance and mental workload in rotary wing aircraft. *Ergonomics*, 36(9), 1121-1140.
- Splawn, J. M., & Miller, M. E.** (2013). *Prediction of perceived workload from task performance and heart rate measures*. Paper presented at the Proceedings of the Human Factors and Ergonomics Society Annual Meeting.
- Tac, U., Tavacioglu, L., Bolat, P., Kora, O. K., & Bolat, F.** (2013). Monitoring Seafarers' Cognitive Performance Under Stressor Factors During a Voyage by Automated Neuropsychological Assessment Metrics. *Universitatii Maritime Constanta. Analele*, 14(20), 291.
- Tavacıoğlu, L.** (1999). Bilişsel Değerlendirmeler. *Bağırçan Yayınevi*.
- TRANSAS.** (2012). *TechSim/LCHS 5000 Chemical Tanker and Chemical Terminal Trainee Manual* (1.1 ed.). Transas MIP Ltd.

- TRANSAS.** (2014). *Navi-Trainer Professional 5000 Instructor Manual* (5.35 ed.). Transas MIP Ltd.
- URL-1** <<https://pupil-labs.com/products/core/tech-specs>>, date retrieved 25.03.2020
- Veltman, J., & Gaillard, A.** (1996). Physiological indices of workload in a simulated flight task. *Biological Psychology*, 42(3), 323-342.
- Veltman, J., & Gaillard, A.** (1998). Physiological workload reactions to increasing levels of task difficulty. *Ergonomics*, 41(5), 656-669.
- Wahlström, M., Hakulinen, J., Karvonen, H., & Lindborg, I.** (2015). Human factors challenges in unmanned ship operations—insights from other domains. *Procedia Manufacturing*, 3, 1038-1045.
- Wickens, C. D.** (2008). Multiple resources and mental workload. *Human factors*, 50(3), 449-455.
- Wierwille, W. W., & Eggemeier, F. T.** (1993). Recommendations for mental workload measurement in a test and evaluation environment. *Human factors*, 35(2), 263-281.
- Wilson, G. F.** (2002). An analysis of mental workload in pilots during flight using multiple psychophysiological measures. *The international journal of aviation psychology*, 12(1), 3-18.
- Wilson, G. F., & Russell, C. A.** (2003). Operator functional state classification using multiple psychophysiological features in an air traffic control task. *Human factors*, 45(3), 381-389.
- Wu, Y., Miwa, T., & Uchida, M.** (2017). Using physiological signals to measure operator's mental workload in shipping—an engine room simulator study. *Journal of Marine Engineering & Technology*, 16(2), 61-69.
- Yan, S., Wei, Y., & Tran, C. C.** (2019). Evaluation and prediction mental workload in user interface of maritime operations using eye response. *International Journal of Industrial Ergonomics*, 71, 117-127.
- Yerkes, R. M., & Dodson, J. D.** (1908). The relation of strength of stimulus to rapidity of habit-formation. *Journal of comparative neurology and psychology*, 18(5), 459-482.
- Yıldırım, U., Başar, E., & Uğurlu, Ö.** (2019). Assessment of collisions and grounding accidents with human factors analysis and classification system (HFACS) and statistical methods. *Safety science*, 119, 412-425.
- Yılmaz, H., Başar, E., & Yüksekıldız, E.** (2013). Investigation of Watchkeeping Officers' Watches Under The Working Hours Ineligible to STCW Regulation. *TransNav: International Journal on Marine Navigation and Safety of Sea Transportation*, 7(4).
- Yin, Z., & Zhang, J.** (2014). Identification of temporal variations in mental workload using locally-linear-embedding-based EEG feature reduction and support-vector-machine-based clustering and classification techniques. *Computer methods and programs in biomedicine*, 115(3), 119-134.
- Young, M. S., Brookhuis, K. A., Wickens, C. D., & Hancock, P. A.** (2015). State of science: mental workload in ergonomics. *Ergonomics*, 58(1), 1-17.

Young, M. S., & Stanton, N. A. (2002). Malleable attentional resources theory: a new explanation for the effects of mental underload on performance. *Human factors*, 44(3), 365-375.



APPENDICES

APPENDIX A: Voluntary Participation Form

APPENDIX B: NASA Task Load Index (Rating)

APPENDIX C: NASA Task Load Index (Weighting)

APPENDIX D: All Subjective Assessments of the Subjects

APPENDIX E: SPSS ANOVA Analysis Outputs of NASA-TLX Scores

APPENDIX F: Calculation Details of Performance Scores

APPENDIX G: Coordinates of the ROC Curves of Developed Officer Performance Model

APPENDIX H: Data Collected During the Study

APPENDIX I: SPSS t-Test Outputs of Physiological Data Between Low and High Task Load

APPENDIX J: Divergence Values of Physiological Features

APPENDIX K: Matlab Code for Eye Features

APPENDIX L: Matlab Code for ANN Classification

APPENDIX M: *MSE* Values of Validation Data Sets

APPENDIX A: Voluntary Participation Form

Voluntary Participation Form

This study is a PhD thesis, named as “*Design of Seafarer-Centric Safety System; Mental Workload (MWL) Prediction*”, conducted by Barış ÖZSEVER, postgraduate student in Maritime Transportation Engineering Department of Istanbul Technical University Graduate School of Science, Engineering and Technology and thesis advisor Prof. Dr. Leyla TAVACIOĞLU. Main aim of the thesis is designing the mental workload prediction system for seafarers. The physiological data of the officer will be recorded according to the design. By being correlated with the performance of the officer, the change of physiological responses of the subjects will be analysed in low and high task load levels.

Your participation in this study is entirely voluntary. No personal identification is required during the research. For the purpose of the study, the data collected from you in the simulator environment will be used only for scientific purposes and will not be shared with others. You have the right to review the data collected from you, if you wish.

The data collection process does not contain any requests or activities that may cause you discomfort. However, if you feel uncomfortable during this process, you can leave at any time. In this case, the data collected from you will be excluded from the study.

You are asked to fill in the following parameters which are thought to have an impact on the data collected during the study:

1. Year of birth:
2. Total duration of sea service as an officer:
3. Ship type you have worked as an officer:
4. Coffee consumption since last night:
5. Alcohol consumption since last morning:
6. Usage of anti-depressant medicine:
7. Total sleep duration of last night:

For more information about the study, you can contact Prof. Dr. Leyla TAVACIOĞLU (tavaciog@itu.edu.tr) or Barış ÖZSEVER (barisozsever@yahoo.com).

I take part in this research as a volunteer and I know that I can withdraw from this research whenever I want. I accept the use of data collected from me for scientific purposes.

Subject ID:

Date:

Signature:

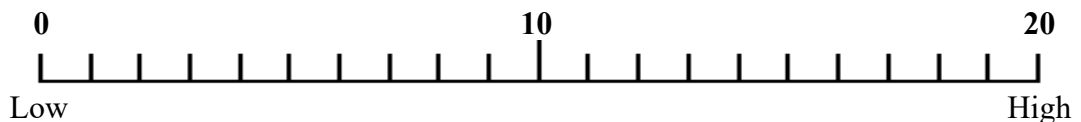
APPENDIX B: NASA Task Load Index (Rating)

NASA Task Load Index (Rating)

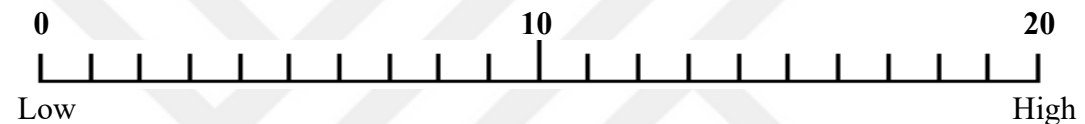
Subject ID:	Task ID:	Date:
-------------	----------	-------

Evaluate the following workload factors within the defined task by giving a score between 0 and 20.

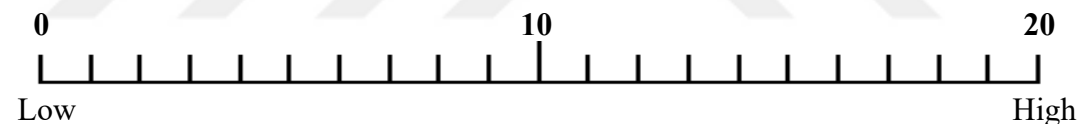
Mental Demand: How much mental and perceptual activity, was required (e.g., thinking, deciding, calculating, remembering, looking, searching, etc.)? Was the task easy or demanding, simple or complex, exacting or forgiving?



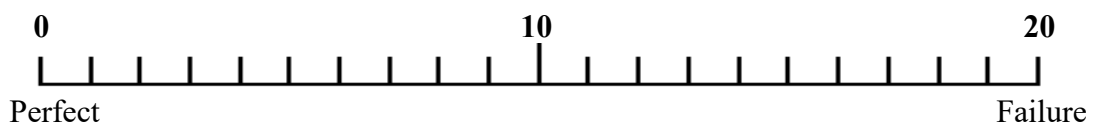
Physical Demand: How much physical activity was required (e.g. pushing, pulling, turning, controlling, activating, etc.)? Was the task easy or demanding, slow or brisk, slack or strenuous, restful or laborious?



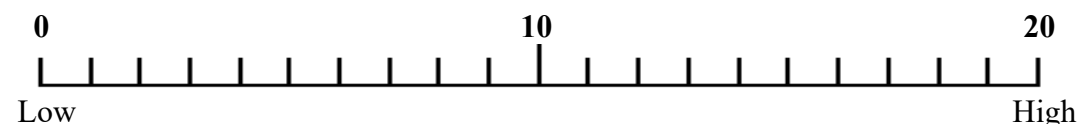
Temporal Demand: How much time pressure did you feel due to the rate or pace at which the tasks or task elements occurred? Was the pace slow and leisurely or rapid and frantic?



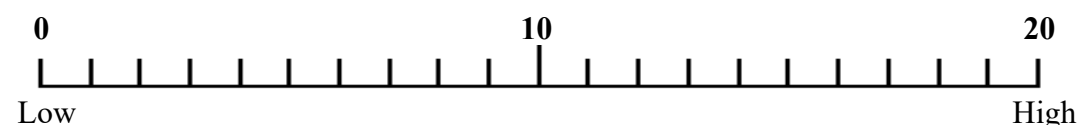
Performance: How successful do you think you were in accomplishing the goals of the task set by the experimenter (or yourself)? How satisfied were you with your performance in accomplishing these goals?



Effort: How hard did you have to work (mentally and physically) to accomplish your level of performance?



Frustration Level: How insecure, discouraged, irritated, stressed and annoyed versus secure, gratified, content, relaxed and complacent did you feel during the task?



APPENDIX C: NASA Task Load Index (Weighting)

NASA Task Load Index (Weighting)

Subject ID:	Task ID:	Date:
-------------	----------	-------

Which of the following workload factors do you think is more effective for the defined job? (Circle the selected workload factor in each row).

	Factor - 1	Factor - 2
1	Mental Demand	Temporal Demand
2	Temporal Demand	Performance
3	Mental Demand	Frustration Level
4	Effort	Performance
5	Mental Demand	Physical Demand
6	Physical Demand	Frustration Level
7	Temporal Demand	Effort
8	Mental Demand	Performance
9	Temporal Demand	Frustration Level
10	Physical Demand	Temporal Demand
11	Performance	Frustration Level
12	Physical Demand	Effort
13	Effort	Frustration Level
14	Mental Demand	Effort
15	Physical Demand	Performance

NASA-TLX workload test completed. Thank you for your co-operation. If you have any assessment about the test and / or testing process, please specify.

.....

.....

.....

.....

APPENDIX D: All Subjective Assessments of the Subjects

Table D.1 : All subjective assessments of the subjects and their calculations.

ID	Step	Scores						Weights						Weighted Scores						Result
		MD	PD	TD	P	E	F	MD	PD	TD	P	E	F	MD	PD	TD	P	E	F	
1	1	3	0	3	1	5	3	4	0	1	4	2	4	4	0	1	1.3	3.3	4	13.66
	2	5	0	4	4	8	4	5	0	1	3	3	3	8.3	0	1.3	4	8	4	25.66
	3	8	0	7	5	10	6	5	0	3	1	4	2	13.3	0	7	1.7	13.3	4	39.33
	4	15	0	18	16	15	13	3	0	5	1	3	3	15	0	30	5.3	15	13	78.33
2	1	5	0	3	9	4	1	5	0	4	3	2	1	8.3	0	4	9	2.7	0.3	24.33
	2	7	0	5	5	7	1	5	0	4	2	2	2	11.7	0	6.7	3.3	4.7	0.7	27
	3	9	0	9	10	9	5	3	0	5	3	2	2	9	0	15	10	6	3.3	43.33
	4	15	0	17	17	14	10	3	0	5	4	2	1	15	0	28.3	22.7	9.3	3.3	78.66
3	1	0	0	0	0	0	0	-	-	-	-	-	-	0	0	0	0	0	0	0
	2	1	0	1	2	2	1	2	0	3	4	5	1	0.7	0	1	2.6	3.3	0.3	8
	3	4	0	3	3	4	3	5	0	2	3	4	1	6.7	0	2	3	5.3	1	18
	4	15	0	9	10	14	9	5	0	2	3	4	1	25	0	6	10	18.7	3	62.66
4	1	2	0	1	4	4	3	3	0	1	5	4	2	2	0	0.3	6.7	5.3	2	16.33
	2	7	0	12	7	8	6	3	0	5	4	1	2	7	0	20	9.3	2.7	4	43
	3	12	0	14	10	6	9	2	0	5	4	1	3	8	0	23.3	13.3	2	9	55.66
	4	15	0	16	12	12	13	2	0	5	2	2	4	10	0	26.7	8	8	17.3	70
5	1	2	0	1	10	9	2	4	0	1	5	3	2	2.7	0	0.3	16.7	9	1.3	30
	2	14	0	13	12	13	13	3	0	4	1	2	5	14	0	17.3	4	8.7	21.7	65.66
	3	13	0	14	14	13	15	4	0	3	2	2	4	17.3	0	14	9.3	8.7	20	69.33
	4	18	0	18	20	20	20	4	0	3	1	2	5	24	0	18	6.7	13.3	33.3	95.33
6	1	1	0	0	0	0	1	3	0	2	5	1	4	1	0	0	0	0	1.33	2.333
	2	6	0	3	0	1	3	5	0	2	4	2	2	10	0	2	0	0.7	2	14.66
	3	12	0	11	6	5	5	4	0	5	2	3	1	16	0	18.3	4	5	1.7	45
	4	18	0	16	10	10	5	5	0	4	2	3	1	30	0	21.3	6.7	10	1.7	69.66
7	1	2	0	0	3	3	3	4	0	1	5	3	2	2.7	0	0	5	3	2	12.66
	2	6	0	0	6	6	6	5	0	1	4	3	2	10	0	0	8	6	4	28
	3	8	0	5	10	9	8	4	0	1	3	5	2	10.7	0	1.7	10	15	5.3	42.66
	4	10	0	5	17	14	10	5	0	1	2	4	3	16.7	0	1.7	11.3	18.7	10	58.33
8	1	5	0	4	10	7	7	4	0	1	2	3	5	6.7	0	1.3	6.7	7	11.7	33.33
	2	10	0	6	10	12	11	4	0	1	2	3	5	13.3	0	2	6.7	12	18.3	52.33
	3	16	0	13	11	10	18	4	0	2	1	3	5	21.3	0	8.7	3.7	10	30	73.66
9	1	2	0	1	2	2	2	4	0	3	1	3	4	2.7	0	1	0.7	2	2.7	9
	2	5	0	2	8	6	8	5	0	2	3	1	4	8.3	0	1.3	8	2	10.7	30.33
	3	9	0	4	5	8	6	5	0	3	1	2	4	15	0	4	1.7	5.3	8	34
	4	13	0	9	20	13	11	5	0	3	2	1	4	21.7	0	9	13.3	4.3	14.7	63
10	1	3	0	3	10	3	3	5	0	2	3	2	3	5	0	2	10	2	3	22
	2	8	0	10	12	10	9	4	0	3	1	4	3	10.7	0	10	4	13.3	9	47
	3	13	0	12	7	10	10	5	0	2	2	3	3	21.7	0	8	4.7	10	10	54.33
	4	18	0	18	6	18	17	4	0	3	2	3	3	24	0	18	4	18	17	81
11	1	5	0	4	7	6	5	4	0	3	2	2	4	6.7	0	4	4.7	4	6.7	26
	2	11	0	12	10	14	12	4	0	3	2	3	3	14.7	0	12	6.7	14	12	59.33
	3	17	0	18	17	17	18	4	0	2	1	3	5	22.7	0	12	5.7	17	30	87.33
12	1	5	0	0	5	4	0	2	0	3	5	4	1	3.3	0	0	8.3	5.3	0	17
	2	10	0	10	7	13	10	4	0	1	4	4	2	13.3	0	3.3	9.3	17.3	6.7	50
	3	14	0	10	10	14	14	4	0	3	4	2	2	18.7	0	10	13.3	9.3	9.3	60.66
	4	20	0	10	7	17	19	2	0	1	3	4	5	13.3	0	3.3	7	22.7	31.7	78

Table D.1 (continued) : All subjective assessments of the subjects and their calculations.

ID	Step	Scores						Weights						Weighted Scores						Result
		MD	PD	TD	P	E	F	MD	PD	TD	P	E	F	MD	PD	TD	P	E	F	
13	1	5	0	2	1	4	1	4	0	3	5	2	1	6.7	0	2	1.7	2.6	0.3	13.33
	2	10	0	11	5	9	6	5	0	4	1	3	2	16.7	0	14.7	1.7	9	4	46
	3	15	0	17	14	18	13	3	0	5	1	4	2	15	0	28.3	4.7	24	8.7	80.66
14	1	2	0	0	1	2	1	5	0	1	4	3	2	3.3	0	0	1.3	2	0.7	7.33
	2	9	0	0	6	7	7	4	0	1	3	3	4	12	0	0	6	7	9.3	34.33
	3	10	0	1	5	10	10	3	0	1	3	5	3	10	0	0.3	5	16.7	10	42
	4	13	0	6	13	14	15	4	0	1	3	4	3	17.3	0	2	13	18.7	15	66
15	1	4	0	5	1	7	4	2	0	2	5	4	2	2.7	0	3.3	1.7	9.3	2.7	19.66
	2	8	0	11	4	10	10	3	0	3	2	5	2	8	0	11	2.7	16.7	6.7	45
	3	16	0	9	4	16	14	3	0	2	3	5	2	16	0	6	4	26.7	9.3	62
16	1	5	0	2	5	4	2	3	0	2	5	4	1	5	0	1.3	8.3	5.3	0.7	20.66
	2	10	0	10	5	10	10	5	0	4	2	3	1	16.7	0	13.3	3.3	10	3.3	46.66
	3	15	0	13	10	12	10	5	0	3	2	4	1	25	0	13	6.7	16	3.3	64
	4	17	0	15	12	15	15	5	0	2	3	4	1	28.3	0	10	12	20	5	75.33
17	1	4	0	4	5	5	2	4	0	3	5	2	1	5.3	0	4	8.3	3.3	0.7	21.66
	2	7	0	6	6	8	5	3	0	5	4	2	1	7	0	10	8	5.3	1.7	32
	3	15	0	16	10	14	10	3	0	5	1	4	2	15	0	26.7	3.3	18.7	6.7	70.33

APPENDIX E: SPSS ANOVA Analysis Outputs of NASA-TLX Scores

		Descriptives							
		N	Mean	Std. Deviation	Std. Error	95% Confidence Interval for Mean		Minimum	Maximum
						Lower Bound	Upper Bound		
MD	1	12	3.3333	2.14617	.61955	1.9697	4.6969	.00	8.33
	2	12	10.2222	4.04353	1.16727	7.6531	12.7914	.67	16.67
	3	12	14.2778	5.71341	1.64932	10.6476	17.9079	6.67	25.00
	4	12	20.0278	6.33805	1.82964	16.0008	24.0548	10.00	30.00
	Total	48	11.9653	7.72709	1.11531	9.7216	14.2090	.00	30.00
P	1	12	5.6111	5.16365	1.49062	2.3303	8.8919	.00	16.67
	2	12	5.1667	2.94220	.84934	3.2973	7.0361	.00	9.33
	3	12	6.8889	4.20998	1.21532	4.2140	9.5638	1.67	13.33
	4	12	10.0000	5.03924	1.45470	6.7982	13.2018	4.00	22.67
	Total	48	6.9167	4.69067	.67704	5.5546	8.2787	.00	22.67
TD	1	12	.8333	1.19342	.34451	.0751	1.5916	.00	4.00
	2	12	6.3611	7.11444	2.05376	1.8408	10.8814	.00	20.00
	3	12	9.7222	7.21227	2.08200	5.1398	14.3047	.33	23.33
	4	12	14.5278	10.52794	3.03915	7.8386	21.2169	1.67	30.00
	Total	48	7.8611	8.70120	1.25591	5.3345	10.3877	.00	30.00
E	1	12	3.3333	2.56235	.73969	1.7053	4.9614	.00	9.00
	2	12	6.9722	4.89374	1.41270	3.8629	10.0816	.67	17.33
	3	12	9.3889	4.88831	1.41113	6.2830	12.4948	2.00	16.67
	4	12	14.7222	5.67972	1.63959	11.1135	18.3309	4.33	22.67
	Total	48	8.6042	6.14585	.88708	6.8196	10.3887	.00	22.67
F	1	12	1.5000	1.26730	.36584	.6948	2.3052	.00	4.00
	2	12	6.3056	5.89548	1.70188	2.5597	10.0514	.33	21.67
	3	12	7.0833	5.22644	1.50874	3.7626	10.4041	1.00	20.00
	4	12	13.7500	10.40797	3.00452	7.1371	20.3629	1.67	33.33
	Total	48	7.1597	7.72732	1.11534	4.9159	9.4035	.00	33.33
Total	1	12	14.6111	8.96777	2.58877	8.9133	20.3090	.00	30.00
	2	12	35.0278	16.16484	4.66639	24.7571	45.2984	8.00	65.67
	3	12	47.3611	14.24423	4.11196	38.3108	56.4115	18.00	69.33
	4	12	73.0278	10.20146	2.94491	66.5461	79.5095	58.33	95.33
	Total	48	42.5069	24.67059	3.56089	35.3434	49.6705	.00	95.33

Figure E.1 : Descriptives of NASA-TLX scores for navigation scenario.

		ANOVA				
		Sum of Squares	df	Mean Square	F	Sig.
MD	Between Groups	1774.803	3	591.601	25.236	.000
	Within Groups	1031.472	44	23.443		
	Total	2806.275	47			
P	Between Groups	171.296	3	57.099	2.912	.045
	Within Groups	862.815	44	19.609		
	Total	1034.111	47			
TD	Between Groups	1194.574	3	398.191	7.412	.000
	Within Groups	2363.833	44	53.723		
	Total	3558.407	47			
E	Between Groups	821.896	3	273.965	12.644	.000
	Within Groups	953.361	44	21.667		
	Total	1775.257	47			
F	Between Groups	914.396	3	304.799	7.088	.001
	Within Groups	1892.046	44	43.001		
	Total	2806.442	47			
Total	Between Groups	21470.396	3	7156.799	44.131	.000
	Within Groups	7135.602	44	162.173		
	Total	28605.998	47			

Figure E.2 : ANOVA of NASA-TLX scores for navigation scenario.

		Descriptives							
		N	Mean	Std. Deviation	Std. Error	95% Confidence Interval for Mean		Minimum	Maximum
						Lower Bound	Upper Bound		
MD	1	5	5.6000	1.73845	.77746	3.4414	7.7586	2.67	6.67
	2	5	11.9333	4.23215	1.89268	6.6784	17.1882	7.00	16.67
	3	5	18.0000	3.70435	1.65664	13.4004	22.5996	15.00	22.67
	Total	15	11.8444	6.11253	1.57825	8.4594	15.2294	2.67	22.67
TD	1	5	2.9333	1.21106	.54160	1.4296	4.4371	1.33	4.00
	2	5	9.9333	4.76329	2.13021	4.0189	15.8477	2.00	14.67
	3	5	16.3333	10.42966	4.66429	3.3832	29.2835	6.00	28.33
	Total	15	9.7333	8.37058	2.16128	5.0979	14.3688	1.33	28.33
P	1	5	4.6000	2.97583	1.33083	.9050	8.2950	1.67	8.33
	2	5	5.1333	2.78488	1.24544	1.6754	8.5912	1.67	8.00
	3	5	4.2667	.92496	.41366	3.1182	5.4152	3.33	5.67
	Total	15	4.6667	2.26428	.58464	3.4127	5.9206	1.67	8.33
E	1	5	5.2667	2.81267	1.25786	1.7743	8.7591	2.67	9.33
	2	5	11.4000	4.39949	1.96751	5.9373	16.8627	5.33	16.67
	3	5	19.2667	6.49102	2.90287	11.2070	27.3263	10.00	26.67
	Total	15	11.9778	7.41670	1.91498	7.8705	16.0850	2.67	26.67
F	1	5	4.4000	4.78075	2.13802	-1.5361	10.3361	.33	11.67
	2	5	8.5333	6.69411	2.99370	.2215	16.8452	1.67	18.33
	3	5	16.9333	11.96848	5.35247	2.0725	31.7942	6.67	30.00
	Total	15	9.9556	9.45488	2.44124	4.7196	15.1915	.33	30.00
Total	1	5	22.8000	7.44834	3.33100	13.5517	32.0483	13.33	33.33
	2	5	46.9333	10.13081	4.53064	34.3543	59.5124	32.00	59.33
	3	5	74.8000	9.70281	4.33923	62.7524	86.8476	62.00	87.33
	Total	15	48.1778	23.57456	6.08692	35.1226	61.2329	13.33	87.33

Figure E.3 : Descriptives of NASA-TLX scores for cargo operation scenario.

		ANOVA				
		Sum of Squares	df	Mean Square	F	Sig.
MD	Between Groups	384.459	2	192.230	16.641	.000
	Within Groups	138.622	12	11.552		
	Total	523.081	14			
TD	Between Groups	449.200	2	224.600	5.069	.025
	Within Groups	531.733	12	44.311		
	Total	980.933	14			
P	Between Groups	1.911	2	.956	.164	.851
	Within Groups	69.867	12	5.822		
	Total	71.778	14			
E	Between Groups	492.504	2	246.252	10.645	.002
	Within Groups	277.600	12	23.133		
	Total	770.104	14			
F	Between Groups	407.881	2	203.941	2.901	.094
	Within Groups	843.644	12	70.304		
	Total	1251.526	14			
Total	Between Groups	6771.615	2	3385.807	40.266	.000
	Within Groups	1009.022	12	84.085		
	Total	7780.637	14			

Figure E.4 : ANOVA of NASA-TLX scores for cargo operation scenario.

APPENDIX F: Calculation Details of Performance Scores

		Weights ($w\alpha, w\psi$)	Scores ($\gamma\alpha, \eta\psi$)	Product	Weighted Sum			Weights ($w\alpha, w\psi$)	Scores ($\gamma\alpha, \eta\psi$)	Product	Weighted Sum			Weights ($w\alpha, w\psi$)	Scores ($\gamma\alpha, \eta\psi$)	Product	Weighted Sum			Weights ($w\alpha, w\psi$)	Scores ($\gamma\alpha, \eta\psi$)	Product	Weighted Sum		
Step 1	T1	ψ_{13}	0.32	1	0.32	Step 2	T1	ψ_{13}	0.24	1	0.24	Step 3	T1	ψ_{13}	0.16	0.5	0.08	Step 4	T1	ψ_{13}	0.31	1	0.31		
		η_{31}	0.18	1	0.18			ψ_{15}	0.22	1	0.22			ψ_{14}	0.16	0	0			η_{31}	0.16	1	0.16		
		η_4	0.25	1	0.25			η_1	0.16	1	0.16			ψ_{15}	0.16	0	0			η_{31}	0.23	1	0.23		
		ψ_{14}	0.25	1	0.25			η_4	0.22	1	0.22			ψ_3	0.16	1	0.16			η_4	0.3	1	0.3		
	T2	ψ_{15}	0.25	1	0.25		T2	ψ_{12}	0.2	1	0.2		T2	η_{31}	0.11	1	0.11		T2	η_{32}	0.32	1	0.32		
		η_1	0.12	1	0.12			ψ_{14}	0.22	1	0.22			η_4	0.14	1	0.14			η_4	0.31	1	0.31		
		η_{31}	0.17	1	0.17			η_{31}	0.15	1	0.15			T3	ψ_{13}	0.2	1			0.2	T3	ψ_{11}	0.21	0	0
		η_4	0.21	1	0.21			ψ_{15}	0.23	1	0.23				ψ_{15}	0.2	1			0.2		ψ_{14}	0.22	0	0
	ψ_{12}	0.22	1	0.22	η_4		0.2	1	0.2	ψ_3	0.19		1		0.19	ψ_{15}	0.22		1	0.22					
	ψ_{14}	0.22	0.5	0.11	ψ_{11}		0.22	1	0.22	η_1	0.12		0.5		0.06	η_{31}	0.17		1	0.17					
	T3	ψ_{15}	0.22	1	0.22		T3	ψ_{12}	0.21	1	0.21		T3	η_{31}	0.12	1	0.12		T3	η_4	0.18	1	0.18		
		η_{31}	0.17	1	0.17			ψ_{13}	0.22	1	0.22			η_4	0.17	1	0.17			ψ_{11}	0.25	0	0		
		η_4	0.17	1	0.17			η_{31}	0.14	1	0.14			T4	ψ_{11}	0.25	0			0	T4	ψ_3	0.27	0	0
		ψ_{11}	0.43	1	0.43			η_4	0.21	1	0.21				ψ_{12}	0.22	0			0		η_{31}	0.23	1	0.23
	T4	η_{31}	0.25	1	0.25		T4	ψ_{11}	0.29	1	0.29		T4		ψ_3	0.16	1		0.16	T4		η_4	0.25	1	0.25
η_4		0.32	1	0.32	ψ_{12}	0.27		1	0.27	η_4	0.22	1			0.22	ψ_{13}	0.28	1	0.28						
ψ_{11}		0.27	1	0.27	η_4	0.25		1	0.25	η_{31}	0.15	1		0.15	η_4	0.25	1	0.25							
T5	η_2	0.27	1	0.27	T5	ψ_{11}	0.21	1	0.21	T5	ψ_{13}	0.28	0.5	0.14	T5	ψ_{11}	0.28	0.5	0.14						
	η_{31}	0.22	1	0.22		ψ_{12}	0.2	1	0.2		T5	ψ_3	0.28	1		0.28	T5	η_{31}	0.23	1	0.23				
	η_4	0.24	1	0.24		ψ_{31}	0.16	1	0.16			η_4	0.26	1		0.26		η_4	0.24	1	0.24				
	ψ_{11}	0.27	1	0.27		η_4	0.2	1	0.2			T6	ψ_{15}	0.26		1		0.26	T6	ψ_{11}	0.15	1	0.15		
η_2	0.27	1	0.27	ψ_3	0.24	1	0.24	T6	ψ_3	0.28			1	0.28	T6	ψ_{14}		0.15		1	0.15				
η_{31}	0.22	1	0.22	η_{31}	0.22	1	0.22		T6	η_{31}	0.2		1	0.2		T6	ψ_{15}	0.15		1	0.15				
η_4	0.24	1	0.24	η_4	0.26	1	0.26			T6	ψ_2		0.13	1			0.13	T6		ψ_2	0.14	1	0.14		
ψ_{11}	0.27	1	0.27	ψ_3	0.28	1	0.28				T6	ψ_{13}	0.13	1			0.13		T6	ψ_3	0.14	1	0.14		
η_2	0.27	1	0.27	ψ_{14}	0.13	1	0.13	T6				ψ_{14}	0.13	1	0.13		T6			η_3	0.14	1	0.14		
η_{31}	0.22	1	0.22	ψ_{15}	0.14	1	0.14		T6			ψ_{15}	0.14	1	0.14	T6				η_4	0.13	1	0.13		
η_4	0.24	1	0.24	ψ_2	0.13	1	0.13			T6		η_4	0.13	1	0.13			T6		ψ_2	0.21	1	0.21		
ψ_{11}	0.27	1	0.27	η_{31}	0.1	1	0.1				T6	ψ_3	0.22	1	0.22				T6	η_1	0.16	1	0.16		
η_2	0.27	1	0.27	η_4	0.12	1	0.12	T6				η_{31}	0.21	1	0.21		T6			η_{31}	0.21	1	0.21		
η_{31}	0.22	1	0.22	η_4	0.12	1	0.12		T6			η_4	0.2	1	0.2	T6				η_4	0.2	1	0.2		
η_4	0.24	1	0.24	η_4	0.12	1	0.12			T6		η_4	0.2	1	0.2			T6		η_4	0.2	1	0.2		

Subject ID 01

Figure F.1 : Calculation details of performance score for navigation tasks.

		Weights (w α , w ν)	Scores ($\gamma\alpha$, $\eta\nu$)	Product	Weighted Sum			Weights (w α , w ν)	Scores ($\gamma\alpha$, $\eta\nu$)	Product	Weighted Sum			Weights (w α , w ν)	Scores ($\gamma\alpha$, $\eta\nu$)	Product	Weighted Sum			Weights (w α , w ν)	Scores ($\gamma\alpha$, $\eta\nu$)	Product	Weighted Sum																		
Step 1	T1	$\gamma 13$	0.32	1	0.32	1	Step 2	T1	$\gamma 13$	0.24	1	0.24	0.78	Step 3	T1	$\gamma 13$	0.16	1	0.16	0.785	Step 4	T1	$\gamma 13$	0.31	1	0.31	1														
		$\eta 1$	0.25	1	0.25				$\gamma 15$	0.22	0	0				$\eta 1$	0.16	1	0.16				$\eta 1$	0.16	1	0.16															
		$\eta 31$	0.18	1	0.18				$\eta 31$	0.16	1	0.16				$\gamma 15$	0.16	0	0				$\eta 31$	0.23	1	0.23		$\eta 31$	0.23	1	0.23										
		$\eta 4$	0.25	1	0.25				$\eta 4$	0.22	1	0.22				$\gamma 3$	0.16	1	0.16				$\eta 4$	0.3	1	0.3		$\eta 4$	0.3	1	0.3										
	T2	$\gamma 14$	0.25	1	0.25	1		T2	$\gamma 12$	0.2	0	0	0.71		T2	$\gamma 13$	0.2	1	0.2	0.94		T3	$\gamma 11$	0.21	0	0	0.83	T4	$\gamma 11$	0.25	0	0	0.5								
		$\gamma 15$	0.25	1	0.25				$\gamma 14$	0.22	1	0.22				$\gamma 15$	0.2	1	0.2				$\eta 1$	0.11	0.5	0.055			$\gamma 12$	0.22	0	0		$\eta 31$	0.11	1	0.11				
		$\eta 1$	0.12	1	0.12				$\gamma 15$	0.23	1	0.23				$\eta 31$	0.11	1	0.11				$\eta 1$	0.11	0.5	0.055			$\eta 31$	0.12	1	0.12		$\eta 4$	0.14	1	0.14				
		$\eta 4$	0.21	1	0.21				$\eta 31$	0.15	1	0.15				$\eta 4$	0.14	1	0.14				$\eta 4$	0.12	0.5	0.06			$\eta 4$	0.17	1	0.17		$\eta 4$	0.17	1	0.17				
	T3	$\gamma 12$	0.22	1	0.22	1		T3	$\gamma 11$	0.22	0.5	0.11	0.47		T4	$\gamma 11$	0.25	0	0	0.53		T5	$\gamma 11$	0.15	1	0.15	0.8	T6	$\gamma 11$	0.13	0.5	0.065	0.13								
		$\gamma 14$	0.22	1	0.22				$\gamma 12$	0.21	0	0				$\gamma 12$	0.22	1	0.22				$\gamma 3$	0.19	1	0.19			$\gamma 12$	0.22	0	0		$\gamma 13$	0.13	1	0.13				
		$\gamma 15$	0.22	1	0.22				$\gamma 13$	0.22	1	0.22				$\eta 31$	0.14	1	0.14				$\eta 4$	0.21	0	0			$\eta 31$	0.14	1	0.14		$\gamma 14$	0.13	0	0	$\gamma 13$	0.13	1	0.13
		$\eta 31$	0.17	1	0.17				$\eta 4$	0.2	0	0				$\eta 4$	0.21	0	0				$\gamma 11$	0.29	1	0.29			$\eta 4$	0.25	0	0		$\eta 4$	0.26	1	0.26	$\gamma 15$	0.14	1	0.14
	T4	$\gamma 11$	0.43	1	0.43	1		T4	$\gamma 11$	0.29	1	0.29	0.48		T5	$\gamma 3$	0.16	1	0.16	0.58		T6	$\gamma 3$	0.28	0	0	1	T7	$\gamma 3$	0.28	1	0.28	0.805								
		$\eta 31$	0.25	1	0.25				$\gamma 12$	0.27	0	0				$\eta 4$	0.22	1	0.22				$\eta 4$	0.22	1	0.22			$\eta 4$	0.22	1	0.22		$\gamma 31$	0.18	1	0.18				
		$\eta 4$	0.32	1	0.32				$\eta 31$	0.19	1	0.19				$\gamma 13$	0.28	0.5	0.14				$\eta 4$	0.22	1	0.22			$\eta 4$	0.26	1	0.26		$\eta 4$	0.26	1	0.26	$\gamma 31$	0.28	1	0.28
		$\gamma 11$	0.27	1	0.27				$\eta 4$	0.25	0	0				$\gamma 3$	0.28	0	0				$\gamma 15$	0.26	1	0.26			$\gamma 31$	0.28	1	0.28		$\eta 4$	0.26	1	0.26	$\eta 4$	0.26	1	0.26
	T5	$\eta 2$	0.27	1	0.27	1		T5	$\gamma 2$	0.23	1	0.23	0.8		T6	$\gamma 31$	0.15	1	0.15	0.58		T7	$\gamma 31$	0.15	1	0.15	0.75	T8	$\gamma 31$	0.15	1	0.15	0.45								
		$\eta 31$	0.22	1	0.22				$\gamma 12$	0.2	1	0.2				$\eta 4$	0.22	1	0.22				$\gamma 3$	0.25	0	0			$\gamma 31$	0.23	1	0.23		$\gamma 31$	0.23	1	0.23				
		$\eta 4$	0.24	1	0.24				$\eta 31$	0.16	1	0.16				$\gamma 13$	0.28	0.5	0.14				$\eta 4$	0.24	1	0.24			$\eta 4$	0.23	1	0.23		$\eta 4$	0.24	1	0.24	$\eta 4$	0.24	1	0.24
		$\gamma 11$	0.27	1	0.27				$\eta 4$	0.2	0	0				$\gamma 14$	0.28	1	0.28				$\gamma 11$	0.28	1	0.28			$\eta 4$	0.24	1	0.24		$\gamma 11$	0.28	1	0.28	$\gamma 11$	0.28	1	0.28
T6	$\gamma 11$	0.27	1	0.27	1	T6	$\gamma 2$	0.23	1	0.23	0.8	T7	$\gamma 31$	0.18	1	0.18	0.58	T8	$\gamma 31$	0.18	1	0.18	0.75	T9	$\gamma 31$	0.18	1	0.18	0.45												
	$\eta 2$	0.27	1	0.27			$\eta 31$	0.16	1	0.16			$\gamma 15$	0.26	1	0.26			$\gamma 31$	0.18	1	0.18			$\gamma 15$	0.26	1	0.26		$\gamma 31$	0.21	1	0.21								
	$\eta 31$	0.22	1	0.22			$\eta 4$	0.2	0	0			$\gamma 15$	0.26	1	0.26			$\eta 4$	0.22	1	0.22			$\gamma 15$	0.26	1	0.26		$\eta 4$	0.24	1	0.24								
	$\eta 4$	0.24	1	0.24			$\gamma 11$	0.21	1	0.21			$\gamma 15$	0.26	1	0.26			$\gamma 31$	0.28	1	0.28			$\gamma 15$	0.26	1	0.26		$\gamma 31$	0.28	1	0.28								
T7	$\gamma 11$	0.27	1	0.27	1	T7	$\gamma 2$	0.23	1	0.23	0.8	T8	$\gamma 31$	0.15	1	0.15	0.58	T9	$\gamma 31$	0.15	1	0.15	0.75	T10	$\gamma 31$	0.15	1	0.15	0.45												
	$\eta 2$	0.27	1	0.27			$\gamma 12$	0.2	1	0.2			$\gamma 31$	0.15	1	0.15			$\gamma 31$	0.15	1	0.15			$\gamma 31$	0.15	1	0.15		$\gamma 31$	0.15	1	0.15								
	$\eta 31$	0.22	1	0.22			$\eta 31$	0.16	1	0.16			$\gamma 13$	0.28	0.5	0.14			$\gamma 31$	0.15	1	0.15			$\gamma 31$	0.15	1	0.15		$\gamma 31$	0.15	1	0.15								
	$\eta 4$	0.24	1	0.24			$\eta 4$	0.2	0	0			$\gamma 14$	0.28	1	0.28			$\gamma 31$	0.15	1	0.15			$\gamma 31$	0.15	1	0.15		$\gamma 31$	0.15	1	0.15								
T8	$\gamma 11$	0.27	1	0.27	1	T8	$\gamma 2$	0.23	1	0.23	0.8	T9	$\gamma 31$	0.18	1	0.18	0.58	T10	$\gamma 31$	0.18	1	0.18	0.75	T11	$\gamma 31$	0.18	1	0.18	0.45												
	$\eta 2$	0.27	1	0.27			$\eta 31$	0.16	1	0.16			$\gamma 15$	0.26	1	0.26			$\gamma 31$	0.18	1	0.18			$\gamma 31$	0.18	1	0.18		$\gamma 31$	0.18	1	0.18								
	$\eta 31$	0.22	1	0.22			$\eta 4$	0.2	0	0			$\gamma 15$	0.26	1	0.26			$\gamma 31$	0.18	1	0.18			$\gamma 31$	0.18	1	0.18		$\gamma 31$	0.18	1	0.18								
	$\eta 4$	0.24	1	0.24			$\gamma 11$	0.21	1	0.21			$\gamma 15$	0.26	1	0.26			$\gamma 31$	0.18	1	0.18			$\gamma 31$	0.18	1	0.18		$\gamma 31$	0.18	1	0.18								
T9	$\gamma 11$	0.27	1	0.27	1	T9	$\gamma 2$	0.23	1	0.23	0.8	T10	$\gamma 31$	0.15	1	0.15	0.58	T11	$\gamma 31$	0.15	1	0.15	0.75	T12	$\gamma 31$	0.15	1	0.15	0.45												
	$\eta 2$	0.27	1	0.27			$\gamma 12$	0.2	1	0.2			$\gamma 31$	0.15	1	0.15			$\gamma 31$	0.15	1	0.15			$\gamma 31$	0.15	1	0.15		$\gamma 31$	0.15	1	0.15								
	$\eta 31$	0.22	1	0.22			$\eta 31$	0.16	1	0.16			$\gamma 13$	0.28	0.5	0.14			$\gamma 31$	0.15	1	0.15			$\gamma 31$	0.15	1	0.15		$\gamma 31$	0.15	1	0.15								
	$\eta 4$	0.24	1	0.24			$\eta 4$	0.2	0	0			$\gamma 14$	0.28	1	0.28			$\gamma 31$	0.15	1	0.15			$\gamma 31$	0.15	1	0.15		$\gamma 31$	0.15	1	0.15								
T10	$\gamma 11$	0.27	1	0.27	1	T10	$\gamma 2$	0.23	1	0.23	0.8	T11	$\gamma 31$	0.18	1	0.18	0.58	T12	$\gamma 31$	0.18	1	0.18	0.75	T13	$\gamma 31$	0.18	1	0.18	0.45												
	$\eta 2$	0.27	1	0.27			$\gamma 12$	0.2	1	0.2			$\gamma 31$	0.18	1	0.18			$\gamma 31$	0.18	1	0.18			$\gamma 31$	0.18	1	0.18		$\gamma 31$	0.18	1	0.18								
	$\eta 31$	0.22	1	0.22			$\eta 31$	0.16	1	0.16			$\gamma 13$	0.28	0.5	0.14			$\gamma 31$	0.18	1	0.18			$\gamma 31$	0.18	1	0.18		$\gamma 31$	0.18	1	0.18								
	$\eta 4$	0.24	1	0.24			$\eta 4$	0.2	0	0			$\gamma 14$	0.28	1	0.28			$\gamma 31$	0.18	1	0.18			$\gamma 31$	0.18	1	0.18		$\gamma 31$	0.18	1	0.18								
T11	$\gamma 11$	0.27	1	0.27	1	T11	$\gamma 2$	0.23	1	0.23	0.8	T12	$\gamma 31$	0.15	1	0.15	0.58	T13	$\gamma 31$	0.15	1	0.15	0.75	T14	$\gamma 31$	0.15	1	0.15	0.45												
	$\eta 2$	0.27	1	0.27			$\gamma 12$	0.2	1	0.2			$\gamma 31$	0.15	1	0.15			$\gamma 31$	0.15	1	0.15			$\gamma 31$	0.15	1	0.15		$\gamma 31$	0.15	1	0.15								
	$\eta 31$	0.22	1	0.22			$\eta 31$	0.16	1	0.16			$\gamma 13$	0.28	0.5	0.14			$\gamma 31$	0.15	1	0.15			$\gamma 31$	0.15	1	0.15		$\gamma 31$	0.15	1	0.15								
	$\eta 4$	0.24	1	0.24			$\eta 4$	0.2	0	0			$\gamma 14$	0.28	1	0.28			$\gamma 31$	0.15	1	0.15			$\gamma 31$	0.15	1	0.15		$\gamma 31$	0.15	1	0.15								
T12	$\gamma 11$	0.27	1	0.27	1	T12	$\gamma 2$	0.23	1	0.23	0.																														

		Weights (w α , w ν)	Scores ($\gamma\alpha$, $\eta\nu$)	Product	Weighted Sum			Weights (w α , w ν)	Scores ($\gamma\alpha$, $\eta\nu$)	Product	Weighted Sum			Weights (w α , w ν)	Scores ($\gamma\alpha$, $\eta\nu$)	Product	Weighted Sum			Weights (w α , w ν)	Scores ($\gamma\alpha$, $\eta\nu$)	Product	Weighted Sum									
Step 1	T1	$\gamma 13$	0.32	1	0.32	1	Step 2	T1	$\gamma 13$	0.24	1	0.24	Step 3	T1	$\gamma 13$	0.16	1	0.16	Step 4	T1	$\gamma 13$	0.31	1	0.31								
		$\eta 1$	0.25	1	0.25				$\gamma 15$	0.22	1	0.22			$\gamma 14$	0.16	1	0.16			$\eta 1$	0.16	1	0.16	$\eta 1$	0.16	1	0.16				
		$\eta 31$	0.18	1	0.18				$\eta 31$	0.16	1	0.16			$\gamma 15$	0.16	1	0.16			$\eta 31$	0.23	1	0.23	$\eta 31$	0.23	1	0.23				
		$\eta 4$	0.25	1	0.25				$\eta 4$	0.22	1	0.22			$\gamma 3$	0.16	1	0.16			$\eta 4$	0.3	0	0	$\eta 4$	0.3	0	0				
	T2	$\gamma 14$	0.25	1	0.25	1		T2	$\gamma 12$	0.2	1	0.2		0.8	T2	$\eta 1$	0.11	1		0.11	0.73	T2	$\gamma 13$	0.2	0.5	0.1	T2	$\gamma 13$	0.37	1	0.37	
		$\eta 1$	0.12	1	0.12				$\gamma 14$	0.22	1	0.22				$\eta 4$	0.14	0		0			$\gamma 15$	0.2	1	0.2		$\eta 32$	0.32	1	0.32	
		$\eta 31$	0.17	1	0.17				$\eta 31$	0.15	1	0.15				$\gamma 3$	0.19	1		0.19			$\eta 4$	0.31	1	0.31		$\eta 4$	0.31	1	0.31	
	T3	$\gamma 12$	0.22	1	0.22	1		T3	$\gamma 11$	0.22	1	0.22		0.79	T3	$\eta 31$	0.12	1		0.12	0.655	T3	$\gamma 11$	0.22	1	0.22	1	T3	$\gamma 15$	0.22	1	0.22
		$\gamma 14$	0.22	1	0.22				$\eta 4$	0.2	0	0				$\eta 1$	0.12	1		0.12			$\gamma 3$	0.19	1	0.19			$\eta 31$	0.17	1	0.17
		$\gamma 15$	0.22	1	0.22				$\gamma 11$	0.21	1	0.21				$\eta 31$	0.12	1		0.12			$\eta 4$	0.17	0	0			$\eta 4$	0.18	1	0.18
	T4	$\eta 31$	0.17	1	0.17	1		T4	$\gamma 13$	0.22	1	0.22		0.75	T4	$\eta 4$	0.17	0		0	0.73	T4	$\gamma 11$	0.25	0.5	0.125	0.655	T4	$\gamma 11$	0.21	1	0.21
		$\eta 4$	0.17	1	0.17				$\eta 31$	0.14	1	0.14				$\gamma 12$	0.22	0		0			$\gamma 12$	0.22	0	0			$\gamma 3$	0.16	1	0.16
		$\gamma 11$	0.43	1	0.43				$\eta 4$	0.21	0	0				$\eta 31$	0.14	1		0.14			$\eta 4$	0.22	1	0.22			$\eta 31$	0.15	1	0.15
	T5	$\eta 31$	0.25	1	0.25	1		T5	$\gamma 11$	0.29	1	0.29		0.75	T5	$\eta 4$	0.22	1		0.22	0.655	T5	$\gamma 11$	0.25	0.5	0.125	0.655	T5	$\gamma 11$	0.29	1	0.29
		$\eta 4$	0.32	1	0.32				$\gamma 12$	0.27	1	0.27				$\gamma 3$	0.16	1		0.16			$\gamma 12$	0.22	0	0			$\gamma 12$	0.27	1	0.27
$\gamma 11$		0.27	1	0.27	$\eta 4$		0.25		0	0	$\eta 4$	0.22	1			0.22	$\eta 4$	0.26	1	0.26			$\eta 4$	0.25	0	0						
T6	$\eta 2$	0.27	1	0.27	1	T6	$\gamma 11$	0.21	1	0.21	0.8	T6	$\gamma 11$	0.21	1	0.21	0.655	T6	$\gamma 11$	0.28	1	0.28	0.655	T6	$\gamma 11$	0.28	1	0.28				
	$\eta 31$	0.22	1	0.22			$\gamma 12$	0.2	1	0.2			$\gamma 3$	0.18	1	0.18			$\gamma 3$	0.18	1	0.18			$\gamma 3$	0.18	1	0.18				
	$\eta 4$	0.24	1	0.24			$\gamma 2$	0.23	1	0.23			$\eta 4$	0.26	1	0.26			$\eta 4$	0.26	1	0.26			$\eta 4$	0.26	1	0.26				
T7	$\gamma 11$	0.27	1	0.27	1	T7	$\gamma 2$	0.24	1	0.24	0.8	T7	$\gamma 11$	0.13	0.5	0.065	0.805	T7	$\gamma 11$	0.13	0.5	0.065	0.805	T7	$\gamma 11$	0.13	0.5	0.065				
	$\eta 2$	0.27	1	0.27			$\gamma 12$	0.12	1	0.12			$\gamma 12$	0.12	1	0.12			$\gamma 12$	0.12	1	0.12			$\gamma 12$	0.12	1	0.12				
	$\eta 31$	0.22	1	0.22			$\gamma 13$	0.13	1	0.13			$\gamma 13$	0.13	1	0.13			$\gamma 13$	0.13	1	0.13			$\gamma 13$	0.13	1	0.13				
	$\eta 4$	0.24	1	0.24			$\gamma 14$	0.13	1	0.13			$\gamma 14$	0.13	1	0.13			$\gamma 14$	0.13	1	0.13			$\gamma 14$	0.13	1	0.13				
T8	$\gamma 11$	0.27	1	0.27	1	T8	$\gamma 3$	0.28	1	0.28	0.74	T8	$\gamma 14$	0.13	1	0.13	0.805	T8	$\gamma 14$	0.13	1	0.13	0.805	T8	$\gamma 14$	0.13	1	0.13				
	$\eta 2$	0.27	1	0.27			$\eta 32$	0.22	1	0.22			$\gamma 15$	0.14	1	0.14			$\gamma 15$	0.14	1	0.14			$\gamma 15$	0.14	1	0.14				
	$\eta 31$	0.22	1	0.22			$\eta 4$	0.26	0	0			$\gamma 2$	0.13	0	0			$\gamma 2$	0.13	0	0			$\gamma 2$	0.13	0	0				
	$\eta 4$	0.24	1	0.24			$\eta 4$	0.26	0	0			$\eta 31$	0.1	1	0.1			$\eta 31$	0.1	1	0.1			$\eta 31$	0.1	1	0.1				
T9	$\gamma 11$	0.27	1	0.27	1	T9	$\gamma 4$	0.26	0	0	0.74	T9	$\eta 4$	0.12	1	0.12	0.805	T9	$\gamma 4$	0.26	1	0.26	0.805	T9	$\eta 4$	0.12	1	0.12				
	$\eta 2$	0.27	1	0.27			$\gamma 11$	0.13	0.5	0.065			$\gamma 11$	0.13	0.5	0.065			$\gamma 11$	0.13	0.5	0.065			$\gamma 11$	0.13	0.5	0.065				
	$\eta 31$	0.22	1	0.22			$\gamma 12$	0.12	1	0.12			$\gamma 12$	0.12	1	0.12			$\gamma 12$	0.12	1	0.12			$\gamma 12$	0.12	1	0.12				
	$\eta 4$	0.24	1	0.24			$\gamma 13$	0.13	1	0.13			$\gamma 13$	0.13	1	0.13			$\gamma 13$	0.13	1	0.13			$\gamma 13$	0.13	1	0.13				
T10	$\gamma 11$	0.27	1	0.27	1	T10	$\gamma 14$	0.13	1	0.13	0.74	T10	$\gamma 14$	0.13	1	0.13	0.805	T10	$\gamma 14$	0.13	1	0.13	0.805	T10	$\gamma 14$	0.13	1	0.13				
	$\eta 2$	0.27	1	0.27			$\gamma 15$	0.14	1	0.14			$\gamma 15$	0.14	1	0.14			$\gamma 15$	0.14	1	0.14			$\gamma 15$	0.14	1	0.14				
	$\eta 31$	0.22	1	0.22			$\gamma 2$	0.13	0	0			$\gamma 2$	0.13	0	0			$\gamma 2$	0.13	0	0			$\gamma 2$	0.13	0	0				
	$\eta 4$	0.24	1	0.24			$\eta 31$	0.1	1	0.1			$\eta 31$	0.1	1	0.1			$\eta 31$	0.1	1	0.1			$\eta 31$	0.1	1	0.1				
T11	$\gamma 11$	0.27	1	0.27	1	T11	$\gamma 15$	0.14	1	0.14	0.74	T11	$\gamma 15$	0.14	1	0.14	0.805	T11	$\gamma 15$	0.14	1	0.14	0.805	T11	$\gamma 15$	0.14	1	0.14				
	$\eta 2$	0.27	1	0.27			$\gamma 2$	0.13	0	0			$\gamma 2$	0.13	0	0			$\gamma 2$	0.13	0	0			$\gamma 2$	0.13	0	0				
	$\eta 31$	0.22	1	0.22			$\eta 31$	0.1	1	0.1			$\eta 31$	0.1	1	0.1			$\eta 31$	0.1	1	0.1			$\eta 31$	0.1	1	0.1				
	$\eta 4$	0.24	1	0.24			$\eta 4$	0.12	1	0.12			$\eta 4$	0.12	1	0.12			$\eta 4$	0.12	1	0.12			$\eta 4$	0.12	1	0.12				
T12	$\gamma 11$	0.27	1	0.27	1	T12	$\eta 4$	0.12	1	0.12	0.74	T12	$\eta 4$	0.12	1	0.12	0.805	T12	$\eta 4$	0.12	1	0.12	0.805	T12	$\eta 4$	0.12	1	0.12				
	$\eta 2$	0.27	1	0.27			$\gamma 11$	0.13	0.5	0.065			$\gamma 11$	0.13	0.5	0.065			$\gamma 11$	0.13	0.5	0.065			$\gamma 11$	0.13	0.5	0.065				
	$\eta 31$	0.22	1	0.22			$\gamma 12$	0.12	1	0.12			$\gamma 12$	0.12	1	0.12			$\gamma 12$	0.12	1	0.12			$\gamma 12$	0.12	1	0.12				
	$\eta 4$	0.24	1	0.24			$\gamma 13$	0.13	1	0.13			$\gamma 13$	0.13	1	0.13			$\gamma 13$	0.13	1	0.13			$\gamma 13$	0.13	1	0.13				
T13	$\gamma 11$	0.27	1	0.27	1	T13	$\gamma 14$	0.13	1	0.13	0.74	T13	$\gamma 14$	0.13	1	0.13	0.805	T13	$\gamma 14$	0.13	1	0.13	0.805	T13	$\gamma 14$	0.13	1	0.13				
	$\eta 2$	0.27	1	0.27			$\gamma 15$	0.14	1	0.14			$\gamma 15$	0.14	1	0.14			$\gamma 15$	0.14	1	0.14			$\gamma 15$	0.14	1	0.14				
	$\eta 31$	0.22	1	0.22			$\gamma 2$	0.13	0	0			$\gamma 2$	0.13	0	0			$\gamma 2$	0.13	0	0			$\gamma 2$	0.13	0	0				
	$\eta 4$	0.24	1	0.24			$\eta 31$	0.1	1	0.1			$\eta 31$	0.1	1	0.1			$\eta 31$	0.1	1	0.1			$\eta 31$	0.1	1	0.1				
T14	$\gamma 11$	0.27	1	0.27	1	T14	$\eta 4$	0.12	1	0.12	0.74	T14	$\eta 4$	0.12	1	0.12	0.805	T14	$\eta 4$	0.12	1	0.12	0.805	T14	$\eta 4$	0.12	1	0.12				
	$\eta 2$	0.27	1	0.27			$\gamma 11$	0.13	0.5	0.065			$\gamma 11$	0.13	0.5	0.065			$\gamma 11$	0.13	0.5	0.065			$\gamma 11$	0.13	0.5	0.065				
	$\eta 31$	0.22	1	0.22			$\gamma 12$	0.12	1	0.12			$\gamma 12$	0.12	1	0.12			$\gamma 12$	0.12	1	0.12			$\gamma 12$	0.12	1	0.12				
	$\eta 4$	0.24	1	0.24			$\gamma 13$	0.13	1	0.13			$\gamma 13$	0.13	1	0.13			$\gamma 13</$													

		Weights (w_a, w_v)	Scores (γ_a, η_v)	Product	Weighted Sum			Weights (w_a, w_v)	Scores (γ_a, η_v)	Product	Weighted Sum			Weights (w_a, w_v)	Scores (γ_a, η_v)	Product	Weighted Sum													
Step 1	T1	γ_{13}	0.32	1	0.32	1	Step 2	T1	γ_{13}	0.24	1	0.24	Step 3	T1	γ_{13}	0.16	0.5	0.08	Step 4	T1	γ_{13}	0.31	1	0.31						
		η_{11}	0.25	1	0.25				γ_{15}	0.22	1	0.22			γ_{14}	0.16	0	0			η_{11}	0.16	1	0.16	η_{11}	0.16	1	0.16		
		η_{31}	0.18	1	0.18				η_{31}	0.16	1	0.16			γ_{15}	0.16	0	0			η_{31}	0.23	1	0.23	η_{31}	0.23	1	0.23		
		η_4	0.25	1	0.25				η_4	0.22	1	0.22			η_4	0.16	1	0.16			η_4	0.3	1	0.3	η_4	0.3	1	0.3		
	T2	γ_{14}	0.25	1	0.25	1		T2	γ_{12}	0.2	1	0.2		1	T2	γ_3	0.11	0.5		0.055	T2	γ_{13}	0.37	0	0	T2	γ_{13}	0.37	0	0
		γ_{15}	0.25	1	0.25				γ_{14}	0.22	1	0.22				η_{31}	0.11	1		0.11		η_4	0.14	1	0.14		η_{31}	0.17	1	0.17
		η_{11}	0.12	1	0.12				η_{31}	0.15	1	0.15				η_4	0.21	1		0.21		γ_{15}	0.2	1	0.2		η_4	0.31	1	0.31
	T3	γ_{12}	0.22	1	0.22	1		T3	γ_{11}	0.22	1	0.22		1	T3	η_{11}	0.12	0.5		0.06	T3	γ_{11}	0.22	0	0	T3	γ_{11}	0.21	0	0
		γ_{14}	0.22	1	0.22				γ_{12}	0.21	1	0.21				γ_3	0.19	1		0.19		η_{31}	0.12	1	0.12		γ_{15}	0.22	1	0.22
		γ_{15}	0.22	1	0.22				γ_{13}	0.22	1	0.22				η_{11}	0.12	0.5		0.06		η_{31}	0.12	1	0.12		η_{31}	0.22	1	0.22
		η_4	0.21	1	0.21				η_4	0.15	1	0.15				η_4	0.17	1		0.17		η_4	0.18	1	0.18		η_4	0.17	1	0.17
	T4	γ_{11}	0.43	0.5	0.215	0.785		T4	η_{31}	0.14	1	0.14		0.855	T4	γ_{11}	0.25	0		0	T4	γ_{11}	0.25	0	0	T4	γ_3	0.27	1	0.27
		η_{31}	0.25	1	0.25				η_{31}	0.14	1	0.14				γ_{12}	0.22	1		0.22		η_{31}	0.14	1	0.14		η_{31}	0.23	0	0
		η_4	0.32	1	0.32				η_4	0.21	1	0.21				η_4	0.17	1		0.17		η_4	0.25	1	0.25		η_4	0.25	1	0.25
	T5	γ_{11}	0.27	0.5	0.135	0.865		T5	γ_{11}	0.29	0.5	0.145		0.855	T5	γ_{11}	0.25	1		0.25	T5	γ_{11}	0.28	1	0.28	T5	γ_{11}	0.28	1	0.28
		η_4	0.27	1	0.27				γ_{12}	0.27	1	0.27				γ_{12}	0.27	1		0.27		η_4	0.26	1	0.26		η_4	0.26	1	0.26
η_2		0.27	1	0.27	η_{31}		0.19		1	0.19	η_{31}	0.19	1			0.19	γ_{13}	0.28	1	0.28		γ_{13}	0.28	1	0.28					
η_{31}		0.22	1	0.22	η_4		0.25		1	0.25	η_4	0.25	1			0.25	η_{31}	0.18	1	0.18		η_{31}	0.18	1	0.18					
T6	γ_4	0.24	1	0.24	1	T6	γ_2	0.23	1	0.23	1	T6	γ_2	0.13	1	0.13	T6	γ_2	0.28	1	0.28	T6	γ_2	0.28	1	0.28				
	η_4	0.24	1	0.24			η_{31}	0.16	1	0.16			η_4	0.26	1	0.26		η_4	0.26	1	0.26		η_4	0.26	1	0.26				
	η_4	0.24	1	0.24			η_4	0.2	1	0.2			γ_3	0.28	1	0.28		γ_3	0.28	1	0.28		γ_3	0.28	1	0.28				
	η_4	0.24	1	0.24			γ_4	0.2	1	0.2			η_4	0.26	1	0.26		η_4	0.26	1	0.26		η_4	0.26	1	0.26				
T7	γ_2	0.28	1	0.28	1	T7	γ_3	0.28	1	0.28	1	T7	γ_3	0.28	1	0.28	T7	γ_3	0.28	1	0.28	T7	γ_3	0.28	1	0.28				
	η_{32}	0.22	1	0.22			γ_4	0.26	1	0.26			γ_4	0.26	1	0.26		γ_4	0.26	1	0.26		γ_4	0.26	1	0.26				
	η_4	0.26	1	0.26			γ_4	0.26	1	0.26			γ_4	0.26	1	0.26		γ_4	0.26	1	0.26		γ_4	0.26	1	0.26				
	η_4	0.26	1	0.26			γ_4	0.26	1	0.26			γ_4	0.26	1	0.26		γ_4	0.26	1	0.26		γ_4	0.26	1	0.26				
	η_4	0.26	1	0.26			γ_4	0.26	1	0.26			γ_4	0.26	1	0.26		γ_4	0.26	1	0.26		γ_4	0.26	1	0.26				
	η_4	0.26	1	0.26			γ_4	0.26	1	0.26			γ_4	0.26	1	0.26		γ_4	0.26	1	0.26		γ_4	0.26	1	0.26				
	η_4	0.26	1	0.26			γ_4	0.26	1	0.26			γ_4	0.26	1	0.26		γ_4	0.26	1	0.26		γ_4	0.26	1	0.26				
	η_4	0.26	1	0.26			γ_4	0.26	1	0.26			γ_4	0.26	1	0.26		γ_4	0.26	1	0.26		γ_4	0.26	1	0.26				
T8	γ_2	0.21	0	0	0.5	T8	γ_2	0.21	0	0	0.5	T8	γ_2	0.21	0	0	T8	γ_2	0.21	0	0	T8	γ_2	0.21	0	0				
	γ_3	0.22	1	0.22			γ_3	0.22	1	0.22			γ_3	0.22	1	0.22		γ_3	0.22	1	0.22		γ_3	0.22	1	0.22				
	η_{31}	0.21	0	0			η_{31}	0.21	0	0			η_{31}	0.21	0	0		η_{31}	0.21	0	0		η_{31}	0.21	0	0				
	η_4	0.2	1	0.2			η_4	0.2	1	0.2			η_4	0.2	1	0.2		η_4	0.2	1	0.2		η_4	0.2	1	0.2				
	η_4	0.2	1	0.2			η_4	0.2	1	0.2			η_4	0.2	1	0.2		η_4	0.2	1	0.2		η_4	0.2	1	0.2				
	η_4	0.2	1	0.2			η_4	0.2	1	0.2			η_4	0.2	1	0.2		η_4	0.2	1	0.2		η_4	0.2	1	0.2				
	η_4	0.2	1	0.2			η_4	0.2	1	0.2			η_4	0.2	1	0.2		η_4	0.2	1	0.2		η_4	0.2	1	0.2				
	η_4	0.2	1	0.2			η_4	0.2	1	0.2			η_4	0.2	1	0.2		η_4	0.2	1	0.2		η_4	0.2	1	0.2				

Subject ID 04

Figure F.1 (continued) : Calculation details of performance score for navigation tasks.

		Weights (w α , w ν)	Scores ($\gamma\alpha$, $\eta\nu$)	Product	Weighted Sum			Weights (w α , w ν)	Scores ($\gamma\alpha$, $\eta\nu$)	Product	Weighted Sum			Weights (w α , w ν)	Scores ($\gamma\alpha$, $\eta\nu$)	Product	Weighted Sum			Weights (w α , w ν)	Scores ($\gamma\alpha$, $\eta\nu$)	Product	Weighted Sum														
Step 1	T1	$\gamma 13$	0.32	1	0.32	1	Step 2	T1	$\gamma 13$	0.24	1	0.24	Step 3	T1	$\gamma 13$	0.16	0.5	0.08	0.46	Step 4	T1	$\gamma 13$	0.31	1	0.31	1											
		$\eta 1$	0.25	1	0.25				$\gamma 15$	0.22	1	0.22			$\gamma 14$	0.16	0	0				$\eta 1$	0.16	1	0.16		$\eta 1$	0.16	1	0.16							
		$\eta 31$	0.18	1	0.18				$\eta 4$	0.25	1	0.25			$\gamma 3$	0.16	1	0.16				$\eta 31$	0.23	1	0.23		$\eta 31$	0.23	1	0.23							
		$\eta 4$	0.25	1	0.25				$\eta 1$	0.12	1	0.12			$\eta 1$	0.11	1	0.11				$\eta 4$	0.3	1	0.3		$\eta 4$	0.3	1	0.3							
	T2	$\gamma 14$	0.25	1	0.25	1		T2	$\gamma 12$	0.2	1	0.2		0.8	T2	$\gamma 13$	0.2	1	0.2		0.71	T2	$\gamma 13$	0.21	0.5	0.105	0.505	T2	$\eta 32$	0.32	0	0	0.31				
		$\gamma 15$	0.25	1	0.25				$\gamma 14$	0.22	1	0.22				$\eta 1$	0.17	1	0.17				$\gamma 15$	0.22	1	0.22			$\gamma 14$	0.22	0	0					
		$\eta 1$	0.12	1	0.12				$\eta 4$	0.21	1	0.21				$\eta 4$	0.14	0	0				$\eta 1$	0.12	0	0			$\gamma 15$	0.22	1	0.22		$\eta 31$	0.17	0	0
	T3	$\gamma 12$	0.22	1	0.22	0.89		T3	$\gamma 11$	0.22	0.5	0.11		0.68	T3	$\eta 1$	0.12	0	0		0.71	T3	$\eta 31$	0.17	0	0	0.505	T3	$\eta 4$	0.18	1	0.18	0.505				
		$\gamma 14$	0.22	0.5	0.11				$\eta 4$	0.2	0	0				$\gamma 3$	0.19	1	0.19				$\eta 1$	0.12	0	0			$\gamma 11$	0.21	0.5	0.105		$\gamma 14$	0.22	0	0
		$\gamma 15$	0.22	1	0.22				$\gamma 11$	0.22	1	0.22				$\eta 31$	0.12	1	0.12				$\eta 4$	0.17	0	0			$\gamma 15$	0.22	1	0.22		$\eta 31$	0.17	0	0
		$\eta 31$	0.17	1	0.17				$\gamma 12$	0.21	1	0.21				$\eta 4$	0.17	0	0				$\eta 4$	0.17	0	0			$\eta 31$	0.17	0	0		$\eta 4$	0.18	1	0.18
	T4	$\gamma 11$	0.43	1	0.43	1		T4	$\eta 4$	0.21	0	0		0.68	T4	$\gamma 11$	0.25	0.5	0.125		0.655	T4	$\gamma 11$	0.25	1	0.25	0.5	T4	$\gamma 3$	0.27	0	0	0.5				
		$\eta 31$	0.25	1	0.25				$\gamma 11$	0.22	1	0.22				$\gamma 3$	0.19	1	0.19				$\eta 31$	0.23	0	0			$\eta 31$	0.23	0	0		$\eta 4$	0.25	1	0.25
		$\eta 4$	0.32	1	0.32				$\gamma 12$	0.27	0	0				$\eta 4$	0.22	0	0				$\eta 4$	0.22	0	0			$\eta 4$	0.24	1	0.24		$\gamma 3$	0.27	0	0
	T5	$\gamma 11$	0.27	1	0.27	1		T5	$\eta 4$	0.25	0	0		0.335	T5	$\gamma 11$	0.29	0.5	0.145		0.655	T5	$\gamma 13$	0.28	0.5	0.14	0.86	T5	$\gamma 13$	0.28	0.5	0.14	0.24				
		$\eta 2$	0.27	1	0.27				$\gamma 12$	0.2	1	0.2				$\gamma 3$	0.28	1	0.28				$\gamma 3$	0.28	1	0.28			$\eta 31$	0.23	0	0		$\eta 31$	0.23	0	0
$\eta 31$		0.22	1	0.22	$\gamma 2$		0.23		1	0.23	$\eta 4$	0.22	0			0	$\eta 4$	0.22	0	0			$\eta 4$	0.24	1	0.24			$\eta 4$	0.24	1	0.24					
$\eta 4$		0.24	1	0.24	$\eta 31$		0.16		1	0.16	$\eta 4$	0.25	0			0	$\eta 4$	0.26	1	0.26			$\eta 4$	0.26	1	0.26			$\gamma 11$	0.28	1	0.28					
T6	$\gamma 11$	0.21	0.5	0.105	0.895	T6	$\gamma 11$	0.21	0.5	0.105	0.895	T6	$\gamma 11$	0.25	0.5	0.125	0.655	T6	$\gamma 11$	0.25	0.5	0.125	0.86	T6	$\gamma 11$	0.28	0.5	0.14	0.72								
	$\gamma 12$	0.2	1	0.2			$\gamma 12$	0.2	1	0.2			$\gamma 12$	0.2	1	0.2			$\gamma 12$	0.2	1	0.2			$\gamma 12$	0.2	1	0.2		$\gamma 12$	0.2	1	0.2				
	$\gamma 2$	0.23	1	0.23			$\gamma 2$	0.23	1	0.23			$\gamma 2$	0.23	1	0.23			$\gamma 2$	0.23	1	0.23			$\gamma 2$	0.23	1	0.23		$\gamma 2$	0.23	1	0.23				
	$\eta 31$	0.16	1	0.16			$\eta 31$	0.16	1	0.16			$\eta 31$	0.16	1	0.16			$\eta 31$	0.16	1	0.16			$\eta 31$	0.16	1	0.16		$\eta 31$	0.16	1	0.16				
T7	$\gamma 2$	0.24	1	0.24	0.72	T7	$\gamma 3$	0.28	0	0	0.72	T7	$\gamma 3$	0.28	0	0	0.72	T7	$\gamma 3$	0.28	0	0	0.72	T7	$\gamma 3$	0.28	0	0	0.72								
	$\eta 32$	0.22	1	0.22			$\eta 32$	0.22	1	0.22			$\eta 32$	0.22	1	0.22			$\eta 32$	0.22	1	0.22			$\eta 32$	0.22	1	0.22		$\eta 32$	0.22	1	0.22				
	$\eta 4$	0.26	1	0.26			$\eta 4$	0.26	1	0.26			$\eta 4$	0.26	1	0.26			$\eta 4$	0.26	1	0.26			$\eta 4$	0.26	1	0.26		$\eta 4$	0.26	1	0.26				
	$\gamma 3$	0.28	0	0			$\gamma 3$	0.28	0	0			$\gamma 3$	0.28	0	0			$\gamma 3$	0.28	0	0			$\gamma 3$	0.28	0	0		$\gamma 3$	0.28	0	0				
T8	$\gamma 11$	0.13	0	0	0.52	T8	$\gamma 11$	0.13	0	0	0.52	T8	$\gamma 11$	0.13	0	0	0.52	T8	$\gamma 11$	0.13	0	0	0.52	T8	$\gamma 11$	0.13	0	0	0.52								
	$\gamma 12$	0.12	0	0			$\gamma 12$	0.12	0	0			$\gamma 12$	0.12	0	0			$\gamma 12$	0.12	0	0			$\gamma 12$	0.12	0	0		$\gamma 12$	0.12	0	0				
	$\gamma 13$	0.13	1	0.13			$\gamma 13$	0.13	1	0.13			$\gamma 13$	0.13	1	0.13			$\gamma 13$	0.13	1	0.13			$\gamma 13$	0.13	1	0.13		$\gamma 13$	0.13	1	0.13				
	$\gamma 14$	0.13	0	0			$\gamma 14$	0.13	0	0			$\gamma 14$	0.13	0	0			$\gamma 14$	0.13	0	0			$\gamma 14$	0.13	0	0		$\gamma 14$	0.13	0	0				
T9	$\gamma 15$	0.14	1	0.14	0.79	T9	$\gamma 15$	0.14	1	0.14	0.79	T9	$\gamma 15$	0.14	1	0.14	0.79	T9	$\gamma 15$	0.14	1	0.14	0.79	T9	$\gamma 15$	0.14	1	0.14	0.79								
	$\gamma 2$	0.13	1	0.13			$\gamma 2$	0.13	1	0.13			$\gamma 2$	0.13	1	0.13			$\gamma 2$	0.13	1	0.13			$\gamma 2$	0.13	1	0.13		$\gamma 2$	0.13	1	0.13				
	$\eta 31$	0.1	0	0			$\eta 31$	0.1	0	0			$\eta 31$	0.1	0	0			$\eta 31$	0.1	0	0			$\eta 31$	0.1	0	0		$\eta 31$	0.1	0	0				
	$\eta 4$	0.12	1	0.12			$\eta 4$	0.12	1	0.12			$\eta 4$	0.12	1	0.12			$\eta 4$	0.12	1	0.12			$\eta 4$	0.12	1	0.12		$\eta 4$	0.12	1	0.12				
T10	$\gamma 11$	0.15	0	0	0.43	T10	$\gamma 11$	0.15	0	0	0.43	T10	$\gamma 11$	0.15	0	0	0.43	T10	$\gamma 11$	0.15	0	0	0.43	T10	$\gamma 11$	0.15	0	0	0.43								
	$\gamma 14$	0.15	0	0			$\gamma 14$	0.15	0	0			$\gamma 14$	0.15	0	0			$\gamma 14$	0.15	0	0			$\gamma 14$	0.15	0	0		$\gamma 14$	0.15	0	0				
	$\gamma 15$	0.15	1	0.15			$\gamma 15$	0.15	1	0.15			$\gamma 15$	0.15	1	0.15			$\gamma 15$	0.15	1	0.15			$\gamma 15$	0.15	1	0.15		$\gamma 15$	0.15	1	0.15				
	$\eta 2$	0.14	1	0.14			$\eta 2$	0.14	1	0.14			$\eta 2$	0.14	1	0.14			$\eta 2$	0.14	1	0.14			$\eta 2$	0.14	1	0.14		$\eta 2$	0.14	1	0.14				
T11	$\gamma 2$	0.21	0	0	0.2	T11	$\gamma 2$	0.21	0	0	0.2	T11	$\gamma 2$	0.21	0	0	0.2	T11	$\gamma 2$	0.21	0	0	0.2	T11	$\gamma 2$	0.21	0	0	0.2								
	$\gamma 3$	0.22	0	0			$\gamma 3$	0.22	0	0			$\gamma 3$	0.22	0	0			$\gamma 3$	0.22	0	0			$\gamma 3$	0.22	0	0		$\gamma 3$	0.22	0	0				
	$\eta 1$	0.16	0	0			$\eta 1$	0.16	0	0			$\eta 1$	0.16	0	0			$\eta 1$	0.16	0	0			$\eta 1$	0.16	0	0		$\eta 1$	0.16	0	0				
	$\eta 31$	0.21	0	0			$\eta 31$	0.21	0	0			$\eta 31$	0.21	0	0			$\eta 31$	0.21	0	0			$\eta 31$	0.21	0	0		$\eta 31$	0.21	0	0				
T12	$\eta 4$	0.2	1	0.2	0.2	T12	$\eta 4$	0.2	1	0.2	0.2	T12	$\eta 4$	0.2	1	0.2	0.2	T12	$\eta 4$	0.2	1	0.2	0.2	T12	$\eta 4$	0.2	1	0.2	0.2								
	$\gamma 2$	0.21	0	0			$\gamma 2$	0.21	0	0			$\gamma 2$	0.21	0	0			$\gamma 2$	0.21	0	0			$\gamma 2$	0.21	0	0		$\gamma 2$	0.21	0	0				
	$\gamma 3$	0.22	0	0			$\gamma 3$	0.22	0	0			$\gamma 3$	0.22	0	0			$\gamma 3$	0.22	0	0			$\gamma 3$	0.22	0	0		$\gamma 3$	0.22	0	0				
	$\eta 31$	0.21	0	0			$\eta 31$	0.21	0	0			$\eta 31$	0.21	0	0			$\eta 31$	0.21	0	0			$\eta 31$	0.21	0	0		$\eta 31$	0.21	0	0				

Subject ID 05

Figure F.1 (continued

		Weights (w α , w ν)	Scores ($\gamma\alpha$, $\eta\nu$)	Product	Weighted Sum			Weights (w α , w ν)	Scores ($\gamma\alpha$, $\eta\nu$)	Product	Weighted Sum			Weights (w α , w ν)	Scores ($\gamma\alpha$, $\eta\nu$)	Product	Weighted Sum			Weights (w α , w ν)	Scores ($\gamma\alpha$, $\eta\nu$)	Product	Weighted Sum													
Step 1	T1	$\gamma 13$	0.32	1	0.32	1	Step 2	T1	$\gamma 13$	0.24	1	0.24	Step 3	T1	$\gamma 13$	0.16	1	0.16	Step 4	T1	$\gamma 13$	0.31	1	0.31												
		$\eta 1$	0.25	1	0.25				$\gamma 15$	0.22	1	0.22			$\gamma 14$	0.16	0	0			$\eta 1$	0.16	1	0.16	$\eta 1$	0.16	1	0.16								
		$\eta 31$	0.18	1	0.18				$\eta 1$	0.16	1	0.16			$\gamma 15$	0.16	0	0			$\eta 31$	0.23	1	0.23	$\eta 31$	0.23	1	0.23								
		$\eta 4$	0.25	1	0.25				$\eta 4$	0.22	1	0.22			$\gamma 3$	0.16	1	0.16			$\eta 4$	0.3	0	0	$\eta 4$	0.3	0	0								
	T2	$\gamma 14$	0.25	1	0.25	1		T2	$\gamma 12$	0.2	1	0.2		0.8	T2	$\gamma 13$	0.2	1		0.2	0.77	T3	$\gamma 11$	0.21	1	0.21	1	T4	$\gamma 11$	0.21	1	0.21				
		$\gamma 15$	0.25	1	0.25				$\gamma 14$	0.22	1	0.22				$\eta 1$	0.11	0.5		0.055			$\gamma 15$	0.23	1	0.23			$\eta 31$	0.11	1	0.11	$\gamma 14$	0.22	1	0.22
		$\eta 1$	0.12	1	0.12				$\eta 4$	0.22	1	0.22				$\eta 4$	0.14	0		0			$\eta 1$	0.12	0.5	0.06			$\eta 4$	0.31	1	0.31	$\gamma 11$	0.21	1	0.21
	T3	$\gamma 12$	0.22	1	0.22	1		T3	$\eta 31$	0.15	1	0.15		0.89	T3	$\gamma 3$	0.19	1		0.19	0.655	T4	$\eta 31$	0.17	1	0.17	0.5	T5	$\gamma 11$	0.25	1	0.25				
		$\eta 31$	0.17	1	0.17				$\eta 4$	0.21	1	0.21				$\eta 1$	0.12	1		0.12			$\gamma 12$	0.22	0.5	0.11			$\eta 4$	0.17	0	0	$\gamma 15$	0.2	1	0.2
		$\eta 4$	0.21	1	0.21				$\gamma 11$	0.22	1	0.22				$\gamma 3$	0.19	1		0.19			$\eta 4$	0.22	0	0			$\eta 4$	0.18	1	0.18	$\gamma 11$	0.22	1	0.22
	T4	$\gamma 11$	0.43	1	0.43	1		T4	$\gamma 12$	0.21	1	0.21		1	T4	$\eta 1$	0.12	0.5		0.06	0.72	T5	$\eta 31$	0.17	1	0.17	0.77	T6	$\gamma 11$	0.25	0.5	0.125				
		$\eta 4$	0.32	1	0.32				$\gamma 12$	0.21	1	0.21				$\eta 4$	0.17	0		0			$\gamma 12$	0.22	0	0			$\gamma 12$	0.22	0	0	$\gamma 11$	0.22	1	0.22
		$\gamma 11$	0.27	1	0.27				$\gamma 13$	0.22	0.5	0.11				$\eta 4$	0.21	1		0.21			$\eta 4$	0.17	0	0			$\gamma 11$	0.25	0.5	0.125	$\gamma 15$	0.2	1	0.2
	T5	$\eta 2$	0.27	1	0.27	1		T5	$\eta 4$	0.25	1	0.25		1	T5	$\gamma 11$	0.22	1		0.22	1	T6	$\gamma 11$	0.25	0.5	0.125	0.5	T7	$\gamma 11$	0.25	1	0.25				
		$\eta 31$	0.22	1	0.22				$\gamma 12$	0.27	1	0.27				$\gamma 12$	0.21	1		0.21			$\gamma 12$	0.27	1	0.27			$\gamma 12$	0.22	0	0	$\gamma 11$	0.25	1	0.25
$\eta 4$		0.24	1	0.24	$\eta 4$		0.21		1	0.21	$\eta 4$	0.25	1			0.25	$\eta 4$	0.22	1	0.22			$\gamma 12$	0.22	0	0			$\gamma 15$	0.2	1	0.2				
$\gamma 2$		0.23	1	0.23	$\gamma 11$		0.29		1	0.29	$\gamma 11$	0.27	1			0.27	$\eta 4$	0.22	1	0.22			$\gamma 12$	0.27	1	0.27			$\gamma 11$	0.25	1	0.25				
T6	$\gamma 2$	0.24	1	0.24	1	T6	$\gamma 2$	0.23	1	0.23	1	T6	$\gamma 13$	0.28	1	0.28	0.805	T7	$\gamma 13$	0.28	1	0.28	0.77	T8	$\gamma 13$	0.28	1	0.28								
	$\eta 4$	0.2	1	0.2			$\gamma 31$	0.19	1	0.19			$\eta 4$	0.25	1	0.25			$\gamma 3$	0.16	1	0.16			$\gamma 3$	0.25	1	0.25	$\gamma 3$	0.25	1	0.25				
	$\gamma 3$	0.28	1	0.28			$\eta 4$	0.25	1	0.25			$\gamma 3$	0.16	1	0.16			$\gamma 3$	0.25	1	0.25			$\gamma 3$	0.25	1	0.25	$\gamma 3$	0.25	1	0.25				
	$\eta 32$	0.22	1	0.22			$\gamma 11$	0.21	1	0.21			$\eta 4$	0.25	1	0.25			$\eta 31$	0.23	0	0			$\gamma 3$	0.25	1	0.25	$\eta 31$	0.23	0	0				
T7	$\eta 31$	0.22	1	0.22	1	T7	$\gamma 31$	0.16	1	0.16	1	T8	$\gamma 13$	0.28	1	0.28	0.72	T8	$\gamma 13$	0.28	1	0.28	0.24	T9	$\gamma 13$	0.28	1	0.28								
	$\eta 4$	0.24	1	0.24			$\gamma 2$	0.23	1	0.23			$\gamma 13$	0.28	1	0.28			$\gamma 13$	0.28	1	0.28			$\gamma 13$	0.28	1	0.28	$\gamma 13$	0.28	1	0.28				
	$\gamma 2$	0.23	1	0.23			$\eta 4$	0.25	1	0.25			$\gamma 3$	0.28	1	0.28			$\gamma 13$	0.28	1	0.28			$\gamma 13$	0.28	1	0.28	$\gamma 13$	0.28	1	0.28				
	$\gamma 31$	0.16	1	0.16			$\gamma 11$	0.21	1	0.21			$\eta 4$	0.25	1	0.25			$\gamma 13$	0.28	1	0.28			$\gamma 13$	0.28	1	0.28	$\gamma 13$	0.28	1	0.28				
T8	$\gamma 2$	0.24	1	0.24	1	T9	$\gamma 2$	0.24	1	0.24	1	T10	$\gamma 11$	0.13	0.5	0.065	0.805	T11	$\gamma 11$	0.13	0.5	0.065	0.42	T12	$\gamma 11$	0.13	0.5	0.065								
	$\eta 4$	0.2	1	0.2			$\gamma 12$	0.24	1	0.24			$\gamma 12$	0.24	1	0.24			$\gamma 12$	0.12	1	0.12			$\gamma 12$	0.12	1	0.12	$\gamma 12$	0.12	1	0.12				
	$\gamma 3$	0.28	1	0.28			$\gamma 13$	0.22	1	0.22			$\gamma 13$	0.13	1	0.13			$\gamma 13$	0.13	1	0.13			$\gamma 13$	0.13	1	0.13	$\gamma 13$	0.13	1	0.13				
	$\eta 32$	0.22	1	0.22			$\gamma 14$	0.13	0	0			$\gamma 14$	0.13	0	0			$\gamma 14$	0.13	0	0			$\gamma 14$	0.13	0	0	$\gamma 14$	0.13	0	0				
T9	$\gamma 2$	0.27	1	0.27	1	T11	$\gamma 14$	0.13	0	0	1	T12	$\gamma 14$	0.13	0	0	0.72	T13	$\gamma 14$	0.13	0	0	0.72	T14	$\gamma 14$	0.13	0	0								
	$\eta 4$	0.2	1	0.2			$\gamma 15$	0.14	1	0.14			$\gamma 15$	0.14	1	0.14			$\gamma 15$	0.14	1	0.14			$\gamma 15$	0.14	1	0.14	$\gamma 15$	0.14	1	0.14				
	$\gamma 31$	0.16	1	0.16			$\gamma 2$	0.13	1	0.13			$\gamma 2$	0.13	1	0.13			$\gamma 2$	0.13	1	0.13			$\gamma 2$	0.13	1	0.13	$\gamma 2$	0.13	1	0.13				
	$\gamma 2$	0.24	1	0.24			$\eta 31$	0.1	1	0.1			$\eta 31$	0.1	1	0.1			$\eta 31$	0.1	1	0.1			$\eta 31$	0.1	1	0.1	$\eta 31$	0.1	1	0.1				
T10	$\gamma 2$	0.27	1	0.27	1	T12	$\eta 4$	0.2	1	0.2	1	T13	$\eta 4$	0.12	1	0.12	0.805	T14	$\eta 4$	0.12	1	0.12	0.72	T15	$\eta 4$	0.12	1	0.12								
	$\eta 31$	0.22	1	0.22			$\gamma 31$	0.19	1	0.19			$\gamma 31$	0.19	1	0.19			$\gamma 31$	0.19	1	0.19			$\gamma 31$	0.19	1	0.19	$\gamma 31$	0.19	1	0.19				
	$\eta 4$	0.25	1	0.25			$\gamma 11$	0.21	1	0.21			$\gamma 11$	0.21	1	0.21			$\gamma 11$	0.21	1	0.21			$\gamma 11$	0.21	1	0.21	$\gamma 11$	0.21	1	0.21				
	$\gamma 11$	0.27	1	0.27			$\gamma 12$	0.2	1	0.2			$\gamma 12$	0.2	1	0.2			$\gamma 12$	0.2	1	0.2			$\gamma 12$	0.2	1	0.2	$\gamma 12$	0.2	1	0.2				
T11	$\gamma 2$	0.27	1	0.27	1	T13	$\gamma 12$	0.2	1	0.2	1	T14	$\gamma 12$	0.2	1	0.2	0.72	T15	$\gamma 12$	0.2	1	0.2	0.72	T16	$\gamma 12$	0.2	1	0.2								
	$\eta 31$	0.22	1	0.22			$\gamma 13$	0.22	0.5	0.11			$\gamma 13$	0.22	0.5	0.11			$\gamma 13$	0.22	0.5	0.11			$\gamma 13$	0.22	0.5	0.11	$\gamma 13$	0.22	0.5	0.11				
	$\eta 4$	0.25	1	0.25			$\eta 4$	0.21	1	0.21			$\eta 4$	0.21	1	0.21			$\eta 4$	0.21	1	0.21			$\eta 4$	0.21	1	0.21	$\eta 4$	0.21	1	0.21				
	$\gamma 11$	0.27	1	0.27			$\gamma 11$	0.29	1	0.29			$\gamma 11$	0.29	1	0.29			$\gamma 11$	0.29	1	0.29			$\gamma 11$	0.29	1	0.29	$\gamma 11$	0.29	1	0.29				
T12	$\gamma 2$	0.27	1	0.27	1	T14	$\gamma 11$	0.29	1	0.29	1	T15	$\gamma 11$	0.29	1	0.29	0.655	T16	$\gamma 11$	0.29	1	0.29	0.5	T17	$\gamma 11$	0.29	1	0.29								
	$\eta 31$	0.25	1	0.25			$\gamma 12$	0.27	1	0.27			$\gamma 12$	0.27	1	0.27			$\gamma 12$	0.27	1	0.27			$\gamma 12$	0.27	1	0.27	$\gamma 12$	0.27	1	0.27				
	$\eta 4$	0.32	1	0.32			$\gamma 12$	0.27	1	0.27			$\gamma 12$	0.27	1	0.27			$\gamma 12$	0.27	1	0.27			$\gamma 12$	0.27	1	0.27	$\gamma 12$	0.27	1	0.27				
	$\gamma 11$	0.27	1	0.27			$\eta 4$	0.25	1	0.25			$\eta 4$	0.25	1	0.25			$\eta 4$	0.25	1	0.25			$\eta 4$	0.25	1	0.25	$\eta 4$	0.25	1	0.25				
T13	$\gamma 2$	0.27	1	0.27	1	T16	$\gamma 11$	0.25	1	0.25	1	T17	$\gamma 11$	0.25	1	0.25	0.655	T18	γ																	

		Weights (wa, wv)	Scores (ya, ηv)	Product	Weighted Sum			Weights (wa, wv)	Scores (ya, ηv)	Product	Weighted Sum			Weights (wa, wv)	Scores (ya, ηv)	Product	Weighted Sum															
Step 1	T1	γ13	0.32	1	0.32	1	Step 2	T1	γ13	0.24	1	0.24	Step 3	T1	γ13	0.16	1	0.16	Step 4	T1	γ13	0.31	1	0.31								
		η1	0.25	1	0.25				γ15	0.22	1	0.22			γ14	0.16	0	0			η1	0.16	1	0.16	η1	0.16	1	0.16				
		η31	0.18	1	0.18				η31	0.16	1	0.16			γ15	0.16	0	0			η31	0.23	1	0.23	η31	0.23	1	0.23				
		η4	0.25	1	0.25				η4	0.22	1	0.22			γ3	0.16	1	0.16			η4	0.3	1	0.3	η4	0.3	1	0.3				
	γ14	0.25	1	0.25	γ12	0.2			1	0.2	η1	0.11			1	0.11	γ13	0.37		1	0.37	γ13	0.37	1	0.37							
	T2	γ15	0.25	1	0.25	1		T2	γ14	0.22	1	0.22		0.8	T2	η31	0.11	1		0.11	η32	0.32	1	0.32	1	T2	η32	0.32	1	0.32		
		η1	0.12	1	0.12				η4	0.14	1	0.14				η4	0.31	1		0.31	γ11	0.21	1	0.21			1	T3	γ11	0.21	1	0.21
		η31	0.17	1	0.17				γ15	0.23	1	0.23				γ15	0.19	1		0.19	γ14	0.22	1	0.22					γ15	0.22	1	0.22
		η4	0.21	1	0.21				η31	0.15	1	0.15				η1	0.12	0.5		0.06	η31	0.17	1	0.17					η31	0.17	1	0.17
	γ12	0.22	1	0.22	η4	0.2			0	0	η31	0.12				1	0.12	η4		0.18	1	0.18	η4	0.18	1	0.18						
	T3	γ14	0.22	1	0.22	1		T3	γ11	0.22	1	0.22		0.58	T3	η4	0.17	1		0.17	0.94	T3	γ11	0.25	0.5	0.125	1	T4	γ11	0.25	0.5	0.125
		γ15	0.22	1	0.22				γ12	0.21	0	0				γ12	0.22	0		0			γ12	0.22	0	0			γ12	0.22	0	0
		η31	0.17	1	0.17				γ13	0.22	1	0.22				γ3	0.19	1		0.19			γ3	0.16	1	0.16			γ3	0.16	1	0.16
		η4	0.17	1	0.17				η31	0.14	1	0.14				η1	0.12	0.5		0.06			η31	0.15	1	0.15			η31	0.15	1	0.15
	T4	γ11	0.43	1	0.43	1			T4	η4	0.21	0				0	0.48	T4		η4	0.22	1	0.22	0.655	T4	γ11	0.25	0.5	0.125	0.61	T5	γ11
η31		0.25	1	0.25	γ11		0.29	1		0.29	γ12	0.22	0	0	γ12	0.22			0	0	γ12	0.22	0			0						
η4		0.32	1	0.32	γ12		0.27	0		0	γ3	0.16	1	0.16	γ3	0.16			1	0.16	γ3	0.16	1			0.16						
γ11		0.27	1	0.27	η31		0.19	1		0.19	η4	0.22	1	0.22	η4	0.22			1	0.22	η4	0.22	1			0.22						
T5	η2	0.27	1	0.27	1	T5	η4	0.25		0	0	0.8	T5	γ13	0.28	1			0.28	1	T5	γ13	0.28	1	0.28	0.72	T6	γ13	0.28	1	0.28	
	η31	0.22	1	0.22			γ11	0.21	1	0.21	γ15			0.26	1	0.26	γ15	0.26	1			0.26	γ15	0.26	1			0.26				
	η4	0.24	1	0.24			γ12	0.2	1	0.2	γ3			0.28	0	0	γ3	0.28	0			0	γ3	0.28	0			0				
	γ2	0.27	1	0.27			γ2	0.23	1	0.23	η31			0.2	1	0.2	η31	0.2	1			0.2	η31	0.2	1			0.2				
T6	γ3	0.28	1	0.28	1		T6	η31	0.16	1	0.16			0.74	T6	η4	0.26	1	0.26	0.72	T6	η4	0.26	1	0.26	0.72	T6	η4	0.26	1	0.26	
	η4	0.24	1	0.24		γ2		0.24	1	0.24	γ11	0.13	0.5			0.065	γ11	0.13	0.5			0.065	γ11	0.13	0.5			0.065				
	γ3	0.28	1	0.28		γ12		0.12	1	0.12	γ12	0.12	1			0.12	γ12	0.12	1			0.12	γ12	0.12	1			0.12				
	η32	0.22	1	0.22		γ13		0.13	1	0.13	γ13	0.13	1			0.13	γ13	0.13	1			0.13	γ13	0.13	1			0.13				
T7	γ2	0.24	1	0.24	1	T7		γ2	0.23	1	0.23	0.8	T7			γ14	0.13	0	0	0.675	T7	γ14	0.13	0	0	0.675	T7	γ14	0.13	0	0	
	γ3	0.28	1	0.28			γ3	0.23	1	0.23	γ15			0.14	1	0.14	γ15	0.14	1			0.14	γ15	0.14	1			0.14				
	η4	0.26	0	0			η4	0.2	0	0	γ2			0.13	0	0	γ2	0.13	0			0	γ2	0.13	0			0				
	γ32	0.22	1	0.22			η31	0.16	1	0.16	η31			0.1	1	0.1	η31	0.1	1			0.1	η31	0.1	1			0.1				
T8	γ4	0.26	0	0	1		T8	η4	0.26	0	0			0.74	T8	η4	0.12	1	0.12	0.675	T8	η4	0.12	1	0.12	0.675	T8	η4	0.12	1	0.12	
	γ2	0.24	1	0.24		γ11		0.13	0.5	0.065	γ11	0.13	0.5			0.065	γ11	0.13	0.5			0.065	γ11	0.13	0.5			0.065				
	γ3	0.28	1	0.28		γ12		0.12	1	0.12	γ12	0.12	1			0.12	γ12	0.12	1			0.12	γ12	0.12	1			0.12				
	η32	0.22	1	0.22		γ13		0.13	1	0.13	γ13	0.13	1			0.13	γ13	0.13	1			0.13	γ13	0.13	1			0.13				
T9	γ2	0.24	1	0.24	1	T9		γ2	0.23	1	0.23	0.8	T9			γ2	0.23	1	0.23	0.675	T9	γ2	0.23	1	0.23	0.675	T9	γ2	0.23	1	0.23	
	γ3	0.28	1	0.28			γ3	0.23	1	0.23	γ3			0.23	1	0.23	γ3	0.23	1			0.23	γ3	0.23	1			0.23				
	η4	0.26	0	0			η4	0.2	0	0	η4			0.2	0	0	η4	0.2	0			0	η4	0.2	0			0				
	γ4	0.26	0	0			η4	0.26	0	0	η4			0.26	0	0	η4	0.26	0			0	η4	0.26	0			0				
T10	γ2	0.24	1	0.24	1		T10	γ2	0.23	1	0.23			0.8	T10	γ2	0.23	1	0.23	0.675	T10	γ2	0.23	1	0.23	0.675	T10	γ2	0.23	1	0.23	
	γ3	0.28	1	0.28		γ3		0.23	1	0.23	γ3	0.23	1			0.23	γ3	0.23	1			0.23	γ3	0.23	1			0.23				
	η4	0.26	0	0		η4		0.2	0	0	η4	0.2	0			0	η4	0.2	0			0	η4	0.2	0			0				
	γ4	0.26	0	0		η4		0.26	0	0	η4	0.26	0			0	η4	0.26	0			0	η4	0.26	0			0				
T11	γ2	0.24	1	0.24	1	T11		γ2	0.23	1	0.23	0.8	T11			γ2	0.23	1	0.23	0.675	T11	γ2	0.23	1	0.23	0.675	T11	γ2	0.23	1	0.23	
	γ3	0.28	1	0.28			γ3	0.23	1	0.23	γ3			0.23	1	0.23	γ3	0.23	1			0.23	γ3	0.23	1			0.23				
	η4	0.26	0	0			η4	0.2	0	0	η4			0.2	0	0	η4	0.2	0			0	η4	0.2	0			0				
	γ4	0.26	0	0			η4	0.26	0	0	η4			0.26	0	0	η4	0.26	0			0	η4	0.26	0			0				
T12	γ2	0.24	1	0.24	1		T12	γ2	0.23	1	0.23			0.8	T12	γ2	0.23	1	0.23	0.675	T12	γ2	0.23	1	0.23	0.675	T12	γ2	0.23	1	0.23	
	γ3	0.28	1	0.28		γ3		0.23	1	0.23	γ3	0.23	1			0.23	γ3	0.23	1			0.23	γ3	0.23	1			0.23				
	η4	0.26	0	0		η4		0.2	0	0	η4	0.2	0			0	η4	0.2	0			0	η4	0.2	0			0				
	γ4	0.26	0	0		η4		0.26	0	0	η4	0.26	0			0	η4	0.26	0			0	η4	0.26	0			0				
T13	γ2	0.24	1	0.24	1	T13		γ2	0.23	1	0.23	0.8	T13			γ2	0.23	1	0.23	0.675	T13	γ2	0.23	1	0.23	0.675	T13	γ2	0.23	1	0.23	
	γ3	0.28	1	0.28			γ3	0.23	1	0.23	γ3			0.23	1	0.23	γ3	0.23	1			0.23	γ3	0.23	1			0.23				
	η4	0.26	0	0			η4	0.2	0	0	η4			0.2	0	0	η4	0.2	0			0	η4	0.2	0			0				
	γ4	0.26	0	0			η4	0.26	0	0	η4			0.26	0	0	η4	0.26	0			0	η4	0.26	0			0				
T14	γ2	0.24	1	0.24	1		T14	γ2	0.23	1	0.23			0.8	T14	γ2	0.23	1	0.23	0.675	T14	γ2	0.23	1	0.23	0.675	T14	γ2	0.23	1	0.23	
	γ3	0.28	1	0.28		γ3		0.23	1	0.23	γ3	0.23	1			0.23	γ3	0.23	1			0.23	γ3	0.23	1			0.23				
	η4	0.26	0	0		η4		0.2	0	0	η4	0.2	0			0	η4	0.2	0			0	η4	0.2	0			0				
	γ4	0.26	0	0		η4		0.26	0	0	η4	0.26	0			0	η4	0.26	0			0	η4	0.26	0			0				
T15	γ2	0.24	1	0.24	1	T15		γ2	0.23	1	0.23	0.8	T15			γ2	0.23	1	0.23	0.675	T15	γ2	0.23	1	0.23	0.675	T15	γ2	0.23	1	0.23	
	γ3	0.28	1	0.28																												

		Weights (w_a, w_v)	Scores (γ_a, η_v)	Product	Weighted Sum			Weights (w_a, w_v)	Scores (γ_a, η_v)	Product	Weighted Sum			Weights (w_a, w_v)	Scores (γ_a, η_v)	Product	Weighted Sum																
Step 1	T1	γ_{13}	0.32	1	0.32	0.78	T1	γ_{13}	0.24	1	0.24	0.8	T1	γ_{13}	0.16	0.5	0.08	0.545	T1	γ_{13}	0.31	1	0.31										
		η_1	0.25	1	0.25			γ_{15}	0.22	0	0			η_1	0.16	1	0.16			η_1	0.16	1	0.16	η_1	0.16	1	0.16						
		η_{31}	0.18	1	0.18			η_{31}	0.16	1	0.16			γ_3	0.16	1	0.16			η_{31}	0.23	1	0.23	η_4	0.3	1	0.3	η_{31}	0.23	1	0.23		
		η_4	0.25	1	0.25			η_4	0.22	1	0.22			η_1	0.11	0.5	0.055			η_4	0.37	1	0.37	η_4	0.3	1	0.3	η_4	0.3	1	0.3		
	T2	γ_{14}	0.25	1	0.25	1	T2	γ_{12}	0.2	0	0	0.68	T2	γ_{13}	0.2	1	0.2	0.94	T2	γ_{13}	0.21	1	0.21	1	T2	γ_{32}	0.32	1	0.32				
		η_1	0.12	1	0.12			γ_{14}	0.22	1	0.22			η_4	0.14	1	0.14			η_4	0.31	1	0.31			η_4	0.31	1	0.31	η_4	0.31	1	0.31
		η_{31}	0.17	1	0.17			η_{31}	0.15	1	0.15			γ_3	0.19	1	0.19			γ_{14}	0.22	1	0.22			γ_{15}	0.22	1	0.22	γ_{15}	0.22	1	0.22
	T3	γ_{15}	0.25	1	0.25	1	T3	η_4	0.2	1	0.2	0.585	T3	η_1	0.12	0.5	0.06	0.655	T3	η_1	0.12	0.5	0.06	0.73	T3	η_4	0.18	1	0.18				
		η_4	0.21	1	0.21			γ_{11}	0.22	1	0.22			η_{31}	0.12	1	0.12			η_{31}	0.12	1	0.12			η_{31}	0.17	1	0.17	η_{31}	0.17	1	0.17
		η_{31}	0.17	1	0.17			γ_{12}	0.21	0	0			η_4	0.17	1	0.17			η_4	0.17	1	0.17			η_4	0.18	1	0.18	η_4	0.18	1	0.18
	T4	γ_{11}	0.43	1	0.43	1	T4	η_{31}	0.14	1	0.14	0.895	T4	γ_{11}	0.25	0.5	0.125	0.72	T4	γ_{11}	0.25	1	0.25	0.38	T4	γ_{11}	0.25	1	0.25				
		η_4	0.25	1	0.25			γ_{12}	0.27	0	0			γ_3	0.16	1	0.16			γ_3	0.16	1	0.16			γ_3	0.16	1	0.16	γ_3	0.16	1	0.16
		η_4	0.32	1	0.32			η_{31}	0.19	1	0.19			η_4	0.22	1	0.22			η_4	0.22	1	0.22			η_4	0.22	1	0.22	η_4	0.22	1	0.22
	T5	γ_{11}	0.27	1	0.27	0.73	T5	η_4	0.25	1	0.25	0.78	T5	γ_{11}	0.25	0.5	0.125	1	T5	γ_{11}	0.25	0.5	0.125	0.51	T5	γ_{11}	0.25	0.5	0.125				
		η_2	0.27	0	0			γ_{12}	0.27	0	0			γ_3	0.15	1	0.15			γ_3	0.15	1	0.15			γ_3	0.15	1	0.15	γ_3	0.15	1	0.15
η_{31}		0.22	1	0.22	η_{31}			0.19	1	0.19	η_4			0.22	1	0.22	η_4			0.22	1	0.22	η_4			0.22	1	0.22	η_4	0.22	1	0.22	
T6	η_4	0.24	1	0.24	0.73	T6	γ_{11}	0.21	0.5	0.105	0.895	T6	γ_{11}	0.21	0.5	0.105	0.52	T6	γ_{11}	0.21	0.5	0.105	0.28	T6	γ_{11}	0.21	0.5	0.105					
	η_4	0.24	1	0.24			γ_{12}	0.2	1	0.2			γ_{12}	0.2	1	0.2			γ_{12}	0.2	1	0.2			γ_{12}	0.2	1	0.2	γ_{12}	0.2	1	0.2	
	η_4	0.24	1	0.24			γ_{12}	0.2	1	0.2			γ_{12}	0.2	1	0.2			γ_{12}	0.2	1	0.2			γ_{12}	0.2	1	0.2	γ_{12}	0.2	1	0.2	
Step 2	T1	γ_{13}	0.24	1	0.24	0.78	T1	γ_{13}	0.24	1	0.24	0.78	T1	γ_{13}	0.16	0.5	0.08	0.545	T1	γ_{13}	0.16	0.5	0.08	0.545	T1	γ_{13}	0.16	0.5	0.08				
		γ_{15}	0.22	0	0			γ_{15}	0.22	0	0			η_1	0.16	1	0.16			η_1	0.16	1	0.16			η_1	0.16	1	0.16				
		η_1	0.16	1	0.16			η_1	0.16	1	0.16			η_1	0.16	1	0.16			η_1	0.16	1	0.16			η_1	0.16	1	0.16				
		η_{31}	0.16	1	0.16			η_{31}	0.16	1	0.16			η_{31}	0.16	1	0.16			η_{31}	0.16	1	0.16			η_{31}	0.16	1	0.16				
	T2	γ_{14}	0.25	1	0.25	1	T2	γ_{12}	0.2	0	0	0.8	T2	γ_{12}	0.2	0	0	0.94	T2	γ_{12}	0.2	0	0	1	T2	γ_{12}	0.2	0	0				
		η_1	0.12	1	0.12			γ_{14}	0.22	1	0.22			η_4	0.14	1	0.14			η_4	0.14	1	0.14			η_4	0.14	1	0.14				
		η_{31}	0.17	1	0.17			γ_{15}	0.23	1	0.23			η_4	0.14	1	0.14			η_4	0.14	1	0.14			η_4	0.14	1	0.14				
	T3	γ_{14}	0.25	1	0.25	1	T3	η_4	0.2	1	0.2	0.68	T3	γ_3	0.19	1	0.19	0.94	T3	γ_3	0.19	1	0.19	1	T3	γ_3	0.19	1	0.19				
		η_4	0.21	1	0.21			η_1	0.12	0.5	0.06			η_1	0.12	0.5	0.06			η_1	0.12	0.5	0.06			η_1	0.12	0.5	0.06				
		η_{31}	0.17	1	0.17			γ_{11}	0.22	0.5	0.11			η_{31}	0.12	1	0.12			η_{31}	0.12	1	0.12			η_{31}	0.12	1	0.12				
	T4	γ_{11}	0.43	1	0.43	1	T4	γ_{13}	0.22	1	0.22	0.68	T4	η_4	0.17	1	0.17	0.655	T4	η_4	0.17	1	0.17	0.73	T4	η_4	0.17	1	0.17				
		η_4	0.25	1	0.25			η_{31}	0.14	1	0.14			γ_{11}	0.25	0.5	0.125			γ_{11}	0.25	0.5	0.125			γ_{11}	0.25	0.5	0.125				
		η_4	0.32	1	0.32			η_{31}	0.14	1	0.14			γ_{12}	0.22	0	0			γ_{12}	0.22	0	0			γ_{12}	0.22	0	0				
	T5	γ_{11}	0.27	1	0.27	0.73	T5	γ_{11}	0.29	0.5	0.145	0.895	T5	γ_{11}	0.29	0.5	0.145	0.655	T5	γ_{11}	0.29	0.5	0.145	0.38	T5	γ_{11}	0.29	0.5	0.145				
		η_2	0.27	0	0			γ_{12}	0.27	0	0			γ_3	0.16	1	0.16			γ_3	0.16	1	0.16			γ_3	0.16	1	0.16				
η_{31}		0.22	1	0.22	η_{31}			0.19	1	0.19	η_4			0.22	1	0.22	η_4			0.22	1	0.22	η_4			0.22	1	0.22					
T6	η_4	0.24	1	0.24	0.73	T6	η_4	0.25	1	0.25	0.895	T6	γ_{11}	0.25	0.5	0.125	1	T6	γ_{11}	0.25	0.5	0.125	0.51	T6	γ_{11}	0.25	0.5	0.125					
	η_4	0.24	1	0.24			γ_{12}	0.27	0	0			γ_3	0.15	1	0.15			γ_3	0.15	1	0.15			γ_3	0.15	1	0.15					
	η_4	0.24	1	0.24			η_{31}	0.19	1	0.19			η_4	0.22	1	0.22			η_4	0.22	1	0.22			η_4	0.22	1	0.22					
Step 3	T1	γ_{13}	0.16	0.5	0.08	0.545	T1	γ_{13}	0.16	0.5	0.08	0.545	T1	γ_{13}	0.16	0.5	0.08	0.545	T1	γ_{13}	0.16	0.5	0.08	0.545	T1	γ_{13}	0.16	0.5	0.08				
		γ_{14}	0.16	0	0			γ_{14}	0.16	0	0			η_1	0.16	1	0.16			η_1	0.16	1	0.16			η_1	0.16	1	0.16				
		γ_{15}	0.16	0	0			η_1	0.16	1	0.16			η_1	0.16	1	0.16			η_1	0.16	1	0.16			η_1	0.16	1	0.16				
		η_1	0.16	1	0.16			η_1	0.16	1	0.16			η_1	0.16	1	0.16			η_1	0.16	1	0.16			η_1	0.16	1	0.16				
	T2	γ_{14}	0.25	1	0.25	1	T2	γ_{12}	0.2	0	0	0.8	T2	γ_{12}	0.2	0	0	0.94	T2	γ_{12}	0.2	0	0	1	T2	γ_{12}	0.2	0	0				
		η_1	0.12	1	0.12			γ_{14}	0.22	1	0.22			η_4	0.14	1	0.14			η_4	0.14	1	0.14			η_4	0.14	1	0.14				
		η_{31}	0.17	1	0.17			γ_{15}	0.23	1	0.23			η_4	0.14	1	0.14			η_4	0.14	1	0.14			η_4	0.14	1	0.14				
	T3	γ_{14}	0.25	1	0.25	1	T3	η_4	0.2	1	0.2	0.68	T3	γ_3	0.19	1	0.19	0.94	T3	γ_3	0.19	1	0.19	1	T3	γ_3	0.19	1	0.19				
		η_4	0.21	1	0.21			η_1	0.12	0.5	0.06			η_1	0.12	0.5	0.06			η_1	0.12	0.5	0.06			η_1	0.12	0.5	0.06				
		η_{31}	0.17	1	0.17			γ_{11}	0.22	0.5	0.11			η_{31}	0.12	1	0.12			η_{31}	0.12	1	0.12			η_{31}	0.12	1	0.12				
	T4	γ_{1																															

		Weights (w _a , w _v)	Scores (γ _a , η _v)	Product	Weighted Sum			Weights (w _a , w _v)	Scores (γ _a , η _v)	Product	Weighted Sum			Weights (w _a , w _v)	Scores (γ _a , η _v)	Product	Weighted Sum			Weights (w _a , w _v)	Scores (γ _a , η _v)	Product	Weighted Sum								
Step 1	T1	γ13	0.32	1	0.32	1	Step 2	T1	γ13	0.24	1	0.24	1	Step 3	T1	γ13	0.16	1	0.16	0.68	Step 4	T1	γ13	0.31	1	0.31	1				
		η1	0.25	1	0.25				γ15	0.22	1	0.22				γ14	0.16	0	0				η1	0.16	1	0.16		η1	0.16	1	0.16
		η31	0.18	1	0.18				η1	0.16	1	0.16				γ15	0.16	0	0				η31	0.11	1	0.11		η31	0.23	1	0.23
		η4	0.25	1	0.25				η4	0.22	1	0.22				η31	0.11	1	0.11				η4	0.3	1	0.3		η4	0.3	1	0.3
	T2	γ14	0.25	1	0.25	1		T2	γ12	0.2	0	0	0.6		T2	γ13	0.2	1	0.2	1		T2	γ13	0.37	1	0.37	0.68				
		γ15	0.25	1	0.25				γ14	0.22	1	0.22				γ15	0.2	1	0.2				η32	0.32	0	0		γ14	0.22	0	0
		η1	0.12	1	0.12				η4	0.2	0	0				η1	0.19	1	0.19				η4	0.31	1	0.31		γ15	0.22	1	0.22
	T3	γ14	0.22	1	0.22	1		T3	γ11	0.22	0.5	0.11	0.47		T3	γ11	0.2	1	0.2	1		T3	γ11	0.21	1	0.21	0.61				
		η31	0.17	1	0.17				γ12	0.21	0	0				η1	0.12	1	0.12				γ14	0.22	0	0		γ15	0.22	1	0.22
		η4	0.21	1	0.21				η4	0.2	0	0				η31	0.12	1	0.12				η4	0.18	1	0.18		η31	0.17	0	0
		γ11	0.43	1	0.43				γ13	0.22	1	0.22				η4	0.17	1	0.17				γ11	0.25	0.5	0.125		η4	0.18	1	0.18
	T4	η31	0.25	1	0.25	1		T4	γ11	0.29	0.5	0.145	0.605		T4	γ11	0.25	0.5	0.125	0.655		T4	γ3	0.27	0	0	0.375				
		η4	0.32	1	0.32				γ12	0.27	1	0.27				γ31	0.16	1	0.16				η4	0.25	1	0.25		η31	0.23	0	0
		γ11	0.27	1	0.27				η4	0.21	0	0				η4	0.22	1	0.22				γ13	0.28	0	0		η4	0.25	1	0.25
	T5	η2	0.27	0.5	0.135	0.865		T5	γ12	0.2		0.605	T5		γ3	0.16	1	0.16	0.655	T5		γ13	0.28	1	0.28	0.49					
		η31	0.22	1	0.22				γ12	0.2					η4	0.22	1	0.22				γ31	0.15	1	0.15		γ13	0.23	0	0	
η4		0.24	1	0.24	γ11		0.21			γ4	0.22			1	0.22	η4	0.24	1			0.24	η4	0.24	1	0.24						
					γ2		0.23			γ3	0.28			1	0.28	γ11	0.28	0			0	γ11	0.28								
T6	γ2	0.24	1	0.24	0.24	T6	γ2	0.24	1	0.24	0.24	T6	γ15	0.26	0	0	0.82	T6	γ15	0.26	0	0	0.26								
	γ3	0.28	0	0			γ31	0.16		γ11			0.25	0.5	0.125	γ3			0.28	0	0	γ15		0.26	0	0					
	η32	0.22	0	0			η4	0.2		γ12			0.22	0	0	γ31			0.2	0	0	γ3		0.28	0	0					
	η4	0.26	0	0			γ4	0.26	1	0.26			η4	0.17	1	0.17			η4	0.26	1	0.26		η4	0.24	1	0.24				
T7	γ11	0.13	0.5	0.065	0.705	T7	γ11	0.13	0.5	0.065	0.705	T7	γ11	0.13	0.5	0.065	0.705	T7	γ11	0.15	0	0	0.43								
	γ12	0.12	1	0.12			γ12	0.12	1	0.12			γ12	0.12	1	0.12			γ12	0.12	1	0.12		γ15	0.15	1	0.15				
	γ13	0.13	1	0.13			γ13	0.13	1	0.13			γ13	0.13	1	0.13			γ13	0.13	1	0.13		γ2	0.14	1	0.14				
	γ14	0.13	0	0			γ14	0.13	0	0			γ14	0.13	0	0			γ14	0.13	0	0		γ3	0.14	1	0.14				
	γ15	0.14	1	0.14			γ15	0.14	1	0.14			γ15	0.14	1	0.14			γ15	0.14	1	0.14		η3	0.14	0	0				
	γ2	0.13	1	0.13			γ2	0.13	1	0.13			γ2	0.13	1	0.13			γ2	0.13	1	0.13		η4	0.13	0	0				
	η31	0.1	0	0			η31	0.1	0	0			η31	0.1	0	0			η31	0.1	0	0		γ2	0.21	0	0				
η4	0.12	1	0.12	η4	0.12	1	0.12	η4	0.12	1	0.12	η4	0.12	1	0.12	γ3	0.22	0	0												
T8	η1	0.16	0	0	0.2	T8	η1	0.16	0	0	0.2	T8	η1	0.16	0	0	0.2	T8	η1	0.16	0	0	0.2								
	η31	0.21	0	0			η31	0.21	0	0			η31	0.21	0	0			η31	0.21	0	0		η31	0.21	0	0				
	η4	0.2	1	0.2			η4	0.2	1	0.2			η4	0.2	1	0.2			η4	0.2	1	0.2		η4	0.2	1	0.2				

Subject ID 10

Figure F.1 (continued) : Calculation details of performance score for navigation tasks.

		Weights (w α , w ν)	Scores ($\gamma\alpha$, $\eta\nu$)	Product	Weighted Sum			Weights (w α , w ν)	Scores ($\gamma\alpha$, $\eta\nu$)	Product	Weighted Sum			Weights (w α , w ν)	Scores ($\gamma\alpha$, $\eta\nu$)	Product	Weighted Sum			Weights (w α , w ν)	Scores ($\gamma\alpha$, $\eta\nu$)	Product	Weighted Sum									
Step 1	T1	$\gamma 13$	0.32	1	0.32	1	Step 2	T1	$\gamma 13$	0.24	1	0.24	1	Step 3	T1	$\gamma 13$	0.16	1	0.16	0.68	Step 4	T1	$\gamma 13$	0.31	1	0.31	0.84					
		$\eta 1$	0.25	1	0.25				$\gamma 15$	0.22	1	0.22				$\gamma 14$	0.16	0	0				$\eta 1$	0.16	0	0		$\eta 1$	0.16	0	0	
		$\eta 31$	0.18	1	0.18				$\eta 31$	0.16	1	0.16				$\gamma 3$	0.16	1	0.16				$\eta 31$	0.23	1	0.23		$\eta 31$	0.23	1	0.23	
		$\eta 4$	0.25	1	0.25				$\eta 4$	0.22	1	0.22				$\eta 1$	0.11	1	0.11				$\eta 4$	0.3	1	0.3		$\eta 4$	0.3	1	0.3	
	T2	$\gamma 14$	0.25	1	0.25	1		T2	$\gamma 12$	0.2	0	0	0.6		T2	$\eta 31$	0.11	1	0.11	0.57		T2	$\gamma 13$	0.37	0.5	0.185	0.495	T3	$\gamma 11$	0.21		
		$\gamma 15$	0.25	1	0.25				$\gamma 14$	0.22	1	0.22				$\gamma 15$	0.2	1	0.2				$\eta 1$	0.12	0	0			$\gamma 14$	0.22		
		$\eta 1$	0.12	1	0.12				$\eta 31$	0.15	1	0.15				$\eta 3$	0.19	0	0				$\eta 31$	0.17					$\gamma 15$	0.22		
		$\eta 31$	0.17	1	0.17				$\eta 4$	0.2	0	0				$\eta 1$	0.12	0	0				$\eta 4$	0.18					$\eta 31$	0.17		
	T3	$\gamma 12$	0.22	1	0.22	1		T3	$\gamma 11$	0.22	0.5	0.11	0.57		T3	$\eta 4$	0.17	1	0.17	1		T3	$\gamma 11$	0.25	1	0.25	0.52	T4	$\gamma 11$	0.25	0	0
		$\gamma 14$	0.22	1	0.22				$\gamma 12$	0.21	1	0.21				$\gamma 12$	0.22	1	0.22				$\eta 31$	0.12	0	0			$\gamma 12$	0.22	1	0.22
		$\gamma 15$	0.22	1	0.22				$\gamma 13$	0.22	0.5	0.11				$\gamma 3$	0.16	1	0.16				$\eta 4$	0.17	1	0.17			$\eta 31$	0.15	1	0.15
		$\eta 31$	0.17	1	0.17				$\eta 31$	0.14	1	0.14				$\eta 4$	0.22	1	0.22				$\eta 4$	0.25	1	0.25			$\eta 4$	0.25	1	0.25
	T4	$\gamma 11$	0.43	0.5	0.215	0.785		T4	$\gamma 11$	0.29	0.5	0.145	0.605		T4	$\gamma 11$	0.25	1	0.25	1		T4	$\gamma 12$	0.28	1	0.28	0.28	T5	$\gamma 3$	0.25	0	0
		$\eta 31$	0.17	1	0.17				$\gamma 12$	0.27	1	0.27				$\eta 31$	0.15	1	0.15				$\eta 31$	0.18	0	0			$\gamma 3$	0.25	0	0
		$\eta 4$	0.32	1	0.32				$\eta 4$	0.21	0	0				$\eta 4$	0.22	1	0.22				$\eta 4$	0.26	1	0.26			$\eta 4$	0.24	0	0
		$\gamma 11$	0.27	0.5	0.135				$\gamma 11$	0.21	0.5	0.105				$\gamma 11$	0.28	0	0				$\gamma 11$	0.28	0	0			$\gamma 11$	0.28	0	0
T5	$\eta 2$	0.27	1	0.27	0.865	T5	$\gamma 12$	0.2	1	0.2	0.695	T5	$\gamma 3$	0.28	0	0	0.26	T5	$\gamma 3$	0.28	0	0	0.26	T6	$\gamma 11$	0.28	0	0				
	$\eta 31$	0.22	1	0.22			$\gamma 2$	0.23	1	0.23			$\eta 31$	0.18	0	0			$\gamma 11$	0.28	0	0			$\gamma 11$	0.28	0	0				
	$\eta 4$	0.24	1	0.24			$\eta 31$	0.16	1	0.16			$\eta 4$	0.26	1	0.26			$\eta 4$	0.26	1	0.26			$\gamma 15$	0.26	0	0				
	$\gamma 11$	0.27	0.5	0.135			$\eta 4$	0.2	0	0			$\gamma 2$	0.24	1	0.24			$\gamma 3$	0.28	0	0			$\gamma 3$	0.28	0	0				
T6	$\eta 2$	0.27	1	0.27	0.865	T6	$\gamma 3$	0.28	1	0.28	0.74	T6	$\gamma 11$	0.13	0	0	0.52	T6	$\gamma 11$	0.15	0	0	0.27	T7	$\gamma 11$	0.15	0	0				
	$\eta 31$	0.22	1	0.22			$\gamma 12$	0.2	1	0.2			$\gamma 12$	0.12	0	0			$\gamma 14$	0.15	0	0			$\gamma 14$	0.15	0	0				
	$\eta 4$	0.24	1	0.24			$\gamma 13$	0.23	1	0.23			$\gamma 13$	0.13	1	0.13			$\gamma 15$	0.15	0	0			$\gamma 15$	0.15	0	0				
	$\gamma 11$	0.27	0.5	0.135			$\eta 31$	0.16	1	0.16			$\eta 4$	0.26	1	0.26			$\eta 31$	0.2	0	0			$\gamma 2$	0.14	1	0.14				
T7	$\eta 2$	0.27	1	0.27	0.865	T7	$\eta 4$	0.26	0	0	0.74	T7	$\gamma 14$	0.13	0	0	0.52	T7	$\gamma 2$	0.14	1	0.14	0.28	T8	$\gamma 3$	0.14	1	0.14				
	$\eta 31$	0.22	1	0.22			$\gamma 15$	0.14	1	0.14			$\gamma 3$	0.13	1	0.13			$\eta 3$	0.14	1	0.14			$\eta 3$	0.14	0	0				
	$\eta 4$	0.24	1	0.24			$\eta 2$	0.24	1	0.24			$\eta 31$	0.1	0	0			$\eta 4$	0.13	0	0			$\eta 4$	0.13	0	0				
	$\gamma 11$	0.27	0.5	0.135			$\gamma 3$	0.28	1	0.28			$\eta 4$	0.12	1	0.12			$\gamma 2$	0.13	1	0.13			$\gamma 3$	0.22						
T8	$\eta 2$	0.27	1	0.27	0.865	T8	$\eta 4$	0.26	0	0	0.74	T8	$\eta 4$	0.12	1	0.12	0.52	T8	$\gamma 3$	0.22			0.27	T8	$\eta 1$	0.16						
	$\eta 31$	0.22	1	0.22			$\gamma 11$	0.13	0	0			$\eta 4$	0.2					$\eta 1$	0.16					$\eta 31$	0.21						
	$\eta 4$	0.24	1	0.24			$\gamma 12$	0.12	0	0			$\gamma 11$	0.13	0	0			$\eta 31$	0.21					$\eta 4$	0.2						
	$\gamma 11$	0.27	0.5	0.135			$\gamma 13$	0.13	1	0.13			$\gamma 14$	0.13	0	0			$\eta 4$	0.2					$\eta 4$	0.2						

Subject ID 12

Figure F.1 (continued) : Calculation details of performance score for navigation tasks.

Step 1						Step 2						Step 3						Step 4											
		Weights (w α , w ν)	Scores ($\gamma\alpha$, $\eta\nu$)	Product	Weighted Sum			Weights (w α , w ν)	Scores ($\gamma\alpha$, $\eta\nu$)	Product	Weighted Sum			Weights (w α , w ν)	Scores ($\gamma\alpha$, $\eta\nu$)	Product	Weighted Sum			Weights (w α , w ν)	Scores ($\gamma\alpha$, $\eta\nu$)	Product	Weighted Sum						
Step 1	T1	$\gamma13$	0.32	1	0.32	1	T1	$\gamma13$	0.24	1	0.24	1	T1	$\gamma13$	0.16	1	0.16	0.68	T1	$\gamma13$	0.31	1	0.31	1	T1	$\eta1$	0.25	1	0.25
		$\eta31$	0.18	1	0.18			$\eta1$	0.16	1	0.16			$\gamma14$	0.16	0	0			$\eta1$	0.16	1	0.16			$\eta31$	0.23	1	0.23
		$\eta4$	0.25	1	0.25			$\eta31$	0.16	1	0.16			$\eta1$	0.11	1	0.11			$\eta4$	0.3	1	0.3			$\eta4$	0.37	1	0.37
		$\gamma14$	0.25	1	0.25			$\eta4$	0.22	1	0.22			$\eta31$	0.11	1	0.11			$\eta32$	0.32	1	0.32			$\eta4$	0.31	1	0.31
	T2	$\gamma15$	0.25	1	0.25	1	T2	$\gamma12$	0.2	1	0.2	1	T2	$\gamma13$	0.2	0.5	0.1	0.9	T3	$\gamma11$	0.21	1	0.21	1	T3	$\gamma14$	0.22	1	0.22
		$\eta1$	0.12	1	0.12			$\gamma14$	0.22	1	0.22			$\eta1$	0.12	1	0.12			$\gamma15$	0.23	1	0.23			$\eta1$	0.12	1	0.12
		$\eta31$	0.17	1	0.17			$\eta31$	0.15	1	0.15			$\gamma3$	0.19	1	0.19			$\eta31$	0.12	1	0.12			$\eta31$	0.17	1	0.17
		$\eta4$	0.21	1	0.21			$\eta4$	0.2	1	0.2			$\eta4$	0.17	1	0.17			$\eta4$	0.18	1	0.18			$\eta4$	0.18	1	0.18
	T3	$\gamma12$	0.22	1	0.22	1	T3	$\gamma11$	0.22	1	0.22	0.89	T3	$\eta1$	0.12	1	0.12	0.655	T4	$\gamma11$	0.25	0.5	0.125	0.75	T4	$\gamma3$	0.27	1	0.27
		$\gamma14$	0.22	1	0.22			$\gamma13$	0.22	0.5	0.11			$\gamma12$	0.22	0	0			$\eta31$	0.12	1	0.12			$\eta31$	0.23	1	0.23
		$\gamma15$	0.22	1	0.22			$\eta31$	0.14	1	0.14			$\eta4$	0.17	1	0.17			$\eta4$	0.25	1	0.25			$\eta4$	0.25	1	0.25
		$\eta31$	0.17	1	0.17			$\eta4$	0.21	1	0.21			$\gamma11$	0.29	1	0.29			$\gamma12$	0.22	0	0			$\gamma31$	0.23	1	0.23
	T4	$\gamma11$	0.43	1	0.43	1	T4	$\gamma12$	0.27	0	0	0.73	T4	$\gamma3$	0.16	1	0.16	0.82	T5	$\gamma12$	0.27	1	0.27	0.86	T5	$\gamma13$	0.28	1	0.28
		$\eta31$	0.25	1	0.25			$\eta31$	0.19	1	0.19			$\eta4$	0.22	1	0.22			$\eta4$	0.26	1	0.26			$\eta4$	0.24	1	0.24
		$\eta4$	0.32	1	0.32			$\eta4$	0.25	1	0.25			$\gamma13$	0.28	1	0.28			$\gamma31$	0.15	1	0.15			$\gamma15$	0.26	1	0.26
		$\gamma11$	0.27	1	0.27			$\eta4$	0.2	1	0.2			$\eta4$	0.22	1	0.22			$\eta4$	0.22	1	0.22			$\gamma3$	0.28	0	0
T5	$\eta2$	0.27	0.5	0.135	0.865	T5	$\gamma11$	0.21	1	0.21	1	T5	$\gamma13$	0.28	1	0.28	0.52	T6	$\gamma13$	0.28	1	0.28	0.72	T6	$\gamma13$	0.28	1	0.28	
	$\eta31$	0.22	1	0.22			$\gamma12$	0.2	1	0.2			$\gamma31$	0.18	0	0			$\gamma15$	0.26	1	0.26			$\gamma31$	0.23	1	0.23	
	$\eta4$	0.24	1	0.24			$\gamma2$	0.23	1	0.23			$\eta4$	0.22	1	0.22			$\eta4$	0.26	1	0.26			$\eta4$	0.24	1	0.24	
							$\eta31$	0.16	1	0.16			$\gamma3$	0.28	0	0			$\gamma11$	0.28	0	0			$\gamma15$	0.27	1	0.27	
T6	$\gamma2$	0.24	1	0.24	0.72	T6	$\gamma11$	0.29	1	0.29	0.73	T6	$\gamma11$	0.13	0.5	0.065	0.935	T7	$\gamma11$	0.28	0	0	0.41	T7	$\gamma11$	0.28	0	0	
	$\gamma3$	0.28	0	0			$\gamma12$	0.27	0	0			$\gamma12$	0.12	1	0.12			$\gamma14$	0.15	0	0			$\gamma14$	0.15	0	0	
	$\eta32$	0.22	1	0.22			$\gamma13$	0.23	1	0.23			$\gamma13$	0.13	1	0.13			$\gamma15$	0.15	0	0			$\gamma14$	0.15	0	0	
	$\eta4$	0.26	1	0.26			$\gamma14$	0.16	1	0.16			$\gamma14$	0.13	1	0.13			$\gamma2$	0.14	1	0.14			$\gamma2$	0.14	1	0.14	
T7	$\gamma2$	0.24	1	0.24	0.72	T7	$\gamma12$	0.2	1	0.2	0.89	T7	$\gamma15$	0.14	1	0.14	0.935	T8	$\gamma2$	0.14	1	0.14	0.41	T8	$\gamma3$	0.14	1	0.14	
	$\gamma3$	0.28	0	0			$\gamma15$	0.23	1	0.23			$\gamma15$	0.14	1	0.14			$\gamma3$	0.14	0	0			$\eta3$	0.14	0	0	
	$\eta32$	0.22	1	0.22			$\eta4$	0.2	1	0.2			$\gamma2$	0.13	1	0.13			$\eta4$	0.13	1	0.13			$\eta4$	0.13	1	0.13	
	$\eta4$	0.26	1	0.26			$\eta4$	0.2	1	0.2			$\eta4$	0.12	1	0.12			$\gamma31$	0.1	1	0.1			$\gamma2$	0.21			
T8	$\gamma2$	0.24	1	0.24	0.72	T8	$\gamma13$	0.24	1	0.24	0.89	T8	$\gamma31$	0.1	1	0.1	0.935	T8	$\gamma3$	0.22			0.41	T8	$\gamma3$	0.22			
	$\gamma3$	0.28	0	0			$\gamma15$	0.23	1	0.23			$\eta4$	0.12	1	0.12			$\eta4$	0.2					$\eta1$	0.16			
	$\eta32$	0.22	1	0.22			$\eta4$	0.2	1	0.2			$\eta4$	0.12	1	0.12			$\eta4$	0.2					$\eta31$	0.21			
	$\eta4$	0.26	1	0.26			$\eta4$	0.2	1	0.2			$\eta4$	0.12	1	0.12			$\eta4$	0.2					$\eta4$	0.2			

Subject ID 16

Figure F.1 (continued) : Calculation details of performance score for navigation tasks.

Step 1					Step 2					Step 3							
		Weights (w_a, w_v)	Scores (γ_a, η_v)	Product	Weighted Sum			Weights (w_a, w_v)	Scores (γ_a, η_v)	Product	Weighted Sum			Weights (w_a, w_v)	Scores (γ_a, η_v)	Product	Weighted Sum
Step 1	T1	y1	0.11	1	0.11	Step 2	T1	y1	0.1	1	0.1	Step 3	T1	y1	0.11	1	0.11
		y2	0.1	1	0.1			y2	0.08	1	0.08			y2	0.12	0	0
		y3	0.2	1	0.2			y3	0.15	1	0.15			y3	0.14	1	0.14
		y4	0.22	1	0.22			y4	0.14	1	0.14			y4	0.14	1	0.14
		y5	0.21	1	0.21			y5	0.12	1	0.12			y5	0.12	1	0.12
	T2	η2	0.16	1	0.16		T2	η2	0.15	1	0.15		T2	η1	0.13	1	0.13
		y1	0.12	1	0.12			y1	0.09	1	0.09			η2	0.11	1	0.11
		y2	0.08	1	0.08			y2	0.05	1	0.05			η2	0.11	1	0.11
		y3	0.13	1	0.13			y3	0.1	1	0.1			η4	0.13	0.5	0.065
		y4	0.15	1	0.15			y4	0.11	1	0.11			y1	0.1	1	0.1
	T3	η1	0.15	0	0		T3	η1	0.13	1	0.13		T3	y2	0.11	0	0
		η2	0.1	1	0.1			y2	0.08	1	0.08			y3	0.14	1	0.14
		η4	0.16	1	0.16			y7	0.13	1	0.13			y4	0.14	1	0.14
		y1	0.12	0	0			η1	0.13	1	0.13			y5	0.1	1	0.1
		y2	0.08	1	0.08			η2	0.09	1	0.09			η1	0.13	1	0.13
	T4	y3	0.17	1	0.17		T4	η3	0.1	1	0.1		T4	η2	0.15	1	0.15
		y4	0.15	1	0.15			η4	0.12	0	0			η4	0.13	0.5	0.065
		y5	0.17	1	0.17			y1	0.07	1	0.07			y1	0.1	1	0.1
		y6	0.15	0	0			y2	0.04	1	0.04			y2	0.1	0	0
		η2	0.16	1	0.16			y3	0.11	1	0.11			y3	0.12	1	0.12
T4	y1	0.12	0	0	T4	y4	0.12	1	0.12	T4	y4	0.13	1	0.13			
	y2	0.08	1	0.08		y5	0.11	1	0.11		y5	0.08	1	0.08			
	y3	0.15	1	0.15		y7	0.09	1	0.09		η8	0.16	0	0			
	y4	0.15	1	0.15		η8	0.13	0	0		η1	0.09	1	0.09			
	y5	0.1	1	0.1		η1	0.07	1	0.07		η2	0.13	0	0			
T5	η1	0.15	0.5	0.075	T5	η2	0.1	0	0	T5	η4	0.09	0.5	0.045			
	η2	0.1	1	0.1		η3	0.07	0.5	0.035		y1	0.07	1	0.07			
	η4	0.15	0.5	0.075		η4	0.09	0.5	0.045		y2	0.07	0	0			
	y1	0.12	0	0		y1	0.07	1	0.07		y3	0.12	1	0.12			
	y2	0.08	1	0.08		y2	0.02	1	0.02		y4	0.13	1	0.13			
T6	y3	0.15	1	0.15	T6	y3	0.1	1	0.1	T6	y5	0.14	1	0.14			
	y4	0.15	1	0.15		y4	0.11	1	0.11		y6	0.15	0	0			
	y5	0.1	1	0.1		y5	0.12	1	0.12		η1	0.09	1	0.09			
	η1	0.15	0.5	0.075		y7	0.08	1	0.08		η2	0.13	0	0			
	η2	0.1	1	0.1		η8	0.13	0	0		η4	0.1	0.5	0.05			
T7	η3	0.17	1	0.17	T7	η1	0.08	1	0.08	T7	y1	0.08	1	0.08			
	η4	0.16	1	0.16		η2	0.12	0	0		y2	0.1	0	0			
	y1	0.12	0	0		η3	0.07	0.5	0.035		y3	0.11	1	0.11			
	y2	0.08	1	0.08		η4	0.1	0	0		y3	0.11	1	0.11			
	y3	0.15	1	0.15		y1	0.08	1	0.08		η1	0.08	1	0.08			
T8	y4	0.15	1	0.15	T8	y2	0.03	1	0.03	T8	η3	0.11	1	0.11			
	y5	0.1	1	0.1		y3	0.11	1	0.11		y4	0.13	1	0.13			
	η1	0.15	0.5	0.075		y4	0.13	1	0.13		y5	0.1	1	0.1			
	η2	0.1	1	0.1		y5	0.1	1	0.1		η2	0.11	1	0.11			
	η4	0.15	0.5	0.075		y7	0.11	0	0		η4	0.1	0	0			
T9	y1	0.12	0	0	T9	η1	0.1	0	0	T9	y1	0.07	1	0.07			
	y2	0.08	1	0.08		η2	0.12	1	0.12		y2	0.06	0	0			
	y3	0.15	1	0.15		η3	0.11	0.5	0.055		y3	0.13	1	0.13			
	y4	0.15	1	0.15		η4	0.11	0	0		y4	0.13	1	0.13			
	y5	0.1	1	0.1		y1	0.05	1	0.05		y5	0.14	0	0			
T10	η1	0.15	0.5	0.075	T10	y2	0.06	1	0.06	T10	η1	0.11	0	0			
	η2	0.1	1	0.1		y3	0.12	1	0.12		η2	0.11	1	0.11			
	η4	0.15	0.5	0.075		y4	0.12	1	0.12		η4	0.13	0	0			
	y1	0.12	0	0		y5	0.13	0	0		y1	0.07	1	0.07			
	y2	0.08	1	0.08		η2	0.12	1	0.12		y2	0.07	0	0			
T11	y3	0.15	1	0.15	T11	η3	0.07	0	0	T11	y3	0.13	1	0.13			
	y4	0.15	1	0.15		η4	0.09	0	0		y4	0.13	1	0.13			
	y5	0.1	1	0.1		y1	0.04				y5	0.14	0	0			
	η1	0.15	0.5	0.075		y2	0.06				η1	0.08	0	0			
	η2	0.1	1	0.1		y3	0.12				η2	0.13	0	0			
T12	η4	0.15	0.5	0.075	T12	y4	0.14			T12	y4	0.13					
	y1	0.12	0	0		y5	0.11				y5	0.11					
	y2	0.08	1	0.08		y7	0.1				y6	0.13					
	y3	0.15	1	0.15		η1	0.08				y8	0.13					
	y4	0.15	1	0.15		η2	0.14				η1	0.06					
T13	η1	0.15	0.5	0.075	T13	η3	0.1			T13	η2	0.1					
	η2	0.1	1	0.1		η4	0.11				η2	0.1					
	η4	0.15	0.5	0.075		y1	0.04				η4	0.1					
	y1	0.12	0	0		y2	0.06				y1	0.07					
	y2	0.08	1	0.08		y3	0.12				y2	0.07					
T14	y3	0.15	1	0.15	T14	y4	0.14			T14	y3	0.12					
	y4	0.15	1	0.15		y5	0.11				y4	0.11					
	y5	0.1	1	0.1		y7	0.1				y5	0.11					
	η1	0.15	0.5	0.075		η1	0.08				y6	0.13					
	η2	0.1	1	0.1		η2	0.14				y8	0.13					
T15	η4	0.15	0.5	0.075	T15	η3	0.1			T15	η1	0.06					
	y1	0.12	0	0		η4	0.11				η2	0.1					
	y2	0.08	1	0.08		y1	0.04				η4	0.1					
	y3	0.15	1	0.15		y2	0.06				y1	0.07					
	y4	0.15	1	0.15		y3	0.12				y2	0.07					
T16	η1	0.15	0.5	0.075	T16	y4	0.14			T16	y3	0.12					
	η2	0.1	1	0.1		y5	0.11				y4	0.11					
	η4	0.15	0.5	0.075		y7	0.1				y5	0.11					
	y1	0.12	0	0		η1	0.08				y6	0.13					
	y2	0.08	1	0.08		η2	0.14				y8	0.13					
T17	y3	0.15	1	0.15	T17	η3	0.1			T17	η1	0.06					
	y4	0.15	1	0.15		η4	0.11				η2	0.1					
	y5	0.1	1	0.1		y1	0.04				η4	0.1					
	η1	0.15	0.5	0.075		y2	0.06				y1	0.07					
	η2	0.1	1	0.1		y3	0.12				y2	0.07					
T18	η4	0.15	0.5	0.075	T18	y4	0.14			T18	y3	0.12					
	y1	0.12	0	0		y5	0.11				y4	0.11					
	y2	0.08	1	0.08		y7	0.1				y5	0.11					
	y3	0.15	1	0.15		η1	0.08				y6	0.13					
	y4	0.15	1	0.15		η2	0.14				y8	0.13					
T19	η1	0.15	0.5	0.075	T19	η3	0.1			T19	η1	0.06					
	η2	0.1	1	0.1		η4	0.11				η2	0.1					
	η4	0.15	0.5	0.075		y1	0.04				η4	0.1					
	y1	0.12	0	0		y2	0.06				y1	0.07					
	y2	0.08	1	0.08		y3	0.12				y2	0.07					
T20	y3	0.15	1	0.15	T20	y4	0.14			T20	y3	0.12					
	y4	0.15	1	0.15		y5	0.11				y4	0.11					
	y5	0.1	1	0.1		y7	0.1				y5	0.11					
	η1	0.15	0.5	0.075		η1	0.08				y6	0.13					
	η2	0.1	1	0.1		η2	0.14				y8	0.13					
T21	η4	0.15	0.5	0.075	T21	η3	0.1			T21	η1	0.06					
	y1	0.12	0	0		η4	0.11				η2	0.1					
	y2	0.08	1	0.08		y1	0.04				η4	0.1					
	y3	0.15	1	0.15		y2	0.06				y1	0.07					
	y4	0.15	1	0.15		y3	0.12				y2	0.07					

Step 1					Step 2					Step 3																						
		Weights ($w\alpha, w\upsilon$)	Scores ($\gamma\alpha, \eta\upsilon$)	Product	Weighted Sum			Weights ($w\alpha, w\upsilon$)	Scores ($\gamma\alpha, \eta\upsilon$)	Product	Weighted Sum			Weights ($w\alpha, w\upsilon$)	Scores ($\gamma\alpha, \eta\upsilon$)	Product	Weighted Sum															
Step 1	T1	$\gamma 1$	0.11	1	0.11	Step 2	T1	$\gamma 1$	0.1	1	0.1	Step 3	T1	$\gamma 1$	0.11	1	0.11	Step 3	T1	$\gamma 1$	0.11	1	0.11									
		$\gamma 2$	0.1	1	0.1			$\gamma 2$	0.08	1	0.08			$\gamma 2$	0.12	1	0.12			$\gamma 2$	0.12	1	0.12									
		$\gamma 3$	0.2	1	0.2			$\gamma 3$	0.15	1	0.15			$\gamma 3$	0.14	1	0.14			$\gamma 3$	0.14	1	0.14	$\gamma 3$	0.14	1	0.14					
		$\gamma 4$	0.22	1	0.22			$\gamma 4$	0.14	1	0.14			$\gamma 4$	0.14	1	0.14			$\gamma 4$	0.14	1	0.14	$\gamma 4$	0.14	1	0.14					
		$\gamma 5$	0.21	1	0.21			$\gamma 5$	0.12	1	0.12			$\gamma 5$	0.12	1	0.12			$\gamma 5$	0.12	1	0.12	$\gamma 5$	0.12	1	0.12					
	T2	$\eta 2$	0.16	1	0.16		$\eta 2$	0.15	1	0.15	$\eta 2$		0.15	1	0.15	$\eta 2$	0.15		1	0.15	$\eta 2$	0.15	1	0.15	$\eta 2$	0.15	1	0.15				
		$\gamma 1$	0.12	1	0.12		T2	$\gamma 1$	0.09	1	0.09		T2	$\gamma 1$	0.1	1	0.1		T2	$\gamma 1$	0.1	1	0.1	T2	$\gamma 1$	0.1	1	0.1				
		$\gamma 2$	0.08	1	0.08			$\gamma 2$	0.05	1	0.05			$\gamma 2$	0.11	1	0.11			$\gamma 2$	0.11	1	0.11		$\gamma 2$	0.11	1	0.11				
		$\gamma 3$	0.13	1	0.13			$\gamma 3$	0.1	1	0.1			$\gamma 3$	0.14	1	0.14			$\gamma 3$	0.14	1	0.14		$\gamma 3$	0.14	1	0.14				
		$\gamma 4$	0.15	1	0.15			$\gamma 4$	0.11	1	0.11			$\gamma 4$	0.14	1	0.14			$\gamma 4$	0.14	1	0.14		$\gamma 4$	0.14	1	0.14				
	$\gamma 5$	0.11	1	0.11	$\gamma 5$			0.08	1	0.08	$\gamma 5$			0.1	1	0.1	$\gamma 5$			0.1	1	0.1	$\gamma 5$		0.1	1	0.1					
	T3	$\eta 1$	0.15	0.5	0.075		$\eta 1$	0.13	1	0.13	$\eta 1$		0.13	1	0.13	$\eta 1$	0.13		0	0	$\eta 1$	0.13	0	0	$\eta 1$	0.13	0	0				
		$\eta 2$	0.1	1	0.1		$\eta 2$	0.09	0	0	$\eta 2$		0.09	0	0	$\eta 2$	0.15		0	0	$\eta 2$	0.15	0	0	$\eta 2$	0.15	0	0				
		$\eta 4$	0.16	0.5	0.08		$\eta 3$	0.1	1	0.1	$\eta 3$		0.1	1	0.1	$\eta 3$	0.13		0	0	$\eta 3$	0.13	0	0	$\eta 3$	0.13	0	0				
		$\gamma 1$	0.12	1	0.12		$\eta 4$	0.12	1	0.12	$\eta 4$		0.12	1	0.12	$\eta 4$	0.13		0	0	$\eta 4$	0.13	0	0	$\eta 4$	0.13	0	0				
		$\gamma 2$	0.08	1	0.08		$\gamma 1$	0.07	1	0.07	$\gamma 1$		0.07	1	0.07	$\gamma 1$	0.07		1	0.07	$\gamma 1$	0.07	1	0.07	$\gamma 1$	0.07	1	0.07				
	T4	$\gamma 3$	0.17	1	0.17		T3	$\gamma 2$	0.04	1	0.04		T3	$\gamma 2$	0.04	1	0.04		T3	$\gamma 2$	0.12	1	0.12	T3	$\gamma 2$	0.12	1	0.12				
		$\gamma 4$	0.15	1	0.15			$\gamma 3$	0.11	0	0			$\gamma 3$	0.11	0	0			$\gamma 3$	0.11	0	0		$\gamma 3$	0.11	0	0	$\gamma 3$	0.11	0	0
		$\gamma 5$	0.15	0	0			$\gamma 4$	0.12	1	0.12			$\gamma 4$	0.12	1	0.12			$\gamma 4$	0.12	1	0.12		$\gamma 4$	0.12	1	0.12	$\gamma 4$	0.12	1	0.12
		$\eta 2$	0.16	1	0.16			$\gamma 5$	0.11	0	0			$\gamma 5$	0.11	0	0			$\gamma 5$	0.11	0	0		$\gamma 5$	0.11	0	0	$\gamma 5$	0.11	0	0
$\gamma 1$		0.12	1	0.12	$\eta 1$	0.07		1	0.07	$\eta 1$	0.07	1		0.07	$\eta 1$	0.07	1	0.07		$\eta 1$	0.07	1	0.07		$\eta 1$	0.07	1	0.07				
T4	$\gamma 2$	0.08	1	0.08	T4	$\eta 2$	0.1	0	0	T4	$\eta 2$	0.1	0	0	T4	$\eta 2$	0.1	0	0	T4	$\eta 2$	0.1	0	0								
	$\gamma 3$	0.15	1	0.15		$\eta 3$	0.07	1	0.07		$\eta 3$	0.07	1	0.07		$\eta 3$	0.07	1	0.07		$\eta 3$	0.07	1	0.07	$\eta 3$	0.07	1	0.07				
	$\gamma 4$	0.15	1	0.15		$\eta 4$	0.09	1	0.09		$\eta 4$	0.09	1	0.09		$\eta 4$	0.09	1	0.09		$\eta 4$	0.09	1	0.09	$\eta 4$	0.09	1	0.09				
	$\gamma 5$	0.1	1	0.1		$\gamma 1$	0.07	1	0.07		$\gamma 1$	0.07	1	0.07		$\gamma 1$	0.07	1	0.07		$\gamma 1$	0.07	1	0.07	$\gamma 1$	0.07	1	0.07				
	$\eta 1$	0.15	1	0.15		$\gamma 2$	0.02	1	0.02		$\gamma 2$	0.02	1	0.02		$\gamma 2$	0.02	1	0.02		$\gamma 2$	0.02	1	0.02	$\gamma 2$	0.02	1	0.02				
T4	$\eta 2$	0.1	1	0.1	T4	$\gamma 3$	0.1	1	0.1	T4	$\gamma 3$	0.1	1	0.1	T4	$\gamma 3$	0.1	1	0.1	T4	$\gamma 3$	0.1	1	0.1								
	$\eta 4$	0.15	1	0.15		$\gamma 4$	0.11	1	0.11		$\gamma 4$	0.11	1	0.11		$\gamma 4$	0.11	1	0.11		$\gamma 4$	0.11	1	0.11	$\gamma 4$	0.11	1	0.11				
	$\gamma 1$	0.08	1	0.08		$\gamma 5$	0.12	0	0		$\gamma 5$	0.12	0	0		$\gamma 5$	0.12	0	0		$\gamma 5$	0.12	0	0	$\gamma 5$	0.12	0	0				
	$\gamma 2$	0.03	1	0.03		$\eta 1$	0.08	0.5	0.04		$\eta 1$	0.08	0.5	0.04		$\eta 1$	0.08	0.5	0.04		$\eta 1$	0.08	0.5	0.04	$\eta 1$	0.08	0.5	0.04				
	$\gamma 3$	0.11	1	0.11		$\eta 2$	0.12	1	0.12		$\eta 2$	0.12	1	0.12		$\eta 2$	0.12	1	0.12		$\eta 2$	0.12	1	0.12	$\eta 2$	0.12	1	0.12				
T5	$\gamma 4$	0.13	1	0.13	T5	$\eta 3$	0.07	0.5	0.035	T5	$\eta 3$	0.07	0.5	0.035	T5	$\eta 3$	0.07	0.5	0.035	T5	$\eta 3$	0.07	0.5	0.035								
	$\gamma 5$	0.1	0	0		$\eta 4$	0.1	1	0.1		$\eta 4$	0.1	1	0.1		$\eta 4$	0.1	1	0.1		$\eta 4$	0.1	1	0.1	$\eta 4$	0.1	1	0.1				
	$\gamma 7$	0.11	1	0.11		$\gamma 1$	0.08	1	0.08		$\gamma 1$	0.08	1	0.08		$\gamma 1$	0.08	1	0.08		$\gamma 1$	0.08	1	0.08	$\gamma 1$	0.08	1	0.08				
	$\eta 1$	0.1	0.5	0.05		$\gamma 2$	0.03	1	0.03		$\gamma 2$	0.03	1	0.03		$\gamma 2$	0.03	1	0.03		$\gamma 2$	0.03	1	0.03	$\gamma 2$	0.03	1	0.03				
	$\eta 2$	0.12	0	0		$\gamma 3$	0.11	1	0.11		$\gamma 3$	0.11	1	0.11		$\gamma 3$	0.11	1	0.11		$\gamma 3$	0.11	1	0.11	$\gamma 3$	0.11	1	0.11				
T6	$\eta 3$	0.11	0.5	0.055	T6	$\gamma 4$	0.13	1	0.13	T6	$\gamma 4$	0.13	1	0.13	T6	$\gamma 4$	0.13	1	0.13	T6	$\gamma 4$	0.13	1	0.13								
	$\eta 4$	0.11	0.5	0.055		$\gamma 5$	0.1	0	0		$\gamma 5$	0.1	0	0		$\gamma 5$	0.1	0	0		$\gamma 5$	0.1	0	0	$\gamma 5$	0.1	0	0				
	$\gamma 1$	0.05	1	0.05		$\gamma 7$	0.11	1	0.11		$\gamma 7$	0.11	1	0.11		$\gamma 7$	0.11	1	0.11		$\gamma 7$	0.11	1	0.11	$\gamma 7$	0.11	1	0.11				
	$\gamma 2$	0.06	1	0.06		$\eta 1$	0.1	0.5	0.05		$\eta 1$	0.1	0.5	0.05		$\eta 1$	0.1	0.5	0.05		$\eta 1$	0.1	0.5	0.05	$\eta 1$	0.1	0.5	0.05				
	$\gamma 3$	0.12	1	0.12		$\eta 2$	0.12	0	0		$\eta 2$	0.12	0	0		$\eta 2$	0.12	0	0		$\eta 2$	0.12	0	0	$\eta 2$	0.12	0	0				
T6	$\gamma 4$	0.12	1	0.12	T6	$\eta 3$	0.11	0.5	0.055	T6	$\eta 3$	0.11	0.5	0.055	T6	$\eta 3$	0.11	0.5	0.055	T6	$\eta 3$	0.11	0.5	0.055								
	$\gamma 5$	0.13	1	0.13		$\eta 4$	0.11	0.5	0.055		$\eta 4$	0.11	0.5	0.055		$\eta 4$	0.11	0.5	0.055		$\eta 4$	0.11	0.5	0.055	$\eta 4$	0.11	0.5	0.055				
	$\gamma 6$	0.13	1	0.13		$\gamma 1$	0.05	1	0.05		$\gamma 1$	0.05	1	0.05		$\gamma 1$	0.05	1	0.05		$\gamma 1$	0.05	1	0.05	$\gamma 1$	0.05	1	0.05				
	$\gamma 7$	0.06	1	0.06		$\gamma 2$	0.06	1	0.06		$\gamma 2$	0.06	1	0.06		$\gamma 2$	0.06	1	0.06		$\gamma 2$	0.06	1	0.06	$\gamma 2$	0.06	1	0.06				
	$\eta 1$	0.07	1	0.07		$\gamma 3$	0.12	1	0.12		$\gamma 3$	0.12	1	0.12		$\gamma 3$	0.12	1	0.12		$\gamma 3$	0.12	1	0.12	$\gamma 3$	0.12	1	0.12				
T7	$\eta 2$	0.1	1	0.1	T7	$\gamma 4$	0.12	1	0.12	T7	$\gamma 4$	0.12	1	0.12	T7	$\gamma 4$	0.12	1	0.12	T7	$\gamma 4$	0.12	1	0.12								
	$\eta 3$	0.07	0.5	0.035		$\gamma 5$	0.13	1	0.13		$\gamma 5$	0.13	1	0.13		$\gamma 5$	0.13	1	0.13		$\gamma 5$	0.13	1	0.13	$\gamma 5$	0.13	1	0.13				
	$\eta 4$	0.09	0.5	0.045		$\gamma 6$	0.13	1	0.13		$\gamma 6$	0.13	1	0.13		$\gamma 6$	0.13	1	0.13		$\gamma 6$	0.13	1	0.13	$\gamma 6$	0.13	1	0.13				
	$\gamma 1$	0.04	1	0.04		$\gamma 7$	0.06	1	0.06		$\gamma 7$	0.06	1	0.06		$\gamma 7$	0.06	1	0.06		$\gamma 7$	0.06	1	0.06	$\gamma 7$	0.06	1	0.06				
	$\gamma 2$	0.06	1	0.06		$\eta $																										

Step 1					Step 2					Step 3								
		Weights (w α , wv)	Scores ($\gamma\alpha$, ηv)	Product	Weighted Sum			Weights (w α , wv)	Scores ($\gamma\alpha$, ηv)	Product	Weighted Sum			Weights (w α , wv)	Scores ($\gamma\alpha$, ηv)	Product	Weighted Sum	
Step 1	T1	y1	0.11	1	0.11	1	T1	y1	0.1	1	0.1	0.85	T1	y1	0.11	1	0.11	0.74
		y2	0.1	1	0.1			y2	0.08	1	0.08			y2	0.12	1	0.12	
		y3	0.2	1	0.2			y3	0.15	1	0.15			y3	0.14	1	0.14	
		y4	0.22	1	0.22			y4	0.14	1	0.14			y4	0.14	1	0.14	
		y5	0.21	1	0.21			y5	0.12	1	0.12			y5	0.12	1	0.12	
	T2	y2	0.12	1	0.12	1	T2	y2	0.11	1	0.11	1	T2	y2	0.11	1	0.11	1
		y2	0.08	1	0.08			y3	0.1	1	0.1			y3	0.14	1	0.14	
		y3	0.13	1	0.13			y4	0.11	1	0.11			y4	0.14	1	0.14	
		y4	0.15	1	0.15			y5	0.08	1	0.08			y5	0.1	1	0.1	
		y5	0.11	1	0.11			y7	0.13	1	0.13			y7	0.13	1	0.13	
	T3	y1	0.15	1	0.15	0.85	T3	y1	0.13	1	0.13	0.745	T3	y1	0.13	1	0.13	0.87
		y2	0.1	1	0.1			y2	0.09	1	0.09			y2	0.15	1	0.15	
		y3	0.17	1	0.17			y3	0.1	1	0.1			y3	0.12	1	0.12	
		y4	0.15	1	0.15			y4	0.12	1	0.12			y4	0.13	1	0.13	
		y5	0.17	1	0.17			y5	0.11	0	0			y5	0.13	1	0.13	
	T4	y6	0.15	0	0	1	T4	y6	0.12	1	0.12	0.87	T4	y6	0.16	1	0.16	0.58
		y6	0.16	1	0.16			y7	0.09	1	0.09			y7	0.08	1	0.08	
		y1	0.12	1	0.12			y8	0.13	1	0.13			y8	0.16	1	0.16	
		y2	0.08	1	0.08			y7	0.09	1	0.09			y7	0.16	1	0.16	
		y3	0.15	1	0.15			y8	0.13	1	0.13			y8	0.16	1	0.16	
Step 2	T1	y4	0.15	1	0.15	1	T1	y4	0.13	1	0.13	0.745	T1	y4	0.13	1	0.13	0.87
		y5	0.1	1	0.1			y5	0.07	0.5	0.035			y5	0.13	1	0.13	
		y5	0.15	1	0.15			y6	0.1	1	0.1			y6	0.13	1	0.13	
		y6	0.1	1	0.1			y7	0.07	1	0.07			y7	0.13	1	0.13	
		y6	0.1	1	0.1			y8	0.09	1	0.09			y8	0.13	1	0.13	
	T2	y1	0.12	1	0.12	0.85	T2	y1	0.1	1	0.1	0.87	T2	y1	0.12	1	0.12	0.735
		y2	0.08	1	0.08			y2	0.12	1	0.12			y2	0.13	1	0.13	
		y3	0.17	1	0.17			y3	0.07	1	0.07			y3	0.13	1	0.13	
		y4	0.15	1	0.15			y4	0.1	0.5	0.05			y4	0.13	1	0.13	
		y5	0.17	1	0.17			y5	0.08	0	0			y5	0.13	1	0.13	
	T3	y1	0.07	1	0.07	0.745	T3	y6	0.12	1	0.12	0.87	T3	y6	0.13	1	0.13	0.735
		y2	0.04	1	0.04			y7	0.08	1	0.08			y7	0.13	1	0.13	
		y3	0.11	0	0			y8	0.13	1	0.13			y8	0.13	1	0.13	
		y4	0.12	1	0.12			y8	0.13	1	0.13			y8	0.13	1	0.13	
		y5	0.11	0	0			y9	0.08	0	0			y9	0.13	1	0.13	
	T4	y7	0.09	1	0.09	0.87	T4	y9	0.13	1	0.13	0.87	T4	y9	0.13	1	0.13	0.735
		y8	0.13	1	0.13			y1	0.07	1	0.07			y1	0.13	1	0.13	
		y9	0.08	0	0			y2	0.07	1	0.07			y2	0.13	1	0.13	
		y1	0.07	1	0.07			y3	0.12	1	0.12			y3	0.13	1	0.13	
		y2	0.07	1	0.07			y4	0.12	1	0.12			y4	0.13	1	0.13	
T5	y3	0.12	1	0.12	0.87	T5	y5	0.12	1	0.12	0.87	T5	y5	0.13	1	0.13	0.735	
	y4	0.11	1	0.11			y6	0.07	1	0.07			y6	0.13	1	0.13		
	y5	0.12	1	0.12			y7	0.12	1	0.12			y7	0.13	1	0.13		
	y6	0.11	1	0.11			y8	0.12	1	0.12			y8	0.13	1	0.13		
	y7	0.12	1	0.12			y9	0.12	1	0.12			y9	0.13	1	0.13		
T6	y1	0.09	1	0.09	0.745	T6	y1	0.07	1	0.07	0.745	T6	y1	0.07	1	0.07	0.735	
	y2	0.1	1	0.1			y2	0.07	1	0.07			y2	0.07	1	0.07		
	y3	0.11	1	0.11			y3	0.12	1	0.12			y3	0.07	1	0.07		
	y4	0.13	1	0.13			y4	0.13	1	0.13			y4	0.07	1	0.07		
	y5	0.1	1	0.1			y5	0.13	1	0.13			y5	0.07	1	0.07		
T7	y6	0.13	1	0.13	0.9	T7	y6	0.13	1	0.13	0.9	T7	y6	0.13	1	0.13	0.63	
	y7	0.06	1	0.06			y7	0.06	1	0.06			y7	0.13	1	0.13		
	y8	0.13	1	0.13			y8	0.13	1	0.13			y8	0.13	1	0.13		
	y9	0.11	1	0.11			y9	0.13	1	0.13			y9	0.13	1	0.13		
	y1	0.05	1	0.05			y1	0.07	1	0.07			y1	0.13	1	0.13		
T8	y2	0.06	1	0.06	0.76	T8	y2	0.06	1	0.06	0.76	T8	y2	0.07	1	0.07	0.6	
	y3	0.12	1	0.12			y3	0.12	1	0.12			y3	0.07	1	0.07		
	y4	0.12	1	0.12			y4	0.12	1	0.12			y4	0.12	1	0.12		
	y5	0.13	1	0.13			y5	0.12	1	0.12			y5	0.12	1	0.12		
	y6	0.13	1	0.13			y6	0.14	1	0.14			y6	0.12	1	0.12		
T9	y7	0.06	1	0.06	0.9	T9	y7	0.06	1	0.06	0.9	T9	y7	0.11	1	0.11	0.6	
	y8	0.13	1	0.13			y8	0.11	1	0.11			y8	0.11	1	0.11		
	y9	0.11	1	0.11			y9	0.11	1	0.11			y9	0.11	1	0.11		
	y1	0.07	1	0.07			y1	0.11	1	0.11			y1	0.11	1	0.11		
	y2	0.1	0	0			y2	0.1	0	0			y2	0.11	1	0.11		
T10	y3	0.07	1	0.07	0.76	T10	y3	0.07	1	0.07	0.76	T10	y3	0.11	1	0.11	0.6	
	y4	0.09	1	0.09			y4	0.07	1	0.07			y4	0.11	1	0.11		
	y5	0.11	1	0.11			y5	0.07	1	0.07			y5	0.11	1	0.11		
	y6	0.13	1	0.13			y6	0.11	1	0.11			y6	0.11	1	0.11		
	y7	0.06	1	0.06			y7	0.11	1	0.11			y7	0.11	1	0.11		
T11	y8	0.13	1	0.13	0.9	T11	y8	0.13	1	0.13	0.9	T11	y8	0.11	1	0.11	0.6	
	y9	0.11	1	0.11			y9	0.11	1	0.11			y9	0.11	1	0.11		
	y1	0.04	1	0.04			y1	0.11	1	0.11			y1	0.11	1	0.11		
	y2	0.06	1	0.06			y2	0.11	1	0.11			y2	0.11	1	0.11		
	y3	0.12	1	0.12			y3	0.11	1	0.11			y3	0.11	1	0.11		
T12	y4	0.14	1	0.14	0.76	T12	y4	0.14	1	0.14	0.76	T12	y4	0.11	1	0.11	0.6	
	y5	0.11	1	0.11			y5	0.11	1	0.11			y5	0.11	1	0.11		
	y6	0.1	0	0			y6	0.1	0	0			y6	0.11	1	0.11		
	y7	0.1	0	0			y7	0.1	0	0			y7	0.11	1	0.11		
	y8	0.08	1	0.08			y8	0.1	0	0			y8	0.11	1	0.11		
T13	y9	0.14	1	0.14	0.76	T13	y9	0.14	1	0.14	0.76	T13	y9	0.11	1	0.11	0.6	
	y1	0.14	1	0.14			y1	0.14	1	0.14			y1	0.11	1	0.11		
	y2	0.14	1	0.14			y2	0.14	1	0.14			y2	0.11	1	0.11		
	y3	0.14	1	0.14			y3	0.14	1	0.14			y3	0.11	1	0.11		
	y4	0.14	1	0.14			y4	0.14	1	0.14			y4	0.11	1	0.11		

Subject ID 13

Figure F.2 (continued) : Calculation details of performance score for cargo operation tasks.

Step 1					Step 2					Step 3								
		Weights (w α , wv)	Scores (y α , η v)	Product	Weighted Sum			Weights (w α , wv)	Scores (y α , η v)	Product	Weighted Sum			Weights (w α , wv)	Scores (y α , η v)	Product	Weighted Sum	
Step 1	T1	y1	0.11	1	0.11	1	T1	y1	0.1	1	0.1	1	T1	y1	0.11	1	0.11	1
		y2	0.1	1	0.1			y2	0.08	1	0.08			y2	0.12	1	0.12	
		y3	0.2	1	0.2			y3	0.15	1	0.15			y3	0.14	1	0.14	
		y4	0.22	1	0.22			y4	0.14	1	0.14			y4	0.14	1	0.14	
		y5	0.21	1	0.21			y5	0.12	1	0.12			y5	0.12	1	0.12	
	T2	η 2	0.16	1	0.16	0.765	T2	η 2	0.15	1	0.15	1	T2	η 2	0.13	1	0.13	1
		y1	0.12	1	0.12			y1	0.09	1	0.09			y1	0.1	1	0.1	
		y2	0.08	1	0.08			y2	0.05	1	0.05			y2	0.11	1	0.11	
		y3	0.13	1	0.13			y3	0.1	1	0.1			y3	0.14	1	0.14	
		y4	0.15	1	0.15			y4	0.11	1	0.11			y4	0.14	1	0.14	
	T3	y5	0.11	1	0.11	0.85	T3	y5	0.08	1	0.08	1	T3	y5	0.1	1	0.1	0.87
		η 1	0.15	0.5	0.075			η 1	0.13	1	0.13			η 1	0.13	1	0.13	
		η 2	0.1	1	0.1			η 2	0.09	1	0.09			η 2	0.15	1	0.15	
		η 4	0.16	0	0			η 3	0.1	1	0.1			η 4	0.13	1	0.13	
		y1	0.12	1	0.12			η 4	0.12	1	0.12			y1	0.1	1	0.1	
	T4	y2	0.08	1	0.08	0.85	T4	y2	0.07	1	0.07	1	T4	y2	0.12	1	0.12	0.73
		y3	0.17	1	0.17			y3	0.11	1	0.11			y3	0.12	1	0.12	
		y4	0.15	1	0.15			y4	0.12	1	0.12			y4	0.13	1	0.13	
		y5	0.17	1	0.17			y5	0.11	1	0.11			y5	0.08	1	0.08	
		η 2	0.16	1	0.16			y7	0.09	1	0.09			η 1	0.09	1	0.09	
Step 2	T5	y1	0.12	1	0.12	0.775	T5	η 1	0.07	1	0.07	0.775	T5	y1	0.07	1	0.07	0.745
		y2	0.08	1	0.08			η 2	0.1	1	0.1			y2	0.07	1	0.07	
		y3	0.17	1	0.17			η 3	0.07	1	0.07			y3	0.12	1	0.12	
		y4	0.15	1	0.15			η 4	0.09	1	0.09			y4	0.13	1	0.13	
		y5	0.17	1	0.17			y1	0.07	0	0			y5	0.14	0	0	
	T6	η 2	0.16	1	0.16	0.54	T6	y2	0.02	1	0.02	0.54	T6	y6	0.15	1	0.15	0.935
		y1	0.12	1	0.12			y3	0.1	1	0.1			η 1	0.09	1	0.09	
		y2	0.08	1	0.08			y4	0.11	1	0.11			η 2	0.13	0	0	
		y3	0.17	1	0.17			y5	0.12	1	0.12			η 4	0.1	1	0.1	
		y4	0.15	1	0.15			y7	0.08	1	0.08			y1	0.08	1	0.08	
T7	η 1	0.15	0.5	0.075	0.85	T7	η 1	0.08	1	0.08	0.9	T7	y2	0.15	1	0.15	0.775	
	η 2	0.1	1	0.1			η 2	0.12	0	0			y3	0.11	1	0.11		
	η 4	0.15	0.5	0.075			η 3	0.07	0.5	0.035			y4	0.13	1	0.13		
	η 1	0.12	1	0.12			η 4	0.1	1	0.1			y5	0.14	1	0.14		
	η 2	0.1	1	0.1			y1	0.08	1	0.08			y8	0.17	1	0.17		
Step 3	T8	y1	0.12	1	0.12	0.87	T8	y2	0.03		0.775	T8	η 1	0.11	0.5	0.055	0.775	
		y2	0.08	1	0.08			y3	0.11	1			0.11	η 2	0.11	0		0
		y3	0.17	1	0.17			y4	0.13	1			0.13	η 4	0.1	1		0.1
		y4	0.15	1	0.15			y5	0.1	1			0.1	y1	0.07	1		0.07
		y5	0.17	1	0.17			y7	0.11					y2	0.07	1		0.07
	T9	η 2	0.16	1	0.16	0.87	T9	η 1	0.07	1	0.07	0.775	T9	y3	0.13	1	0.13	0.935
		y1	0.12	1	0.12			η 2	0.12	0	0			y4	0.13	1	0.13	
		y2	0.08	1	0.08			η 3	0.07	0.5	0.035			y5	0.14	1	0.14	
		y3	0.17	1	0.17			η 4	0.1	1	0.1			y6	0.14	1	0.14	
		y4	0.15	1	0.15			y1	0.05	0	0			η 1	0.08	1	0.08	
T10	η 1	0.15	0.5	0.075	0.85	T10	y2	0.06	0	0	0.54	T10	η 2	0.13	0.5	0.065	0.775	
	η 2	0.1	1	0.1			y3	0.12	0	0			y1	0.07	1	0.07		
	η 4	0.15	0.5	0.075			y4	0.12	1	0.12			y2	0.07	1	0.07		
	η 1	0.12	1	0.12			y5	0.13	0	0			y3	0.13	1	0.13		
	η 2	0.1	1	0.1			y6	0.13	1	0.13			y4	0.13	1	0.13		
Step 3	T11	y1	0.12	1	0.12	0.87	T11	y7	0.06	1	0.06	0.54	T11	y5	0.1	1	0.1	0.775
		y2	0.08	1	0.08			η 1	0.07	1	0.07			y8	0.17	0	0	
		y3	0.17	1	0.17			η 2	0.1	0	0			η 1	0.09	1	0.09	
		y4	0.15	1	0.15			η 3	0.07	1	0.07			η 2	0.11	0.5	0.055	
		y5	0.17	1	0.17			η 4	0.09	1	0.09			η 4	0.13	1	0.13	
	T12	η 2	0.16	1	0.16	0.87	T12	y1	0.04	0	0	0.9	T12	y1	0.07	1	0.07	0.9
		y1	0.12	1	0.12			y2	0.06	0	0			y2	0.07	1	0.07	
		y2	0.08	1	0.08			y3	0.12	1	0.12			y3	0.12	1	0.12	
		y3	0.17	1	0.17			y4	0.14	1	0.14			y4	0.11	1	0.11	
		y4	0.15	1	0.15			y5	0.11	1	0.11			y5	0.11	1	0.11	
T13	y5	0.17	1	0.17	0.85	T13	y7	0.1	1	0.1	0.9	T13	y6	0.13	1	0.13	0.9	
	η 1	0.15	0.5	0.075			η 1	0.08	1	0.08			y8	0.13	1	0.13		
	η 2	0.1	1	0.1			η 2	0.14	1	0.14			η 1	0.06	1	0.06		
	η 4	0.15	0.5	0.075			η 3	0.1	1	0.1			η 2	0.1	0	0		
	η 1	0.12	1	0.12			η 4	0.11	1	0.11			η 4	0.1	1	0.1		

Subject ID 15

Figure F.2 (continued) : Calculation details of performance score for cargo operation tasks.

		Weights (w α , wv)	Scores (y α , η v)	Product	Weighted Sum			Weights (w α , wv)	Scores (y α , η v)	Product	Weighted Sum			Weights (w α , wv)	Scores (y α , η v)	Product	Weighted Sum		
Step 1	T1	y1	0.11	1	0.11	1	Step 2	T1	y1	0.1	1	0.1	1	T1	y1	0.11	1	0.11	0.74
		y2	0.1	1	0.1				y2	0.08	1	0.08			y2	0.12	1	0.12	
		y3	0.2	1	0.2				y3	0.15	1	0.15			y3	0.14	1	0.14	
		y4	0.22	1	0.22				y4	0.14	1	0.14			y4	0.14	1	0.14	
		y5	0.21	1	0.21				y5	0.12	1	0.12			y5	0.12	1	0.12	
	T2	y2	0.12	1	0.12	0.84		T2	y2	0.11	1	0.11	1	T2	y2	0.11	1	0.11	0.74
		y2	0.08	1	0.08				y3	0.15	1	0.15			y3	0.14	1	0.14	
		y3	0.13	1	0.13				y4	0.11	1	0.11			y4	0.14	1	0.14	
		y4	0.15	1	0.15				y5	0.08	1	0.08			y5	0.1	1	0.1	
		y5	0.11	1	0.11				y7	0.13	1	0.13			y7	0.13	0	0	
	T3	y2	0.15	1	0.15	0.85		T3	y2	0.09	1	0.09	1	T3	y2	0.15	1	0.15	0.82
		y3	0.17	1	0.17				y3	0.1	1	0.1			y3	0.13	0	0	
		y4	0.15	1	0.15				y4	0.11	1	0.11			y4	0.13	1	0.13	
		y5	0.17	1	0.17				y5	0.11	1	0.11			y5	0.08	1	0.08	
		y6	0.15	0	0				y7	0.09	1	0.09			y8	0.16	1	0.16	
	T4	y1	0.12	1	0.12	1		T4	y1	0.07	1	0.07	1	T4	y1	0.09	0	0	0.81
		y2	0.08	1	0.08				y2	0.1	1	0.1			y2	0.09	0	0	
		y3	0.15	1	0.15				y3	0.11	1	0.11			y3	0.12	1	0.12	
		y4	0.15	1	0.15				y4	0.12	1	0.12			y4	0.13	1	0.13	
		y5	0.1	1	0.1				y5	0.11	1	0.11			y5	0.14	1	0.14	
Step 3	T1	y1	0.15	1	0.15	0.93	Step 3	T1	y1	0.07	0	0	0.92	T1	y1	0.07	1	0.07	0.79
		y2	0.15	1	0.15				y2	0.02	1	0.02			y2	0.07	1	0.07	
		y3	0.17	1	0.17				y3	0.1	1	0.1			y3	0.12	1	0.12	
		y4	0.15	1	0.15				y4	0.11	1	0.11			y4	0.13	1	0.13	
		y5	0.16	1	0.16				y5	0.12	1	0.12			y5	0.14	1	0.14	
	T2	y2	0.07	1	0.07	0.92		T2	y2	0.04	1	0.04	1	T2	y2	0.13	1	0.13	0.8
		y3	0.17	1	0.17				y3	0.11	1	0.11			y3	0.13	1	0.13	
		y4	0.15	1	0.15				y4	0.12	1	0.12			y4	0.13	1	0.13	
		y5	0.16	1	0.16				y5	0.11	1	0.11			y5	0.14	1	0.14	
		y6	0.15	0	0				y7	0.08	1	0.08			y6	0.14	1	0.14	
	T3	y1	0.12	1	0.12	0.92		T3	y1	0.08	0	0	1	T3	y1	0.08	1	0.08	0.78
		y2	0.08	1	0.08				y2	0.03	1	0.03			y2	0.11	1	0.11	
		y3	0.15	1	0.15				y3	0.11	1	0.11			y3	0.11	1	0.11	
		y4	0.15	1	0.15				y4	0.13	1	0.13			y4	0.13	1	0.13	
		y5	0.1	1	0.1				y5	0.1	1	0.1			y5	0.13	1	0.13	
	T4	y2	0.12	1	0.12	0.93		T4	y2	0.11	1	0.11	1	T4	y2	0.13	1	0.13	0.87
		y3	0.17	1	0.17				y3	0.11	1	0.11			y3	0.13	1	0.13	
		y4	0.15	1	0.15				y4	0.11	1	0.11			y4	0.13	1	0.13	
		y5	0.16	1	0.16				y5	0.13	1	0.13			y5	0.11	1	0.11	
		y6	0.15	0	0				y7	0.11	1	0.11			y6	0.13	0	0	
T5	y1	0.08	1	0.08	0.92	T5	y1	0.08	0	0	1	T5	y1	0.07	1	0.07	0.78		
	y2	0.03	1	0.03			y2	0.03	1	0.03			y2	0.07	1	0.07			
	y3	0.11	1	0.11			y3	0.11	1	0.11			y3	0.13	1	0.13			
	y4	0.13	1	0.13			y4	0.13	1	0.13			y4	0.13	1	0.13			
	y5	0.1	1	0.1			y5	0.1	1	0.1			y5	0.14	1	0.14			
T6	y2	0.12	1	0.12	0.92	T6	y2	0.11	1	0.11	1	T6	y2	0.14	1	0.14	0.8		
	y3	0.17	1	0.17			y3	0.11	1	0.11			y3	0.14	1	0.14			
	y4	0.15	1	0.15			y4	0.11	1	0.11			y4	0.14	1	0.14			
	y5	0.16	1	0.16			y5	0.11	1	0.11			y5	0.14	1	0.14			
	y6	0.15	0	0			y7	0.11	1	0.11			y6	0.14	1	0.14			
T7	y1	0.08	0	0	0.92	T7	y1	0.08	0	0	1	T7	y1	0.08	0	0	0.78		
	y2	0.03	1	0.03			y2	0.03	1	0.03			y2	0.11	1	0.11			
	y3	0.11	1	0.11			y3	0.11	1	0.11			y3	0.11	1	0.11			
	y4	0.13	1	0.13			y4	0.13	1	0.13			y4	0.13	1	0.13			
	y5	0.1	1	0.1			y5	0.13	1	0.13			y5	0.14	1	0.14			
T8	y2	0.12	1	0.12	0.92	T8	y2	0.11	1	0.11	1	T8	y2	0.14	1	0.14	0.8		
	y3	0.17	1	0.17			y3	0.11	1	0.11			y3	0.14	1	0.14			
	y4	0.15	1	0.15			y4	0.11	1	0.11			y4	0.14	1	0.14			
	y5	0.16	1	0.16			y5	0.11	1	0.11			y5	0.14	1	0.14			
	y6	0.15	0	0			y7	0.11	1	0.11			y6	0.14	1	0.14			
T9	y1	0.05	1	0.05	0.92	T9	y1	0.05	1	0.05	1	T9	y1	0.07	1	0.07	0.78		
	y2	0.06	1	0.06			y2	0.06	1	0.06			y2	0.11	1	0.11			
	y3	0.12	1	0.12			y3	0.12	1	0.12			y3	0.11	1	0.11			
	y4	0.12	1	0.12			y4	0.12	1	0.12			y4	0.13	1	0.13			
	y5	0.13	1	0.13			y5	0.13	1	0.13			y5	0.13	1	0.13			
T10	y6	0.13	1	0.13	0.92	T10	y6	0.13	1	0.13	1	T10	y6	0.13	1	0.13	0.87		
	y7	0.06	1	0.06			y7	0.06	1	0.06			y7	0.13	1	0.13			
	y8	0.06	1	0.06			y8	0.06	1	0.06			y8	0.13	1	0.13			
	y9	0.07	1	0.07			y9	0.07	1	0.07			y9	0.13	1	0.13			
	y10	0.07	1	0.07			y10	0.07	1	0.07			y10	0.13	1	0.13			
T11	y1	0.07	1	0.07	0.92	T11	y1	0.07	1	0.07	1	T11	y1	0.07	1	0.07	0.87		
	y2	0.12	1	0.12			y2	0.12	1	0.12			y2	0.07	1	0.07			
	y3	0.17	1	0.17			y3	0.12	1	0.12			y3	0.07	1	0.07			
	y4	0.15	1	0.15			y4	0.12	1	0.12			y4	0.07	1	0.07			
	y5	0.16	1	0.16			y5	0.12	1	0.12			y5	0.07	1	0.07			
T12	y6	0.13	1	0.13	0.92	T12	y6	0.13	1	0.13	1	T12	y6	0.13	1	0.13	0.87		
	y7	0.06	1	0.06			y7	0.13	1	0.13			y7	0.07	1	0.07			
	y8	0.06	1	0.06			y8	0.13	1	0.13			y8	0.07	1	0.07			
	y9	0.07	1	0.07			y9	0.13	1	0.13			y9	0.07	1	0.07			
	y10	0.07	1	0.07			y10	0.13	1	0.13			y10	0.07	1	0.07			
T13	y1	0.04	1	0.04	0.92	T13	y1	0.04	1	0.04	1	T13	y1	0.07	1	0.07	0.87		
	y2	0.06	1	0.06			y2	0.06	1	0.06			y2	0.07	1	0.07			
	y3	0.12	1	0.12			y3	0.12	1	0.12			y3	0.07	1	0.07			
	y4	0.14	1	0.14			y4	0.14	1	0.14			y4	0.07	1	0.07			
	y5	0.11	1	0.11			y5	0.11	1	0.11			y5	0.07	1	0.07			
T14	y7	0.1	1	0.1	0.92	T14	y7	0.1	1	0.1	1	T14	y7	0.13	0	0	0.87		
	y8	0.08	1	0.08			y8	0.1	1	0.1			y8	0.13	0	0			
	y9	0.08	1	0.08			y9	0.14	1	0.14			y9	0.13	0	0			
	y10	0.14	1	0.14			y10	0.14	1	0.14			y10	0.13	0	0			
	y11	0.1	1	0.1			y11	0.1	1	0.1			y11	0.13	0	0			
T15	y2	0.14	1	0.14	0.92	T15	y2	0.14	1	0.14	1	T15	y2	0.1	1	0.1	0.87		
	y3	0.1	1	0.1			y3	0.14	1	0.14			y3	0.1	1	0.1			
	y4	0.08	1	0.08			y4	0.1	1	0.1			y4	0.1	1	0.1			
	y5	0.14	1	0.14			y5	0.1	1	0.1			y5	0.1	1	0.1			
	y6	0.1	1	0.1			y6	0.11	1	0.11			y6	0.1	1	0.1			

Subject ID 17

Figure F.2 (continued) : Calculation details of performance score for cargo operation tasks.

APPENDIX G: Coordinates of the ROC Curves of Developed Officer Performance Model



Figure G.1 : Coordinates of the ROC curves for navigation tasks (a) and cargo operation tasks (b).

APPENDIX H: Data Collected During the Study

Participant ID	Step No	Task No	Time Interval	Performance result (safe/risky)	Performance score (1-100)	Task loading (1-10)	NASA_TLX score	HRV																							
								Time-based							Frequency-based Welch periodogram							Frequency-based Lomb-Scargle periodogram									
								meanHR	SDNN	RMSSD	pNNx	HRVTI	TINN	aLF	aHF	aTotal	pLF	pHF	nLF	nHF	LFHF	peakLF	peakHF	aLF	aHF	aTotal	pLF				
								(bpm)	(ms)	(ms)	(%)	(ms)	(ms)	(ms ²)	(ms ²)	(ms ²)	(%)	(%)	(%)	(%)		(Hz)	(Hz)	(ms ²)	(ms ²)	(ms ²)	(%)				
1	1	1	0-70	Safe	100	3	13.67	79.4	41.2	23.7	2.2	7.1	30.5	204.54	149.13	356.36	57.4	41.8	0.578	0.422	1.372	0.1	0.37	0.039	0.035	0.074	52.8				
		2	70-270	Safe	100	4		73.1	41.2	34.6	11.7	11.4	162.8	483.8	283.03	842.37	57.4	33.6	0.631	0.369	1.709	0.08	0.38	0.038	0.019	0.059	64.7				
		3	270-720	Safe	89	4		75.6	52.2	35.8	14.1	6.9	102.1	790.59	372.29	1224.32	64.6	30.4	0.68	0.32	2.124	0.09	0.35	0.023	0.018	0.042	55.1				
		4	720-870	Safe	100	2		70.8	48.5	43.8	26.6	6.4	102.5	435.33	401.78	887.37	49.1	45.3	0.52	0.48	1.084	0.07	0.38	0.025	0.028	0.054	46.3				
		5	870-1045	Safe	100	2		70.6	49.3	42.1	25.2	11.3	179.4	518.42	452.73	1016.45	51	44.5	0.534	0.466	1.145	0.11	0.16	0.033	0.023	0.058	57				
	2	1	0-180	Safe	100	4	25.67	96.3	48.1	21.6	1.7	14.4	204.3	454.34	215.57	709.68	64	30.4	0.678	0.322	2.108	0.13	0.37	0.032	0.015	0.047	67.3				
		2	180-300	Safe	100	4		85.2	36.5	23.4	3.6	7.6	91.6	417.26	129.67	601.64	69.4	21.6	0.763	0.237	3.218	0.07	0.28	0.031	0.009	0.041	75.9				
		3	300-360	Safe	100	6		84	42.2	26.4	10	10.1	112.3	116.68	112	248.47	47	45.1	0.51	0.49	1.042	0.06	0.17	0.023	0.021	0.045	50.3				
		4	360-660	Safe	100	4		87.4	55.7	27.4	7.4	11.1	202.1	489.81	300.22	828.5	59.1	36.2	0.62	0.38	1.632	0.09	0.32	0.029	0.018	0.048	61.3				
		5	660-900	Safe	100	3		87.2	70.3	28.5	7.1	14.2	272.5	588.89	222.87	856.7	68.7	26	0.725	0.275	2.642	0.08	0.22	0.017	0.005	0.022	76.7				
	3	3	1	900-1108	Safe	100	5	39.33	83.7	34.3	27.4	5.9	9.3	122.1	380.27	234.82	655.84	58	35.8	0.618	0.382	1.619	0.12	0.33	0.037	0.03	0.068	54.3			
			2	1108-1200	Safe	60	6		85.4	38.3	28	8.3	7.7	82	203.06	581.83	789.93	25.7	73.7	0.259	0.741	0.349	0.15	0.19	0.013	0.036	0.049	26.3			
		4	1	0-60	Safe	94	8		79.1	49.2	33.6	14.5	8	124.5	930.59	383.5	1378.22	67.5	27.8	0.708	0.292	2.427	0.1	0.16	0.031	0.008	0.04	78.3			
			2	60-360	Risky	53	8		77.9	39.9	32.5	13	7.8	99.6	939.64	726.42	1693.33	55.5	42.9	0.564	0.436	1.294	0.15	0.32	0.038	0.022	0.059	63.5			
		5	1	420-540	Safe	86	6		80.7	38.1	28.7	6.3	9.4	133.4	540.52	274.94	864.53	62.5	31.8	0.663	0.337	1.966	0.09	0.22	0.043	0.019	0.064	66.8			
			2	540-870	Safe	100	7		84	51.2	27.7	8.3	7.9	132.8	787.87	387.85	1261.02	62.5	30.8	0.67	0.33	2.031	0.08	0.17	0.035	0.017	0.054	64.4			
		4	6	1	870-1104	Safe	88		7	87.7	42.4	21.7	2.1	11	164.1	441.23	200.49	708.72	62.3	28.3	0.688	0.312	2.201	0.06	0.33	0.028	0.01	0.04	71.6		
				2	1104-1200	Safe	100		8	94.8	20.2	18.1	0.8	6.1	5.9	38.11	26.84	67.3	56.6	39.9	0.587	0.413	1.42	0.11	0.25	0.034	0.03	0.064	52.2		
			7	1	0-90	Safe	82		9	91.2	29.1	21.6	1.7	7.7	78.1	158.93	92.8	264.56	60.1	35.1	0.631	0.369	1.713	0.09	0.24	0.036	0.025	0.062	58.4		
				2	90-330	Risky	57		7	86.2	47.9	30.3	7.6	11.4	181.6	597.61	431.44	1105.67	54	39	0.581	0.419	1.385	0.07	0.27	0.033	0.02	0.054	61.1		
			8	1	330-510	Safe	48		10	86.7	33	24.8	5.6	8.4	85.4	238.52	305.75	561.96	42.4	54.4	0.438	0.562	0.78	0.1	0.19	0.012	0.019	0.031	39.7		
				2	510-720	Risky	86		9	81.5	36.9	30.1	9.3	9.6	102.1	650.67	351.78	1021.21	63.7	34.4	0.649	0.351	1.85	0.12	0.28	0.027	0.02	0.047	57.6		
			9	1	720-840	Safe	86		9	82.8	34.2	26.2	4.4	8	101.6	795.18	222.34	1141.82	69.6	19.5	0.781	0.219	3.576	0.07	0.36	0.026	0.028	0.058	45.6		
				2	840-960	Safe	100		9	85.1	42.5	27.1	6.6	10.7	177.2	444.67	311.33	790	56.3	39.4	0.588	0.412	1.428	0.12	0.23	0.029	0.02	0.05	59.2		
			10	1	960-1200	Safe	100		8	81.8	50.1	31.3	9.6	13	209.5	751.7	524.39	1328.79	56.6	39.5	0.589	0.411	1.433	0.09	0.17	0.033	0.021	0.054	60.2		
				2	1200-1401	Safe	100		3	89.5	55.6	28.3	6.9	8.1	156.3	1397.77	318.32	1815.65	77	17.5	0.815	0.185	4.391	0.09	0.29	0.026	0.01	0.038	69.6		
			2	1	1	0-300	Safe		100	3	24.33	89.6	50.4	28.4	4.8	11.1	183.1	1583	400.2	2078.13	76.2	19.3	0.798	0.202	3.955	0.08	0.25	0.03	0.01	0.04	75
					2	300-430	Safe		100	4		89.7	35.1	20.1	1	8.5	85.9	546.64	163.68	720.23	75.9	22.7	0.77	0.23	3.34	0.1	0.3	0.024	0.012	0.036	67.1
3	430-570				Safe	100	4	94.2	41.2	18.6		1.6	10.4	157.2	931.62	132.24	1128.45	82.6	11.7	0.876	0.124	7.045	0.09	0.2	0.018	0.003	0.021	87.1			
4	570-780				Safe	100	2	90.3	44.2	23.8		4.8	10.7	148.7	979.26	202.89	1251.27	78.3	16.2	0.828	0.172	4.826	0.09	0.34	0.044	0.007	0.051	86.5			
5	780-1030	Safe			100	2	84	64.6	38	16.5		6.9	256.3	2384.79	523.69	3142.12	75.9	16.7	0.82	0.18	4.554	0.09	0.32	0.022	0.004	0.027	81.4				
2	1	0-80		Safe	78	4	89.6	54.5	27.1	8.7	11.6	164.1	871.06	378.22	1305.97	66.7	29	0.697	0.303	2.303	0.11	0.32	0.032	0.013	0.046	70					
	2	80-160		Safe	71	4	88.3	50.9	32.7	12.8	14.8	225.6	1235.35	411.62	1722.65	71.7	23.9	0.75	0.25	3.001	0.09	0.33	0.034	0.03	0.064	52.4					
	3	160-360		Safe	47	6	86.4	51.8	37.3	8.8	9.4	144.5	1533.55	616.72	2276.93	67.4	27.1	0.713	0.287	2.487	0.1	0.2	0.037	0.013	0.05	73.9					
	4	360-480		Safe	48	4	86.1	44.4	31.5	10.5	9.8	153.1	661.15	395.64	1128.72	58.6	35.1	0.626	0.374	1.671	0.09	0.32	0.029	0.01	0.039	73.8					
	5	480-800		Safe	80	3	87	47.7	34.6	10.8	7.8	145.3	969.83	495.52	1507.75	64.3	32.9	0.662	0.338	1.957	0.1	0.32	0.031	0.018	0.05	62.6					
3	1	800-1109		Safe	100	5	94.3	51.3	31.4	8.3	10.3	175.8	1223.72	494.13	1837.79	66.6	26.9	0.712	0.288	2.477	0.11	0.37	0.035	0.017	0.052	66.3					
	2	1109-1200		Safe	94	8	88.8	48	30.3	8.7	12.4	193.4	749.25	388.54	1193.95	62.8	32.5	0.659	0.341	1.928	0.11	0.34	0.033	0.009	0.043	78					
	3	1200-1380		Risky	53	8	95.1	48.4	28.2	3.3	13.1	184.1	883.82	363.5	1281.96	68.9	28.4	0.709	0.291	2.431	0.1	0.32	0.041	0.019	0.06	68.2					
	4	1380-1680		Risky	58	6	93.9	43.2	23.5	2.2	8.9	134.5	855.71	231.69	1109.13	77.2	20.9	0.787	0.213	3.693	0.1	0.34	0.022	0.004	0.026	84.4					
	5	1680-1902		Risky	45	9	94.7	53.4	31.5	5.2	9.2	171.4	1199.68	503.95	1751.34	68.5	28.8	0.704	0.296	2.381	0.1	0.27	0.044	0.013	0.057	77.4					
4	5	1		840-1160	Safe	80	7	78.67	94.5	50.4	25.1	5.1	13.4	217.5	1190.49	358.75	1642.74	72.5	21.8	0.768	0.232	3.318	0.09	0.29	0.028	0.007	0.035	80			
		2		1160-1200	Safe	100	8		90.7	54.5	33.1	10.7	6.8	123.8	1115.63	526.32	1706.95	65.4	30.8	0.679	0.321	2.12	0.1	0.23	0.033	0.016	0.049	67.1			
	6	1		0-360	Safe	100	9		90.1	56.5	36.8	13.5	9	144.5	1767.12	492.75	2297.24	76.9	21.4	0.782	0.218	3.586	0.1	0.35	0.021	0.005	0.026	79.7			
		2		360-540	Safe	100	9		90.3	49.8	29.3	5.6	10	92	1371.59	317.46	1720.75	79.7	18.4	0.812	0.188	4.321	0.11	0.38	0.04	0.013	0.053	74.9			
	7	1		540-600	Safe	83	7		91	42.6	26.1	5.6	11.9	187.5	524.56	268.42	816.69	64.2	32.9	0.662	0.338	1.954	0.11	0.35	0.026	0.017	0.043	59.9			
		2		600-1200	Safe	50	10		88	52.9	37.1	10.9	7.8	114.3	1452.78	763.27	2268.33	64	33.6	0.656	0.344	1.903	0.1	0.31	0.027	0.014	0.042	65.4			
	8	1		1200-1380	Safe	75	9		90.7	51.8	32.3	10.1	6.6	127	1208.33	555.82	1803.34	67	30.8	0.685	0.315	2.174	0.1	0.24							

HRV																								
Frequency-based						Non-linear						Time-frequency						Time-frequency						
Lomb-Scargle periodogram												Lomb-Scargle periodogram						Wavelet transform						
pHF	nLF	nHF	LFHF	peakLF	peakHF	SD1	SD2	sampen	alpha1	alpha2	aLF	aHF	aTotal	pLF	pHF	nLF	nHF	LFHF	peakLF	peakHF	aLF	aHF	aTotal	pLF
(%)	(%)	(%)	(Hz)	(Hz)	(ms)	(ms)					(ms ²)	(ms ²)	(ms ²)	(%)	(%)	(%)	(%)		(Hz)	(Hz)	(ms ²)	(ms ²)	(ms ²)	(%)
46.9	0.674	0.47	1.126	0.1	0.18	16.8	55.8	2.075	1.028	1.326	6.52	4.93	11.53	56.5	42.8	0.569	0.431	1.321	0.1	0.38	915.97	732.71	1649.99	55.5
31.3	0.674	0.326	2.066	0.08	0.37	24.5	52.9	2.661	1.162	0.986	11.63	9.1	22.84	50.9	39.8	0.561	0.439	1.278	0.08	0.24	2561.36	1311.67	3923.11	65.3
43.1	0.561	0.439	1.278	0.1	0.27	25.3	69.4	1.559	1.257	0.834	24.96	13.4	39.92	62.5	33.6	0.651	0.349	1.863	0.09	0.34	4341.48	1995.96	6363.84	68.2
52.4	0.469	0.531	0.884	0.09	0.18	31.1	61.1	2.767	0.923	0.814	14.55	15.34	30.78	47.3	49.8	0.487	0.513	0.949	0.08	0.38	2793.56	1999.93	4820.42	58
39.2	0.593	0.407	1.454	0.09	0.36	29.8	63	2.667	1.201	1.107	14.53	16	31.99	45.4	50	0.476	0.524	0.908	0.14	0.28	2604.09	2439.09	5077.31	51.3
32.2	0.676	0.324	2.091	0.14	0.18	15.3	66.3	2.159	1.647	0.982	15.85	7.62	24.32	65.2	31.3	0.675	0.325	2.079	0.13	0.2	2581.64	1105.31	3695.69	69.9
22.4	0.772	0.228	3.383	0.06	0.21	16.6	48.9	2.327	1.329	1.114	10.83	4.8	17.01	63.6	28.2	0.693	0.307	2.258	0.06	0.19	2145.68	875.09	3044.87	70.5
45.8	0.523	0.477	1.096	0.1	0.17	18.8	56.7	2.358	0.964	1.305	3.2	3.34	6.97	45.9	47.9	0.489	0.511	0.958	0.08	0.17	603.92	517.09	1129.75	53.5
38.2	0.616	0.384	1.606	0.09	0.21	19.4	76.3	1.362	1.262	1.023	14.92	10.12	26.02	57.3	38.9	0.596	0.404	1.474	0.08	0.21	2728.82	1726.47	4469.44	61.1
22.2	0.776	0.224	3.463	0.09	0.23	20.2	97.3	1.376	1.449	1.063	18.83	9.07	29.31	64.2	30.9	0.675	0.325	2.077	0.09	0.17	3535.59	1347.1	4903.41	72.1
44.6	0.549	0.451	1.216	0.1	0.2	19.4	44.5	2.292	1.344	0.704	10.54	8.73	20.39	51.7	42.8	0.547	0.453	1.207	0.09	0.19	2089.32	1432.94	3543.68	59
73.6	0.263	0.737	0.358	0.11	0.19	19.9	50.4	2.669	1.065	0.973	6.32	17.88	24.29	26	73.6	0.261	0.739	0.354	0.11	0.2	933.17	2773	3706.47	25.2
20.5	0.793	0.207	3.823	0.09	0.17	23.8	65.4	2.629	1.42	0.836	27.27	12.5	41.91	65.1	29.8	0.686	0.314	2.181	0.11	0.21	5069.99	2199.9	7308.74	69.4
36.5	0.635	0.365	1.741	0.14	0.2	23.1	51.5	2.337	1.583	0.326	27.92	21.42	50.05	55.8	42.8	0.566	0.434	1.303	0.14	0.25	3795.83	3159.34	6956.24	54.6
29.9	0.691	0.309	2.237	0.08	0.24	20.3	49.8	2.511	1.348	0.744	15.96	8.32	25.84	61.8	32.2	0.657	0.343	1.919	0.07	0.19	2716.45	1291.03	4041.19	67.2
31.2	0.673	0.327	2.063	0.1	0.22	19.6	69.7	2.477	1.426	0.925	26.06	13.45	41.56	62.7	32.4	0.66	0.34	1.937	0.07	0.18	4619.69	2097.29	6752.62	68.4
24	0.749	0.251	2.979	0.11	0.22	15.4	57.9	2.33	1.385	1.014	13.93	6.93	22.47	62	30.8	0.668	0.332	2.011	0.11	0.17	2585.98	1146.4	3764.77	68.7
47.1	0.526	0.474	1.108	0.11	0.37	12.8	25.6	2.217	0.839	1.21	1.38	1.04	2.47	55.9	42.2	0.57	0.43	1.323	0.11	0.2	205.9	189.28	396.24	52
40.6	0.59	0.41	1.437	0.14	0.26	15.3	38.3	2.205	1	1.002	5.1	3.02	8.35	61.1	36.2	0.628	0.372	1.69	0.11	0.24	843.31	509.46	1355.85	62.2
37.5	0.619	0.381	1.628	0.07	0.28	21.5	64.3	2.429	1.317	0.753	18.63	15.51	37.16	50.1	41.7	0.546	0.454	1.201	0.07	0.2	3907.69	2408.84	6355.58	61.5
59.6	0.4	0.6	0.667	0.1	0.2	17.6	43.2	2.224	1.182	0.851	7.12	10.59	18.32	38.9	57.8	0.402	0.598	0.672	0.1	0.19	1297.63	1912.98	3219.19	40.3
42.1	0.578	0.422	1.368	0.13	0.17	21.3	47.6	2.351	1.477	0.65	19.73	12.27	32.72	60.3	37.5	0.617	0.383	1.608	0.13	0.27	2954.27	2116.57	5073.4	58.2
48.3	0.486	0.514	0.944	0.06	0.2	18.6	44.7	2.37	1.143	0.641	11.75	12.73	26.13	45	48.7	0.48	0.52	0.923	0.05	0.2	4167.99	1243.02	5516.1	75.6
39.4	0.6	0.4	1.501	0.07	0.17	19.2	56.9	2.387	1.285	0.907	14.79	10.9	26.79	55.2	40.7	0.576	0.424	1.358	0.08	0.17	2413.98	1794.98	4225.35	57.1
39.2	0.605	0.395	1.534	0.11	0.18	22.2	67.2	2.946	1.209	0.803	22.25	17.38	40.76	54.6	42.6	0.561	0.439	1.28	0.08	0.17	3780.91	2794.81	6593.97	57.3
27.7	0.715	0.285	2.511	0.08	0.29	20	76	1.132	1.368	0.763	40.4	12.21	54.59	74	22.4	0.768	0.232	3.309	0.09	0.2	7483.76	1994.82	9527.33	78.6
24.9	0.751	0.249	3.017	0.08	0.26	20.2	68.4	2.352	1.462	0.65	40.93	16.08	58.6	69.8	27.4	0.718	0.282	2.544	0.08	0.24	8179.03	1954.17	10155.81	80.5
32.6	0.673	0.327	2.061	0.11	0.29	14.3	47.6	1.961	1.568	0.753	13.28	7.3	20.76	64	35.2	0.645	0.355	1.818	0.1	0.23	2504.99	857.11	3364.44	74.5
12.6	0.873	0.127	6.895	0.1	0.2	13.2	56.8	1.971	1.794	0.769	27.96	6.3	35.11	79.6	17.9	0.816	0.184	4.44	0.09	0.21	5052.41	752.96	5818.01	86.8
13.3	0.866	0.134	6.484	0.09	0.22	16.9	60.2	2.294	1.564	0.628	27.97	6.65	36.32	77	18.3	0.808	0.192	4.204	0.09	0.34	5378.26	1037.18	6424.65	83.7
15.5	0.84	0.16	5.249	0.09	0.3	27	87.3	1.553	1.494	0.865	79.11	19.54	103.93	76.1	18.8	0.802	0.198	4.05	0.09	0.18	13617.55	2825.13	16524.68	82.4
29	0.707	0.293	2.412	0.11	0.18	19.2	74.6	1.243	1.566	1.131	18.46	9.59	29.29	63	32.7	0.658	0.342	1.924	0.1	0.31	4456.12	1705.06	6185.85	72
46.3	0.531	0.469	1.132	0.06	0.32	23.2	68.2	2.542	1.43	0.816	33.69	15.21	50	67.4	30.4	0.689	0.311	2.215	0.09	0.18	6789.31	2236.56	9042.03	75.1
25.8	0.741	0.259	2.865	0.1	0.19	26.5	68.3	2.35	1.364	0.859	47.85	19.67	69.78	68.6	28.2	0.709	0.291	2.432	0.1	0.19	7032.41	2753.84	9794.42	71.8
25.4	0.744	0.256	2.906	0.1	0.32	22.3	58.6	2.432	1.152	0.825	18.69	15.28	35	53.4	43.7	0.55	0.45	1.223	0.1	0.32	3917.91	2193.3	6144.37	63.8
37.2	0.628	0.372	1.685	0.07	0.25	24.5	62.9	2.559	1.265	0.76	26.84	17.16	44.85	59.8	38.3	0.61	0.39	1.564	0.09	0.32	4609.87	2583.78	7200.25	64
32.2	0.673	0.327	2.062	0.11	0.17	22.2	69.1	2.49	1.483	0.524	39.07	18.27	60.01	65.1	30.4	0.681	0.319	2.138	0.12	0.17	7238.11	2676.62	10006.68	72.3
21.8	0.781	0.219	3.571	0.12	0.35	21.5	64.4	2.432	1.56	0.887	20.57	12.31	33.19	62	37.1	0.626	0.374	1.671	0.12	0.35	5022.4	2209.3	7250.76	69.3
30.9	0.688	0.312	2.21	0.12	0.32	20	65.5	2.406	1.196	0.977	28.54	13.46	42.73	66.8	31.5	0.68	0.32	2.12	0.09	0.22	4438.83	1900.23	6354.45	69.9
15.4	0.846	0.154	5.477	0.11	0.2	16.7	58.7	2.2	1.579	0.704	23.9	7.01	31.79	75.2	22	0.773	0.227	3.412	0.1	0.19	4581.98	1185.09	5772.83	79.4
22.4	0.775	0.225	3.45	0.12	0.26	22.3	72.2	1.388	1.449	0.73	37.04	17.16	55.36	66.9	31	0.683	0.317	2.158	0.09	0.26	6458.95	2850.89	9316.94	69.3
19.7	0.802	0.198	4.055	0.09	0.3	17.7	69.1	2.3	1.465	0.934	29.87	12.46	43.49	68.7	28.6	0.706	0.294	2.398	0.09	0.17	6024.9	1848.64	7895.88	76.3
31.9	0.678	0.322	2.103	0.08	0.23	23.4	73.4	1.359	1.376	0.71	32.73	15.93	50.57	64.7	31.5	0.673	0.327	2.054	0.12	0.21	6588.29	2997.24	9605.59	68.6
20.2	0.798	0.202	3.943	0.1	0.36	26.1	75.5	1.362	1.409	0.549	51.3	15.7	68.86	74.5	22.8	0.766	0.234	3.267	0.1	0.35	8808.61	2709.3	11520.27	76.5
23.8	0.759	0.241	3.148	0.1	0.21	20.8	67.3	2.767	1.447	0.788	45.69	12.38	59.04	77.4	21	0.787	0.213	3.692	0.11	0.2	5485.81	1594.48	7094.36	77.3
39.6	0.602	0.398	1.511	0.11	0.34	18.4	57.3	2.366	1.339	0.931	16.3	9.38	26.51	61.5	35.4	0.635	0.365	1.737	0.12	0.36	2997.51	1422.85	4427.94	67.7
34.4	0.655	0.345	1.9	0.09	0.27	26.3	70.1	1.467	1.32	0.66	42.14	19.34	62.56	67.4	30.9	0.685	0.315	2.179	0.1	0.26	6921.27	3704.25	10634.28	65.1
38.5	0.615	0.385	1.599	0.1	0.23	22.9	69.5	2.538	1.285	0.706	38.82	16.49	56.23	69	29.3	0.702	0.298	2.354	0.1	0.24	6556.3	3		

HRV										EDA										Eye									
Time-frequency Wavelet transform										Continuous decomposition analysis										Trough-to-peak analysis					Pupil diameter			Blink frequency	
pHF	nLF	nHF	LFHF	peakLF	peakHF	CDA.nSCR frequency	CDA.Amp Sum [µs]	CDA.Amp Sum [µs]	CDA.SCR (avg.) [µs]	CDA.SCR (max.) [µs]	CDA.ISCR (avg.) [µs]	CDA.ISCR (max.) [µs]	CDA.Phasic Max (avg.) [µs]	CDA.Phasic Max (max.) [µs]	CDA.Tonic (avg.) [µs]	CDA.Tonic (max.) [µs]	TTP.nSCR frequency	TTP.Amps um (avg.) [µs]	TTP.Amps um (max.) [µs]	Global. Mean (avg.) [µs]	Global. Mean (max.) [µs]	mean	std	PerLPD	freq	AEC5	PERCLOS		
(%)	(%)	(%)	(%)	(Hz)	(Hz)																								
44.4	0.556	0.444	1.25	0.09	0.38	0.085714	0.124948	0.275153	0.02726	0.059687	0.654251	1.432492	0.761189	1.2675588	1.868926	2.103187	0.071429	0.153465	0.280204	2.103641	2.411333	30.6381	2.8569	-0.0053	0.2286	0.2581	0.059		
33.4	0.661	0.339	1.953	0.05	0.38	0	0	0	0.000233	0.000233	0.005604	0.005604	0.025695	0.025695	0.895126	0.895126	0	0	0	0.900927	0.900927	31.0181	2.8685	0.0071	0.21	0.3088	0.0649		
31.4	0.685	0.315	2.175	0.09	0.36	0.035556	0.047508	0.13486	0.009794	0.030904	0.235058	0.741699	0.2425756	0.486144	1.166494	1.319026	0.044444	0.067389	0.395154	1.206844	1.386347	30.6229	3.2098	-0.0058	0.3133	0.4189	0.1313		
41.5	0.583	0.417	1.397	0.07	0.38	0	0	0	0.000255	0.000597	0.006132	0.014325	0.010337	0.042345	0.791912	0.804431	0	0	0	0.796413	0.807115	30.8083	2.6364	0.0003	0.34	0.4843	0.1647		
48	0.516	0.484	1.068	0.11	0.38	0.011429	0.013702	0.014486	0.001863	0.002099	0.044717	0.050387	0.0307422	0.0308993	0.718624	0.727401	0.011429	0.013616	0.014761	0.730149	0.740229	28.622	3.3363	-0.0707	0.3086	0.5258	0.1623		
29.9	0.7	0.3	2.336	0.06	0.15	0.05	0.057992	0.101245	0.016202	0.025609	0.388848	0.614617	0.3311539	0.4241999	2.858867	3.09798	0.072222	0.119711	0.28409	2.996895	3.218673	29.8732	2.3673	-0.3001	0.485	0.3156	0.142		
28.7	0.71	0.29	2.452	0.06	0.15	0	0	0	0	0	0	0	0	0	0	0	0	0	0	0	0	31.24	2.6502	0.1043	0.3917	1.983	0.0777		
45.8	0.539	0.461	1.168	0.05	0.17	0.066667	0.076412	0.14031	0.021334	0.033164	0.512027	0.795928	0.3392081	0.4987477	2.6929	2.710995	0.05	0.060039	0.133357	2.748232	2.792636	30.3545	2.4534	-0.0145	0.2833	0.8104	0.2296		
38.6	0.612	0.388	1.581	0.07	0.15	0.03	0.071907	0.14376	0.021129	0.044169	0.507099	1.060044	0.4282594	0.6902714	2.683155	2.82431	0.036667	0.149829	0.844669	2.684197	3.021169	30.0888	2.5453	-0.2331	0.3667	0.3037	0.1114		
27.5	0.724	0.276	2.625	0.09	0.15	0.05	0.079263	0.379972	0.018923	0.056989	0.454146	1.367744	0.5455043	2.4291097	3.228086	3.723736	0.054167	0.130129	0.52441	3.323168	3.844291	32.9476	3.6415	0.0697	0.3708	0.4286	0.159		
40.4	0.593	0.407	1.458	0.05	0.15	0.033654	0.072627	0.170337	0.025386	0.042542	0.609262	1.021012	0.4327914	0.6142424	2.725359	3.009309	0.091346	0.079013	0.308539	2.918271	3.257107	34.3453	2.8239	0.1151	0.3462	0.4803	0.1662		
74.8	0.252	0.748	0.337	0.09	0.19	0.05	0.129274	0.201454	0.032356	0.057583	0.776535	1.381985	0.8852109	1.3163062	2.423383	2.459202	0.05	0.166124	0.347269	2.631484	2.866029	32.1231	2.7085	0.043	0.3	0.2292	0.0687		
30.1	0.697	0.303	2.305	0.1	0.15	0.006667	0.041933	0.041933	0.019707	0.019707	0.472975	0.472975	0.2058393	0.2058393	2.140429	2.140429	0.013333	0.041811	0.074011	1.321272	2.746368	31.7984	3.3299	0.0324	0.2933	0.4606	0.1351		
45.4	0.546	0.454	1.201	0.14	0.15	0	0	0	0.00019	0.00019	0.004551	0.004551	0.0181468	0.0181468	1.821998	1.821998	0	0	0	1.824307	1.824307	29.5486	3.3041	-0.0406	0.25	0.6109	0.1527		
31.9	0.678	0.322	2.104	0.07	0.23	0.016667	0.13316	0.255211	0.049136	0.089825	1.179265	2.155796	0.7301279	1.3409224	1.692175	1.733231	0.016667	0.206626	0.376233	1.750484	1.753446	32.0422	2.756	0.0403	0.25	0.799	0.1997		
31.1	0.688	0.312	2.203	0.06	0.15	0.024242	0.080845	0.364545	0.018452	0.074015	0.442845	1.776361	0.3106268	1.172131	1.962616	2.11133	0.033333	0.114235	0.620717	1.973222	2.306882	29.826	2.8108	-0.0316	0.3091	0.338	0.1045		
30.5	0.693	0.307	2.256	0.05	0.15	0.017094	0.228335	0.635715	0.050033	0.135533	1.200793	3.252796	0.6862566	1.7513028	1.841928	1.890003	0.021368	0.170999	0.746777	1.894781	2.112048	29.7994	2.6407	-0.0325	0.3248	0.4175	0.1356		
47.8	0.521	0.479	1.088	0.11	0.18	0.133333	0.120066	0.420844	0.039116	0.115009	0.938785	2.760211	1.0839396	2.807792	3.310859	3.430828	0.088889	0.125137	0.377687	3.523605	3.924248	30.1287	2.1139	-0.0218	0.3111	0.4877	0.1517		
37.6	0.623	0.377	1.655	0.06	0.24	0.033333	0.116522	0.192485	0.041373	0.061146	0.992942	1.467499	0.6975574	0.9386215	3.359623	3.567173	0.070833	0.148405	0.512123	3.440304	3.827913	32.4965	2.7582	0.0551	0.2833	0.407	0.1153		
37.9	0.619	0.381	1.622	0.06	0.15	0.016667	0.123204	0.215808	0.037863	0.063985	0.908702	1.53564	0.6183676	1.015729	3.236833	3.281453	0.044444	0.096355	0.23296	3.233918	3.405013	33.677	3.0917	0.0394	0.3934	0.4444	0.1217		
59.4	0.404	0.596	0.678	0.09	0.19	0.028571	0.121595	0.374501	0.043899	0.124926	1.053855	2.998227	0.6144226	1.5389089	2.650186	2.836902	0.019048	0.161305	0.463287	2.716496	2.933534	31.6951	2.6848	0.0291	0.3	0.394	0.1182		
41.7	0.583	0.417	1.396	0.12	0.27	0	0	0	0.011246	0.011246	0.269907	0.269907	0.3280888	0.3280888	2.412815	2.412815	0.008333	0.049715	0.049715	2.447673	2.447673	31.181	2.5751	0.0124	0.4	0.3261	0.1304		
22.5	0.77	0.23	3.353	0.06	0.15	0	0	0	0.001039	0.001039	0.024931	0.024931	0.0094703	0.0094703	2.117721	2.117721	0	0	0	1.25765	1.25765	30.7151	2.1635	-0.0028	0	0	0		
42.5	0.574	0.426	1.345	0.07	0.15	0.054167	0.194984	0.418737	0.068659	0.111745	1.647807	2.681873	1.0198602	1.8565185	2.364119	2.80342	0.0375	0.348545	0.592837	2.488401	3.155397	30.0989	2.3325	-0.0228	0.3542	0.608	0.1278		
42.4	0.575	0.425	1.353	0.08	0.16	0.024876	0.141868	0.359605	0.033241	0.078324	0.797779	1.879778	0.7274022	1.8686146	2.534857	2.764465	0.029851	0.096991	0.419729	2.676488	2.942406	30.3636	2.4037	-0.0142	0.3383	0.6879	0.2327		
20.9	0.79	0.21	3.752	0.09	0.27	0.09	0.147474	0.787869	0.026232	0.08887	0.629559	2.613291	0.6565688	2.7422868	2.571803	2.920773	0.1	0.166489	0.753976	2.786429	3.336371	35.1428	3.6824	0.0701	0.06	0.3084	0.0185		
19.2	0.807	0.193	4.185	0.08	0.25	0.115385	0.23828	0.579427	0.041528	0.079475	0.996662	1.907408	1.121609	2.0520893	3.283337	3.567878	0.130769	0.232973	0.615154	3.58627	4.04401	36.9961	3.9094	0.1174	0.1692	0.7946	0.1345		
25.5	0.745	0.255	2.923	0.1	0.3	0.042857	0.083877	0.139645	0.019385	0.029105	0.465236	0.698531	0.5439978	1.02433	2.837504	3.230767	0.078571	0.084973	0.17279	2.963498	3.492876	32.8396	3.893	0.0000	0.1143	0.5985	0.0684		
12.9	0.87	0.13	6.71	0.09	0.18	0.142857	0.248083	0.975291	0.035598	0.132004	0.854354	3.168096	0.8825283	2.5696964	3.130888	3.550816	0.12381	0.220131	0.839993	3.367145	3.962069	32.2109	3.6667	-0.0192	0.2857	0.4153	0.1187		
16.1	0.838	0.162	5.185	0.09	0.33	0.05	0.267478	0.61397	0.059448	0.143679	1.426763	3.448287	1.20602	2.5620314	2.957921	3.89185	0.072	0.257282	0.779705	3.274899	4.137716	30.4265	3.8413	-0.0735	0.128	0.2283	0.0292		
17.1	0.828	0.172	4.82	0.09	0.31	0.05	0.14503	0.33406	0.033023	0.056448	0.792543	1.354762	1.2094963	1.8774907	3.621917	3.859775	0.0875	0.194974	0.50909	3.747176	4.21477	33.6194	3.3452	0.0237	0.0375	0.1939	0.0048		
27.6	0.723	0.277	2.613	0.11	0.32	0.0625	0.252922	0.569104	0.073961	0.107904	1.775604	2.589691	1.8721892	3.5084577	3.240096	3.478913	0.075	0.349082	0.852309	3.771207	4.472701	31.849	3.6931	-0.0302	0.125	0.8046	0.1006		
24.7	0.752	0.248	3.036	0.09	0.32	0.08	0.352467	0.943612	0.064433	0.18787	1.546399	4.508876	1.507061	2.837208	3.63325	3.860929	0.11	0.258673	1.005892	3.861902	4.483336	33.1622	4.1124	0.0098	0.15	0.197	0.0296		
28.1	0.719	0.281	2.554	0.1	0.19	0.108333	0.361205	0.77269	0.053249	0.100758	1.277985	2.418186	1.4476864	2.454887	4.001787	4.25497	0.1	0.309862	0.640068	4.339085	4.851835	31.765	4.235	-0.0327	0.1833	0.1994	0.0366		
35.7	0.641	0.359	1.786	0.1	0.31	0.103125	0.220794	1.54581	0.044044	0.218956	1.057059	2.549933	0.9450041	3.5987963	3.476133	3.778935	0.09375	0.189287	1.212541	3.705129	4.256839	29.6459	3.6892	-0.0973	0.1531	0.2003	0.0307		
35.9	0.641	0.359	1.784	0.09	0.31	0.106796	0.230098	1.122225	0.041637	0.173991	0.999299	4.175788	0.9053271	2.8775662	3.892523	4.198759	0.132686	0.252354	1.15553	4.158649	4.836134	31.2965	4.069	-0.0					

Participant ID	Step No	Task No	Time interval	Performance result (safe/risky)	Performance score (1-100)	Task loading (1-10)	NASA_TLX score	HRV																			
								Time-based								Frequency-based Welch periodogram						Frequency-based Lomb-Scargle periodogram					
								meanHR	SDNN	RMSSD	pNNx	HRVTi	TINN	aLF	aHF	aTotal	pLF	pHF	nLF	nHF	LFHF	peakLF	peakHF	aLF	aHF	aTotal	pLF
								(bpm)	(ms)	(ms)	(%)	(ms)	(ms)	(ms ²)	(ms ²)	(ms ²)	(%)	(%)	(%)	(%)	(Hz)	(Hz)	(ms ²)	(ms ²)	(ms ²)	(%)	
1	1	1	0-300	Safe	100	3	0	100.8	49.1	26.8	5.9	10.7	190.9	776.58	439.07	1247.85	2.6	35.2	0.639	0.361	1.769	0.1	0.33	0.034	0.014	0.049	70.1
		2	300-420	Safe	100	4		100.6	65.6	30.3	8.1	7.7	68.4	1660.41	503.68	2210.75	75.1	22.8	0.767	0.233	3.297	0.09	0.36	0.031	0.007	0.038	81.3
		3	420-600	Safe	100	4		97.5	38.8	30.5	7	8.7	129.9	424.36	404.3	840	50.5	48.1	0.512	0.488	1.05	0.11	0.16	0.023	0.025	0.048	47.3
		4	600-720	Safe	100	2		98	38.2	31.9	11.8	9.4	128.2	339.34	394.92	773.35	43.9	51.1	0.462	0.538	0.859	0.08	0.27	0.031	0.027	0.058	53.6
		5	720-1114	Safe	100	2		94.2	42.6	32.9	10.4	10.9	166.5	425.64	516.95	956.81	44.5	54	0.452	0.548	0.823	0.14	0.27	0.017	0.036	0.053	32.5
	2	1	0-65	Safe	100	4		96.3	61.2	41.6	21.1	10.7	161.1	928.14	710.77	1667.42	55.7	42.6	0.566	0.434	1.306	0.08	0.28	0.03	0.015	0.046	66.6
		2	65-140	Safe	80	4		89.8	57.3	49.1	33.3	8	124.5	1215.66	882.8	2131.4	57	41.4	0.579	0.421	1.377	0.13	0.23	0.027	0.018	0.045	59
		3	140-360	Safe	79	6		92.6	58.8	39.7	19.7	7.4	133.3	903.38	679.98	1643.47	55	41.4	0.571	0.429	1.329	0.14	0.16	0.042	0.027	0.069	60.1
		4	360-480	Safe	75	4		91.3	49.8	33.9	11.8	12.8	203.1	294.22	617.89	930.43	31.6	66.4	0.323	0.677	0.476	0.09	0.2	0.025	0.051	0.077	33.2
		5	480-800	Safe	80	3		91.4	52.2	35.8	13.9	8.7	162.6	979.1	462.64	1490.92	65.7	31	0.679	0.321	2.116	0.09	0.26	0.036	0.02	0.057	64
		6	800-1128	Safe	74	5		92.1	47.7	33.1	10.9	10.3	156.3	941.35	490.91	1519.38	62	32.3	0.657	0.343	1.918	0.11	0.19	0.033	0.016	0.049	66.3
	3	1	0-130	Safe	86	6		95.9	63.8	34	13.2	9.8	200.2	1055.66	662.79	1772.07	59.6	37.4	0.614	0.386	1.593	0.13	0.36	0.04	0.017	0.057	70.5
			2	130-300	Safe	73		8	91.8	50.3	34.6	14	13.6	204.3	1041.55	724.63	1825.49	57.1	39.7	0.59	0.41	1.437	0.08	0.35	0.036	0.028	0.064
		3	300-420	Safe	65	8		93.1	60.3	37.7	17.4	11.9	203.1	1492.68	565.32	2206.27	67.7	25.6	0.725	0.275	2.64	0.11	0.16	0.032	0.021	0.054	59.8
			4	420-540	Safe	100		6	94.8	65.3	40.1	18.9	10.3	189.7	1239.26	939.11	2234.63	55.5	42	0.569	0.431	1.32	0.1	0.28	0.038	0.018	0.056
		5	540-840	Safe	100	7		92.8	62.8	36.6	14.2	10.6	230.2	1656.85	787.45	2543.48	65.1	31	0.678	0.322	2.104	0.08	0.3	0.03	0.023	0.053	57
			6	840-1126	Safe	81		7	88.8	62.2	34.5	12.3	9.5	215.3	1658.84	638.27	2361.87	70.2	27	0.722	0.278	2.599	0.11	0.16	0.022	0.007	0.03
		1	0-360	Safe	70	8		95.4	55.8	34	14.2	7.9	123	1055.56	638.74	1737.14	60.8	36.8	0.623	0.377	1.653	0.09	0.22	0.034	0.016	0.05	67.6
			2	360-540	Safe	100		9	102.1	52.6	26.7	7.3	13.8	207.5	399.03	467.48	882.23	45.2	53	0.46	0.54	0.854	0.11	0.18	0.029	0.041	0.07
	4	3	540-720	Safe	100	7		100.6	53.4	29.1	8.8	17.4	249.8	1218.69	368.53	1638.88	74.4	22.5	0.768	0.232	3.307	0.09	0.33	0.038	0.011	0.05	76.4
4			720-1130	Risky	25	10	99.3	50.3	28.3	7.2	16.8	210.9	952.86	490.95	1522.16	62.6	32.3	0.66	0.34	1.941	0.08	0.28	0.029	0.008	0.038	77.1	
5		1130-1380	Risky	38	9	102.8	49.6	28.8	6.5	13.9	233.6	1044.89	440.18	1535.82	68	28.7	0.704	0.296	2.374	0.1	0.28	0.018	0.004	0.022	82.1		
		6	1380-1590	Risky	38	9	99.9	51.9	31.6	9.6	10.8	205.1	1062.9	501.56	1614.04	65.9	31.1	0.679	0.321	2.119	0.1	0.33	0.04	0.021	0.061	65.4	
7		1590-2040	Safe	86	9	99.9	56.1	28.9	6.7	7.3	129.9	1382.06	515.59	1957.55	70.6	26.3	0.728	0.272	2.681	0.11	0.16	0.034	0.01	0.044	77.1		
		8	2040-2280	Risky	20	8	94.3	62	35.3	12.6	11.6	213.6	2117.66	670.43	2861.65	74	23.4	0.76	0.24	3.159	0.1	0.16	0.041	0.014	0.054	74.6	
1		1	0-380	Safe	100	3	75.1	55	30.9	8.2	7.1	117.2	1535.89	211.93	1854.75	82.8	11.4	0.879	0.121	7.247	0.09	0.29	0.031	0.005	0.039	80.4	
			2	380-510	Safe	100	4	75.7	58	29.8	8.6	12.5	234.6	1506.21	194.3	1880.3	80.1	10.3	0.886	0.114	7.752	0.09	0.25	0.036	0.005	0.045	81.2
	3		510-680	Safe	100	4	77.8	52.9	25.6	4.3	7.4	170.2	970.93	210.57	1231.67	78.8	17.1	0.822	0.178	4.611	0.09	0.16	0.034	0.01	0.045	76.7	
	4		680-780	Safe	78	2	79.3	78.2	32.3	7.6	9.2	142.8	2089.28	258.58	2748.38	76	9.4	0.89	0.11	8.08	0.06	0.16	0.036	0.004	0.042	87	
	5		780-1021	Safe	87	2	79.7	70.1	30	8.1	7.6	195.3	1984.22	225.96	2580.66	76.9	8.8	0.898	0.102	8.781	0.07	0.16	0.023	0.003	0.026	87.6	
	2	1	0-240	Safe	100	4	78.1	63.1	28.2	6.3	11.1	180.7	1182.78	219.77	1491.5	79.3	14.7	0.843	0.157	5.382	0.11	0.22	0.025	0.003	0.029	87.5	
		2	240-345	Safe	100	4	75.5	53	28.2	5.4	8.1	107.9	1581.4	235.51	1962.58	80.6	12	0.87	0.13	6.715	0.09	0.26	0.026	0.003	0.03	86.2	
		3	345-480	Safe	100	6	77.1	38.9	23	4.7	8.7	76.2	1121.35	110.64	1276.63	87.8	8.7	0.91	0.09	10.136	0.11	0.26	0.017	0.001	0.018	92.1	
	3	4	480-720	Safe	86	4	78.3	55.3	24.3	3.5	9.7	190.4	1660.03	186.44	1997.44	83.1	9.3	0.899	0.101	8.904	0.09	0.16	0.027	0.002	0.03	90	
		5	720-810	Safe	100	3	78.3	43.4	26.8	4.5	8.6	113.3	1383.51	233.02	1758.06	78.7	13.3	0.856	0.144	5.937	0.13	0.24	0.035	0.006	0.041	84.3	
		6	810-1027	Safe	100	5	77.1	67.9	35	8.3	11.5	205.1	1524.1	351.96	2092.31	72.8	16.8	0.812	0.188	4.33	0.1	0.37	0.039	0.01	0.052	74.6	
		1	0-240	Safe	55	6	81.1	69.6	30.4	8.4	7.5	164.1	1230.65	208.91	1589	77.4	13.1	0.855	0.145	5.891	0.1	0.27	0.025	0.002	0.029	89.1	
2		240-340	Safe	84	8	74.5	66.3	39.3	14.8	7.8	115.5	1586.78	370.85	2009.47	79	18.5	0.811	0.189	4.279	0.11	0.16	0.031	0.004	0.035	88.7		
4	3	340-420	Safe	75	8	73.8	60.1	24.5	5.2	14	227.1	1310.72	155.83	1530.87	85.6	10.2	0.894	0.106	8.411	0.09	0.22	0.023	0.003	0.026	86.7		
	4	420-540	Safe	100	6	75.3	53	28.8	7.7	11.9	196.8	1101.36	256.6	1460.05	75.4	17.6	0.811	0.189	4.292	0.1	0.18	0.035	0.011	0.048	72		
	5	540-780	Safe	100	7	74	63.5	30.3	7.8	14.8	278.3	1314.95	266.01	1765.85	74.5	15.1	0.832	0.168	4.943	0.09	0.31	0.051	0.011	0.066	77.3		
	6	780-1103	Risky	50	7	74	65.5	30.5	8.5	11	215.3	1320.3	286.26	1797.57	73.4	15.9	0.822	0.178	4.612	0.1	0.38	0.024	0.004	0.031	78.9		
	1	0-360	Safe	100	8	74.1	73.8	35.2	12.6	12	317.4	2641.37	294.99	3308.89	79.8	8.9	0.9	0.1	8.954	0.1	0.33	0.019	0.002	0.021	88.8		
4	2	360-570	Safe	63	9	71.6	57	38	14.6	9.5	167	1229.71	468.74	2053.31	59.9	22.8	0.724	0.276	2.623	0.05	0.21	0.025	0.009	0.038	63.9		
		3	570-960	Risky	40	7	70.9	67.4	34.4	13.3	12.3	293.9	1982.76	350.67	2510.82	79	14	0.85	0.15	5.654	0.09	0.27	0.033	0.007	0.043	78.2	
	4	960-1080	Safe	52	10	73	59.4	35	10.4	13.6	232.4	2108.67	193.38	2608.15	80.8	7.4	0.916	0.084	10.904	0.09	0.25	0.026	0.002	0.03	85.2		
	5	1080-1260	Safe	52	9	75.4	69.9	34.9	14	11.6	256.3	2622.35	353.47	3188.74	82.2	11.1	0.881	0.119	7.419	0.1	0.38	0.033	0.004	0.037	89.1		
	6	1260-1350	Safe	65	9	74.7	99.4	44.7	19.6	10.9	258.8	3669.88	448.22	4359.94	84.2	10.3	0.891	0.109	8.188	0.09	0.32	0.027	0.004	0.032	84.7		
	7	1350-1590	Safe	100	9	74.5	88	40.4	12.4	11.5	339.8	3155.8	432.6	4017.8	78.5	10.8	0.879	0.121	7.295	0.08	0.16	0.043	0.005	0.049	87.2		
	8	1590-1992	Safe	50	8	70.3	50.2	25	5.4	12.6	201.4	826.85	152.11	1041.49	79.4	14.6	0.845	0.155	5.436	0.1	0.28	0.021	0.003	0.025	86.8		

Figure H.1 (continued) :

HRV

Frequency-based																							Non-linear					Time-frequency										Time-frequency				
Lomb-Scargle periodogram											Lomb-Scargle periodogram												Wavelet transform																			
pHF	nLF	nHF	LFHF	peakLF	peakHF	SD1	SD2	sampen	alpha1	alpha2	aLF	aHF	aTotal	pLF	pHF	nLF	nHF	LFHF	peakLF	peakHF	aLF	aHF	aTotal	pLF																		
(%)	(%)	(%)	(Hz)	(Hz)	(ms)	(ms)	(ms)	(ms)	(ms)	(ms)	(ms ²)	(ms ²)	(ms ²)	(%)	(%)	(%)	(%)	(%)	(%)	(Hz)	(Hz)	(ms ²)	(ms ²)	(ms ²)	(%)																	
29.7	0.298	2.358	0.07	0.17	19	66.8	2.261	1.389	0.683	25.61	13.29	40.04	64	33.2	0.658	0.342	1.928	0.1	0.21	4229.65	2262.42	6498.39	65.1																			
18.5	0.814	0.186	4.383	0.08	0.19	21.5	90.2	1.411	1.541	0.816	55.33	17.3	74.16	74.6	23.3	0.762	0.238	3.199	0.08	0.36	8081.66	2866.26	10957.47	73.8																		
52.5	0.474	0.526	0.9	0.1	0.19	21.6	50.5	2.468	1.249	0.967	13.94	12.72	27	51.6	47.1	0.523	0.477	1.096	0.1	0.19	2165.1	2156.57	4324.55	50.1																		
46.2	0.537	0.463	1.16	0.1	0.21	22.6	49.1	2.601	1.07	0.713	11.92	11.63	24.18	49.3	48.1	0.506	0.494	1.025	0.09	0.2	1827.92	2005.33	3844.37	47.5																		
67.4	0.325	0.675	0.482	0.09	0.27	23.3	55.5	2.536	1.178	0.764	13.53	16.85	30.84	43.9	54.6	0.445	0.555	0.803	0.15	0.2	2292.55	2850.47	5148.08	44.5																		
33.1	0.668	0.332	2.013	0.09	0.2	29.6	81.4	1.817	1.727	0.994	30.43	22	52.6	57.9	41.8	0.58	0.42	1.384	0.09	0.2	5158.81	4130.36	9295.27	55.5																		
40.8	0.591	0.409	1.446	0.13	0.21	34.9	73.1	1.958	0.993	0.937	33.36	26.02	61.26	54.5	42.5	0.562	0.438	1.282	0.14	0.21	5137.93	4223.21	9371.19	54.8																		
39.5	0.603	0.397	1.52	0.14	0.17	28.1	78.3	1.747	1.483	0.826	28.28	21.99	51.6	54.8	42.6	0.563	0.437	1.286	0.13	0.21	5209.41	3828.53	9048.62	57.6																		
66.4	0.333	0.667	0.5	0.06	0.21	24	66.2	2.683	1.323	0.963	10.95	21.52	33.04	33.1	65.1	0.337	0.663	0.909	0.08	0.21	1558.34	3392.23	4952.08	31.5																		
35.6	0.642	0.358	1.796	0.13	0.18	25.4	69.4	1.589	1.39	0.849	29.51	15.22	45.95	64.2	33.1	0.66	0.34	1.939	0.09	0.26	5221.85	2480.11	7713.66	67.7																		
33.3	0.666	0.334	1.992	0.06	0.17	23.4	63.2	2.565	1.36	0.693	29.34	19.57	50.13	58.5	39	0.6	0.4	1.5	0.12	0.18	5224.44	2784.1	8030.85	65.1																		
29.1	0.707	0.293	2.417	0.06	0.19	24.1	86.9	1.607	1.595	1.006	37.31	21.44	60	62.2	35.7	0.635	0.365	1.74	0.12	0.19	6083.11	3479.03	9569.28	63.6																		
43.8	0.562	0.438	1.281	0.14	0.24	24.5	66.8	2.561	1.401	0.486	38.49	25.14	64.86	59.3	38.8	0.605	0.395	1.531	0.08	0.18	5652.67	4091.05	9750.87	58																		
38.6	0.608	0.392	1.551	0.13	0.19	26.7	81	1.692	1.346	0.777	42.87	23.14	69.91	61.3	33.1	0.649	0.351	1.852	0.13	0.18	8697.72	3803.22	12558.79	69.3																		
31.7	0.682	0.318	2.15	0.09	0.17	28.4	87.8	1.483	1.42	0.716	38.95	30.85	71.62	54.4	43.1	0.558	0.442	1.262	0.09	0.21	6661.05	4888.1	11565.83	57.6																		
42.6	0.572	0.428	1.338	0.09	0.19	25.9	85	1.616	1.52	0.611	53.62	24.94	81.66	65.7	30.5	0.683	0.317	2.15	0.08	0.18	9562.7	4287.74	13870.97	68.9																		
24.3	0.755	0.245	3.09	0.13	0.19	24.4	84.5	1.604	1.592	0.691	49.93	25.63	77.43	64.5	33.1	0.661	0.339	1.948	0.12	0.19	8928.79	3577.75	12522.31	71.3																		
31.9	0.679	0.321	2.116	0.09	0.25	24.1	75.2	1.555	1.393	0.762	35.73	21.31	57.86	61.8	36.8	0.626	0.374	1.677	0.09	0.21	5667.08	3547.9	9222.12	61.5																		
58.5	0.415	0.585	0.708	0.12	0.17	18.9	71.9	1.398	1.434	1.088	11.65	16.5	28.61	40.7	57.7	0.414	0.586	0.706	0.11	0.18	2156.68	2531.35	4690.43	46																		
22.7	0.771	0.229	3.363	0.09	0.17	20.6	72.7	1.421	1.513	0.714	37.41	13.91	53.23	70.3	26.1	0.729	0.271	2.69	0.08	0.17	7094.91	2400.19	9508.49	74.6																		
22.3	0.775	0.225	3.452	0.06	0.18	20	68.3	2.466	1.526	0.712	33.8	16.34	51.77	65.3	31.6	0.674	0.326	2.068	0.07	0.24	5773.17	2731.57	8523.24	67.7																		
17.8	0.822	0.178	4.623	0.1	0.2	20.4	67.1	2.434	1.436	0.72	33.54	15.48	50.25	66.7	30.8	0.684	0.316	2.167	0.1	0.2	5858.45	2681.8	8549.81	68.5																		
34.3	0.656	0.344	1.908	0.11	0.19	22.4	69.9	2.587	1.422	0.624	32.82	16.35	50.39	65.1	32.4	0.668	0.332	2.008	0.1	0.24	6053.18	3339.79	9408.44	64.3																		
22.8	0.771	0.229	3.375	0.07	0.17	20.5	76.7	1.305	1.493	0.567	43.12	17.41	61.58	70	28.3	0.712	0.288	2.477	0.1	0.19	7748.28	3146.5	10905.71	71																		
24.8	0.751	0.249	3.009	0.14	0.17	25	84	1.499	1.488	0.59	64.34	24.4	90.04	71.5	27.1	0.725	0.275	2.636	0.09	0.21	11020.21	4088.42	15119.73	72.9																		
13.5	0.856	0.144	5.959	0.08	0.17	21.9	74.7	1.353	1.595	0.701	47.64	10.23	60.5	78.7	16.9	0.823	0.177	4.656	0.09	0.18	8585.09	1332.99	10003.82	85.8																		
11	0.881	0.119	7.396	0.11	0.17	21.1	79.2	1.452	1.686	0.602	48.1	9.49	61.82	77.8	15.3	0.835	0.165	5.071	0.09	0.24	8329.7	1234.45	9770.42	85.3																		
21.7	0.78	0.22	3.537	0.08	0.17	18.1	72.6	1.292	1.41	0.757	28.44	7.21	36.95	77	19.5	0.798	0.202	3.948	0.09	0.19	5614.42	1380.5	7005.48	80.1																		
10.6	0.891	0.109	8.193	0.06	0.25	23	108.2	1.233	1.287	1.012	55.96	12.11	75.6	74	16	0.822	0.178	4.621	0.06	0.24	11365.48	1331.85	12768	89																		
9.5	0.902	0.098	9.253	0.1	0.21	21.2	96.8	1.308	1.558	0.812	66.22	9.37	83.81	79	11.2	0.876	0.124	7.066	0.09	0.21	13803.14	1509.84	15622.65	88.4																		
10.6	0.892	0.108	8.241	0.11	0.18	20	86.9	1.271	1.58	1.048	37.71	8.09	49.11	76.8	16.5	0.823	0.177	4.661	0.11	0.21	6693	1140.71	7873.21	85																		
11.5	0.882	0.118	7.485	0.1	0.17	20	72.2	1.304	1.736	0.705	44.1	6.14	52.23	84.4	11.8	0.878	0.122	7.183	0.09	0.27	8133.86	1240.09	9432.54	86.2																		
7	0.929	0.071	13.123	0.11	0.26	16.3	52.6	2.194	1.77	0.48	38.03	4.82	43.76	86.9	11	0.888	0.112	7.897	0.11	0.19	5618.49	720.66	6355.16	88.4																		
8	0.918	0.082	11.2	0.09	0.21	17.2	76.3	1.196	1.627	0.668	54.33	7.57	66.21	82.1	11.4	0.878	0.122	7.178	0.09	0.22	9112.19	978.8	10191.92	89.4																		
14.9	0.85	0.15	5.661	0.13	0.21	19	58.4	2.328	1.468	0.659	42.94	7.95	55.77	77	14.3	0.844	0.156	5.4	0.12	0.31	6951.09	1503.15	8503.36	81.7																		
19.1	0.796	0.204	3.903	0.1	0.19	24.8	92.7	1.484	1.366	1.015	54.01	15.21	75.21	71.8	20.2	0.78	0.22	3.552	0.1	0.24	9330.88	2135.13	11626.54	80.3																		
7.2	0.926	0.074	12.437	0.11	0.18	21.5	96.1	1.288	1.719	1.258	37.81	7.21	49.64	76.2	14.5	0.84	0.16	5.242	0.1	0.26	7961.72	1265.65	9352.69	85.1																		
10.7	0.893	0.107	8.324	0.09	0.18	27.9	89.5	1.551	1.552	0.476	51.66	9.45	62.51	82.6	15.1	0.845	0.155	5.466	0.09	0.21	13878.65	2311.59	16199.96	85.7																		
12.3	0.876	0.124	7.039	0.1	0.31	17.4	83.2	1.372	1.83	0.626	36.17	5.92	43.11	83.9	13.7	0.859	0.141	6.111	0.1	0.31	6082.8	927.86	7021.91	86.6																		
23.5	0.754	0.246	3.068	0.11	0.18	20.4	72.1	1.369	1.728	0.679	35.63	11.39	48.45	73.5	23.5	0.758	0.242	3.127	0.1	0.17	5657.72	1625.76	7358.23	76.9																		
16.9	0.821	0.179	4.577	0.07	0.2	21.5	87.1	1.468	1.626	0.89	38.36	10.91	55.01	69.7	19.8	0.779	0.221	3.515	0.12	0.19	7633.54	1795.81	9579.45	79.7																		
12.4	0.864	0.136	6.375	0.1	0.17	21.6	90.1	1.473	1.678	1.012	42.01	12.85	60.43	69.5	21.3	0.766	0.234	3.27	0.1	0.17	7808.72	1512.61	9526.82	82																		
10	0.899	0.101	8.895	0.09	0.26	24.9	101.4	1.596	1.519	0.706	83.6	12.09	105.12	79.5	11.5	0.874	0.126	6.916	0.1	0.23	15451.64	1659.78	17309	89.3																		
22.3	0.741	0.259	2.865	0.09	0.21	26.9	76	1.66	1.368	0.689	42.38	18.91	71.16	59.6	26.6	0.691	0.309	2.241	0.09	0.21	7543.55	2579.17	10447.56	72.2																		
17	0.821	0.179	4.592	0.08	0.18	24.3	92.1	1.6	1.551	0.76	65.25	13.51	83.59	78.1	16.2	0.828	0.172	4.829	0.09	0.22	10920.76	2015.4	13067.73	83.6																		
7	0.924	0.076	12.107	0.09	0.18	24.8	80.2	1.524	1.598	0.538	66.82	7.88	81.51	82	9.7	0.895	0.105	8.48	0.09	0.19	11465.09	1289.66	13069.33	87.7																		
10	0.899	0.101	8.936	0.1	0.25	24.7	95.7	1.684	1.703	0.689	88.13	15.55	109.2	80.7	14.2	0.85	0.15	5.668	0.1	0.21	13997.85	2237.03	16308.92	85.8																		
12.3	0.873	0.127	6.895	0.09	0.21	31.7	136.9	1.795	1.777	0.644	120.27	16.71	146.41	82.1	11.4	0.878	0.122	7.																								

HRV							EDA														Eye									
Time-frequency Wavelet transform							Continuous decomposition analysis														Trough-to-peak analysis					Pupil diameter		Blink frequency		
pHF	nLF	nHF	LFHF	peakLF	peakHF		CDA.nSCR	CDA.Amp Sum (avg.)	CDA.Amp Sum (max.)	CDA.SCR (avg.)	CDA.SCR (max.)	CDA.iSCR (avg.)	CDA.iSCR (max.)	CDA.Phasic (avg.)	CDA.Phasic (max.)	CDA.Tonic (avg.)	CDA.Tonic (max.)	TTP.nSCR um (avg.)	TTP.nSCR um (max.)	TTP.Amp um (avg.)	TTP.Amp um (max.)	Global. Mean (avg.)	Global. Mean (max.)	mean	std	PerLPD	freq	AEC5	PERCLOS	
(%)	(%)	(%)	(%)	(Hz)	(Hz)		frequency	[µS]	[µS]	[µS]	[µS]	[µSxs]	[µSxs]	[µS]	[µS]	[µS]	[µS]	frequency	S]	[m]	[m]	[µS]	[µS]							
34.8	0.652	0.348	1.87	0.1	0.15	0.036667	0.187526	0.571701	0.035259	0.131269	0.846206	3.150453	0.7206894	2.3285099	1.550396	2.271123	0.043333	0.123717	0.615399	1.641618	2.640092	47.147	3.3214	0.065	0.31	0.2286	0.0709			
26.2	0.738	0.262	2.82	0.08	0.15	0.058333	0.204026	0.419548	0.03311	0.064863	0.794637	1.556707	0.9266986	1.5669431	1.451199	1.688636	0.058333	0.247264	0.863287	1.674276	2.125715	49.718	3.9931	0.1231	0.1833	0.4157	0.0762			
49.9	0.501	0.499	1.004	0.1	0.15	0.022222	0.06595	0.07485	0.017493	0.020053	0.419824	0.481284	0.3263887	0.364899	1.01651	1.030463	0.027778	0.047611	0.07065	1.096297	1.147396	46.0632	3.4242	0.0405	0.2722	0.2319	0.0631			
52.2	0.477	0.523	0.912	0.05	0.15	0.016667	0.060216	0.060216	0.024557	0.024557	0.589378	0.589378	0.3665169	0.3665169	0.685949	0.685949	0.008333	0.060074	0.060074	0.716657	0.716657	44.2487	3.0846	-0.0005	0.3167	0.2509	0.0794			
55.4	0.446	0.554	0.804	0.14	0.27	0.007614	0.072016	0.128671	0.02152	0.037634	0.516474	0.903215	0.3375265	0.5623186	0.502907	0.509284	0.010152	0.054007	0.147632	0.535713	0.565024	44.2639	3.631	-0.0001	0.2538	0.2438	0.0619			
44.4	0.555	0.445	1.249	0.14	0.15	0	0	0	0.005275	0.005275	0.126591	0.126591	0.1850232	0.1850232	1.358721	1.358721	0.015385	0.029431	0.029431	1.441746	1.441746	45.9669	2.1029	0.0383	0.2462	0.213	0.0524			
45.1	0.549	0.451	1.217	0.13	0.21	0.026667	0.074862	0.074862	0.02838	0.02838	0.681115	0.681115	0.7777761	0.7777761	0.926708	0.926708	0.026667	0.082652	0.108561	1.026613	1.068894	42.6297	4.4288	-0.0371	0.28	0.3052	0.0854			
42.3	0.576	0.424	1.361	0.13	0.15																	40.863	4.1072	-0.077	0.25	0.2361	0.059			
68.5	0.315	0.685	0.459	0.06	0.21	0.004545	0.016799	0.016799	0.02879	0.02879	0.690965	0.690965	0.7230638	0.7230638	1.198549	1.198549	0.004545	0.323833	0.323833	1.227819	1.227819	41.0946	3.9818	-0.0717	0.3	0.2344	0.0703			
32.2	0.678	0.322	2.105	0.09	0.26	0.0125	0.223052	0.396155	0.066261	0.119671	1.590266	2.872103	1.7538983	0.892642	0.978434	0.009375	0.19209	0.513879	1.055407	1.217401	39.132	3.769	-0.1161	0.3031	0.2269	0.0688				
34.7	0.652	0.348	1.877	0.06	0.15	0.009146	0.124267	0.218113	0.053396	0.096156	1.281508	2.307747	0.6350288	1.1365996	0.706407	0.707119	0.009146	0.324051	0.533304	0.725623	0.808101	41.4045	3.1716	-0.0647	0.2896	0.2141	0.062			
36.4	0.636	0.364	1.749	0.12	0.15																	47.1313	3.5063	0.0646	0.2462	0.2111	0.052			
42	0.58	0.42	1.382	0.07	0.15	0.023529	0.049509	0.059924	0.015608	0.02236	0.374586	0.560642	0.2171212	0.266917	0.958132	0.998289	0.023529	0.05516	0.104195	1.007071	1.117028	47.0153	2.8694	0.062	0.2176	0.2115	0.046			
30.3	0.696	0.304	2.287	0.05	0.15	0.041667	0.055555	0.074212	0.014124	0.021211	0.338971	0.509294	0.3669445	0.6536569	0.905192	0.924043	0.038912	0.056082	0.128102	0.952488	1.022231	47.074	4.2466	0.0633	0.2417	0.2145	0.018			
42.3	0.577	0.423	1.363	0.09	0.15	0.025	0.040755	0.072487	0.011978	0.018433	0.287464	0.442394	0.2746284	0.4845368	0.848268	0.867551	0.033333	0.043089	0.090699	0.877556	0.925419	46.2504	2.9725	0.0447	0.2333	0.2108	0.0492			
30.9	0.69	0.31	2.23	0.08	0.15	0.02	0.096628	0.164363	0.020606	0.033805	0.494542	0.811322	0.2936504	0.4435161	0.84679	0.970321	0.016667	0.114771	0.407452	0.839155	1.0502	45.0198	4.4201	0.0169	0.21	0.2121	0.0445			
28.6	0.714	0.286	2.496	0.11	0.15	0.027972	0.044497	0.092589	0.011264	0.022784	0.27033	0.546819	0.1941532	0.5064813	0.658554	0.772884	0.024476	0.074318	0.22457	0.674665	0.88958	42.1743	4.5572	-0.0473	0.2238	0.2118	0.0474			
38.5	0.615	0.385	1.597	0.09	0.15	0.022222	0.151924	0.661631	0.028741	0.119583	0.689795	2.869984	0.4327078	1.697476	1.287854	1.545556	0.016667	0.109926	0.559479	1.377237	1.818073	44.7659	3.9285	0.0112	0.2083	0.2583	0.0538			
54	0.46	0.54	0.852	0.11	0.17	0.027778	0.105225	0.266061	0.016231	0.003614	0.389539	0.885948	0.2441973	0.4115381	0.779454	0.873289	0.022222	0.132283	0.278634	0.836941	1.01994	43.5724	3.6339	-0.0158	0.1722	0.2144	0.0669			
25.2	0.747	0.253	2.956	0.09	0.15	0.011111	0.011623	0.013228	0.022121	0.002309	0.050970	0.055412	0.0239221	0.0256992	0.738464	0.757419	0.016667	0.011389	0.011743	0.780236	0.846125			0.2333	0.2005	0.0468				
32	0.679	0.321	2.113	0.06	0.15	0.026829	0.028305	0.090872	0.008445	0.017762	0.202681	0.42628	0.2847094	0.6311256	0.721788	0.78179	0.031707	0.042521	0.187547	0.737327	0.820419			0.2366	0.1988	0.047				
31.4	0.686	0.314	2.185	0.1	0.15	0.072	0.083878	0.254396	0.018596	0.046016	0.446312	1.104395	0.3659209	0.8895821	1.058093	1.287225	0.076	0.083044	0.289148	1.132507	1.408548	46.0543	2.9403	0.0403	0.196	0.1923	0.0377			
35.5	0.644	0.356	1.812	0.1	0.15	0.033333	0.026862	0.083398	0.006286	0.015758	0.150862	0.378199	0.1190959	0.2711883	0.919325	0.959459	0.052381	0.029806	0.096954	0.978098	1.087433	44.5199	2.8337	0.0056	0.2143	0.198	0.0424			
28.9	0.711	0.289	2.463	0.1	0.15	0.044444	0.080283	0.224831	0.016581	0.046051	0.397939	1.105213	0.3390004	0.970377	0.905523	1.048989	0.037778	0.083395	0.395021	0.955387	1.164786	44.0352	3.3526	-0.0053	0.2378	0.2102	0.05			
27	0.729	0.271	2.695	0.09	0.15	0.038961	0.067742	0.214205	0.013008	0.041281	0.312202	0.990747	0.3490724	1.1782638	0.939919	1.099691	0.046753	0.077156	0.346606	0.992215	1.286672	43.7475	3.57	-0.0118	0.2958	0.2037	0.0603			
13.3	0.866	0.134	6.44	0.09	0.15	0.168421	0.188385	0.689571	0.02378	0.091708	0.570713	2.200999	0.7347668	1.733721	3.900019	4.085417	0.207895	0.186228	0.57773	4.112857	4.562935	22.0578	2.3972	-0.0334	0.25	0.1959	0.049			
12.6	0.871	0.129	6.748	0.09	0.15	0.184615	0.164318	0.625584	0.022024	0.070438	0.52857	1.690522	0.624193	1.8393165	3.81745	4.083411	0.207692	0.125833	0.449196	3.984754	4.381343	20.2505	1.8886	-0.1126	0.2385	0.1804	0.043			
19.7	0.803	0.197	4.067	0.09	0.15	0.135294	0.244722	0.93384	0.029389	0.143575	0.705329	3.44581	0.7140469	2.5585375	3.782704	4.015636	0.164706	0.196305	0.958906	3.95712	4.480659	20.7137	2.1197	-0.0923	0.2118	0.2121	0.0449			
10.4	0.895	0.105	8.534	0.06	0.27	0.13	0.23502	0.62588	0.032496	0.056603	0.779897	1.358466	0.8637193	1.8205673	3.71444	3.87255	0.18	0.16948	0.64297	3.898061	4.154448	22.826	1.8398	0.0003	0.42	0.2357	0.099			
9.7	0.901	0.099	9.142	0.04	0.15	0.120332	0.219054	0.762953	0.030386	0.120369	0.729254	2.888847	0.7266879	2.0516096	3.644189	3.951619	0.141079	0.181143	0.824914	3.871162	4.52176	20.9122	1.9059	-0.0836	0.2365	0.337	0.0797			
14.5	0.854	0.146	5.867	0.11	0.22	0.15	0.232214	0.86626	0.031826	0.104944	0.763818	2.518646	1.0547185	2.8813974	4.104435	4.251399	0.195833	0.253796	0.859943	4.387804	4.961749	23.0027	2.3788	0.008	0.2458	0.2843	0.0699			
13.1	0.868	0.132	6.559	0.09	0.15	0.152381	0.206316	0.761515	0.024213	0.070838	0.581119	1.700108	0.5779337	1.5222344	4.062571	4.351033	0.219048	0.14795	0.774455	4.252028	4.906017	23.2797	2.4662	0.0201	0.2857	0.2037	0.0582			
11.3	0.886	0.114	7.996	0.11	0.26																	22.5832	1.8838	-0.0104	0.2519	0.1972	0.0497			
9.6	0.903	0.097	9.31	0.09	0.15	0.170833	0.130004	0.592277	0.021224	0.08476	0.509381	2.034234	0.5616387	1.6610169	3.814421	3.975789	0.1875	0.154675	0.665886	3.9919	4.422237	21.8003	1.6481	-0.0447	0.1917	0.1915	0.0367			
17.7	0.822	0.178	4.624	0.12	0.15	0.222222	0.228628	0.58637	0.032785	0.062201	0.786837	1.492819	0.8590369	1.5986739	3.964365	4.190921	0.255556	0.201872	0.519589	4.214324	4.497567	21.8169	1.5735	-0.044	0.2222	0.1763	0.0392			
18.4	0.814	0.186	4.37	0.05	0.15	0.138249	0.221943	0.860275	0.030397	0.118525	0.729524	2.844603	0.6854412	1.5208065	3.888977	4.108276	0.175115	0.19554	0.686514	4.089579	4.50948	21.8662	1.7154	-0.0418	0.2028	0.2209	0.0448			
13.5	0.863	0.137	6.291	0.1	0.15	0.095833	0.124936	0.412083	0.023069	0.072872	0.595651	1.748919	0.5063201	1.212																

Participant ID	Step No	Task No	Time interval	Performance result (safe/risky)	Performance score (1-100)	Task loading (1-10)	NASA_TLX score	HRV																									
								Time-based								Frequency-based Welch periodogram						Frequency-based Lomb-Scargle periodogram											
								meanHR	SDNN	RMSSD	pNNx	HRVTI	TINN	aLF	aHF	aTotal	pLF	pHF	nLF	nHF	LFHF	peakLF	peakHF	aLF	aHF	aTotal	pLF						
								(bpm)	(ms)	(ms)	(%)	(ms)	(ms)	(ms ²)	(ms ²)	(ms ²)	(%)	(%)	(%)	(%)	(%)	(Hz)	(Hz)	(ms ²)	(ms ²)	(ms ²)	(%)						
1	1	1	0-360	Safe	100	3	30	95.5	26.1	18.9	0.7	8.3	8.8	222.15	76.5	315.38	70.4	24.3	0.744	0.256	2.904	0.1	0.28	0.026	0.01	0.035	72.3						
		2	360-570	Safe	100	4		95.4	16.9	17	0	5.2	5.9	86.77	35.02	126.8	68.4	27.6	0.712	0.288	2.478	0.09	0.39	0.024	0.005	0.029	81.5						
		3	570-760	Safe	89	4		94.7	18.7	16.8	0	5.6	30.8	124.21	68.5	205.41	60.5	33.3	0.645	0.355	1.813	0.08	0.17	0.022	0.011	0.033	66.5						
		4	760-820	Safe	100	2		93.1	17.1	17.7	0	5.1	4.4	26.99	35.99	68.87	39.2	52.3	0.429	0.571	0.75	0.05	0.18	0.01	0.01	0.021	48.5						
	2	1	1	0-120	Safe	100	2	65.66	94.4	27.9	18.1	1	7.1	48.8	384.01	55.6	467.73	82.1	11.9	0.874	0.126	6.907	0.09	0.16	0.031	0.004	0.035	87.1					
			2	120-210	Safe	80	4		88.9	26.6	21.1	0.6	8	54	248.18	91.56	356.63	69.6	25.7	0.73	0.27	2.71	0.09	0.24	0.031	0.012	0.043	72.2					
			3	210-360	Safe	68	6		88.8	20	22.7	0	5.9	5.4	48.83	52.58	103.98	47	50.6	0.482	0.518	0.929	0.1	0.23	0.011	0.006	0.017	65.8					
			4	360-480	Safe	33	4		88.4	26.5	22	1.9	6.5	48.8	343.52	137.71	563.51	61	24.4	0.714	0.286	2.495	0.09	0.39	0.024	0.019	0.043	54.6					
		5	2	4	480-800	Safe	89	3	69.33	86.5	36.2	23.9	2.3	8.6	78.6	517.16	154.93	697.17	74.2	22.2	0.769	0.231	3.338	0.1	0.33	0.036	0.011	0.048	75.8				
				5	800-1133	Safe	72	5		86.6	38.5	22.6	3.1	11.7	175.8	525.31	144.03	727.21	72.2	19.8	0.785	0.215	3.647	0.08	0.27	0.038	0.012	0.05	76.2				
				6	1133-1320	Safe	72	5		86.4	34	23.6	2.3	10.4	123	351.33	154.15	535.44	65.6	28.8	0.695	0.305	2.279	0.09	0.38	0.032	0.017	0.05	64.4				
				7	1320-1440	Safe	46	6		85.7	30	26.7	3.9	8.5	78.9	246.69	94.68	359.63	68.6	26.3	0.723	0.277	2.605	0.08	0.28	0.031	0.011	0.042	74				
			6	3	2	90-270	Safe	71	8	95.33	89	39.3	24.6	3.4	11.5	152.6	664.1	163.26	892.55	74.4	18.3	0.803	0.197	4.068	0.07	0.32	0.021	0.004	0.025	82.6			
					3	270-420	Safe	66	8		88.5	27.9	20.5	2.3	6.7	37.1	92.19	106.26	207.44	44.4	51.2	0.465	0.535	0.868	0.07	0.35	0.031	0.039	0.07	43.9			
					4	420-540	Safe	86	6		84.2	29.2	26.6	5.5	7.5	52.7	320.73	131	477.49	67.2	27.4	0.71	0.29	2.448	0.09	0.22	0.022	0.011	0.034	65.3			
					5	540-840	Safe	72	7		85.2	28.7	23.8	1.7	8.6	96.7	240.62	148.76	422.04	57	35.2	0.618	0.382	1.617	0.07	0.31	0.025	0.015	0.04	62			
				7	4	6	840-1170	Risky	52	7	2.33	86.7	31.2	23.9	2.8	8	101.6	474.31	132.07	676.58	70.1	19.5	0.782	0.218	3.591	0.1	0.16	0.028	0.013	0.042	67.5		
						1	0-360	Safe	100	8		85.6	29.7	24.2	2	9.2	10.7	238.12	101.62	364.49	65.3	27.9	0.701	0.299	2.343	0.08	0.39	0.016	0.004	0.02	81.8		
						2	360-540	Risky	31	9		88.9	40.6	23	2.3	9.2	120.4	403.2	116.31	569.94	70.7	20.4	0.776	0.224	3.467	0.07	0.22	0.022	0.005	0.027	81.9		
						3	540-800	Risky	51	7		87.5	37.8	23.5	2.7	10.3	127.4	462.26	136.68	691.46	66.9	19.8	0.772	0.228	3.382	0.06	0.28	0.012	0.006	0.018	66.7		
					8	5	4	800-960	Risky	50	10	14.66	87	45.2	23.1	5.8	9.4	136.2	1049.02	93.19	1336.34	78.5	7	0.918	0.082	11.257	0.07	0.29	0.02	0.004	0.024	83.3	
							5	960-1320	Safe	24	9		84.5	41.1	25.7	4.1	9.2	145.3	700.85	240.04	1055.66	66.4	22.7	0.745	0.255	2.92	0.08	0.16	0.046	0.018	0.065	71	
							6	1320-1440	Safe	79	9		83.8	49.7	34.4	13.5	9.9	169.2	501.03	259.44	790.52	63.4	32.8	0.659	0.341	1.931	0.08	0.25	0.027	0.01	0.037	72.3	
							7	1440-1600	Risky	43	9		84.9	46.4	26.9	5	11	148.7	618.08	178.31	940.14	65.7	19	0.776	0.224	3.466	0.06	0.38	0.022	0.007	0.031	71.8	
						9	6	8	1600-2017	Risky	20	8	45	87.8	45.8	23.4	3.6	7.6	116.2	754.8	181.46	1043.69	72.3	17.4	0.806	0.194	4.16	0.07	0.37	0.03	0.008	0.038	79
								1	0-90	Safe	100	3		81.5	42.2	23.8	3.3	9.4	129.9	686.88	135.18	829.94	82.8	16.3	0.836	0.164	5.081	0.11	0.33	0.02	0.004	0.024	84
								2	90-270	Safe	100	4		82.7	37.6	22	3.3	10.7	97.4	682.6	226.95	965.45	70.7	23.5	0.75	0.25	3.008	0.12	0.31	0.032	0.008	0.039	80.2
								3	270-480	Safe	100	4		82.6	35.4	20	1.8	8.4	103.8	704.92	129.23	901.4	78.2	14.3	0.845	0.155	5.455	0.11	0.32	0.03	0.006	0.037	81.1
10							7	4	480-780	Safe	100	2	14.66	80.9	40	23.8	3	10.3	151.4	905.77	186.8	1140.19	79.4	16.4	0.829	0.171	4.849	0.11	0.29	0.025	0.004	0.029	87.1
								5	780-1097	Safe	100	2		80.6	36.6	21.5	1.2	10.9	146	694.15	166.12	895.84	77.5	18.5	0.807	0.193	4.178	0.11	0.31	0.027	0.003	0.031	89.3
								1	0-120	Safe	100	4		78.8	32.3	22.4	2	8.1	105.5	677.53	176.05	879.52	77	20	0.794	0.206	3.849	0.11	0.31	0.015	0.004	0.019	78.6
								2	120-240	Safe	80	4		80.2	27.8	17.7	0	6.6	48.8	329.27	128.99	477.05	69	27	0.719	0.281	2.553	0.12	0.31	0.036	0.01	0.048	75.6
	11						8	3	240-390	Safe	89	6	45	81.2	46.3	25.6	4.1	10.3	141.6	701.53	209.59	962.47	72.9	21.8	0.77	0.23	3.347	0.12	0.32	0.034	0.004	0.039	88
								4	390-540	Safe	100	4		79.5	40.9	23.1	2	7.9	102.5	708.62	208.9	990.69	71.5	21.1	0.772	0.228	3.392	0.12	0.3	0.029	0.003	0.033	88.1
								5	540-800	Safe	100	3		78.9	43	21.9	1.8	10.2	164.1	815.59	146.68	990.15	82.4	14.8	0.848	0.152	5.56	0.11	0.32	0.022	0.007	0.029	74.4
								6	800-1197	Safe	100	5		81.6	43.7	22	3	11.5	166.5	667.13	187.48	905.64	73.7	20.7	0.781	0.219	3.558	0.12	0.3	0.028	0.009	0.037	75.8
		12					9	1	0-210	Safe	49	6	69.66	80.2	58.4	30.7	9.1	8.6	314.9	920.84	405.27	1346.01	68.4	30.1	0.694	0.306	2.272	0.11	0.32	0.017	0.006	0.023	73.6
								2	210-300	Safe	77	8		74.4	36.1	32	9.3	6.8	70.3	725.2	429.88	1206.84	60.1	35.6	0.628	0.372	1.687	0.12	0.33	0.022	0.013	0.035	61.2
								3	300-420	Safe	65	8		76.2	41.9	27.3	6.1	11.5	168.5	613.18	185.19	833.89	73.5	22.2	0.768	0.232	3.311	0.12	0.33	0.038	0.011	0.05	76.3
								4	420-540	Safe	100	6		80	70	38.7	9.2	14	300.8	1928.98	449.93	2398.96	80.4	18.8	0.811	0.189	4.287	0.12	0.34	0.016	0.004	0.019	80.7
			13				10	5	540-840	Safe	72	7	69.66	80.3	61.2	27.2	6.2	9.2	140.6	854.07	232.52	1140.9	74.9	20.4	0.786	0.214	3.673	0.12	0.32	0.024	0.007	0.032	74.6
								6	840-1175	Safe	80	7		76.2	51.5	29.6	9	7.9	152.3	768.83	315.16	1127.94	68.2	27.9	0.709	0.291	2.44	0.12	0.31	0.03	0.015	0.046	64.9
								1	0-360	Safe	70	8		75.4	43.6	27.8	6.6	11.1	164.1	820.1	275.12	1147.49	71.5	24	0.749	0.251	2.981	0.11	0.31	0.032	0.011	0.043	74.5
								2	360-720	Safe	100	9		76.9	48.4	26.1	4.7	7.1	114.3	880.27	269.49	1239.03	71	21.7	0.766	0.234	3.266	0.11	0.31	0.04	0.009	0.048	81.9
				14			11	3	720-880	Safe	100	7	69.66	75.8	36.8	21.1	1	10.6	134.8	432.38	155.15	612.62	70.6	25.3	0.736	0.264	2.787	0.1	0.31	0.037	0.008	0.046	81.2
								4	880-1200	Safe	50	10		76.6	40.3	25.3	2.7	10.9	134.5	712.43	213.22	970.92	73.4	22	0.77	0.23	3.341	0.11	0.31	0.016	0.003	0.019	82.1
								5	1200-1420	Safe	77	9		78	41.7	23.3	4	8.6	131.8	697.66	160.86	878.82	79.4	18.3	0.813	0.187	4.337	0.11	0.3	0.023	0.008	0.031	72.2
								6	1420-1680	Risky	24	9		76.5	41	25.9	3.1	9.5	14.6	651.87	266.56	957.04	68.1	27.9	0.71	0.29	2.445	0.11	0.3	0.016	0.012	0.029	56.3
					15		12	7	1680-2040	Safe	72	9	69.66	78.4	53.4	26.2	5.2	8.8	171.4	884.61	236.08	1163.47	76	20.3	0.789	0.211	3.747	0.11	0.3	0.033	0.013	0.047	70.5
								8	2040-2255	Risky	42	8		77.7	38.6	26.4	3.4	11.2	151.6	598.74	196.55	826.3	72.5										

HRV																								
Frequency-based							Non-linear					Time-frequency							Time-frequency					
Lomb-Scargle periodogram												Lomb-Scargle periodogram							Wavelet transform					
pHF	nLF	nHF	LFHF	peakLF	peakHF	SD1	SD2	sampen	alpha1	alpha2	aLF	aHF	aTotal	pLF	pHF	nLF	nHF	LFHF	peakLF	peakHF	aLF	aHF	aTotal	pLF
(%)	(%)	(%)	(Hz)	(Hz)	(ms)	(ms)					(ms ²)	(ms ²)	(ms ²)	(%)	(%)	(%)	(%)	(Hz)	(Hz)	(ms ²)	(ms ²)	(ms ²)	(%)	
27.1	0.727	0.273	2.667	0.12	0.21	13.4	34.4	2.075	1.181	0.995	5.63	2.23	8.1	69.6	27.6	0.716	0.284	2.522	0.09	0.21	1290.02	435.63	1732.08	74.5
18	0.819	0.181	4.519	0.07	0.35	12.1	20.7	1.876	0.864	0.763	2.69	1.28	4.03	66.7	31.7	0.678	0.322	2.104	0.1	0.24	501.45	230.42	733.2	68.4
32.8	0.67	0.33	2.026	0.08	0.26	11.9	23.6	1.834	0.984	0.797	3.17	2.32	5.65	56.1	41.1	0.577	0.423	1.866	0.08	0.21	718.74	371.16	1093.44	65.7
50.5	0.49	0.51	0.961	0.1	0.18	12.6	20.7	1.976	0.486	0.652	0.94	1.38	2.43	38.7	57	0.405	0.595	0.68	0.13	0.35	177.94	227.52	407.38	43.7
12.7	0.873	0.127	6.859	0.07	0.21	12.8	37.3	1.961	1.423	0.703	10.21	1.91	12.72	80.3	15	0.843	0.157	5.357	0.09	0.2	1994.96	350.25	2349.45	84.9
26.9	0.729	0.271	2.689	0.09	0.36	15	34.5	2.19	0.989	1.126	7.67	2.89	10.94	70.2	26.4	0.727	0.273	2.66	0.09	0.34	1243.19	472.19	1720.22	72.3
33.5	0.663	0.337	1.964	0.12	0.36	16.1	23.3	1.98	0.506	0.62	1.7	1.35	3.09	54.9	43.7	0.557	0.443	1.256	0.07	0.36	246.72	292.95	539.97	45.7
44.5	0.551	0.449	1.225	0.07	0.22	15.6	34.1	1.894	0.889	0.849	3.34	3.9	7.34	45.5	53.1	0.461	0.539	0.857	0.09	0.33	2086.76	778.86	2896.96	72
23.6	0.763	0.237	3.217	0.08	0.21	16.9	48.2	2.252	1.418	0.841	16.38	6.59	23.26	70.4	28.3	0.713	0.287	2.486	0.08	0.17	2559.96	904.35	3469.45	73.8
23.7	0.762	0.238	3.209	0.06	0.25	16	52	2.179	1.4	0.923	14.27	4.91	20.03	71.3	24.5	0.744	0.256	2.909	0.07	0.25	2983.73	848.68	3839.61	77.7
34.6	0.65	0.35	1.86	0.11	0.19	16.7	45.1	2.336	1.175	0.922	10.94	5.34	17.05	64.2	31.3	0.672	0.328	2.048	0.09	0.22	1916.1	863.72	2794.81	68.6
24.9	0.748	0.252	2.972	0.09	0.38	19	38	2.448	0.869	0.828	6.32	3.26	9.86	64.1	33.1	0.66	0.34	1.937	0.08	0.38	1134.35	485.37	1623.92	69.9
16.2	0.836	0.164	5.084	0.07	0.17	17.5	52.8	2.273	1.529	0.812	20.82	5.98	27.63	75.4	21.6	0.777	0.223	3.482	0.07	0.18	3866.09	891.85	4775.36	81
55.7	0.441	0.559	0.788	0.12	0.17	14.5	36.7	2.086	1.155	0.943	3.23	4.49	6.92	46.6	50.5	0.48	0.52	0.924	0.07	0.34	730.59	678.76	1412.08	51.7
33.2	0.663	0.337	1.966	0.09	0.17	18.9	36.8	2.348	1.025	0.572	11.2	4.53	16.61	67.5	27.3	0.712	0.288	2.474	0.09	0.18	1878.87	854.79	2741.36	68.5
37.5	0.623	0.377	1.651	0.06	0.3	16.9	36.9	2.297	0.983	0.788	7.19	4.81	12.79	56.3	37.6	0.599	0.401	1.495	0.07	0.21	1426.07	823.56	2265.62	62.9
31.9	0.679	0.321	2.119	0.1	0.38	16.9	40.8	2.229	1.151	0.826	10.18	4.87	15.66	65	31.1	0.677	0.323	2.092	0.1	0.36	2612.74	717.35	3351.91	77.9
17.7	0.822	0.178	4.622	0.09	0.34	17.1	38.3	2.271	0.963	0.918	6.37	3.39	10.2	62.4	33.2	0.653	0.347	1.879	0.09	0.35	1342.44	577.16	1932.89	69.5
17	0.828	0.172	4.824	0.07	0.38	16.3	55.1	2.254	1.143	0.926	13.11	4.38	18.5	70.9	23.7	0.75	0.25	2.992	0.07	0.18	2499.54	710.43	3217.4	77.7
30.9	0.683	0.317	2.156	0.13	0.24	16.7	50.8	2.273	1.24	0.978	11.33	4.86	17.94	63.1	27.1	0.7	0.3	2.332	0.1	0.2	2942.66	756.98	3750.25	78.5
14.8	0.849	0.151	5.634	0.07	0.17	16.4	61.9	2.206	1.474	0.996	23.1	6.17	30.06	76.9	20.5	0.789	0.211	3.742	0.07	0.18	5979.26	532.29	6533.43	91.5
28.4	0.714	0.286	2.498	0.09	0.21	18.2	55.2	2.22	1.393	0.873	14.75	9.33	25.12	58.7	37.1	0.613	0.387	1.581	0.07	0.24	4366.14	1338.83	5727.92	76.2
27.3	0.726	0.274	2.65	0.08	0.26	24.4	65.9	2.579	1.331	1.277	13.35	7.61	21.53	62	35.4	0.637	0.363	1.753	0.08	0.26	2814.92	1304.7	4123.56	68.3
23.3	0.755	0.245	3.087	0.1	0.3	19.1	62.8	2.439	1.334	0.999	20.86	6.52	30.19	69.1	21.6	0.762	0.238	3.197	0.06	0.36	3940.31	939.58	4948.29	79.6
20.2	0.797	0.203	3.915	0.07	0.21	16.6	62.7	2.192	1.469	0.93	21.58	6.22	29.98	72	20.7	0.776	0.224	3.47	0.07	0.2	4406.65	1040.96	5480.35	80.4
15.8	0.842	0.158	5.317	0.11	0.31	16.9	57.2	2.052	1.473	0.965	22.42	5.56	28.26	79.3	19.7	0.801	0.199	4.03	0.11	0.17	4202.06	964.05	5167.95	81.3
19.2	0.807	0.193	4.175	0.13	0.31	15.6	50.8	2.155	1.548	0.774	22.4	6.47	30.11	74.4	21.5	0.776	0.224	3.461	0.12	0.31	3659.55	1255.78	4941.33	74.1
15.7	0.838	0.162	5.176	0.1	0.17	14.1	48	2.077	1.514	0.749	18.62	4.96	25.57	72.8	19.4	0.79	0.21	3.756	0.11	0.2	3803.6	759.02	4615.41	82.4
12.3	0.876	0.124	7.066	0.12	0.29	16.8	54	2.331	1.514	0.69	27.12	6.81	35.44	76.5	19.2	0.799	0.201	3.983	0.11	0.22	5041.84	1072.87	6127.92	82.3
10.3	0.897	0.103	8.682	0.12	0.31	15.2	49.4	2.298	1.452	0.728	22.78	6.1	30.01	75.9	20.3	0.789	0.211	3.736	0.12	0.31	3815.15	911.72	4747.31	80.4
20.8	0.791	0.209	3.789	0.11	0.3	15.9	42.9	2.244	1.493	0.65	17.28	5.93	23.68	73	25	0.745	0.255	2.917	0.11	0.3	3328.84	954.1	4285.23	77.6
21.8	0.776	0.224	3.472	0.11	0.31	12.5	37.2	2.043	1.414	0.677	10.66	3.96	15.09	70.6	26.3	0.729	0.271	2.689	0.11	0.32	1722.69	638.42	2374.28	72.7
10.8	0.891	0.109	8.185	0.12	0.3	18.1	62.9	2.313	1.338	0.723	25.28	7.84	34.06	74.2	23	0.763	0.237	3.226	0.12	0.32	4279.76	1330.37	5642.02	75.9
9.5	0.903	0.097	9.261	0.13	0.3	16.4	55.4	2.213	1.446	0.727	20.81	6.49	29.99	69.4	21.7	0.762	0.238	3.205	0.13	0.31	4186.92	1181.72	5408.92	77.4
23.1	0.763	0.237	3.219	0.11	0.32	15.5	58.8	2.25	1.563	0.872	25.07	5.5	31.38	79.9	17.5	0.82	0.18	4.555	0.11	0.32	4191.14	797.71	5008.73	83.7
24.1	0.759	0.241	3.145	0.12	0.18	15.6	59.7	2.128	1.499	0.837	20.1	6.5	27.76	72.4	23.4	0.756	0.244	3.094	0.12	0.31	3602.92	1011.88	4645.79	77.6
26.2	0.738	0.262	2.811	0.1	0.31	21.8	79.7	1.437	1.448	0.947	30.61	12.44	44.04	69.5	28.2	0.711	0.289	2.46	0.1	0.32	4723.15	2222.21	6955.59	67.9
36.2	0.628	0.372	1.691	0.11	0.34	22.8	45.7	2.368	1.175	0.428	18.61	12.72	32.18	57.8	39.5	0.594	0.406	1.463	0.1	0.34	3635.88	2028.91	5706.04	63.7
22.9	0.769	0.231	3.327	0.12	0.34	19.3	56	2.735	1.172	0.821	18.41	6.88	26.13	70.4	26.3	0.728	0.272	2.674	0.12	0.34	3362.58	1089.51	4467.93	75.3
18.2	0.816	0.184	4.435	0.12	0.17	27.5	95.2	1.542	1.796	0.891	72.17	17.46	90.89	79.4	19.2	0.805	0.195	4.134	0.12	0.21	9382.36	2610.73	12014.46	78.1
21.6	0.776	0.224	3.456	0.11	0.17	19.2	84.4	1.346	1.439	0.947	27.37	8.13	36.94	74.1	22	0.771	0.229	3.367	0.12	0.32	4763.43	1418.22	6214.54	76.6
31.4	0.674	0.326	2.066	0.12	0.2	21	69.7	2.384	1.428	0.786	25.32	10.72	37.13	68.2	28.9	0.703	0.297	2.363	0.12	0.19	4180.03	2005.33	6233.92	67.1
24.3	0.754	0.246	3.065	0.06	0.31	19.7	58.5	2.423	1.412	0.774	24.79	9.16	35.12	70.6	26.1	0.73	0.27	2.707	0.11	0.31	4463	1507.52	5989.46	74.5
17.7	0.822	0.178	4.623	0.09	0.21	18.5	65.8	2.423	1.439	0.931	25.9	9.15	37.37	69.3	24.5	0.739	0.261	2.832	0.1	0.31	5029.72	1366.16	6438.66	78.1
16.9	0.827	0.173	4.791	0.11	0.32	15	49.8	2.233	1.491	0.996	13.84	5.24	19.52	70.9	26.8	0.725	0.275	2.642	0.11	0.31	2326.5	836.47	3171.37	73.4
17.2	0.827	0.173	4.774	0.11	0.19	17.9	54.2	2.334	1.412	0.781	21.64	8.21	30.7	70.5	26.7	0.725	0.275	2.637	0.11	0.31	3965.84	1135.63	5118.75	77.5
27.1	0.727	0.273	2.666	0.11	0.3	16.5	56.6	2.166	1.514	0.847	21.05	7.23	28.69	73.4	25.2	0.744	0.256	2.911	0.12	0.3	3721.47	956.34	4682.54	79.5
43	0.567	0.433	1.309	0.12	0.18	18.3	55	2.349	1.411	0.792	19.19	8.26	28.36	67.7	29.1	0.699	0.301	2.323	0.12	0.31	3452.89	1442.11	4900.59	70.5

HRV							EDA														Eye									
Time-frequency							Continuous decomposition analysis														Trough-to-peak analysis					Pupil diameter			Blink frequency	
Wavelet transform																														
pHF	nLF	nHF	LFHF	peakLF	peakHF		CDA.nSCR	CDA.Amp	CDA.Amp	CDA.SCR	CDA.SCR	CDA.ISCR	CDA.ISCR	CDA.Phasic	CDA.Phasic	CDA.Tonic	CDA.Tonic	TTP.nSCR	TTP.Amp	TTP.Amp	Global.	Global.								
(%)	(%)	(%)	(Hz)	(Hz)		frequency	frequency	Sum	Sum	[muS]	[muS]	[muSxs]	[muSxs]	[muS]	[muS]	[muS]	[muS]	frequency	um	um	Mean	Mean	mean	std	PerLPD	freq	AEC5	PERCLOS		
								[muS]	[muS]	[muS]	[muS]	[muSxs]	[muSxs]	[muS]	[muS]	[muS]	[muS]	[S]	[muS]	[m	[m	[muS]	[muS]							
25.2	0.748	0.252	2.961	0.09	0.15	0.172222	0.286917	1.08857	0.043467	0.137496	1.043202	3.2999	1.2229034	2.5891812	4.696064	5.052127	0.188889	0.252145	0.883921	5.059349	5.59755	36.3585	3.7637	0.0651	0.2222	0.298	0.0662			
31.4	0.685	0.315	2.176	0.07	0.4	0.038095	0.240451	0.724465	0.060998	0.220363	1.463953	5.288724	1.1425685	2.6331877	3.720741	4.89854	0.095238	0.225721	1.196418	4.353594	5.704811	35.5298	3.3814	0.0409	0.2	0.3908	0.0782			
33.9	0.659	0.341	1.936	0.08	0.17	0.089474	0.323497	1.079184	0.069747	0.253375	1.673918	6.081003	1.3442965	5.0457804	4.137706	4.547083	0.094737	0.347962	1.137141	4.467407	5.32653	33.4551	2.202	-0.0199	0.3105	0.3608	0.112			
55.9	0.439	0.561	0.782	0.06	0.18	0.066667	0.543903	1.572056	0.071979	0.178802	1.727503	4.291239	1.3561903	2.5921411	3.949021	4.568413	0.066667	0.596296	1.63454	4.428905	5.024841	34.0961	3.232	-0.0011	0.1833	0.6672	0.1223			
14.9	0.851	0.149	5.696	0.07	0.15																	33.8726	2.5945	-0.0077	0.33	0.4081	0.1347			
27.4	0.725	0.275	2.633	0.09	0.22	0.058333	1.074904	3.660116	0.191827	0.567171	4.603858	13.61209	2.4837247	5.957083	4.581598	5.052101	0.075	0.570464	3.110741	5.084592	6.389481	34.5707	2.9772	0.0128	0.2417	0.3536	0.0854			
54.3	0.457	0.543	0.842	0.11	0.2	0.022222	0.464046	0.856829	0.130713	0.248403	3.137103	5.961675	2.6851899	4.8723353	3.240766	3.669307	0.055556	0.326846	1.312332	3.408164	3.88953	32.9122	2.961	-0.0258	0.1667	0.2737	0.0456			
26.9	0.728	0.272	2.679	0.07	0.39	0.053333	0.370137	0.722897	0.073077	0.159758	1.753855	3.834196	1.5085428	3.1057896	3.225972	3.782163	0.066667	0.320322	0.769751	3.473772	3.912064	34.1586	2.6629	0.0007	0.1733	0.3464	0.06			
26.1	0.739	0.261	2.831	0.08	0.38	0.1	0.231942	0.796908	0.051407	0.150165	1.233763	3.603956	1.4456021	3.1247306	4.239423	5.196739	0.108333	0.433111	1.237455	4.572746	5.624821	32.7082	2.5073	-0.0418	0.1333	0.7866	0.1049			
22.1	0.779	0.221	3.516	0.06	0.28																	33.1119	2.4447	-0.03	0.2281	0.5327	0.1215			
30.9	0.689	0.311	2.218	0.07	0.39	0.039039	0.526082	1.940969	0.093403	0.302589	2.241669	7.26213	1.8224794	4.7017635	4.368744	5.688375	0.087087	0.419713	2.016601	5.089661	6.67107	32.8431	2.2883	-0.0378	0.2162	0.5772	0.1248			
29.9	0.7	0.3	2.337	0.09	0.4	0.066667	0.42565	0.685894	0.104911	0.144652	2.517868	3.471657	1.7611601	2.7884492	4.84701	5.296654	0.044444	0.268807	0.631084	5.527204	6.314031	33.8328	2.3327	-0.0089	0.1111	0.2863	0.0318			
18.7	0.813	0.187	4.335	0.07	0.15	0.038889	0.121223	0.305855	0.038574	0.085763	0.925785	2.058319	5.498111	1.166554	3.301647	3.340496	0.044444	0.089138	0.336276	3.519984	4.046505	34.7135	2.1483	0.0169	0.1833	0.221	0.0405			
48.1	0.518	0.482	1.076	0.07	0.37	0.046667	0.150561	0.299198	0.031163	0.067942	0.74792	1.630613	0.6184684	0.8865307	3.312723	3.426967	0.053333	0.19585	0.738435	3.417553	3.608065	32.5435	1.7804	-0.0466	0.18	0.405	0.0613			
31.2	0.687	0.313	2.198	0.08	0.4	0.05	0.215121	0.5103	0.045989	0.123092	1.103726	2.954209	0.6409766	1.57463	3.339409	3.573364	0.05	0.206188	0.675291	3.55131	3.720137	33.1388	2.5292	-0.0292	0.1917	0.3064	0.0587			
36.4	0.634	0.366	1.732	0.07	0.39	0.046667	0.346363	1.053486	0.067451	0.229142	1.618824	5.499413	1.2438767	3.4565129	3.397946	3.704853	0.06	0.289667	1.071445	3.662409	4.149115	32.684	2.0034	-0.0425	0.16	0.3374	0.054			
21.4	0.785	0.215	3.642	0.09	0.39	0.048485	0.372167	2.360999	0.072926	0.269337	1.750217	6.464077	1.5445269	5.6188164	3.845445	6.812275	0.057576	0.911932	5.473316	1.545503	8.616134	33.4173	2.2838	-0.021	0.1197	0.3826	0.0754			
29.9	0.699	0.301	2.626	0.09	0.4	0.033333	0.621571	2.044474	0.113063	0.345501	2.713524	8.292022	1.6595717	4.2144903	4.149095	6.061254	0.044444	0.712158	3.884736	4.969143	6.708805	32.88	2.546	-0.0268	0.2129	0.3956	0.0846			
22.1	0.779	0.221	3.518	0.06	0.15	0.066667	0.485436	1.083158	0.077012	0.147582	1.848285	3.541979	2.2570495	4.7341412	5.533153	6.337387	0.105556	0.511438	1.59592	5.764685	7.109341	34.3457	2.5698	0.0062	0.25	0.3582	0.0895			
20.2	0.795	0.205	3.887	0.05	0.29	0.069231	0.794651	2.385776	0.146686	0.442155	3.52047	10.61172	2.7619613	7.2717294	4.923309	5.44163	0.096154	0.656887	2.329589	5.667199	7.356622	34.0648	2.3216	-0.0021	0.2346	0.4089	0.0959			
8.1	0.918	0.082	11.233	0.07	0.28	0.05	1.014576	2.179988	0.197506	0.484272	4.740134	11.62252	3.9780589	7.6006883	4.901058	5.17585	0.075	0.687544	2.285512	5.575649	5.953266	33.1851	2.1849	-0.0278	0.2437	0.4897	0.1194			
23.4	0.765	0.235	3.261	0.07	0.38	0.066667	0.542782	2.212789	0.117697	0.395197	2.82473	9.484734	2.3112168	5.1029686	4.861573	5.325562	0.086111	0.508984	2.297548	5.3758	6.062018	33.542	1.9797	-0.0174	0.2194	0.4936	0.1083			
31.6	0.683	0.317	2.158	0.08	0.31	0.075	0.282022	0.559464	0.046718	0.089057	1.121243	2.137359	1.1415541	1.7873079	4.045158	4.737633	0.075	0.264751	0.576897	4.355365	4.869235	32.2264	2.356	-0.0559	0.275	0.5606	0.1542			
19	0.807	0.193	4.194	0.06	0.36	0.05625	0.679752	3.058444	0.155943	0.71437	3.742634	17.14488	2.3001197	7.8167592	4.461939	5.887678	0.08125	0.531886	3.53855	5.103438	6.25106	34.5065	2.6006	0.0109	0.2326	0.5671	0.1843			
19	0.809	0.191	4.233	0.06	0.15	0.088729	0.46605	2.310782	0.093361	0.403752	2.406668	9.690052	1.9815635	7.2298756	4.874856	5.615418	0.131894	0.425502	2.220257	5.370067	7.06334	35.0133	2.7217	0.0257	0.2206	0.5456	0.1204			
18.7	0.813	0.187	4.359	0.11	0.33	0.177778	0.454712	1.079959	0.062888	0.160403	1.509303	3.849681	1.6363229	3.3000163	4.889911	5.402907	0.222222	0.396397	1.020264	5.399173	6.429782	28.5621	2.4147	0.0367	0.2667	0.3768	0.1005			
25.4	0.745	0.255	2.914	0.12	0.31	0.166667	0.393647	1.644191	0.050911	0.189573	1.221867	4.549746	1.2190346	4.3454099	4.534814	5.390197	0.188889	0.452648	1.653378	5.100337	6.163959	27.7091	2.307	0.0058	0.3222	0.2689	0.0867			
16.4	0.834	0.166	5.011	0.11	0.32	0.190476	0.232179	1.505275	0.027276	0.168804	0.654627	4.051305	0.8302775	4.1389229	4.106914	4.483906	0.195238	0.335542	1.813991	4.383634	5.496583	29.0641	2.3161	0.055	0.3143	0.2533	0.0796			
17.5	0.825	0.175	4.699	0.11	0.29	0.123333	0.552149	2.258097	0.069812	0.25036	1.675487	6.008643	1.5817467	4.9131928	4.026537	4.866345	0.136667	0.369804	1.993125	4.505548	6.067327	27.2132	2.0489	-0.0122	0.48	0.2619	0.1257			
19.2	0.807	0.193	4.185	0.11	0.31	0.123028	0.402452	1.29327	0.057664	0.188002	1.383944	4.512057	1.4963182	4.9050675	3.727147	4.532086	0.141956	0.356055	1.229884	4.106624	5.720769	28.1007	2.1664	0.0200	0.3817	0.269	0.1027			
22.3	0.777	0.223	3.489	0.11	0.31	0.133333	0.346317	1.299805	0.04374	0.184121	1.049761	4.41891	1.001861	3.7790652	4.312136	4.784629	0.141667	0.303313	1.191055	4.550674	5.822092	27.5502	1.9937	0.0000	0.3917	0.2368	0.0928			
26.9	0.73	0.27	2.698	0.11	0.31	0.108333	0.239491	0.756842	0.036156	0.119491	0.867738	6.867793	1.25756	4.0749535	3.786115	3.934216	0.158333	0.168698	0.80852	4.071779	4.453783	28.4149	2.1271	0.0314	0.3583	0.2459	0.0881			
23.6	0.763	0.237	3.217	0.11	0.32	0.233333	1.052485	3.158321	0.107993	0.313132	2.591834	7.515164	2.5116017	5.7894878	5.449321	7.159534	0.206667	0.762302	2.632944	6.409173	9.34848	29.0907	2.4116	0.0559	0	0	0			
21.8	0.78	0.22	3.543	0.12	0.31	0.153333	0.696109	1.885485	0.07665	0.186252	1.839598	4.470044	2.3011064	4.0261442	5.294204	5.685987	0.153333	0.575491	1.326736	5.797512	6.546433	28.4148	1.9993	0.0314	0.4	0.2427	0.0971			
15.9	0.84	0.16	5.254	0.1	0.32	0.138462	0.402953	1.689084	0.048264	0.182054	1.158338	4.369302	1.1763573	4.2345434	4.972606	5.740497	0.176923	0.371748	1.911364	5.344701	6.454573	28.3878	2.0543	0.0304	0.3846	0.2286	0.0879			
21.8	0.781	0.219	3.561	0.12	0.3	0.211587	0.659834	2.866411	0.0																					

Participant ID	Step No	Task No	Time Interval	Performance result (safe/risky)	Performance score (-100)	Task loading (1-10)	NASA_TLX score	HRV																				
								Time-based						Frequency-based Welch periodogram						Frequency-based Lomb-Scargle periodogram								
								meanHR	SDNN	RMSSD	pNNx	HRVTI	TINN	aLF	aHF	aTotal	pLF	pHF	nLF	nHF	LFHF	peakLF	peakHF	aLF	aHF	aTotal	pLF	
								(bpm)	(ms)	(ms)	(%)	(ms)	(ms)	(ms ²)	(ms ²)	(ms ²)	(%)	(%)	(%)	(%)		(Hz)	(Hz)	(ms ²)	(ms ²)	(ms ²)	(%)	
7	1	1	0-300	Safe	100	3	12.66	117.9	25.3	14.5	0.2	7	54	138.57	245.91	393.77	35.2	62.4	0.36	0.64	0.564	0.15	0.2	0.023	0.033	0.055	40.8	
		2	300-500	Safe	100	4		119.4	19.7	11.1	0	5.6	6.3	81.25	107.24	189.65	42.8	56.5	0.431	0.569	0.758	0.11	0.25	0.02	0.016	0.037	55.2	
		3	500-720	Safe	100	4		119.6	16.9	10.2	0	5.1	6.3	52.08	65.11	119.31	43.7	54.6	0.444	0.556	0.8	0.1	0.23	0.034	0.024	0.058	58.8	
		4	720-870	Safe	100	2		115.1	20.6	12.6	0.4	5.4	7.3	77.11	108.6	188.83	40.8	57.5	0.415	0.585	0.71	0.12	0.22	0.025	0.019	0.044	57.6	
		5	870-1097	Safe	100	2		110.7	25.8	16.3	0.2	8.4	62.3	287.02	225.41	523.98	54.8	43	0.56	0.44	1.273	0.12	0.16	0.031	0.029	0.06	51.6	
	2	1	0-120	Safe	100	4	110.8	17.7	12.9	0	5.2	5.4	61.97	101.67	166.76	37.2	61	0.379	0.621	0.61	0.11	0.28	0.025	0.04	0.065	38.2		
		2	120-240	Safe	80	4	111.1	23.8	12.9	0	6.9	39.1	101.58	125.66	230.93	44	54.4	0.447	0.553	0.808	0.15	0.25	0.026	0.041	0.068	38.5		
		3	240-360	Safe	58	6	106.2	23.6	15.4	0	6	23.4	166.43	216.01	384.98	43.2	56.1	0.435	0.565	0.77	0.15	0.22	0.011	0.019	0.03	36		
		4	360-480	Safe	48	4	105.9	23.4	16.4	0	6	31.3	150.56	243.61	395.34	38.1	61.6	0.382	0.618	0.618	0.14	0.25	0.032	0.044	0.076	42.4		
		5	480-750	Safe	80	3	103.3	35.2	20.9	3.1	8.2	88.9	484.08	357.4	865.98	55.9	41.3	0.575	0.425	1.354	0.11	0.24	0.034	0.015	0.049	68.9		
		6	750-1096	Safe	74	5	102.2	24.6	16.9	0.3	7.2	60.3	175.97	194.59	380.91	46.2	51.1	0.475	0.525	0.904	0.12	0.27	0.028	0.021	0.049	58		
	3	1	0-240	Safe	68	6	110.8	34.9	19.4	1.6	8.9	69.8	161.66	292.93	459.03	35.2	63.8	0.356	0.644	0.552	0.13	0.22	0.025	0.037	0.062	40		
		2	240-300	Safe	94	8	104.9	36.7	24.3	5	7.2	61.5	376.53	328.78	732.35	51.4	44.9	0.534	0.466	1.145	0.11	0.22	0.04	0.028	0.069	58.5		
		3	300-420	Safe	65	8	105.2	30.9	19.6	0.5	7.5	85.9	315.8	323.47	646.68	48.8	50	0.494	0.506	0.976	0.11	0.23	0.031	0.035	0.066	46.7		
		4	420-510	Safe	100	6	104.2	19.9	15.9	0	6.5	5.9	76.78	266.79	344.75	22.3	77.4	0.223	0.777	0.288	0.15	0.21	0.019	0.04	0.059	31.9		
		5	510-720	Safe	72	7	103.3	29.8	19.8	1.1	8.9	106.7	276.96	279.37	572.62	48.4	48.8	0.498	0.502	0.991	0.13	0.22	0.022	0.033	0.055	40.6		
		6	720-1106	Safe	67	7	100.1	33.2	22.7	3.6	7.5	95.7	354.37	433.56	819.45	43.2	52.9	0.45	0.55	0.817	0.1	0.22	0.035	0.042	0.077	45.7		
	4	1	0-360	Safe	100	8	102.3	31.7	21.4	1.7	8.6	87.2	243.27	386.2	648.14	37.5	59.6	0.386	0.614	0.63	0.12	0.24	0.015	0.022	0.037	40		
		2	360-450	Safe	100	9	101.8	29	19.6	1.3	7.6	53.7	214.32	250.69	467.71	45.8	53.6	0.461	0.539	0.855	0.12	0.21	0.027	0.03	0.057	47.7		
		3	450-660	Safe	100	7	101.4	31.7	22.8	3.5	7.3	78.6	258.18	392.47	668.35	38.6	58.7	0.397	0.603	0.658	0.08	0.27	0.03	0.032	0.062	48.1		
		4	660-990	Safe	73	10	101.6	31	21.4	2.6	8.9	95.5	240.65	311.17	571.16	42.1	54.5	0.436	0.564	0.773	0.1	0.19	0.017	0.027	0.045	38.8		
		5	990-1250	Safe	61	9	99.6	42.1	26	5.9	9.7	129.9	525.6	469.55	1023.12	51.4	45.9	0.528	0.472	1.119	0.11	0.27	0.044	0.041	0.086	51.8		
		6	1250-1350	Safe	86	9	96.5	40.8	28.3	5.1	9.9	158.7	738.3	546.7	1311.08	56.3	41.7	0.575	0.425	1.35	0.11	0.25	0.022	0.015	0.038	59.2		
		7	1350-1656	Risky	28	9	97.3	42.5	26.6	6.1	11.9	197.8	579.72	496.21	1096.94	52.8	45.2	0.539	0.461	1.168	0.12	0.25	0.033	0.018	0.052	64.4		
	8	1	1	0-240	Safe	100	2	33.33	91.5	47.4	53.7	35.3	12.2	195.3	430.13	824.9	1270.29	33.9	64.9	0.343	0.657	0.521	0.12	0.27	0.01	0.029	0.039	25.7
			2	240-480	Safe	85	4		89.5	44.9	52.5	35.5	11	168.5	383.68	840.11	1244.09	30.8	67.5	0.314	0.686	0.457	0.1	0.24	0.025	0.063	0.088	28.3
			3	480-742	Safe	73	5		88.7	58.7	48.6	26.1	9.3	200	1266.37	1030.02	2414.6	52.4	42.7	0.551	0.449	1.229	0.09	0.23	0.043	0.025	0.069	61.7
			4	742-1070	Safe	73	4		83.4	66.9	60.2	38.4	10.7	340.6	1398.38	1898.44	3373.61	41.5	56.3	0.424	0.576	0.737	0.11	0.24	0.025	0.034	0.06	42
2		1	0-100	Safe	100	3	84.6	60.5	67.1	43.5	9.9	280	1096.53	1630.96	2755.04	39.8	59.2	0.402	0.598	0.672	0.1	0.22	0.024	0.04	0.064	37.8		
		2	100-280	Safe	88	5	85.1	58.4	57.1	37.3	9.8	205.1	592.01	1161.65	1802.7	32.8	64.4	0.338	0.662	0.51	0.08	0.26	0.025	0.066	0.091	27.8		
		3	280-600	Safe	69	7	84.6	61.7	61.4	43.5	7.9	157.5	743.21	1698.54	2526.48	29.4	67.2	0.304	0.696	0.438	0.07	0.25	0.009	0.039	0.047	17.9		
		4	600-720	Safe	61	8	80.8	69.7	70.2	47.1	12	244.1	804.49	2859.11	3729.72	21.6	76.7	0.22	0.78	0.281	0.1	0.24	0.006	0.031	0.038	15.8		
		5	720-1080	Safe	62	5	82.5	65.3	61.3	39	8.4	206.5	836.4	1966.23	2872.62	29.1	68.4	0.298	0.702	0.425	0.12	0.25	0.012	0.025	0.037	32.8		
		6	1080-1473	Risky	41	7	82	73.8	63.8	40.2	11.3	386	1467.48	1940.59	3528.51	41.6	55	0.431	0.569	0.756	0.09	0.23	0.01	0.031	0.041	23.7		
3		1	0-290	Safe	82	4	85.4	60.9	76.6	49	7.3	191.4	380.43	1267.26	1717.36	22.2	73.8	0.231	0.769	0.3	0.14	0.28	0.013	0.06	0.074	17.5		
		2	290-540	Safe	82	4	86.3	54.8	66	45.8	6.6	111.3	727.97	1051.32	1890.75	38.5	55.6	0.409	0.591	0.692	0.1	0.24	0.023	0.032	0.056	40.6		
		3	540-630	Safe	56	6	82.3	68.1	81	60	9.3	295.2	436.29	3123.06	3701.97	11.8	84.4	0.123	0.877	0.14	0.1	0.27	0.015	0.053	0.07	21.7		
		4	630-720	Safe	60	8	86.8	47.5	58.6	46.2	11.3	13.2	118.84	1075.18	1206.54	9.8	89.1	0.1	0.9	0.111	0.15	0.24	0.014	0.044	0.058	24.3		
		5	720-1620	Safe	52	7	82.6	73.2	77.3	52.9	10.9	273.9	1523.29	1901.8	3609.92	42.2	52.7	0.445	0.555	0.801	0.11	0.22	0.027	0.057	0.086	31.9		
		6	1620-2097	Risky	33	9	79.8	80.5	86.1	56.8	11.5	311.5	1255.56	2488.23	3913.48	32.1	63.6	0.335	0.665	0.505	0.09	0.23	0.021	0.038	0.06	34.9		

Figure H.1 (continued) : Data collected during the study.

HRV

Frequency-based Lomb-Scargle periodogram																								Non-linear						Time-frequency Lomb-Scargle periodogram										Time-frequency Wavelet transform					
pHF	nLF	nHF	LFHF	peakLF	peakHF	SD1	SD2	sampen	alpha1	alpha2	aLF	aHF	aTotal	pLF	pHF	nLF	nHF	LFHF	peakLF	peakHF	aLF	aHF	aTotal	pLF																					
(%)	(%)	(%)	(%)	(Hz)	(Hz)	(ms)	(ms)				(ms ²)	(ms ²)	(ms ²)	(%)	(%)	(%)	(%)		(Hz)	(Hz)	(ms ²)	(ms ²)	(ms ²)	(%)																					
59.2	0.408	0.592	0.688	0.12	0.22	10.3	34.3	1.726	1.48	0.713	4.31	7.7	12.15	35.5	63.4	0.359	0.641	0.56	0.14	0.22	862.22	1339.64	2203.63	39.1																					
44.7	0.553	0.447	1.236	0.1	0.26	7.9	26.8	1.601	1.497	0.768	2.74	3.38	6.17	44.5	54.9	0.448	0.552	0.81	0.1	0.25	420.52	579.39	1000.2	42																					
41.1	0.589	0.411	1.43	0.09	0.25	7.2	22.8	1.448	1.243	0.937	1.59	2	3.64	43.7	55.1	0.442	0.558	0.793	0.09	0.21	272.97	336.9	610.04	44.7																					
42.1	0.578	0.422	1.37	0.11	0.22	8.9	27.7	1.67	1.429	0.709	2.14	3.37	5.63	38.1	59.9	0.389	0.611	0.636	0.11	0.22	719.59	697.86	1418.91	50.7																					
48.4	0.516	0.484	1.066	0.13	0.26	11.5	34.5	1.891	1.302	0.741	7.09	7.16	14.35	49.4	49.9	0.498	0.502	0.99	0.12	0.23	1348.7	1197.6	2550.45	52.9																					
61.8	0.382	0.618	0.618	0.11	0.28	9.1	23.4	1.663	1.347	1.014	1.85	2.84	4.76	38.9	59.7	0.394	0.606	0.651	0.08	0.28	319.68	509.24	829.44	38.5																					
61.2	0.386	0.614	0.63	0.11	0.22	9.1	32.4	1.643	1.57	0.906	2.75	3.82	6.7	41	57	0.419	0.581	0.72	0.12	0.25	636.87	824.5	1462	43.6																					
63.9	0.361	0.639	0.564	0.1	0.23	10.9	31.5	1.843	1.498	0.646	5.3	7.23	12.59	42.1	57.4	0.423	0.577	0.733	0.11	0.23	840.21	1247.25	2087.82	40.2																					
57.5	0.425	0.575	0.738	0.14	0.26	11.6	31.1	1.901	1.358	0.601	4.85	7.23	12.12	40	59.7	0.401	0.599	0.67	0.13	0.26	737.72	1265.65	2003.47	36.8																					
31	0.69	0.31	2.224	0.09	0.26	14.8	47.6	2.047	1.403	0.751	13.61	11.22	25.3	53.8	44.3	0.548	0.452	1.213	0.08	0.18	2483.86	1933.65	4422.84	56.2																					
41.9	0.581	0.419	1.386	0.09	0.29	12	32.6	1.826	1.309	0.667	5.01	6	11.22	44.6	53.5	0.455	0.545	0.834	0.13	0.21	932.98	1029.46	1964.2	47.5																					
59.9	0.401	0.599	0.668	0.12	0.21	13.8	47.4	1.993	1.319	1.051	4.66	8.82	13.65	34.1	64.6	0.346	0.654	0.529	0.13	0.21	822.35	1520.53	2343.37	35.1																					
41	0.588	0.412	1.425	0.11	0.22	17.3	48.9	1.795	1.699	0.732	16.85	11.01	28.84	58.4	38.2	0.605	0.395	1.53	0.1	0.21	2311.42	1922.93	4237.14	54.6																					
53.3	0.467	0.533	0.876	0.1	0.24	13.9	41.5	2.088	1.347	0.645	9.26	9.64	19.05	48.6	50.6	0.49	0.51	0.961	0.1	0.25	1463.89	1654.4	3118.9	46.9																					
68	0.319	0.681	0.469	0.14	0.27	11.3	25.8	1.963	1.423	0.45	3.08	8.53	11.64	26.5	73.3	0.265	0.735	0.361	0.14	0.21	462.72	1237.12	1699.91	27.2																					
59.3	0.406	0.594	0.683	0.12	0.22	14	39.8	2.024	1.419	0.595	6.7	8.55	15.46	43.3	55.3	0.439	0.561	0.784	0.11	0.23	1417.63	1666	3087.46	45.9																					
54.2	0.458	0.542	0.845	0.07	0.21	16.1	44.2	2.093	1.325	0.747	7.78	13.14	21.14	36.8	62.2	0.372	0.628	0.592	0.11	0.24	1975.56	2413.66	4403.28	44.9																					
59.9	0.4	0.6	0.668	0.13	0.21	15.1	42.3	2.118	1.114	0.712	7.07	11.74	19.07	37.1	61.6	0.376	0.624	0.602	0.12	0.25	1351.7	2047.63	3402.82	39.7																					
51.8	0.48	0.52	0.922	0.11	0.21	13.9	38.6	1.958	1.329	0.82	7.35	9.43	16.85	43.6	56	0.438	0.562	0.78	0.12	0.21	1044.12	1236.06	2281.46	45.8																					
51.5	0.483	0.517	0.933	0.06	0.28	16.1	41.9	2.097	1.313	0.824	7.21	12.82	20.4	35.3	62.9	0.36	0.64	0.562	0.08	0.17	1323.56	2167.79	3499.1	37.8																					
61.1	0.389	0.611	0.636	0.12	0.21	15.2	41.2	2.05	1.259	0.727	7.91	9.93	18.15	43.6	54.7	0.444	0.556	0.797	0.09	0.21	1353.04	1689.07	3045.14	44.4																					
47.9	0.519	0.481	1.081	0.11	0.19	18.4	56.6	2.185	1.427	0.612	13.85	14.06	28.56	48.5	49.2	0.496	0.504	0.985	0.12	0.28	3140.06	2676.62	5821.89	53.9																					
40.5	0.593	0.407	1.46	0.12	0.24	20.1	54	2.294	1.493	0.71	21.1	14.45	36.22	58.3	39.9	0.594	0.406	1.461	0.11	0.25	3525.04	2687.43	6219.51	56.7																					
35	0.648	0.352	1.838	0.12	0.17	18.8	57.1	2.257	1.254	0.557	17.43	15.39	33.42	52.2	46	0.531	0.469	1.133	0.12	0.24	3391.44	2868.92	6271.36	54.1																					
74.1	0.257	0.743	0.347	0.08	0.27	38	55.1	3.139	0.845	0.9	12.58	26.54	39.61	31.7	67	0.322	0.678	0.474	0.1	0.28	2106.55	4306.4	6417.7	32.8																					
71.4	0.284	0.716	0.397	0.12	0.28	37.2	51.5	2.873	0.774	0.766	9.72	26.42	36.65	26.5	72.1	0.269	0.731	0.368	0.1	0.27	1976.08	4379.69	6359.82	31.1																					
36.5	0.628	0.372	1.688	0.12	0.21	34.4	75.5	1.9	1.194	0.654	37.4	31.9	71.95	52	44.3	0.54	0.46	1.172	0.08	0.21	7092.47	5438.3	12590.87	56.3																					
57.8	0.421	0.579	0.726	0.09	0.24	42.6	84.4	2.066	1.091	0.691	38.03	60.37	101.46	37.5	59.5	0.386	0.614	0.63	0.11	0.24	7658.67	9665.14	17347.46	44.1																					
61.7	0.38	0.62	0.613	0.12	0.23	47.7	71.1	2.243	1.045	0.236	28.35	52.55	82.43	34.4	63.8	0.35	0.65	0.54	0.1	0.23	5046.82	8158.44	13212.14	38.2																					
72	0.279	0.721	0.386	0.07	0.17	40.5	72	2.013	0.77	0.866	19.78	37.44	58.58	33.8	63.9	0.346	0.654	0.528	0.07	0.27	3573.07	6071.31	9654.11	37																					
81.4	0.181	0.819	0.22	0.14	0.24	43.5	75.7	1.901	0.871	0.762	20.09	53.83	76.13	26.4	70.7	0.272	0.728	0.373	0.06	0.25	4566.93	9310.54	13905.6	32.8																					
82	0.162	0.838	0.193	0.1	0.25	49.8	85.1	2.065	0.829	0.714	30.91	99.7	132.87	23.3	75	0.237	0.763	0.31	0.1	0.25	4448.41	14660.69	19191.11	23.2																					
66.6	0.33	0.67	0.493	0.07	0.27	43.4	81.5	1.953	0.984	0.708	31.55	64.18	97.68	32.3	65.7	0.33	0.67	0.492	0.12	0.25	5611.59	10430.11	16062.82	34.9																					
75.9	0.238	0.762	0.312	0.09	0.26	45.2	94.1	1.988	1.054	0.745	45.81	68.13	117.09	39.1	58.2	0.402	0.598	0.672	0.09	0.21	8598.92	10220.98	18874.03	45.6																					
80.5	0.179	0.821	0.218	0.14	0.25	54.3	66.9	2.141	0.617	0.977	13.08	46.37	61.4	21.3	75.5	0.22	0.78	0.282	0.14	0.34	2774.64	7486.16	10337.65	26.8																					
57.4	0.414	0.586	0.706	0.11	0.25	46.8	61.8	2.115	0.749	0.606	20.36	34.32	57.31	35.5	59.9	0.372	0.628	0.593	0.1	0.25	4551.59	5488.05	10112.16	45																					
75.9	0.222	0.778	0.286	0.13	0.28	57.8	77.1	2.558	0.753	0.6	20.06	102.93	127.05	15.8	81	0.163	0.837	0.195	0.11	0.28	9043.36	13768.69	22942.63	39.4																					
75.3	0.244	0.756	0.323	0.13	0.24	41.7	52.7	2.959	0.731	0.202	4.18	30.93	35.37	11.8	87.4	0.119	0.881	0.135	0.08	0.25	1362.08	5961.86	7332.56	18.6																					
66.7	0.323	0.677	0.478	0.13	0.24	54.7	87.8	2.323	1.014	0.746	46.22	66.26	116.84	39.6	56.7	0.411	0.589	0.698	0.12	0.23	8914.47	10231.59	19294.61	46.2																					
62.4	0.359	0.641	0.559	0.11	0.18	61	96.1	2.389	0.856	0.778	37.15	91.71	133.18	27.9	68.9	0.288	0.712	0.405	0.09	0.23	6805.2	13063.04	20028.56	34																					

Figure H.1 (continued) : Data collected during the study.

Participant ID	Step No	Task No	Time Interval	Performance result (safe/risky)	Performance score (1-100)	Task loading (1-10)	NASA_TLX score	HRV																				
								Time-based						Frequency-based Welch periodogram						Frequency-based Lomb-Scargle periodogram								
								meanHR	SDNN	RMSSD	pNNx	HRVtI	TINN	aLF	aHF	aTotal	pLF	pHF	nLF	nHF	LFHF	peakLF	peakHF	aLF	aHF	aTotal	pLF	
								(bpm)	(ms)	(ms)	(%)	(ms)	(ms)	(ms ²)	(ms ²)	(ms ²)	(%)	(%)	(%)	(%)	(%)	(%)	(%)	(ms ²)	(ms ²)	(ms ²)	(%)	
9	1	1	0-420	Safe	100	3	9	91.5	47.4	53.7	35.3	12.2	195.3	430.13	824.9	1270.29	33.9	64.9	0.343	0.657	0.521	0.12	0.27	0.01	0.029	0.039	25.7	
		2	420-600	Safe	100	4		89.5	44.9	52.5	35.5	11	168.5	383.68	840.11	1244.09	30.8	67.5	0.314	0.686	0.457	0.1	0.24	0.025	0.063	0.088	28.3	
		3	600-720	Safe	100	4		86.5	36.9	23.8	2.3	10.2	134.8	360.21	320.05	707.82	50.9	45.2	0.53	0.47	1.125	0.09	0.27	0.025	0.027	0.052	47.3	
		4	720-900	Safe	100	2		82.8	43	25.5	2.4	9.9	127	597.13	299.79	965.44	61.9	31.1	0.666	0.334	1.992	0.07	0.29	0.031	0.015	0.047	65.5	
	2	1	900-1077	Safe	73	2	30.33	80.7	42.2	28	5.6	10.7	168.5	810.43	361.86	1212.79	66.8	29.8	0.691	0.309	2.24	0.1	0.27	0.041	0.023	0.065	63.7	
		5	0-120	Safe	78	4		83.1	42.4	30.7	9.1	10.4	155.8	442.11	614.16	1066.73	41.4	57.6	0.419	0.581	0.72	0.12	0.24	0.02	0.032	0.053	38.4	
		2	120-270	Safe	80	4		84.3	52.5	27.3	4.3	13.1	195.3	1030.73	456.22	1529.05	67.4	29.8	0.693	0.307	2.259	0.09	0.22	0.029	0.01	0.039	72.9	
		3	270-360	Safe	68	6		82.2	33.4	26.3	1.6	9.5	136.2	117.02	405.88	535.39	21.9	75.8	0.224	0.776	0.288	0.14	0.26	0.014	0.036	0.051	27.9	
		4	360-540	Safe	58	4		82.1	40.8	26.3	4.5	11.7	181.6	521.5	372.62	920.83	56.6	40.5	0.583	0.417	1.4	0.09	0.27	0.032	0.02	0.052	61.1	
		5	540-720	Safe	89	3		81.2	38.3	26	2.9	11	146	506.65	376.31	936.69	54.1	40.2	0.574	0.426	1.346	0.08	0.23	0.026	0.026	0.053	49.5	
	3	1	720-1168	Safe	78	5	34	80.9	44.3	27.7	5.2	13.1	189.2	652.2	399.08	1118.94	58.3	35.7	0.62	0.38	1.634	0.09	0.28	0.021	0.011	0.033	64.4	
		2	0-240	Safe	55	6		88.4	40.1	26.3	4.4	10.1	109.9	402.58	309.99	731.94	55	42.4	0.565	0.435	1.299	0.1	0.31	0.039	0.023	0.062	62.8	
		2	240-300	Safe	94	8		86.4	22.3	22.4	0	5.7	75.2	79.14	249.04	335.47	23.6	74.2	0.241	0.759	0.318	0.09	0.3	0.006	0.027	0.034	18.1	
		3	300-400	Safe	65	8		87.4	33.1	23.1	0.7	7.3	61.8	340.88	339.68	690.29	49.4	49.2	0.501	0.499	1.004	0.1	0.29	0.034	0.026	0.059	56.2	
		4	400-540	Safe	72	6		89.3	41.2	25.6	2	12	158.7	330.49	337.18	678.03	48.7	49.7	0.495	0.505	0.98	0.11	0.27	0.026	0.021	0.047	55.5	
		5	540-840	Safe	100	7		83.4	41.4	28.8	6.8	11.2	119.7	778.92	465.22	1287.86	60.5	36.1	0.626	0.374	1.674	0.1	0.29	0.03	0.023	0.054	56.1	
	4	6	840-1149	Risky	52	7	63	82.6	56.8	29.5	7.1	10.8	196.5	577.85	536.09	1143.54	50.5	46.9	0.519	0.481	1.078	0.09	0.25	0.028	0.03	0.058	47.6	
		1	0-360	Safe	100	8		88.8	61.2	27.1	5.2	9.6	176.3	876.93	363.98	1273.36	68.9	28.6	0.707	0.293	2.409	0.1	0.16	0.036	0.012	0.049	74.7	
		2	360-600	Safe	100	9		89.2	38.9	24.1	2.5	9.1	116	446.64	365.73	843.51	52.9	43.4	0.55	0.45	1.221	0.1	0.25	0.035	0.023	0.058	60.5	
		3	600-700	Safe	100	7		90.1	32.6	22.7	1.4	6.8	37.6	372.03	327.45	714.36	52.1	45.8	0.532	0.468	1.136	0.11	0.25	0.03	0.024	0.054	55	
		4	700-960	Safe	73	10		89.3	35	25.4	3.2	9.1	118.7	489.76	338.81	867.96	56.4	39	0.591	0.409	1.446	0.12	0.23	0.035	0.017	0.053	65.9	
		5	960-1290	Risky	38	9		85.8	55.4	29.3	8.1	7.5	111.1	793.44	453.08	1325.17	59.9	34.2	0.637	0.363	1.751	0.07	0.22	0.024	0.012	0.036	65.7	
		6	1290-1380	Risky	51	9		82.3	32.6	27.9	4.1	8.7	71.8	555.39	404.07	977.4	56.8	41.3	0.579	0.421	1.374	0.11	0.24	0.029	0.022	0.051	55.9	
	7	1380-1699	Risky	28	9	83.6	51.4	31.8	8.5	9.1	149.4	589.34	453.49	1091.04	54	41.6	0.565	0.435	1.3	0.09	0.27	0.037	0.021	0.058	64.2			
	10	1	1	0-300	Safe	100	3	22	95.6	29.1	18.9	1.5	7.7	63.5	347.87	225.57	580.66	59.9	38.8	0.607	0.393	1.542	0.11	0.24	0.028	0.005	0.033	83.5
			2	300-420	Safe	100	4		103.9	39.8	23.1	4.7	10.7	134.3	418.41	335	794.65	52.7	42.2	0.555	0.445	1.249	0.08	0.19	0.037	0.029	0.067	55.8
			3	420-653	Safe	100	4		95.8	36.4	24.5	4.6	10.2	112.8	679.67	347.83	1051.45	64.6	33.1	0.661	0.339	1.954	0.13	0.37	0.02	0.015	0.035	56.5
			4	653-740	Safe	100	2		97.4	24.1	15.9	0	7.1	5.9	232.76	103.18	339.86	68.5	30.4	0.693	0.307	2.256	0.13	0.26	0.036	0.015	0.052	70.2
2		5	740-1074	Safe	86	2	47	95.4	25.9	16.8	0	8.1	70.6	300.75	171.27	485.42	62	35.3	0.637	0.363	1.756	0.11	0.16	0.017	0.009	0.026	63.5	
		1	0-120	Safe	100	4		95	33	19.5	2.1	8.6	112.8	659.77	283.04	955.15	69.1	29.6	0.7	0.3	2.331	0.1	0.16	0.03	0.013	0.043	70.3	
		2	120-240	Safe	60	4		98	46.4	22.4	2.2	11.4	140.4	373.11	301.73	718.9	51.9	42	0.553	0.447	1.237	0.14	0.22	0.044	0.035	0.08	55	
		3	240-360	Safe	47	6		94.4	26.7	19.4	2.7	7.1	60.3	277.27	265.78	554.98	50	47.9	0.511	0.489	1.043	0.13	0.22	0.015	0.019	0.035	43.5	
		4	360-630	Safe	61	4		95.3	20.9	13.8	0	6.2	7.3	108.61	115.73	229.42	47.3	50.4	0.484	0.516	0.938	0.13	0.24	0.025	0.028	0.053	47.6	
		6	630-957	Risky	24	5		98.1	36.4	18	1.9	10.1	138.4	311.37	163.97	496.52	62.7	33	0.655	0.345	1.899	0.11	0.16	0.04	0.013	0.054	75.6	
3		1	0-240	Safe	68	6	54.33	97.6	22.3	14.5	0	6.7	30.8	227.45	125.98	360.46	63.1	34.9	0.644	0.356	1.805	0.12	0.27	0.035	0.014	0.049	70.3	
		2	240-300	Safe	100	8		99.6	28.8	15.5	0	5.5	7.8	211.45	106.01	329.99	64.1	32.1	0.666	0.334	1.995	0.08	0.29	0.03	0.016	0.046	65.3	
		3	300-420	Safe	65	8		98.8	21.7	14.2	0.5	7.2	6.8	223.11	117.88	348.45	64	33.8	0.654	0.346	1.893	0.09	0.25	0.031	0.013	0.044	69.4	
		4	420-540	Safe	82	6		97.3	17	13.1	0	5	5.4	71.69	97.41	170.66	42	57.1	0.424	0.576	0.736	0.1	0.18	0.025	0.026	0.051	49.5	
		5	540-810	Risky	26	7		95	24.5	18.3	0.7	6.9	60.3	265.73	188.74	470.47	56.5	40.1	0.585	0.415	1.408	0.13	0.24	0.029	0.016	0.046	63.7	
		6	810-1119	Safe	70	7		94	40.4	21.3	2.7	8	99.1	431.71	316.2	767.87	56.2	41.2	0.577	0.423	1.365	0.1	0.16	0.03	0.018	0.048	62	
4		1	0-360	Safe	100	8	81	90.8	31.9	18.8	0.7	9.6	111.3	415.43	143.02	576.76	72	24.8	0.744	0.256	2.905	0.11	0.29	0.045	0.015	0.059	75.4	
		2	360-600	Safe	68	9		93.3	39.4	22	3.3	8.3	92.3	521.02	243.73	822.47	63.3	29.6	0.681	0.319	2.138	0.12	0.31	0.026	0.013	0.039	66.3	
		3	600-720	Safe	61	7		89.6	30.4	19.1	0.6	7.1	64.5	482.5	151.2	679.73	71	22.2	0.761	0.239	3.191	0.12	0.36	0.023	0.008	0.031	73.7	
		4	720-1200	Risky	37	10		89.2	39.7	21.3	2.5	12.6	184.1	480.57	236.67	738.02	65.1	32.1	0.67	0.33	2.031	0.11	0.16	0.038	0.017	0.055	69.5	
		5	1200-1320	Safe	49	9		92.5	46	19.3	1.6	8.3	109.9	256.13	190.1	468.94	54.6	40.5	0.574	0.426	1.347	0.1	0.21	0.042	0.034	0.076	54.5	
		7	1320-1680	Risky</																								

HRV

Frequency-based																							Non-linear					Time-frequency										Time-frequency				
Lomb-Scargle periodogram						SD1						SD2						Lomb-Scargle periodogram						Wavelet transform																		
pHF	nLF	nHF	LFHF	peakLF	peakHF	SD1	SD2	sampen	alpha1	alpha2	aLF	aHF	aTotal	pLF	pHF	nLF	nHF	LFHF	peakLF	peakHF	aLF	aHF	aTotal	pLF																		
(%)	(%)	(%)	(Hz)	(Hz)	(ms)	(ms)	(ms)				(ms ²)	(ms ²)	(ms ²)	(%)	(%)	(%)	(%)	(%)	(%)	(Hz)	(Hz)	(ms ²)	(ms ²)	(ms ²)	(%)																	
74.1	0.257	0.743	0.347	0.08	0.27	38	55.1	3.139	0.845	0.9	12.58	26.54	39.61	31.7	67	0.322	0.678	0.474	0.1	0.28	2106.55	4306.4	6417.7	32.8																		
71.4	0.284	0.716	0.397	0.12	0.28	37.2	51.5	2.873	0.774	0.766	9.72	26.42	36.65	26.5	72.1	0.269	0.731	0.368	0.1	0.27	1976.08	4379.69	6359.82	31.1																		
51.9	0.477	0.523	0.911	0.09	0.28	16.8	49.4	1.964	1.086	0.803	10.09	10.97	22.25	45.4	49.3	0.479	0.521	0.92	0.08	0.27	1730.37	1751.04	3495.66	49.5																		
32.6	0.668	0.332	2.011	0.08	0.28	18	58.1	2.43	1.463	1.019	18.68	10.33	30.81	60.6	33.5	0.644	0.356	1.809	0.07	0.29	3645.59	1495.22	5148.46	70.8																		
35.7	0.641	0.359	1.786	0.07	0.27	19.9	56.4	2.573	1.375	0.785	21.16	11.93	33.73	62.7	35.4	0.639	0.361	1.773	0.11	0.27	4194.6	1923.29	6129.29	68.4																		
61.1	0.386	0.614	0.628	0.1	0.19	21.7	55.9	2.635	1.324	0.936	12.37	21.64	34.55	35.8	62.6	0.364	0.636	0.572	0.09	0.17	2143.17	3689.39	5834.84	36.7																		
26.3	0.735	0.265	2.774	0.09	0.21	19.3	71.7	1.436	1.583	0.748	30.17	16.28	48.15	62.7	33.8	0.649	0.351	1.853	0.09	0.22	4661.32	2407.47	7092.25	65.7																		
70.9	0.283	0.717	0.394	0.14	0.25	18.7	43.4	2.621	0.897	1.045	4.6	13.33	18.49	24.9	72.1	0.257	0.743	0.345	0.13	0.25	780.41	2204.23	2991.12	26.1																		
38.1	0.616	0.384	1.605	0.08	0.27	18.6	54.7	2.464	1.054	0.809	17.42	11.39	29.67	58.7	38.4	0.605	0.395	1.53	0.09	0.28	2634.42	1867.16	4517.85	58.3																		
49.9	0.498	0.502	0.992	0.09	0.22	18.4	50.9	2.621	1.243	0.943	15.38	12.91	29.54	52	43.7	0.544	0.456	1.191	0.07	0.23	2749.64	2009.65	4773.8	57.6																		
34.9	0.648	0.352	1.844	0.1	0.29	19.6	59.5	2.52	1.313	0.914	20.82	13.75	36.71	56.7	37.5	0.602	0.398	1.514	0.1	0.28	3763.59	2106.62	5922.32	63.5																		
36.8	0.63	0.37	1.706	0.08	0.3	18.7	53.6	2.451	1.115	0.699	12.1	10.17	22.7	53.3	44.8	0.543	0.457	1.19	0.1	0.31	2184.51	1630.46	3820.57	57.2																		
80.9	0.183	0.817	0.224	0.07	0.29	15.9	27.2	2.277	0.836	2.08	8.43	10.13	12.91	19	77.3	0.198	0.802	0.246	0.14	0.3	332.85	1418.15	1756.24	19.9																		
43.3	0.566	0.434	1.304	0.09	0.29	16.4	43.8	2.421	1.272	0.411	11.46	9.71	21.57	53.1	45	0.541	0.459	1.18	0.09	0.29	1831.59	1562.37	3395.28	53.9																		
44.6	0.553	0.447	1.237	0.09	0.28	18.2	55.4	2.434	1.257	1.103	9.51	11	20.68	46	53.2	0.464	0.536	0.865	0.1	0.27	1694.72	1746.76	3442.53	49.2																		
43.1	0.565	0.435	1.301	0.1	0.31	20.4	54.9	2.537	1.357	0.56	24.74	14.96	40.8	60.6	36.7	0.623	0.377	1.654	0.11	0.29	4153.28	2617.89	6789.4	61.2																		
52	0.478	0.522	0.915	0.08	0.26	20.9	77.6	1.474	1.174	0.885	18.21	18.46	37.6	48.4	49.1	0.497	0.503	0.987	0.08	0.25	3012.33	2839.68	5861.59	51.4																		
24.7	0.751	0.249	3.018	0.08	0.21	19.2	84.4	1.424	1.572	1.026	27.32	12.61	40.97	66.7	30.8	0.684	0.316	2.166	0.09	0.21	4837.75	2206.03	7055.58	68.6																		
39.3	0.606	0.394	1.539	0.1	0.26	17.1	52.3	2.301	1.163	0.833	15.82	12.63	29.32	53.9	43.1	0.556	0.444	1.252	0.1	0.27	2540.11	1881.36	4433.76	57.3																		
44.9	0.55	0.45	1.223	0.11	0.25	16.1	43.2	2.157	1.248	0.724	11.59	11.32	23.27	49.8	48.7	0.506	0.494	1.024	0.12	0.25	1848.82	1679.86	3529.5	52.4																		
33.1	0.666	0.334	1.993	0.06	0.2	18	46	2.297	1.287	0.579	12.94	11.17	24.98	51.8	44.7	0.537	0.463	1.158	0.11	0.23	3243.9	1812.72	5073.89	63.9																		
33.6	0.662	0.338	1.956	0.07	0.24	20.7	75.5	1.445	1.326	0.876	23.16	17.36	41.89	55.3	41.4	0.572	0.428	1.334	0.07	0.21	4393.93	2481.71	6883.62	63.8																		
43.6	0.562	0.438	1.281	0.12	0.25	19.8	41.6	2.604	1.12	0.596	18.5	12.54	31.21	59.3	40.2	0.596	0.404	1.475	0.11	0.24	2447.35	1943.54	4396.29	55.7																		
35.6	0.643	0.357	1.804	0.11	0.31	22.5	69.1	2.618	1.153	0.922	18.24	15.64	34.94	52.2	44.8	0.538	0.462	1.166	0.11	0.27	3418.79	2356.87	5791.01	59																		
16.4	0.836	0.164	5.099	0.1	0.23	13.4	38.9	2.006	1.441	0.643	9.99	6.84	16.99	58.8	40.3	0.593	0.407	1.46	0.1	0.19	1842.79	1227.63	3072.8	60																		
44	0.559	0.441	1.268	0.06	0.2	16.4	53.9	2.02	1.071	0.896	12.15	10.59	23.39	51.9	45.3	0.534	0.466	1.147	0.09	0.19	2678.21	2070.06	4751.79	56.4																		
43.5	0.565	0.435	1.299	0.12	0.18	17.4	48.5	2.147	1.512	0.54	19.26	10.97	31.05	62	35.3	0.637	0.363	1.756	0.12	0.17	3460.03	2092.6	5556.47	62.3																		
29.7	0.703	0.297	2.367	0.14	0.18	11.3	32.1	1.923	1.604	0.5	7.98	3.55	11.58	68.9	30.7	0.692	0.308	2.245	0.13	0.25	1061.74	632.92	1695.68	62.6																		
36.4	0.636	0.364	1.744	0.09	0.18	11.9	34.7	1.96	1.539	0.643	8.74	5.71	14.74	59.3	38.7	0.605	0.395	1.532	0.11	0.23	1595.57	965.28	2565.45	62.2																		
29.6	0.704	0.296	2.375	0.09	0.19	13.8	44.5	2.078	1.774	0.449	21.86	9.74	31.89	68.5	30.5	0.692	0.308	2.244	0.1	0.2	3033.09	1510.52	4545.32	66.7																		
44.5	0.553	0.447	1.235	0.08	0.21	15.9	63.6	2.125	1.15	0.861	10.18	9.07	19.48	52.3	46.5	0.529	0.471	1.123	0.08	0.23	2314.69	1565.08	3891.01	59.5																		
56	0.437	0.563	0.777	0.14	0.21	13.7	35.2	1.787	1.204	0.477	8.18	9.72	18.08	45.3	53.8	0.457	0.543	0.842	0.14	0.21	1506.41	1596.72	3110.34	48.4																		
52.2	0.477	0.523	0.912	0.14	0.18	9.8	27.9	1.779	1.265	0.807	3.57	3.57	7.26	49.2	49.1	0.5	0.5	1.001	0.13	0.2	630.62	665.54	1297.61	48.6																		
24.3	0.756	0.244	3.107	0.07	0.19	12.7	49.8	1.869	1.455	0.733	10.13	5.18	15.58	65	33.2	0.662	0.338	1.956	0.08	0.18	2059.76	1053.74	3119.97	66																		
29.2	0.707	0.293	2.41	0.11	0.3	10.3	29.9	1.756	1.481	0.516	7.14	4.27	11.51	62	37.2	0.625	0.375	1.67	0.11	0.28	1181.46	728.09	1911.58	61.8																		
34.6	0.654	0.346	1.887	0.08	0.17	11	39.2	1.38	1.823	0.496	5.56	4.15	10.02	55.5	41.4	0.573	0.427	1.34	0.08	0.21	1786.66	953.93	2741.6	65.2																		
30.5	0.695	0.305	2.274	0.1	0.28	10	28.9	1.77	1.563	0.775	6.25	3.64	10.1	61.9	36.1	0.632	0.368	1.714	0.08	0.25	1039.64	614.81	1655.24	62.8																		
50.5	0.495	0.505	0.979	0.11	0.18	9.3	22.2	1.75	1.393	0.483	1.91	3.31	5.31	35.9	62.3	0.366	0.634	0.576	0.09	0.18	413.3	523.33	936.78	44.1																		
35.4	0.643	0.357	1.8	0.13	0.3	13	32.1	1.983	1.322	0.662	5.55	6.07	11.84	46.8	51.3	0.478	0.522	0.914	0.12	0.24	1500.75	1040.55	2541.85	59																		
37.8	0.621	0.379	1.641	0.11	0.17	15.1	55.1	2.021	1.41	0.771	12.88	9.43	22.75	56.6	41.4	0.577	0.423	1.365	0.09	0.19	2293.76	1721.72	4019.78	57.1																		
24.5	0.755	0.245	3.075	0.1	0.27	13.3	43.1	2.023	1.372	0.814	10.88	4.96	16.15	67.4	30.7	0.687	0.313	2.193	0.12	0.23	2281.2	855.17	3140.58	72.6																		
32.9	0.668	0.332	2.014	0.14	0.26	15.6	53.6	1.969	1.379	0.827	12	6.74	19.39	61.9	34.8	0.64	0.36	1.78	0.14	0.31	3124.93	1476.09	4628.31	67.5																		
26.2	0.738	0.262	2.818	0.12	0.18	13.5	40.8	2.009	1.584	0.874	10.69	5.12	16.2	66	31.6	0.676	0.324	2.087	0.12	0.2	2416.42	867.82	3292.85	73.4																		
29.9	0.699	0.301	2.325	0.13	0.22	15	54.2	2.112	1.385	0.885	14.29	7.04	21.73	65.8	32.4	0.67	0.33	2.029	0.1	0.21	2594.92	1335.88	3938.64	65.9																		
43.9	0.554	0.446	1.241	0.08	0.22	13.7	63.5	1.794	1.206	1.231	8.47	6.66	15.77	53.7	42.2	0.56	0.44	1.272	0.1	0.21	1359.63	1199.71	2568.65	52.9																		
40.4	0.595	0.405	1.469	0.13	0.18	14.5	56.9	2.066	1.461	0.78	17.92	7.06	25.31	60.8	27.9	0.717	0.283	2.539	0.14	0.21	2997.22	1359.76	4359.61	68.7																		
20.8	0.791	0.209	3.781	0.13	0.18	20.6	70.6	2.424	1.237	0.904	24.91	10.64	36.99	67.3	28.8	0.701	0.299	2.342	0.14	0.19	4238.76	2207.71	6456.96	65.6																		

Figure H.1 (continued) : Data collected during the study.

HRV										EDA										Eye													
Time-frequency										Continuous decomposition analysis										Trough-to-peak analysis						Pupil diameter			Blink frequency				
Wavelet transform																																	
pHF	nLF	nHF	LFHF	peakLF	peakHF		CDA.nSCR	CDA.Amp	CDA.Amp	CDA.SCR	CDA.SCR	CDA.ISCR	CDA.ISCR	CDA.Phasic	CDA.Phasic	CDA.Tonic	CDA.Tonic	TTP.nSCR	TTP.Amp5	TTP.Amp5	Global.	Global.											
(%)	(%)	(%)	(Hz)	(Hz)	(Hz)		frequency	[μs]	[μs]	[μs]	[μs]	[μs]	[μs]	[μs]	[μs]	[μs]	[μs]	frequency	[μs]	[μs]	[μs]	[μs]	mean	std	PerLPD	freq	AECs	PERCLOS					
67.1	0.328	0.672	0.489	0.1	0.27	0.038095	0.052988	0.140748	0.016614	0.038655	0.398732	0.927722	0.3373394	0.8444661	2.392675	2.458564	0.059524	0.051454	0.163869	2.45059	2.569108	26.8769	1.8919	0.0421	0.2548	0.2313	0.0589						
68.9	0.311	0.689	0.451	0.08	0.26	0.077778	0.106039	0.22753	0.026702	0.063693	0.640844	1.528624	0.5384568	1.1285573	2.485819	2.630501	0.066667	0.095423	0.262326	2.597962	2.863571	25.8686	1.9517	0.003	0.3278	0.2091	0.0685						
50.1	0.497	0.503	0.988	0.08	0.28	0.025	0.036114	0.057266	0.010032	0.013402	0.240772	0.321637	0.2024538	0.3138127	2.479353	2.494122	0.05	0.056193	0.156278	2.518474	2.575148	25.7902	1.5092	0.0000	0.3333	0.249	0.083						
29	0.709	0.291	2.438	0.06	0.3	0.038889	0.117621	0.358591	0.027148	0.076897	0.651552	1.845536	0.5259221	1.1080904	2.521391	2.664887	0.088889	0.122911	0.343563	2.718348	2.963123	0	0	0	0	0	0						
31.4	0.686	0.314	2.181	0.1	0.28	0.050847	0.143551	0.319637	0.03303	0.087102	0.792713	2.090458	0.6400006	1.0874136	2.812409	3.10368	0.090395	0.145943	0.423209	2.959467	3.468622	24.6523	1.8616	-0.0441	0.4237	0.2415	0.1023						
63.2	0.367	0.633	0.581	0.1	0.17	0.125	0.096799	0.217101	0.02189	0.04924	0.525368	1.181765	0.5495595	1.124119	3.753422	3.862992	0.175	0.058034	0.243069	3.842665	4.035252	29.2539	1.3089	1.0343	0.1583	0.2144	0.0339						
33.9	0.659	0.341	1.936	0.09	0.15	0.106667	0.120805	0.397095	0.021793	0.073584	0.523032	1.766013	0.5078107	1.3964759	3.684291	3.795538	0.14	0.10016	0.367317	3.79481	4.003466	28.4162	1.9523	0.1018	0.2267	0.2098	0.0476						
73.7	0.261	0.739	0.354	0.06	0.26	0.077778	0.09985	0.249351	0.013525	0.041766	0.324593	1.002385	0.3836299	0.8313877	3.654164	3.67459	0.122222	0.074045	0.27498	3.708651	3.792258	27.8479	1.7418	0.0798	0.2333	0.2233	0.0521						
41.3	0.585	0.415	1.411	0.09	0.27	0.083333	0.165035	0.399337	0.029555	0.078062	0.70933	1.873493	0.6662007	1.7709591	3.71131	3.876235	0.122222	0.126979	0.343114	3.844233	4.237702	27.8914	1.2775	0.0815	0.25	0.2371	0.0593						
42.1	0.578	0.422	1.368	0.05	0.25	0.061111	0.143357	0.331068	0.02674	0.073332	0.64175	1.759972	0.6689766	1.423968	3.663233	4.10805	0.088889	0.16705	0.188903	3.799634	4.15602	28.1037	1.4825	0.0897	0.2722	0.2126	0.0579						
35.6	0.641	0.359	1.787	0.09	0.27	0.078125	0.152787	0.465945	0.028165	0.104328	0.675956	2.503869	0.7530635	2.2210291	3.751076	4.088392	0.129464	0.132278	0.557263	3.9301	4.493368	27.2052	1.4545	0.0549	0.1964	0.2426	0.0477						
42.7	0.573	0.427	1.34	0.1	0.31	0.154167	0.142858	0.671359	0.018055	0.094026	0.433313	2.256617	0.4005041	1.842151	5.033416	5.193298	0.083333	0.099952	0.57141	5.176152	5.83049	27.8763	1.4011	0.0809	0.2375	0.2258	0.0536						
80.7	0.19	0.81	0.235	0.05	0.29	0.033333	0.058072	0.058072	0.013414	0.013414	0.321947	0.1824028	0.1824028	0.1824028	4.734859	4.734859	0.05	0.03402	0.049283	4.790528	4.827722	27.3548	1.1789	0.0607	0.3	0.1899	0.057						
46	0.54	0.46	1.172	0.09	0.29	0.04	0.069614	0.070233	0.017261	0.020064	0.414274	0.481532	0.4564919	0.5972006	4.60714	4.653196	0.02	0.065256	0.067657	4.649935	4.703054	27.9556	1.2565	0.084	0.2	0.2033	0.0407						
50.7	0.492	0.508	0.97	0.1	0.28	0.1	0.155429	0.416403	0.030869	0.08022	0.740851	1.925289	0.5883826	1.7083295	4.664176	4.929605	0.078571	0.121658	0.892786	4.834265	5.097484	28.298	1.353	0.0972	0.3214	0.2139	0.0688						
38.6	0.613	0.387	1.586	0.11	0.28	0.063333	0.094206	0.240894	0.02275	0.05913	0.546	1.41911	0.4391659	1.0699831	4.720616	4.771778	0.076667	0.088406	0.244839	4.811262	4.96303	27.3298	1.3765	0.0597	0.2733	0.1968	0.0538						
48.4	0.515	0.485	1.061	0.08	0.25	0.12945	0.148134	0.788798	0.019361	0.083638	0.464662	2.007309	0.29529	1.0915961	4.656759	5.05291	0.106796	0.09768	0.627749	4.825505	5.449441	27.6305	1.5462	0.0714	0.2848	0.2005	0.0571						
31.3	0.687	0.313	2.193	0.09	0.15	0.080556	0.153245	0.505352	0.030335	0.074571	0.728041	1.789699	0.7098626	1.8258442	4.690502	5.098003	0.094444	0.160315	0.641561	4.874981	5.457297	27.4232	1.6356	0.0633	0.2806	0.1985	0.0557						
42.4	0.574	0.426	1.35	0.1	0.25	0.075	0.111537	0.653159	0.021156	0.107415	0.50774	2.577964	0.4264873	1.6182445	4.768082	5.058299	0.104167	0.093668	0.58838	4.902076	5.312496	27.1231	1.5821	0.0517	0.3333	0.2017	0.0672						
47.6	0.524	0.476	1.101	0.11	0.25	0.05	0.03571	0.1004	0.0061	0.015727	0.146408	0.37746	0.2088394	0.5273663	4.572628	4.708935	0.11	0.066325	0.221505	4.661807	4.94231	27.5365	1.4008	0.0677	0.25	0.2025	0.0506						
35.7	0.642	0.358	1.79	0.11	0.23	0.119231	0.18585	0.478154	0.038984	0.100965	0.935624	2.423164	0.9084701	1.7787587	4.473099	4.724049	0.107692	0.183495	0.573166	4.64406	5.130064	26.9522	1.3298	0.0451	0.3038	0.1981	0.0602						
36.1	0.639	0.361	1.771	0.07	0.22	0.10303	0.128099	0.494741	0.025628	0.108484	0.61506	2.603609	0.6012844	2.7820331	4.168403	4.298247	0.112121	0.135029	0.467133	4.316588	4.709052	27.8038	1.3334	0.0781	0.2788	0.1871	0.0522						
44.2	0.557	0.443	1.259	0.11	0.26	0.133333	0.117472	0.261144	0.020608	0.056612	0.49459	1.358684	0.6510252	2.06117	3.928247	3.9575	0.111111	0.102599	0.268827	4.058072	4.214178	26.5618	1.18	0.0299	0.1667	0.1808	0.0301						
40.7	0.592	0.408	1.451	0.07	0.28	0.144201	0.122131	0.490572	0.022653	0.088583	0.543663	2.126001	0.5243574	1.3863397	3.800797	4.044895	0.134796	0.111092	0.494571	3.91558	4.204628	27.6989	1.9342	0.074	0	0	0						
40	0.6	0.4	1.501	0.09	0.15	0.053333	0.029776	0.057761	0.008471	0.018351	0.203295	0.440424	0.2129976	0.3653631	1.562993	1.590171	0.07	0.034502	0.075151	1.590906	1.639473	30.3558	2.3073	-0.0034	0.1333	0.2257	0.0301						
43.6	0.564	0.436	1.294	0.06	0.18	0.066667	0.031187	0.084769	0.007154	0.014822	0.171688	0.355719	0.23555	0.2873702	1.768392	1.858438	0.083333	0.039151	0.074845	1.813867	1.913994	31.2827	1.9562	0.027	0.2167	0.2796	0.0606						
37.7	0.623	0.377	1.653	0.12	0.15	0.055794	0.030518	0.059055	0.009703	0.013784	0.232877	0.330814	0.177472	0.2301039	1.791425	1.819626	0.04721	0.037129	0.06564	1.823446	1.861415	30.4565	2.61	-0.0001	0.1416	0.2572	0.0364						
37.3	0.627	0.373	1.678	0.13	0.27																	31.3338	2.3513	0.0287	0.069	0.2022	0.0139						
37.6	0.623	0.377	1.653	0.11	0.15	0.023952	0.039592	0.093212	0.011565	0.02709	0.277554	0.650151	0.2123421	0.39647	1.786247	1.804817	0.035928	0.035785	0.113441	1.807244	1.854056	28.2925	2.4199	-0.0712	0.1168	0.2325	0.0272						
33.2	0.668	0.332	2.008	0.09	0.18																	29.2184	1.9048	-0.0408	0.1167	0.1942	0.0227						
40.2	0.597	0.403	1.479	0.11	0.22	0.075	0.028129	0.055805	0.006534	0.015582	0.156813	0.373975	0.186961	0.2717513	2.030294	2.145041	0.066667	0.04061	0.121202	2.093747	2.19001	29.875	1.9573	-0.0192	0.125	0.1957	0.0245						
51.3	0.485	0.515	0.943	0.13	0.21	0.058333	0.045148	0.06309	0.009113	0.013603	0.218716	0.326469	0.1986936	0.2863207	1.887362	1.901609	0.041667	0.04195	0.066565	1.908865	1.921264	27.8517	1.9623	-0.0856	0.075	0.1827	0.0137						
51.3	0.487	0.513	0.948	0.13	0.15	0.040741	0.032356	0.097519	0.008032	0.020491	0.192775	0.491781	0.1636729	0.3848612	1.846813	1.94614	0.059259	0.031514	0.109274	1.850742	1.992184	28.4693	2.5154	-0.0654	0.0926	0.212	0.0196						
33.8	0.662	0.338	1.955	0.12	0.15	0.051988	0.03943	0.096326	0.009416	0.025493	0.225987	0.611826	0.2110104	0.3877646	1.996986	2.063979																	

Participant ID	Step No	Task No	Time interval	Performance result (safe/risky)	Performance score (1-100)	Task loading (1-10)	NASA_TLX score	HRV																				
								Time-based						Frequency-based Welch periodaogram						Frequency-based Lomb-Scargle periodaogram								
								meanHR	SDNN	RMSSD	pNNx	HRVTi	TINN	aLF	aHF	aTotal	pLF	pHF	nLF	nHF	LFHF	peakLF	peakHF	aLF	aHF	aTotal	pLF	
								(bpm)	(ms)	(ms)	(%)	(ms)	(ms)	(ms^2)	(ms^2)	(ms^2)	(%)	(%)	(%)	(%)		(Hz)	(Hz)	(ms^2)	(ms^2)	(ms^2)	(%)	
11	1	1	0-120	Safe	100	2	26	90.3	35.2	17.9	0.6	7.8	61.5	537.08	135.82	680.81	78.9	20	0.798	0.202	3.954	0.1	0.28	0.02	0.005	0.025	79	
		2	120-360	Safe	84	4		88.5	32.8	19.3	0.9	9.3	102.5	421.98	174.89	611.26	69	28.6	0.707	0.293	2.413	0.11	0.31	0.029	0.013	0.043	69	
		3	360-600	Safe	85	5		89.5	37	21.5	2.9	11.3	152.6	1113.87	276.89	1723.38	64.6	16.1	0.801	0.199	4.023	0.08	0.38	0.033	0.025	0.058	57	
		4	600-936	Safe	100	4		87.6	36.5	18.7	0.6	9.4	109.9	389.48	234.69	649.92	59.9	36.1	0.624	0.376	1.66	0.1	0.16	0.022	0.017	0.039	56.1	
	2	1	0-360	Safe	100	3	59.33	91.2	37	22.4	3.2	8.2	95.7	762.15	205.15	1004.33	75.9	20.4	0.788	0.212	3.715	0.11	0.38	0.025	0.005	0.029	83.2	
		2	360-510	Safe	91	5		90.5	49.1	25.7	4.5	12.3	183.1	1293.7	355.12	1700.8	76.1	20.9	0.785	0.215	3.643	0.1	0.23	0.03	0.005	0.035	84.5	
		3	510-660	Safe	68	7		91.6	47.1	41.3	15.7	6.4	94	1126.17	654.18	1887.54	59.7	34.7	0.633	0.367	1.721	0.09	0.17	0.03	0.016	0.046	64.3	
		4	660-870	Safe	67	8		91	61.6	32.8	8.6	7.3	126.5	2862.79	295.35	3307.54	86.6	8.9	0.906	0.094	9.693	0.09	0.16	0.032	0.004	0.036	89.6	
		5	870-1080	Safe	62	5		89.8	64.4	29.4	8.4	8.3	193.4	1820.78	360.94	2330.87	78.1	15.5	0.835	0.165	5.044	0.12	0.16	0.031	0.008	0.039	79.8	
		6	1080-1380	Safe	92	7		89.3	48.7	24.8	4.5	11	185.3	729.22	278.61	1070.82	68.1	26	0.724	0.276	2.617	0.07	0.16	0.027	0.01	0.039	70.9	
		7	1380-1660	Safe	95	5		90	56.9	29.7	9.1	8	140.6	2639.33	377.56	3402.97	77.6	11.1	0.875	0.125	6.991	0.09	0.16	0.026	0.009	0.036	72.7	
		8	1660-1920	Safe	74	4		92.3	45.5	35.1	11.6	7.3	98.4	1425.38	337.93	1825.95	78.1	18.5	0.808	0.192	4.218	0.12	0.16	0.021	0.004	0.026	82.6	
	3	1	0-120	Safe	74	4	87.33	89.1	46.5	36.5	13.9	9.8	161.1	1306.95	420.69	1768.21	73.9	23.8	0.756	0.244	3.107	0.12	0.27	0.032	0.008	0.041	78.6	
		2	120-240	Safe	59	4		90.8	47.1	40.6	20.6	12.2	148.7	1538.06	338.03	1884.88	81.6	17.9	0.82	0.18	4.55	0.11	0.16	0.029	0.006	0.034	83.5	
		3	240-360	Safe	75	6		88.4	51.6	36.1	14.5	7.7	153.6	1785.24	288.54	2178.05	82	13.2	0.861	0.139	6.187	0.11	0.16	0.03	0.007	0.037	80.3	
		4	360-780	Risky	49	8		87.9	56.4	33.9	9.8	10.2	167	2062.47	434.59	2583.2	79.8	16.8	0.826	0.174	4.746	0.11	0.33	0.028	0.006	0.034	81.8	
5		780-1170	Risky	28	7	86.1		52.2	29	7.8	7.3	140.1	989.71	374.11	1422.94	69.6	26.3	0.726	0.274	2.645	0.13	0.16	0.028	0.017	0.046	61.1		
6		1170-1725	Risky	43	11																							
12	1	1	0-240	Safe	100	3	17																					
		2	240-360	Safe	100	4																						
		3	360-540	Safe	100	4																						
		4	540-840	Safe	78	2																						
		5	840-1168	Safe	87	2																						
	2	1	0-120	Safe	100	4	50																					
		2	120-240	Safe	60	4																						
		3	240-480	Safe	57	6																						
		4	480-720	Safe	61	4																						
		5	720-820	Safe	70	3																						
		6	820-1088	Safe	74	5																						
	3	1	0-120	Safe	68	6	60.66																					
		2	120-540	Safe	57	8																						
		3	540-720	Safe	100	8																						
		4	720-970	Risky	26	6																						
		5	970-1080	Risky	26	7																						
		6	1080-1468	Safe	52	7																						
	4	1	0-480	Safe	84	8	78																					
		2	480-915	Safe	50	9																						
		4	915-1170	Safe	52	10																						
5		1170-1350	Risky	28	9																							
6		1350-1590	Risky	27	9																							
7		1590-1726	Risky	28	9																							

Figure H.1 (continued) : Data collected during the study.

HRV							EDA														Eye											
Time-frequency Wavelet transform							Continuous decomposition analysis														Trough-to-peak analysis						Pupil diameter			Blink frequency		
pHF	nLF	nHF	LFHF	peakLF	peakHF		CDA.nSCR	CDA.Amp	CDA.Amp	CDA.SCR	CDA.SCR	CDA.ISCR	CDA.ISCR	CDA.Phasic	CDA.Phasic	CDA.Tonic	CDA.Tonic	TTP.nSCR	TTP.AmpS	TTP.AmpS	Global.	Global.										
(%)	(%)	(%)		(Hz)	(Hz)		frequency	(avg.)	(max.)	(avg.)	(max.)	(avg.)	(max.)	Max (avg.)	Max (max.)	(avg.)	(max)	frequency	(avg.)	(max.)	Mean	Mean	mean	std	PerLPD	freq	A ECS	PERCLOS				
							[muS]	[muS]	[muS]	[muS]	[muS]	[muSxs]	[muSxs]	[muS]	[muS]	[muS]	[muS]	[muS]	[muS]	[muS]	[muS]	[muS]	[muS]									
22.2	0.778	0.222	3.511	0.09	0.28	0.025	0.019587	0.026237	0.007352	0.007397	0.176444	0.177537	0.1427916	0.1523119	0.892798	0.903369	0.033333	0.029558	0.056163	0.921023	0.939837	29.1124	1.5868	0.0151	0.1417	0.3724	0.0528					
29.3	0.707	0.293	2.409	0.11	0.3	0.0125	0.016468	0.022655	0.00468	0.007476	0.112312	0.179416	0.0949652	0.1371407	0.812319	0.855798	0.020833	0.039318	0.09174	0.844821	0.884571	28.6856	1.2111	0.0002	0.1125	0.35	0.0394					
21.5	0.783	0.217	3.602	0.09	0.21	0.033333	0.029264	0.06079	0.005501	0.012135	0.132028	0.291244	0.260632	0.5535881	0.916319	0.947562	0.041667	0.029031	0.06651	0.931783	0.991198	29.2391	1.402	0.0195	0.1875	0.4127	0.0774					
39.2	0.607	0.393	1.544	0.09	0.15	0.008929	0.027725	0.042391	0.007408	0.010069	0.17779	0.241657	0.1754539	0.2852527	0.856999	0.896138	0.020833	0.036626	0.077327	0.887243	0.926794	28.1887	1.4881	-0.0171	0.0863	0.509	0.0439					
22.9	0.771	0.229	3.359	0.1	0.15	0	0	0	0.000458	0.000458	0.010993	0.010993	0.0058477	0.0058477	0.686265	0.686265	0.002778	0.013011	0.013011	0.689909	0.689909	26.286	1.3369	-0.0835	0.1806	0.8827	0.1594					
22.7	0.772	0.228	3.391	0.09	0.15	0	0	0	0.001231	0.001317	0.029549	0.03161	0.0159948	0.0194801	0.699373	0.707655	0.013333	0.021921	0.026522	0.705042	0.713366	26.8583	1.2793	-0.0635	0.2	0.754	0.1508					
33.7	0.661	0.339	1.952	0.08	0.15	0.006667	0.010204	0.010204	0.002466	0.002466	0.059182	0.059182	0.0351551	0.0351551	0.762675	0.762675	0.033333	0.018778	0.034024	0.744265	0.775375	27.3724	1.3561	-0.0456	0.38	0.7735	0.2939					
10.5	0.895	0.105	8.501	0.09	0.15	0	0	0	0.000536	0.000726	0.012859	0.01743	0.0074973	0.0107031	0.771932	0.774373	0.014286	0.012464	0.01372	0.776186	0.776545	26.3023	1.244	-0.0829	0.2952	0.7837	0.2314					
19.3	0.806	0.194	4.156	0.12	0.15	0	0	0	0.001244	0.001784	0.029855	0.042812	0.0163024	0.0251824	0.8168	0.838755	0.019048	0.029722	0.050983	0.821729	0.846645	26.7252	1.5462	-0.0682	0.219	0.611	0.1338					
25.3	0.747	0.253	2.947	0.06	0.15	0.006667	0.015404	0.018336	0.004206	0.004524	0.10094	0.108575	0.0669716	0.0781823	0.845633	0.847276	0.02	0.031373	0.062886	0.856992	0.880312	26.4417	1.0612	-0.078	0.0567	0.422	0.0239					
13.9	0.86	0.14	6.147	0.08	0.15	0.014286	0.01268	0.015299	0.004113	0.004822	0.098714	0.115739	0.0602818	0.0629682	0.887123	0.903284	0.032143	0.019988	0.03672	0.900288	0.924809	25.9487	1.1762	-0.0952	0.0571	0.1997	0.0114					
21.7	0.782	0.218	3.59	0.12	0.15	0	0	0	0.000086	0.000086	0.002052	0.002052	0.0022118	0.0022118	0.679489	0.679489	0.008333	0.020571	0.020571	0.680224	0.680224	26.757	0.9753	-0.0671	0.0417	0.2009	0.0084					
25.8	0.742	0.258	2.873	0.13	0.15																	27.2956	1.0805	-0.0483	0.025	0.1581	0.0026					
23	0.77	0.23	3.353	0.1	0.15	0	0	0	0.000284	0.000284	0.006825	0.006825	0.0037655	0.0037655	0.681223	0.681223	0.008333	0.016724	0.016724	0.683546	0.683546	27.2778	0.9275	-0.0489	0	0	0					
16.1	0.839	0.161	5.208	0.11	0.15	0.002381	0.011118	0.011118	0.003038	0.003038	0.072908	0.072908	0.0493496	0.0493496	0.675939	0.675939	0.004762	0.02207	0.023146	0.681143	0.681226	27.3423	1.1833	-0.0466	0.0357	0.1714	0.0061					
20.3	0.796	0.204	3.909	0.11	0.15	0.002564	0.011412	0.011412	0.003306	0.003306	0.079354	0.079354	0.0604067	0.0604067	0.707471	0.707471	0.025641	0.022014	0.04996	0.694525	0.735443	26.8461	1.5133	-0.0639	0.0718	0.1958	0.0141					
28.8	0.711	0.289	2.463	0.12	0.15	0.005405	0.012479	0.015344	0.007569	0.010666	0.181666	0.255973	0.1504338	0.2369871	0.764472	0.90345	0.014414	0.045213	0.106767	0.773433	0.933165	27.2239	1.6403	-0.0508	0.0541	0.2403	0.013					

Figure H.1 (continued) : Data collected during the study.

Participant ID	Step No	Task No	Time Interval	Performance result (safe/risky)	Performance score (1-100)	Task loading (1-10)	NASA_TLX score	HRV																			
								Time-based						Frequency-based Welch periodogram						Frequency-based Lomb-Scargle periodogram							
								meanHR	SDNN	RMSSD	pNNx	HRVTi	TINN	aLF	aHF	aTotal	pLF	pHF	nLF	nHF	LFHF	peakLF	peakHF	aLF	aHF	aTotal	pLF
								(bpm)	(ms)	(ms)	(%)	(ms)	(ms)	(ms ²)	(ms ²)	(ms ²)	(%)	(%)	(%)	(%)		(Hz)	(Hz)	(ms ²)	(ms ²)	(ms ²)	(%)
13	1	1	0-120	Safe	100	2	13.33	70.6	54.9	46.3	30	8.3	126.5	1516.59	764.88	2402.36	63.1	31.8	0.665	0.335	1.983	0.1	0.3	0.037	0.019	0.057	64.3
		2	120-340	Safe	100	4		70.1	55.6	45.2	25.2	7.3	79.1	980.62	783.06	1847.01	53.1	42.4	0.556	0.444	1.252	0.1	0.29	0.019	0.01	0.03	63.2
		3	340-500	Safe	85	5		73.1	51.5	42.7	25.5	9	153.8	948.96	792.33	1819.35	52.2	43.6	0.545	0.455	1.198	0.09	0.27	0.027	0.014	0.042	64.9
		4	500-690	Safe	100	4		71.1	58.8	47.8	25.7	8.1	148.4	1035.85	900.46	2034.52	50.9	44.3	0.535	0.465	1.15	0.11	0.3	0.05	0.036	0.088	57.3
	2	1	0-180	Safe	85	3	46	88.2	48.2	28.9	5.1	12.1	177.2	1274.05	307.72	1620.63	78.6	19	0.805	0.195	4.14	0.11	0.33	0.017	0.004	0.021	79.9
		2	180-420	Safe	100	5		83.2	60.7	27.9	6.7	11	184.6	1092.99	322.99	1463.98	74.7	22.1	0.772	0.228	3.384	0.12	0.32	0.032	0.011	0.044	74
		3	420-690	Safe	74	7		77.9	62.3	35.6	14.7	8.9	197.8	2078.79	457.42	2616.57	79.4	17.5	0.82	0.18	4.545	0.11	0.27	0.021	0.003	0.024	85.8
		4	690-1560	Safe	87	8		76.2	62.5	39.3	16.4	9.6	234.4	2125.31	519.17	2746.13	77.4	18.9	0.804	0.196	4.094	0.11	0.3	0.032	0.01	0.042	75.3
		5	1560-1680	Safe	100	5		74.2	74.3	51.1	27	9.5	231.9	3833.05	928.19	4822.89	79.5	19.2	0.805	0.195	4.13	0.11	0.27	0.024	0.004	0.028	86.6
		6	1680-1980	Safe	90	7		74	61	40.2	21.3	9.3	190.2	2531.29	581.64	3229.5	78.4	18	0.813	0.187	4.352	0.11	0.16	0.036	0.011	0.047	75.8
		7	1980-2349	Safe	76	5		73.5	77.7	50.4	21.8	9.5	246.1	2891.12	838.08	3969.97	72.8	21.1	0.775	0.225	3.45	0.12	0.16	0.018	0.005	0.024	74.2
		8	0-150	Safe	74	4		77.8	55.9	34.8	13.5	8.4	129.9	1313.48	589	1961.58	67	30	0.69	0.31	2.23	0.12	0.34	0.021	0.008	0.03	71.1
	3	2	150-300	Safe	100	4	80.66	77.9	80.7	44.4	20.5	9.8	251.2	3275.52	548.97	3853.78	85	14.2	0.856	0.144	5.967	0.11	0.34	0.029	0.006	0.036	82.6
		3	300-420	Safe	87	6		75	53.6	35.8	15.5	12.4	234.6	986.89	465.14	1535.22	64.3	30.3	0.68	0.32	2.122	0.11	0.27	0.026	0.014	0.041	62.4
		4	420-600	Safe	58	8		76.2	83.1	44.5	19.5	11.4	349.1	2369.2	669.3	3170.61	74.7	21.1	0.78	0.22	3.54	0.1	0.16	0.061	0.013	0.074	82.3
		5	600-900	Safe	74	7		74.1	61.6	41.4	18.8	9.1	180.2	1580.05	799.73	2469.02	64	32.4	0.664	0.336	1.976	0.12	0.16	0.021	0.006	0.027	77.3
14	1	1	0-300	Safe	100	3	7.33	80.7	35.4	19.6	1.3	9.1	99.6	413.39	136.66	585.93	70.6	23.3	0.752	0.248	3.025	0.07	0.31	0.008	0.008	0.016	51.5
		2	300-420	Safe	100	4		82.9	38.7	20.6	1.8	10.9	129.2	730.48	114.6	907.74	80.5	12.6	0.864	0.136	6.374	0.1	0.21	0.031	0.005	0.037	84.1
		3	420-780	Safe	100	4		84.6	39	18.1	2	9.9	120.4	462.18	101	643.37	71.8	15.7	0.821	0.179	4.576	0.06	0.16	0.039	0.01	0.049	79.3
		4	780-960	Safe	100	2		84.5	29.8	16.8	1.6	8.7	83	405.65	86.57	524.59	77.3	16.5	0.824	0.176	4.686	0.11	0.27	0.034	0.01	0.045	76.5
	2	5	960-1140	Safe	86	2	34.33	83.8	33.6	17.8	0.8	9.9	112.3	630.18	77.68	792.76	79.5	9.8	0.89	0.11	8.113	0.07	0.35	0.035	0.014	0.05	69.3
		1	0-120	Safe	100	4		83.3	33.7	19.3	1.8	6.7	15.4	526.58	136.4	690.03	76.3	19.8	0.794	0.206	3.861	0.11	0.28	0.026	0.007	0.033	78.8
		2	120-240	Safe	57	4		84	47.6	23	4.8	11.1	166.5	943.2	223.63	1214.16	77.7	18.4	0.808	0.192	4.218	0.12	0.31	0.028	0.006	0.034	81
		3	240-360	Safe	46	6		84.7	41.3	21.1	1.2	9.9	127	910.49	131.34	1151.51	79.1	11.4	0.874	0.126	6.932	0.1	0.31	0.04	0.004	0.045	89.3
		4	360-600	Safe	61	4		84.1	50.1	31	5.5	6.4	102.1	1377.83	267.07	1733.29	79.5	15.4	0.838	0.162	5.159	0.1	0.16	0.03	0.004	0.034	88.5
		6	600-984	Risky	46	5		82.2	69.9	32.8	9.7	9.9	246.1	2237.74	273.08	2724.99	82.1	10	0.891	0.109	8.194	0.09	0.16	0.025	0.006	0.031	79.7
		1	0-240	Safe	54	6		82.2	46.1	23.4	4	9.6	113.3	1038.96	141.16	1244.83	83.5	11.3	0.88	0.12	7.36	0.09	0.37	0.037	0.005	0.043	86.5
		2	240-300	Safe	63	8		83	39.9	21.3	2.5	5.9	9.3	290.11	234.26	531.57	54.6	44.1	0.553	0.447	1.238	0.1	0.18	0.028	0.025	0.053	52.9
	3	3	300-420	Safe	66	8	42	84	51.9	27.2	7.2	12	181.6	1224.48	194.94	1463.18	83.7	13.3	0.863	0.137	6.281	0.11	0.34	0.041	0.007	0.048	85.3
		4	420-540	Safe	74	6		85.5	61	32.1	10.8	11.2	190.4	2073.84	193.14	2413.78	85.9	8	0.915	0.085	10.737	0.09	0.26	0.028	0.003	0.031	90.5
5		540-840	Risky	0	7	78.9		62.7	27.3	7.4	10.9	228.5	1495.25	210.67	1820.51	82.1	11.6	0.877	0.123	7.097	0.09	0.16	0.033	0.008	0.041	80.3	
6		840-1083	Safe	68	7	75.2		40.7	24.8	4.3	7.4	99.1	585.7	219.99	878.78	66.6	25	0.727	0.273	2.662	0.09	0.32	0.042	0.011	0.056	75.6	
4	1	0-390	Safe	100	8	66	78.6	47.4	23.8	3.2	13.5	205.3	756.19	180.36	1018.2	74.3	17.7	0.807	0.193	4.193	0.09	0.33	0.034	0.008	0.043	77.8	
	2	390-720	Safe	63	9		78.1	42.7	22.8	3.8	10.4	141.6	549.35	212.61	795.74	69	26.7	0.721	0.279	2.584	0.1	0.33	0.017	0.006	0.023	73.5	
	3	720-900	Safe	51	7		78	50.8	22.1	3.4	9.3	170.9	584.9	183.17	866.92	67.5	21.1	0.762	0.238	3.193	0.08	0.28	0.022	0.01	0.034	64	
	4	900-1200	Risky	25	10		77	52.6	25.2	5.8	10.2	180.7	835.7	193.95	1137.56	73.5	17	0.812	0.188	4.309	0.07	0.34	0.039	0.012	0.052	73.6	
	5	1200-1380	Safe	77	9		78.3	62	30.3	9.7	7.1	149.2	1755.76	348.88	2350.76	74.7	14.8	0.834	0.166	5.033	0.07	0.22	0.039	0.009	0.049	78.4	
	7	1380-1800	Risky	42	9		77.1	54	26	5.4	9.6	180.9	965.05	237.94	1287.73	74.9	18.5	0.802	0.198	4.056	0.08	0.37	0.046	0.011	0.058	79.1	
	8	1800-2056	Risky	49	8		77.5	77.8	30.9	9.3	9.3	250.5	1104.01	270.2	1573.53	70.2	17.2	0.803	0.197	4.086	0.06	0.28	0.038	0.011	0.052	72.3	

Figure H.1 (continued) : Data collected during the study.

HRV

HRV																									
Frequency-based Lomb-Scargle periodogram						Non-linear						Time-frequency Lomb-Scargle periodogram								Time-frequency Wavelet transform					
pHF	nLF	nHF	LFHF	peakLF	peakHF	SD1	SD2	sampen	alpha1	alpha2	aLF	aHF	aTotal	pLF	pHF	nLF	nHF	LFHF	peakLF	peakHF	aLF	aHF	aTotal	pLF	
(%)	(%)	(%)	(Hz)	(Hz)	(ms)	(ms)					(ms ²)	(ms ²)	(ms ²)	(%)	(%)	(%)	(%)			(Hz)	(Hz)	(ms ²)	(ms ²)	(ms ²)	(%)
32.6	0.664	0.336	1.976	0.09	0.3	32.9	70.3	1.842	1.077	0.372	37.45	26.6	67.21	55.7	39.6	0.585	0.415	1.408	0.11	0.29	7145.49	4107.44	11318.35	63.1	
33.6	0.653	0.347	1.882	0.1	0.25	32.1	71.9	1.8	1.125	1.028	32.81	26.61	62.38	52.6	42.7	0.552	0.448	1.233	0.1	0.28	5978.98	4213.37	10271.51	58.2	
34.2	0.655	0.345	1.896	0.1	0.28	30.3	66.2	2.929	1.092	0.564	28.07	24.92	55.05	51	45.3	0.53	0.47	1.126	0.09	0.28	5323.58	4084.75	9440.09	56.4	
41.3	0.581	0.419	1.389	0.09	0.28	33.9	76	1.745	1.198	0.875	29.96	31.31	63.33	47.3	49.4	0.489	0.511	0.957	0.12	0.3	5712.33	4720.9	10490.63	54.5	
20	0.799	0.201	3.987	0.12	0.17	20.5	65.1	2.144	1.448	0.54	33.55	9.57	44.06	76.2	21.7	0.778	0.222	3.505	0.12	0.24	6014.12	1804.77	7827.05	76.8	
24.9	0.748	0.252	2.975	0.1	0.17	19.7	83.5	1.329	1.479	0.915	35.28	10.15	46.5	75.9	21.8	0.777	0.223	3.476	0.12	0.33	5730.49	1776.28	7529.97	76.1	
12.7	0.871	0.129	6.74	0.12	0.21	25.2	84.5	1.594	1.491	0.729	59.51	16.56	78.67	75.6	21	0.782	0.218	3.594	0.12	0.2	10483.2	2660	13208.69	79.4	
23.9	0.759	0.241	3.155	0.12	0.21	27.8	83.9	1.669	1.47	0.629	63.68	19.2	84.83	75.1	22.6	0.768	0.232	3.316	0.11	0.3	11556.05	3122.48	14748.97	78.4	
13.2	0.868	0.132	6.55	0.11	0.21	36.2	98.6	1.783	1.451	0.609	114.92	33.45	149.71	76.8	22.3	0.775	0.225	3.436	0.11	0.19	17640.83	5284.86	22941.01	76.9	
23.4	0.764	0.236	3.245	0.1	0.17	28.4	81.5	1.761	1.409	0.557	71.05	24.72	99.33	71.5	24.9	0.742	0.258	2.874	0.11	0.17	13110.77	3465.82	16601.42	79	
22.5	0.767	0.233	3.297	0.13	0.21	35.7	104	1.777	1.333	0.781	90.6	28.16	125.64	72.1	22.4	0.763	0.237	3.217	0.12	0.24	16123.33	4999.03	21362.99	75.5	
25.5	0.736	0.264	2.781	0.11	0.19	24.7	75.1	1.644	1.296	0.66	44.08	19.2	64.42	68.4	29.8	0.697	0.303	2.295	0.11	0.3	6970.37	3038.89	10057.31	69.3	
17	0.829	0.171	4.861	0.1	0.17	31.5	109.8	1.768	1.678	0.732	104.33	24.96	131.72	79.2	18.9	0.807	0.193	4.18	0.1	0.24	15762.53	3697.67	19467.06	81	
34.5	0.644	0.356	1.807	0.11	0.28	25.4	71.4	1.691	1.657	0.618	36.86	15.39	55.49	66.4	27.7	0.705	0.295	2.395	0.1	0.28	6514.84	2906.17	9451.45	68.9	
17.1	0.828	0.172	4.827	0.11	0.2	31.6	113.2	1.838	1.53	0.694	76.18	27.11	106.99	71.2	25.3	0.738	0.262	2.81	0.11	0.18	14090.4	4183.21	18322.18	76.9	
22.4	0.775	0.225	3.452	0.13	0.21	29.3	82	1.667	1.386	0.539	49.43	26.66	78.12	63.3	34.1	0.65	0.35	1.854	0.13	0.18	8218.86	4373.57	12620.55	65.1	
17.3	0.823	0.177	4.655	0.12	0.2	34.3	86	1.855	1.382	0.523	82.87	28.91	115.11	72	25.1	0.741	0.259	2.867	0.11	0.19	13742.71	4648.18	18518.81	74.2	
18.9	0.806	0.194	4.156	0.08	0.21	29.2	86.7	1.69	1.442	0.606	66.34	21.33	92.27	71.9	23.1	0.757	0.243	3.11	0.11	0.29	11421.06	3484.83	15012.09	76.1	
47.3	0.521	0.479	1.089	0.07	0.17	13.9	48.2	1.968	1.454	0.869	13.11	4.81	19.08	68.7	25.2	0.731	0.269	2.723	0.06	0.31	2316.25	753.01	3073.78	75.4	
12.4	0.872	0.128	6.799	0.09	0.17	14.6	52.8	2.113	1.603	0.706	25.09	4.96	31.74	79	15.6	0.835	0.165	5.06	0.09	0.22	3873.04	803.46	4733.76	81.8	
19.8	0.8	0.2	4.005	0.06	0.17	12.8	53.6	1.871	1.552	0.86	14.97	4.1	20.88	71.7	19.6	0.785	0.215	3.653	0.06	0.22	2836.31	587.31	3469.46	81.8	
22.9	0.77	0.23	3.341	0.07	0.2	11.9	40.5	1.859	1.515	0.825	13.64	3.2	17.53	77.8	18.2	0.81	0.19	4.269	0.11	0.25	2160.25	489.82	2673.75	80.8	
28.3	0.71	0.29	2.449	0.11	0.22	12.6	45.9	2.029	1.457	0.959	12.66	5.54	19.64	64.5	28.2	0.696	0.304	2.285	0.07	0.22	3499.12	445.93	3974.27	88	
21	0.79	0.21	3.758	0.11	0.17	13.7	45.6	2.146	1.606	0.731	18.14	4.93	23.56	77	20.9	0.786	0.214	3.682	0.12	0.21	2639.89	906.81	3549.33	74.4	
17.8	0.819	0.181	4.538	0.12	0.17	16.3	65.3	2.254	1.703	0.885	29.36	6.55	36.96	79.4	17.7	0.818	0.182	4.482	0.13	0.25	4625.39	1274.35	5922.32	78.1	
9	0.908	0.092	9.872	0.11	0.2	15	56.4	2.403	1.547	0.659	28.35	4.47	34.69	81.7	12.9	0.864	0.136	6.348	0.1	0.21	5167.79	784.5	5979.21	86.4	
11	0.889	0.111	8.035	0.11	0.18	22	67.4	2.358	1.428	0.701	43.14	9.98	54.87	78.6	18.2	0.812	0.188	4.323	0.11	0.2	7579.15	1678.6	9281.12	81.7	
18.9	0.808	0.192	4.21	0.09	0.22	23.2	96.2	1.474	1.67	0.775	73.99	11.72	91.01	81.3	12.9	0.863	0.137	6.316	0.09	0.23	12909.16	1615.25	14584.32	88.5	
11.7	0.881	0.119	7.369	0.08	0.25	16.6	63.1	2.1	1.691	0.744	31.45	6.04	39.46	79.7	15.3	0.839	0.161	5.204	0.08	0.22	5454.56	788.5	6265	87.1	
46.5	0.532	0.468	1.138	0.11	0.18	15.2	54.4	2.056	1.597	1.063	11.36	9.23	21.03	54	43.9	0.552	0.448	1.231	0.11	0.18	1204.41	1049.37	2256.51	53.4	
14	0.859	0.141	6.081	0.11	0.19	19.3	70.8	2.281	1.589	0.722	34.53	6.58	42.01	82.2	15.7	0.84	0.16	5.25	0.11	0.2	6226.64	1044.63	7283.64	85.5	
8.2	0.917	0.083	11.063	0.09	0.18	22.8	83.3	1.527	1.585	0.725	51.08	8.1	62.03	82.3	13.1	0.863	0.137	6.306	0.09	0.18	10450.89	1119.64	11611	90	
18.6	0.812	0.188	4.317	0.09	0.17	19.4	86.5	1.34	1.689	0.813	46.69	8.34	59.2	78.9	14.1	0.848	0.152	5.595	0.11	0.18	8455.76	1316.04	9800.81	86.3	
19.7	0.794	0.206	3.843	0.09	0.18	17.6	54.8	2.244	1.32	0.83	17.72	7.78	27.84	63.7	28	0.695	0.305	2.278	0.09	0.18	3427.64	1276.33	4760.58	72	
19.1	0.803	0.197	4.065	0.08	0.18	16.8	64.9	2.305	1.543	0.955	23.41	6.83	32.49	72.1	21	0.774	0.226	3.426	0.09	0.22	4323.43	1042.11	5414.48	79.8	
26.2	0.738	0.262	2.811	0.11	0.35	16.2	58.2	2.21	1.521	0.843	17.84	6.82	25.69	69.5	26.6	0.723	0.277	2.615	0.11	0.19	2950.85	1101.2	4070.06	72.5	
28.8	0.689	0.311	2.22	0.1	0.22	15.7	70	2.256	1.408	0.93	19.34	6.86	29.12	66.4	23.6	0.738	0.262	2.818	0.1	0.22	3278.07	973.1	4328.2	75.7	
23.1	0.761	0.239	3.188	0.11	0.21	17.8	72.2	1.214	1.598	0.983	25.31	7.74	35.45	71.4	21.8	0.766	0.234	3.271	0.07	0.21	5004.02	1102.79	6179.02	81	
18.9	0.805	0.195	4.138	0.06	0.18	21.5	85	1.432	1.531	0.905	52.24	12.63	69.78	74.9	18.1	0.805	0.195	4.137	0.1	0.22	9791.81	1748.69	11618.82	84.3	
19.6	0.801	0.199	4.029	0.07	0.2	18.4	74.2	1.348	1.48	0.963	31.37	8.01	41.79	75.1	19.2	0.797	0.203	3.915	0.08	0.19	5331.21	1338.4	6724.89	79.3	
21.7	0.769	0.231	3.325	0.09	0.18	21.9	107.9	1.368	1.727	1.192	34.34	8.85	49	70.1	18.1	0.795	0.205	3.879	0.09	0.28	6754.06	1553.83	8489.35	79.6	

Figure H.1 (continued) : Data collected during the study.

HRV							EDA														Eye											
Time-frequency Wavelet transform							Continuous decomposition analysis														Trough-to-peak analysis						Pupil diameter			Blink frequency		
pHF	nLF	nHF	LFHF	peakLF	peakHF		CDA.nSCR	CDA.Amp Sum	CDA.Amp Sum	CDA.SCR (avg.)	CDA.SCR (max.)	CDA.ISCR (avg.)	CDA.ISCR (max.)	CDA.Phasic Max (avg.)	CDA.Phasic Max (max.)	CDA.Tonic (avg.)	CDA.Tonic (max.)	TTP.nSCR	TTP.AmpSum (avg.)	TTP.AmpSum (max.)	Global Mean (avg.)	Global Mean (max.)	mean	std	PerLPD	freq	AECS	PERCLOS				
(%)	(%)	(%)	(Hz)	(Hz)			frequency	[muS]	[muS]	[muS]	[muS]	[muS]	[muS]	[muS]	[muS]	[muS]	[muS]	frequency	[mu uS]	[m uS]	[muS]	[muS]										
36.3	0.635	0.365	1.74	0.1	0.3	0.15	0.53704	1.567462	0.069105	0.166441	1.658527	3.994572	1.8698881	4.1432638	2.697105	2.9566	0.166667	0.48039	1.19869	3.189885	3.782157	27.6409	2.2383	-0.0156	0.325	0.4185	0.136					
41	0.587	0.413	1.419	0.1	0.28	0.163636	0.282176	1.352069	0.039952	0.178184	0.958844	4.276408	1.1662451	3.7122232	2.38551	2.820549	0.154545	0.367453	1.1687	2.789567	4.04318	28.0791	2.0607	0.0000	0.3409	0.3119	0.1063					
43.3	0.566	0.434	1.303	0.09	0.27	0.069231	0.271763	0.840347	0.030843	0.088817	0.740236	2.131599	0.8783979	2.1902847	2.704053	3.106938	0.103846	0.253238	0.870504	2.934618	4.050158	28.5092	1.9135	0.0153	0.2385	0.2969	0.0708					
45	0.548	0.452	1.21	0.11	0.28	0.121053	0.359752	1.157025	0.052072	0.150438	1.249736	3.610524	1.2545186	3.4185851	2.586684	2.984261	0.142105	0.311087	1.171918	2.959488	3.667967	28.4183	2.1982	0.012	0.4	0.2895	0.1158					
23.1	0.769	0.231	3.332	0.11	0.15	0.205556	0.336299	0.823654	0.04114	0.124351	0.987368	2.984428	1.258625	2.6996474	9.361836	9.492713	0.261111	0.302149	0.790683	9.713619	10.16088	27.6743	1.6261	-0.0144	0.2667	0.4951	0.132					
23.6	0.763	0.237	3.226	0.12	0.32	0.208333	0.387018	1.369516	0.045334	0.137488	1.088027	3.299722	1.200723	3.3388449	9.401474	9.673366	0.25	0.306387	1.141863	9.775865	10.45785	27.3535	1.5962	-0.0259	0.375	0.4121	0.1545					
20.1	0.798	0.202	3.941	0.11	0.15	0.181481	0.52826	1.505837	0.062989	0.189085	1.511729	4.538043	1.7748541	4.4935599	9.443761	9.905925	0.248148	0.424081	1.452653	9.891641	10.69035	27.3018	1.5275	-0.0277	0.2704	0.4148	0.1122					
21.2	0.787	0.213	3.701	0.11	0.15	0.186207	0.509012	1.842524	0.057841	0.25025	1.388194	6.005991	1.5678683	4.6904939	9.119192	9.67267	0.225287	0.495882	1.782038	9.608795	10.58301	27.3126	1.7514	-0.0273	0.3437	0.3659	0.1258					
23	0.769	0.231	3.338	0.11	0.15	0.158333	0.823106	2.213048	0.088369	0.226711	2.120853	5.441062	2.5096424	6.1256645	8.760659	8.973255	0.175	0.743579	2.153886	9.453879	10.2703	26.8786	1.7977	-0.0428	0.2833	0.2808	0.0796					
20.9	0.791	0.209	3.783	0.11	0.15	0.196667	0.688882	2.840433	0.072275	0.249702	1.734593	5.992853	1.8496844	5.3940237	8.587268	9.121835	0.21	0.593281	2.377752	9.185618	10.33785	26.5536	1.5564	-0.0544	0.2333	0.2892	0.0675					
23.4	0.763	0.237	3.225	0.12	0.15	0.195122	0.818975	3.539697	0.103266	0.435736	2.478374	10.88967	2.3465922	8.7358702	9.47054	13.07799	0.203252	0.69985	4.34114	10.35553	15.59543	26.7624	1.7115	-0.0469	0.3225	0.2865	0.0924					
30.2	0.696	0.304	2.294	0.11	0.33	0.173333	0.515313	2.017456	0.068777	0.167102	1.650647	4.010451	1.8761452	5.2346514	10.83659	11.13801	0.186667	0.580178	2.158464	11.41855	12.68043	28.3404	1.6472	0.0093	0.18	0.51	0.0918					
19	0.81	0.19	4.263	0.1	0.15	0.206667	0.564524	2.269568	0.067788	0.279839	1.62692	6.716141	1.4384156	3.7065982	10.74704	11.17199	0.206667	0.56517	2.620924	11.37427	13.23196	27.7121	1.7469	-0.0131	0.34	0.4236	0.144					
30.7	0.692	0.308	2.242	0.1	0.26	0.208333	0.322426	1.186581	0.045117	0.149956	1.08281	3.598951	1.1974669	3.2314539	10.5186	11.1131	0.216667	0.388595	1.242832	10.9677	12.29538	27.0486	1.2982	-0.0367	0.3083	0.4152	0.128					
22.8	0.771	0.229	3.368	0.1	0.15	0.144444	0.664148	4.502024	0.091665	0.491047	2.199968	11.78513	2.4707746	6.7478448	10.38356	10.94113	0.177778	0.752788	3.314611	11.11444	12.96424	26.9319	1.7392	-0.0409	0.2333	0.4625	0.1079					
34.7	0.653	0.347	1.879	0.12	0.15	0.156667	0.753144	2.439784	0.08938	0.268225	2.14513	6.437388	2.2026862	6.4140354	9.920398	10.61371	0.19	0.622479	2.396379	10.58665	12.3356	26.4984	1.9112	-0.0563	0.3133	0.2612	0.0818					
25.1	0.747	0.253	2.957	0.11	0.15	0.175	0.836368	4.057095	0.096755	0.308095	2.322114	7.394289	2.4318045	7.3967221	9.457335	9.95581	0.181818	0.769446	3.005899	10.25237	12.21994	26.8595	1.7798	-0.0435	0.325	0.3143	0.1021					
23.2	0.766	0.234	3.277	0.11	0.15	0.159836	0.749277	4.393286	0.087218	0.431683	2.093229	10.36038	2.3251484	9.6325584	8.330899	9.011608	0.159836	0.751461	4.198792	9.081669	11.34746	25.9482	1.6618	-0.0759	0.3484	0.3601	0.1254					
24.5	0.755	0.245	3.076	0.06	0.15	0.256667	0.284301	1.550736	0.03937	0.225005	0.944871	5.400116	1.1651593	2.8810482	9.331796	10.77847	0.206667	0.28908	1.955256	9.684388	11.2757	24.3268	2.0057	-0.0159	0.1033	0.2574	0.0266					
17	0.828	0.172	4.82	0.09	0.15	0.25	0.34438	1.12153	0.051182	0.1542	1.22836	3.700797	1.5552884	2.9392208	10.63461	11.18747	0.225	0.349267	1.442404	11.05113	11.86608	27.0124	2.5241	0.0927	0.1917	0.2758	0.0529					
16.9	0.828	0.172	4.829	0.05	0.15	0.263889	0.284066	1.102324	0.03779	0.131239	0.906956	3.149728	1.0655919	2.460647	11.246	12.08309	0.2	0.27784	1.156344	11.55635	12.88396	26.2986	2.2702	0.0639	0.1889	0.3205	0.0605					
18.3	0.815	0.185	4.41	0.11	0.28	0.172222	0.398068	1.545406	0.055388	0.219239	1.32993	5.261728	1.2666123	3.0368575	11.40023	11.83827	0.166667	0.319145	1.476792	11.83805	12.61359	24.7202	1.7626	0.0000	0.2222	0.3389	0.0753					
11.2	0.887	0.113	7.847	0.06	0.15																	25.3814	1.9243	0.0268	0.2	0.25	0.05					
25.5	0.744	0.256	2.911	0.11	0.15	0.158333	0.186133	0.868289	0.026874	0.121034	0.644978	2.904808	0.7503214	2.1430024	13.12419	13.8917	0.141667	0.167029	0.770776	13.35837	14.38958	24.1555	1.6713	-0.0228	0.0833	0.196	0.0163					
21.5	0.784	0.216	3.63	0.12	0.15	0.225	0.327394	1.728303	0.051929	0.18763	1.246305	4.503126	1.4574179	2.6945082	13.80945	14.55457	0.208333	0.307372	1.69466	14.21063	15.1523	25.1495	1.84	0.0174	0.15	0.2248	0.0337					
13.1	0.868	0.132	6.587	0.06	0.15	0.291667	0.244522	0.71639	0.033753	0.121183	0.810072	2.908382	0.8934041	1.7964612	13.76874	14.06453	0.266667	0.18376	1.181199	14.00627	14.48701	23.9006	1.2786	-0.0331	0	0	0					
18.1	0.819	0.181	4.515	0.1	0.15	0.241667	0.254213	0.899056	0.037464	0.137823	0.899146	3.307759	1.0276926	2.6688646	13.80532	14.44461	0.220833	0.200295	0.906641	14.02652	14.8727	24.5505	2.096	-0.0069	0.2	0.2106	0.0421					
11.1	0.889	0.111	7.992	0.09	0.15	0.260417	0.257852	0.695684	0.035835	0.112271	0.860039	2.694515	0.9251443	2.4272082	14.7403	15.20835	0.221354	0.213577	1.026281	15.0357	15.84687	25.4787	1.5883	0.0307	0.2214	0.2103	0.0466					
12.6	0.874	0.126	6.918	0.08	0.15	0.208333	0.129791	0.338684	0.024924	0.057891	0.598185	1.389376	0.6438972	1.6102948	16.81111	17.85127	0.1125	0.15197	0.696644	16.85087	18.18306	30.7799	1.586	0.2451	0	0	0					
46.5	0.534	0.466	1.148	0.1	0.17	0.15	0.225365	0.512001	0.042178	0.107504	1.012272	2.580103	0.9225106	1.7251308	18.44448	19.04542	0.15	0.281678	1.348809	18.7036	19.29592	29.9285	1.994	0.2107	0.2167	0.2077	0.045					
14.3	0.856	0.144	5.961	0.11	0.33	0.266667	0.282778	0.815166	0.046095	0.115005	1.106287	2.760124	1.1718875	2.0690559	19.65303	20.78305	0.191667	0.251221	0.693792	19.97655	21.12099	31.0294	2.0684	0.2552	0.175	0.2143	0.0375					
9.6	0.903	0.097	9.334	0.09	0.15																	31.1368	2.6911	0.2596	0.1667	0.2216	0.0369					
13.4	0.865	0.135	6.425	0.1	0.15	0.276667	0.275948	1.065976	0.03789	0.161668	0.909357	3.880036	0.9594338	2.3389614	20.78988	21.35684	0.17	0.261642	1.63173	21.09203	21.75045	30.352	2.3062	0.2278	0.1467	0.2166	0.0318					
26.8	0.729	0.271	2.886	0.05	0.31	0.279833	0.299301	1.706463	0.039695	0.235004	0.952682	5.640107	1.1792522	2.9386471	20.7807	21.52813	0.226337	0.28207	1.681198	21.0797	22.62981	28.5243	1.8696	0.1539	0.1646	0.2069	0.0341					
19.2	0.806	0.194	4.149	0.09	0.32	0.312821	0.266936	0.939397	0.034901	0.145956	0.837634	3.502937	0.8608854	1.9771232	21.36998	22.17248	0.241026	0.205949	1.050354	21.63011	22.56503	28.9346	1.7442	0.1705	0.1667	0.2139	0.0357					
27.1	0.728	0.272	2.68	0.1	0.15	0.372727	0.245542	1.385189	0.031331	0.170641	0.751936	4.09538	0.6796139	1.6507159	20.80808	21.33834	0.236364	0.181601	1.552849	21.05296	21.74762	28.1274	1.9525	0.1378	0.1273	0.2006	0.0255					
22.5	0.771	0																														

Participant ID	Step No	Task No	Time Interval	Performance result (safe/risky)	Performance score (1-100)	Task loading (1-10)	NASA_TLX score	HRV																			
								Time-based						Frequency-based Welch periodaogram						Frequency-based Lomb-Scargle periodaogram							
								meanHR	SDNN	RMSSD	pNNx	HRVTI	TINN	aLF	aHF	aTotal	pLF	pHF	nLF	nHF	LFHF	peakLF	peakHF	aLF	aHF	aTotal	pLF
								(bpm)	(ms)	(ms)	(%)	(ms)	(ms)	(ms ²)	(ms ²)	(ms ²)	(%)	(%)	(%)	(%)		(Hz)	(Hz)	(ms ²)	(ms ²)	(ms ²)	(%)
15	1	1	0-240	Safe	100	2	16.66	89	30.4	17.1	0.6	7.9	85.9	443.46	80.58	543.37	81.6	14.8	0.846	0.154	5.504	0.1	0.26	0.037	0.007	0.045	82.8
		2	240-360	Safe	76	4		86.3	34.2	18.1	2.3	8.6	102.1	522.98	107.7	645.64	81	16.7	0.829	0.171	4.856	0.1	0.35	0.019	0.004	0.023	83
		3	360-480	Safe	85	5		87.4	35	18.4	0.6	9.2	101.6	637.47	198.1	909.44	70.1	21.8	0.763	0.237	3.218	0.08	0.17	0.03	0.01	0.041	74.1
		4	480-703	Safe	85	4		86.7	37	20.6	1.9	10.3	138.4	750.44	110.39	911.29	82.3	12.1	0.872	0.128	6.798	0.1	0.23	0.02	0.007	0.027	73
	2	1	0-90	Safe	100	3	45	85.1	39	18.2	0	8.5	79.3	846.71	106.95	995.01	85.1	10.7	0.888	0.112	7.917	0.09	0.31	0.018	0.002	0.021	87
		2	90-360	Safe	100	5		85.5	39.3	20.6	1.8	9.6	139.2	805.57	166.84	1050.55	76.7	15.9	0.828	0.172	4.828	0.08	0.16	0.03	0.008	0.039	77.7
		3	360-960	Safe	100	7		83.6	38	18.5	0.7	10.8	146	521.49	110.76	681.27	76.5	16.3	0.825	0.175	4.708	0.09	0.32	0.032	0.007	0.039	80.7
		4	960-1180	Safe	78	8		81.3	36.2	20.5	2	8.7	114.3	675.14	158.53	887.83	76	17.9	0.81	0.19	4.259	0.11	0.3	0.051	0.009	0.063	80.8
	3	6	1180-1650	Risky	54	7	62	81.5	41	22.2	2.6	10.9	156.3	850.1	167.39	1063.65	79.9	15.7	0.835	0.165	5.078	0.1	0.34	0.03	0.011	0.041	72.5
		7	1650-1756	Safe	90	5		80.4	51.2	26.5	4.3	10.1	174.1	1455.41	292.06	1907.84	76.3	15.3	0.833	0.167	4.983	0.09	0.16	0.025	0.006	0.031	79.2
		1	0-150	Safe	100	4		85.6	54.6	23	3.8	11.8	177.2	1428.08	137.41	1656.74	86.2	8.3	0.912	0.088	10.393	0.09	0.3	0.046	0.004	0.05	91.9
		2	150-240	Safe	100	4		83	44.2	22.8	2.4	10.3	150.4	1421.14	221.25	1695.66	83.8	13	0.865	0.135	6.423	0.1	0.34	0.037	0.006	0.043	86.1
		3	240-360	Safe	87	6		83.2	32.5	20.4	2.5	9.4	78.9	417.41	177.94	612.81	68.1	29	0.701	0.299	2.346	0.1	0.22	0.042	0.012	0.055	76.2
		4	360-510	Safe	73	8		81.2	37	21	3	10.2	114.3	583.75	144.92	771.06	75.7	18.8	0.801	0.199	4.028	0.12	0.31	0.027	0.004	0.031	85.6
		5	510-580	Safe	74	7		82.5	43.7	25.6	5.3	10.7	150.4	788.23	203.67	1024.62	76.9	19.9	0.795	0.205	3.87	0.12	0.29	0.045	0.014	0.06	74.4
		6	580-1260	Safe	93	9		82.3	55	25.3	5.7	10.2	205.1	1256.74	191.81	1541.88	81.5	12.4	0.868	0.132	6.552	0.09	0.16	0.015	0.006	0.021	68.6
16	1	7	1260-1680	Safe	77	6	20.66	80.3	50.2	27.9	7.5	7.9	107.9	1449.33	250.86	1819.83	79.6	13.8	0.852	0.148	5.777	0.09	0.16	0.03	0.004	0.035	85.6
		8	1680-1842	Safe	90	11		80.5	59.5	27.3	7	12.7	226.6	1275.39	223.84	1648.12	77.4	13.6	0.851	0.149	5.698	0.08	0.18	0.026	0.006	0.034	77.1
		1	0-300	Safe	100	3		81.1	48.5	26.2	6.7	11.2	170.9	916.73	268.18	1273.5	72	21.1	0.774	0.226	3.418	0.08	0.28	0.026	0.013	0.039	66.6
		2	300-600	Safe	100	4		84.6	63.1	28.1	5.7	11.1	225.8	1213.6	330.33	1671.1	72.6	19.8	0.786	0.214	3.674	0.1	0.26	0.022	0.011	0.034	66.1
	2	3	600-840	Safe	100	4	83.6	49.2	24.6	5.1	12.3	191.2	912.43	247.29	1202.25	75.9	20.6	0.787	0.213	3.69	0.09	0.16	0.033	0.013	0.046	71.3	
		4	840-960	Safe	100	2	81.4	35.1	22	4.3	9.6	97.7	356.59	215.12	605.94	58.8	35.5	0.624	0.376	1.658	0.1	0.28	0.021	0.012	0.034	60.8	
		5	960-1197	Safe	86	2	84.5	49.9	24.1	3.9	11.9	195.3	1042.89	221.19	1372.73	76	16.1	0.825	0.175	4.715	0.08	0.28	0.029	0.004	0.033	87.3	
		1	0-120	Safe	100	4	84.7	68.6	38.5	11.5	12.1	250.2	1934.22	682.14	2782.92	69.5	24.5	0.739	0.261	2.836	0.08	0.36	0.025	0.009	0.034	73.7	
		2	120-270	Safe	100	4	89.7	58.3	29.6	3.7	13.8	224.1	1174.38	313.34	1591.93	73.8	19.7	0.789	0.211	3.748	0.08	0.22	0.033	0.007	0.041	82	
		3	270-380	Safe	89	6	83.6	53.6	28.9	9.9	7.7	116.2	1540.87	293.81	1944.26	79.3	15.1	0.84	0.16	5.244	0.08	0.25	0.03	0.007	0.037	81.7	
		4	380-480	Safe	73	4	86.4	43.5	28.8	6.4	10.9	164.1	913.4	225.88	1186.09	77	19	0.802	0.198	4.044	0.1	0.28	0.03	0.012	0.043	71.3	
		5	480-780	Safe	100	3	86.5	47.5	27.3	5.5	12.4	218.8	705.98	242.06	991.4	71.2	24.4	0.745	0.255	2.917	0.11	0.26	0.017	0.003	0.02	83.8	
	3	6	780-1083	Safe	72	5	86.2	56.9	27.7	5.8	13.1	240.7	763.76	207.74	1001.03	76.3	20.8	0.786	0.214	3.677	0.1	0.26	0.017	0.005	0.023	75.1	
		1	0-90	Safe	68	6	84.3	37.7	26.6	4.8	10.5	112.8	776.12	227.49	1052.93	73.7	21.6	0.773	0.227	3.412	0.08	0.21	0.036	0.012	0.048	74.2	
		2	90-300	Safe	90	8	85.3	55.3	29.4	9.2	9.2	205.1	638.16	449.47	1133.53	56.3	39.7	0.587	0.413	1.42	0.08	0.16	0.033	0.014	0.047	69.1	
		3	300-420	Safe	65	8	85	54.9	29.7	6.1	11.9	171.9	845.17	377.12	1312.34	64.4	28.7	0.691	0.309	2.241	0.1	0.28	0.049	0.021	0.071	69.4	
4		420-540	Safe	82	6	87.4	46.7	26.7	5.4	8.4	92.3	488.91	275.54	791.45	61.8	34.8	0.64	0.36	1.774	0.09	0.28	0.032	0.024	0.056	57.4		
5		540-740	Risky	52	7	83.9	57.2	34.6	8.5	10.5	198.7	855.12	392.65	1325.63	64.5	29.6	0.685	0.315	2.178	0.11	0.26	0.044	0.017	0.062	70.4		
6		740-1088	Safe	94	7	80.2	47.7	32.8	11.5	13	210.9	1024.76	333.99	1428.1	71.8	23.4	0.754	0.246	3.068	0.1	0.28	0.033	0.01	0.043	76.1		
7		1088-1380	Safe	100	8	85.5	51.7	28.2	6.6	13.2	217.5	1083.2	242.77	1394.41	77.7	17.4	0.817	0.183	4.462	0.1	0.36	0.032	0.007	0.04	80.3		
4	2	300-540	Safe	100	9	75.33	88.4	49.9	25.8	4.7	9.8	179.4	773.75	210.62	1022.54	75.7	20.6	0.786	0.214	3.674	0.09	0.26	0.036	0.013	0.049	74.1	
	3	540-720	Safe	100	7		84.1	38.7	26.3	6.6	10.1	162.8	785.24	160.4	1001.57	78.4	16	0.83	0.17	4.895	0.1	0.28	0.031	0.012	0.044	70.4	
	4	720-1160	Safe	75	10		85.5	43.8	26.4	5.1	11.4	177.2	856.37	258.78	1159.19	73.9	22.3	0.768	0.232	3.309	0.09	0.16	0.026	0.004	0.031	84.7	
	5	1160-1280	Safe	86	9		85.1	37.6	24.8	4.3	9.1	73	582.78	309.69	919.47	63.4	33.7	0.653	0.347	1.882	0.12	0.27	0.033	0.014	0.048	69.8	
	6	1280-1380	Safe	72	9		86	47.4	31.7	9.6	10.5	145	1101	156.08	1276.8	86.2	12.2	0.876	0.124	7.054	0.11	0.29	0.04	0.005	0.045	88.3	
	7	1380-1630	Risky	41	9		82.6	47.4	25.6	4.5	7.8	132.8	813.4	232.66	1108.22	73.4	21	0.778	0.222	3.496	0.1	0.24	0.024	0.007	0.032	77	

Figure H.1 (continued) : Data collected during the study.

HRV

Frequency-based																								Non-linear						Time-frequency										Time-frequency					
Lomb-Scargle periodogram												Lomb-Scargle periodogram										Wavelet transform																							
pHF	nLF	nHF	LFHF	peakLF	peakHF	SD1	SD2	sampen	alpha1	alpha2	aLF	aHF	aTotal	pLF	pHF	nLF	nHF	LFHF	peakLF	peakHF	aLF	aHF	aTotal	pLF																					
(%)	(%)	(%)	(Hz)	(Hz)	(ms)	(ms)					(ms ²)	(ms ²)	(ms ²)	(%)	(%)	(%)	(%)		(Hz)	(Hz)	(ms ²)	(ms ²)	(ms ²)	(%)																					
16.5	0.834	0.166	5.016	0.11	0.19	12.1	12.1	41.2	1.955	1.578	0.605	15.08	3.17	18.74	80.5	16.9	0.826	0.174	4.75	0.12	0.22	2609.12	514.92	3126.18	83.5																				
16.6	0.833	0.167	4.991	0.1	0.18	12.8	12.8	46.7	2.021	1.514	0.737	16.61	3.96	20.93	79.4	18.9	0.808	0.192	4.197	0.1	0.21	2526.49	640.62	3170.66	79.7																				
25.4	0.744	0.256	2.913	0.06	0.18	13	13	47.7	1.964	1.691	0.679	17.43	6.87	25.72	67.8	26.7	0.717	0.283	2.537	0.06	0.26	3257.87	1085.17	4362.17	74.7																				
26.1	0.737	0.263	2.801	0.1	0.21	14.6	14.6	50.3	2.119	1.527	0.746	19.5	5.77	25.83	75.5	22.3	0.772	0.228	3.382	0.1	0.21	4278.5	915.43	5205.21	82.2																				
11.7	0.882	0.118	7.467	0.1	0.19	12.9	12.9	53.6	2.04	1.685	1.152	22.39	5.02	28.33	79	17.7	0.817	0.183	4.462	0.1	0.18	3773.32	555.55	4342.42	86.9																				
21.6	0.782	0.218	3.59	0.09	0.18	14.6	14.6	53.6	2.073	1.359	0.763	24.02	6.16	31.9	75.3	19.3	0.796	0.204	3.899	0.09	0.19	4379.74	972.58	5370.7	81.5																				
16.6	0.829	0.171	4.848	0.12	0.21	13.1	13.1	52.1	2.023	1.502	0.857	16.89	4.66	22.76	74.2	20.5	0.784	0.216	3.627	0.11	0.21	3127.61	650.72	3787.17	82.6																				
14.2	0.851	0.149	5.707	0.14	0.2	14.5	14.5	49.1	2.088	1.582	0.695	20.58	5.21	27.15	75.8	19.2	0.798	0.202	3.947	0.1	0.33	3610.25	876.51	4535.6	79.6																				
27.1	0.728	0.272	2.677	0.09	0.22	15.7	15.7	55.9	2.233	1.489	0.753	24.38	7.53	32.88	74.2	22.9	0.764	0.236	3.239	0.1	0.21	4636.81	990.09	5633.54	82.3																				
18	0.815	0.185	4.403	0.09	0.2	18.8	18.8	69.9	2.551	1.609	0.634	37.99	11.15	52.38	72.5	21.3	0.773	0.227	3.406	0.1	0.2	7695.46	1728.71	9491.65	81.1																				
7.4	0.925	0.075	12.393	0.08	0.19	16.3	16.3	75.4	1.192	1.659	0.769	46.25	7.71	56.06	82.5	13.8	0.857	0.143	5.999	0.08	0.19	7015.15	816.74	7866.83	89.2																				
13.6	0.864	0.136	6.331	0.11	0.18	16.2	16.2	60.4	2.122	1.644	0.569	51.45	7.4	60.24	85.4	12.3	0.874	0.126	6.953	0.1	0.19	6351.61	1114.03	7479.79	84.9																				
22.6	0.771	0.229	3.365	0.09	0.24	14.5	14.5	43.6	2.263	1.501	0.916	12.5	7	20.18	62	34.7	0.641	0.359	1.785	0.09	0.23	2107.72	950.7	3068.25	68.7																				
14.1	0.859	0.141	6.078	0.12	0.2	14.9	14.9	50.2	2.171	1.666	0.636	20.72	5.41	27.06	76.6	20	0.793	0.207	3.83	0.12	0.19	3897.75	897.75	4800.81	81.2																				
23.9	0.757	0.243	3.117	0.08	0.22	18.2	18.2	59.1	1.972	1.593	0.739	22.69	6.07	29.98	75.7	20.2	0.789	0.211	3.741	0.08	0.29	3707.72	1405.69	5127.96	72.3																				
29.7	0.698	0.302	2.314	0.09	0.18	17.9	17.9	75.7	1.293	1.698	0.845	39.3	7.43	49.3	79.7	15.1	0.841	0.159	5.289	0.1	0.2	7295.13	1177.57	8493.59	85.9																				
11.5	0.882	0.118	7.444	0.1	0.19	19.7	19.7	68.2	2.44	1.701	0.509	49.56	10.02	62.19	79.7	16.1	0.832	0.168	4.948	0.09	0.28	8728.95	1476.05	10264.95	85																				
19	0.802	0.198	4.05	0.08	0.17	19.4	19.4	81.9	1.352	1.671	0.926	42.36	8.86	54.51	77.7	16.3	0.827	0.173	4.779	0.07	0.19	7689.26	1322.84	9077.85	84.7																				
32.9	0.669	0.331	2.023	0.07	0.18	18.6	18.6	66.1	2.227	1.423	0.715	29.91	8.6	41.04	72.9	20.9	0.777	0.223	3.479	0.08	0.18	6342.15	1511.56	7866.73	80.4																				
32.7	0.669	0.331	2.018	0.12	0.2	19.9	19.9	87	1.441	1.516	0.732	38.91	11.86	54.16	71.8	21.9	0.766	0.234	3.281	0.1	0.2	7048.43	1888.45	8986.88	78.4																				
27.9	0.718	0.282	2.552	0.1	0.26	17.4	17.4	67.4	2.32	1.482	0.991	26.66	9.4	37.18	71.7	25.3	0.739	0.261	2.836	0.09	0.21	4456.65	1435	5900.48	75.5																				
34.8	0.636	0.364	1.747	0.1	0.29	15.6	15.6	47.1	2.285	1.369	0.589	10.57	6.56	17.49	60.5	37.5	0.617	0.383	1.612	0.1	0.28	1927.13	1123.74	3074.63	62.7																				
11.8	0.881	0.119	7.394	0.1	0.2	17	17	68.5	2.356	1.556	0.828	33.77	9	45.62	74	19.7	0.79	0.21	3.754	0.08	0.2	6082.59	1366.89	7499.2	81.1																				
25.8	0.741	0.259	2.857	0.11	0.21	27.3	27.3	93	1.536	1.741	0.677	69.81	26.91	100.98	69.1	26.6	0.722	0.278	2.595	0.11	0.21	11611.2	3235.81	14860.17	78.1																				
17.9	0.821	0.179	4.58	0.09	0.21	21	21	79.8	1.234	1.301	0.832	39.51	14.28	55.91	70.7	25.5	0.734	0.266	2.766	0.09	0.17	6608.66	2076.32	8704.14	75.9																				
17.6	0.823	0.177	4.643	0.08	0.17	20.5	20.5	72.9	1.362	1.495	0.826	47.83	11.78	61.86	77.3	19	0.802	0.198	4.061	0.08	0.17	7371.23	1523.15	8924.2	82.6																				
27.7	0.72	0.28	2.572	0.1	0.27	20.5	20.5	58	2.692	1.507	0.76	30.28	10.51	41.93	72.2	25.1	0.742	0.258	2.881	0.1	0.17	4146.31	1387.7	5556.78	74.6																				
14.4	0.853	0.147	5.811	0.12	0.26	19.3	19.3	64.3	2.389	1.493	1.016	23.72	9.05	33.87	70	26.7	0.724	0.276	2.619	0.12	0.2	3990.11	1366.76	5381.31	74.1																				
23.7	0.76	0.24	3.173	0.11	0.26	19.6	19.6	78	1.333	1.414	0.971	24.95	7.51	33.18	75.2	22.6	0.769	0.231	3.324	0.1	0.26	4137.19	1111.56	5263.2	78.6																				
24.8	0.75	0.25	2.994	0.09	0.21	18.9	18.9	49.9	2.613	1.313	0.471	23.29	8.1	32.08	72.6	25.3	0.742	0.258	2.874	0.08	0.21	3570.71	1214.58	4788.57	74.6																				
29.7	0.699	0.301	2.325	0.06	0.2	20.8	20.8	75.4	1.45	1.311	1.002	19.59	13.16	33.95	57.7	38.7	0.598	0.402	1.489	0.09	0.23	3803.92	2288.56	6104.98	62.3																				
29.3	0.703	0.297	2.366	0.11	0.28	21.1	21.1	74.7	1.46	1.278	1.117	23.47	11.47	37.67	62.3	30.5	0.672	0.328	2.046	0.06	0.28	4415.24	1983.56	6437.8	68.6																				
42.5	0.574	0.426	1.349	0.07	0.27	19	19	63.3	2.494	1.475	1.12	16.41	9.47	26.63	61.6	35.6	0.634	0.366	1.732	0.08	0.28	2698.82	1407.52	4107.84	65.7																				
28.1	0.715	0.285	2.504	0.1	0.28	24.5	24.5	77.1	1.448	1.491	0.771	26.73	13.66	42.21	63.3	32.4	0.662	0.338	1.956	0.12	0.22	4411.78	2019.58	6492.89	67.9																				
23.5	0.764	0.236	3.239	0.08	0.27	23.2	23.2	63.4	2.626	1.386	0.703	32.52	11.69	45.72	71.1	25.6	0.736	0.264	2.782	0.09	0.22	5645.97	1757.25	7427.32	76																				
18.3	0.814	0.186	4.388	0.11	0.21	20	20	70.3	2.409	1.496	0.704	37.76	9.1	48.3	78.2	18.8	0.806	0.194	4.15	0.11	0.23	6055.5	1472.8	7544.83	80.3																				
25.7	0.742	0.258	2.879	0.11	0.18	18.3	18.3	68.1	2.473	1.477	0.882	23.62	8.23	32.95	71.7	25	0.742	0.258	2.869	0.09	0.27	4576.28	1145.01	5730.63	79.9																				
27	0.722	0.278	2.601	0.09	0.18	18.6	18.6	51.4	2.328	1.426	0.666	26.8	5.99	34.45	77.8	17.4	0.817	0.183	4.472	0.1	0.27	4306.35	914.11	5260.64	81.9																				
14.6	0.853	0.147	5.816	0.08	0.22	18.7	18.7	59	2.403	1.473	0.705	27.07	10.18	38.26	70.7	26.6	0.727	0.273	2.658	0.09	0.18	4640.51	1415.3	6069.41	76.5																				
29.6	0.702	0.298	2.357	0.12	0.17	17.6	17.6	50.2	2.264	1.322	0.79	18.71	11.41	30.74	60.9	37.1	0.621	0.379	1.641	0.12	0.29	2904.1	1562.12	4468.88	65																				
11.3	0.886	0.114	7.806	0.1	0.29	22.5	22.5	63.2	2.698	1.444	0.541	34.43	6.27	41.1	83.8	15.3	0.846	0.154	5.488	0.11	0.28	5333.07	1010.99	6347.39	84																				
22.2	0.776	0.224	3.461	0.11	0.21	18.1	18.1	64.5	2.447	1.508	0.868	25.86	7.18	35.1	73.7	20.5	0.783	0.217	3.599	0.09	0.21	4465.08	1228.24	5714.77	78.1																				

Figure H.1 (continued) : Data collected during the study.

HRV							EDA														Eye											
Time-frequency Wavelet transform							Continuous decomposition analysis														Trough-to-peak analysis						Pupil diameter			Blink frequency		
pHF	nLF	nHF	LFHF	peakLF	peakHF		CDA.nSCR	CDA.Amp Sum (avg.)	CDA.Amp Sum (max.)	CDA.SCR (avg.)	CDA.SCR (max.)	CDA.ISCR (avg.)	CDA.ISCR (max.)	CDA.Phasic Max (avg.)	CDA.Phasic Max (max.)	CDA.Tonic (avg.)	CDA.Tonic (max.)	TTP.nSCR frequency	TTP.Amp5 um (avg.)	TTP.Amp5 um (max.)	Global Mean (avg.)	Global Mean (max.)	mean	std	PerLPD	freq	AEC5	PERCLOS				
(%)	(%)	(%)		(Hz)	(Hz)		[muS]	[muS]	[muS]	[muS]	[muS]	[muS]	[muS]	[muS]	[muS]	[muS]	[muS]	[muS]	[muS]	[muS]	[m uS]	[m uS]	[muS]	[muS]								
16.5	0.835	0.165	5.067	0.11	0.15	0.3375	0.431079	1.483218	0.058702	0.188542	1.40886	4.524996	1.4747171	5.5795464	18.55684	20.21475	0.275	0.306626	2.400777	19.02351	20.93602	23.2703	1.1835	-0.0396	0.1125	0.1933	0.0217					
20.2	0.798	0.202	3.944	0.1	0.34	0.291667	0.470899	1.863887	0.065901	0.281747	1.581633	6.76192	1.5430117	3.5936902	19.52941	20.2007	0.233333	0.341641	1.903022	20.05082	20.90708	23.0544	1.1659	-0.0485	0.0833	0.2184	0.0182					
24.9	0.75	0.25	3.002	0.06	0.16	0.341667	0.353596	1.185186	0.048892	0.202133	1.173413	4.851185	1.5312865	3.1569359	20.31838	21.21128	0.25	0.279728	1.70739	20.78026	21.78758	24.2291	1.1351	0.0000	0.15	0.2111	0.0317					
17.6	0.824	0.176	4.674	0.1	0.15	0.295964	0.313693	1.060451	0.04643	0.136955	1.114328	3.28691	1.4958328	4.0759187	20.2494	21.8715	0.2287	0.256763	0.857599	20.52543	22.36642	23.3977	1.2464	-0.0343	0.1883	0.2133	0.0402					
12.8	0.872	0.128	6.792	0.09	0.31	0.355556	0.256115	0.730726	0.03424	0.107826	0.821762	2.587834	1.3227954	2.5046897	22.24319	22.54278	0.322222	0.163784	0.55275	22.55473	23.26088	23.5294	1.153	-0.0289	0.1222	0.2182	0.0267					
18.1	0.818	0.182	4.503	0.06	0.15	0.37037	0.283921	0.818609	0.041681	0.156202	1.000355	3.748848	1.1938158	3.5722314	22.92263	23.7806	0.251852	0.238513	1.229889	23.25651	24.13777	23.292	1.1044	-0.0387	0.1037	0.2133	0.0221					
17.2	0.828	0.172	4.806	0.05	0.15	0.258333	0.332067	1.438393	0.057211	0.283249	1.373061	6.797977	1.5922047	5.5684355	23.59548	24.7125	0.211667	0.272227	1.64886	24.00169	25.5287	23.6471	1.3777	-0.0241	0.12	0.2187	0.0262					
19.3	0.805	0.195	4.119	0.1	0.15	0.263636	0.266833	1.195869	0.044305	0.220125	1.063323	5.282996	1.1186323	3.2328249	24.52331	25.17293	0.213636	0.262496	1.668195	24.91266	25.98072	23.2409	1.2738	-0.0408	0.1818	0.196	0.0356					
17.6	0.824	0.176	4.683	0.1	0.15	0.261702	0.30433	1.633952	0.045031	0.214775	1.080736	5.154603	1.0987292	4.3999373	25.08638	25.89202	0.2	0.278189	1.522735	25.41286	26.54053	23.4052	1.1537	-0.034	0.134	0.205	0.0275					
18.2	0.817	0.183	4.452	0.09	0.15	0.207547	0.219247	1.112121	0.041873	0.122398	1.004957	2.937561	1.1206593	2.6818516	24.79012	25.19136	0.169811	0.390748	0.82371	25.30262	26.05719	24.2875	1.5622	0.0024	0.2642	0.2032	0.0537					
10.4	0.896	0.104	8.589	0.07	0.29	0.206667	0.348678	1.970596	0.059216	0.267079	1.421192	6.409893	1.7547646	5.4923593	22.71744	23.58232	0.146667	0.442988	0.202516	23.2685	24.58424	26.6899	1.5482	0.1015	0.1733	0.2092	0.0363					
14.9	0.851	0.149	5.701	0.1	0.34	0.255556	0.272643	0.696527	0.041163	0.114628	0.987917	2.751064	1.1886136	2.1665989	22.85602	23.57843	0.2	0.249224	0.428423	23.2018	24.19229	25.8067	1.4515	0.0651	0.2778	0.2424	0.0673					
31	0.689	0.311	2.217	0.09	0.22	0.175	0.466462	1.526921	0.079758	0.27768	1.914187	6.664332	2.0767038	5.9057713	23.27081	23.79726	0.175	0.43707	2.42974	23.86855	24.61886	25.9641	1.6715	0.0716	0.1917	0.2001	0.0383					
18.7	0.813	0.187	4.342	0.12	0.15	0.226667	0.201251	1.265366	0.035765	0.173535	0.858357	4.164833	0.9854916	2.4081361	23.26362	23.76608	0.153333	0.2703	1.177389	23.54892	24.59847	25.5754	1.0592	0.0555	0.1467	0.192	0.0282					
27.4	0.725	0.275	2.638	0.08	0.15	0.328571	0.441916	1.376873	0.064234	0.191764	1.54161	4.602335	1.3807418	2.4407296	24.12931	25.73525	0.214286	0.477357	2.431341	24.62498	26.47741	25.8625	1.4294	0.0674	0.1714	0.1939	0.0332					
13.9	0.861	0.139	6.195	0.09	0.15	0.269118	0.353559	1.548786	0.054351	0.208846	1.304415	5.012307	1.4108075	3.6991203	24.7713	25.62617	0.195588	0.316218	1.480548	25.21715	26.88263	26.5191	1.2991	0.0945	0.1647	0.2116	0.0348					
14.4	0.855	0.145	5.914	0.09	0.15	0.359524	0.316671	1.544408	0.049697	0.214425	1.192733	5.141398	1.3586107	3.7685787	25.2334	26.3164	0.280952	0.298874	2.161768	25.60007	27.43921	26.1919	1.2245	0.081	0.2167	0.2157	0.0467					
14.6	0.853	0.147	5.813	0.07	0.15	0.320988	0.548552	1.777689	0.069588	0.195059	1.670105	4.681415	1.4554078	2.7233042	26.45085	27.12388	0.228395	0.414267	1.640886	26.90658	28.34174	26.9769	1.3762	0.1134	0.3457	0.2235	0.0773					
19.2	0.808	0.192	4.196	0.07	0.18	0.1	0.073956	0.267992	0.014769	0.040456	0.354461	0.970946	0.2752589	0.6275669	1.088876	1.256794	0.106667	0.073844	0.258267	1.173543	1.34425	29.4653	2.8765	-0.032	0.3533	0.1816	0.0642					
21	0.789	0.211	3.732	0.05	0.15	0.106667	0.113108	0.269276	0.021404	0.044318	0.513694	1.063644	0.5052439	0.9706682	1.432076	1.86234	0.133333	0.101599	0.279749	1.547339	2.074023	29.9817	2.7945	-0.0151	0.3333	0.1817	0.0606					
24.3	0.756	0.244	3.106	0.09	0.15	0.054167	0.130279	0.258521	0.026361	0.055402	0.63266	1.329658	0.5965885	1.1179881	1.569363	1.846192	0.1125	0.088191	0.333376	1.630669	1.959211	29.2215	2.7153	-0.04	0.3792	0.2016	0.0764					
36.5	0.632	0.368	1.715	0.1	0.28	0.05	0.057166	0.114383	0.015971	0.031657	0.383296	0.75977	0.3473352	0.5703964	1.281779	1.327342	0.091667	0.0611	0.230037	1.334994	1.454508	30.44	2.356	0.0000	0.2833	0.1725	0.0489					
18.2	0.817	0.183	4.45	0.07	0.15	0.067511	0.050396	0.118817	0.012077	0.028152	0.289851	0.675659	0.3075663	0.5976278	1.347031	1.418082	0.109705	0.058552	0.14753	1.395716	1.501747	-	-	-	-	-	-					
21.8	0.782	0.218	3.588	0.11	0.15	0.183333	0.107939	0.370851	0.020136	0.074581	0.483259	1.789943	0.6402811	1.3856938	2.158956	2.259189	0.166667	0.119704	0.311429	2.31593	2.47111	30.672	2.2682	0.0076	0.1583	0.1803	0.0285					
23.9	0.761	0.239	3.183	0.06	0.15	0.12	0.089042	0.281268	0.014744	0.052606	0.353857	1.262536	0.4102841	0.8900791	2.386555	2.573512	0.193333	0.107022	0.359706	2.507894	2.818266	30.9201	2.2151	0.0158	0.2067	0.1805	0.0373					
17.1	0.829	0.171	4.839	0.08	0.25	0.127273	0.083419	0.142662	0.017769	0.035076	0.42645	0.841827	0.5311703	0.9304081	2.239207	2.422141	0.154545	0.096327	0.21502	2.380182	2.647269	29.5558	1.855	-0.029	0	0	0					
25	0.749	0.251	2.988	0.1	0.28	0.08	0.061626	0.176826	0.014699	0.042434	0.352776	1.018417	0.3560123	0.783066	2.23251	2.336228	0.16	0.065772	0.124724	2.370568	2.550607	29.749	2.2473	-0.0227	0.22	0.1726	0.038					
25.4	0.745	0.255	2.919	0.12	0.25	0.143333	0.091963	0.370749	0.016431	0.073844	0.394356	1.772263	0.4063095	1.0051171	2.292641	2.585584	0.183333	0.078601	0.422794	2.422873	2.655555	29.1796	2.3522	-0.0414	0.18	0.1866	0.0336					
21.1	0.788	0.212	3.722	0.1	0.26	0.079208	0.117949	0.505953	0.022546	0.096542	0.541107	2.317018	0.4420528	1.3299134	2.059631	2.485785	0.112211	0.076771	0.511165	2.221046	2.622366	29.2332	2.4281	-0.0396	0.2178	0.1891	0.0412					
25.4	0.746	0.254	2.944	0.08	0.2	0.122222	0.103614	0.316183	0.024711	0.069095	0.593065	1.658284	0.6587357	1.4202818	3.104662	3.247794	0.144444	0.136229	0.305515	3.301128	3.579089	30.4243	2.3414	-0.0005	0.1667	0.1764	0.0294					
37.5	0.624	0.376	1.662	0.09	0.15	0.052381	0.183656	0.401554	0.043333	0.111765	1.039995	2.682358	0.9401858	1.6721979	3.368635	3.626846	0.12381	0.158218	0.55244	3.553886	3.838972	30.617	2.4857	0.0058	0.2524	0.184	0.0464					
30.8	0.69	0.31	2.226	0.06	0.28	0.1	0.187339	0.785325	0.033807	0.16709	0.811361	4.010158	0.5918817	1.9661574	3.330662	3.517384	0.191667	0.115136	0.807804	3.479665	3.885464	29.8106	1.8259	-0.0207	0.25	0.1755	0.0439					
34.3	0.657	0.343	1.917	0.1	0.28	0.15	0.113967	0.380681	0.022276	0.054458	0.534631	1.306985	0.6014266	1.5315896	3.363627	3.590531	0.141667	0.102994	0.341157	3.527815	3.77545	30.8815	2.5606	0.0145	0.2	0.1839	0.0368					
31.1	0.686	0.314	2.185	0.12	0.26	0.13	0.137369	0.525279	0.024084	0.076982	0.578006	1.84756	0.5411686	1.1936689	3.046148	3.262519	0.13	0.117197	0.571481	3.210359	3.568419	31.9621	2.5198	0.05	0.14	0.1667	0.0233					
23.7	0.763	0.237	3.213	0.08	0.25	0.071839	0.107069	0.500122	0.022208	0.091814	0.532988	2.303537	0.4884886	1.2250133	2.731437	2.96382	0.109195	0.088384	0.474434	2.775155	3.159581	28.6655	2.8504	-0.0583	0.2615	0.18	0.0471					
19.5	0.804	0.196	4.112	0.1	0.15	0																										

Participant ID	Step No	Task No	Time Interval	Performance result (safe/risky)	Performance score (1-100)	Task loading (1-10)	NASA_TLX score	HRV																			
								Time-based						Frequency-based Welch periodaogram								Frequency-based Lomb-Scargle periodaogram					
								meanHR	SDNN	RMSSD	pNNx	HRVTi	TINN	aLF	aHF	aTotal	pLF	pHF	nLF	nHF	LFHF	peakLF	peakHF	aLF	aHF	aTotal	pLF
								(bpm)	(ms)	(ms)	(%)	(ms)	(ms)	(ms ²)	(ms ²)	(ms ²)	(%)	(%)	(%)	(%)		(Hz)	(Hz)	(ms ²)	(ms ²)	(ms ²)	(%)
17	1	1	0-240	Safe	100	2	21.66	75.5	56.2	37.4	14.3	8.2	148.4	821.96	407.38	1274.49	64.5	32	0.669	0.331	2.018	0.12	0.23	0.026	0.013	0.04	64.9
		2	240-360	Safe	84	4		74.7	35.4	25.7	4.7	7.5	70.3	322.86	200.84	557.86	57.9	36	0.616	0.384	1.608	0.07	0.23	0.022	0.014	0.036	60
		3	360-600	Safe	85	5		78.7	55.4	34	12.2	12.2	190.9	1101.82	476.22	1610.87	68.4	29.6	0.698	0.302	2.314	0.1	0.23	0.033	0.018	0.051	64.9
		4	600-987	Safe	100	4		75	52.2	30	7.3	12.3	190.9	975.27	307.64	1396.24	69.8	22	0.76	0.24	3.17	0.09	0.19	0.027	0.006	0.034	80.4
	2	1	0-150	Safe	100	3	32	78.5	59.8	39.7	16.1	6.7	52.7	1722.23	611.87	2376.15	72.5	25.8	0.738	0.262	2.815	0.12	0.16	0.022	0.004	0.026	85.5
		2	150-360	Safe	100	5		80.3	51.8	41.8	16.2	7.3	120.6	995.75	619.19	1719.23	57.9	36	0.617	0.383	1.608	0.11	0.2	0.039	0.023	0.064	60.7
		3	360-900	Safe	100	7		77.1	61.4	53.3	29.5	9.4	199.5	1135.56	837.25	2099.3	54.1	39.9	0.576	0.424	1.356	0.12	0.26	0.038	0.033	0.072	52.7
		4	900-1320	Safe	93	8		74.1	50.2	44.8	22.8	8.4	175.8	694.06	618.29	1403.96	49.4	44	0.529	0.471	1.123	0.11	0.16	0.039	0.047	0.088	45
		5	1320-1440	Safe	92	5		75.3	53.3	36.7	16.4	10.8	177.2	974.34	449.8	1472.68	66.2	30.5	0.684	0.316	2.166	0.11	0.22	0.036	0.019	0.056	64.3
		6	1440-1920	Safe	100	7		74.7	49.7	35.9	14.5	10.3	166	1002.01	419.87	1508.41	66.4	27.8	0.705	0.295	2.386	0.1	0.16	0.036	0.018	0.055	65.5
		7	1920-2051	Safe	100	5		74.1	54.2	39.5	16.7	9.1	174.3	789.36	486.99	1345.1	58.7	36.2	0.618	0.382	1.621	0.08	0.23	0.024	0.012	0.037	64.4
		8	2051-2060	Safe	74	4		73.9	46	29.7	8.3	8.5	106.2	715.7	166.61	937.36	76.4	17.8	0.811	0.189	4.296	0.09	0.35	0.034	0.014	0.049	70.5
	3	1	0-90	Safe	74	4	70.33	72	48.5	43.3	17	10.6	168.5	663.49	406.83	1294.1	51.3	31.4	0.62	0.38	1.631	0.06	0.28	0.02	0.017	0.04	49.4
		2	90-180	Safe	82	6		74.6	49.5	44.4	16	10.5	136.7	685.58	467.13	1393.82	49.2	33.5	0.595	0.405	1.468	0.12	0.27	0.02	0.018	0.043	45.8
		3	180-300	Safe	82	6		74.2	56.8	46.5	23.7	7.4	150.1	818.37	574.3	1501.47	54.5	38.2	0.588	0.412	1.425	0.08	0.24	0.047	0.02	0.067	69.5
		4	300-520	Safe	81	8		74.1	53.5	46.6	22.6	11.1	195.3	1021.96	628	1713.55	59.6	36.6	0.619	0.381	1.627	0.11	0.24	0.032	0.018	0.05	62.7
		5	520-900	Safe	79	7		75.3	63.8	51.5	26.9	9.5	210	1538.13	752.85	2388.51	64.4	31.5	0.671	0.329	2.043	0.11	0.16	0.047	0.015	0.064	72.2
		6	900-1320	Safe	80	9		73.7	54.4	39.3	18.9	7.1	94	940.88	508.48	1493.4	63	34	0.649	0.351	1.85	0.11	0.16	0.022	0.014	0.036	59.8
		7	1320-1740	Safe	78	6		72.8	53.1	36.9	13.4	8.3	241.7	1041.88	442.37	1674.24	62.2	26.4	0.702	0.298	2.355	0.06	0.18	0.022	0.008	0.031	71.1
		8	1740-2060	Safe	87	11																					

Figure H.1 (continued) : Data collected during the study.

HRV

Frequency-based Lomb-Scargle periodaogram						Non-linear						Time-frequency Lomb-Scargle periodaogram										Time-frequency Wavelet transform			
pHF	nLF	nHF	LFHF	peakLF	peakHF	SD1	SD2	sampen	alpha1	alpha2	aLF	aHF	aTotal	pLF	pHF	nLF	nHF	LFHF	peakLF	peakHF	aLF	aHF	aTotal	pLF	
(%)	(%)	(%)	(%)	(Hz)	(Hz)	(ms)	(ms)				(ms ²)	(ms ²)	(ms ²)	(%)	(%)	(%)	(%)			(Hz)	(Hz)	(ms ²)	(ms ²)	(ms ²)	(%)
33.4	0.66	0.34	1.945	0.13	0.19	26.5	74.9	1.613	1.47	0.949	29.72	15.32	46.45	64	33	0.66	0.34	1.94	0.12	0.19	4889.32	2370.26	7279.86	67.2	
38.9	0.607	0.393	1.543	0.08	0.29	18.3	46.6	2.337	1.235	0.585	10.52	7.14	18	58.4	39.7	0.596	0.404	1.474	0.07	0.23	1971.71	1026.69	3012.32	65.5	
34.1	0.655	0.345	1.903	0.12	0.17	24.1	74.6	1.52	1.305	0.923	34.01	19.91	54.85	62	36.3	0.631	0.369	1.708	0.1	0.17	5587.66	2514.02	8123.43	68.8	
17.6	0.821	0.179	4.575	0.09	0.21	21.3	70.6	1.405	1.459	0.868	33.78	11.91	48.67	69.4	24.5	0.739	0.261	2.835	0.09	0.2	5758.06	1782.62	7605.32	75.7	
13.4	0.864	0.136	6.357	0.12	0.21	28.2	79.8	1.685	1.556	0.48	53.13	17.79	73.5	72.3	24.2	0.749	0.251	2.987	0.12	0.21	9919.94	3164.97	13107.27	75.7	
36.5	0.624	0.376	1.662	0.09	0.2	29.6	67	2.833	1.31	0.863	29.5	23.39	56.19	52.5	41.6	0.558	0.442	1.261	0.12	0.2	5061.12	3676.6	8860.77	57.1	
46.4	0.532	0.468	1.136	0.1	0.19	37.7	78.2	1.94	1.175	0.875	35.4	28.69	67.3	52.6	42.6	0.552	0.448	1.234	0.12	0.17	6148.52	4585.3	10849.86	56.7	
53.3	0.458	0.542	0.845	0.13	0.17	31.7	63.5	2.868	1.144	0.716	23.19	23.44	49.2	47.1	47.7	0.497	0.503	0.989	0.12	0.22	4160.45	3494.24	7729.33	53.8	
33.3	0.658	0.342	1.928	0.11	0.21	26.1	70.7	1.607	1.381	0.921	26.54	17.45	45.42	58.4	38.4	0.603	0.397	1.521	0.11	0.19	4634.77	2346.45	7019.79	66	
33.1	0.664	0.336	1.979	0.08	0.24	25.4	65.6	2.691	1.316	0.657	31.86	14.86	48.91	65.1	30.4	0.682	0.318	2.143	0.09	0.24	5542.51	2256.03	7841.18	70.7	
33.9	0.655	0.345	1.898	0.08	0.17	28	71.3	1.507	1.275	1.022	26.95	15.06	43.61	61.8	34.5	0.642	0.358	1.789	0.08	0.21	4823.27	2615.23	7467.86	64.6	
27.8	0.717	0.283	2.531	0.13	0.18	21.1	61.5	2.246	1.242	1.06	22.02	6.72	29.64	74.3	22.7	0.766	0.234	3.278	0.12	0.21	3364.32	1239.66	4620.08	72.8	
41.4	0.544	0.456	1.194	0.06	0.31	30.8	61.3	2.823	1.052	0.743	16.8	19.05	39.12	42.9	48.7	0.469	0.531	0.882	0.05	0.3	3740.65	2173.2	6037.62	62	
42.5	0.519	0.481	1.078	0.06	0.26	31.6	62.5	2.305	1.2	0.598	21.25	18.09	44.71	47.5	40.5	0.54	0.46	1.175	0.12	0.27	4146.04	2970.11	7348.39	56.4	
29.3	0.703	0.297	2.37	0.08	0.18	33	73.3	1.685	1.173	0.8	28	20.71	51.34	54.5	40.4	0.575	0.425	1.352	0.09	0.19	4770.28	3279.72	8122.14	58.7	
35.5	0.639	0.361	1.768	0.11	0.21	33.1	68.1	1.758	0.996	0.862	32.93	23.71	57.76	57	41	0.581	0.419	1.389	0.11	0.25	5315.63	3279.67	8620.79	61.7	
23.8	0.752	0.248	3.028	0.08	0.21	36.4	82.5	1.855	1.301	0.651	52.38	24.38	78.5	66.7	31.1	0.682	0.318	2.149	0.12	0.22	8342.21	4063.35	12461.76	66.9	
39.6	0.602	0.398	1.51	0.14	0.22	27.8	71.8	1.561	1.263	0.727	29.11	17.97	48.54	60	37	0.618	0.382	1.62	0.11	0.19	4996.98	2928.24	7937.79	63	
27	0.725	0.275	2.637	0.07	0.24	26.2	70.4	1.43	1.32	0.612	37.22	18.91	62.04	60	30.5	0.663	0.337	1.968	0.09	0.18	6726.92	2551.95	9370.35	71.8	

Figure H.1 (continued) : Data collected during the study.

HRV							EDA														Eye									
Time-frequency Wavelet transform							Continuous decomposition analysis														Trough-to-peak analysis				Pupil diameter			Blink frequency		
pHF	nLF	nHF	LFHF	peakLF	peakHF		CDA.nSCR	CDA.Amp	CDA.Amp	CDA.SCR	CDA.SCR	CDA.ISCR	CDA.ISCR	CDA.Phasic	CDA.Phasic	CDA.Tonic	CDA.Tonic	TTP.nSCR	TTP.AmpS	TTP.AmpS	Global.	Global.								
(%)	(%)	(%)	(%)	(Hz)	(Hz)		frequency	(avg.)	(max.)	(avg.)	(max.)	(avg.)	(max.)	Max (avg.)	Max (max.)	(avg.)	(max)	frequency	um	um	Mean	Mean	mean	std	PerLPD	freq	AECS	PERCLOS		
32.6	0.673	0.327	2.063	0.1	0.15	0.041667	0.040301	0.063444	0.009541	0.017095	0.228996	0.41027	0.2672067	0.3751465	0.837048	0.945612	0.104167	0.041175	0.102157	0.874137	1.025915	27.6369	1.3916	0.0225	0.2125	0.2112	0.0449			
34.1	0.658	0.342	1.92	0.08	0.26	0.016667	0.017456	0.021592	0.003071	0.006142	0.073702	0.147404	0.1487419	0.1554633	0.595628	0.61416	0.05	0.046794	0.191449	0.61895	0.647297	27.027	1.2068	-0.0001	0.1917	0.1857	0.0356			
30.9	0.69	0.31	2.223	0.1	0.22	0.058333	0.03721	0.076138	0.005981	0.014299	0.143539	0.343175	0.1852894	0.3046795	0.609032	0.700629	0.0875	0.028113	0.086279	0.655924	0.736139	27.7311	1.1733	0.0259	0.2292	0.1787	0.041			
23.4	0.764	0.236	3.23	0.09	0.19	0.02584	0.02285	0.067838	0.005967	0.016845	0.14321	0.404274	0.1478735	0.2436168	0.608469	0.635512	0.03876	0.03081	0.089313	0.620309	0.681092	27.3808	1.3119	0.013	0.2377	0.177	0.0421			
24.1	0.758	0.242	3.134	0.12	0.15	0.066667	0.102506	0.21622	0.017866	0.049097	0.428773	1.178321	0.4097382	0.8217691	1.577515	1.619847	0.166667	0.080279	0.266071	1.646426	1.757407	28.7255	1.4532	0.0627	0.2867	0.223	0.0639			
41.5	0.579	0.421	1.377	0.12	0.2	0.071429	0.042163	0.134603	0.009633	0.028551	0.231196	0.685218	0.2072292	0.4835132	1.457719	1.581791	0.109524	0.055169	0.149132	1.488479	1.654482	27.6909	1.3275	0.0245	0.1952	0.1997	0.039			
42.3	0.573	0.427	1.341	0.12	0.15	0.044444	0.033412	0.08478	0.00742	0.01854	0.178079	0.444952	0.2779277	0.4457768	1.18796	1.371312	0.094444	0.041019	0.130486	1.229543	1.444997	27.9075	1.2628	0.0325	0.2556	0.1965	0.0502			
45.2	0.544	0.456	1.191	0.05	0.15	0.028571	0.031133	0.049065	0.008098	0.013049	0.194342	0.313169	0.1608735	0.2371743	0.941793	1.030869	0.054762	0.028508	0.066589	0.966011	1.05476	26.9143	1.2451	-0.0043	0.2714	0.2008	0.0545			
33.4	0.664	0.336	1.975	0.1	0.15	0.016667	0.01625	0.019473	0.004341	0.008682	0.10418	0.208359	0.1440097	0.1670054	0.795751	0.815532	0.041667	0.014971	0.022477	0.802046	0.825741	25.9814	1.5473	-0.0388	0.1917	0.1648	0.0316			
28.8	0.711	0.289	2.457	0.1	0.15	0.020833	0.046332	0.113459	0.006721	0.026875	0.161311	0.645007	0.4964851	1.4162972	0.569857	0.780942	0.029167	0.036769	0.102173	0.617532	0.801603	26.8988	1.4409	-0.0049	0.2854	0.1762	0.0503			
35	0.648	0.352	1.844	0.08	0.23	0	0	0.004096	0.00603	0.098297	0.144721	0.0900468	0.1323303	0.608941	0.672044	0.030534	0.046613	0.135712	0.617912	0.685913	27.0886	1.4545	0.0022	0.2901	0.1993	0.0578				
26.8	0.731	0.269	2.714	0.11	0.15	0.088889	0.090922	0.122807	0.024653	0.032043	0.591667	0.769032	0.4163983	0.5205317	0.957828	0.98562	0.055556	0.075234	0.157292	1.033507	1.105677	28.7945	1.4858	0.0653	0.2556	0.2158	0.0551			
36	0.633	0.367	1.721	0.06	0.16	0.055556	0.047776	0.100913	0.018169	0.034206	0.436051	0.820943	0.2405032	0.4366217	0.946796	1.011959	0.055556	0.037164	0.092968	0.952092	1.036809	28.8317	1.4645	0.0667	0.3111	0.2191	0.0682			
40.4	0.583	0.417	1.396	0.1	0.19	0.058333	0.031397	0.086406	0.01162	0.029131	0.278884	0.699155	0.1801206	0.2548486	0.731532	0.805964	0.05	0.045728	0.145741	0.80378	0.835187	28.1026	1.3967	0.0397	0.3333	0.191	0.0637			
40.4	0.593	0.407	1.454	0.08	0.15	0.023684	0.026279	0.034793	0.010263	0.026235	0.246301	0.629639	0.4269198	1.873588	0.586302	0.726315	0.031579	0.019361	0.031862	0.630521	0.7539	26.7441	1.2001	-0.0106	0.2211	0.1895	0.0419			
38	0.618	0.382	1.621	0.11	0.24	0.022727	0.034176	0.072102	0.012056	0.027355	0.289352	0.65652	0.2020438	0.3631005	0.788281	0.790719	0.027273	0.034048	0.078649	0.797842	0.81204	27.0313	1.2659	0.0000	0.3273	0.223	0.073			
32.6	0.672	0.328	2.053	0.11	0.15	0.035714	0.034684	0.056782	0.011327	0.016549	0.271853	0.397173	0.1727258	0.2413608	0.544112	0.610251	0.035714	0.029268	0.0748	0.582488	0.66615	27.2503	1.2628	0.0082	0.2286	0.1796	0.041			
36.9	0.631	0.369	1.706	0.11	0.15	0.02619	0.064317	0.111554	0.010757	0.021559	0.258172	0.517423	0.4210294	1.0041825	0.443154	0.490251	0.016667	0.039959	0.088772	0.516245	0.534652	27.6236	1.7955	0.022	0.2262	0.1757	0.0397			
27.2	0.725	0.275	2.636	0.05	0.18	0.059375	0.067579	0.120012	0.017017	0.048341	0.408401	1.160185	0.9905771	2.4699213	0.341505	0.416999	0.040625	0.046214	0.091298	0.432778	0.480198	27.303	1.5706	0.0101	0.2719	0.1952	0.0531			

Figure H.1 (continued) : Data collected during the study.

APPENDIX I: SPSS t-Test Outputs of Physiological Data Between Low and High Task Load

		Independent Samples Test								
		Levene's Test for Equality of Variances				t-test for Equality of Means				
		F	Sig.	t	df	Sig. (2-tailed)	Mean Difference	Std. Error Difference	95% Confidence Interval of the Difference	
									Lower	Upper
n_hrv_hr	Equal variances assumed	2.041	.155	3.016	201	.003	.11972641	.03969603	.04145233	-.19800049
	Equal variances not assumed			2.978	176.049	.003	.11972641	.04020233	.04038588	-.19906694
n_hrv_sdnn	Equal variances assumed	.008	.928	-3.427	201	.001	-.12739130	.03717573	-.20069576	-.05408685
	Equal variances not assumed			-3.396	178.959	.001	-.12739130	.03750778	-.20140572	-.05337689
n_hrv_rmssd	Equal variances assumed	.116	.734	-2.442	201	.015	-.08870636	.03632958	-.16034236	-.01707036
	Equal variances not assumed			-2.412	176.544	.017	-.08870636	.03676961	-.16127090	-.01614182
n_hrv_pnn50	Equal variances assumed	.487	.486	-2.685	201	.008	-.10950057	.04078801	-.18992786	-.02907327
	Equal variances not assumed			-2.682	184.726	.008	-.10950057	.04082734	-.19004838	-.02895275
n_hrv_hvnti	Equal variances assumed	.033	.856	-1.518	201	.130	-.06173487	.04065895	-.14190768	.01843794
	Equal variances not assumed			-1.514	183.464	.132	-.06173487	.04077140	-.14217597	.01870623
n_hrv_tinn	Equal variances assumed	.035	.852	-3.058	201	.003	-.12202069	.03990075	-.20069846	-.04334293
	Equal variances not assumed			-3.039	180.830	.003	-.12202069	.04015666	-.20125659	-.04278480
n_hrv_fwalf	Equal variances assumed	.374	.542	-3.566	201	.000	-.13522013	.03791568	-.20998366	-.06045660
	Equal variances not assumed			-3.565	185.051	.000	-.13522013	.03793441	-.21005966	-.06038061
n_hrv_fwahf	Equal variances assumed	.028	.867	-2.739	201	.007	-.10191676	.03721425	-.17529719	-.02853633
	Equal variances not assumed			-2.745	186.944	.007	-.10191676	.03712837	-.17516119	-.02867233
n_hrv_fwatotal	Equal variances assumed	.502	.479	-3.487	201	.001	-.13021795	.03734198	-.20385023	-.05658567
	Equal variances not assumed			-3.492	186.407	.001	-.13021795	.03728594	-.20377460	-.05666130
hrv_fwplf	Equal variances assumed	8.622	.004	-2.128	201	.035	-3.8664	1.8166	-7.4485	-.2843
	Equal variances not assumed			-2.049	155.346	.042	-3.8664	1.8869	-7.5936	-.1391
hrv_fwphf	Equal variances assumed	6.095	.014	2.204	201	.029	4.4945	2.0391	.4738	8.5153
	Equal variances not assumed			2.129	157.905	.035	4.4945	2.1114	.3242	8.6648
hrv_fwnlf	Equal variances assumed	6.284	.013	-2.171	201	.031	-.044374	.020443	-.084683	-.004064
	Equal variances not assumed			-2.098	158.516	.038	-.044374	.021152	-.086150	-.002597
hrv_fwnhf	Equal variances assumed	6.284	.013	2.171	201	.031	.044374	.020443	.004064	.084683
	Equal variances not assumed			2.098	158.516	.038	.044374	.021152	.002597	.086150
n_hrv_fwlfhf	Equal variances assumed	.087	.768	-1.683	201	.094	-.06388099	.03794678	-.13870584	.01094386
	Equal variances not assumed			-1.683	185.116	.094	-.06388099	.03796194	-.13877466	.01101267
n_hrv_fwpeaklf	Equal variances assumed	7.607	.006	2.450	201	.015	.09927477	.04052479	.01936650	.17918303
	Equal variances not assumed			2.382	163.592	.018	.09927477	.04167714	.01698028	.18156925
n_hrv_fwpeakhf	Equal variances assumed	.111	.739	.042	201	.966	.00187448	.04457188	-.08601398	.08976294
	Equal variances not assumed			.042	188.547	.966	.00187448	.04435896	-.08562915	.08937811
n_hrv_flalf	Equal variances assumed	.368	.545	-2.670	201	.008	-.10297572	.03857217	-.17903373	-.02691771
	Equal variances not assumed			-2.690	190.252	.008	-.10297572	.03828188	-.17848716	-.02746428
n_hrv_flahf	Equal variances assumed	2.491	.116	.520	201	.603	.02128955	.04090450	-.05936744	.10194655
	Equal variances not assumed			.510	169.953	.611	.02128955	.04174377	-.06111352	.10369262

Figure I.1 : t-Test of physiological data between low and high task load for navigation tasks.

		Independent Samples Test										
		Levene's Test for Equality of Variances				t-test for Equality of Means						
		F	Sig.	t	df	Sig. (2-tailed)	Mean Difference	Std. Error Difference	95% Confidence Interval of the Difference			
									Lower	Upper		
n_hrv_flsatotal	Equal variances assumed	1.593	.208	-1.549	201	.123	-.06047196	.03902724	-1.13742729	.01648337		
	Equal variances not assumed			-1.568	192.709	.119	-.06047196	.03856714	-1.13653987	.01559595		
hrv_flsplf	Equal variances assumed	3.752	.054	-1.926	201	.056	-3.9103	2.0305	-7.9141	.0935		
	Equal variances not assumed			-1.874	164.385	.063	-3.9103	2.0862	-8.0296	.2089		
hrv_flsphf	Equal variances assumed	3.044	.083	2.007	201	.046	4.2124	2.0987	.0741	8.3507		
	Equal variances not assumed			1.957	165.994	.052	4.2124	2.1521	-.0367	8.4614		
hrv_flsnlf	Equal variances assumed	3.222	.074	-1.986	201	.048	-.041632	.020964	-.082971	-.000294		
	Equal variances not assumed			-1.936	165.695	.055	-.041632	.021506	-.084093	.000829		
hrv_flsnhf	Equal variances assumed	3.222	.074	1.986	201	.048	.041632	.020964	.000294	.082971		
	Equal variances not assumed			1.936	165.695	.055	.041632	.021506	-.000829	.084093		
n_hrv_flslfhf	Equal variances assumed	.398	.529	-1.468	201	.144	-.05397506	.03677958	-1.2649839	.01854826		
	Equal variances not assumed			-1.453	178.298	.148	-.05397506	.03714036	-1.2726629	.01931617		
n_hrv_flspeaklf	Equal variances assumed	.010	.919	-.153	201	.879	-.00622605	.04077083	-.08661946	.07416735		
	Equal variances not assumed			-.153	186.501	.879	-.00622605	.04070389	-.08652528	.07407317		
n_hrv_flspeakhf	Equal variances assumed	.168	.682	.372	201	.710	.01788390	.04806402	-.07689048	.11265829		
	Equal variances not assumed			.372	184.545	.711	.01788390	.04812294	-.07705795	.11282575		
n_hrv_nlsd1	Equal variances assumed	.151	.698	-2.405	201	.017	-.08731750	.03630313	-1.5890134	-.01573366		
	Equal variances not assumed			-2.376	176.309	.019	-.08731750	.03675394	-1.5895178	-.01478321		
n_hrv_nlsd2	Equal variances assumed	.019	.890	-3.565	201	.000	-1.13216706	.03707388	-.20527070	-.05906343		
	Equal variances not assumed			-3.543	180.949	.001	-1.13216706	.03730570	-.20577720	-.05855693		
n_hrv_nlsampen	Equal variances assumed	2.179	.141	-.755	201	.451	-.03416809	.04527034	-1.2343379	.05509762		
	Equal variances not assumed			-.744	174.378	.458	-.03416809	.04594533	-1.2484862	.05651244		
n_hrv_nlalpa1	Equal variances assumed	.676	.412	-.652	201	.515	-.02472538	.03792875	-.09951467	.05006392		
	Equal variances not assumed			-.644	176.409	.520	-.02472538	.03839480	-.10049762	.05104687		
n_hrv_nlalpa2	Equal variances assumed	4.394	.037	.830	201	.408	.03110820	.03747895	-.04279416	.10501055		
	Equal variances not assumed			.810	166.630	.419	.03110820	.03840341	-.04471177	.10692816		
n_hrv_tflsalf	Equal variances assumed	.966	.327	-3.596	201	.000	-1.13672017	.03802469	-.21169865	-.06174169		
	Equal variances not assumed			-3.619	189.601	.000	-1.13672017	.03777907	-.21124146	-.06219889		
n_hrv_tflsahf	Equal variances assumed	.930	.336	-2.763	201	.006	-1.0967817	.03969467	-1.8794957	-.03140677		
	Equal variances not assumed			-2.725	175.214	.007	-1.0967817	.04024382	-1.8910321	-.03025314		
n_hrv_tflsatotal	Equal variances assumed	.984	.322	-3.545	201	.000	-1.13480247	.03802343	-.20977846	-.05982647		
	Equal variances not assumed			-3.569	189.707	.000	-1.13480247	.03777128	-.20930812	-.06029681		
hrv_tflsplf	Equal variances assumed	8.294	.004	-2.171	201	.031	-3.9454	1.8175	-7.5293	-.3615		
	Equal variances not assumed			-2.098	158.629	.037	-3.9454	1.8804	-7.6592	-.2316		
hrv_tflsphf	Equal variances assumed	7.178	.008	2.247	201	.026	4.4204	1.9675	.5409	8.3000		
	Equal variances not assumed			2.174	159.395	.031	4.4204	2.0337	.4040	8.4368		

Figure I.1 (continued) : t-Test of physiological data between low and high task load for navigation tasks.

		Independent Samples Test								
		Levene's Test for Equality of Variances				t-test for Equality of Means			95% Confidence Interval of the Difference	
		F	Sig.	t	df	Sig. (2-tailed)	Mean Difference	Std. Error Difference	Lower	Upper
hrv_tflsnlf	Equal variances assumed	7.348	.007	-2.207	201	.028	-.043603	.019757	-.082560	-.004647
	Equal variances not assumed			-2.136	159.666	.034	-.043603	.020414	-.083921	-.003286
hrv_tflsnhf	Equal variances assumed	7.348	.007	2.207	201	.028	.043603	.019757	.004647	.082560
	Equal variances not assumed			2.136	159.666	.034	.043603	.020414	.003286	.083921
n_hrv_tflsflhf	Equal variances assumed	.040	.842	-2.345	201	.020	-.08773233	.03740600	-.16149085	-.01397381
	Equal variances not assumed			-2.353	187.548	.020	-.08773233	.03728533	-.16128485	-.01417981
n_hrv_tflspeaklf	Equal variances assumed	.395	.530	.633	201	.527	.02709360	.04277527	-.05725224	.11143943
	Equal variances not assumed			.628	179.148	.531	.02709360	.04314656	-.05804727	.11223446
n_hrv_tflspeakhf	Equal variances assumed	.727	.395	.723	201	.470	.03303625	.04568920	-.05705539	.12312789
	Equal variances not assumed			.720	182.691	.472	.03303625	.04586518	-.05745731	.12352981
n_hrv_tflwalf	Equal variances assumed	.733	.393	-4.005	201	.000	-.15918527	.03974773	-.23756130	-.08080924
	Equal variances not assumed			-4.023	188.418	.000	-.15918527	.03956594	-.23723440	-.08113614
n_hrv_tflwahf	Equal variances assumed	.071	.790	-3.287	201	.001	-.12685221	.03859513	-.20295549	-.05074892
	Equal variances not assumed			-3.278	183.504	.001	-.12685221	.03869970	-.20320577	-.05049864
n_hrv_tflwatotal	Equal variances assumed	1.426	.234	-3.952	201	.000	-.15670792	.03965201	-.23489521	-.07852063
	Equal variances not assumed			-3.986	190.887	.000	-.15670792	.03931142	-.23424848	-.07916735
hrv_tflwplf	Equal variances assumed	5.469	.020	-2.241	201	.026	-4.5101	2.0126	-8.4785	-.5416
	Equal variances not assumed			-2.176	162.456	.031	-4.5101	2.0726	-8.6028	-.4173
hrv_tflwphf	Equal variances assumed	5.100	.025	2.240	201	.026	4.5716	2.0409	.5473	8.5958
	Equal variances not assumed			2.177	163.017	.031	4.5716	2.1003	.4242	8.7189
hrv_tflwnlf	Equal variances assumed	5.149	.024	-2.239	201	.026	-.045658	.020388	-.085860	-.005457
	Equal variances not assumed			-2.176	162.998	.031	-.045658	.020983	-.087091	-.004225
hrv_tflwnhf	Equal variances assumed	5.149	.024	2.239	201	.026	.045658	.020388	.005457	.085860
	Equal variances not assumed			2.176	162.998	.031	.045658	.020983	.004225	.087091
n_hrv_tflwflhf	Equal variances assumed	.007	.934	-1.771	201	.078	-.07079321	.03997658	-.14962050	.00803407
	Equal variances not assumed			-1.759	180.506	.080	-.07079321	.04025059	-.15021541	.00862898
n_hrv_tflwpeaklf	Equal variances assumed	.662	.417	1.919	201	.056	.08652048	.04509123	-.00239204	.17543300
	Equal variances not assumed			1.908	181.361	.058	.08652048	.04534776	-.00295656	.17599752
n_hrv_tflwpeakhf	Equal variances assumed	.021	.886	1.241	201	.216	.06841799	.05514536	-.04031965	.17715563
	Equal variances not assumed			1.239	184.596	.217	.06841799	.05520889	-.04050353	.17733951
eda_cdanscr	Equal variances assumed	3.443	.065	-.975	201	.331	-.00939777	.00964010	-.02840646	.00961092
	Equal variances not assumed			-1.003	199.497	.317	-.00939777	.00936776	-.02787031	.00907477
n_eda_cdaampsuma	Equal variances assumed	2.608	.108	-.013	201	.990	-.00050168	.03988056	-.07913962	.07813625
	Equal variances not assumed			-.012	173.588	.990	-.00050168	.04051550	-.08046811	.07946474
n_eda_cdaampsumm	Equal variances assumed	2.344	.127	-1.905	201	.058	-.07597969	.03989019	-.15463661	.00267724
	Equal variances not assumed			-1.942	196.396	.054	-.07597969	.03912019	-.15312926	.00116988

Figure I.1 (continued) : t-Test of physiological data between low and high task load for navigation tasks.

		Levene's Test for Equality of Variances				t-Test for Equality of Means				95% Confidence Interval of the Difference	
		F	Sig.	t	df	Sig. (2-tailed)	Mean Difference	Std. Error Difference	Lower	Upper	
n_eda_cdascra	Equal variances assumed	1.757	.187	.313	201	.755	.01202469	.03840872	-.06371102	.08776039	
	Equal variances not assumed			.307	171.719	.759	.01202469	.03911138	-.06517630	.08922567	
n_eda_cdascrm	Equal variances assumed	.639	.425	-1.318	201	.189	-.05436938	.04125536	-.13571821	.02697946	
	Equal variances not assumed			-1.334	192.855	.184	-.05436938	.04075797	-.13475800	.02601925	
n_eda_cdaiscra	Equal variances assumed	1.757	.187	.313	201	.755	.01202469	.03840872	-.06371102	.08776039	
	Equal variances not assumed			.307	171.719	.759	.01202469	.03911138	-.06517630	.08922567	
n_eda_cdaiscrm	Equal variances assumed	.639	.425	-1.318	201	.189	-.05436938	.04125536	-.13571821	.02697946	
	Equal variances not assumed			-1.334	192.855	.184	-.05436938	.04075797	-.13475800	.02601925	
n_eda_cdamaxa	Equal variances assumed	.479	.489	.977	201	.330	.03708490	.03797244	-.03779053	.11196034	
	Equal variances not assumed			.971	181.171	.333	.03708490	.03819834	-.03828594	.11245575	
eda_cdamaxm	Equal variances assumed	1.918	.168	-9.009	201	.364	-.22007481	.24210434	-.69746498	.25731536	
	Equal variances not assumed			-.939	200.384	.349	-.22007481	.23426084	-.68200749	.24185787	
n_eda_cdatonica	Equal variances assumed	.010	.920	-2.004	201	.046	-.08835699	.04408010	-.17527574	-.00143825	
	Equal variances not assumed			-1.990	180.099	.048	-.08835699	.04440647	-.17598088	-.00073311	
n_eda_cdatonicm	Equal variances assumed	.895	.345	-2.125	201	.035	-.08856153	.04166758	-.17072319	-.00639988	
	Equal variances not assumed			-2.100	176.710	.037	-.08856153	.04216319	-.17176973	-.00535334	
eda_ttpnsr	Equal variances assumed	.028	.868	-.464	201	.643	-.00407134	.00877931	-.02138271	.01324002	
	Equal variances not assumed			-.465	187.830	.642	-.00407134	.00874718	-.02132668	.01318400	
n_eda_ttpampsuma	Equal variances assumed	.039	.844	-.145	201	.885	-.00589026	.04062833	-.08600270	.07422217	
	Equal variances not assumed			-.145	184.137	.885	-.00589026	.04070188	-.08619226	.07441173	
n_eda_ttpampsumm	Equal variances assumed	1.657	.199	-1.460	201	.146	-.05765370	.03948184	-.13550543	.02019802	
	Equal variances not assumed			-1.478	192.957	.141	-.05765370	.03899838	-.13457156	.01926415	
n_eda_sca	Equal variances assumed	.236	.627	-1.898	201	.059	-.08292610	.04368062	-.16905713	.00320494	
	Equal variances not assumed			-1.895	184.270	.060	-.08292610	.04375140	-.16924417	.00339198	
n_eda_scm	Equal variances assumed	.516	.474	-2.308	201	.022	-.09618826	.04166963	-.17835396	-.01402255	
	Equal variances not assumed			-2.280	176.439	.024	-.09618826	.04218002	-.17943054	-.01294597	
n_pd_mean	Equal variances assumed	2.751	.099	-1.809	201	.072	-.0717695	.0396630	-.1499785	.0064395	
	Equal variances not assumed			-1.789	177.109	.075	-.0717695	.04011142	-.1509327	.0073938	
pd_std	Equal variances assumed	.110	.741	-.263	201	.793	-.0275917	.1049992	-.2346330	.1794497	
	Equal variances not assumed			-.262	182.891	.794	-.0275917	.1053743	-.2354972	.1803138	
pd_lpd	Equal variances assumed	11.453	.001	-2.951	201	.004	-.0285733	.0096822	-.0476650	-.0094815	
	Equal variances not assumed			-3.110	199.371	.002	-.0285733	.0091884	-.0466921	-.0104544	
n_br_freq	Equal variances assumed	1.916	.168	.617	201	.538	.0239138	.0386768	-.0525299	.1003575	
	Equal variances not assumed			.607	172.875	.545	.0239138	.0394202	-.0538930	.1017206	
n_br_aecs	Equal variances assumed	5.942	.016	3.589	201	.000	.1556740	.0433694	.0701566	.2411913	
	Equal variances not assumed			3.513	168.922	.001	.1556740	.0443153	.0681909	.2431570	
n_br_perclos	Equal variances assumed	.608	.436	2.020	201	.045	.0767484	.0379857	.0018467	.1516501	
	Equal variances not assumed			2.006	180.385	.046	.0767484	.0382523	.0012688	.1522280	

Figure I.1 (continued) : t-Test of physiological data between low and high task load for navigation tasks.

		Levene's Test for Equality of Variances				t-test for Equality of Means				95% Confidence Interval of the Difference	
		F	Sig.	t	df	Sig. (2-tailed)	Mean Difference	Std. Error Difference	Lower	Upper	
n_hrv_hr	Equal variances assumed	8.238	.005	2.689	78	.009	.16857462	.06267983	.04378866	.29336059	
	Equal variances not assumed			2.872	77.578	.005	.16857462	.05869198	.05171786	.28543138	
n_hrv_sdn	Equal variances assumed	.070	.791	-2.512	78	.014	-.15667600	.06236432	-.28083383	-.03251817	
	Equal variances not assumed			-2.528	67.973	.014	-.15667600	.06198326	-.28036254	-.03298946	
n_hrv_rmssd	Equal variances assumed	1.748	.190	-2.479	78	.015	-.16096567	.06494395	-.29025916	-.03167219	
	Equal variances not assumed			-2.570	74.015	.012	-.16096567	.06263373	-.28576568	-.03616567	
n_hrv_pnn50	Equal variances assumed	2.387	.126	-2.821	78	.006	-.17722495	.06282553	-.30230098	-.05214893	
	Equal variances not assumed			-2.973	76.362	.004	-.17722495	.05961886	-.29595710	-.05849280	
n_hrv_hrvti	Equal variances assumed	.013	.908	-.987	78	.327	-.06469964	.06558140	-.19526218	.06586289	
	Equal variances not assumed			-.997	69.019	.322	-.06469964	.06487245	-.19411599	.06471670	
n_hrv_tinn	Equal variances assumed	.014	.907	-2.670	78	.009	-.16192229	.06064492	-.28265705	-.04118754	
	Equal variances not assumed			-2.655	65.306	.010	-.16192229	.06098530	-.28370753	-.04013706	
n_hrv_fwalf	Equal variances assumed	1.997	.162	-.947	78	.347	-.06577814	.06949433	-.20413073	.07257445	
	Equal variances not assumed			-.984	74.509	.328	-.06577814	.06682253	-.19890981	.06735354	
n_hrv_fwahf	Equal variances assumed	1.197	.277	-1.438	78	.154	-.09230420	.06417358	-.22006400	.03545559	
	Equal variances not assumed			-1.492	74.115	.140	-.09230420	.06185400	-.21554779	.03093938	
n_hrv_fwatotal	Equal variances assumed	.884	.350	-1.465	78	.147	-.10155371	.06929784	-.23951511	.03640769	
	Equal variances not assumed			-1.500	71.666	.138	-.10155371	.06768651	-.23649505	.03338763	
hrv_fwplf	Equal variances assumed	.097	.757	-.042	78	.967	-.1760	4.2326	-8.6025	8.2504	
	Equal variances not assumed			-.041	62.983	.967	-.1760	4.2991	-8.7672	8.4151	
hrv_fwphf	Equal variances assumed	.190	.664	-.030	78	.976	-.1313	4.3709	-8.8331	8.5706	
	Equal variances not assumed			-.030	62.673	.977	-.1313	4.4455	-9.0159	8.7534	
hrv_fwnif	Equal variances assumed	.128	.721	-.001	78	.999	-.000042	.044772	-.089176	.089092	
	Equal variances not assumed			-.001	62.975	.999	-.000042	.045477	-.090921	.090838	
hrv_fwnhf	Equal variances assumed	.128	.721	.001	78	.999	.000042	.044772	-.089092	.089176	
	Equal variances not assumed			.001	62.975	.999	.000042	.045477	-.090838	.090921	
n_hrv_fwlfhf	Equal variances assumed	.534	.467	.509	78	.612	.03015037	.05922898	-.08776548	.14806622	
	Equal variances not assumed			.524	72.568	.602	.03015037	.05758348	-.08462484	.14492558	
n_hrv_fwpeaklf	Equal variances assumed	.937	.336	-.359	78	.720	-.02560764	.07128104	-.16751728	.11630200	
	Equal variances not assumed			-.352	62.042	.726	-.02560764	.07269442	-.17091977	.11970449	
n_hrv_fwpeakhf	Equal variances assumed	.427	.516	1.916	78	.059	.15523104	.08102846	-.00608424	.31654631	
	Equal variances not assumed			1.947	70.112	.056	.15523104	.07974596	-.00381281	.31427488	
n_hrv_flsalf	Equal variances assumed	.385	.537	-1.819	78	.073	-.12231597	.06725924	-.25621883	.01158688	
	Equal variances not assumed			-1.778	61.375	.080	-.12231597	.06878955	-.25985218	.01522024	
n_hrv_flsahf	Equal variances assumed	.165	.686	-.592	78	.555	-.03793317	.06405915	-.16546515	.08959880	
	Equal variances not assumed			-.603	70.678	.548	-.03793317	.06287474	-.16331174	.08744540	

Figure I.2 : t-Test of physiological data between low and high task load for cargo operation tasks.

		Independent Samples Test										
		Levene's Test for Equality of Variances		t-test for Equality of Means							95% Confidence Interval of the Difference	
		F	Sig.	t	df	Sig. (2-tailed)	Mean Difference	Std. Error Difference	Lower	Upper		
n_hrv_flsatotal	Equal variances assumed	.112	.738	-.994	78	.323	-.06369541	.06405643	-.19122196	.06383114		
	Equal variances not assumed			-.985	64.340	.328	-.06369541	.06468514	-.19290567	.06551485		
hrv_flsplf	Equal variances assumed	.515	.475	.245	78	.807	1.1167	4.5605	-7.9627	10.1960		
	Equal variances not assumed			.239	60.628	.812	1.1167	4.6793	-8.2414	10.4747		
hrv_flsphf	Equal variances assumed	.876	.352	-.291	78	.772	-1.3208	4.5356	-10.3505	7.7089		
	Equal variances not assumed			-.283	59.671	.778	-1.3208	4.6730	-10.6693	8.0276		
hrv_flsnlf	Equal variances assumed	.727	.396	.258	78	.797	.011854	.046001	-.079726	.103435		
	Equal variances not assumed			.250	59.988	.803	.011854	.047329	-.082819	.106528		
hrv_flsnhf	Equal variances assumed	.727	.396	-.258	78	.797	-.011854	.046001	-.103435	.079726		
	Equal variances not assumed			-.250	59.988	.803	-.011854	.047329	-.106528	.082819		
n_hrv_flslfhf	Equal variances assumed	.800	.374	.604	78	.548	.03704759	.06136680	-.08512433	.15921951		
	Equal variances not assumed			.616	70.875	.540	.03704759	.06017476	-.08294114	.15703632		
n_hrv_flspeakf	Equal variances assumed	.238	.627	-1.622	78	.109	-1.1104911	.06844885	-.24732030	.02522208		
	Equal variances not assumed			-1.616	65.735	.111	-1.1104911	.06870513	-.24823367	.02613545		
n_hrv_flspeakhf	Equal variances assumed	6.203	.015	1.082	78	.283	.07806256	.07213706	-.06555128	.22167641		
	Equal variances not assumed			1.153	77.426	.252	.07806256	.06769945	-.05673245	.21285757		
n_hrv_nlsd1	Equal variances assumed	1.732	.192	-2.456	78	.016	-1.6015704	.06520325	-.28996675	-.03034733		
	Equal variances not assumed			-2.547	74.032	.013	-1.6015704	.06287758	-.28544246	-.03487162		
n_hrv_nlsd2	Equal variances assumed	.101	.752	-2.343	78	.022	-1.5211131	.06491930	-.28135571	-.02286691		
	Equal variances not assumed			-2.361	68.270	.021	-1.5211131	.06443667	-.28068348	-.02353915		
n_hrv_nlsampen	Equal variances assumed	.108	.743	.270	78	.788	.01965369	.07286814	-.12541564	.16472302		
	Equal variances not assumed			.269	66.381	.788	.01965369	.07293506	-.12595026	.16525764		
n_hrv_nlalpha1	Equal variances assumed	2.540	.115	-.296	78	.768	-.01893886	.06390677	-.14616746	.10828974		
	Equal variances not assumed			-.309	74.813	.758	-.01893886	.06133226	-.14112401	.10324628		
n_hrv_nlalpha2	Equal variances assumed	1.241	.269	1.294	78	.200	.08620482	.06664295	-.04647111	.21888074		
	Equal variances not assumed			1.342	74.125	.184	.08620482	.06423031	-.04177328	.21418291		
n_hrv_tflsalf	Equal variances assumed	1.435	.235	-1.462	78	.148	-.09902358	.06771936	-.23384247	.03579532		
	Equal variances not assumed			-1.508	73.049	.136	-.09902358	.06566843	-.22989909	.03185194		
n_hrv_tflsahf	Equal variances assumed	.832	.365	-1.650	78	.103	-1.0874075	.06589690	-.23993141	.02244991		
	Equal variances not assumed			-1.696	72.464	.094	-1.0874075	.06410146	-.23651071	.01902920		
n_hrv_tflsatotal	Equal variances assumed	.891	.348	-1.860	78	.067	-1.2996273	.06985592	-.26903518	.00910973		
	Equal variances not assumed			-1.898	70.993	.062	-1.2996273	.06845963	-.26646759	.00654214		
hrv_tflsplf	Equal variances assumed	.053	.818	-.185	78	.854	-.7635	4.1379	-9.0014	7.4744		
	Equal variances not assumed			-.182	63.480	.856	-.7635	4.1940	-9.1433	7.6162		
hrv_tflsphf	Equal variances assumed	.161	.689	.228	78	.820	.9531	4.1845	-7.3775	9.2837		
	Equal variances not assumed			.223	62.090	.824	.9531	4.2665	-7.5753	9.4816		

Figure I.2 (continued) : t-Test of physiological data between low and high task load for cargo operation tasks.

		Levene's Test for Equality of Variances					t-test for Equality of Means			95% Confidence Interval of the Difference	
		F	Sig.	t	df	Sig. (2-tailed)	Mean Difference	Std. Error Difference	Lower	Upper	
hrv_tflsnlf	Equal variances assumed	.100	.752	-.240	78	.811	-.010281	.042878	-.095645	.075083	
	Equal variances not assumed			-.236	62.725	.814	-.010281	.043601	-.097418	.076855	
hrv_tflsnhf	Equal variances assumed	.100	.752	.240	78	.811	.010281	.042878	-.075083	.095645	
	Equal variances not assumed			.236	62.725	.814	.010281	.043601	-.076855	.097418	
n_hrv_tflslfhf	Equal variances assumed	2.223	.140	.159	78	.874	.00985870	.06213640	-.11384536	.13356277	
	Equal variances not assumed			.167	76.299	.868	.00985870	.05899583	-.10763423	.12735163	
n_hrv_tflspeaklf	Equal variances assumed	.022	.884	-.535	78	.594	-.03578869	.06686832	-.16891328	.09733590	
	Equal variances not assumed			-.530	64.464	.598	-.03578869	.06748871	-.17059422	.09901684	
n_hrv_tflspeakhf	Equal variances assumed	.342	.561	1.400	78	.165	.09221135	.06586375	-.03891331	.22333601	
	Equal variances not assumed			1.413	68.728	.162	.09221135	.06523836	-.03794479	.22236748	
n_hrv_tfwalf	Equal variances assumed	2.434	.123	-1.377	78	.173	-.09352185	.06792769	-.22875548	.04171179	
	Equal variances not assumed			-1.441	75.492	.154	-.09352185	.06489410	-.22278373	.03574004	
n_hrv_tfwahf	Equal variances assumed	.818	.369	-2.189	78	.032	-.13504623	.06168956	-.25786070	-.01223175	
	Equal variances not assumed			-2.258	73.083	.027	-.13504623	.05981027	-.25424565	-.01584680	
n_hrv_tfwatotal	Equal variances assumed	2.292	.134	-1.978	78	.051	-.12989566	.06567854	-.26065158	.00086027	
	Equal variances not assumed			-2.078	75.977	.041	-.12989566	.06252050	-.25441662	-.00537469	
hrv_tfwplf	Equal variances assumed	.567	.454	-.019	78	.985	-.0740	3.9299	-7.8977	7.7498	
	Equal variances not assumed			-.018	59.298	.986	-.0740	4.0555	-8.1882	8.0402	
hrv_tfwphf	Equal variances assumed	.594	.443	-.001	78	.999	-.0031	3.9232	-7.8137	7.8074	
	Equal variances not assumed			-.001	59.325	.999	-.0031	4.0482	-8.1026	8.0963	
hrv_tfwnlf	Equal variances assumed	.581	.448	-.006	78	.995	-.000250	.039405	-.078699	.078199	
	Equal variances not assumed			-.006	59.350	.995	-.000250	.040655	-.081591	.081091	
hrv_tfwnhf	Equal variances assumed	.581	.448	.006	78	.995	.000250	.039405	-.078199	.078699	
	Equal variances not assumed			.006	59.350	.995	.000250	.040655	-.081091	.081591	
n_hrv_tfwlfhf	Equal variances assumed	.134	.716	.217	78	.828	.01409494	.06484052	-.11499262	.14318249	
	Equal variances not assumed			.217	66.250	.829	.01409494	.06493730	-.11554743	.14373730	
n_hrv_tfwpeaklf	Equal variances assumed	1.098	.298	.492	78	.624	.03278770	.06666343	-.09992900	.16550440	
	Equal variances not assumed			.477	59.585	.635	.03278770	.06870880	-.10467006	.17024546	
n_hrv_tfwpeakhf	Equal variances assumed	11.920	.001	2.993	78	.004	.25312500	.08456550	.08476802	.42148198	
	Equal variances not assumed			3.162	76.623	.002	.25312500	.08006406	.09368458	.41256542	
eda_cdanscr	Equal variances assumed	.152	.697	.240	78	.811	.00602758	.02506551	-.04387402	.05592918	
	Equal variances not assumed			.241	66.670	.811	.00602758	.02505676	-.04399047	.05604563	
n_eda_cdaampsuma	Equal variances assumed	3.763	.056	-1.009	78	.316	-.06932710	.06872701	-.20615206	.06749786	
	Equal variances not assumed			-1.073	77.274	.287	-.06932710	.06462630	-.19800722	.05935303	
n_eda_cdaampsumm	Equal variances assumed	.792	.376	-1.156	78	.251	-.08052247	.06962997	-.21914510	.05810015	
	Equal variances not assumed			-1.194	73.218	.236	-.08052247	.06745858	-.21496049	.05391554	

Figure I.2 (continued) : t-Test of physiological data between low and high task load for cargo operation tasks.

Independent Samples Test										
		Levene's Test for Equality of Variances		t-Test for Equality of Means						
		F	Sig.	t	df	Sig. (2-tailed)	Mean Difference	Std. Error Difference	95% Confidence Interval of the Difference	
									Lower	Upper
n_eda_cdascra	Equal variances assumed	1.528	.220	-1.547	78	.126	-10707125	.06920003	-24483793	.03069543
	Equal variances not assumed			-1.605	74.083	.113	-10707125	.06671161	-23999456	.02585206
n_eda_cdascrm	Equal variances assumed	1.214	.274	-1.962	78	.053	-13846684	.07056850	-27895793	.00202426
	Equal variances not assumed			-2.000	70.758	.049	-13846684	.06923723	-27653016	-.00040352
n_eda_cdaiscra	Equal variances assumed	1.528	.220	-1.547	78	.126	-10707125	.06920003	-24483793	.03069543
	Equal variances not assumed			-1.605	74.083	.113	-10707125	.06671161	-23999456	.02585206
n_eda_cdaiscrm	Equal variances assumed	1.214	.274	-1.962	78	.053	-13846684	.07056850	-27895793	.00202426
	Equal variances not assumed			-2.000	70.758	.049	-13846684	.06923723	-27653016	-.00040352
n_eda_cdamaxa	Equal variances assumed	.017	.897	-.843	78	.402	-.05919288	.07018748	-.19892541	.08053965
	Equal variances not assumed			-.852	68.903	.397	-.05919288	.06946579	-.19777683	.07939107
eda_cdamaxm	Equal variances assumed	.672	.415	-.851	78	.397	-.44194729	.51906310	-1.47532253	.59142796
	Equal variances not assumed			-.830	60.644	.410	-.44194729	.53254672	-1.50696684	.62307226
n_eda_cdatonica	Equal variances assumed	2.101	.151	-.567	78	.572	-.04241700	.07476528	-.19126324	.10642924
	Equal variances not assumed			-.587	73.582	.559	-.04241700	.07228659	-.18646480	.10163079
n_eda_cdatonicm	Equal variances assumed	.518	.474	-1.084	78	.282	-.07750134	.07149087	-.21982873	.06482604
	Equal variances not assumed			-1.101	70.089	.274	-.07750134	.07036690	-.21784057	.06283788
eda_tpnscr	Equal variances assumed	.116	.734	.600	78	.550	.01214377	.02023336	-.02813774	.05242529
	Equal variances not assumed			.602	67.359	.549	.01214377	.02016489	-.02810158	.05238913
n_eda_tppampsuma	Equal variances assumed	.899	.346	-.603	78	.548	-.04155647	.06892889	-.17878334	.09567040
	Equal variances not assumed			-.613	70.277	.542	-.04155647	.06778476	-.17673955	.09362661
n_eda_tppampsumm	Equal variances assumed	.222	.639	-1.044	78	.300	-.06969784	.06677911	-.20264485	.06324916
	Equal variances not assumed			-1.049	67.661	.298	-.06969784	.06646376	-.20233623	.06294055
n_eda_sca	Equal variances assumed	1.405	.240	-.470	78	.640	-.03568654	.07598065	-.18695240	.11557931
	Equal variances not assumed			-.483	72.587	.630	-.03568654	.07386234	-.18290807	.11515499
n_eda_scm	Equal variances assumed	.108	.744	-1.165	78	.247	-.08107489	.06958069	-.21959940	.05744962
	Equal variances not assumed			-1.180	69.353	.242	-.08107489	.06872289	-.21816087	.05601108
n_pd_mean	Equal variances assumed	4.588	.035	2.591	78	.011	.1676861	.0647288	.0388210	.2965513
	Equal variances not assumed			2.708	75.304	.008	.1676861	.0619191	.0443450	.2910273
pd_std	Equal variances assumed	.012	.913	.602	78	.549	.0348635	.0578964	-.0803993	.1501263
	Equal variances not assumed			.597	64.617	.553	.0348635	.0583949	-.0817721	.1514992
pd_lpd	Equal variances assumed	.165	.686	1.393	78	.168	.0143271	.0102860	-.0061509	.0348050
	Equal variances not assumed			1.371	62.959	.175	.0143271	.0104488	-.0065535	.0352076
n_br_freq	Equal variances assumed	.722	.398	.493	78	.623	.0330934	.0671097	-.1005118	.1666985
	Equal variances not assumed			.481	60.841	.632	.0330934	.0687946	-.1044771	.1706639
n_br_aecs	Equal variances assumed	.036	.850	.871	78	.386	.0597130	.0685465	-.0767526	.1961786
	Equal variances not assumed			.879	68.517	.383	.0597130	.0679610	-.0758825	.1953085
n_br_perclos	Equal variances assumed	.839	.362	.564	78	.575	.0380345	.0674798	-.0963075	.1723766
	Equal variances not assumed			.545	58.856	.588	.0380345	.0697710	-.1015842	.1776532

Figure I.2 (continued) : t-Test of physiological data between low and high task load for cargo operation tasks.

APPENDIX J: Divergence Values of Physiological Features

Table J.1 : Divergence values of features for navigation tasks.

Feature	D_i	Feature	D_i	Feature	D_i
n_hrv_hr	0.046	n_hrv_flspk1f	0.000	n_hrv_tfwlfhf	0.016
n_hrv_sdn	0.060	n_hrv_flspk2f	0.001	n_hrv_tfwpeaklf	0.019
n_hrv_rmssd	0.030	n_hrv_nlsd1	0.029	n_hrv_tfwpeakhf	0.008
n_hrv_pnn50	0.037	n_hrv_nlsd2	0.065	eda_cdanscr	0.005
n_hrv_hrvti	0.012	n_hrv_nlsampen	0.003	n_eda_cdaampsuma	0.000
n_hrv_tinn	0.048	n_hrv_nlalpha1	0.002	n_eda_cdaampsumm	0.019
n_hrv_fwalf	0.065	n_hrv_nlalpha2	0.003	n_eda_cdascra	0.000
n_hrv_fwahf	0.039	n_hrv_tflsalf	0.067	n_eda_cdascrm	0.009
n_hrv_fwatotal	0.062	n_hrv_tflsahf	0.039	n_eda_cdaiscra	0.000
hrv_fwplf	0.022	n_hrv_tflsatotal	0.065	n_eda_cdaiscrm	0.009
hrv_fwphf	0.024	hrv_tflsplf	0.023	n_eda_cdamaxa	0.005
hrv_fwnlf	0.023	hrv_tflsphf	0.025	eda_cdamaxm	0.004
hrv_fwnhf	0.023	hrv_tflsnlf	0.024	n_eda_cdatonica	0.020
n_hrv_fwlhf	0.015	hrv_tflsnhf	0.024	n_eda_cdatonicm	0.023
n_hrv_fwpeaklf	0.030	n_hrv_tflslfhf	0.028	eda_tpnscr	0.001
n_hrv_fwpeakhf	0.000	n_hrv_tflspeaklf	0.002	n_eda_ttpampsuma	0.000
n_hrv_flself	0.037	n_hrv_tflspeakhf	0.003	n_eda_ttpampsumm	0.011
n_hrv_flself	0.001	n_hrv_tfwalf	0.083	n_eda_sca	0.018
n_hrv_flself	0.012	n_hrv_tfwahf	0.055	n_eda_scm	0.027
hrv_flself	0.019	n_hrv_tfwatotal	0.081	n_pd_mean	0.017
hrv_flself	0.020	hrv_tfwplf	0.025	pd_std	0.000
hrv_flself	0.020	hrv_tfwphf	0.025	pd_lpd	0.047
hrv_flself	0.020	hrv_tfwnlf	0.025	n_br_freq	0.002
n_hrv_flself	0.011	hrv_tfwnhf	0.025	n_br_aecd	0.065
				n_br_perclos	0.021

Table J.2 : Divergence values of features for cargo operation tasks.

Feature	D_i	Feature	D_i	Feature	D_i
n_hrv_hr	0.104	n_hrv_flpeaklf	0.036	n_hrv_tfwlfhf	0.001
n_hrv_sdn	0.086	n_hrv_flpeakhf	0.017	n_hrv_tfwpeaklf	0.003
n_hrv_rmssd	0.086	n_hrv_nlsd1	0.085	n_hrv_tfwpeakhf	0.128
n_hrv_pnn50	0.113	n_hrv_nlsd2	0.075	eda_cdanscr	0.001
n_hrv_hrvti	0.013	n_hrv_nlsampen	0.001	n_eda_cdaampsuma	0.015
n_hrv_tinn	0.096	n_hrv_nlalpha1	0.001	n_eda_cdaampsumm	0.019
n_hrv_fwalf	0.013	n_hrv_nlalpha2	0.024	n_eda_cdascra	0.034
n_hrv_fwahf	0.029	n_hrv_tflsalf	0.030	n_eda_cdascrm	0.053
n_hrv_fwatotal	0.030	n_hrv_tflsahf	0.038	n_eda_cdaiscra	0.034
hrv_fwplf	0.000	n_hrv_tflsatotal	0.048	n_eda_cdaiscrm	0.053
hrv_fwphf	0.000	hrv_tflsplf	0.000	n_eda_cdamaxa	0.010
hrv_fwnlf	0.000	hrv_tflsphf	0.001	eda_cdamaxm	0.010
hrv_fwnhf	0.000	hrv_tflsnlf	0.001	n_eda_cdatonica	0.005
n_hrv_fwlfhf	0.004	hrv_tflsnhf	0.001	n_eda_cdatonicm	0.016
n_hrv_fwpeaklf	0.002	n_hrv_tflslfhf	0.000	eda_ttpnsr	0.005
n_hrv_fwpeakhf	0.051	n_hrv_tflspeaklf	0.004	n_eda_ttpampsuma	0.005
n_hrv_flsalf	0.044	n_hrv_tflspeakhf	0.027	n_eda_ttpampsumm	0.015
n_hrv_flsahf	0.005	n_hrv_tfwalf	0.027	n_eda_sca	0.003
n_hrv_flsatotal	0.013	n_hrv_tfwahf	0.067	n_eda_scm	0.019
hrv_flsplf	0.001	n_hrv_tfwatotal	0.056	n_pd_mean	0.095
hrv_flsphf	0.001	hrv_tfwplf	0.000	pd_std	0.005
hrv_flsnlf	0.001	hrv_tfwphf	0.000	pd_lpd	0.026
hrv_flsnhf	0.001	hrv_tfwnlf	0.000	n_br_freq	0.003
n_hrv_flslfhf	0.005	hrv_tfwnhf	0.000	n_br_aecd	0.010
				n_br_perclos	0.004

APPENDIX K: Matlab Code for Eye Features

```
%pupil diameter%
clc
clear
A=load('17_Pd_S3_T8.txt');
A0 = downsample(A,2,0);
Time=A0(:,2);
Pupil=A0(:,1);

%mean%
avg1=mean(Pupil);
disp('pd_mean=');
disp(avg1)

%std%
stddev=std(Pupil);
disp('pd_std=');
disp(stddev)

%PerLPD%
Dmean=27.03;
PerLPD=(A0(:,1)-Dmean)./Dmean;

avg2=mean(PerLPD);
disp('pd_lpd=');
disp(avg2)

%blink frequency%
%blink rate%
B=load('17_Br_S3_T8.txt');
t=320;
br_freq=length(B)./t;
disp('br_freq=');
disp(br_freq)

%average eye closure duration%
duration=B(:,1);
avg3=mean(duration);
disp('br_aecd=');
disp(avg3)

%percentage of eye closure%
close=sum(B(:,1));
perclos=close./t;
disp('br_perclos=');
disp(perclos)
```

APPENDIX L: Matlab Code for ANN Classification

```
function [output_test]=ann(Y, X, neuron, iteration)

[obs, col]= size(X);
[obs1, col1]= size(Y);

%[trainInd,valInd,testInd] = divideind(obs,75:203,38:74,1:37);
[trainInd,valInd,testInd] = divideind(obs,38:169,170:203,1:37);
%[trainInd,valInd,testInd] = divideind(obs,1:130,170:203,131:169);
%[trainInd,valInd,testInd] = divideind(obs,1:130,131:169,170:203);
%[trainInd,valInd,testInd] = divideind(obs,38:169,1:37,170:203);
%[trainInd,valInd,testInd] = divideind(obs,75:203,1:37,38:74);

for i=1:length(trainInd)
    train_Y(i,1:col1)= Y(trainInd(i),:);
    train_X(i,:)= X(trainInd(i),:);
end

for i=1:length(testInd)
    test_tar(i,1:col1)= Y(testInd(i),:);
    test_inp(i,:)= X(testInd(i),:);
end

for i=1:length(valInd)
    val_Y(i,1:col1)= Y(valInd(i),:);
    val_X(i,:)= X(valInd(i),:);
end

hiddenLayerSize = [neuron neuron];
net = patternnet(hiddenLayerSize);
net.performFcn = 'mse';
net.trainFcn = 'trainlm';

net.layers{1}.transferFcn = 'tansig';

net.divideFcn= 'divideind'; % divide data into three parts with
respect to their indices.
net.divideParam.trainInd = 38:169; %75:203; %38:169; %1:130; %1:130;
%38:169; %75:203
net.divideParam.valInd = 170:203; %38:74; %170:203; %170:203;
%131:169; %1:37; %1:37;
net.divideParam.testInd = 1:37; %1:37; %1:37; %131:169; %170:203;
%170:203; %38:74;

net.trainParam.lr = 0.5; % for GD GD

net.trainParam.epochs=iteration;
%net.trainParam.goal=0;
%net.trainParam.max_fail=10;

net.trainParam.min_grad=1e-10;

[net,TR]=train(net,X',Y');
x=getwb(net)';
view(net)

outputs = net(train_X');
output_test = net(test_inp');
output_all = net(X');
```

```

output_val = net(val_X');

perf = mse(net,train_Y',outputs);
test_mse_perf = mse(net,test_tar',output_test);
val_mse_perf = mse(net,val_Y',output_val);
all_mse_perf= mse(net,Y',output_all);

entropy_train = perform(net,train_Y',outputs);
entropy_test = perform(net,test_tar',output_test);
entropy_all = perform(net,Y',output_all);

%par_fix= (neuron*(col +2)+1); % the number of paramters

par_fix= net.numWeightElements;

fprintf('mse of training data is %6.4f\n',perf);
fprintf('mse of test data is %6.4f\n',test_mse_perf);
fprintf('mse of val data is %6.4f\n',val_mse_perf);
fprintf('mse of all data is %6.4f\n',all_mse_perf);

fprintf('entropy_train is %6.4f\n',entropy_train);
fprintf('entropy_all is %6.4f\n',entropy_all);
fprintf('entropy_test is %6.4f\n',entropy_test);

fprintf('AIC is %6.4f\n',numel(train_Y)*log(perf)+ 2*par_fix);
fprintf('AICc %6.4f\n',numel(train_Y)*log(perf)+ 2*par_fix +
(2*(par_fix+1)*(par_fix+2)/ (numel(train_Y) - par_fix-2)) );
fprintf('bic %6.4f\n',numel(train_Y)*log(perf)+ par_fix+
par_fix*log(numel(train_Y)) );

end

```

APPENDIX M: MSE Values of Validation Data Sets

Table M.1 : *MSE* values of validation data sets (navigation task without feature selection).

Network structure	Partition 1	Partition 2	Partition 3	Partition 4	Partition 5	Partition 6
73-1-1-1	0.2355	0.2285	0.2041	0.2467	0.227	0.2452
73-2-2-1	0.2567	0.2235	0.2474	0.1871	0.2468	0.2468
73-3-3-1	0.2663	0.2653	0.236	0.2512	0.2659	0.3309
73-4-4-1	0.2209	0.2116	0.2543	0.286	0.2876	0.2811
73-5-5-1	0.2638	0.2066	0.2066	0.2637	0.2528	0.2586
73-6-6-1	0.2443	0.2184	0.2611	0.2372	0.2148	0.2757
73-7-7-1	0.2689	0.2278	0.2609	0.2686	0.2644	0.2817
73-8-8-1	0.3292	0.208	0.2972	0.2556	0.278	0.2875
73-9-9-1	0.2453	0.2635	0.2679	0.2643	0.2424	0.1945
73-10-10-1	0.2549	0.1791	0.1353	0.2772	0.3075	0.3071
73-11-11-1	0.2368	0.2515	0.2665	0.2497	0.2088	0.2867
73-12-12-1	0.2758	0.2607	0.2938	0.2688	0.2613	0.3543
73-13-13-1	0.2466	0.2377	0.2011	0.2255	0.2502	0.2827
73-14-14-1	0.3064	0.2021	0.2287	0.24	0.2634	0.2363
73-15-15-1	0.2658	0.2108	0.3498	0.2921	0.2467	0.2712
73-16-16-1	0.3005	0.2396	0.2575	0.2835	0.239	0.2592
73-17-17-1	0.2171	0.2368	0.2375	0.2199	0.2977	0.2533
73-18-18-1	0.2354	0.2719	0.276	0.254	0.2444	0.2533
73-19-19-1	0.2782	0.2182	0.3253	0.2565	0.259	0.2897
73-20-20-1	0.2493	0.2329	0.2483	0.2036	0.245	0.2453
73-21-21-1	0.3219	0.2514	0.3068	0.2413	0.2674	0.2599
73-22-22-1	0.2312	0.1958	0.2732	0.2824	0.2329	0.2743
73-23-23-1	0.26	0.2227	0.3154	0.2826	0.2493	0.266
73-24-24-1	0.2942	0.1632	0.1632	0.2555	0.2724	0.2482
73-25-25-1	0.2494	0.2259	0.2259	0.2731	0.2475	0.2978
73-26-26-1	0.292	0.1993	0.2001	0.236	0.2446	0.3276
73-27-27-1	0.2398	0.2669	0.2986	0.2194	0.2645	0.3068
73-28-28-1	0.2663	0.2547	0.2547	0.2643	0.2333	0.3094
73-29-29-1	0.3233	0.2062	0.31324	0.2709	0.2213	0.3157
73-30-30-1	0.2182	0.2966	0.2468	0.2045	0.2724	0.264
73-31-31-1	0.2605	0.2688	0.2777	0.2615	0.2743	0.3243
73-32-32-1	0.3433	0.3412	0.2681	0.2833	0.2717	0.3035
73-33-33-1	0.3525	0.2652	0.3012	0.272	0.2635	0.2958
73-34-34-1	0.1874	0.265	0.3205	0.2495	0.2359	0.2359
73-35-35-1	0.2804	0.2914	0.2704	0.2731	0.2621	0.3022

Table M.2 : *MSE* values of validation data sets (navigation task with feature selection).

Network structure	Partition 1	Partition 2	Partition 3	Partition 4	Partition 5	Partition 6
13-1-1-1	0.2819	0.2068	0.2001	0.284	0.2819	0.2811
13-2-2-1	0.2639	0.2403	0.2486	0.2784	0.2454	0.2488
13-3-3-1	0.3091	0.2852	0.2845	0.2602	0.2517	0.2482
13-4-4-1	0.2688	0.2207	0.2531	0.2279	0.2441	0.2688
13-5-5-1	0.2616	0.2199	0.217	0.2459	0.2616	0.2616
13-6-6-1	0.2867	0.2139	0.2401	0.2561	0.2465	0.2465
13-7-7-1	0.3383	0.1664	0.1699	0.2507	0.2569	0.2478
13-8-8-1	0.358	0.2103	0.2307	0.2511	0.2577	0.2785
13-9-9-1	0.2614	0.2206	0.2341	0.2573	0.2648	0.2614
13-10-10-1	0.2761	0.257	0.2395	0.2268	0.2336	0.2756
13-11-11-1	0.2782	0.2469	0.2469	0.2775	0.2768	0.275
13-12-12-1	0.2418	0.1972	0.2083	0.2715	0.24	0.2418
13-13-13-1	0.3125	0.2233	0.2617	0.2564	0.2706	0.3125
13-14-14-1	0.3151	0.2271	0.1993	0.2518	0.2379	0.2379
13-15-15-1	0.3423	0.1756	0.2137	0.2679	0.2636	0.2839
13-16-16-1	0.3209	0.2213	0.1673	0.2571	0.3008	0.2587
13-17-17-1	0.2884	0.2619	0.2467	0.2715	0.2726	0.2884
13-18-18-1	0.2665	0.2177	0.1732	0.3182	0.2686	0.2665
13-19-19-1	0.3418	0.2129	0.2362	0.2786	0.1862	0.2579
13-20-20-1	0.3275	0.2224	0.2334	0.3031	0.3066	0.3275
13-21-21-1	0.3367	0.2202	0.2215	0.276	0.3172	0.3091
13-22-22-1	0.334	0.197	0.2231	0.3232	0.2844	0.3003
13-23-23-1	0.3128	0.2327	0.2378	0.2181	0.312	0.271
13-24-24-1	0.275	0.1899	0.1681	0.2874	0.2924	0.275
13-25-25-1	0.2839	0.2253	0.2516	0.3313	0.2843	0.2839
13-26-26-1	0.2881	0.2513	0.2207	0.2868	0.2608	0.2881

Table M.3 : *MSE* values of validation data sets (cargo operation task without feature selection).

Network structure	Partition 1	Partition 2	Partition 3	Partition 4	Partition 5	Partition 6
73-1-1-1	0.1906	0.2495	0.2209	0.241	0.2839	0.2406
73-2-2-1	0.1964	0.1863	0.1732	0.2584	0.2425	0.254
73-3-3-1	0.17	0.2059	0.1748	0.1765	0.2428	0.1733
73-4-4-1	0.1714	0.253	0.1165	0.2634	0.325	0.251
73-5-5-1	0.2406	0.1568	0.1858	0.2382	0.2763	0.2886
73-6-6-1	0.2622	0.2427	0.1935	0.2273	0.301	0.2972
73-7-7-1	0.2201	0.261	0.2261	0.2598	0.3161	0.2861
73-8-8-1	0.2644	0.2389	0.2185	0.1182	0.2271	0.2209
73-9-9-1	0.2624	0.2057	0.1557	0.1507	0.2681	0.2568
73-10-10-1	0.2596	0.1532	0.1502	0.2071	0.2863	0.2727
73-11-11-1	0.2568	0.1971	0.1756	0.2638	0.1816	0.1871
73-12-12-1	0.2663	0.131	0.2085	0.2143	0.2203	0.2203
73-13-13-1	0.2281	0.1422	0.1504	0.3191	0.1846	0.2284
73-14-14-1	0.1717	0.1824	0.2274	0.3267	0.3245	0.2648
73-15-15-1	0.193	0.1933	0.1818	0.1929	0.3845	0.2864
73-16-16-1	0.2276	0.196	0.1653	0.2403	0.2779	0.2471
73-17-17-1	0.141	0.249	0.1757	0.2223	0.213	0.2413
73-18-18-1	0.1892	0.169	0.2452	0.2868	0.1772	0.2026
73-19-19-1	0.1968	0.1395	0.2639	0.2382	0.1907	0.2441
73-20-20-1	0.2193	0.2458	0.2023	0.236	0.2301	0.2197
73-21-21-1	0.2312	0.1144	0.1903	0.2912	0.2246	0.2465
73-22-22-1	0.25	0.1581	0.1756	0.2571	0.2034	0.2135
73-23-23-1	0.1963	0.2073	0.211	0.2851	0.2311	0.1712
73-24-24-1	0.245	0.2073	0.1987	0.1816	0.2564	0.2022
73-25-25-1	0.2728	0.1275	0.1606	0.2743	0.2292	0.2259
73-26-26-1	0.2716	0.2212	0.0899	0.203	0.2075	0.2075
73-27-27-1	0.1927	0.1678	0.1075	0.2428	0.2468	0.1985
73-28-28-1	0.194	0.2423	0.1319	0.2068	0.3062	0.223
73-29-29-1	0.2073	0.1824	0.2379	0.1925	0.2925	0.2734
73-30-30-1	0.1899	0.1441	0.1511	0.178	0.2361	0.2131
73-31-31-1	0.2732	0.1998	0.2361	0.2798	0.2937	0.3035
73-32-32-1	0.1616	0.1578	0.2417	0.2278	0.2482	0.2781
73-33-33-1	0.1961	0.1553	0.2507	0.2527	0.2532	0.2754
73-34-34-1	0.1975	0.1777	0.1634	0.2686	0.1813	0.2149
73-35-35-1	0.224	0.1627	0.2069	0.2874	0.2041	0.2333

Table M.4 : *MSE* values of validation data sets (cargo operation task with feature selection).

Network structure	Partition 1	Partition 2	Partition 3	Partition 4	Partition 5	Partition 6
10-1-1-1	0.2068	0.1759	0.1811	0.1764	0.2457	0.1899
10-2-2-1	0.2419	0.2086	0.1498	0.1445	0.2564	0.181
10-3-3-1	0.1887	0.1717	0.1715	0.2349	0.1817	0.168
13-4-4-1	0.2236	0.1522	0.1585	0.2031	0.1925	0.1668
10-5-5-1	0.1937	0.1762	0.1552	0.2535	0.1611	0.2588
10-6-6-1	0.1455	0.2044	0.2759	0.2575	0.2558	0.2043
10-7-7-1	0.1737	0.1494	0.1494	0.1376	0.1951	0.1638
10-8-8-1	0.1705	0.2289	0.2289	0.1961	0.2197	0.214
10-9-9-1	0.1893	0.2396	0.2259	0.1224	0.2537	0.1901
10-10-10-1	0.1863	0.2484	0.2255	0.2381	0.2359	0.2354
10-11-11-1	0.1761	0.161	0.1817	0.1745	0.2315	0.2172
10-12-12-1	0.1738	0.2078	0.1659	0.1165	0.247	0.2163
10-13-13-1	0.1795	0.1582	0.1855	0.2052	0.2386	0.1957
10-14-14-1	0.1368	0.2655	0.1594	0.2168	0.2367	0.2009
10-15-15-1	0.1506	0.2323	0.2531	0.1992	0.304	0.2247
10-16-16-1	0.2149	0.2356	0.1502	0.1887	0.2466	0.2571
10-17-17-1	0.1605	0.239	0.1632	0.1758	0.221	0.2733
10-18-18-1	0.1654	0.1999	0.2088	0.2181	0.2575	0.2687
10-19-19-1	0.1541	0.1646	0.1646	0.1721	0.2075	0.2075
10-20-20-1	0.0837	0.2528	0.1952	0.1093	0.2077	0.1835

CURRICULUM VITAE

Name Surname : Barış ÖZSEVER

EDUCATION :

- **B.Sc.** : 2012, Karadeniz Technical University, Sürmene Faculty of Marine Sciences, Maritime Transportation Management Engineering
- **M.Sc.** : 2015, Istanbul Technical University, Maritime Transportation Engineering Department, Maritime Transportation Engineering

PROFESSIONAL EXPERIENCE AND REWARDS:

- 2012-2013 Third Officer, ACE Tankers BV (Chemical Tanker)
- 2013-2013 Second Officer, ACE Tankers BV (Chemical Tanker)
- 2016-2016 Second Officer, Atlantik Denizcilik (Chemical Tanker)
- 2014-Present Research Assistant, Piri Reis University

PUBLICATIONS, PRESENTATIONS AND PATENTS ON THE THESIS:

- **Özsever, B.** & Tavacıoğlu, L. (2019). *An Extensive Research into Possibility of a Human-Centered Safety System for Fatigue Detection at Sea*. III. Global Conference on Innovation in Marine Technology and the Future of Maritime Transportation, İzmir, Turkey.
- Solmaz, M.S., **Özsever, B.**, Ölmez, K., & Demirkol, M. (2019). *Development of Evaluation Procedures for Chemical Tanker Officers Using Liquefied Cargo Handling Simulator*. International Maritime Lecturer Association Conference (IMLA 26), Batumi, Georgia.
- Solmaz, M. S., **Özsever, B.**, Güllü, A., & Meşe, C. (2020). Development of Evaluation Procedures for Watchkeeping Officers Using Bridge Simulator. *TransNav, the International Journal on Marine Navigation and Safety of Sea Transportation*, 14(3)
- **Özsever, B.** & Tavacıoğlu, L. (2021). Measuring mental workload and heart rate variability of officers during different navigation conditions. *Marine Science and Technology Bulletin*, 10(3), 306-312.
- **Özsever, B.** & Tavacıoğlu, L. (2021). Mental Workload (MWL) Measurement of Officers in Simulated Ship Navigation; Determining the Redlines of Performance. *International Journal of Maritime Engineering ...(..), ...-... (accepted)*

OTHER PUBLICATIONS, PRESENTATIONS AND PATENTS:

- **Özsever, B.**, Solmaz, M.S., Eyüpoglu A., & Karabulut N. (2017). *Decision Making in Cargo Tank Coatings for Chemical Tanker Companies*. IAMU 18th Annual General Assembly.
- **Özsever, B.**, & Tavacıođlu, L. (2018). Analysing the effects of working period on psychophysiological states of seafarers. *International Maritime Health*, 69(2), 84-93.

